frontiers | Research Topics

Clinical metagenomics-based diagnostics for infectious diseases

Edited by
Sathyavathi Sundararaju, Arun Prasath Lakshmanan, Pushpanathan Muthuirulan and Jeyaprakash Rajendhran

Published in
Frontiers in Cellular and Infection Microbiology

ISSN 1664-8714
ISBN 978-2-8325-5335-0
DOI 10.3389/978-2-8325-5335-0

About Frontiers

Frontiers is more than just an open access publisher of scholarly articles: it is a pioneering approach to the world of academia, radically improving the way scholarly research is managed. The grand vision of Frontiers is a world where all people have an equal opportunity to seek, share and generate knowledge. Frontiers provides immediate and permanent online open access to all its publications, but this alone is not enough to realize our grand goals.

Frontiers journal series

The Frontiers journal series is a multi-tier and interdisciplinary set of open-access, online journals, promising a paradigm shift from the current review, selection and dissemination processes in academic publishing. All Frontiers journals are driven by researchers for researchers; therefore, they constitute a service to the scholarly community. At the same time, the *Frontiers journal series* operates on a revolutionary invention, the tiered publishing system, initially addressing specific communities of scholars, and gradually climbing up to broader public understanding, thus serving the interests of the lay society, too.

Dedication to quality

Each Frontiers article is a landmark of the highest quality, thanks to genuinely collaborative interactions between authors and review editors, who include some of the world's best academicians. Research must be certified by peers before entering a stream of knowledge that may eventually reach the public - and shape society; therefore, Frontiers only applies the most rigorous and unbiased reviews. Frontiers revolutionizes research publishing by freely delivering the most outstanding research, evaluated with no bias from both the academic and social point of view. By applying the most advanced information technologies, Frontiers is catapulting scholarly publishing into a new generation.

What are Frontiers Research Topics?

Frontiers Research Topics are very popular trademarks of the *Frontiers journals series*: they are collections of at least ten articles, all centered on a particular subject. With their unique mix of varied contributions from Original Research to Review Articles, Frontiers Research Topics unify the most influential researchers, the latest key findings and historical advances in a hot research area.

Find out more on how to host your own Frontiers Research Topic or contribute to one as an author by contacting the Frontiers editorial office: frontiersin.org/about/contact

Clinical metagenomics-based diagnostics for infectious diseases

Topic editors

Sathyavathi Sundararaju — Sidra Medicine, Qatar
Arun Prasath Lakshmanan — Sidra Medicine, Qatar
Pushpanathan Muthuirulan — Harvard University, United States
Jeyaprakash Rajendhran — Madurai Kamaraj University, India

Citation

Sundararaju, S., Lakshmanan, A. P., Muthuirulan, P., Rajendhran, J., eds. (2024). *Clinical metagenomics-based diagnostics for infectious diseases*. Lausanne: Frontiers Media SA. doi: 10.3389/978-2-8325-5335-0

Table of contents

frontiers | Frontiers in Cellular and Infection Microbiology

TYPE Editorial
PUBLISHED 07 August 2024
DOI 10.3389/fcimb.2024.1459621

OPEN ACCESS

EDITED AND REVIEWED BY
Nahed Ismail,
University of Illinois Chicago, United States

*CORRESPONDENCE
Jeyaprakash Rajendhran
jrajendhran@gmail.com;
rajendhran.biological@mkuniversity.ac.in

†PRESENT ADDRESS
Sathyavathi Sundararaju,
Department of Civil Engineering, Monash University, Melbourne, VIC, Australia

RECEIVED 04 July 2024
ACCEPTED 29 July 2024
PUBLISHED 07 August 2024

CITATION
Rajendhran J, Muthuirulan P, Lakshmanan AP and Sundararaju S (2024) Editorial: Clinical metagenomics-based diagnostics for infectious diseases.
Front. Cell. Infect. Microbiol. 14:1459621.
doi: 10.3389/fcimb.2024.1459621

Editorial: Clinical metagenomics-based diagnostics for infectious diseases

Jeyaprakash Rajendhran[1]*, Pushpanathan Muthuirulan[2], Arun Prasath Lakshmanan[3] and Sathyavathi Sundararaju[4†]

[1]Department of Genetics, School of Biological Sciences, Madurai Kamaraj University, Madurai, India, [2]Department of Human Evolutionary Biology, Harvard University, Cambridge, MA, United States, [3]Precision Nutrition, Research Department, Sidra Medicine, Doha, Qatar, [4]Department of Pathology, Sidra Medicine, Doha, Qatar

KEYWORDS

clinical metagenomics, next-generation sequencing (NGS), metagenomic NGS (mNGS), infectious diseases, diagnosis, pathogen detection

Editorial on the Research Topic
Clinical metagenomics-based diagnostics for infectious diseases

Infectious diseases remain a significant global public health challenge, leading to over 13 million deaths annually (Cohen, 2000). The development of rapid and dependable diagnostic tools for infectious diseases is crucial. Traditionally, the diagnosis of infectious diseases typically involves culture-based methods, serological tests, or PCR assays. However, these methods have limitations, including time consumption, lack of specificity, and unculturability of certain organisms. Metagenomic approaches, particularly clinical metagenomics using metagenomic next-generation sequencing (mNGS) technology, offer a promising solution (Batool and Galloway-Peña, 2023). This emerging method, with its potential to significantly reduce the global burden of morbidity and mortality, instills hope and optimism in our fight against infectious diseases.

Clinical mNGS is revolutionizing diagnostics, particularly in intensive care units (ICUs), where rapid and precise pathogen identification is critical (Liang et al., 2023). It can identify a wide range of pathogens, including bacteria, viruses, fungi, and parasites, and is adept at detecting co-infections and delineating complex microbial ecosystems often missed by conventional methods. This comprehensive diagnostic capability of mNGS provides reassurance in the face of complex infectious diseases. The application of mNGS, with its role in promoting targeted therapeutic interventions, empowers healthcare professionals and significantly enhances therapeutic decision-making and optimizing antibiotic use. Importantly, deploying mNGS in clinical settings supports antimicrobial stewardship by helping to avoid the overuse of broad-spectrum antibiotics and promoting the use of more appropriate, targeted therapies.

Clinical mNGS uses NGS to analyze genetic material from clinical samples, providing a comprehensive snapshot of the microbial communities. mNGS produces a large amount of data, which can be challenging to interpret and definitively identify the causative agent.

Standard operating procedures for sample processing, sequencing, quality control, and subsequent bioinformatic analyses must be established to make mNGS suitable for regular clinical use. This Research Topic included articles covering advances from sample processing to data analysis and clinical applications of mNGS in diagnosing and treating infectious diseases.

He et al. presented a bibliometric analysis using the Web of Science on the application of mNGS in pathogen diagnosis. Their analysis revealed that 325 mNGS studies were published between 2009 and 2022. The most studied infections included pneumonia, tuberculosis, central nervous system infections, and infections in children. The number of publications on mNGS has been increasing every year, indicating the expansion of research in this field.

Du et al. have reported a case study where a 30-year-old woman was initially misdiagnosed with tuberculosis. The anti-tuberculosis treatment did not work, and eventually, she developed sepsis. Subsequently, through mNGS, she was diagnosed with talaromycosis caused by *Talaromyces marneffei*. After receiving appropriate antifungal treatment, her health condition improved. Xu et al. reported another case study where *T. marneffei* infection was diagnosed in a renal transplant patient. They detected *T. marneffei* sequences in blood and bronchoalveolar lavage fluid using mNGS and then confirmed it with a blood culture. This study showed the value of using mNGS for diagnosis and highlighted the importance of starting antifungal treatment promptly, which helped the patient recover successfully.

Wu et al. have reported that mNGS was used to diagnose pneumonia caused by *Chlamydia psittaci*. Four patients were admitted with pneumonia symptoms, and their bronchoalveolar lavage fluid (BALF) samples underwent multiple tests, such as acid-fast bacteria, fungal, galactomannans tests, and tumor marker tests, and found all the tests were negative. However, chest CT scans revealed multiple infectious lesions in both lungs. Also, serum inflammatory markers like C-reactive protein (CRP) were elevated in all patients. Subsequently, mNGS testing was performed on BALF samples obtained through bronchoscopy, which revealed *Chlamydia psittaci* infection. As a result of the diagnosis, the antibiotic treatments were modified, leading to the successful treatment of the patients. Xie et al. investigated the microbiomes in the lower respiratory tracts of patients with chlamydial pneumonia using mNGS. They found that patients infected with *C. psittaci* had more co-infecting pathogens than those infected with *Chlamydia abortus*. Furthermore, they observed that different clinical subgroups exhibited significantly distinct profiles of lower respiratory tract microbiomes. Mixed infections involving *C. psittaci* and *C. abortus* were linked to lower lung microbiome diversity, indicating that chlamydial infections shape the unique lung microbiome and pathology. Wu et al. also reported that mNGS significantly improved the accuracy and detection rate of pathogens in patients with pulmonary infections after examining more than 500 BALF samples.

Chen et al. analyzed sputum samples from 50 patients with pulmonary infections following cardiac surgery using conventional culture testing and mNGS. They identified 64 bacterial pathogens, ten fungal pathogens, and three viruses. Importantly, they distinguished between opportunistic pathogenic and colonizing strains in the individual samples. These findings offer valuable insights into the precise diagnosis of pathogens, particularly opportunistic pathogens, in a clinical setting.

Zhao et al. conducted a study comparing a new mNGS tool called Quality/Quantity mNGS (QmNGS) with the standard mNGS for diagnosing pulmonary pathogens. They evaluated the bronchoalveolar lavage fluid from 36 patients with suspected pulmonary infection using both UmNGS and QmNGS. The study found that the sensitivity of QmNGS was similar to that of mNGS, while the specificity of QmNGS was slightly higher. However, it was noted that the depth and coverage of the QmNGS sequencing were lower than those of UmNGS. Chen et al. introduced a 16S rDNA nanopore sequencing method called NB16S-seq by adding pathogen-specific barcodes to the 16S rRNA gene primers. This improved mNGS tool enabled the rapid identification of common pulmonary bacterial pathogens in bronchoalveolar lavage fluid samples from children with severe pneumonia.

Zhang et al. assessed the clinical advantages of mNGS in hematological patients with and without hematopoietic stem cell transplantation (HSCT). They found that mNGS is highly sensitive in detecting pathogens and can be a basis for anti-infective therapies in hematological diseases. However, they noted that mNGS cannot wholly replace traditional detection methods. They suggested that mNGS of peripheral blood can serve as a valuable complementary detection method when traditional tests are negative or when specimens are challenging to obtain. In a study, Liu et al. assessed the diagnostic accuracy and clinical significance of blood mNGS in ICU patients suspected of having mono- and polymicrobial bloodstream infections. The research revealed that mNGS demonstrated better diagnostic accuracy and higher sensitivity than blood culture, particularly for polymicrobial infections. Consequently, mNGS has the potential to play a crucial role in accurately diagnosing and treating infections in critically ill patients. Cao et al. analyzed circulating cell-free DNA using mNGS from blood samples of ICU patients at high risk of bloodstream infections. They aimed to determine if a modified mNGS (mcfDNA-seq) version could detect pathogens before blood cultures indicated any positive infection. The results showed a higher diagnostic and overall predictive sensitivity of mcfDNA-seq, suggesting its potential use in identifying pathogens before the onset of bloodstream infections.

The application of mNGS of urine samples has been reported by Huang et al. for diagnosing urinary tract infections (UTIs) among patients undergoing cutaneous ureterostomy (CU). The study found that mNGS could efficiently detect pathogens and assist in the early diagnosis of UTI in CU patients, making it helpful for monitoring microbial changes in their urine. Additionally, mNGS could detect the presence of genes coding for virulence factors and antimicrobial resistance, facilitating appropriate antimicrobial therapy. It's essential to ensure that metagenomic DNA extraction is reliable and reproducible so that mNGS can be used effectively for pathogen detection. Zhang et al. compared three DNA extraction methods for urine samples with microbial infections to address this.

They used long-read nanopore sequencing to evaluate metagenomic DNA yield, integrity, and microbial diversity. Based on their findings, they recommend using an enzyme-based method for metagenomic DNA extraction from urine for mNGS-based pathogen detection.

Zhang et al. evaluated the use of mNGS in detecting pathogens responsible for spinal infections. They used the infected tissue and pus samples for mNGS and culturing. Pathogenic organisms like *Mycobacterium tuberculosis* complex, *Staphylococcus aureus*, *Mycoplasma hominis*, and *Brucella* spp. were identified in multiple samples through mNGS analysis. The results emphasized its superior sensitivity and specificity compared to microbial culture, reaffirming mNGS's importance in guiding treatment decisions and enhancing patient outcomes. Xu et al. also reported the superiority of mNGS over culture methods in detecting pathogens responsible for spinal infections using blood and tissue samples. Notably, novel pathogens, including non-tuberculosis mycobacteria, other fungi, and bacterial species, were detected using mNGS. Sepsis is a leading cause of death in patients with cervical spine injury (CSI). Wan et al. conducted a study to assess the effectiveness of mNGS in identifying pathogens in CSI patients with sepsis. They tested 27 blood samples from 17 patients using mNGS and found that it could detect a wide range of pathogens, including 129 bacterial species, eight viral species, and 51 fungal species. The authors concluded that while mNGS does not have prognostic value, it can help guide antibiotic therapy in CSI patients diagnosed with sepsis.

Central nervous system (CNS) infections can be fatal and require rapid medical intervention. However, accurate detection of pathogens in cerebrospinal fluid (CSF) samples has been challenging due to the small sample volumes and low detection efficiency of traditional culture methods. Yu et al. evaluated the effectiveness of mNGS in diagnosing CNS infections using CSF samples from 390 patients. They analyzed both cell-free and whole-cell DNA from the CSF and found that mNGS outperformed traditional methods in detecting pathogens, especially in viral and mycobacterial CNS infections. Zhang et al. also performed mNGS of CSF samples from patients infected with community-acquired central nervous system infections (CA-CNS). The study identified various pathogens responsible for CA-CNS infections, many of which could not be detected by conventional methods.

Cancer patients, particularly those with weakened immune systems, are at high risk of developing infections. Having reliable and fast diagnostic methods for identifying infections in these patients is crucial. In a study by Deng et al., the effectiveness of nanopore amplicon sequencing in detecting pathogens in immunocompromised cancer patients with suspected infections was evaluated. The researchers tested samples of BALF, blood, sputum, urine, and peritoneal fluid from the suspected patients. It is a modified version of mNGS, where PCR-amplified products are sequenced with barcodes. The results demonstrated that nanopore amplicon sequencing enables early detection of infections and facilitates precise treatment with anti-infective medications. Colorectal cancer (CRC) is one of the most prevalent cancers. Following surgery to resect the primary tumor in CRC patients, stoma construction is typically performed. Sakai et al. compared the microbiome of CRC patients with and without a stoma using fecal mNGS. Their findings revealed a reduction in anaerobic microbial composition in patients with a stoma. Additionally, they observed an underrepresentation of genes associated with methane and short-chain fatty acid production in stoma patients.

Preeclampsia (PE) is a pregnancy complication with severe hypertension and multiple organ damage. In a study by Lv et al., the fecal samples from 40 early-onset PE patients and 37 healthy pregnant women were analyzed using mNGS. The study found that the presence of certain species, such as *Blautia*, *Pauljensenia*, *Ruminococcus*, and *Collinsella*, as well as specific microbial functions, were associated with PE. Zhang et al. assessed the diagnostic accuracy of mNGS, Xpert, and droplet digital PCR (ddPCR) in detecting Mycobacterium tuberculosis (MTB) in various clinical samples such as BALF, pleural effusion, pericardial effusion, and ascites. Their findings revealed that ddPCR exhibited the highest sensitivity compared to mNGS and Xpert for diagnosing active MTB cases. In a study by Huang et al., fungal co-infections in critically ill patients during the Omicron variant outbreak of COVID-19 from December 2022 to January 2023 were investigated using BALF and blood mNGS. The study revealed that mNGS detected a significantly higher number of pathogenic microorganisms than traditional methods, especially in detecting fungi and viruses. Aspergillus infection was the most common; most patients had concurrent bacterial or viral infections. The study emphasized the superior detection rates of mNGS compared to conventional methods and highlighted the importance of early intervention for fungal infections in COVID-19 patients.

The use of clinical mNGS for diagnostics is a groundbreaking advancement in the field of infectious disease. Articles on this Research Topic discuss using mNGS to identify bacterial, fungal, and viral infections in the blood, BALF, CSF, sputum, peritoneal fluid, urine, and fecal samples. mNGS can also be used to detect microbiome dysbiosis. There is potential to expand the use of mNGS to diagnose any infectious disease from any biological sample. However, it is crucial to establish a standard protocol for diagnosing various diseases using mNGS. mNGS offers comprehensive, rapid, and accurate pathogen identification, potentially significantly improving patient outcomes, mainly when traditional methods are insufficient. While challenges remain, ongoing innovation and collaboration among the scientific and medical communities will enhance the robustness and feasibility of mNGS in combating infectious diseases.

Author contributions

JR: Writing – original draft, Writing – review & editing. PM: Writing – original draft, Writing – review & editing. AL: Writing – original draft, Writing – review & editing. SS: Writing – original draft, Writing – review & editing.

Funding

The author(s) declare that financial support was received for the research, authorship, and/or publication of this article. This work was supported by the MKU-RUSA program (File No.012/RUSA/MKU/2020-2021) of Madurai Kamaraj University.

Acknowledgments

We extend our gratitude to all the authors who contributed to this Research Topic and the reviewers for their meticulous peer review. JR acknowledges MKU-RUSA program (File No.012/RUSA/MKU/2020-2021) of Madurai Kamaraj University.

Conflict of interest

The authors declare that the research was conducted in the absence of any commercial or financial relationships that could be construed as a potential conflict of interest.

Publisher's note

References

Batool, M., and Galloway-Peña, J. (2023). Clinical metagenomics-challenges and future prospects. *Front. Microbiol.* 14. doi: 10.3389/fmicb.2023.1186424

Cohen, M. (2000). Changing patterns of infectious disease. *Nature* 406, 762–767. doi: 10.1038/35021206

Liang, Y., Feng, Q., Wei, K., Hou, X., Song, X., and Li, Y. (2023). Potential of metagenomic next-generation sequencing in detecting infections of ICU patients. *Mol. Cell Probes.* 68, 101898. doi: 10.1016/j.mcp.2023.101898

frontiers in Cellular and Infection Microbiology

ORIGINAL RESEARCH
published: 03 March 2022
doi: 10.3389/fcimb.2022.855839

Metagenomic Assessment of the Pathogenic Risk of Microorganisms in Sputum of Postoperative Patients With Pulmonary Infection

Junji Chen[1†], Lianjie Sun[2†], Xiaoying Liu[1], Qixiang Yu[1], Kaijie Qin[1], Xuejie Cao[2] and Jianwei Gu[1]*

[1] Department of Cardiovascular Surgery, Ruijin Hospital, Shanghai Jiao Tong University School of Medicine, Shanghai, China, [2] Genoxor Medical Science and Technology Inc., Zhejiang, China

OPEN ACCESS

Edited by:
Costas C. Papagiannitsis, University of Thessaly, Greece

Reviewed by:
Ibrahim Bitar, Charles University, Czechia
Ana Elena Pérez-Cobas, Ramón y Cajal Institute for Health Research, Spain

***Correspondence:**
Jianwei Gu
gjw11428@rjh.com.cn

[†]These authors have contributed equally to this work

Specialty section:
This article was submitted to Clinical Microbiology, a section of the journal Frontiers in Cellular and Infection Microbiology

Received: 16 January 2022
Accepted: 11 February 2022
Published: 03 March 2022

Citation:
Chen J, Sun L, Liu X, Yu Q, Qin K, Cao X and Gu J (2022) Metagenomic Assessment of the Pathogenic Risk of Microorganisms in Sputum of Postoperative Patients With Pulmonary Infection. Front. Cell. Infect. Microbiol. 12:855839. doi: 10.3389/fcimb.2022.855839

Respiratory infections are complicated biological processes associated with an unbalanced microbial community and a wide range of pathogens. To date, robust approaches are still required for distinguishing the pathogenic microorganisms from the colonizing ones in the clinical specimens with complex infection. In this study, we retrospectively analyzed the data of conventional culture testing and metagenomic next-generation sequencing (mNGS) of the sputum samples collected from 50 pulmonary infected patients after cardiac surgery from December 2020 and June 2021 in Ruijin Hospital. Taxonomic classification of the sputum metagenomes showed that the numbers of species belonging to bacteria, fungi, and viruses were 682, 58, and 21, respectively. The full spectrum of microorganisms present in the sputum microbiome covered all the species identified by culture, including 12 bacterial species and two fungal species. Based on species-level microbiome profiling, a reference catalog of microbial abundance detection limits was constructed to assess the pathogenic risks of individual microorganisms in the specimens. The proposed screening procedure detected 64 bacterial pathogens, 10 fungal pathogens, and three viruses. In particular, certain opportunistic pathogenic strains can be distinguished from the colonizing ones in the individual specimens. Strain-level identification and phylogenetic analysis were further performed to decipher molecular epidemiological characteristics of four opportunistic etiologic agents, including *Klebsiella pneumoniae*, *Corynebacterium striatum*, *Staphylococcus aureus*, and *Candida albicans*. Our findings provide a novel metagenomic insight into precision diagnosis for clinically relevant microbes, especially for opportunistic pathogens in the clinical setting.

Keywords: pulmonary infection, sputum microbiome, metagenomic next-generation sequencing, pathogen risk, limit of detection, opportunistic pathogen, strain profiling

INTRODUCTION

As is well known, postoperative pulmonary infections are characterized by cough, phlegm, shortness of breath, chest pain, and temperature above 38 degrees (Conde and Lawrence, 2008). The etiological agents causing respiratory tract infections (RTIs) are usually related to a wide variety of pathogenic microbes (Cappelletty, 1998; Chowdhary et al., 2016; Kutter et al., 2018). For instance, a study on 426 patients with suspected lower RTIs has revealed that the most prevalent bacterial species isolated from the specimens (i.e. sputum, endotracheal secretion, and bronchial washing) were *Pseudomonas aeruginosa* and *Haemophilus influenzae* from Gram-negative organisms, and *Streptococcus pneumonia* and *Staphylococcus aureus* from Gram-positive (Khan et al., 2015). Several studies on respiratory infections have reported that *Schizophyllum commune* belonging to filamentous basidiomycetes is an emerging fungal pathogen, and its culture and species identification need a couple of weeks under specific culture media (Chowdhary et al., 2013; Chowdhary et al., 2016). Although traditional culture methods are still the gold standard for clinically microbiological testing, the new omics approaches particularly metagenomics have facilitated culture-free, faster detection for different types of pathogens (e.g. bacteria, viruses, and fungi) in complicated infectious diseases (Deurenberg et al., 2017; Ferone et al., 2020). Besides, many members of the human respiratory tract microbiota are colonizing opportunistic pathogens that are normally harmless and, when the microbial homeostasis becomes disrupted, can cause infections (Price et al., 2017).

Taxonomic profiling *via* metagenomic next-generation sequencing (mNGS) techniques has enabled higher sensitivity and resolution than does conventional culture approaches for better understanding of microbial compositions present in the sputum specimens (Human Microbiome Project Consortium, 2012; Finch et al., 2015; Yan et al., 2016; Ditz et al., 2020; Dicker et al., 2021b). According to 16S rRNA gene amplicon sequencing of sputum samples and clinically measured phenotypes of patients with bronchiectasis, a prospective observational study has revealed that the risk of exacerbation and long-term outcomes are associated with the reduced diversity of sputum microbiome, particularly dominated by bacterial genera *Pseudomonas*, *Enterobacteriaceae*, and *Stenotrophomonas* (Dicker et al., 2021b). Another study has also demonstrated that the dominance of *Proteobacteria* in the sputum microbiome is significantly associated with the neutrophil activation pathway and increased mortality in chronic obstructive pulmonary disease (Dicker et al., 2021a). Besides, Yan et al., have reported that the "near-complete" bacterial genomes could be reconstructed for the highest-abundant pathogens through sputum massive metagenomic sequencing (Yan et al., 2016).

To date, how to distinguish microbial colonization and/or infection is still a vital issue for pathogen identification under hospital settings. To address the above issue, the sputum microbiota of a cohort of postoperative patients with pulmonary infection were investigated based on the data of mNGS and culture testing. Metagenomic analysis was performed to reveal the taxonomic diversity of the sputum microbial community. Based on species-level microbiome profiling, a reference catalog of abundance detection limits was constructed to assess the pathogenic risk of individual microorganisms, which was further compared with the species detected by culture. Subsequently, strain-level identification and phylogenetic analysis were carried out to characterize the clinically relevant pathogens. The scheme of microbial abundance detection limits proposed in this manuscript may provide a useful reference to metagenomic surveillance for opportunistic pathogenic microbes.

MATERIALS AND METHODS

Patients and Samples

This retrospective analysis was performed for the patients with suspected lung infections after cardiac surgery in Ruijin Hospital. In this study, the postoperative patients were enrolled based on abnormal imaging changes represented by chest X-ray, including chest infiltration, consolidation, cavity, and pleural effusion. Pulmonary infection was determined if at least two of the following three options were satisfied: 1) fever greater than 38℃, 2) the number of white blood cells beyond the routine detection limits, 3) occurrence of purulent airway secretion. Sputum specimens of the patients were collected from December 2020 and June 2021 (**Table S1**).

Specimen Culture

According to the cultivation procedure for bacteria and fungi in the diagnostic laboratory of Ruijin Hospital, the routine isolation media were used, including blood agar, eosin methylene-blue (EMB) agar, chocolate agar, Mueller-Hinton agar, sabouraud dextrose agar, and cooked meat medium (Oxoid, UK). Chocolate agar and EMB agar plates were incubated in 5-10% CO_2 at 37°C for 48-72 hours; blood agar, Mueller-Hinton agar, and cooked meat medium plates were incubated at 37°C for 24-48 hours. Sabouraud dextrose agar plates suitable for the isolation of *Candida albicans* were incubated at 28°C and 35°C for 24-48 hours, respectively. Species identification of isolated strains was then carried out using the VITEK-2 Compact Instrument (bioMérieux, France) (Melhem et al., 2014).

Experiments of mNGS

For the preprocessing of specimens, sputum samples were homogenized by the dithiothreitol (DTT) treatment as proposed by Terranova et al. (Terranova et al., 2018). Approximately 200 μL sputum per sample was resuspended by 600 μL of DTT solution (1% concentration) and 20 μL of proteinase K (20 mg mL^{-1}), followed by incubation at 56°C for 20 mins. Cells were removed by centrifugation to reduce host-background nucleic acid. Total DNA was extracted using HostZERO Microbial DNA Kit (Zymo Research, USA) following the manufacturer's instructions. DNA extraction yield was quantified using a Quant-iT dsDNA HS Assay Kit and Qubit 3.0 Fluorometer (Thermo Scientific, USA). Enzymatic

shearing was employed for the fragmentation (~200 bp) of DNA molecules and the libraries were then constructed using the Nextera XT DNA Library Preparation Kit (Illumina, USA). A certain number of PCR cycles (5-7) were applied to produce 1 μg of the metagenomic library. The quality of the libraries was assessed by a 2100 Bioanalyzer using the High Sensitivity DNA Assay (Agilent Technologies, USA). Metagenome shotgun sequencing in a single-end 75-bp mode was performed using the NextSeq 500/550 High Output Kit (92 cycles) on an Illumina NextSeq 550 sequencer. The samples as the No-Template Control (NTC) were sequenced simultaneously to assess contaminations during the wet-lab experiments.

Bioinformatics Analysis of Species-Level Abundance Profiling

Raw sequencing data were first subjected to a quality control process for trimming adapter sequences, removing low-quality tails and reads by Trimmomatic v0.36 (Bolger et al., 2014). Next, the reads mapping to the human reference genome GRCh37 were excluded using the short-read alignment tool Bowtie v2.2.6 (Langmead and Salzberg, 2012). To remove identical duplicated reads considered as technical artifacts by PCR (Martin et al., 2018), de-duplication was performed using an in-house Perl script. Taxonomic classification of microbial reads was conducted using Kraken v2.0.9-beta (Wood et al., 2019) and a custom *k*-mer database constructed using 51,543 genomes of ~27,000 species from the NCBI assembly databases (Kitts et al., 2016). To produce species-level abundance estimates, the number of reads in the Kraken classification report was further estimated by the Bayesian algorithm implemented by Bracken v2.2 (Lu et al., 2017). The microbial taxa bearing putative contamination during the experiments were removed from the final profiles based on the information of NTC samples in each batch: the ratio of read count (sputum sample)/read count (NTC) less than 10 for a specified species. Using a similar way to TPM (transcripts per million) described by Li et al. (Li et al., 2009), the estimates of percentage relative abundance of each species were computed for bacteria, viruses (excluding phages), and fungi, respectively.

To investigate pathogenic signals in the sputum microbiome, we proposed a rule of thumb to evaluate detection limits of pathogenic risks for individual organisms through species-level abundance profiling. Briefly, the values of the mean and standard deviation of relative abundances were calculated according to the estimates of each species across the samples. In this study, limits of detection (LOD) for prompting pathogenic potential of a specified species were estimated through the filtering criteria below: read count > 100; relative abundance > 0.05; presence in at least three samples; the mean plus the standard deviation of the abundance values as the LOD of the pathogenic risk.

Strain-Level Phylogenetic Analysis

Strain-level profiling analysis was conducted based on single-nucleotide variants (SNVs) using the StrainPhlAn v3.0 package (Truong et al., 2017). Briefly, metagenomic reads per sample were first aligned to the marker gene database of MetaPhlAn v3.0 (Beghini et al., 2021). The sample-specific consensus sequences from the markers were reconstructed for each species' most abundant strain and the species-specific markers were extracted from MetaPhlAn for identifying the homologous sequences in the reference isolate genomes using blastn (Altschul et al., 1990). Based on sequence alignment, maximum-likelihood phylogenetic trees were reconstructed using RAxML (Stamatakis, 2014) and then visualized using MEGA10 (Kumar et al., 2018). Genome sequences of the isolated strains were retrieved from the NCBI Assembly database and were used for phylogenetic reconstruction together with the strains detected in the metagenomic samples. The program MetaMLST v1.2.2 was employed to predict the known and novel Sequence Type (ST) of the most abundant strains in metagenomic samples (Zolfo et al., 2017). Since it is complicated to resolve the phylogeny of the diploid fungi, an alternative pipeline was used to build the phylogenetic tree according to multilocus sequence typing (MLST) analysis of seven loci (Hirakawa et al., 2015b). Seven MLST allele sequences were reconstructed from the metagenomes using MetaMLST, and the related gene sequences from the isolate genomes were processed using FastMLST (Guerrero-Araya et al., 2021). Multiple sequence alignment was performed with MUSCLE (Edgar, 2004), and the phylogeny was inferred with RAxML.

Statistical Analysis of Community Diversity

The analysis of α-diversity and two sample T-test were conducted using the package fossil v0.4.0 (Chao, 1987) based on the Chao1 index representing community richness. To estimate the community compositional variation of the samples between groups, β-diversity was measured by calculating the Bray-Curtis distance matrix using Vegan v2.5-7 (Dixon, 2003). Differences in the rank dissimilarities within and between groups were inferred using the non-parametric ANOSIM test of 1,000 permutations. All statistical analyses and visualizations were performed in R v4.1.0 (R Core Team, 2021).

RESULTS

Characteristics of Patients and Samples

In this retrospective study, we analyzed the data of microbiological testing on sputum samples from postoperative patients that were diagnosed with pulmonary infection. During the 7-month study, the specimens were collected from 50 adults aged from 34 to 81 years with a median of 64 years. Approximately three quarters (n = 36; 72%) were male. Participant characteristics are listed in **Table S1**, including body mass index (BMI), dates of both cardiac surgery and specimen sampling, patient outcomes, National Early Warning Score (NEWS) (Smith et al., 2013), and Sequential Organ Failure Assessment (SOFA) scores upon admission (Vincent et al., 1998). The median time of sample collection was day 3 after the cardiac surgery. The samples were then subject to conventional culture and mNGS testing for species

identification. DNA mNGS testing yielded an average of 22.9 million reads for each specimen (**Table S2**).

Species Identification and Pathogenic Risk

As shown in **Table S1**, the culture testing reported 12 bacterial species and two fungal species across all the samples. It resulted in one species detected in each of the 16 sputum samples, two species in five samples, and three species in one sample (**Table 1**). None of the microorganisms was detected in the remaining tested samples (n = 28; 56%) by the culture method. On the contrary, a substantial number of microorganisms were identified by mNGS testing. The numbers of microorganisms assigned to the domains bacteria, fungi, and viruses were 682, 58, 21, respectively. Particularly, the numbers of bacterial and fungal

TABLE 1 | Summary of the number of microorganisms detected by culture and mNGS testing for the individual sputum specimens.

ID	Culture testing		mNGS testing					
			Screening by read count			Screening by LOD		
	Bacteria	Fungi	Bacteria	Fungi	Viruses	Bacteria	Fungi	Viruses
S1	1	0	120	3	0	1	0	0
S2	1	1	8	2	1	1	1	0
S3	1	0	34	3	1	3	0	0
S4	0	0	139	3	0	1	1	0
S5	0	0	26	6	0	1	0	0
S6	0	0	132	11	4	4	2	1
S7	1	0	125	11	4	3	1	0
S8	1	0	128	13	3	2	1	1
S9	0	0	173	5	1	2	0	0
S10	1	0	175	3	1	1	0	0
S11	0	0	19	4	8	3	1	0
S12	0	2	7	6	0	1	2	0
S13	0	1	151	17	2	4	1	0
S14	1	0	79	11	4	2	1	0
S15	1	0	176	14	2	1	0	0
S16	1	0	39	1	0	1	0	0
S17	0	0	63	6	1	3	1	0
S18	1	0	77	4	0	4	1	0
S19	0	0	97	5	3	4	1	0
S20	0	0	138	14	1	2	1	0
S21	1	0	219	5	1	4	0	0
S22	0	0	46	4	3	1	0	0
S23	0	0	79	2	0	5	1	0
S24	0	0	207	5	0	3	0	0
S25	1	0	15	5	1	1	1	1
S26	0	0	25	3	1	3	0	0
S27	0	0	141	5	6	1	1	1
S28	0	0	192	3	1	4	1	0
S29	2	1	42	5	3	1	1	1
S30	0	0	42	2	0	1	0	0
S31	0	0	43	6	1	3	1	0
S32	2	0	197	3	1	2	0	0
S33	0	0	47	4	0	4	0	0
S34	0	0	85	2	0	4	0	0
S35	0	0	98	2	1	5	0	0
S36	1	0	4	2	0	2	0	0
S37	2	0	4	5	0	1	1	0
S38	1	0	216	4	0	2	0	0
S39	0	0	196	13	0	3	1	0
S40	1	0	15	6	1	1	0	0
S41	1	0	46	2	2	2	1	0
S42	0	0	101	2	1	7	0	1
S43	0	0	163	3	1	7	1	0
S44	1	1	50	4	3	2	2	1
S45	0	0	125	2	1	2	0	1
S46	0	0	103	2	0	5	0	0
S47	0	0	22	6	1	0	1	0
S48	0	0	24	3	0	1	0	0
S49	0	0	42	4	0	0	0	0
S50	0	0	14	3	0	1	0	0

species detected by mNGS testing were much higher than those by culture in the individual samples (**Table 1**). The average number of bacterial species in each sample was 90 with a range from 4 to 219. The average number of fungal species in each sample was 5 with a range from 1 to 17. Besides, the viral species were identified in more than half (n = 31; 62%) of the samples through mNGS; whereas the routine culture approach used in our study can support isolation and identification for bacteria and fungi, but not for viruses.

To assess the pathogenic risk of individual microorganisms, we proposed the abundance LOD for screening candidate pathogens based on mNGS assays and species-level abundance profiles of bacteria, fungi, and viruses, respectively (**Table S3**). Most of the bacterial and fungal species detected by the culture approach were present in the list of the pathogens that were screened out in the individual samples (**Table 2**; the full list shown in **Table S1**). For instance, both culture and mNGS testing for patient #2 identified *B. cenocepacia* and *C. albicans*, which were predominant pathogens in the bacterial (86.3% abundance) and fungal community (98.7%), respectively. For patient #44, the mNGS approach identified five pathogens *C. striatum* (56.2%), *S. aureus* (39.2%), *C. albicans* (93.1%), *A. flavus* (5.5%), and Human alphaherpesvirus 1 (99.8%). Of these, *S. aureus* and *C. albicans* were also detected by culture. According to the LOD (30.8%) of *K. pneumoniae*, this bacterium was assessed as a pathogen in the four patients: 85.4% for #1, 87.1% for #4, 97.7% for #16, and 72.1% for #40. The sputum culture was positive for *K. pneumoniae* in these patients except for #4. The mNGS approach for patient #4 identified *K. pneumoniae* (87.1%) and *C. albicans* (97.8%) as pathogens; whereas, none of them was detected by culture. *C. albicans*, an opportunistic pathogenic yeast, was the most prevalent fungal pathogen detected in the sputum metagenomes of 15 patients (**Table S1**). In addition, human alphaherpesvirus 1 was the most frequently detected pathogen that was identified in six patients. Generally, according to our proposed mNGS screening criteria, the predicted microbial targets bearing pathogenic risk not only well matched the ones detected by culture, but also provided additional and prioritized pathogens missed by culture. It should provide complementary evidence for microbiological diagnosis in the clinical setting.

Community Structure of the Sputum Microbiota

To explore organismal composition in the sputum microbiota, the mNGS dataset containing all sequenced metagenomes was analyzed. We focused on the diversity of bacterial communities

TABLE 2 | List of selected sputum specimens from post-surgery infected patients tested in this study.

ID	Patient's sex, age[a]	Culture testing[b]	Pathogens based on mNGS testing with LOD		
			Bacteria	Fungi	Viruses
1	m, 71	*Klebsiella pneumoniae*	*Klebsiella pneumoniae* (85.4%);	–	–
2	m, 67	*Burkholderia cenocepacia*; *Candida albicans*	*Burkholderia cenocepacia* (86.3%);	*Candida albicans* (98.7%);	–
3	f, 77	*Enterobacter cloacae* complex	*Staphylococcus epidermidis* (51.7%); *Enterobacter hormaechei* (23.8%); *Enterococcus faecalis* (5.7%);	–	–
4	m, 49	–	*Klebsiella pneumoniae* (87.1%);	*Candida albicans* (97.8%);	–
7	m, 65	*Stenotrophomonas maltophilia*	*Stenotrophomonas maltophilia* (50.9%); *Mogibacterium timidum* (8.0%); *Enterococcus faecalis* (7.9%);	*Talaromyces marneffei* (31.3%);	–
10	m, 65	*Serratia marcescens*	*Serratia marcescens* (56.8%);	–	–
11	m, 79	–	*Abiotrophia defectiva* (37.0%); *Staphylococcus epidermidis* (30.4%); *Klebsiella oxytoca* (5.1%);	*Candida albicans* (89.8%);	–
14	m, 79	*Acinetobacter baumannii*	*Stenotrophomonas maltophilia* (57.0%); *Acinetobacter baumannii* (21.0%);	*Candida parapsilosis* (98.5%);	–
16	f, 71	*Klebsiella pneumoniae*	*Klebsiella pneumoniae* (97.7%);	–	–
25	m, 46	*Acinetobacter baumannii*	*Acinetobacter baumannii* (99.2%);	*Candida albicans* (99.7%);	Human betaherpesvirus 5 (99.6%);
26	m, 64	–	*Parvimonas micra* (51.7%); *Streptococcus anginosus* (13.1%); *Streptococcus milleri* (13.0%);	–	–
27	m, 70	–	*Corynebacterium striatum* (92.9%);	*Candida albicans* (99.0%);	Human alphaherpesvirus 1 (53.6%);
28	f, 55	–	*Parvimonas micra* (27.9%); *Streptococcus oralis* (23.1%); *Atopobium rimae* (6.6%); *Atopobium parvulum* (5.1%);	*Candida albicans* (89.9%);	–
36	m, 71	*Acinetobacter baumannii*	*Acinetobacter baumannii* (50.8%); *Staphylococcus aureus* (48.9%);	–	–
40	m, 62	*Klebsiella pneumoniae*	*Klebsiella pneumoniae* (72.1%);	–	–
44	f, 66	*Staphylococcus aureus*, *Candida albicans*	*Corynebacterium striatum* (56.2%); *Staphylococcus aureus* (39.2%);	*Candida albicans* (93.1%); *Aspergillus flavus* (5.5%);	Human alphaherpesvirus 1 (99.8%);

[a] 'f' for female and 'm' for male.
[b] '-' denotes none of the organisms is detected.

bearing high species richness compared to the fungal and viral communities (**Table 1**). The species accumulation curve tended to be smooth, indicating that the number of bacterial species would vary slowly with the increase in sample size (**Figure 1A**). The profile of percentage taxonomic abundances across the sputum metagenomes was displayed in **Figure 1B**. According to the average values of abundances, the top five abundant species were *K. pneumonia* (7.3%), *S. maltophilia* (5.6%), *S. epidermidis* (4.9%), *S. infantis* (4.8%), and *A. baumannii* (3.6%) (**Figure 1B**). It was observed that certain species that were remarkably dominating in the community of the individual samples were estimated to be etiologic agents mentioned above, such as *K. pneumonia* in #1/#4/#16/#40, *A. baumannii* in #25/#36, *N. flavescens* in #9/#17/#46, and *S. anginosus* in #13/#19/#21/#24/#26 (**Table S1**). Next, we compared the community structural dynamics of the sputum microbiota between two clinical outcomes: Recovery and Worse. The α-diversity analysis of community richness indicated that no significant difference ($p = 0.125$) was found between the two groups (**Figure 1C**). Based on the β-diversity ANOSIM test (R = 0.173, $p = 0.008$), it was apparent that the mean of ranked dissimilarities between groups was lower than that within the group Worse (**Figure 1D**). Meanwhile, the low R-value suggested a weak effect of clinical outcomes on the microbial communities. Both α- and β-diversity analyses indicated that the bacterial community diversity was less associated with clinical outcomes of postoperative infected patients, probably due to diverse pathogens dominating the individual samples.

Strain-Level Characteristics of Pathogens

Strain identification is of significant importance for better understanding microbial pathogenicity and transmission of clinically relevant microorganisms (Nayfach et al., 2016). According to the pathogen list assessed by mNGS testing (**Table S1**), strain-level profile analysis was performed for four

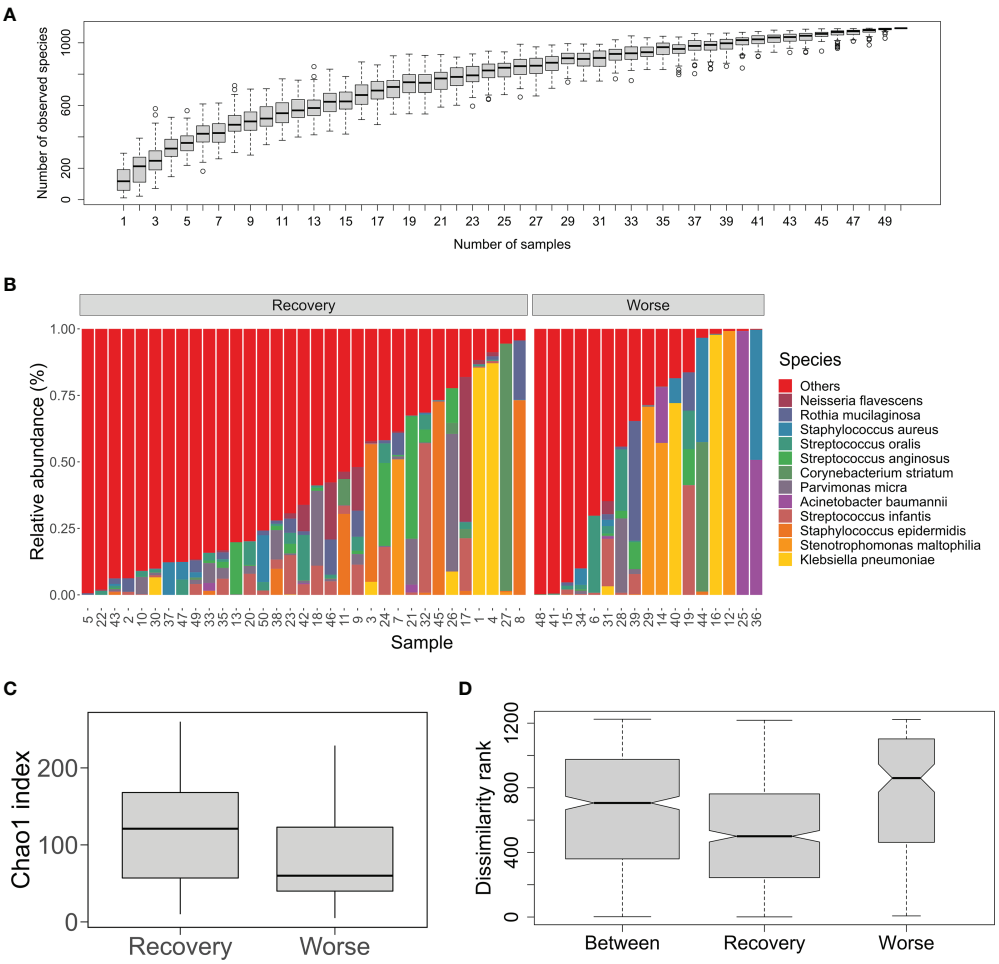

FIGURE 1 | Bacterial community structure and diversity of the sputum microbiota from the post-surgery patients with pulmonary infection. **(A)** An accumulation curve of the microorganisms in the sputum samples. The boxplot denotes the species richness according to the observed species numbers for a given number of samples collected from 100 random permutations of all the samples. **(B)** Percent stacked barplot for species-level taxonomic profiling of the sputum bacterial microbial communities. Labels stand for the top 12 abundant species. The samples are grouped by clinical outcomes Recover and Worse. **(C)** Chao1 index of the sputum microbiota from the two groups Recover and Worse. **(D)** The ANOSIM boxplot ranks between and within the Recover and Worse groups.

opportunistic pathogenic species *K. pneumoniae*, *C. striatum*, *S. aureus*, and *C. albicans*. StrainPhlAn analysis displays strain-level phylogenetic trees visualizing the relatedness between the metagenome-recovered strains and clinical bacterial isolates with publicly genome sequences (**Figure 2**). *K. pneumoniae* strains were reconstructed from the metagenomic samples of three patients #1/#4/#16 (**Figure 2A**). The analysis of metaMLST showed that the strain from patient #4 was *K. pneumoniae* of ST29 and the other two strains were represented by novel STs. Consistently, a *K. pneumoniae* strain derived from #4 was most closely related to a multidrug-resistant ST29 strain (CP024489/INF249) isolated from urinary tract infection (Gorrie et al., 2018) (**Figure 2A**). The strain from #16 was closely related to the *K. pneumoniae* strain NTUH-K2044 (AP006725) causing liver abscess and meningitis (Wu et al., 2009). In addition, two *C. striatum* strains from #27/#44 were phylogenetically placed together (**Figure 2B**), and their closest relatives were the two strains (VCOZ00000000 and VCOY00000000) of *C. striatum* isolated from influenza patients with secondary lower respiratory tract bacterial infections (Qin et al., 2020). Besides, the *S. aureus* strain from #44 was neighboring to the strain 55/2053, which caused the global pandemic of Panton-Valentine leukocidin-producing *S. aureus* in Europe and the United States in the 1950s (Zuo et al., 2021) (**Figure 2C**).

Figure 3 shows the phylogeny of three metagenomic strains of *C. albicans* from #13/#20/#29 together with the isolated strains of *C. albicans*, which is a well-known human fungal pathogen responsible for painful mucosal infections (Kim and Sudbery, 2011; Gulati and Nobile, 2016). Phylogenetic relationships of these fungal strains were investigated by the StrainPhlAn-based tree and the MLST-based tree, respectively. Both trees show that the *C. albicans* strain from #20 was closely related to the strains CHN1, Ca529L, A123, and A67.

DISCUSSION

Rapid species identification followed by assessment of microbial colonization and pathogenesis associated with infections is always a significant issue for public health (Stressmann et al., 2017; Martin

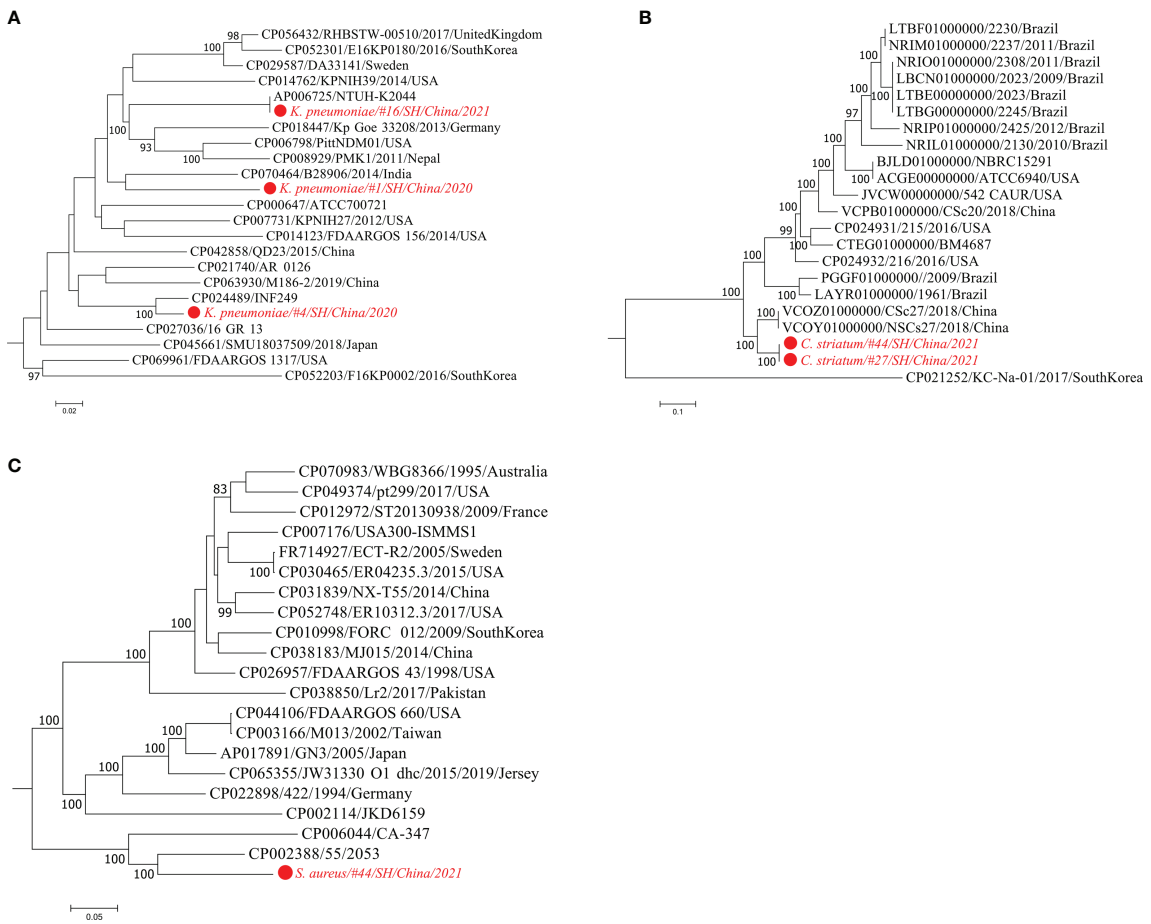

FIGURE 2 | Maximum-likelihood phylogenetic trees of three bacterial pathogens. Using StrainPhlAn trees are built based on the sample-specific consensus sequences of marker genes from *K. pneumoniae* **(A)**, *C. striatum* **(B)**, and *S. aureus* **(C)**, respectively. The strains detected in the metagenomic samples are labeled in red. The isolate genomes are labeled by the GenBank accessions, strain identifiers, isolation country, and year. Bootstrap support values greater than 80% are displayed.

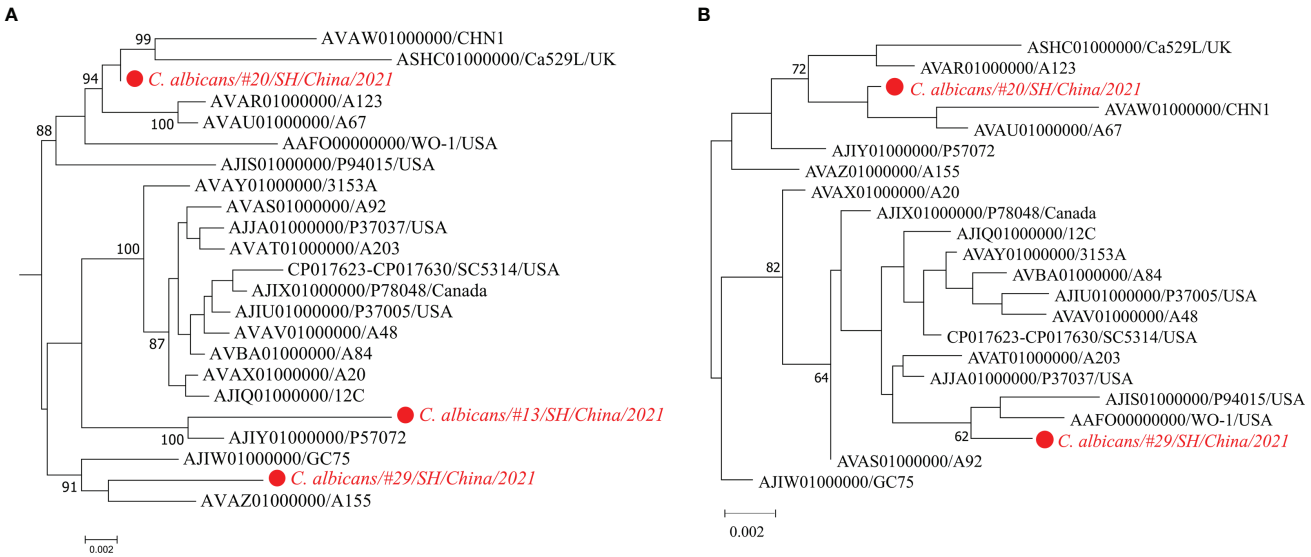

FIGURE 3 | Maximum-likelihood phylogenetic trees of the fungal pathogen *C. albicans*. Trees are built according to the StrainPhlAn analysis **(A)** and MLST analysis **(B)**, respectively. The strain of *C. albicans* in the metagenome sample #13 is excluded from the MLST tree due to its low sequencing depth and failure to reconstruct the MLST loci-sequences.

and Bachman, 2018). In recent years, culture-free high-throughput sequencing methods have successively uncovered many microbial colonizers in the nasopharynx, oropharynx, airway, trachea, and lung of healthy humans, such as *Streptococcus*, *Haemophilus*, *Corynebacterium*, *Staphylococcus*, *Klebsiella*, et al. (Charlson et al., 2011; Martin and Bachman, 2018; Paling et al., 2020). Microbiota balance of specific body sites, including the respiratory tract, is thought to be closely related to host health and disease (Man et al., 2017). Disruption of the microbiota homeostasis underlying the state of diseases enables changing the proportions of certain opportunistic pathogenic strains, thereby facilitating the proliferation of a complex community dominated by these strains and further causing infectious diseases (Haldar et al., 2020; Dicker et al., 2021b). Inference on the risk of colonization and infection by opportunistic pathogens has important implications for the diagnostics of these clinically relevant strains. Thus, we explored the screening procedure of mNGS-based species abundance profiles from the patients with pulmonary infection, further proposing LOD to assess the pathogenic risk in the sputum microbiome in this manuscript.

Microbiome-wide estimation on pathogenic risk for diverse microorganisms is beneficial for distinguishing the pathogenic strains from the colonizing strains in the clinical specimens. In this retrospective analysis, the final pathogen list generated by mNGS-based screening procedures encompassed nearly all the species identified by culture and some additional pathogens associated with infection. Of these pathogens detected in the sputum microbiome, many are human colonizers and also opportunistic etiologic agents, e.g. *K. pneumoniae* (Chung, 2016), *S. marcescens* (Khanna et al., 2013), *S. oralis* (Adams et al., 2017), *S. mitis* (Adams et al., 2017), *C. striatum* (Alibi et al., 2017), and *S. aureus* (Feng et al., 2008). Gram-positive bacterium *S. pneumoniae* is one of the prevalent commensal residents of the nasopharynx and also an opportunistic pathogen that can lead to pneumonia, bacteremia, meningitis, and otitis media (Shak et al., 2013). Herein, *S. pneumoniae* was present in more than half (n = 28) of the samples (**Table S3**). Based on the LOD of 3.6% for this bacterium, it was identified as a pathogen in the three patients: 15.7% abundance in #6; 7.4% in #33; 8.7% in #42. *S. marcescens*, a Gram-negative opportunistic nosocomial pathogen, is commonly involved in catheter-associated bacteremia, urinary tract infections, and wound infections of hospitalized patients (Khanna et al., 2013). *S. marcescens* was detected as a singular pathogen (56.8%) in #10, which was consistent with species identification by culture. *C. albicans* (36.3%) is normally a harmless commensal yeast and also a prevalent opportunistic pathogen that can cause symptomatic infections of mucosal membranes (Kim and Sudbery, 2011). This common fungus was present in about half (n = 23) of the samples (**Table S3**), and it was further assessed as a high-risk pathogen dominating the fungal community of 30% of the samples. These results suggest that the proposed LOD value of pathogenic risk may be a promising clinical indicator for infections caused by opportunistic etiological agents. However, it still needs a bigger sample group to provide robust references of microbial abundances for statistical estimation on LOD of pathogenic risk.

On the other hand, mining metagenomic data can provide more accurate taxonomic classification even at the single-strain resolution, which can be further used to interpret microbial pathogenesis, antimicrobial resistance, and transmission of the newly detected strain (Nayfach et al., 2016; Truong et al., 2017). For example, the sputum culture was negative for *K. pneumoniae* in patient #4, whereas *K. pneumoniae* was identified in the corresponding specimen by mNGS. Interestingly, strain profiling of the sputum metagenome revealed that this highly abundant *K. pneumoniae* strain

was phylogenetically related to the multidrug-resistant and virulent isolate INF249 belonging to *K. pneumoniae* of ST29 and KL30 (Gorrie et al., 2018) (**Figure 2A**). Additionally, the *K. pneumoniae* strain detected in patient #16 was related to NTUH-K2044, a hypervirulent strain bearing the K1 capsule and ST23 (Wu et al., 2009). Besides, for the fungal typing of *C. albicans*, we identified three strains that were distantly related to each other in the phylogenetic tree (**Figure 2D**). The strain of *C. albicans* isolated from patient #13 was most closely related to *C. albicans* strain P57072, which is isolated from a bloodstream infection (Hirakawa et al., 2015). Since opportunistic etiological agents normally include both disease-causing and commensal strains (Paczosa and Mecsas, 2016; Braz et al., 2020), strain-level phylogeny is an alternative to providing accurate detection of whether it is a pathogenic strain or not.

In summary, we utilized mNGS-based species abundance profiling data to propose a practical screening strategy for the assessment of microbial pathogenic risk in sputum of pulmonary infected patients. The strategy enables reducing the disturbance from colonizers in a microbial community; meanwhile, it could also distinguish pathogenic strains from the colonizing strains in specific body sites. Our work provides a novel metagenomic insight into precision diagnosis for clinically relevant microbes, especially for opportunistic pathogens in the clinical setting.

DATA AVAILABILITY STATEMENT

The datasets presented in this study can be found in online repositories. The names of the repository and accession number can be found below: https://www.ncbi.nlm.nih.gov/, PRJNA765792.

ETHICS STATEMENT

The studies involving human participants were reviewed and approved by The Ethics Committee of Ruijin Hospital, Shanghai Jiaotong University School of Medicine Review Board (2021-69). The patients/participants provided their written informed consent to participate in this study.

AUTHOR CONTRIBUTIONS

Conceived and designed the study: JC and JG. Performed the experiments: JC, XL, and QY. Analyzed the data: XC, LS, and KQ. Wrote and revised the manuscript: JC, LS, and JG. All authors contributed to the article and approved the submitted version.

FUNDING

This work was supported by the National Natural Science Foundation of China (81671832).

SUPPLEMENTARY MATERIAL

The Supplementary Material for this article can be found online at: https://www.frontiersin.org/articles/10.3389/fcimb.2022.855839/full#supplementary-material

REFERENCES

Adams, H. M., Joyce, L. R., Guan, Z., Akins, R. L., and Palmer, K. L. (2017). Streptococcus Mitis and S. Oralis Lack a Requirement for CdsA, the Enzyme Required for Synthesis of Major Membrane Phospholipids in Bacteria. *Antimicrobial. Agents Chemother.* 61 (5), e02552–e02516. doi: 10.1128/AAC.02552-16

Alibi, S., Ferjani, A., Boukadida, J., Cano, M. E., Fernández-Martínez, M., Martínez-Martínez, L., et al. (2017). Occurrence of Corynebacterium Striatum as an Emerging Antibiotic-Resistant Nosocomial Pathogen in a Tunisian Hospital. *Sci. Rep.* 7 (1), 9704. doi: 10.1038/s41598-017-10081-y

Altschul, S. F., Gish, W., Miller, W., Myers, E. W., and Lipman, D. J. (1990). Basic Local Alignment Search Tool. *J. Mol. Biol.* 215 (3), 403–410. doi: 10.1016/s0022-2836(05)80360-2

Beghini, F., McIver, L. J., Blanco-Míguez, A., Dubois, L., Asnicar, F., Maharjan, S., et al. (2021). Integrating Taxonomic, Functional, and Strain-Level Profiling of Diverse Microbial Communities With Bobakery 3. *eLife* 10, e65088. doi: 10.7554/eLife.65088

Bolger, A. M., Lohse, M., and Usadel, B. (2014). Trimmomatic: A Flexible Trimmer for Illumina Sequence Data. *Bioinformatics* 30 (15), 2114–2120. doi: 10.1093/bioinformatics/btu170

Braz, V. S., Melchior, K., and Moreira, C. G. (2020). Escherichia Coli as a Multifaceted Pathogenic and Versatile Bacterium. *Front. Cell Infect. Microbiol.* 10 (793). doi: 10.3389/fcimb.2020.548492

Cappelletty, D. (1998). Microbiology of Bacterial Respiratory Infections. *Pediatr. Infect. Dis. J.* 17 (8 Suppl), S55–S61. doi: 10.1097/00006454-199808001-00002

Chao, A. (1987). Estimating the Population Size for Capture-Recapture Data With Unequal Catchability. *Biometrics* 43 (4), 783–791. doi: 10.2307/2531532

Charlson, E. S., Bittinger, K., Haas, A. R., Fitzgerald, A. S., Frank, I., Yadav, A., et al. (2011). Topographical Continuity of Bacterial Populations in the Healthy Human Respiratory Tract. *Am. J. Respir. Crit. Care Med.* 184 (8), 957–963. doi: 10.1164/rccm.201104-0655OC

Chowdhary, A., Agarwal, K., and Meis, J. F. (2016). Filamentous Fungi in Respiratory Infections. What Lies Beyond Aspergillosis and Mucormycosis? *PloS Pathog.* 12 (4), e1005491–e1005491. doi: 10.1371/journal.ppat.1005491

Chowdhary, A., Randhawa, H. S., Gaur, S. N., Agarwal, K., Kathuria, S., Roy, P., et al. (2013). Schizophyllum Commune as an Emerging Fungal Pathogen: A Review and Report of Two Cases. *Mycoses* 56 (1), 1–10. doi: 10.1111/j.1439-0507.2012.02190.x

Chung, P. Y. (2016). The Emerging Problems of Klebsiella Pneumoniae Infections: Carbapenem Resistance and Biofilm Formation. *FEMS Microbiol. Lett.* 363 (20). doi: 10.1093/femsle/fnw219

Conde, M., and Lawrence, V. (2008). Postoperative Pulmonary Infections. *BMJ Clin. Evid.* 2008, fnw219.

Deurenberg, R. H., Bathoorn, E., Chlebowicz, M. A., Couto, N., Ferdous, M., García-Cobos, S., et al. (2017). Application of Next Generation Sequencing in Clinical Microbiology and Infection Prevention. *J. Biotechnol.* 243, 16–24. doi: 10.1016/j.jbiotec.2016.12.022

Dicker, A. J., Huang, J. T. J., Lonergan, M., Keir, H. R., Fong, C. J., Tan, B., et al. (2021a). The Sputum Microbiome, Airway Inflammation, and Mortality in Chronic Obstructive Pulmonary Disease. *J. Allergy Clin. Immunol.* 147 (1), 158–167. doi: 10.1016/j.jaci.2020.02.040

Dicker, A. J., Lonergan, M., Keir, H. R., Smith, A. H., Pollock, J., Finch, S., et al. (2021b). The Sputum Microbiome and Clinical Outcomes in Patients With Bronchiectasis: A Prospective Observational Study. *Lancet Respir. Med.* 9 (8), 885–896. doi: 10.1016/s2213-2600(20)30557-9

Ditz, B., Christenson, S., Rossen, J., Brightling, C., Kerstjens, H. A. M., van den Berge, M., et al. (2020). Sputum Microbiome Profiling in COPD: Beyond Singular Pathogen Detection. *Thorax* 75 (4), 338–344. doi: 10.1136/thoraxjnl-2019-214168

Dixon, P. (2003). VEGAN, a Package of R Functions for Community Ecology. *J. Vegetation. Sci.* 14, 927–930. doi: 10.1111/j.1654-1103.2003.tb02228.x

Edgar, R. C. (2004). MUSCLE: Multiple Sequence Alignment With High Accuracy and High Throughput. *Nucleic Acids Res.* 32 (5), 1792–1797. doi: 10.1093/nar/gkh340

Feng, Y., Chen, C.-J., Su, L.-H., Hu, S., Yu, J., and Chiu, C.-H. (2008). Evolution and Pathogenesis of Staphylococcus Aureus : Lessons Learned From Genotyping and Comparative Genomics. *FEMS Microbiol. Rev.* 32 (1), 23–37. doi: 10.1111/j.1574-6976.2007.00086.x

Ferone, M., Gowen, A., Fanning, S., and Scannell, A. G. M. (2020). Microbial Detection and Identification Methods: Bench Top Assays to Omics Approaches. *Compr. Rev. Food Sci. Food Saf.* 19 (6), 3106–3129. doi: 10.1111/1541-4337.12618

Finch, S., McDonnell, M. J., Abo-Leyah, H., Aliberti, S., and Chalmers, J. D. (2015). A Comprehensive Analysis of the Impact of Pseudomonas Aeruginosa Colonization on Prognosis in Adult Bronchiectasis. *Ann. Am. Thorac. Soc.* 12 (11), 1602–1611. doi: 10.1513/AnnalsATS.201506-333OC

Gorrie, C. L., Mirceta, M., Wick, R. R., Judd, L. M., Wyres, K. L., Thomson, N. R., et al. (2018). Antimicrobial-Resistant Klebsiella Pneumoniae Carriage and Infection in Specialized Geriatric Care Wards Linked to Acquisition in the Referring Hospital. *Clin. Infect. Dis. an Off. Publ. Infect. Dis. Soc. America* 67 (2), 161–170. doi: 10.1093/cid/ciy027

Guerrero-Araya, E., Muñoz, M., Rodríguez, C., and Paredes-Sabja, D. (2021). FastMLST: A Multi-Core Tool for Multilocus Sequence Typing of Draft Genome Assemblies. *Bioinf. Biol. Insights* 15, 11779322211059238. doi: 10.1177/11779322211059238

Gulati, M., and Nobile, C. J. (2016). Candida Albicans Biofilms: Development, Regulation, and Molecular Mechanisms. *Microbes Infect.* 18, 310–321. doi: 10.1016/j.micinf.2016.01.002

Haldar, K., George, L., Wang, Z., Mistry, V., Ramsheh, M. Y., Free, R. C., et al. (2020). The Sputum Microbiome is Distinct Between COPD and Health, Independent of Smoking History. *Respir. Res.* 21 (1), 183. doi: 10.1186/s12931-020-01448-3

Hirakawa, M. P., Martinez, D. A., Sakthikumar, S., Anderson, M. Z., Berlin, A., Gujja, S., et al. (2015). Genetic and Phenotypic Intra-Species Variation in Candida Albicans. *Genome Res.* 25 (3), 413–425. doi: 10.1101/gr.174623.114

Human Microbiome Project Consortium (2012). Structure, Function and Diversity of the Healthy Human Microbiome. *Nature* 486 (7402), 207–214. doi: 10.1038/nature11234

Khanna, A., Khanna, M., and Aggarwal, A. (2013). Serratia Marcescens- a Rare Opportunistic Nosocomial Pathogen and Measures to Limit its Spread in Hospitalized Patients. *J. Clin. Diagn. Res.* 7 (2), 243–246. doi: 10.7860/JCDR/2013/5010.2737

Khan, S., Priti, S., and Ankit, S. (2015). Bacteria Etiological Agents Causing Lower Respiratory Tract Infections and Their Resistance Patterns. *Iran BioMed. J.* 19 (4), 240–246. doi: 10.7508/ibj.2015.04.008

Kim, J., and Sudbery, P. (2011). Candida Albicans, a Major Human Fungal Pathogen. *J. Microbiol. (Seoul. Korea).* 49 (2), 171–177. doi: 10.1007/s12275-011-1064-7

Kitts, P. A., Church, D. M., Thibaud-Nissen, F., Choi, J., Hem, V., Sapojnikov, V., et al. (2016). Assembly: A Resource for Assembled Genomes at NCBI. *Nucleic Acids Res.* 44, D73–D80. doi: 10.1093/nar/gkv1226

Kumar, S., Stecher, G., Li, M., Knyaz, C., and Tamura, K. (2018). MEGA X: Molecular Evolutionary Genetics Analysis Across Computing Platforms. *Mol. Biol. Evol.* 35, 1547–1549. doi: 10.1093/molbev/msy096

Kutter, J. S., Spronken, M. I., Fraaij, P. L., Fouchier, R. A. M., and Herfst, S. (2018). Transmission Routes of Respiratory Viruses Among Humans. *Curr. Opin. Virol.* 28, 142–151. doi: 10.1016/j.coviro.2018.01.001

Langmead, B., and Salzberg, S. L. (2012). Fast Gapped-Read Alignment With Bowtie 2. *Nat. Methods* 9 (4), 357–359. doi: 10.1038/nmeth.1923

Li, B., Ruotti, V., Stewart, R. M., Thomson, J. A., and Dewey, C. N. (2009). RNA-Seq Gene Expression Estimation With Read Mapping Uncertainty. *Bioinformatics* 26 (4), 493–500. doi: 10.1093/bioinformatics/btp692

Lu, J., Breitwieser, F. P., Thielen, P., and Salzberg, S. L. (2017). Bracken: Estimating Species Abundance in Metagenomics Data. *PeerJ. Comput. Sci.* 3, e104. doi: 10.7717/peerj-cs.104

Man, W. H., de Steenhuijsen Piters, W. A. A., and Bogaert, D. (2017). The Microbiota of the Respiratory Tract: Gatekeeper to Respiratory Health. *Nat. Rev. Microbiol.* 15 (5), 259–270. doi: 10.1038/nrmicro.2017.14

Martin, R. M., and Bachman, M. A. (2018). Colonization, Infection, and the Accessory Genome of Klebsiella Pneumoniae. *Front. Cell Infect. Microbiol.* 8. doi: 10.3389/fcimb.2018.00004

Martin, T. C., Visconti, A., Spector, T. D., and Falchi, M. (2018). Conducting Metagenomic Studies in Microbiology and Clinical Research. *Appl. Microbiol. Biotechnol.* 102 (20), 8629–8646. doi: 10.1007/s00253-018-9209-9

Melhem, M. S. C., Bertoletti, A., Lucca, H. R. L., Silva, R. B. O., Meneghin, F. A., and Szeszs, M. W. (2014). Use of the VITEK 2 System to Identify and Test the Antifungal Susceptibility of Clinically Relevant Yeast Species. *Braz. J. Microbiol.* 44 (4), 1257–1266. doi: 10.1590/S1517-83822014005000018

Nayfach, S., Rodriguez-Mueller, B., Garud, N., and Pollard, K. S. (2016). An Integrated Metagenomics Pipeline for Strain Profiling Reveals Novel Patterns of Bacterial Transmission and Biogeography. *Genome Res.* 26 (11), 1612–1625. doi: 10.1101/gr.201863.115

Paczosa, M. K., and Mecsas, J. (2016). *Klebsiella Pneumoniae*: Going on the Offense With a Strong Defense. *Microbiol. Mol. Biol. Rev.* 80 (3), 629–661. doi: 10.1128/MMBR.00078-15

Paling, F. P., Hazard, D., Bonten, M. J. M., Goossens, H., Jafri, H. S., Malhotra-Kumar, S., et al. (2020). Association of Staphylococcus Aureus Colonization and Pneumonia in the Intensive Care Unit. *JAMA Network. Open* 3 (9), e2012741–e2012741. doi: 10.1001/jamanetworkopen.2020.12741

Price, L. B., Hungate, B. A., Koch, B. J., Davis, G. S., and Liu, C. M. (2017). Colonizing Opportunistic Pathogens (COPs): The Beasts in All of Us. *PloS Pathog.* 13 (8), e1006369. doi: 10.1371/journal.ppat.1006369

Qin, T., Geng, T., Zhou, H., Han, Y., Ren, H., Qiu, Z., et al. (2020). Super-Dominant Pathobiontic Bacteria in the Nasopharyngeal Microbiota as Causative Agents of Secondary Bacterial Infection in Influenza Patients. *Emerging. Microbes Infect.* 9, 605–615. doi: 10.1080/22221751.2020.1737578

R Core Team (2021) *R: A Language and Environment for Statistical Computing R Foundation for Statistical Computing* (Vienna, Austria). Available at: https://www.R-project.org/ (Accessed November 1, 2021).

Shak, J. R., Vidal, J. E., and Klugman, K. P. (2013). Influence of Bacterial Interactions on Pneumococcal Colonization of the Nasopharynx. *Trends Microbiol.* 21 (3), 129–135. doi: 10.1016/j.tim.2012.11.005

Smith, G. B., Prytherch, D. R., Meredith, P., Schmidt, P. E., and Featherstone, P. I. (2013). The Ability of the National Early Warning Score (NEWS) to Discriminate Patients at Risk of Early Cardiac Arrest, Unanticipated Intensive Care Unit Admission, and Death. *Resuscitation* 84 (4), 465–470. doi: 10.1016/j.resuscitation.2012.12.016

Stamatakis, A. (2014). RAxML Version 8: A Tool for Phylogenetic Analysis and Post-Analysis of Large Phylogenies. *Bioinformatics* 30, 1312–1313. doi: 10.1093/bioinformatics/btu033

Stressmann, F. A., Couve-Deacon, E., Chainier, D., Chauhan, A., Wessel, A., Durand-Fontanier, S., et al. (2017). Comparative Analysis of Bacterial Community Composition and Structure in Clinically Symptomatic and Asymptomatic Central Venous Catheters. *mSphere* 2 (5), e00146–e00117. doi: 10.1128/mSphere.00146-17

Terranova, L., Oriano, M., Teri, A., Ruggiero, L., Tafuro, C., Marchisio, P., et al. (2018). How to Process Sputum Samples and Extract Bacterial DNA for Microbiota Analysis. *Int. J. Mol. Sci.* 19 (10), 3256. doi: 10.3390/ijms19103256

Truong, D. T., Tett, A., Pasolli, E., Huttenhower, C., and Segata, N. (2017). Microbial Strain-Level Population Structure and Genetic Diversity From Metagenomes. *Genome Res.* 27, 626–638. doi: 10.1101/gr.216242.116

Vincent, J. L., de Mendonça, A., Cantraine, F., Moreno, R., Takala, J., Suter, P. M., et al. (1998). Use of the SOFA Score to Assess the Incidence of Organ Dysfunction/Failure in Intensive Care Units: Results of a Multicenter, Prospective Study. Working Group on "Sepsis-Related Problems" of the European Society of Intensive Care Medicine. *Crit. Care Med.* 26 (11), 1793–1800. doi: 10.1097/00003246-199811000-00016

Wood, D. E., Lu, J., and Langmead, B. (2019). Improved Metagenomic Analysis With Kraken 2. *Genome Biol.* 20 (1), 257. doi: 10.1186/s13059-019-1891-0

Wu, K.-M., Li, L.-H., Yan, J.-J., Tsao, N., Liao, T.-L., Tsai, H.-C., et al. (2009). Genome Sequencing and Comparative Analysis of Klebsiella Pneumoniae NTUH-K2044, a Strain Causing Liver Abscess and Meningitis. *J. Bacteriol.* 191, 4492–4501. doi: 10.1128/JB.00315-09

Yan, Q., Cui, S., Chen, C., Li, S., Sha, S., Wan, X., et al. (2016). Metagenomic Analysis of Sputum Microbiome as a Tool Toward Culture-Independent Pathogen Detection of Patients With Ventilator-Associated Pneumonia. *Am. J. Respir. Crit. Care Med.* 194 (5), 636–639. doi: 10.1164/rccm.201601-0034LE

Zolfo, M., Tett, A., Jousson, O., Donati, C., and Segata, N. (2017). MetaMLST: Multi-Locus Strain-Level Bacterial Typing From Metagenomic Samples. *Nucleic Acids Res.* 45, e7. doi: 10.1093/nar/gkw837

Zuo, H., Uehara, Y., Lu, Y., Sasaki, T., and Hiramatsu, K. (2021). Genetic and Phenotypic Diversity of Methicillin-Resistant Staphylococcus Aureus Among Japanese Inpatients in the Early 1980s. *Sci. Rep.* 11 (1), 5447. doi: 10.1038/s41598-021-84481-6

Conflict of Interest: The authors LS and XC are employed by Genoxor Medical Science and Technology Inc.

The remaining authors declare that the research was conducted in the absence of any commercial or financial relationships that could be construed as a potential conflict of interest.

Publisher's Note: All claims expressed in this article are solely those of the authors and do not necessarily represent those of their affiliated organizations, or those of the publisher, the editors and the reviewers. Any product that may be evaluated in this article, or claim that may be made by its manufacturer, is not guaranteed or endorsed by the publisher.

frontiers | Frontiers in Cellular and Infection Microbiology

ORIGINAL RESEARCH
published: 28 June 2022
doi: 10.3389/fcimb.2022.919903

Comparison Analysis of Different DNA Extraction Methods on Suitability for Long-Read Metagenomic Nanopore Sequencing

Lei Zhang[1†], Ting Chen[1,2†], Ye Wang[1], Shengwei Zhang[1,3], Qingyu Lv[1], Decong Kong[1], Hua Jiang[1], Yuling Zheng[1], Yuhao Ren[1], Wenhua Huang[1], Peng Liu[1*] and Yongqiang Jiang[1*]*

[1] State Key Laboratory of Pathogen and Biosecurity, Beijing Institute of Microbiology and Epidemiology, Academy of Military Medical Sciences, Beijing, China, [2] The Fifth Medical Center of PLA General Hospital, The Fifth School of Clinical Medicine, Anhui Medical University, Hefei, China, [3] Department of Clinical Laboratory, Dongfang Hospital, Beijing University of Chinese Medicine, Beijing, China

OPEN ACCESS

Edited by:
Arun Prasath Lakshmanan, Sidra Medicine, Qatar

Reviewed by:
Selvasankar Murugesan, Sidra Medicine, Qatar
Natalia M Araujo, Oswaldo Cruz Foundation (Fiocruz), Brazil

***Correspondence:**
Wenhua Huang
huangwh1993@163.com
Peng Liu
ammsliupeng@163.com
Yongqiang Jiang
jiangyq@bmi.ac.cn

[†]These authors have contributed equally to this work

Specialty section:
This article was submitted to Clinical Microbiology, a section of the journal Frontiers in Cellular and Infection Microbiology

Received: 14 April 2022
Accepted: 24 May 2022
Published: 28 June 2022

Citation:
Zhang L, Chen T, Wang Y, Zhang S, Lv Q, Kong D, Jiang H, Zheng Y, Ren Y, Huang W, Liu P and Jiang Y (2022) Comparison Analysis of Different DNA Extraction Methods on Suitability for Long-Read Metagenomic Nanopore Sequencing. Front. Cell. Infect. Microbiol. 12:919903. doi: 10.3389/fcimb.2022.919903

Metagenomic next-generation sequencing (mNGS) is a novel useful strategy that is increasingly used for pathogens detection in clinic. Some emerging mNGS technologies with long-read ability are useful to decrease sequencing time and increase diagnosed accuracy, which is of great significance in rapid pathogen diagnosis. Reliable DNA extraction is considered critical for the success of sequencing; hence, there is thus an urgent need of gentle DNA extraction method to get unbiased and more integrate DNA from all kinds of pathogens. In this study, we systematically compared three DNA extraction methods (enzymatic cell lysis based on MetaPolyzyme, mechanical cell lysis based on bead beating, and the control method without pre–cell lysis, respectively) by assessing DNA yield, integrity, and the microbial diversity based on long-read nanopore sequencing of urine samples with microbial infections. Compared with the control method, the enzymatic-based method increased the average length of microbial reads by a median of 2.1-fold [Inter Quartile Range (IQR), 1.7–2.5; maximum, 4.8) in 18 of the 20 samples and the mapped reads proportion of specific species by a median of 11.8-fold (Inter Quartile Range (IQR), 6.9–32.2; maximum, 79.27]. Moreover, it provided fully (20 of 20) consistent diagnosed results to the clinical culture and more representative microbial profiles ($P < 0.05$), which all strongly proves the excellent performance of enzymatic-based method in long-read mNGS–based pathogen identification and potential diseases diagnosis of microbiome related.

Keywords: metagenomics, mechanical lysis, enzymatic lysis, pathogen diagnosis, microbiome

INTRODUCTION

Metagenomic next-generation sequencing (mNGS) is a hypothesis-free and unbiased approach that has the potential to detect all the known and unidentified pathogens yet. Because of its target agnostic nature, mNGS enables the discovery of new organisms in clinical sample and is especially suitable for rare, novel, and atypical etiologies of complicated infectious diseases, as well as the

molecular diagnosis of polymicrobial infections (Goldberg et al., 2015; Cummings et al., 2016; Gu et al., 2019). Although such an unbiased approach appears highly suitable for pathogen diagnosis, difference in pathogens lysis method results in different pathogen distribution (Mattei et al., 2019). Currently, the most common used method is mechanical lysis with hard bead-beating, which may result in excessive DNA fragmentation (Salonen et al., 2010). This method fades the advantage of long sequence reading for the emerging sequencing techniques such as Nanopore and PacBio (Rhoads and Au, 2015; Wang et al., 2021). Furthermore, longer sequence reads can increase taxonomic resolution of sequence classification because they are more readily classified to species or subspecies level; meanwhile, short reads are often difficult to classify to species accurately and can sometimes result in misdiagnoses (Schlaberg et al., 2017). Therefore, there is still an urgent need for optimized cell wall degradation methods that provide DNA with high integrity from all kinds of pathogens.

Urinary tract infections (UTIs) are one of the most common infections in human, which can be caused by the broader microorganisms of bacteria and fungi (Hasman et al., 2014; Zhang et al., 2022). The vast microbial diversity present results in different optimal DNA extraction methods for different cell wall structures and compositions (Maukonen et al., 2012). Therefore, urine metagenomic pathogen diagnosis studies require an optimized DNA extraction method ensuring efficient cell lysis, minimal DNA shearing and unbiased microbial DNA recovery. In addition, it also needs to generate the most representative distribution of present microbial species. Notably, urine can be collected non-invasively in large volumes and therefore represents an attractive target for diagnostic assays. Although there has been much attention and efforts paid on establishment of mNGS-based diagnosed assay for UTI (Imirzalioglu et al., 2008; Schmidt et al., 2017; Li et al., 2020), there has been fewer studies aimed to evaluate the compatibility of DNA extraction methods for emerging long-read mNGS testing.

In this study, we compared three DNA extraction methods of mechanical lysis, enzymatic lysis, and a control method (DNA extracted directly without pre–cell lysis). Using metagenomic nanopore sequencing as the indicator, we assessed the quantity and integrity of the extracted DNA, the microbial diversity recovery, and the proportion of target microbial reads while keeping all the other steps standardized, with the goal of selecting a most compatible DNA extraction method for greater identification of potential pathogens when using long-read mNGS–based pathogen diagnostic analysis.

MATERIALS AND METHODS

Study Design

DNA of the urine samples were extracted with three different methods in this study: Method 1, DNA extracted directly by the IndiSpin Pathogen Kit (Indical Bioscience); Method 2, DNA extracted based on mechanical lysis; Method 3, DNA extracted based on enzymatic lysis. We compared the three DNA extraction methods by evaluating the DNA yield and integrity, DNA recovery of specific species, and microbial diversity. Overview of this study is shown in **Figure 1**.

Subjects and Urine Sample Collection

A clinical diagnosis of UTI required to refer to the culture result and consider indicators including a white blood cell count of > 10^7/L, an epithelial cell count of < 10^7/L, fever, dysuria, frequency of urination, and urgency (Willner et al., 2014; Kumar et al., 2015). In addition, the following criteria were used to determine inclusion in this study: the patients who had a few symptoms including urinary urgency, frequent urination, and painful urination; and the culture results were available and positive. Urine samples with less than 1 ml remained or with more than three species positive in culturation were excluded. There were 20 urine samples finally collected from 20 adults included in this

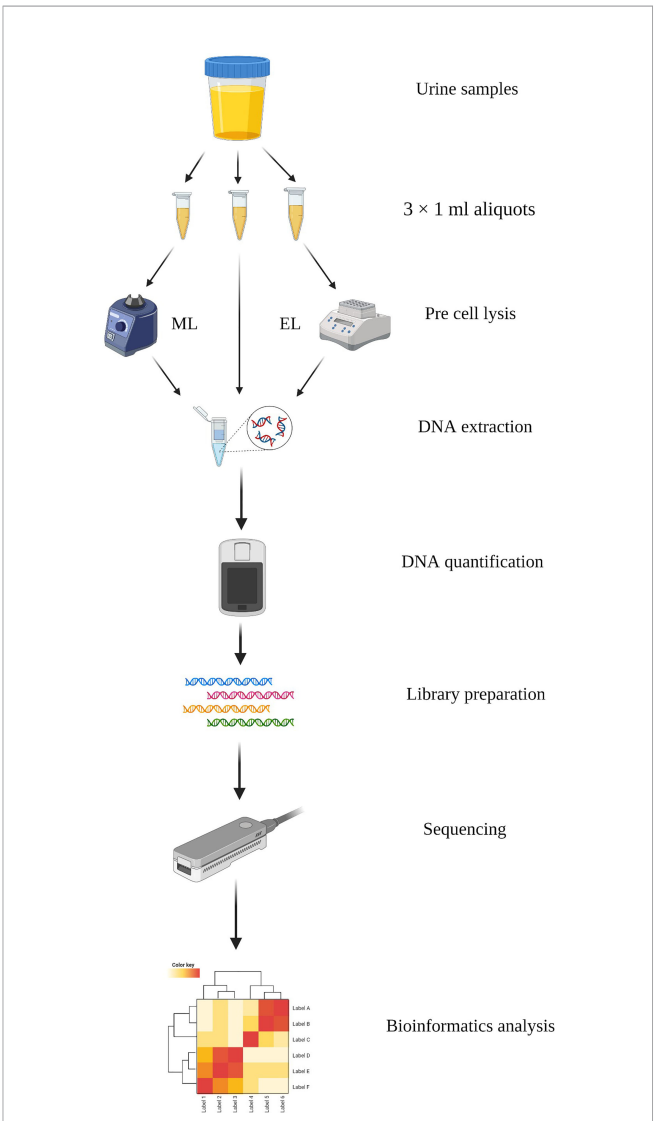

FIGURE 1 | Schematic workflow of the study. DNA was extracted with three methods from urine samples and performed sequencing based on MinION. Created with BioRender.com.

study. Immediately after collection, samples were transported on ice and stored at −80°C prior to DNA extraction by three different methods. This study was approved by the Institutional Review Board (IRB) of the Beijing Dongfang Hospital (reference no. JDF-IRB-2020003101). All samples were obtained with the patient's consent.

DNA Extraction Methods

Each urine sample was aliquoted (1 ml) into three 1.5-ml Eppendorf tubes (Eppendorf) and centrifuged at 20,000 × g for 5 min to enrich for microbes. Then, 800 µl of supernatant was discarded, and the pellet was resuspended in the residual volume (200 µl) by gentle vortex to prepare the enriched urine samples. The detailed methods to extract DNA are listed below.

(i) Method 1. DNA Extraction Directly Without Pre–Cell Lysis

One aliquot of each enriched urine samples (200 µl) was used to extract DNA directly by the IndiSpin Pathogen Kit without pre–cell lysis, to be a method control. Briefly, after 200 µl of urine sample was added to a 20-µl aliquot of Proteinase K, 100 µl of Buffer VXL including 1 µg of Carrier RNA was added to the mixture and incubated for 15 min at 20°C–25°C. After this, 350 µl of Buffer ACB was added to the samples and mixed thoroughly by pulse vortex. Then, all the lysates were transferred to the Mini column and centrifuged at 6,000 × g for 1 min. The collection tubes containing the filtrate were discarded and placed the Mini column in the clean collection tubes. Six hundred microliters of Buffer AW1 was added to the Minin column for washing the DNA by a centrifugation of 6,000 × g for 1 min. The washing step above was repeated using 600 µl of Buffer AW2. After this, the membrane was dried by centrifuging at 20,000 × g for 2 min with clean collection tubes. Finally, the DNA was eluted by 100 µl of Buffer AVE. The concentrations of DNA were measured using Qubit 4.0 fluorometer with the dsDNA HS Assay kit (Thermo Fisher Scientific).

(ii) Method 2. DNA Extraction With Mechanical Lysis

Mechanical lysis of cell walls was accomplished with bead beating. One aliquot of enriched urine samples (200 µl) was transferred into Pathogen Lysis Tubes (Qiagen) with glass beads, and 50 µl of Buffer ATL (containing Reagent DX, Qiagen) was added according to the manufacturer's instructions. The Pathogen Lysis Tubes were then attached to a horizontal platform on a vortex mixer and vortexed for 10 min at maximum speed. After that, the Pathogen Lysis Tubes were removed and briefly spined to collect any drops from the inside of the lid. DNA was extracted from the supernatant using the IndiSpin Pathogen Kit as described in Method 1.

(iii) Method 3. DNA Extraction With Enzymatic Lysis

One aliquot of enriched urine samples (200 µl) was used to extract DNA by enzymatic lysis method. Five microliters of lytic enzyme solution (Qiagen) and 10 µl of MetaPolyzyme [Sigma Aldrich; reconstituted in 750 µl of Phosphate Buffer Saline (PBS)] were added to the 200-µl samples and mixed by gentle pipetting. Mixed samples were incubated at 37°C in shaker for 1 h to lyse microbial cells. DNA was extracted from each post-lysed sample using the IndiSpin Pathogen Kit as described in Method 1.

Library Preparation and Sequencing

All the samples mNGS testing were based on MinION platform (Oxford Nanopore Technology (ONT)). The samples included in this data set were processed and sequenced regardless of microbial DNA concentration to provide an accurate representation of the data that would likely be obtained from metagenomic analysis of urine in clinical settings.

Library preparation was performed using the PCR Barcoding Kit (SQK-PBK004, ONT) according to the manufacturer's instruction, with 2-min extension and 15 cycles in the PCR amplification step. Up to six barcoded samples were loaded per flow cell for each sequencing run. Full details regarding library preparation are provided in **Supplementary Methods**.

Nanopore sequencing was performed using R9.4.1 flow cells (FLO-MIN106) on MinION. A total of 75 µl of library DNA was loaded into the flow cell according to the manufacturer's instructions. ONT MinKNOW GUI software (version 4.2.8) was used to collect raw sequencing data.

Bioinformatic Analysis

The raw sequencing data were processed using our automatic bioinformatics pipeline composed of a set of fixed external software (ont-Guppy, bwa, SAMtools, BLASTn). The processing step consists of (1) trimming adapters using ont-Guppy; (2) subtraction human host sequences mapped to the human reference genome (GRCh38, https://www.ncbi.nlm.nih.gov/data-hub/assembly/GCF_000001405.39/) using Burrows–Wheeler alignment with BWA-MEM algorithm; (3) output SAM file was indexed and sorted with SAMtools (version 1.7) to generate nonhuman reads; (4) all the nonhuman reads were classified by simultaneous alignment to RefSeq microbial genome databases (ftp://ftp.ncbi.nlm.nih.gov/genomes/refseq) consisting of viruses, bacteria, fungi, and parasites using BLASTn (version 2.10.1); (5) species classification result was finally outputted as.csv file after processing by two custom Python scripts and Linux commands. The automatic bioinformatics pipeline is available at https://github.com/gitzl222/APDNS/.

Statistical Analysis

All statistical analyses were performed using GraphPad Prism version 8.4. Normality was tested for all datasets using the D'Agostino Pearson omnibus normality test, and correlation was analyzed using Pearson correlation. All data were log-transformed and further analyzed using Kruskal–Wallis test or the two-tailed paired t-test as appropriate to calculate the statistical significance between the methods. A *P*-value less than 0.05 was considered as statistically significant.

RESULTS

DNA Yield and Integrity

The purpose of this study was to select and statistically validate an optimal method for the microbial DNA extraction to be

applied in long-read mNGS–based pathogen diagnosis of clinical samples. Three extraction methods were compared using clinical urine samples, and their DNA yield, integrity, and the specific species abundance were used as screening criteria to determine the best method. For differences analysis of DNA yield and integrity between the three DNA extraction methods, we counted the DNA concentrations and the average length of microbial reads and found that they varied a lot not only between samples of each method but also between different DNA extraction methods (**Figure 2**). We further investigated the statistical difference among them.

For DNA yield, we found that DNA concentrations extracted by mechanical-based method are significantly lower than the control method ($P < 0.0001$, **Figure 3A**), whereas the enzymatic-based method showed no significant differences with control method ($P > 0.05$, **Figure 3A**). This result indicated that enzymatic-based method has no extra effect, but mechanical lysis with bead-beating has negative effects on DNA yield.

For DNA integrity, we found that the average length of microbial reads generated by enzymatic-based method was significantly longer than the control method ($P < 0.0001$, **Figure 3B**) and mechanical-based method ($P < 0.01$, **Figure 3B**), increased by a median of 2.1-fold (IQR, 1.7–2.5; maximum, 4.8) in 18 of the 20 samples and 1.9-fold (IQR, 1.4–2.3; maximum, 5.0) in 16 of the 20 samples (**Table 1**), respectively.

Abundance Variation for Specific Species

To determine adaption of these three DNA extraction methods for mNGS-based pathogen diagnosis, we counted the consistency between results of culture and mNGS and found that the enzymatic-based method provided a fully consistent result while the other two methods gave 15 of 20 and 14 of 20, respectively (**Table 2**). To evaluate the abundance variation of specific species, we next calculated the mapped reads number and proportion of the specific species that can be identified by culture (**Table 2**). By calculating the sequencing depth of all three DNA extraction methods, we found that the total number of reads generated by MinION of each sample showed no significant difference among all the three DNA extraction methods (all $P > 0.05$, **Figure 3C**). On the basis of the same depth of sequencing, the enzymatic-based method increases the mapped reads proportion of specific species by a median of 11.8-fold (IQR, 6.9–32.2; maximum, 79.27; **Figure 3D**) in 14 of the 20 samples compared with the control method, except one from a gram-negative bacteria *E. coli* infection (P19). In particular, the remaining five samples (P3, P5, P7, P10, and P14) were found of significant increase in reads number of specific species from "no reads detected" to "large number of reads detected". The mechanical-based method showed a decreased proportion of mapped reads in most (9 of 15) samples although no significant difference observed compared with the control method. Furthermore, the five samples with no reads of specific species detected in the control method were also not detected any targeted reads in mechanical-based DNA extraction method. Finally, sample P1, which could be correctly detected by control method, was not detected by mechanical-based method, indicating that this method may lead to loss of microbial DNA sequences.

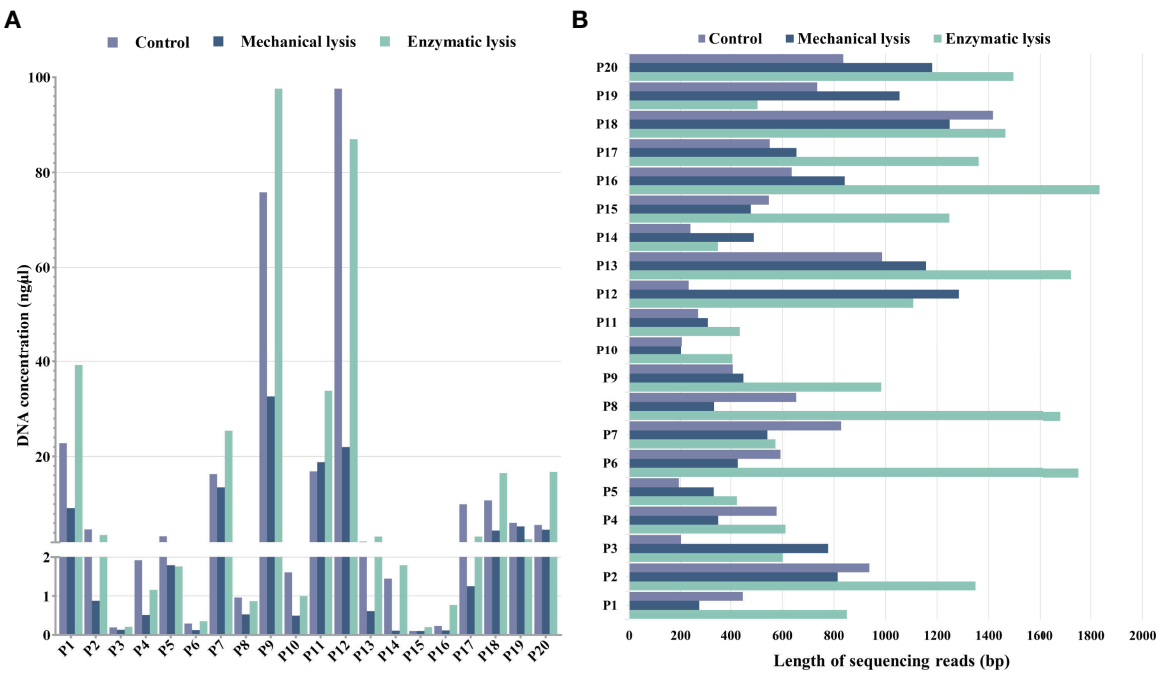

FIGURE 2 | DNA yield and integrity extracted using mechanical lysis and enzymatic lysis. **(A)** DNA concentrations extracted by three different methods. **(B)** The absolute average length of microbial sequencing reads.

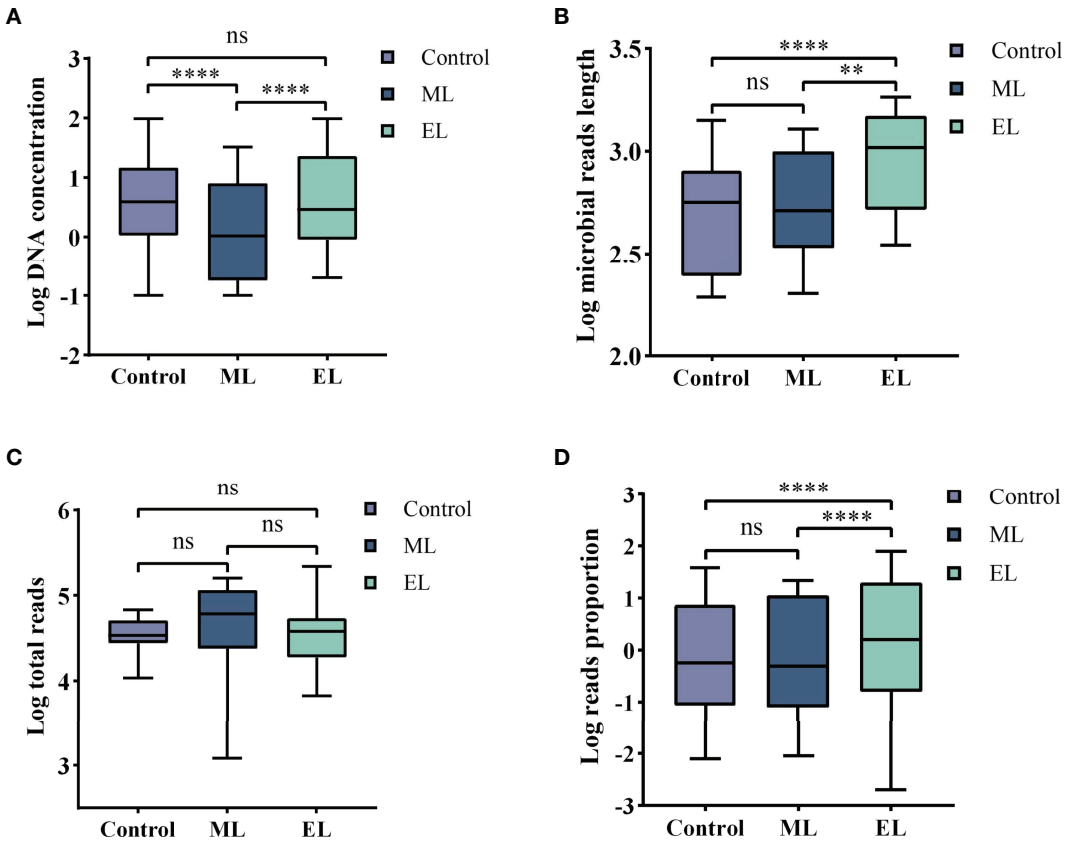

FIGURE 3 | Boxplots demonstrating the statistic difference analysis for the three DNA extraction methods. Median values are indicated by the line within the boxplot. The box extends from the 25th to 75th percentiles, and whiskers indicate the minimum and maximum values. ****$P < 0.0001$; **$P < 0.01$; ns, nonsignificant. **(A)** Log DNA concentration. **(B)** Log average length of microbial reads. **(C)** Log total reads. **(D)** Log mapped reads proportion of the specific species.

TABLE 1 | DNA yield and integrity of the three DNA extraction methods.

SP	Control		ML Method		EL Method	
	Yield(ng/μl)	Length(bp)	Yield(ng/μl)	Length(bp)	Yield(ng/μl)	Length(bp)
P1	22.8	446.2	9.2	273.2	39.2	849.7
P2	4.68	936.9	0.878	814.5	3.5	1348.7
P3	0.198	201.9	0.128	777.7	0.204	602.2
P4	1.92	577.8	0.51	350.9	1.16	612.3
P5	3.28	193.5	1.79	333.6	1.76	423.4
P6	0.294	592	0.126	427.3	0.352	1752.8
P7	16.3	828.7	13.5	541.9	25.4	573.3
P8	0.966	653.8	0.532	334.9	0.872	1682.5
P9	75.8	407.1	32.6	449.1	97.6	983.8
P10	1.61	205.2	0.496	201.5	1	406
P11	16.9	268.3	18.8	311	33.8	435
P12	97.6	231.4	22	1284.1	87	1107.6
P13	2.18	987.2	0.612	1157.1	3.24	1723.6
P14	1.45	238.6	0.11	489.6	1.79	349.6
P15	0.1	547.5	0.1	477.1	0.2	1248
P16	0.232	636.2	0.116	842.2	0.77	1834
P17	10	551.3	1.25	654.9	3.18	1361.3
P18	10.8	1416.9	4.46	1249.4	16.5	1465.5
P19	6.08	735	5.32	1054.9	2.66	503.9
P20	5.64	836.5	4.64	1181.4	16.8	1495.9

SP, sample; ML, mechanical lysis; EL, enzymatic lysis.

TABLE 2 | Abundance variation of specific species by different DNA extraction methods.

SP	Cultureresult	Control		ML Method		EL Method	
		Num	Pro	Num	Pro	Num	Pro
P1	*Candida albicans*	11	0.102%	0	0%	127	1.16%
P2	*Candida glabrata*	25	0.201%	70	0.099%	957	1.32%
P3	*Candida glabrata*	0	0%	0	0%	117	0.47%
P4	*Candida parapsilosis*	174	0.533%	415	0.26%	57069	31.4%
P5	*Candida glabrata*	0	0%	0	0%	32	0.077%
P6	*Candida glabrata*	1202	2.945%	201	1.430%	4212	23.2%
P7	*Candida albicans*	0	0%	0	0%	42	0.02%
P8	*Candida parapsilosis*	116	0.234%	179	0.14%	713	4.07%
P9	*Candida albicans*	2	0.008%	3	0.013%	118	0.27%
P10	*Candida albicans*	0	0%	0	0%	1	0.002%
P11	*Candida albicans*	3	0.008%	11	0.009%	20	0.094%
P12	*Candida glabrata*	3	0.024%	12	0.057%	638	1.39%
P13	*Enterococcus Faecium*	7222	16.52%	12305	22%	15516	45.1%
	Candida albicans	268	0.613%	281	0.5%	4966	14.4%
P14	*Trichosporon asahii*	0	0%	0	0%	53	0.093%
P15	*Candida krusei*	11910	38.571%	252	20.8%	44865	79.1%
P16	*Candida parapsilosis*	1234	2.164%	106	5.8%	17235	59.84%
P17	*Candida albicans*	56	0.082%	36	0.08%	2774	6.5%
P18	*Klebsiella pneumoniae*	3097	10.231%	15168	11.3%	1048	15.6%
P19	*Escherichia coli*	12553	22.157%	5385	20.1%	1503	17.2%
P20	*Candida glabrata*	323	1.139%	429	1.27%	437	1.61%
Con		15/20		14/20		20/20	

SP, sample; Num, number; Pro, proportion; Con, consistency.

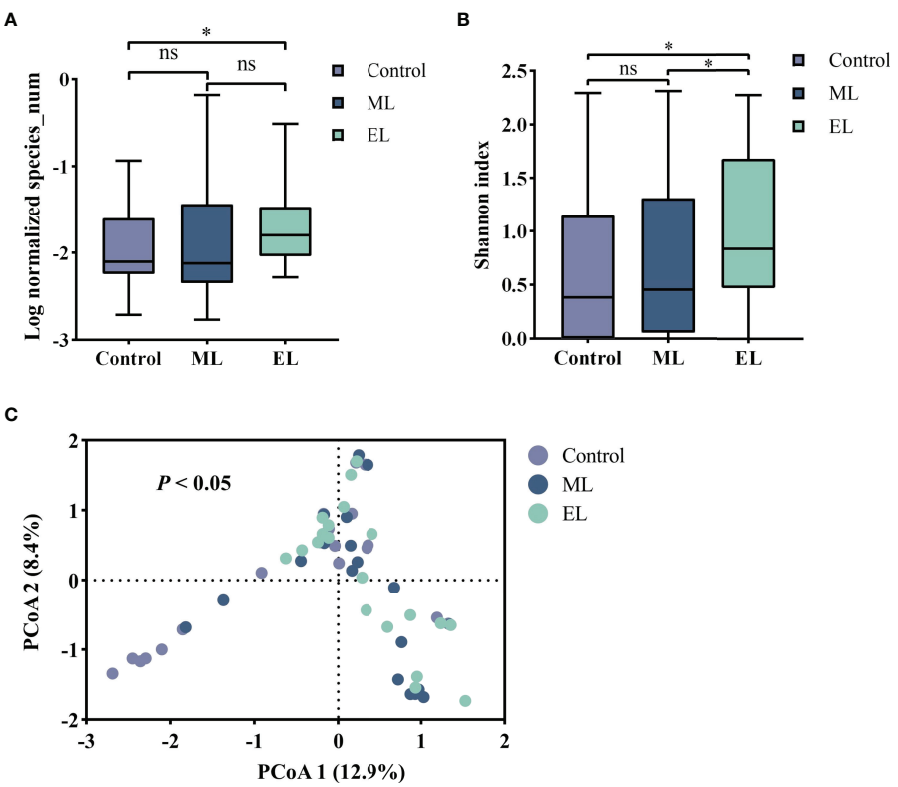

FIGURE 4 | The microbial diversity of the three DNA extraction methods. Median values are indicated by the line within the boxplot. The box extends from the 25th to 75th percentiles, and whiskers indicate the minimum and maximum values. *$P < 0.05$; ns, nonsignificant. **(A)** Log normalized total number of microbial species observed by mNGS. **(B)** Alpha diversity based on the Shannon index. **(C)** Beta diversity with PCoA based on the Bray–Curtis index.

Impact of DNA Extraction Method on Microbial Diversity Composition

To evaluate the impact of DNA extraction method on microbial diversity composition, we quantified the relative abundance of microbial taxa per sample based on nanopore sequencing. We first compared the total number of microbial species for each of the three DNA extraction methods (**Figure 4A**). The total number of microbial species was normalized by the total number of reads per sample and made pairwise comparison across the three DNA extraction methods (see **Supplementary Table S1** for raw data). Enzymatic-based method observed more microbial species in urine samples than the control method ($P < 0.05$), whereas the other two methods gave no significant difference of microbial species diversity ($P > 0.05$). We further evaluated the microbial diversity variation by the alpha and beta diversities. Alpha diversity by Shannon index indicated that significant increase of microbial diversity was observed in enzymatic-based method compared with the other two methods (all $P < 0.05$, **Figure 4B**). The beta diversity with principal coordinate analysis (PCoA) was based on the Bray–Curtis dissimilarity, and the PERMANOVA test showed a significant difference of the microbial composition among these three methods ($P < 0.05$, **Figure 4C**).

For evaluating the microbial DNA extraction efficiency ratio of the three methods, we compared the proportion of total microbial reads per sample for each method (see **Supplementary Table S1** for raw data). Similarly, enzymatic-based method increased the microbial proportion by a median of 9.2-fold (IQR, 3.1–26.0; maximum, 69.0; **Figure 5A**) compared with control group, whereas the mechanical-based method had a median of 0.9-fold (IQR, 0.6–1.2; maximum, 3.3; **Figure 5A**). In addition, compared with the mechanical-based method, enzymatic-based method increased the microbial proportion by a median of 11.9-fold (IQR, 3.3–22.1; maximum, 74.5; **Figure 5A**). To assess which types of species were most impacted by the extraction methods, we investigated the distribution and relative abundance of the most common species (**Figures 5**, **6**). We found that gram-positives had a visible variation and fungi species had a significant variation ($P < 0.0001$, **Figure 5B**) in relative abundance across methods, whereas the variation in gram-negatives abundance was not obvious. These results are in line with previous observations that gram-positive bacteria and fungi are more likely to be affected by DNA extraction methods (McOrist et al., 2002; Santiago et al., 2014; Ackerman et al., 2019). In addition, these results also showed low bacterial abundance in samples from fungal infected patients. Likewise, in samples from bacteria-infected patients (P18 and P19), the fungal abundance was low. We further compared the microbial relative abundance of these three methods using Kruskal–Wallis test and found that significant difference existed between each other (all $P < 0.0001$).

DISCUSSION

In metagenomic sequencing studies, variations in the DNA extraction protocol can have important downstream effects on the observed microbial composition. Maximizing DNA concentration while also minimizing fragmentation are key aspects to consider when selecting an extraction method. This is both because high-quality libraries are required for sequencing, and protocols that consistently recover low-yield or highly fragmented DNA are likely to skew the observed community composition (Costea et al., 2017). The emergence of new long-read sequencing techniques such as nanopore has raised the bar for DNA quality and extraction methods. However, there is a paucity of studies to evaluate performance of different DNA extraction methods for long-read mNGS–based pathogen diagnostic testing. In this study, for selecting a best suited DNA extraction method to support pathogen diagnosis based on long-read mNGS testing, we systematically compared three DNA extraction methods by assessing DNA yield, integrity, and the microbial diversity

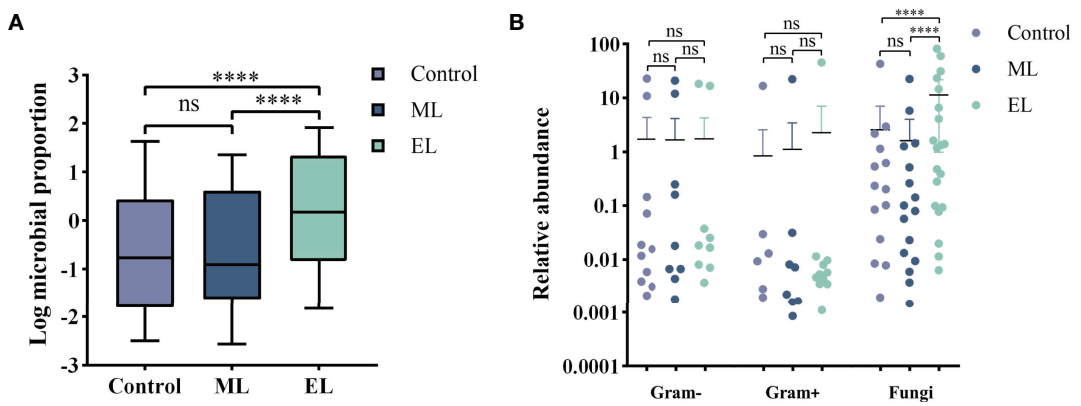

FIGURE 5 | Evaluation of the DNA extraction efficiency for the three DNA extraction methods. ****$P < 0.0001$; ns, nonsignificant. **(A)** Boxplot of Log proportion of microbial reads in total reads generated by MinION. Median values are indicated by the line within the boxplot. The box extends from the 25th to 75th percentiles, and whiskers indicate the minimum and maximum values. **(B)** Relative abundance difference for different types of species by different DNA extraction methods.

FIGURE 6 | Distribution and relative abundance of microbial profile in urine samples with DNA extracted by different methods. Heatmap strip at the left and top are to aid in distinguishing different species types and DNA extraction methods, respectively.

based on metagenomic nanopore sequencing of urine samples from patients with UTI.

Among the three methods, the DNA concentration of the mechanical-based method was significantly lower compared with the other methods, which may be result from the loss of excessive short DNA sequences during DNA purification on silica membrane (Dilley et al., 2021). However, we performed analysis of correlation to compare DNA yield and microbial proportion within each DNA extraction method, and there were no correlations observed (all $P > 0.1$) as host DNA accounts for a large proportion in urine samples. These results are in line with published literature (Yuan et al., 2012). Therefore, DNA yield alone appears to be an unrepresentative measure for extraction efficiency because microbial DNA accounts for a little proportion of total DNA in urine samples (Salonen et al., 2010).

For the comparison of microbial reads length generated by mNGS testing, although there was no significant difference observed between mechanical-based method and control method, enzymatic-based method generated much longer-read length, indicating that the long DNA sequences had been released to a greater extent after the enzymatic cell lysis and resulting in outputted DNA with high integrity. Hence, these results proved the better compatibility of enzymatic-based method to the long-read sequencing technologies. Unusually, this result also seems to show that mechanical-based method did not make excessive shearing of DNA. However, it can also be interpreted with the preference of the silica membrane to capture longer DNA sequences (Doran and Foran, 2014; Dilley et al., 2021), which is also in line with the result of lower DNA yield of mechanical-based method above.

Pathogen diagnosis using MinION-based mNGS testing is common in recent studies (Schmidt et al., 2017; Charalampous et al., 2019; Moon et al., 2019). Unbiased cell lysis and complete DNA extraction of all microbial pathogens are crucial to recover specific pathogenic species accurately in mNGS testing, as reads derived from the normal microbiota in human may influence pathogens identification (Gu et al., 2019). Among the 20 urine samples with microbial infection, enzymatic-based mNGS testing provided a fully consistent result with pathogen detected by culture. In contrast, control method and mechanical-based method missed detection of five and six samples, respectively. All the missed pathogens were fungal pathogens, indicating that some fungal cells are more difficult to lyse, again, in line with the result from a previous study (Ackerman et al., 2019). In addition, on the basis of the detection result of control method and enzymatic method, the cell lysis treatment in advance is necessary and effective for DNA extraction of clinical samples with unknown infectious agents when using sequence-based detection methods, although it increases the turnround time of DNA extraction.

The microorganisms that colonize various anatomical sites of the human body play important roles in human health and

disease (Dethlefsen et al., 2007), it is critical to understand the urinary microbiome comprehensively and accurately to develop novel therapies for UTI (Xiao et al., 2016; Neugent et al., 2020). Enzymatic-based method provided the largest normalized species number and the microbial proportion among the three methods; especially for the recovery of fungi and gram-positive microbiota, the enzymatic-based method obtained a most high abundance, indicating that it can generate a more representative microbial diversity composition from urine samples. These results proved that the enzymatic-based method can serve as an unbiased and reliable procedure for DNA extraction in the future sequence-based metagenomic analyses.

This study presents some limitations. First, it is difficult to assess which DNA extraction method came closest to the biological truth for absence of parallel evaluation of DNA extraction methods with a mock community. Second, we did not investigate any additional factors that may affect the metagenomic results, such as that of reagent and laboratory contamination (Salter et al., 2014).

In conclusion, we proved excellent performance of enzymatic-based method for long-read mNGS testing through systematically comparing three DNA extraction methods. We anticipate that procedures for DNA extraction will likely further improve in the future and propose that using a combination of lytic enzyme solution and MetaPolyzyme for effective lysis of a range of microbes, including both fungi and bacteria with minimal shearing. Although we have only proved the advantage of enzymatic-based DNA extraction method on urine samples, this can probably be extended to other samples such as stool and bronchoalveolar lavage fluid. By combining reliable organism lysis, unbiased sequencing, and comprehensive reference databases, long-read mNGS testing can be applied in real clinical practice for hypothesis-free and universal pathogen detection, promising to improve diagnostic accuracy of all microbiological infections.

DATA AVAILABILITY STATEMENT

The datasets presented in this study can be found in online repositories. The names of the repository/repositories and accession number(s) can be found in the article/**Supplementary Material**.

ETHICS STATEMENT

The studies involving human participants were reviewed and approved by the Institutional Review Board (IRB) of the Beijing Dongfang Hospital (reference no. JDF-IRB-2020003101). The patients/participants provided their written informed consent to participate in this study.

AUTHOR CONTRIBUTIONS

WH, PL, YJ, and LZ conceived and designed the study. LZ and TC carried out the experimental work and analyzed the data. LZ, TC, and YW conceptualized the experimental methods, performed bioinformatics, and wrote the original draft of the manuscript. PL, WH, and YJ participated in the review and editing of the manuscript. All authors contributed to the article and approved the submitted version.

FUNDING

The project was financed by the National Natural Science Foundation of China (82002115).

SUPPLEMENTARY MATERIAL

The Supplementary Material for this article can be found online at: https://www.frontiersin.org/articles/10.3389/fcimb.2022.919903/full#supplementary-material

REFERENCES

Ackerman, A. L., Anger, J. T., Khalique, M. U., Ackerman, J. E., Tang, J., Kim, J., et al. (2019). Optimization of DNA Extraction From Human Urinary Samples for Mycobiome Community Profiling. *PLoS One* 14 (4), e0210306. doi: 10.1371/journal.pone.0210306

Charalampous, T., Kay, G. L., Richardson, H., Aydin, A., Baldan, R., Jeanes, C., et al. (2019). Nanopore Metagenomics Enables Rapid Clinical Diagnosis of Bacterial Lower Respiratory Infection. *Nat. Biotechnol.* 37 (7), 783–792. doi: 10.1038/s41587-019-0156-5

Costea, P. I., Zeller, G., Sunagawa, S., Pelletier, E., Alberti, A., Levenez, F., et al. (2017). Towards Standards for Human Fecal Sample Processing in Metagenomic Studies. *Nat. Biotechnol.* 35 (11), 1069–1076. doi: 10.1038/nbt.3960

Cummings, L. A., Kurosawa, K., Hoogestraat, D. R., SenGupta, D. J., Candra, F., Doyle, M., et al. (2016). Clinical Next Generation Sequencing Outperforms Standard Microbiological Culture for Characterizing Polymicrobial Samples. *Clin. Chem.* 62 (11), 1465–1473. doi: 10.1373/clinchem.2016.258806

Dethlefsen, L., McFall-Ngai, M., and Relman, D. A. (2007). An Ecological and Evolutionary Perspective on Human-Microbe Mutualism and Disease. *Nature* 449 (7164), 811–818. doi: 10.1038/nature06245

Dilley, K., Pagan, F., and Chapman, B. (2021). Methods for Ensuring the Highest DNA Concentration and Yield in Future and Retrospective Trace DNA Extracts. *Sci. Justice.* 61 (2), 193–197. doi: 10.1016/j.scijus.2020.11.005

Doran, A. E., and Foran, D. R. (2014). Assessment and Mitigation of DNA Loss Utilizing Centrifugal Filtration Devices. *Forensic. Sci. Int. Genet.* 13, 187–190. doi: 10.1016/j.fsigen.2014.08.001

Goldberg, B., Sichtig, H., Geyer, C., Ledeboer, N., and Weinstock, G. M. (2015). Making the Leap From Research Laboratory to Clinic: Challenges and Opportunities for Next-Generation Sequencing in Infectious Disease Diagnostics. *mBio* 6 (6), e01888–e01815. doi: 10.1128/mBio.01888-15

Gu, W., Miller, S., and Chiu, C. Y. (2019). Clinical Metagenomic Next-Generation Sequencing for Pathogen Detection. *Annu. Rev. Pathol.* 14, 319–338. doi: 10.1146/annurev-pathmechdis-012418-012751

Hasman, H., Saputra, D., Sicheritz-Ponten, T., Lund, O., Svendsen, C. A., Frimodt-Moller, N., et al. (2014). Rapid Whole-Genome Sequencing for Detection and Characterization of Microorganisms Directly From Clinical Samples. *J. Clin. Microbiol.* 52 (1), 139–146. doi: 10.1128/JCM.02452-13

Imirzalioglu, C., Hain, T., Chakraborty, T., and Domann, E. (2008). Hidden Pathogens Uncovered: Metagenomic Analysis of Urinary Tract Infections. *Andrologia* 40 (2), 66–71. doi: 10.1111/j.1439-0272.2007.00830.x

Kumar, S., Dave, A., Wolf, B., and Lerma, E. V. (2015). Urinary Tract Infections. *Dis. Mon.* 61 (2), 45–59. doi: 10.1016/j.disamonth.2014.12.002

Li, M., Yang, F., Lu, Y., and Huang, W. (2020). Identification of Enterococcus Faecalis in a Patient With Urinary-Tract Infection Based on Metagenomic Next-Generation Sequencing: A Case Report. *BMC Infect. Dis.* 20 (1), 467. doi: 10.1186/s12879-020-05179-0

Mattei, V., Murugesan, S., Al Hashmi, M., Mathew, R., James, N., Singh, P., et al. (2019). Evaluation of Methods for the Extraction of Microbial DNA From Vaginal Swabs Used for Microbiome Studies. *Front. Cell Infect. Microbiol.* 9. doi: 10.3389/fcimb.2019.00197

Maukonen, J., Simoes, C., and Saarela, M. (2012). The Currently Used Commercial DNA-Extraction Methods Give Different Results of Clostridial and Actinobacterial Populations Derived From Human Fecal Samples. *FEMS Microbiol. Ecol.* 79 (3), 697–708. doi: 10.1111/j.1574-6941.2011.01257.x

McOrist, A. L., Jackson, M., and Bird, A. R. (2002). A Comparison of Five Methods for Extraction of Bacterial DNA From Human Faecal Samples. *J. Microbiol. Methods* 50 (2), 131–139. doi: 10.1016/s0167-7012(02)00018-0

Moon, J., Kim, N., Kim, T. J., Jun, J. S., Lee, H. S., Shin, H. R., et al. (2019). Rapid Diagnosis of Bacterial Meningitis by Nanopore 16S Amplicon Sequencing: A Pilot Study. *Int. J. Med. Microbiol.* 309 (6), 151338. doi: 10.1016/j.ijmm.2019.151338

Neugent, M. L., Hulyalkar, N. V., Nguyen, V. H., Zimmern, P. E., and De Nisco, N. J. (2020). Advances in Understanding the Human Urinary Microbiome and Its Potential Role in Urinary Tract Infection. *mBio* 11 (2). doi: 10.1128/mBio.00218-20

Rhoads, A., and Au, K. F. (2015). PacBio Sequencing and Its Applications. *Genomics Proteomics Bioinf.* 13 (5), 278–289. doi: 10.1016/j.gpb.2015.08.002

Salonen, A., Nikkila, J., Jalanka-Tuovinen, J., Immonen, O., Rajilic-Stojanovic, M., Kekkonen, R. A., et al. (2010). Comparative Analysis of Fecal DNA Extraction Methods With Phylogenetic Microarray: Effective Recovery of Bacterial and Archaeal DNA Using Mechanical Cell Lysis. *J. Microbiol. Methods* 81 (2), 127–134. doi: 10.1016/j.mimet.2010.02.007

Salter, S. J., Cox, M. J., Turek, E. M., Calus, S. T., Cookson, W. O., Moffatt, M. F., et al. (2014). Reagent and Laboratory Contamination can Critically Impact Sequence-Based Microbiome Analyses. *BMC Biol.* 12, 87. doi: 10.1186/s12915-014-0087-z

Santiago, A., Panda, S., Mengels, G., Martinez, X., Azpiroz, F., Dore, J., et al. (2014). Processing Faecal Samples: A Step Forward for Standards in Microbial Community Analysis. *BMC Microbiol.* 14, 112. doi: 10.1186/1471-2180-14-112

Schlaberg, R., Chiu, C. Y., Miller, S., Procop, G. W., Weinstock, G., Professional Practice, C., et al. (2017). Validation of Metagenomic Next-Generation Sequencing Tests for Universal Pathogen Detection. *Arch. Pathol. Lab. Med.* 141 (6), 776–786. doi: 10.5858/arpa.2016-0539-RA

Schmidt, K., Mwaigwisya, S., Crossman, L. C., Doumith, M., Munroe, D., Pires, C., et al. (2017). Identification of Bacterial Pathogens and Antimicrobial Resistance Directly From Clinical Urines by Nanopore-Based Metagenomic Sequencing. *J. Antimicrob. Chemother.* 72 (1), 104–114. doi: 10.1093/jac/dkw397

Wang, Y., Zhao, Y., Bollas, A., Wang, Y., and Au, K. F. (2021). Nanopore Sequencing Technology, Bioinformatics and Applications. *Nat. Biotechnol.* 39 (11), 1348–1365. doi: 10.1038/s41587-021-01108-x

Willner, D., Low, S., Steen, J. A., George, N., Nimmo, G. R., Schembri, M. A., et al. (2014). Single Clinical Isolates From Acute Uncomplicated Urinary Tract Infections are Representative of Dominant *in Situ* Populations. *mBio* 5 (2), e01064–e01013. doi: 10.1128/mBio.01064-13

Xiao, B., Niu, X., Han, N., Wang, B., Du, P., Na, R., et al. (2016). Predictive Value of the Composition of the Vaginal Microbiota in Bacterial Vaginosis, a Dynamic Study to Identify Recurrence-Related Flora. *Sci. Rep.* 6, 26674. doi: 10.1038/srep26674

Yuan, S., Cohen, D. B., Ravel, J., Abdo, Z., and Forney, L. J. (2012). Evaluation of Methods for the Extraction and Purification of DNA From the Human Microbiome. *PLoS One* 7 (3), e33865. doi: 10.1371/journal.pone.0033865

Zhang, L., Huang, W., Zhang, S., Li, Q., Wang, Y., Chen, T., et al. (2022). Rapid Detection of Bacterial Pathogens and Antimicrobial Resistance Genes in Clinical Urine Samples With Urinary Tract Infection by Metagenomic Nanopore Sequencing. *Front. Microbiol.* 13. doi: 10.3389/fmicb.2022.858777

Conflict of Interest: The authors declare that the research was conducted in the absence of any commercial or financial relationships that could be construed as a potential conflict of interest.

frontiers | Frontiers in Cellular and Infection Microbiology

TYPE Original Research
PUBLISHED 09 August 2022
DOI 10.3389/fcimb.2022.948602

OPEN ACCESS

EDITED BY
Gaoqian Feng,
Burnet Institute, Australia

REVIEWED BY
Fei Zhao,
University of Toronto, Canada
Yuqing Wang,
Kyushu University, Japan

*CORRESPONDENCE
Degang Yang
degangyang_sh@126.com
Yi Shan
shanyi831@163.com
Zhu Yan
zhuyan2021mise169@126.com

†These authors have contributed equally to the work

SPECIALTY SECTION
This article was submitted to Clinical Microbiology, a section of the journal Frontiers in Cellular and Infection Microbiology

RECEIVED 20 May 2022
ACCEPTED 04 July 2022
PUBLISHED 09 August 2022

CITATION
Wan J, Duan L, Chen Q, Wang L, Bai J, Hu J, Lu X, Zhang T, Song W, Yang D, Shan Y and Yan Z (2022) Potential clinical impact of metagenomic next-generation sequencing of plasma for cervical spine injury with sepsis in intensive care unit: A retrospective study. *Front. Cell. Infect. Microbiol.* 12:948602. doi: 10.3389/fcimb.2022.948602

Potential clinical impact of metagenomic next-generation sequencing of plasma for cervical spine injury with sepsis in intensive care unit: A retrospective study

Jian Wan[1†], Liwei Duan[2†], Qitong Chen[2], Lv Wang[2], Jinxia Bai[1], Jingyun Hu[3], Xinyuan Lu[1], Tao Zhang[1], Wei Song[1], Degang Yang[4*], Yi Shan[2*] and Zhu Yan[2*]

[1]Department of Emergency and Critical Care Medicine, Shanghai Pudong New Area People's Hospital, Shanghai, China, [2]Department of Emergency and Critical Care Medicine, Shanghai Changzheng Hospital, Shanghai, China, [3]Central Lab, Shanghai Key Laboratory of Pathogenic Fungi Medical Testing, Shanghai Pudong New Area People's Hospital, Shanghai, China, [4]Department of Infectious Diseases, Shanghai Skin Disease Hospital, Tongji University School of Medicine, Shanghai, China

Cervical spine injury (CSI) accounts for significant mortality in the intensive care unit (ICU), whereas sepsis remains one of the major causes of death in patients with CSI. However, there is no effective method to diagnose sepsis timely. The aim of this study is to investigate the effect of metagenomic next-generation sequencing (mNGS) on the pathogen features and the prognostic prediction of CSI patients with sepsis. A total of 27 blood samples from 17 included patients were tested by mNGS. Data of mNGS were compared with the conventional culture method. The Kaplan–Meier plots were used to visualize survival curves. A Cox proportional hazards model was used to identify independent prognostic factors for survival. Results showed that mNGS detected a wide spectrum of pathogens in CSI patients with sepsis, including 129 bacterial species, 8 viral species, and 51 fungal species. mNGS indicated 85.2% positive results, while the conventional culture method only showed 11.1% positive results in the blood samples. Further analyses revealed that mNGS had no prognostic effect on the septic CSI patients in ICU, whereas positive results of blood culture were closely correlated with an increased hazard ratio (HR) (HR 77.7067, 95%CI 2.860–2641.4595, p = 0.0155). Our results suggested that the mNGS application may provide evidence for clinicians to use antibiotics when a CSI case is diagnosed with sepsis.

KEYWORDS

cervical spine injury, metagenomic next-generation sequencing, sepsis, ICU, a retrospective study

Introduction

Sepsis is a life-threatening organ dysfunction resulting from dysregulated host response to infection (Singer et al., 2016; Cecconi et al., 2018). In 2017, an estimated 48.9 million cases of sepsis were recorded worldwide, and 11.0 million sepsis-related deaths were reported globally (Rudd et al., 2020). In China, the standardized sepsis-related mortality rate is high, accounting for 66.7 deaths per 100,000 people (Weng et al., 2018). Multiple studies have shown that sepsis is the main cause of intensive care unit (ICU) admission and mortality (Engel et al., 2007; Fleischmann et al., 2016). However, there is no approved specific molecular therapy for sepsis. Timely identification, targeted treatment, and supportive care are necessary to improve clinical outcomes. Sepsis can virtually originate from any infecting pathogens, including bacteria, viruses, fungi, and parasites. Blood culture has been considered the gold standard for sepsis diagnosis. However, microbiological confirmation is difficult to complete when treatment starts. Even when microbiological tests are completed, culture-positive sepsis is observed in only 30%–40% of all cases (Singer et al., 2016). Furthermore, conventional blood culture takes 2–3 days to obtain initial results and up to 1 week for confirmation, resulting in delayed or inadequate targeted antimicrobial therapy (Gu et al., 2019; Han et al., 2019). Alternatively, polymerase chain reaction (PCR)-based techniques have been introduced for pathogen detection in the past decades. However, PCR-based techniques are limited by targeting few numbers of pathogens using specific primers or probes, and a very small portion of the genome (Chiu and Miller, 2019; Gu et al., 2019), and there is also a constant need to update PCR-based methods to include emerging resistance genes and mutations (Buchan and Ledeboer, 2014). Thus, a more sensitive, rapid, and accurate approach for identifying infections of sepsis is needed.

Metagenomic next-generation sequencing (mNGS) is a novel and culture-independent high-throughput sequencing method for evaluating infection and features the advantage of shortened turnaround time, unbiased detection, and semi-quantitative value in follow-up (Gu et al., 2019; Han et al., 2019). The capacity to detect all potential pathogens in a sample and simultaneously interrogate host responses makes it a potential tool in the diagnosis of infectious diseases. To date, several studies have provided a glimpse into the value of mNGS in finding out the causative pathogens and guiding targeted antimicrobial therapy. In 2014, Wilson et al. reported the first use of clinical mNGS for actionable diagnosis and treatment in a critically ill patient with a mysterious neurological infection, as the successful diagnosis prompted appropriate targeted antibiotic treatment and eventual recovery of the patient (Wilson et al., 2014). Increasing data provided by mNGS has been leveraged for detecting pathogens in central nervous system infections, bloodstream infections, respiratory infections, gastrointestinal infections, and ocular infections (Gu et al., 2019). Therefore, mNGS can be a key driver for the precise diagnosis of infectious diseases.

Cervical spine injury (CSI) is defined as the damage to the cervical spinal cord, with traumatic and non-traumatic etiologies. It is associated with significant morbidity and mortality in patients in ICU (Ahuja et al., 2017). The incidence of CSI for the general population is 0.13 per 1,000 (Wu et al., 2012), and mortality in patients with CSI has been reported to be three times more than that in age-matched healthy subjects (Ghajarzadeh et al., 2019). CSI leads to an increased rate of sepsis, which remains to be one of the main causes of death following CSI (Cao et al., 2019; Buzzell et al., 2020; Kamp et al., 2020). Thus, it is necessary to timely diagnose sepsis and deliver the therapeutic actions targeting sepsis to the patients with CSI.

Here we performed a retrospective study to evaluate the potential clinical impact of mNGS on plasma for CSI patients with sepsis in ICU and to investigate the effect of mNGS on the prognosis of these patients. We found a wide spectrum of pathogens in CSI patients with sepsis, including 129 bacterial species, 8 viral species, and 51 fungal species. mNGS indicated 85.2% positive results, while the conventional culture method only showed 11.1% positive results in the blood samples. Further analyses revealed that positive results of blood culture were closely correlated with an increased hazard ratio (HR).

Methods

Study population and specimen collection

The Ethical Review Committee of Changzheng Hospital approved this study. Written informed consent was received from participants or their legal guardians prior to inclusion in this study. All patients in the ICU at Changzheng Hospital from February 2018 to June 2019 were enrolled in this study. The inclusion criteria were 1) patients with complete medical records and with a temperature above 38°C or below 36°C, 2) accompanied with mNGS results for blood samples, and 3) diagnosed with CSI. 4) Patients should also meet one of the following conditions: a) with definite invasive sites or migration foci, b) with rashes or bleeding spots with unknown cause or an increasing blood neutrophil level, and c) systolic pressure below 90 mmHg or decreasing more than 40 mmHg. The exclusion criteria were patients diagnosed with a malignant tumor, blood-related diseases, chronic viral infection, severe major organ dysfunction, or chronic inflammatory diseases.

Patient demographics and clinical features

The demographic data reviewed were based on the information provided by the patients at the time of admission

into ICU, including age and gender. Clinic data observed during the first 24 h of the hospital stay were collected to obtain the following variables: diagnosis, temperature (°C), heart rate, respiratory rate, systolic and mean arterial blood pressure (mmHg), PaO_2 or FiO_2 (mmHg), arterial pH and bicarbonate, serum sodium, potassium, urea and creatinine, urine output, white blood cell count, hematocrit, platelet count and bilirubin, Acute Physiology and Chronic Health Evaluation II (APACHE II) score (Knaus et al., 1985), and sequential [sepsis-related] organ failure assessment (SOFA) score (Vincent et al., 1996). For the patients with multiple blood samples, APACHE II and SOFA scores were timely evaluated when the blood sample was acquired.

Sample preparation and processing

A venous blood sample at a volume of 5 ml was collected in Streck cell-free DNA (cfDNA) tubes and stored at 4°C before use. Samples were collected at the time of suspected or confirmed sepsis diagnosis. The tubes were spun down at 1,600 *g* for 10 min at room temperature to prepare plasma. cfDNA was extracted from plasma using QIAamp (QIAGEN, Valencia, CA, USA) following the manufacturer's operational manual. The extracted DNA was used for the construction of DNA libraries.

Sequencing

Sequencing mNGS libraries were prepared. Negative controls and positive controls were included with patient samples in each batch. The quality of the DNA libraries was evaluated by Agilent 2100 Bioanalyzer (Agilent Technologies, Santa Clara, CA, USA). High-throughput sequencing was conducted using the Illumina NextSeq550Dx platform. On average, twenty-five million reads from the sample were acquired on the sequencer.

Reference database and quality control

Reference genomes for *Homo sapiens* and microorganisms (bacteria, viruses, fungi/molds, and other eukaryotic pathogens) were retrieved from the National Center for Biotechnology Information (NCBI) ftp site (NCBI, U.S. National Library of Medicine (NLM); Human Genome, release GRCh38.p7; and NCBI, U.S. NLM, Microbial Genomes, respectively). Sequence similarities between microorganism references were inspected to identify taxonomic mislabeling and sequence contamination. From the reference genomes passing these quality controls (QCs), a subset was selected to maximize sequence diversity. As part of the selection process, NCBI BioSample data were used to ensure the inclusion of reference genomes from both clinical and non-clinical isolates. Selected sequences were collected into a single FASTA file and used to generate our microorganism reference database.

The selection of MedcareDx's proprietary microorganism reference database was performed as follows. A candidate list was generated by two board-certified infectious disease physicians by including a) DNA viruses, culturable bacteria, additional fastidious and unculturable bacteria, mycobacteria, and eukaryotic pathogens from a number of infectious disease references; b) organisms in the pathogen database referenced in published case reports; c) reference genomes sequenced from human clinical isolates (as indicated by the NCBI BioSample resource) with publications supporting pathogenicity. Organisms from the above list that were associated with high-quality reference genomes, as determined by our reference database QC process (see above), were used to further narrow the range. Finally, organisms observed as sporadic environmental contamination were excluded from the clinical reportable range (CRR) in order to prevent false-positive calls, e.g., *Propionibacterium acnes*, *Acinetobacter lwoffii*, and several *Methylobacterium* spp. The sequence database is continuously curated to minimize human cross-reactivity as well as cross-reactivity between pathogens and is screened to mitigate contamination with sequences from humans or other organisms.

Preprocessing

Raw sequencing output files were processed to generate the demultiplexed sequencing reads files. Reads were filtered based on sequencing quality and trimmed based on partial or full adapter sequence. Low-quality base calls and adapter sequences were trimmed off from the raw reads, retaining reads of trimmed length ≥35 bp, and duplicates were removed. The Burrows-Wheeler Aligner (BWA) tool was used to align the remaining high-quality sequencing reads against the hg19 human reference sequence. Sequencing reads exhibiting strong alignment against the human references were collected, and reads identified as human were excluded from further analysis. The remaining reads were aligned against MedcareDx's proprietary microorganism reference database.

Determination of pathogens

To identify the pathogenic sequences, the remaining unmapped sequences were aligned to a curated pathogen database, including bacterial, viral, fungal, and parasite. The quantity for each organism identified was expressed in normalized number (NN) of DNA sequencing reads from the reported organism present in plasma. An organism in a patient was removed, as the normalized number of strictly mapped

DNA sequencing reads was less than 3. For each discrete viral or bacterial genus, assigned NGS reads are directly mapped to all nucleotide reference sequences corresponding to that genus at the species, strain, or substrain level using BLASTn at an E-value cutoff of 1,020. For each genus, a coverage map of the reference sequence with the highest percent coverage is generated, with priority given to reference sequences in the following order: 1) complete genomes, 2) complete sequences, or 3) partial sequences/individual genes. The parameters for bacteria, viruses, and fungi were annotated with all classified mapped reads. A mixture model was used to assign a likelihood to the complete collection of sequencing reads in the sample. An expectation–maximization algorithm was applied to compute the maximum likelihood estimate of each taxon abundance. Only taxa whose abundances rejected the null hypothesis of originating from environmental contamination (as calculated from the negative controls) at high significance levels were reported. Typically, it took less than 29 h to complete the entire process from DNA extraction to analysis.

Criteria for a positive metagenomic next-generation sequencing result

In this study, positive data were considered as the mapping read number, or relative abundance was more than zero. When categorizing the frequency of pathogens in the blood sample, the positive relative abundance of pathogens in each blood sample was calculated.

Statistical analysis

All statistical analyses were performed using SPSS Statistics (version 25.0) and R (version 3.6.2) with the following main packages: forestplot, survival, survminer, and ggplot2. Continuous data were presented as mean and standard deviation. Categorical data were compared using chi-squared tests. The Kaplan–Meier plots were used to visualize survival curves and compared using the log-rank test. A Cox proportional hazards model was used to identify independent prognostic factors for survival. In stratum-specific analyses of mNGS results, the results of bacteria, viruses, and fungi were counted separately. A p-value of less than 0.05 was considered statistically significant.

Results

Demographic features

From February 2018 to June 2019, a total of 435 patients were admitted to the ICU at Changzheng Hospital, and finally, 17 CSI patients with sepsis were enrolled in this study (Figure 1). Patients' demographics and clinical features are described in Table 1. The median age was 60 (33–74) years, and 76.5% of cases were male. A total of 15/17 (88.2%) cases were traumatic CSI, and the rest two cases were non-traumatic CSI. The median APACHE II score and SOFA score were 19 (8–23) and 6 (3–12), respectively. The length of stay (LOS) in ICU ranged from 6 to 39 days.

Metagenomic information of pathogens in the plasma

A total of 27 blood samples from 17 included patients were tested by mNGS. Figure 2A demonstrates the relative abundance of pathogens in all the blood samples. Overall, 129 bacterial species, 8 viral species, and 51 fungal species were detected by mNGS. Among them, the top 5 abundant bacterial species were *Parvimonas micra*, *Peptostreptococcus stomatis*, *Klebsiella pneumoniae*, *Prevotella intermedia*, and *Mycolicibacterium iranicum*; the top 3 abundant viral species were human parvovirus B19, human herpesvirus 5, and Torque teno virus; and the top 5 abundant fungal species were *Stemphylium lycopersici*, *Nakaseomyces delphensis*, *Aspergillus niger*, *Pseudozyma hubeiensis*, and *Trichophyton mentagrophytes*. We also calculated the frequency of each identified pathogen, as shown in Figures 2B–D (stratum-specific analyses). *Tyzzerella nexilis* was most frequently detected by mNGS in plasma of patients with CSI in ICU.

Comparison of metagenomic next-generation sequencing and conventional culture method

Among the 27 blood samples, blood culture tests were positive only in three (11.1%) of them, while mNGS indicated 23 (85.2%) positive results (reads more than zero). The number of unique reads of pathogens in mNGS-positive samples ranged from three to 5,409. There were two blood samples with both positive blood culture and mNGS results and three with both negative results. Taking blood culture as the gold standard, the sensitivity and specificity of mNGS were 66.7% and 12.5%, respectively, and the positive predictive value (PPV) and negative predictive value (NPV) were 8.7% and 75.0%, respectively (Table 2). Combining results of blood culture and other cultures (sputum, catheter drainage fluid, and urine) as the gold standard, sensitivity and specificity of mNGS were 86.4% and 20.0%, respectively (Table 2).

According to the different thresholds of read number to determine the result of mNGS (positive/negative), we also drew the receiver operating characteristic (ROC) curve. Figures 3A, B show the data based on blood culture and combined culture,

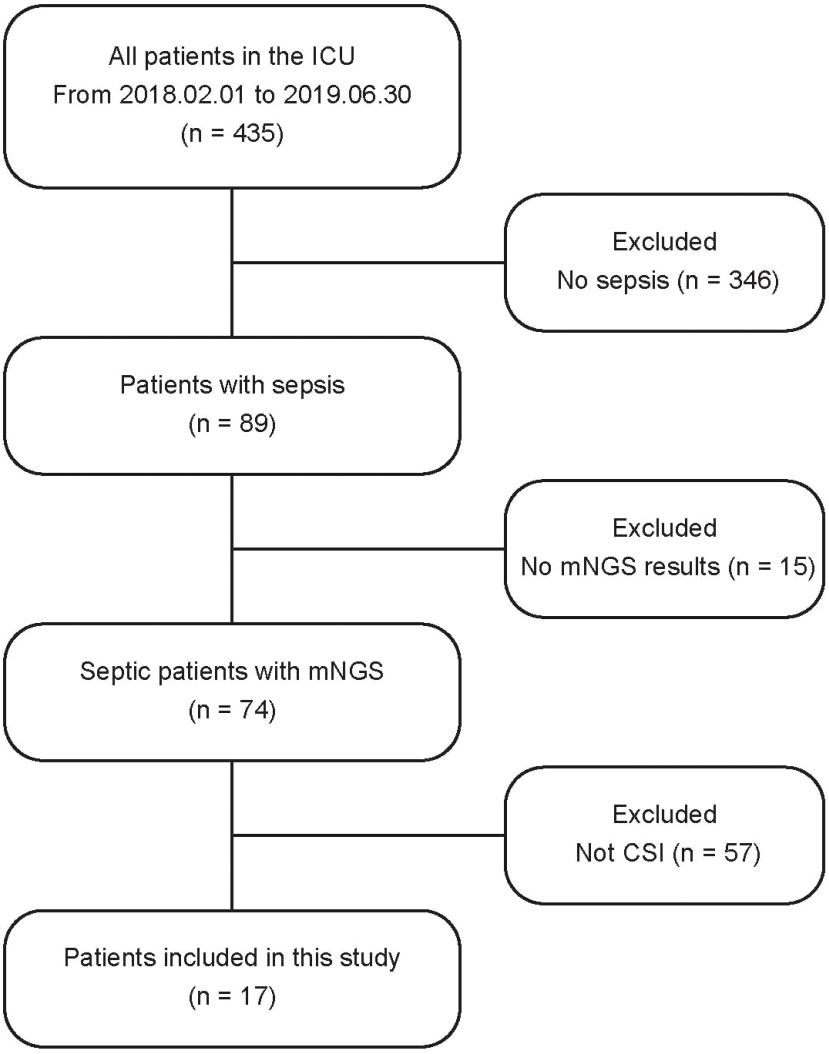

FIGURE 1
Flowchart diagram. The recruiting process of patients in the study.

TABLE 1 Demographics and clinical characteristics of 17 patients enrolled.

Characteristics	
Median age (range) (years)	60 (33–74)
Gender	
Male	13 (76.5%)
Female	4 (23.5%)
Etiologies	
Traumatic	15 (88.24%)
Non-traumatic	2 (11.76%)
Median APACHE II score (range)	19 (8–23)
Median SOFA score (range)	6 (3–12)
Median LOS (range) (day)	19 (6–39)

APACHE, Acute Physiology and Chronic Health Evaluation; SOFA, sequential [sepsis-related] organ failure assessment; LOS, length of stay.

respectively. The area under the curve (AUC) is shown on the graph, which shows low and no significant performance. When the threshold was 10 reads, Youden's index reached the maximum value. Accordingly, we selected 10 reads as the threshold to distinguish the mNGS results in the subsequent analyses. The sensitivity and specificity of mNGS changed to 33.3% and 70.8% based on the new threshold value (Table 2).

Results of metagenomic next-generation sequencing were not correlated with those of conventional culture

To explore the relationship between results of mNGS and those of conventional culture, including blood culture and/or

10.3389/fcimb.2022.948602

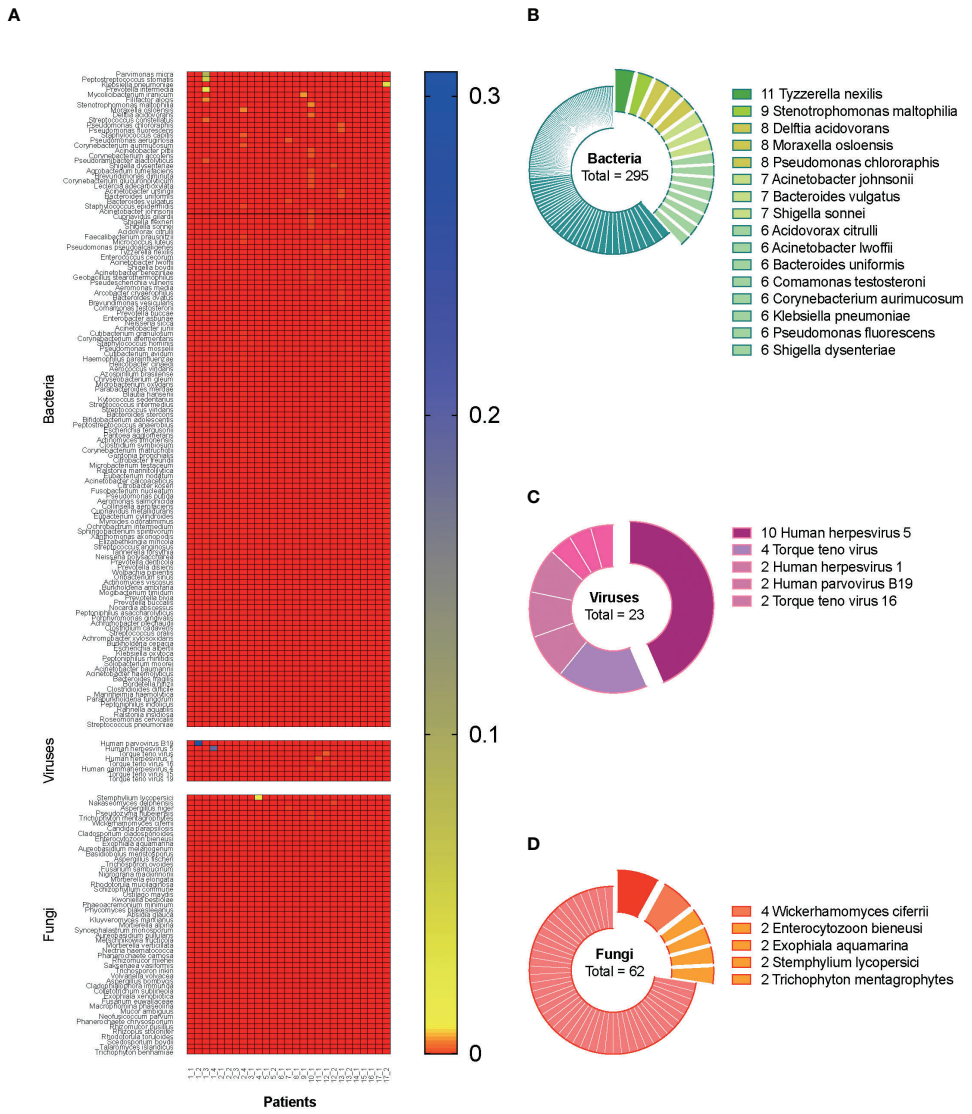

FIGURE 2
Metagenomic information of pathogens in the plasma. A total of 27 blood samples from 17 included septic CSI patients were tested by mNGS. **(A)** Relative abundance of pathogens in all the blood samples. **(B–D)** The frequency of each identified pathogen. Stratum-specific analyses. N = 27. CSI, cervical spine injury; mNGS, metagenomic next-generation sequencing.

other cultures, 10 factors were selected, and correlation analysis was performed. It was out of expectation that mNGS results were not correlated with blood culture or combined culture results (Figure 4). Interestingly, results of conventional culture were negatively correlated with death (Figure 4), suggesting that positive culture results had an indication of poor prognosis of septic CSI patients.

To further explore the underlying factors affecting the prognosis of septic CSI patients in ICU, Cox regression analysis was carried out. As the APACHE II score system was partially coincident with the SOFA score system, only SOFA score on the admission of included patients was selected. Correlation analysis showed that mNGS results were strongly correlated with those of bacteria and viruses, so we chose the results of mNGS-based bacteria (mNGS_BAC) and viruses (mNGS_VIR) to analyze the effects on the prognosis. As shown in Figure 5A, the positive result of blood culture was closely correlated with an increased HR (HR 77.7067, 95%CI 2.860–2641.4595, $p = 0.0155$). By contrast, the positive result of combined culture was correlated with a decreased HR (HR 0.0255, 95%CI 0.0011–0.5714, $p = 0.0207$, Figure 5A). Because of the fact that there were only three positive results of blood

TABLE 2 Diagnostic performance of mNGS.

		Blood culture	Combined culture
mNGS (read 0)	Sensitivity (%)	66.7	86.4
	Specificity (%)	12.5	20.0
	PPV (%)	8.7	82.6
	NPV (%)	75.0	25.0
mNGS (read 10)	Sensitivity (%)	33.3	31.8
	Specificity (%)	70.8	80.0
	PPV (%)	12.5	87.5
	NPV (%)	89.5	21.1

mNGS, metagenomic next-generation sequencing; PPV, positive predictive value; NPV, negative predictive value.

cultures, it was speculated that the septic CSI patients were in the advanced stage when they obtained a positive result of blood culture. In spite of a significant HR of conventional culture being found, neither mNGS_BAC nor mNGS_VIR was shown significantly in the Cox regression analysis, though they appeared to be an increasing trend.

Based on the results of Cox regression analysis, we conducted survival analysis including blood culture and combined culture. The HR for death in the positive results of blood cultures compared with the negative ones was 7.81 (median survival days: 20.0 vs 36.0, $p = 0.0009$, Figure 5B). By contrast, survival probability according to other culture, combined culture, mNGS, mNGS_BAC, and mNGS_VIR were not significantly different (Figures 5C–G, $p = 0.13$, $p = 0.11$, $p = 0.6$, $p = 0.073$, and $p = 0.56$, respectively).

Discussion

Sepsis is a life-threatening disease and the main cause of ICU admission and mortality (Engel et al., 2007; Fleischmann et al., 2016; Singer et al., 2016; Cecconi et al., 2018; Weng et al., 2018). CSI accounts for a majority of patients in ICU with a high mortality (Ahuja et al., 2017; Ghajarzadeh et al., 2019). There is increasing evidence that sepsis remains to be one of the major causes of death in patients with CSI in ICU (Cao et al., 2019; Buzzell et al., 2020; Kamp et al., 2020). Thus, timely diagnosis for sepsis and therapeutic actions targeting sepsis is crucial to improving patient prognosis. In this retrospective study, we illustrated the pathogen abundance and frequency map in blood samples of septic patients with CSI in ICU using mNGS and showed a better diagnostic efficacy of mNGS compared with conventional culture in identifying pathogens. In addition, although there was no correlation between mNGS and survival, we found that septic CSI patients in ICU with a positive blood culture had worse outcomes.

Given the fact that mNGS is a potential tool for broad-range pathogen detection and the non-invasive nature of plasma samples, we tried to identify the causative pathogens in the blood of septic CSI patients in ICU using mNGS. A total of 27 blood samples from 17 included patients in our study were tested by mNGS. Metagenomic results showed a wide spectrum of pathogens, including 129 bacterial species, 8 viral species, and 51 fungal species in total. This finding was in agreement with previous case reports and preliminary studies (Abril et al., 2016; Grumaz et al., 2016; Gosiewski et al., 2017; Pan et al., 2017). Although there were no plasma results from other healthy or non-CSI septic patients as controls, this result provided a reference for clinical antibiotic therapy. It should be important to note that, however, microbial nucleic acids have also been reported in healthy volunteers assessed by mNGS (Gosiewski et al., 2017), raising the issue of potential contamination and the question of the clinical significance of DNA detected in plasma.

Previous evidence has suggested different sensitivities and specificities of mNGS for the identification of different types of

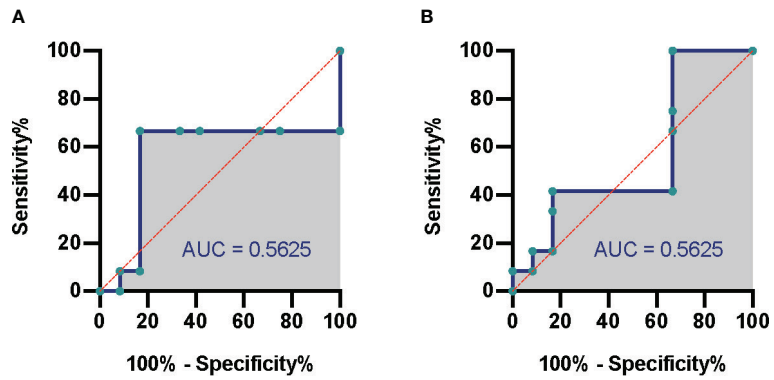

FIGURE 3
Comparison of mNGS and conventional culture method. The ROC of septic CSI patients under different cultural conditions. **(A)** Blood culture. **(B)** Combined culture. N = 27. mNGS, metagenomic next-generation sequencing; ROC, receiver operating characteristic; CSI, cervical spine injury.

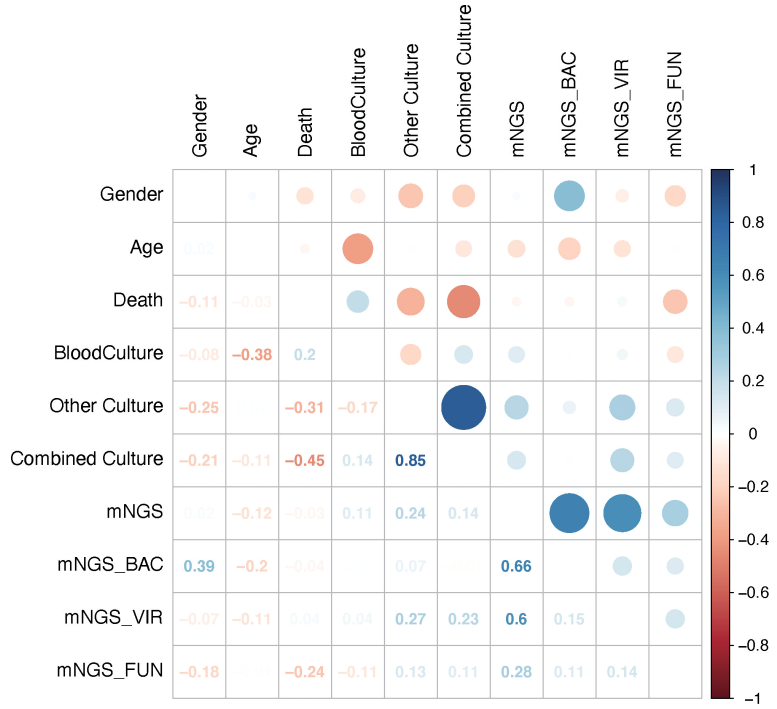

FIGURE 4
Results of mNGS were not correlated with those of conventional culture. The comparison of the mNGS with different cultured conditions. As shown, mNGS results had little correlation with blood or combined culture results. Correlation analysis. N = 27. mNGS, metagenomic next-generation sequencing.

pathogens (bacterial, viral, or fungal), with sensitivity ranging from 36% to 100% and specificity ranging from 76.5% to 87.5% (Parize et al., 2017; Langelier et al., 2018; Li et al., 2018; Miao et al., 2018). In this study, the sensitivity and specificity of mNGS for pathogens detection were relatively low, possibly due to the lower positivity rate of blood culture and the limited scale of samples. Loose positivity criteria for mNGS, defined as the read number of any identified pathogen more than zero, might also result in lower sensitivity. In addition, we did not find a significant correlation between positive results of mNGS and that of conventional culture. Nevertheless, our result suggested that mNGS was superior to conventional culture in recognizing pathogens in blood, with mNGS indicating 85.2% positive results, while blood culture tests were positive only in 11.1% of all the blood samples, which is compatible with a previous report (Blauwkamp et al., 2019). However, when certain organisms were detected *via* mNGS assay, distinguishing a truly positive sample may require a higher organism concentration to be present. Normalizing the detection threshold to background levels can be helpful to establish sample positivity and avoid false-positive calls. One way to achieve this is to divide the number of sequence reads seen in the sample by the number present in negative or no-template controls and then use a threshold for organism detection (Gu et al., 2019). In this case, we also drew the ROC based on the results of blood culture and combined culture. Unfortunately, no noteworthy performance was found in both models.

In addition to comparing the diagnostic efficiency of mNGS, we also analyzed the effect of positive mNGS consequences on the prognosis of septic patients with CSI in ICU. Several attempts have been made to use metagenomic results as a diagnostic and prognostic marker for sepsis outcomes (Dwivedi et al., 2012; Avriel et al., 2014; Jackson Chornenki et al., 2019). However, in the current study, positive results of mNGS had no prognostic effect on the septic CSI patients in ICU. Positive mNGS results were not correlated with prognosis mainly because this was a retrospective study, and we did not use antibiotics specifically based on the results of mNGS. Further study will be focused on evaluating the effect of mNGS-based therapy on prognosis. By contrast, positive blood culture increases the hazard of death of septic CSI patients in ICU, while positive combined culture result was related to a better prognosis. This abnormal phenomenon can be explained, as the septic CSI patients were in the advanced stage when they obtained a positive result from blood culture. When the infection foci were confined to the primary lesion and the pathogens were not detected in the blood, it was still a relatively early stage of infection for the patients, leading to a better prognosis. It was confirmed by the fact that patients had significantly different survival times according to

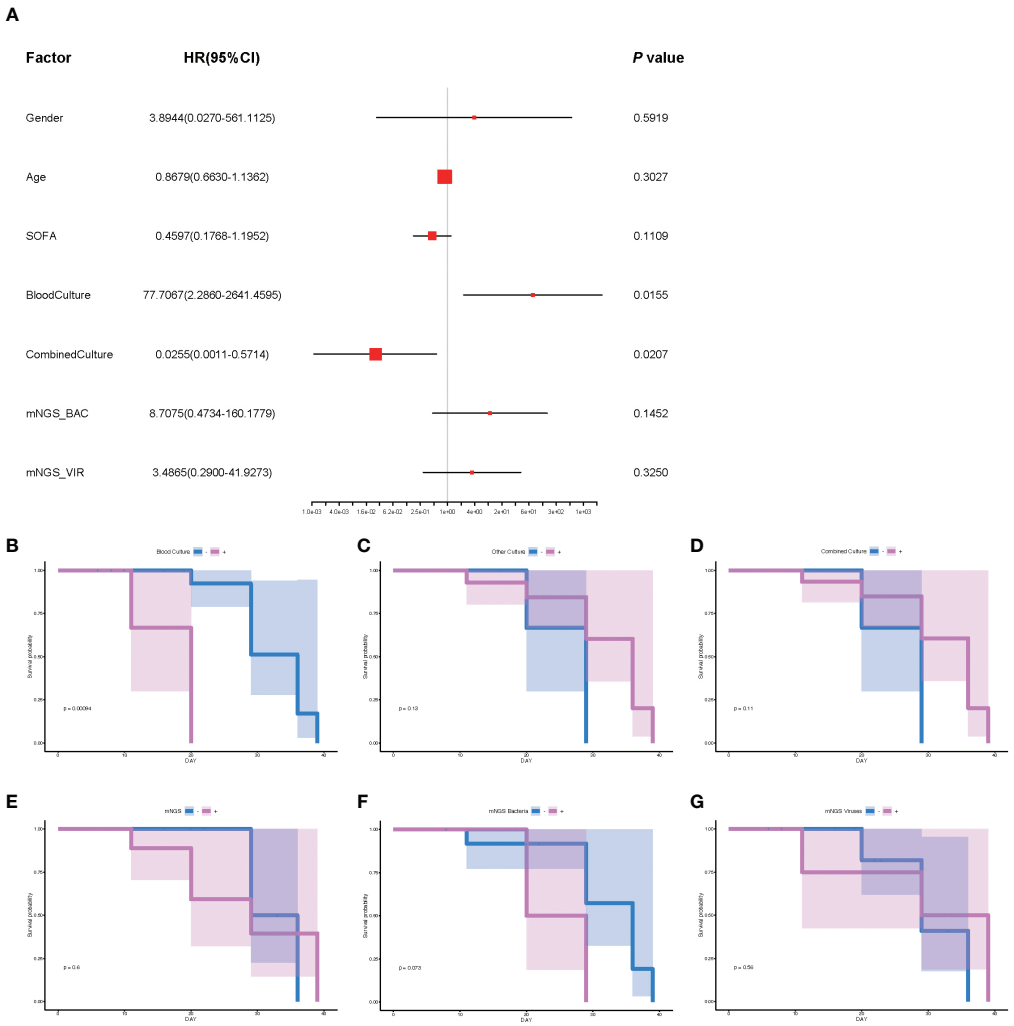

FIGURE 5
The analysis of prognosis based on the results of mNGS_BAC and mNGS_VIR. **(A)** The correlation of different factors with HR. **(B–G)** Survival probability of different cultural conditions and mNGS data. **(B)** Blood culture. **(C)** Other culture. **(D)** Combine culture. **(E)** mNGS. **(F)** mNGS bacteria. **(G)** mNGS viruses. Cox regression analysis for **(A)** and survival analysis for panels B–G. N = 27. HR, hazard ratio; mNGS, metagenomic next-generation sequencing.

the results of blood culture, but not to the results of the combined culture or mNGS, which was demonstrated *via* survival analyses in the current study. Taken together, our results suggested practicing vigilance when treating septic patients with CSI in the ICU when the blood culture is positive. Meanwhile, we could use the mNGS assay when the blood culture is negative to improve sensitivity and reduce the risk of death in advance.

Several limitations exist in the current study. First, this study was retrospective and had a small scale of included cases, which led to a bias of conclusions. Second, the aforementioned lack of targeted use of antibiotics based on the results of mNGS led to an inaccurate evaluation of the effect of mNGS on the prognosis. Third, we lacked mNGS results from non-CSI septic patients or non-septic CSI patients as controls.

In conclusion, our study is the first to apply the mNGS of plasma to evaluate the potential impact for septic patients with CSI in ICU, providing evidence for clinicians to use antibiotics when a CSI case is diagnosed with sepsis. While mNGS holds promise for sepsis diagnosis and management, further clinical study is needed to systemically evaluate the value of mNGS in clinical practice.

Data availability statement

The data presented in the study are deposited in the China National GeneBank DataBase (CNGBdb) repository, accession number CNP0003243.

Ethics statement

This study was reviewed and approved by The Ethical Review Committee of Changzheng Hospital. The patients/participants provided their written informed consent to participate in this study.

Author contributions

YS, DY, and ZY conceived and designed the experiments. JW, LD, and QC performed the experiments, analyzed the data, and wrote the manuscript. They contributed equally and were the co-first authors. LW, JB, JH, XL, TZ, and WS performed confirmation experiments. All authors contributed to the article and approved the submitted version.

Funding

This work is supported by Leading Talent Training in Shanghai Pudong New Area Health System (No. PWRl2018-08), National Natural Science Foundation of China (No. 81872537; 82172183), Project of Clinical Outstanding Clinical Discipline Construction in Shanghai Pudong New Area (No. PWYgy2021-09), Project of Shanghai Municipality Key Medical Specialties Construction (No. ZK2019C08), and Three-year Action Plan for Talent Construction of Changzheng Hospital —Pyramid Talent Project (009).

Conflict of interest

The authors declare that the research was conducted in the absence of any commercial or financial relationships that could be construed as a potential conflict of interest.

Publisher's note

All claims expressed in this article are solely those of the authors and do not necessarily represent those of their affiliated organizations, or those of the publisher, the editors and the reviewers. Any product that may be evaluated in this article, or claim that may be made by its manufacturer, is not guaranteed or endorsed by the publisher.

References

Abril, M. K., Barnett, A. S., Wegermann, K., Fountain, E., Strand, A., Heyman, B. M., et al. (2016). Diagnosis of capnocytophaga canimorsus sepsis by whole-genome next-generation sequencing. *Open Forum Infect. Dis.* 3 (3), ofw144. doi: 10.1093/ofid/ofw144

Ahuja, C. S., Wilson, J. R., Nori, S., Kotter, M. R. N., Druschel, C., Curt, A., et al. (2017). Traumatic spinal cord injury. *Nat. Rev. Dis. Primers* 3, 17018. doi: 10.1038/nrdp.2017.18

Avriel, A., Paryente Wiessman, M., Almog, Y., Perl, Y., Novack, V., Galante, O., et al. (2014). Admission cell free DNA levels predict 28-day mortality in patients with severe sepsis in intensive care. *PloS One* 9 (6), e100514. doi: 10.1371/journal.pone.0100514

Blauwkamp, T. A., Thair, S., Rosen, M. J., Blair, L., Lindner, M. S., Vilfan, I. D., et al. (2019). Analytical and clinical validation of a microbial cell-free DNA sequencing test for infectious disease. *Nat. Microbiol.* 4 (4), 663–674. doi: 10.1038/s41564-018-0349-6

Buchan, B. W., and Ledeboer, N. A. (2014). Emerging technologies for the clinical microbiology laboratory. *Clin. Microbiol. Rev.* 27 (4), 783–822. doi: 10.1128/cmr.00003-14

Buzzell, A., Chamberlain, J. D., Eriks-Hoogland, I., Hug, K., Jordan, X., Schubert, M., et al. (2020). All-cause and cause-specific mortality following non-traumatic spinal cord injury: evidence from a population-based cohort study in Switzerland. *Spinal Cord* 58 (2), 157–164. doi: 10.1038/s41393-019-0361-6

Cao, Y., DiPiro, N., and Krause, J. S. (2019). Health factors and spinal cord injury: a prospective study of risk of cause-specific mortality. *Spinal Cord* 57 (7), 594–602. doi: 10.1038/s41393-019-0264-6

Cecconi, M., Evans, L., Levy, M., and Rhodes, A. (2018). Sepsis and septic shock. *Lancet* 392 (10141), 75–87. doi: 10.1016/s0140-6736(18)30696-2

Chiu, C. Y., and Miller, S. A. (2019). Clinical metagenomics. *Nat. Rev. Genet.* 20 (6), 341–355. doi: 10.1038/s41576-019-0113-7

Dwivedi, D. J., Toltl, L. J., Swystun, L. L., Pogue, J., Liaw, K. L., Weitz, J. I., et al. (2012). Prognostic utility and characterization of cell-free DNA in patients with severe sepsis. *Crit. Care* 16 (4), R151. doi: 10.1186/cc11466

Engel, C., Brunkhorst, F. M., Bone, H. G., Brunkhorst, R., Gerlach, H., Grond, S., et al. (2007). Epidemiology of sepsis in Germany: results from a national prospective multicenter study. *Intensive Care Med.* 33 (4), 606–618. doi: 10.1007/s00134-006-0517-7

Fleischmann, C., Thomas-Rueddel, D. O., Hartmann, M., Hartog, C. S., Welte, T., Heublein, S., et al. (2016). Hospital incidence and mortality rates of sepsis. *Dtsch Arztebl Int.* 113 (10), 159–166. doi: 10.3238/arztebl.2016.0159

Ghajarzadeh, M., Rahimi Foroushani, A., Nedjat, S., Sheikhrezaei, A., and Saberi, H. (2019). Survival analysis in patients with chronic traumatic spinal cord injury. *Iran J. Public Health* 48 (12), 2260–2269.

Gosiewski, T., Ludwig-Galezowska, A. H., Huminska, K., Sroka-Oleksiak, A., Radkowski, P., Salamon, D., et al. (2017). Comprehensive detection and identification of bacterial DNA in the blood of patients with sepsis and healthy volunteers using next-generation sequencing method - the observation of DNAemia. *Eur. J. Clin. Microbiol. Infect. Dis.* 36 (2), 329–336. doi: 10.1007/s10096-016-2805-7

Grumaz, S., Stevens, P., Grumaz, C., Decker, S. O., Weigand, M. A., Hofer, S., et al. (2016). Next-generation sequencing diagnostics of bacteremia in septic patients. *Genome Med.* 8 (1), 73. doi: 10.1186/s13073-016-0326-8

Gu, W., Miller, S., and Chiu, C. Y. (2019). Clinical metagenomic next-generation sequencing for pathogen detection. *Annu. Rev. Pathol.* 14, 319–338. doi: 10.1146/annurev-pathmechdis-012418-012751

Han, D., Li, Z., Li, R., Tan, P., Zhang, R., and Li, J. (2019). mNGS in clinical microbiology laboratories: on the road to maturity. *Crit. Rev. Microbiol.* 45 (5–6), 668–685. doi: 10.1080/1040841x.2019.1681933

Jackson Chornenki, N. L., Coke, R., Kwong, A. C., Dwivedi, D. J., Xu, M. K., McDonald, E., et al. (2019). Comparison of the source and prognostic utility of cfDNA in trauma and sepsis. *Intensive Care Med. Exp.* 7 (1), 29. doi: 10.1186/s40635-019-0251-4

Kamp, O., Jansen, O., Lefering, R., Meindl, R., Waydhas, C., Schildhauer, T. A., et al. (2020). Cervical spinal cord injury shows markedly lower than predicted mortality (>72 hours after multiple trauma) from sepsis and multiple organ failure. *J. Intensive Care Med.* 35 (4), 378–382. doi: 10.1177/0885066617753356

Knaus, W. A., Draper, E. A., Wagner, D. P., and Zimmerman, J. E. (1985). APACHE II: a severity of disease classification system. *Crit. Care Med.* 13 (10), 818–829. doi: 10.1097/00003246-198510000-00009

Langelier, C., Zinter, M. S., Kalantar, K., Yanik, G. A., Christenson, S., O'Donovan, B., et al. (2018). Metagenomic sequencing detects respiratory pathogens in hematopoietic cellular transplant patients. *Am. J. Respir. Crit. Care Med.* 197 (4), 524–528. doi: 10.1164/rccm.201706-1097LE

Li, H., Gao, H., Meng, H., Wang, Q., Li, S., Chen, H., et al. (2018). Detection of pulmonary infectious pathogens from lung biopsy tissues by metagenomic next-generation sequencing. *Front. Cell Infect. Microbiol.* 8. doi: 10.3389/fcimb.2018.00205

Miao, Q., Ma, Y., Wang, Q., Pan, J., Zhang, Y., Jin, W., et al. (2018). Microbiological diagnostic performance of metagenomic next-generation sequencing when applied to clinical practice. *Clin. Infect. Dis.* 67 (suppl_2), S231–s240. doi: 10.1093/cid/ciy693

Pan, W., Ngo, T. T. M., Camunas-Soler, J., Song, C. X., Kowarsky, M., Blumenfeld, Y. J., et al. (2017). Simultaneously monitoring immune response and microbial infections during pregnancy through plasma cfRNA sequencing. *Clin. Chem.* 63 (11), 1695–1704. doi: 10.1373/clinchem.2017.273888

Parize, P., Muth, E., Richaud, C., Gratigny, M., Pilmis, B., Lamamy, A., et al. (2017). Untargeted next-generation sequencing-based first-line diagnosis of infection in immunocompromised adults: a multicentre, blinded, prospective study. *Clin. Microbiol. Infect.* 23 (8), 574.e571–574.e576. doi: 10.1016/j.cmi.2017.02.006

Rudd, K. E., Johnson, S. C., Agesa, K. M., Shackelford, K. A., Tsoi, D., Kievlan, D. R., et al. (2020). Global, regional, and national sepsis incidence and mortality 1990-2017: analysis for the global burden of disease study. *Lancet* 395 (10219), 200–211. doi: 10.1016/s0140-6736(19)32989-7

Singer, M., Deutschman, C. S., Seymour, C. W., Shankar-Hari, M., Annane, D., Bauer, M., et al. (2016). The third international consensus definitions for sepsis and septic shock (Sepsis-3). *Jama* 315 (8), 801–810. doi: 10.1001/jama.2016.0287

Vincent, J. L., Moreno, R., Takala, J., Willatts, S., De Mendonca, A., Bruining, H., et al. (1996). The SOFA (Sepsis-related organ failure assessment) score to describe organ dysfunction/failure. on behalf of the working group on sepsis-related problems of the European society of intensive care medicine. *Intensive Care Med.* 22 (7), 707–710. doi: 10.1007/bf01709751

Weng, L., Zeng, X. Y., Yin, P., Wang, L. J., Wang, C. Y., Jiang, W., et al. (2018). Sepsis-related mortality in China: a descriptive analysis. *Intensive Care Med.* 44 (7), 1071–1080. doi: 10.1007/s00134-018-5203-z

Wilson, M. R., Naccache, S. N., Samayoa, E., Biagtan, M., Bashir, H., Yu, G., et al. (2014). Actionable diagnosis of neuroleptospirosis by next-generation sequencing. *N Engl. J. Med.* 370 (25), 2408–2417. doi: 10.1056/NEJMoa1401268

Wu, J. C., Chen, Y. C., Liu, L., Chen, T. J., Huang, W. C., Cheng, H., et al. (2012). Effects of age, gender, and socio-economic status on the incidence of spinal cord injury: an assessment using the eleven-year comprehensive nationwide database of Taiwan. *J. Neurotrauma* 29 (5), 889–897. doi: 10.1089/neu.2011.1777

frontiers | Frontiers in Cellular and Infection Microbiology

TYPE Original Research
PUBLISHED 14 September 2022
DOI 10.3389/fcimb.2022.933523

OPEN ACCESS

EDITED BY
Steven Gill,
University of Rochester, United States

REVIEWED BY
Matthew Zachariah DeMaere,
iThree Institute, Australia
Yuqing Feng,
China Agricultural University, China
Yuxuan Du,
University of Southern California, United States

*CORRESPONDENCE
Ai-Hua Yin
yinaiwa@vip.126.com
Qiu-Long Yan
qiulongy1988@163.com

†These authors have contributed equally to this work

SPECIALTY SECTION
This article was submitted to Microbiome in Health and Disease, a section of the journal Frontiers in Cellular and Infection Microbiology

RECEIVED 01 May 2022
ACCEPTED 26 August 2022
PUBLISHED 14 September 2022

CITATION
Lv L-J, Li S-H, Wen J-Y, Wang G-Y, Li H, He T-W, Lv Q-B, Xiao M-C, Duan H-L, Chen M-C, Yi Z-T, Yan Q-L and Yin A-H (2022) Deep metagenomic characterization of gut microbial community and function in preeclampsia.
Front. Cell. Infect. Microbiol. 12:933523. doi: 10.3389/fcimb.2022.933523

Deep metagenomic characterization of gut microbial community and function in preeclampsia

Li-Juan Lv[1†], Sheng-Hui Li[2†], Ji-Ying Wen[3], Guang-Yang Wang[4], Hui Li[3], Tian-Wen He[1], Qing-Bo Lv[2], Man-Chun Xiao[4], Hong-Li Duan[3], Min-Chai Chen[1], Zhou-Ting Yi[3], Qiu-Long Yan[4*] and Ai-Hua Yin[1*]

[1]Medical Genetic Center, Guangdong Women and Children Hospital, Guangzhou, China, [2]Puensum Genetech Institute, Wuhan, China, [3]Department of Obstetric, Guangdong Women and Children Hospital, Guangzhou, China, [4]Department of Microbiology, College of Basic Medical Sciences, Dalian Medical University, Dalian, China

Preeclampsia (PE) is a pregnancy complication characterized by severe hypertension and multiple organ damage. Gut microbiota has been linked to PE by previous amplicon sequencing studies. To resolve the PE gut microbiota in a higher taxonomy resolution, we performed shotgun metagenomic sequencing on the fecal samples from 40 early-onset PE and 37 healthy pregnant women. We recovered 1,750 metagenome-assembled genomes (representing 406 species) from the metagenomic dataset and profiled their abundances. We found that PE gut microbiota had enriched in some species belonging to *Blautia*, *Pauljensenia*, *Ruminococcus*, and *Collinsella* and microbial functions such as the bacitracin/lantibiotics transport system, maltooligosaccharide transport system, multidrug efflux pump, and rhamnose transport system. Conversely, the gut microbiome of healthy pregnant women was enriched in species of *Bacteroides* and *Phocaeicola* and microbial functions including the porphyrin and chlorophyll metabolism, pyridoxal-P biosynthesis, riboflavin metabolism, and folate biosynthesis pathway. PE diagnostic potential of gut microbial biomarkers was developed using both species and function profile data. These results will help to explore the relationships between gut bacteria and PE and provide new insights into PE early warning.

KEYWORDS

preeclampsia, gut microbiome, shotgun metagenomic sequencing, pregnancy, microbial dysbiosis, microbial function

Introduction

Preeclampsia (PE) is a complex multi-system disease with maternal hypertension and systemic arteriole spasm as basic pathological changes, leading to the second cause of maternal death worldwide (Brown et al., 2018). In addition to severe complications such as eclampsia, cerebral hemorrhage and multiple organ failure, it can also cause fetal intrauterine growth restriction (FGR), fetal distress, premature delivery, stillbirth, and so on (Ahmadian et al., 2020). It is an important factor in increasing perinatal morbidity and mortality, and a serious burden on patients and families. The etiology of PE is still unknown. It was a widely accepted "two-stage theory" that put forward relative or absolute lack of placental perfusion as the key to the pathogenesis mechanism (Redman, 1991). At present, the disease lacks effective prevention and treatment methods. Termination of pregnancy is usually the final and only effective treatment means, resulting in many iatrogenic preterm births. Therefore, effective diagnosis and treatment methods for preeclampsia are urgently needed.

In recent years, many studies have explored the variability of gut microbiota of PE pregnant women in the late trimester (Lv et al., 2019; Wang et al., 2019; Chang et al., 2020; Chen et al., 2020) and linked the imbalance of the gut microbiome to the pathogenesis of PE (Kell and Kenny, 2016). For example, Wang et al. found that the PE subjects had a reduced diversity of microbial alpha diversity and a substantially different bacterial phylum composition compared with the healthy controls. The fecal microbial gene functions related to lipopolysaccharide (LPS) biosynthesis and LPS concentrations of fecal and plasma were higher in the PE group, indicating the pathogenic potential of gut bacterial LPS (Wang et al., 2019). Our previous study revealed that *Blautia, Ruminococcus, Bilophila*, and *Fusobacterium* were significantly enriched in the antepartum gut samples of PE patients compared to healthy controls (Lv et al., 2019). Chang et al. demonstrated that short-chain fatty acids accompanying changes in the gut microbiome could contribute to the development of hypertension in patients with PE (Chang et al., 2020). Also, Chen et al. found that the PE clinical manifestations could be induced in mice models by fecal microbiota transplantation from PE patients, further suggesting the incidence of PE was related to gut microbiota (Chen et al., 2020). However, these amplicon-based studies using the bacterial 16S rRNA genes could only be accurate to the genus level, which made the gut microbiota of PE not fully understood. As a result, no specifically probiotic or pathogenic candidate strains have yet been identified, which limits the exploration of a mechanism or validation of PE in an animal mode.

Herein, we reconstructed a total of 1,750 bacterial MAGs from the shotgun metagenomic sequencing data of the fecal samples. We found that the gut microbiome structure of PE pregnant women was significantly different from that of normal pregnant women. Exactly, 6 members of *Blautia*, 5 members of *Pauljensenia*, 5 members of *Ruminococcus*, and *Fusobacterium ulcerans* were significantly enriched in the feces of PE patients. In contrast, 14 members of Bacteroidaceae, *Akkermansia muciniphila*, and *Bilophila wadsworthia* were significantly reduced in PE pregnant women. The functional signatures of PE-associated gut bacteria were also analyzed, which could provide us with clues to explore their deep pathogenic mechanism. We also tested the diagnostic potential of the gut microbial biomarkers in predicting PE status using a random forest model.

Methods

Ethics statement

This cohort study was approved by the Ethics Committee of Guangdong Women and Children Hospital (a tertiary referral hospital specializing in maternal and child health) in southern China, and informed consent was obtained from all participants in accordance with the Declaration of Helsinki (Human, 2001; Idanpaan-Heikkila, 2001).

Subject recruitment

This study assessed pregnant women receiving pregnancy care at Guangdong Women and Children Hospital. Inclusion criteria were pregnant women with PE and healthy pregnant women who delivered at the same time without pregnancy complications. Exclusion criteria included multiple pregnancies and pregnancy complications such as fetal malformation, gestational diabetes, intrahepatic cholestasis syndrome, or chorioamnionitis. Preexisting clinical disorders, such as diabetes, hypertension, malignant tumors, and infectious diseases were also excluded. In total, 40 pregnant women diagnosed with severe PE (PE group) and 37 normotensive women (HC group) were included in this study. Normal pregnant women in the third trimester were matched with the PE women for age, gestational age, and parity. PE was diagnosed according to the guideline from the American College of Obstetricians and Gynecologists Croke, L. (2019). PE was defined after the 20th week of gestation as blood pressure (BP) at least 140/90 mmHg on two occasions for at least 4h with previously normal BP; proteinuria at least 300 mg/24-h urine or more collection. In the absence of proteinuria, new onset of any of the following: platelet count less than 100,000 $\times 10^9$/L; serum creatinine concentration more than 1.1 mg/dL or a doubling in the absence of other renal diseases; elevated blood concentrations of liver transaminases to twice normal concentration; pulmonary edema and cerebral or visual

symptoms. The clinical biochemistry parameters of all participants were measured according to the methods described in our previous study (Lv et al., 2019). The detailed information of the clinical and phenotypic characteristics of the participants are summarized in Table 1.

Sample collection, DNA extraction and shotgun metagenomic sequencing

All fecal samples were collected in the third trimester. Fecal samples were collected with sterile feces collection containers and stored rapidly at -80̊ until use. The total DNA of fecal samples (170mg per sample) was extracted using the Tiangen fecal DNA extraction kit (Tiangen, China) according to the manufacturer's instructions. DNA concentration and purity were determined by NanoDrop2000 and Qubit 4.0. Total DNA was fragmented using Covaris M220 (Gene Company Limited, China). The sequencing libraries were prepared using the TruSeq DNA sample prep kit (Illumina, United States). Paired-end shotgun metagenomic sequencing was performed based on the Illumina NovaSeq platform (Novogene Co. Ltd, China), which generated 2 × 150 bp paired-end reads for further analyses. Initial base calling of the metagenomic dataset was performed based on the system default parameters under the sequencing platform.

Bioinformatic analyses

Raw metagenomic sequencing reads were processed for quality controls using fastp (version 0.23.0) (Chen et al., 2018) with parameters "-q 20 -u 30 -n 5 -y -Y 30 -g -x -l 90 -w 20". Low quality (>45 bases with quality score<20, or >5 'N' bases), low complexity, and adapter-containing reads were removed, and the remaining reads were trimmed at the tails for low quality (<Q20) or 'N' bases. Human genomic reads were removed *via* mapping to the reference human genome (GRCh38) using Bowtie2 (version 2.4.4) (Langmead and Salzberg, 2012) with default parameters in the "–end-to-end –fast" mode.

High-quality clean reads were used for *de novo* assembly *via* MEGAHIT (v1.2.9) (Li et al., 2015) with a broad range of k-mer sizes (–k-list 21,41,61,81,101,121,141). Assembled contigs (minimum length threshold 2,000 bp) were binned using MetaBAT 2 (version 2.12.1) (Kang et al., 2019) with default parameters. Only raw bins with a total size >200 kbp were kept for further analyses. The sequencing depth of bins was calculated by mapping the high-quality reads back to the bins with Bowtie2 (version 2.4.4) (Langmead and Salzberg, 2012) based on the formula: $Depth = \frac{Total\_mapped\_reads \times Average\_length\_of\_reads}{Total\_length\_of\_the\_bin}$ .Taxonomic classification of the bins was realized based on the GTDB-Tk toolkit (v1.4.0) (Chaumeil et al., 2019) *via* assigning the sequences of each bin to the Genome Taxonomy Database (version r95) (Parks et al., 2020) with default parameters. The taxonomic name of the bins was manually modified to accord with traditional nomenclatures following the national center for biotechnology information (NCBI) taxonomy. To increase the genomic completeness of bins, in each sample, raw bins were merged if they had approximately equal sequencing depth (± 10% between each other) and G+C content (± 0.02 between each other) and had an identical taxonomic assignment at the species level.

The quality of MAGs was estimated with CheckM (v1.1.3) (Parks et al., 2015) using the *lineage_wf* workflow. The definition of high- and medium-quality MAGs was based on the minimum information about a metagenome-assembled genome (MIMAG) standards (Bowers et al., 2017) (high: ≥90% completeness and<5% contamination; medium: ≥70% completeness and<5% contamination). And the quality score was defined as "QS = completeness – 5 × contamination", following Parks et al. (2017). All high- and medium-quality MAGs with quality score >60 were clustered at the nucleotide level by dRep (v2.2.3) (Olm et al., 2017), for which the MAGs sharing >95% average nucleotide identity (ANI) were treated as redundancies. A MAG with the highest QS was chosen as the representative MAG of each cluster (referred to as "species"). Finally, the high-

TABLE 1 Basic characteristics of the preeclampsia patients and healthy controls included in this study.

	Preeclampsia (n = 40)	Healthy control (n = 37)	*P*-value
Age (y)	31.4 ± 5.0	30.0 ± 4.1	0.178
Gestational age (day)	246 ± 25	273 ± 11	$3.8x10^{-8}$
Pre-pregnancy BMI (kg/m^2)	21.7 ± 3.3	20.5 ± 3.2	0.190
Current BMI	26.6 ± 3.9	26.0 ± 3.0	0.529
SBP (mmHg)	147.6 ± 22.0	114.2 ± 10.6	$1.6x10^{-8}$
DBP (mmHg)	92.8 ± 15.1	68.6 ± 8.9	$2.2x10^{-8}$
GLU (mmol/L)	4.41 ± 0.89	4.27 ± 0.25	0.592
% HbA1c	5.15 ± 0.73	4.99 ± 0.45	0.435

The data for preeclampsia patients and healthy controls were presented as mean ± SD. *P*-values were calculated by Student's *t*-test. SBP, systolic blood pressure; DBP, diastolic blood pressure; GLU, fasting blood glucose.

quality sequencing reads of each sample were mapped against the nonredundant MAG catalog using Bowtie2 (version 2.4.4) (Langmead and Salzberg, 2012) (default parameters in the "–end-to-end –fast" mode) to generate the relative abundance of these MAGs. For the taxonomic profiles at the phylum, class, order, family, and genera levels, we summed the relative abundance of MAGs from the same taxon to yield the abundance of that taxon. A phylogenetic tree of MAGs was built using PhyloPhlAn (version 3.0.58) (Asnicar et al., 2020) and visualized in iTOL (v4) (Letunic and Bork, 2019).

Ab initio microbial genes were identified from the contigs of each MAG using Prodigal (v2.6.3) (Hyatt et al., 2010). The KEGG (The Kyoto Encyclopedia of Genes and Genomes) database (downloaded in June 2021) was used for functional annotation of genes using the BlastKOALA algorithm (Kanehisa et al., 2016). Each protein was assigned a KEGG orthologue (KO) on the basis of the best-hit gene in the database (e-value<1e-10 and covering >50% of the protein length). KOs were assigned into pathways or modules based on the KEGG website (https://www.kegg.jp). The abundance of a functional category (KO, pathway, or module) was calculated from the summation of the relative abundance of its corresponding genes.

Statistical analyses

Statistical analyses were implemented on the R 4.0.1 platform. Principal coordinate analysis (PCoA) was performed with the R *vegan* package, based on the Bray-Curtis dissimilarly, and visualized *via* the R *ade4* package. Permutational multivariate analysis of variance (PERMANOVA, also known as *adonis* analysis) was realized with the R vegan package, and the *adonis P*-value was generated based on 1,000 permutations. Mantel test was performed using the R *ade4* package. Random forest models were analyzed with the R *randomForest* package (1,000 trees). The performance of the predictive model was evaluated using receiver operator characteristic (ROC) analysis which was realized with R *pROC* package. The *q* value was used to evaluate the false discovery rate (FDR) for correction of multiple comparisons and was calculated using the R *fdrtool* package based on the Benjamin-Hochberg method (Strimmer, 2008).

Results

Subjects and construction of metagenome-assembled genomes

To uncover the gut microbial characteristics of PE, we recruited 40 pregnant women with early-onset PE and 37 healthy pregnant women and collected their fecal samples for metagenomic analyses. Patients and controls were matched in their age, pre-pregnancy BMI, and current BMI (Table 1). On average, the gestational age at the sampling time point of the PE patients was approximately 4 weeks less than the healthy controls (35w+1d vs. 39w, $p<0.001$). For the clinical parameters, the systolic blood pressure (SBP) and diastolic blood pressure (DBP) of patients were significantly higher than those of healthy controls, consistent with the clinical feature of PE (Lv et al., 2019). The fasting glucose level and % HbA1c (glycosylated hemoglobin) were approached between two cohorts.

We performed deep shotgun metagenomic sequencing of 77 fecal samples, obtaining a total of 781.0 Gb of high-quality non-human data (on average, 10.1 Gb per sample; Table S1) for analysis. To investigate the gut microbiome at the species and strain levels, we reconstructed a total of 1,750 MAGs from the fecal metagenomes using a recently developed method (Almeida et al., 2019). The genome size of MAGs ranged from 1.07 to 6.63 Mb (on average, 2.51 Mb), with N50 length ranging from 4.2 to 106.1 kb (on average, 66.0 kb; Table S2). Based on the MIMAG standard (Bowers et al., 2017), 59.5% (1,042/1,750) MAGs were high-quality microbial genomes (completeness ≥90%, contamination<5%), 37.9% (663/1,750) MAGs were medium-quality genomes (completeness 70-90%, contamination<5%, and quality score ≥60), while the remaining 2.6% (45/1,750) MAGs were low-quality genomes with completeness 50-70% and contamination 5%.

Based on the genomic similarity threshold (ANI 95%) at the prokaryotic species level (Jain et al., 2018), the 1,750 MAGs were clustered into 406 species-level bins (referred to as "species" hereinafter). For each species, we chose a MAG as the representation of the species based on the highest quality. The phylogenetic tree and the summary of taxonomic assignment of 406 species were shown in Figure 1, and the detailed information of them was provided in Table S3. The species were assigned into 7 bacterial phyla (consisting of 405 species) and 1 archaeal phylum (1 species). The major phyla of all species included Firmicutes (consisting of 282 species), Actinobacteria (58 species), and Bacteroidetes (43 species). At the family level, Lachnospiraceae (93 species), Oscillospiraceae (33 species), Ruminococcaceae (26 species), Bacteroidaceae (25 species), Eggerthellaceae (22 species), and Acutalibacteraceae (Parks et al., 2015) were dominant families of the species catalogue. Notably, only 47.2% (192/406) of the species could be assigned into known species, whereas the others were uncultivated species in the human gut.

Gut microbiome diversity and overall structure in relation to PE

To explore the alteration of diversity and structure in the PE gut microbiome, we profiled the composition of 406 gut species of 77 fecal metagenomes and compared it between the PE

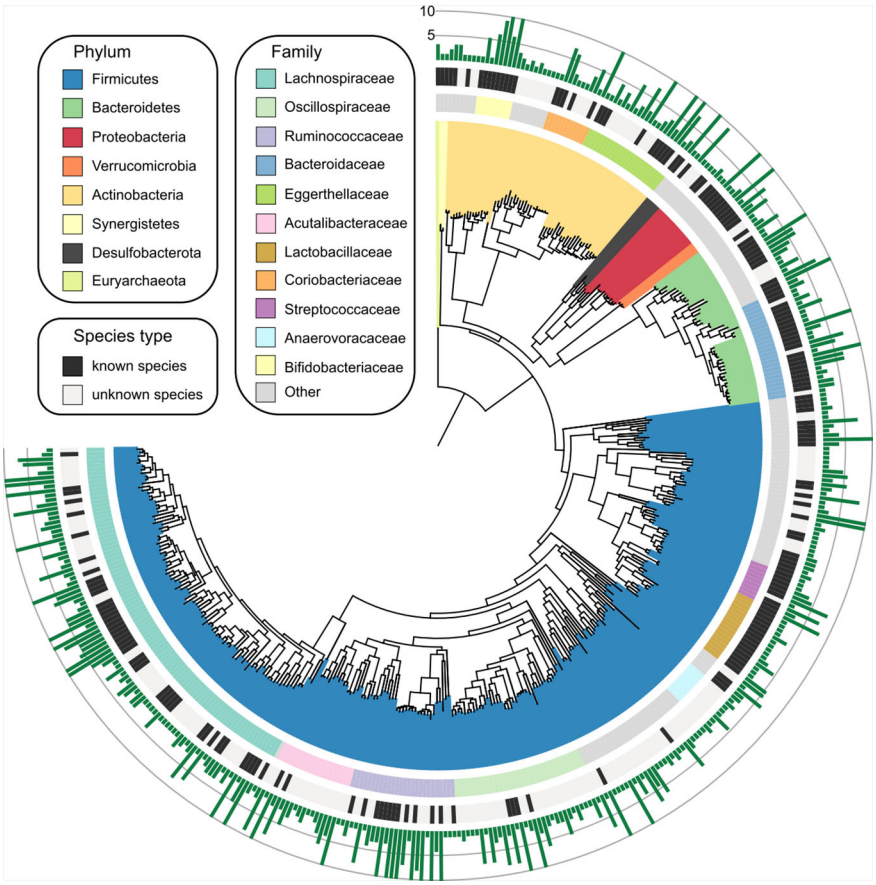

FIGURE 1
Genome-wide representation of 406 prokaryotic species. The innermost circle: phylogenetic tree analysis of 406 species based on their genome sequences. The colors in the tree indicate the phylum-level taxonomic assignment of the species. Circle 2: taxonomic assignment of the species at the family level. Circle 3: the species that could be assigned into known species are labeled in black, and the remaining species are uncultivated. Outermost circle, the number of MAGs for each species. Species with more than 10 MAGs were cropped into 10 for visual clarity, and the detailed information of all species was listed in Table S3.

patients and healthy controls. Rarefaction analysis showed that, under nearly ten samples in PE and control group, the rarefaction curve is approximately saturated (Figure 2A). We then used the Shannon diversity index and Simpson index to assess the microbial richness and evenness at the species level. No significant difference was found in these indexes between the two cohorts (Figure 2B), suggesting that the PE doesn't impact the microbial diversity in the gut microbiome. Next, PCoA analysis based on the Bray-Curtis distance revealed a visible alteration of the overall gut microbial structure between PE patients and the control group (Figure 2C). In addition, PERMANOVA analysis using the distance matrix showed that the PE-status explained 1.4% of microbial variations (permutated p=0.005). As a comparison, the subjects' clinical parameters, including age, pre-pregnancy, current BMI, gestational age, fasting glucose, and %HbA1c, didn't significantly impact the overall microbial variations (Figure 2D). Also, two PE-related clinical indexes, SBP and DBP, significantly acted on the gut microbiota. These results suggested that PE patients undergo profound changes in their gut microbiome.

Identification of PE-associated microbial families and species

We compared the gut microbial composition of PE patients and healthy controls at the family level. Lachnospiraceae, Bifidobacteriaceae, Ruminococcaceae, Enterobacteriaceae, Bacteroidaceae, Coriobacteriaceae, and Eggerthellaceae were the most dominant families, with an accumulative relative abundance of over 81.3% in all analyzed samples (Figure 3A). Of these families, Lachnospiraceae (q=0.026) and Coriobacteriaceae (q=0.048) were significantly enriched in the

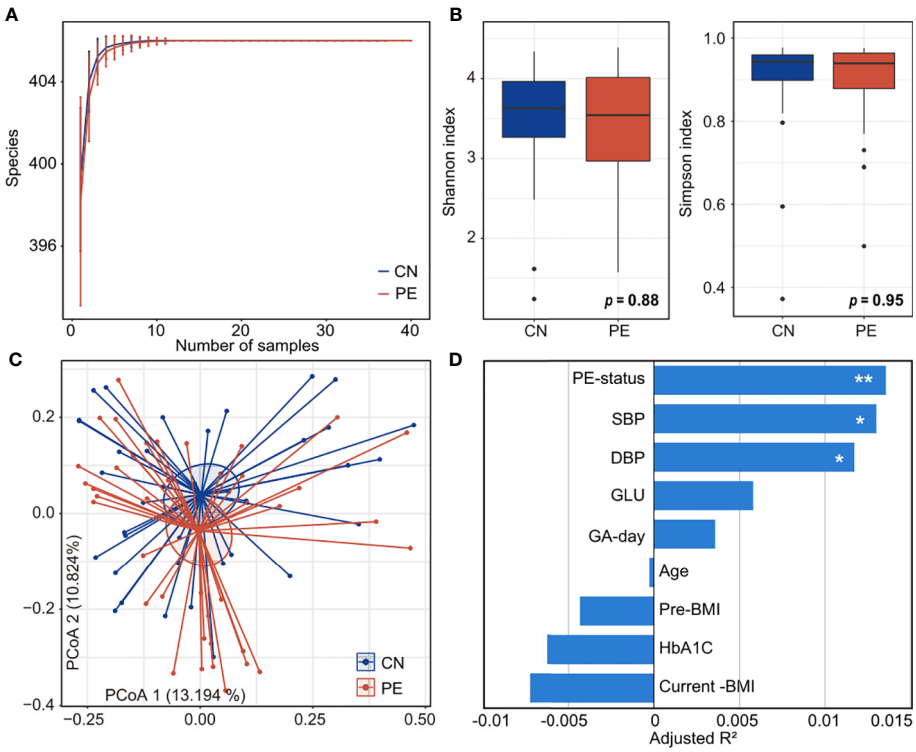

FIGURE 2
Comparison of microbial diversity and structure in PE patients and healthy controls. **(A)** Rarefaction curve analysis of the number of observed species in two groups. The number of species in different groups is calculated based on a randomly selected specific number of samples with 30 replacements, and the median and quartile values are shown. **(B)** Boxplot shows the Shannon and Simpson diversity indexes of gut microbiota that differ among the two groups. Boxes represent the interquartile range between the first and third quartiles and median (internal line); whiskers denote the lowest and highest values within 1.5 times the range of the first and third quartiles, respectively; and nodes represent outliers beyond the whiskers. **(C)** PCoA analysis of Bray-Curtis distance based on the composition of gut microbiota, revealing the separation between the PE patients and healthy controls. The location of samples (represented by nodes) in the first two principal coordinates is shown. Lines connect samples in the same group, and circles cover samples near the center of gravity for each group. **(D)** PERMANOVA analysis showing the effect size of phenotype indexes that contribute to the variance of the overall gut microbiome. Bar plots indicate the explained variation (adjusted R^2) of each factor. *Adonis* test: *, permutated $p<0.05$; **, permutated $p<0.01$. SBP, systolic blood pressure; DBP, diastolic blood pressure; GLU, fasting blood glucose; GA-day, gestational age (day); Pre-BMI, pre-pregnancy body mass index.

gut microbiota of PE patients compared with those of the healthy controls, while Bacteroidaceae ($q<0.001$) were marked depleted in the PE patients (Figure 3B).

At the species level, 74 of 406 species were identified as PE-associated species with significant differences in relative abundance between two cohorts (Wilcoxon rank-sum test, $p<0.05$; corresponding to FDR 12.6%; Table S4). 39 of these species were more abundant in the gut microbiota of PE patients, while 35 were enriched in the healthy controls. The PE-enriched species included 7 members of *Blautia* (unknown at the species level), 5 members of *Pauljensenia* (containing *P. bouchesdurhonensis* and 4 uncultivated species), 5 members of *Ruminococcus* (containing R. gnavus and 4 uncultivated species), *Fusobacterium ulcerans*, and others (Figure 3C). Consistent with the findings at the family level, the control-enriched species included 14 members of Bacteroidaceae, containing 7 *Bacteroides* spp., 4 *Phocaeicola* spp., a *Prevotella bivia*, a *Paraprevotella clara*, and a *Barnesiella intestinihominis* species. Also, an *Akkermansia muciniphila* species and a *Bilophila wadsworthia* species were enriched in the gut microbiota of healthy controls. Of note, several phylogenetically closely related species showed an opposite tendency between PE patients and healthy controls, such as *Phocaeicola coprophilus/sartorii* vs. *Phocaeicola plebeius/vulgatus/barnesiae/dorei* and *Paraprevotella xylaniphila* vs. *Paraprevotella clara* (Figure 3C), suggesting that their difference in functions may relate to PE.

Identification of PE-associated functional signatures

In order to describe the functional characteristics of the PE microbiome, we annotated the functions of 406 species *via* the KEGG database (Kanehisa et al., 2017) and profiled the functions of

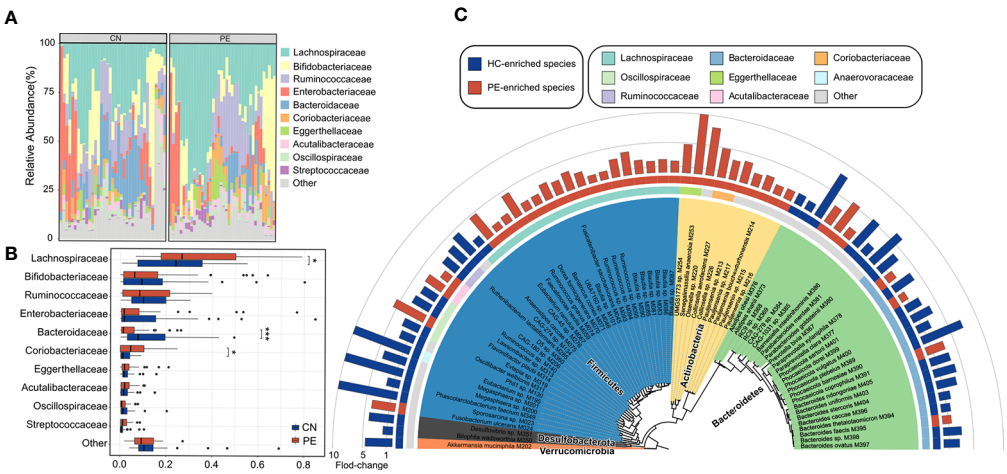

FIGURE 3
Family- and species-level alteration of the gut microbiota in PE patients. **(A)** Composition of gut microbiota at the family level. **(B)** Boxplot shows the dominant families of the gut microbiota when compared between the PE patients and healthy controls. **(C)** Detailed information of 74 species that differed in abundance between the gut microbiota of PE patients and healthy controls. Innermost circle, phylogenetic tree analysis of 74 PE-associated species based on their genome sequences. The colors in the tree indicate the phylum-level taxonomic assignment of the species. Circle 2: taxonomic assignment of the species at the family level. Circle 3: enrichment direction of the species. Red and blue label the species that enriched in the PE patients and controls, respectively. Outermost circle: barplot shows the fold changes of species abundance in PE patients compared with that in healthy subjects.

all fecal samples. A total of 7,399 KOs and 679 KEGG modules were involved. Similar to the aforementioned taxonomic composition, the overall functional capacity of PE patients also changed considerably compared to that of the healthy controls (effect size of KOs = 3.4%, PERMANOVA p=0.023; effect size of modules = 4.7%, PERMANOVA p=0.006; Figures 4A, B). There were significant differences in the relative abundance of 618 KEGG orthologs (KOs) and 107 modules between the patient and control group (Wilcoxon rank-sum test, q<0.05; Figures 4C, D). 115 and 503 KOs were enriched in the gut microbiota of PE patients and healthy controls, respectively. The HC-enriched KOs were frequently involved in the enzymes of core pathways including energy metabolism, amino acid metabolism, carbohydrate metabolism, glycan biosynthesis and metabolism, and lipid metabolism; while the PE-enriched KOs usually participated in functions such as genetic information processing, membrane transport, and signaling and cellular processes (Table S5). We especially focused on the PE-associated KOs involved in the membrane transport and cofactors/vitamins metabolism pathways. The PE-enriched KOs belonging to the cofactors and vitamins metabolism pathway were mainly composed of cobalamin biosynthesis (containing 5 KOs) and molybdenum metabolism (3 KOs), on the other hand, the HC-enriched KOs of cofactors/vitamins metabolism pathway were related to folate biosynthesis (containing 7 KOs), porphyrin and chlorophyll metabolism (6 KOs), pyridoxal-P (vitamin B6) biosynthesis (4 KOs), riboflavin metabolism (4 KOs), and others (Figure 4E). The PE-enriched KOs of the membrane transport pathway contained the transport systems of rhamnose (containing 4 KOs), bacitracin/lantibiotics (4 KOs), molybdate (3 KOs), maltooligosaccharide (3 KOs), lysine (3 KOs), and multidrug efflux pump (2 KOs), while the HC-enriched KOs of membrane transport pathway were dominated by type III secretion (containing 14 KOs), lipopolysaccharide export system (3 KOs), and phospholipid/cholesterol/gamma-HCH transport system (3 KOs). Moreover, we quantified the contribution of 74 PE-associated species on these functions, based on the functional configuration information of the species (Figure 5). This analysis connected the PE-associated species and functions and led to several notable findings. For example, the enzymes of the bacitracin/lantibiotics transport system were mainly encoded by PE-enriched *Collinsella* and *Blautia* species, and the enzymes of rhamnose transport system were encoded by PE-enriched *Blautia* and *Pauljensenia* species. In contrast, functions of porphyrin and chlorophyll metabolism, pyridoxal-P biosynthesis, riboflavin metabolism, and folate biosynthesis were dominantly encoded by the members of *Bacteroides* and *Phocaeicola* that were both more abundant in the gut microbiota of HC subjects.

Diagnostic potential of gut microbial biomarkers

Finally, we used the random forest regression model to evaluate the performance of the gut microbiome in identifying PE status. A random forest model based on the gut species profile obtained the discriminatory power of the area under the

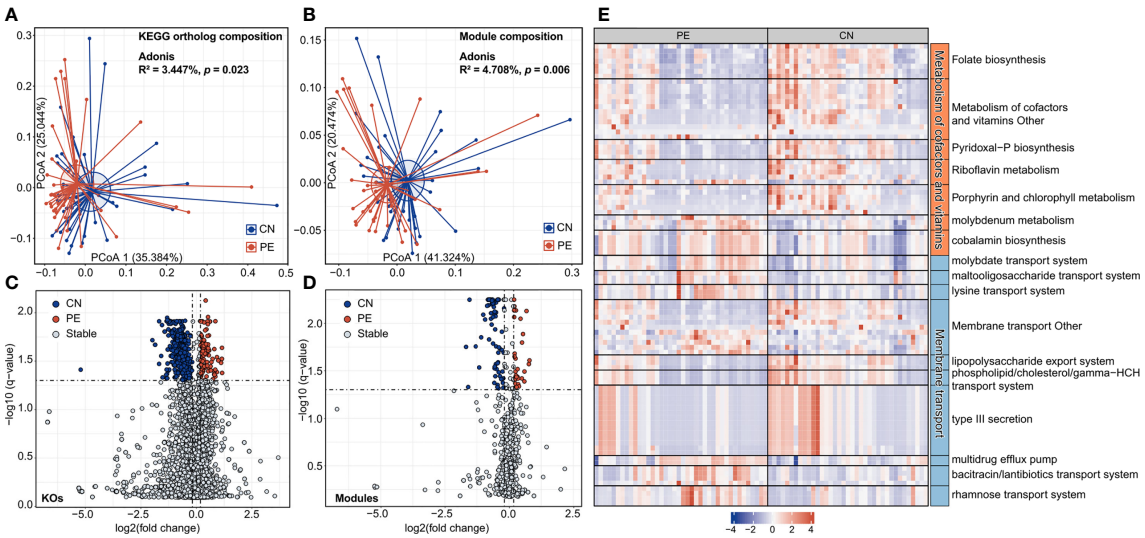

FIGURE 4
Functional comparison of the gut microbiome. **(A, B)** PCoA analysis of Bray-Curtis distance based on the functional composition of gut microbiota at the KO **(A)** and module **(B)** levels. The location of samples (represented by nodes) in the first two principal coordinates is shown. Lines connect samples in the same group, and circles cover samples near the center of gravity for each group. **(C, D)** Volcano plots show the fold change vs. *q*-values for the KOs **(C)** and modules **(D)**. The X-axis shows the ratio (log2 transformed) of function abundance in PE patients compared with that in healthy controls. The Y-axis shows the *q*-value (-log10 transformed) of a function. The functions that were enriched in PE and control subjects are shown in red and blue points, respectively. **(E)** A heatmap showing the abundance of PE-associated KOs involved in the metabolism of cofactors and vitamins and membrane transport pathways. Each column represents an individual and each row represents a KO. The pathway categories of the KOs are grouped and the detailed information of these KOs are shown in Table S5.

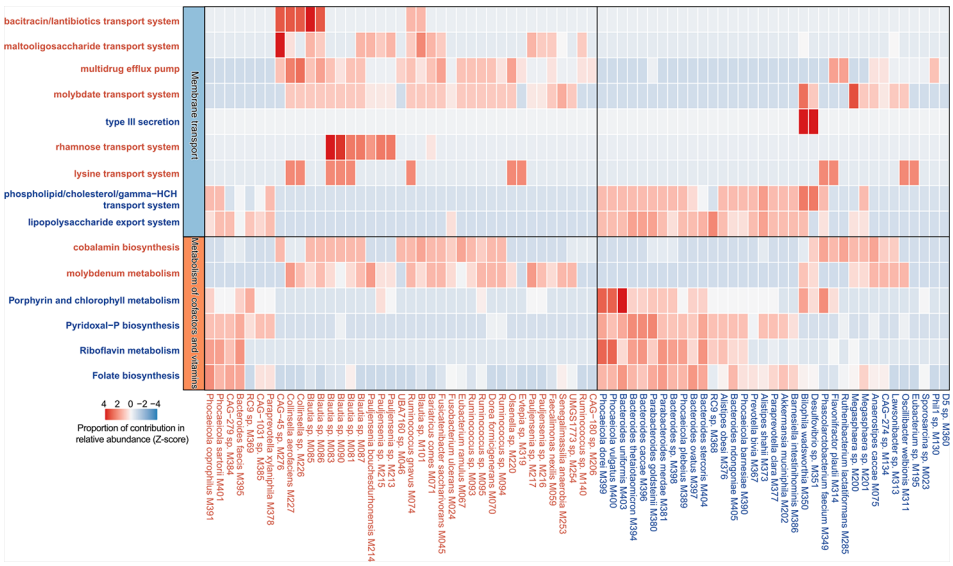

FIGURE 5
Contribution of species on the abundance of functional categories. A heatmap showing the proportional contribution of 74 PE-associated species on the abundance of 15 functional categories shown in Figure 4E. The species that were enriched in the gut microbiota of PE patients and healthy controls are labeled in red and blue, respectively.

receiver operating characteristic curve (AUC) of 0.805 (95% confidence interval [CI] 0.705–0.906; Figure 6A). Several PE-enriched species, including *Olsenella* sp. M220, *Ruminococcus* sp. M094, *Blautia* sp. M090, and *Senegalimassilia anaerobia* M253, as well as several control-enriched species, including *Flavonifractor plautii* M314, *Bacteroides uniformis* M403, and *Bacteroides* sp. M398, featured the highest score for the discrimination of PE patients and healthy controls (Figure 6B). Likewise, a model based on the KO profile obtained the discriminatory power of AUC of 0.764 (95% CI 0.653–0.874; Figure 6C). Several PE-enriched KOs, including K02526 (2-keto-3-deoxygluconate permease), K13954 (alcohol dehydrogenase), and K12511 (tight adherence protein), as well as several control-enriched KOs, including K01241 (AMP nucleosidase), K03404 (magnesium chelatase), K01425 (glutaminase), and K05369 (dihydrobiliverdin/ferredoxin oxidoreductase), featured the highest discrimination score in the model (Figure 6D).

Discussion

Although a series of 16S rRNA gene-based studies have uncovered the relationships between gut microbiota and PE (Lv et al., 2019; Wang et al., 2019; Chang et al., 2020; Chen et al., 2020), deep metagenomic characterization of the PE gut microbiota has still not been reported. In this study, 406 species (as identified from representative MAGs), including 214 human gut uncultivated species indicated the advantages of whole metagenome methods and extended the existing database. More accurate PE-associated bacterial species and functional characteristics of the PE microbiome were identified. For example, PE-enriched multiple strains of genus *Collinsella*, *Pauljensenia*, *Ruminococcus* and *Blautia*, and HC-enriched multiple strains of genus *Bacteroides*, *Phocaeicola*, and *Parabacteroides*, were the potential key strains and typical representative among them (Figure 3C). The enzymes of the

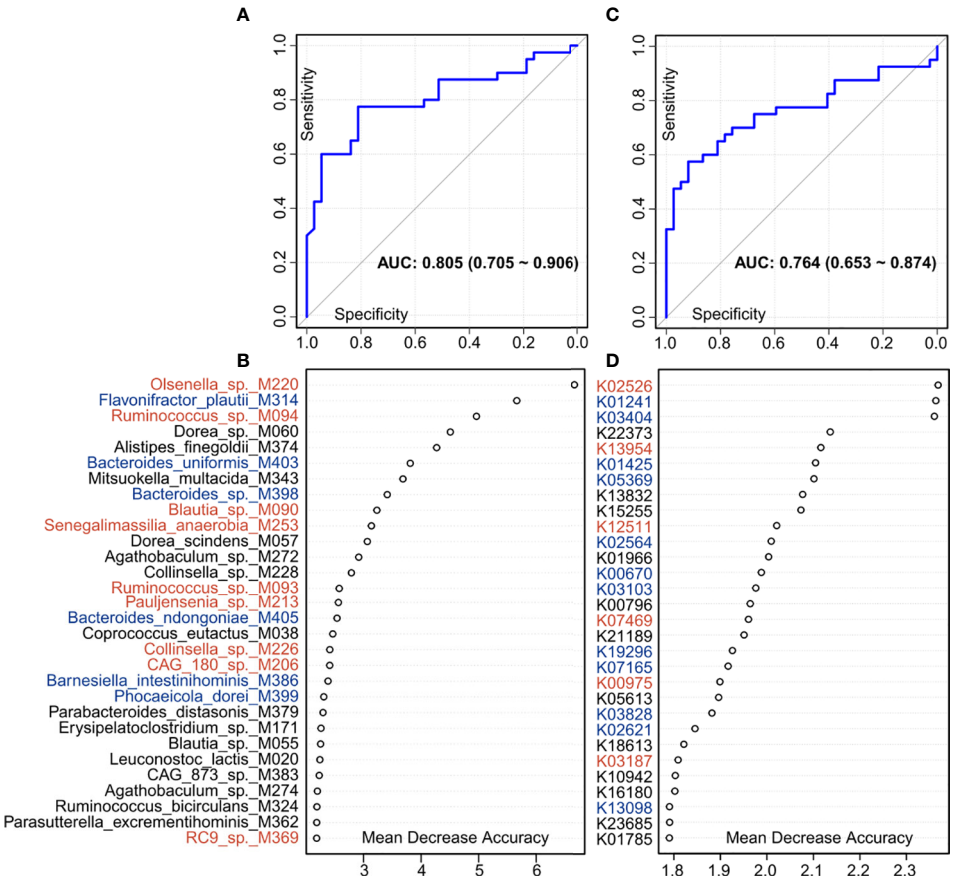

FIGURE 6
Classification of PE status by the relative abundances of gut microbial biomarkers. **(A, C),** ROC analysis for classification of PE patients and healthy controls by species **(A)** and KO **(C)** profiles, assessed by AUC. **(B, D)** The 30 most discriminant species **(B)** and KOs **(D)** in the model classifying patients and controls. Colors represent enrichment in PE patients (red) or healthy controls (blue).

bacitracin/lantibiotics transport system, the rhamnose transport system, and the maltooligosaccharide transport system encoded by PE-enriched *Blautia* and *Collinsella* species, the enzymes of the phospholipid/cholesterol/gamma-HCH transport system, the lipopolysaccharide export system, the porphyrin and chlorophyll metabolism, the Pyridoxal-P biosynthesis, the riboflavin metabolism, and the folate biosynthesis mainly encoded by HC-enriched *Bacteroides* and *Parabacteroides* species, were the importantly PE-associated functional signatures (Figure 5). The well-defined gut microbial biomarkers of PE status will contribute to the PE's early warning.

Eight genera were found enriched in antenatal PE feces in our previous study, of which *Blautia* and *Ruminococcus2* represented the major variances in PE microbiomes and were associated with most PE-enriched functional modules, suggesting their central role in the PE microbiome (Lv et al., 2019). Herein, higher sequencing accuracy reached the species level, uncovering 6 members of *Blautia* and 5 members of *Ruminococcus* (*R. gnavus* and 4 uncultivated species). *Blautia* is a genus containing over 20 anaerobic species that are widely present in the mammalian gut (Liu et al., 2021). As a dominant genus in the intestinal microbiota, the increased abundance of genera *Blautia* (Eckburg et al., 2005; Round and Mazmanian, 2009; Human Microbiome Project, 2012) and *Ruminococcus* was positively correlated with irritable bowel syndrome (Rajilic-Stojanovic et al., 2011), ulcerative colitis (Nishino et al., 2018), gestational diabetes mellitus (Crusell et al., 2018), preeclampsia (Lv et al., 2019; Liu et al., 2021; Miao et al., 2021), pregestational weight, hyperlipidemia (Miao et al., 2021), obesity and dyslipidemia, which involved lipid metabolism, glycosyltransferases, biotin metabolism, and the oxidative-phosphorylation pathway (Miao et al., 2021). Maternal blood pressure and liver enzyme levels were positively correlated to *Ruminococcus* (Lv et al., 2019). *R. gnavus* was a definite species of PE enriched *Ruminococcus* genus. *R. gnavus* were associated with advanced coronary artery diseases (CAD) (Toya et al., 2020), inflammatory bowel disease (Hall et al., 2017), and obesity (Petriz et al., 2014), which could secrete a complex polysaccharide that potently induces inflammatory cytokine (TNF-α) secretion by dendritic cells (Henke et al., 2019).

Previous studies have revealed the enrichment of LPS in peripheral blood of PE women (Lv et al., 2019) which may produce a severe inflammatory response leading to the development of PE (Sanchez-Aranguren et al., 2014). It causes insufficient infiltration of placental trophoblast cells, abnormal spiral artery remodeling, and placental ischemia and hypoxia (Riley and Nelson, 2010). Chen et al. transplanted fecal bacteria from PE patients and found that mice showed PE-like symptoms, increased peripheral blood LPS and increased placental inflammation (Chen et al., 2020). PE enriched *Fusobacterium* contained lipopolysaccharide, and could promote immune abnormalities, stimulate inflammatory response, and damage intestinal barrier function (Lv et al., 2019). Its thermal killing effect on chorionic cells mainly depended on the LPS activity (Barak et al., 2007), which was positively correlated with blood pressure in pregnant women. Due to the increased accuracy of shotgun metagenomic sequencing, *Fusobacterium ulcerans* was a representative species in the PE-enriched gut microbiota in this study, which had confirmed the cytotoxic effect and may contribute to the pathogenesis of tropical ulcers (Adriaans and Garelick, 1989; Veraldi et al., 2021).

Collinsella genus is enriched in the PE gut and belongs to the family Coriobacteriaceae of the phylum Actinobacteria. Members of the family Coriobacteriaceae are frequently considered as pathobionts and can affect metabolism by altering intestinal cholesterol absorption, decreasing glycogenesis in the liver, and increasing triglyceride synthesis. *Collinsella* increases gut permeability by reducing the expression of tight junction proteins ZO-1 (Chen et al., 2016). Its abundance has been associated with type 2 diabetes (T2D), rheumatoid arthritis (Chen et al., 2016), and cholesterol metabolism (Chen et al., 2016). *Collinsella* contributes to the pathogenesis in rheumatoid arthritis by increasing gut permeability, reducing the expression of tight junction proteins in epithelial cells, and inducing the expression of IL-17 cytokines (Chen et al., 2016), which may result in the pathologic effects by recruitment of neutrophils and activation of NF-kB signaling (Derrien et al., 2009). The increased gut permeability leads to leakage of bacteria and endotoxins from the gut lumen to the mesenteric lymph nodes and portal circulation, which will stimulate peritoneal, intestinal and hepatic macrophages (Kim et al., 2006) to release numerous inducer cytokines of PE (Lv et al., 2019; Chen et al., 2020). We found that intestinal fatty acid binding protein, a biomarker of the integrity of the tight junction barrier of peripheral blood intestinal epithelial cells in PE pregnant women, was higher than in the control group, indicating that the intestinal barrier was impaired in PE pregnant women (Lv et al., 2019).

Furthermore, Th17 cellular immunity is dominant in PE (Molvarec et al., 2015; Zhang et al., 2018; Eghbal-Fard et al., 2019). The imbalance of Th17/Treg cells dominated by Th17 cellular immunity can cause exaggerated systemic inflammation (Quinn et al., 2011; Toldi et al., 2015), endothelial dysfunction and placental dysangiogenesis, which are the pathogenesis of PE (Vargas-Rojas et al., 2016). The Th17 response is mainly characterized by the production of inflammatory cytokines, including IL-17A (Eghbal-Fard et al., 2019). IL-17 stimulates fibroblasts, MQs, DCs, endothelial cells and epithelial cells to generate multiple pro-inflammatory mediators, resulting in further inflammatory immune response (Kleinewietfeld and Hafler, 2013). Moreover, IL-17 also induces placental and renal oxidative stress and placental vascular dysfunction resulting in the development of hypertension (Cornelius and Lamarca, 2014). Therefore, we speculated that Collinsella might be related to the increase of IL-17 in PE, but the specific

mechanism needs to be further clarified. Overall, these results suggest that many PE-enriched bacteria were related to the damage of the intestinal barrier, the promotion of immune abnormalities, the activation of inflammatory response, and the metabolic abnormalities of PE patients, and may be involved in the pathogenesis of PE through the entero-placental pathway.

Another strength of this whole metagenome-based study is the precise analysis of functional genes of microorganisms. PE-enriched KOs commonly participated in functions such as genetic information processing, membrane transport, and signaling and cellular processes (Table S5). The membrane transport systems partially mediated the interactions between the gut microbiota and host cells (Konishi et al., 2015). Membrane transport is an indispensable step for importing/exporting essential molecules into/out cells and exists in all tissues of living organisms. The breakdown of transport systems could induce various diseases (Konishi et al., 2015). For example, the changed expression levels of Peptide transporter 1 transporters (PEPT1) lead to the enhanced signaling pathways associated with inflammatory reactions (Konishi et al., 2015). In this study, the PE-enriched KOs of the membrane transport pathway contained the transport systems of rhamnose (containing 4 KOs), bacitracin/lantibiotics (4 KOs), molybdate (3 KOs), maltooligosaccharide (3 KOs), lysine (3 KOs), and multidrug efflux pump (2 KOs). The enzymes of the rhamnose transport system were encoded by PE-enriched *Blautia* and *Pauljensenia* species. The bacitracin/lantibiotics transport system was mainly encoded by PE-enriched *Collinsella* and *Blautia* species (Figure 5). Lantibiotics are produced by many Gram-positive bacteria and kill susceptible cells primarily through membrane pore formation with a strong and wide spectrum of antimicrobial activity against Gram-positive bacteria (Willey and van der Donk, 2007; Lobo-Ruiz and Tulla-Puche, 2018). Some members of the intestinal microbiome, such as *Ruminocossus gnavis* and *Blautia obeum*, can produce lantibiotics, which may cause intestinal microbiota dysbiosis (Guinane et al., 2016; Weiss and Hennet, 2017; Garcia-Gutierrez et al., 2019). The bacteriocins production capability of *Blautia* leads to the reduced intestinal colonization of some pathogenic bacteria (Liu et al., 2021). Yonezawa et al. demonstrated that lantibiotic bacteriocins produced in oral bacteria may be one of the causative factors of intestinal microbiota dysbiosis (Yonezawa et al., 2021). In addition, PE-enriched bacteria, such as *Desulfovibrio* (Korenblum et al., 2005), *Bacteroides* (Guinane et al., 2016), and *Eubacterium* (Le Blay et al., 2007), could be inhibited by the bacitracin/lantibiotics produced by gut microbiota. These suggest that bacitracin/lantibiotics produced by *Collinsella* and *Blautia* species may interfere with the composition of the gut microbiota of PE patients.

The enzymes of the multidrug efflux pump (MDR) and molybdate transport system were mainly encoded by PE-enriched *Blautia* and *Collinsella* species, which were associated with bacteria virulence. For example, *Pseudomonas aeruginosa* improved bacterial competition advantage by promoting molybdate acquisition, and the molybdate transport system is critical to bacterial virulence (Wang et al., 2021). Multidrug efflux pumps are ancient elements encoded in microbial chromosomes. In addition to being mainly related to the pathogenicity of bacteria (Piddock, 2006; Blanco et al., 2016), they are also associated with drug resistance (Piddock, 2006). The expression of MDR efflux pumps is induced by host-produced compounds which can play a role in the virulence of bacterial pathogens (Piddock, 2006). Notably, this efflux pump is involved as well in the bacterial capability for biofilms formation (Baugh et al., 2014; Wang et al., 2021).

In addition, we also found HC-enriched KOs frequently involved in the enzymes of core pathways including energy metabolism, amino acid metabolism, carbohydrate metabolism, glycan biosynthesis and metabolism, and lipid metabolism. More impressively, the enzymes of the pyridoxal-P biosynthesis, Riboflavin metabolism, and folate biosynthesis were more encoded by HC-enriched *Bacteroides caccae*, *Bacteroides thetaiotaomicron*, *Bacteroides uniformis*, *Phocaeicola vulgatus* etc. (Figure 5). Generally, the insufficient synthesis of these vitamins is a potential PE pathogenic factor (Brophy and Siiteri, 1975; Wacker et al., 2000; Singh et al., 2015). The phospholipid/cholesterol/gamma-HCH transport system of HC-enriched *Bacteroides* are important anti-inflammatory bacteria in the gut and could decrease cholesterol levels in the plasma and benefit health (Yazdanyar et al., 2011). In this study, the decreased *Phocaeicola* (former name: *Bacteroides*) *vulgatus* was worth noting, which was not only involved in the folate biosynthesis, etc., but also could fight against LPS-induced acute intestinal injury and DSS-induced colitis (Li et al., 2021; Wang et al., 2022). After all, these are the potential risk factors of PE (Ahmadian et al., 2020).

Conclusion

Deep shotgun metagenomic sequencing significantly improved the accuracy of species identification within the PE gut microbiota. This led to a more comprehensive and in-depth exploration of microbial functional genes and potential pathogenic mechanisms. We observed that *Blautia*, *Ruminococcus, Collinsella*, *Bacteroides*, and *Phocaeicola* might relate to the PE occurrence or development. Moreover, the bacitracin/lantibiotics transport system, maltooligosaccharide transport system, multidrug efflux pump, rhamnose transport system, porphyrin and chlorophyll metabolism, pyridoxal-P biosynthesis, riboflavin metabolism, and folate biosynthesis pathway were also significant changes in the PE gut microbiota. The diagnostic biomarkers of gut microbiota were beneficial to the early warning of PE. The future study might

therefore focus on isolating the PE-associated gut bacteria and applying them to the verification experiments to elucidate these abovementioned pathogeneses.

Data availability statement

The datasets presented in this study can be found in online repositories. The names of the repository/repositories and accession number(s) can be found in the article/Supplementary Material.

Ethics statement

The studies involving human participants were reviewed and approved by Ethics Committee of Guangdong Women and Children Hospital. The patients/participants provided their written informed consent to participate in this study.

Author contributions

A-HY contributed to the conception of the work and manuscript guidance. Q-LY contributed to the experiment and manuscript guidance. L-JL mainly carried out the cohort research performance, data analysis, and drafted the manuscript. S-HL and Q-BL were responsible for statistics, analysis, and functional annotation of bioinformatics data. G-YW, T-WH, and M-CX participated in the implementation of the experiment. J-YW, HL, H-LD, M-CC, and Z-TY were responsible for sample storage and fellow-up of the cohort. All the participants provided approval for publication of the content, agreed to be accountable for all aspects of the work in ensuring that questions related to the accuracy or integrity of any part of the work are appropriately investigated and resolved.

Funding

This work was supported by Guangdong Basic and Applied Basic Research Foundation (2019A1515110389) and Medical Scientific Research Foundation of Guangdong Province (B2019013).

Conflict of interest

The authors declare that the research was conducted in the absence of any commercial or financial relationships that could be construed as a potential conflict of interest.

Publisher's note

All claims expressed in this article are solely those of the authors and do not necessarily represent those of their affiliated organizations, or those of the publisher, the editors and the reviewers. Any product that may be evaluated in this article, or claim that may be made by its manufacturer, is not guaranteed or endorsed by the publisher.

Supplementary material

The Supplementary Material for this article can be found online at: https://www.frontiersin.org/articles/10.3389/fcimb.2022.933523/full#supplementary-material

References

Adriaans, B., and Garelick, H. (1989). Cytotoxicity of fusobacterium ulcerans. *J. Med. Microbiol.* 29 (3), 177–180. doi: 10.1099/00222615-29-3-177

Ahmadian, E., Rahbar Saadat, Y., Hosseiniyan Khatibi, S. M., Nariman-Saleh-Fam, Z., Bastami, M., Zununi Vahed, F., et al. (2020). Pre-eclampsia: Microbiota possibly playing a role. *Pharmacol. Res.* 155, 104692. doi: 10.1016/j.phrs.2020.104692

Almeida, A., Mitchell, A. L., Boland, M., Forster, S. C., Gloor, G. B., Tarkowska, A., et al. (2019). A new genomic blueprint of the human gut microbiota. *Nature* 568 (7753), 499–504. doi: 10.1038/s41586-019-0965-1

Asnicar, F., Thomas, A. M., Beghini, F., Mengoni, C., Manara, S., Manghi, P., et al. (2020). Precise phylogenetic analysis of microbial isolates and genomes from metagenomes using PhyloPhlAn 3. *0. Nat. Commun.* 11 (1), 2500. doi: 10.1038/s41467-020-16366-7

Barak, S., Oettinger-Barak, O., Machtei, E. E., Sprecher, H., and Ohel, G. (2007). Evidence of periopathogenic microorganisms in placentas of women with preeclampsia. *J. Periodontol* 78 (4), 670–676. doi: 10.1902/jop.2007.060362

Baugh, S., Phillips, C. R., Ekanayaka, A. S., Piddock, L. J., and Webber, M. A. (2014). Inhibition of multidrug efflux as a strategy to prevent biofilm formation. *J. Antimicrob. Chemother.* 69 (3), 673–681. doi: 10.1093/jac/dkt420

Blanco, P., Hernando-Amado, S., Reales-Calderon, J. A., Corona, F., Lira, F., Alcalde-Rico, M., et al. (2016). Bacterial multidrug efflux pumps: Much more than antibiotic resistance determinants. *Microorganisms* 4 (1), 14. doi: 10.3390/microorganisms4010014

Bowers, R. M., Kyrpides, N. C., Stepanauskas, R., Harmon-Smith, M., Doud, D., Reddy, T. B. K., et al. (2017). Minimum information about a single amplified genome (MISAG) and a metagenome-assembled genome (MIMAG) of bacteria and archaea. *Nat. Biotechnol.* 35 (8), 725–731. doi: 10.1038/nbt.3893

Brophy, M. H., and Siiteri, P. K. (1975). Pyridoxal phosphate and hypertensive disorders of pregnancy. *Am. J. Obstet Gynecol* 121 (8), 1075–1079. doi: 10.1016/s0002-9378(16)33591-8

Brown, M. A., Magee, L. A., Kenny, L. C., Karumanchi, S. A., McCarthy, F. P., Saito, S., et al. (2018). Hypertensive disorders of pregnancy: ISSHP classification, diagnosis, and management recommendations for international practice. *Hypertension* 72 (1), 24–43. doi: 10.1161/HYPERTENSIONAHA.117.10803

Chang, Y., Chen, Y., Zhou, Q., Wang, C., Chen, L., Di, W., et al. (2020). Short-chain fatty acids accompanying changes in the gut microbiome contribute to the development of hypertension in patients with preeclampsia. *Clin. Sci. (Lond)* 134 (2), 289–302. doi: 10.1042/CS20191253

Chaumeil, P. A., Mussig, A. J., Hugenholtz, P., and Parks, D. H. (2019). GTDB-tk: a toolkit to classify genomes with the genome taxonomy database. *Bioinformatics*. 36 (6), 1925–1927. doi: 10.1093/bioinformatics/btz848

Chen, X., Li, P., Liu, M., Zheng, H., He, Y., Chen, M. X., et al. (2020). Gut dysbiosis induces the development of pre-eclampsia through bacterial translocation. *Gut* 69 (3), 513–522. doi: 10.1136/gutjnl-2019-319101

Chen, J., Wright, K., Davis, J. M., Jeraldo, P., Marietta, E. V., Murray, J., et al. (2016). An expansion of rare lineage intestinal microbes characterizes rheumatoid arthritis. *Genome Med.* 8 (1), 43. doi: 10.1186/s13073-016-0299-7

Chen, S., Zhou, Y., Chen, Y., and Gu, J. (2018). Fastp: an ultra-fast all-in-one FASTQ preprocessor. *Bioinformatics* 34 (17), i884–i890. doi: 10.1093/bioinformatics/bty560

Cornelius, D. C., and Lamarca, B. (2014). TH17- and IL-17- mediated autoantibodies and placental oxidative stress play a role in the pathophysiology of pre-eclampsia. *Minerva Ginecol* 66 (3), 243–249.

Croke, L. (2014). Gestational hypertension and preeclampsia: A practice bulletin from ACOG. American family physician. *Minerva Ginecol* 100:649–650.

Crusell, M. K. W., Hansen, T. H., Nielsen, T., Allin, K. H., Ruhlemann, M. C., Damm, P., et al. (2018). Gestational diabetes is associated with change in the gut microbiota composition in third trimester of pregnancy and postpartum. *Microbiome* 6 (1), 89. doi: 10.1186/s40168-018-0472-x

Derrien, M., Adawi, D., Ahrné, S., Jeppsson, B., Molin, G., Osman, N., et al. (2009). The intestinal mucosa as a habitat of the gut microbiota and a rational target for probiotic functionality and safety. *Microbial Ecol. Health Dis.* 16 (2-3), 137–144. doi: 10.1080/08910600410032286

Eckburg, P. B., Bik, E. M., Bernstein, C. N., Purdom, E., Dethlefsen, L., Sargent, M., et al. (2005). Diversity of the human intestinal microbial flora. *Science* 308 (5728), 1635–1638. doi: 10.1126/science.1110591

Eghbal-Fard, S., Yousefi, M., Heydarlou, H., Ahmadi, M., Taghavi, S., Movasaghpour, A., et al. (2019). The imbalance of Th17/Treg axis involved in the pathogenesis of preeclampsia. *J. Cell Physiol.* 234 (4), 5106–5116. doi: 10.1002/jcp.27315

Garcia-Gutierrez, E., Mayer, M. J., Cotter, P. D., and Narbad, A. (2019). Gut microbiota as a source of novel antimicrobials. *Gut Microbes* 10 (1), 1–21. doi: 10.1080/19490976.2018.1455790

Guinane, C. M., Lawton, E. M., O'Connor, P. M., O'Sullivan, O., Hill, C., Ross, R. P., et al. (2016). The bacteriocin bactofencin a subtly modulates gut microbial populations. *Anaerobe* 40, 41–49. doi: 10.1016/j.anaerobe.2016.05.001

Hall, A. B., Yassour, M., Sauk, J., Garner, A., Jiang, X., Arthur, T., et al. (2017). A novel ruminococcus gnavus clade enriched in inflammatory bowel disease patients. *Genome Med.* 9 (1), 103. doi: 10.1186/s13073-017-0490-5

Henke, M. T., Kenny, D. J., Cassilly, C. D., Vlamakis, H., Xavier, R. J., and Clardy, J. (2019). Ruminococcus gnavus, a member of the human gut microbiome associated with crohn's disease, produces an inflammatory polysaccharide. *Proc. Natl. Acad. Sci. U.S.A.* 116 (26), 12672–12677. doi: 10.1073/pnas.1904099116

Human, D. (2001). Declaration of Helsinki. *Lancet* 357 (9251), 236. doi: 10.1016/S0140-6736(05)71342-8

Human Microbiome Project, C. (2012). Structure, function and diversity of the healthy human microbiome. *Nature* 486 (7402), 207–214. doi: 10.1038/nature11234

Hyatt, D., Chen, G. L., Locascio, P. F., Land, M. L., Larimer, F. W., and Hauser, L. J. (2010). Prodigal: prokaryotic gene recognition and translation initiation site identification. *BMC Bioinf.* 11, 119. doi: 10.1186/1471-2105-11-119

Idanpaan-Heikkila, J. E. (2001). Ethical principles for the guidance of physicians in medical research–the declaration of Helsinki. *Bull. World Health Organ* 79 (4), 279.

Jain, C., Rodriguez, R. L., Phillippy, A. M., Konstantinidis, K. T., and Aluru, S. (2018). High throughput ANI analysis of 90K prokaryotic genomes reveals clear species boundaries. *Nat. Commun.* 9 (1), 5114. doi: 10.1038/s41467-018-07641-9

Kanehisa, M., Furumichi, M., Tanabe, M., Sato, Y., and Morishima, K. (2017). KEGG: new perspectives on genomes, pathways, diseases and drugs. *Nucleic Acids Res.* 45 (D1), D353–D361. doi: 10.1093/nar/gkw1092

Kanehisa, M., Sato, Y., and Morishima, K. (2016). BlastKOALA and GhostKOALA: KEGG tools for functional characterization of genome and metagenome sequences. *J. Mol. Biol.* 428 (4), 726–731. doi: 10.1016/j.jmb.2015.11.006

Kang, D. D., Li, F., Kirton, E., Thomas, A., Egan, R., An, H., et al. (2019). MetaBAT 2: An adaptive binning algorithm for robust and efficient genome reconstruction from metagenome assemblies. *PeerJ* 7, e7359. doi: 10.7717/peerj.7359

Kell, D. B., and Kenny, L. C. (2016). A dormant microbial component in the development of preeclampsia. *Front. Med. (Lausanne)* 3. doi: 10.3389/fmed.2016.00060

Kim, J. M., Lee, J. Y., Yoon, Y. M., Oh, Y. K., Youn, J., and Kim, Y. J. (2006). NF-kappa b activation pathway is essential for the chemokine expression in intestinal epithelial cells stimulated with clostridium difficile toxin a. *Scand. J. Immunol.* 63 (6), 453–460. doi: 10.1111/j.1365-3083.2006.001756.x

Kleinewietfeld, M., and Hafler, D. A. (2013). The plasticity of human treg and Th17 cells and its role in autoimmunity. *Semin. Immunol.* 25 (4), 305–312. doi: 10.1016/j.smim.2013.10.009

Konishi, H., Fujiya, M., and Kohgo, Y. (2015). Host-microbe interactions *via* membrane transport systems. *Environ. Microbiol.* 17 (4), 931–937. doi: 10.1111/1462-2920.12632

Korenblum, E., der Weid, I., Santos, A. L., Rosado, A. S., Sebastian, G. V., Coutinho, C. M., et al. (2005). Production of antimicrobial substances by bacillus subtilis LFE-1, b. firmus HO-1 and b. licheniformis T6-5 isolated from an oil reservoir in Brazil. *J. Appl. Microbiol.* 98 (3), 667–675. doi: 10.1111/j.1365-2672.2004.02518.x

Langmead, B., and Salzberg, S. L. (2012). Fast gapped-read alignment with bowtie 2. *Nat. Methods* 9 (4), 357–359. doi: 10.1038/nmeth.1923

Le Blay, G., Lacroix, C., Zihler, A., and Fliss, I. (2007). *In vitro* inhibition activity of nisin a, nisin z, pediocin PA-1 and antibiotics against common intestinal bacteria. *Lett. Appl. Microbiol.* 45 (3), 252–257. doi: 10.1111/j.1472-765X.2007.02178.x

Letunic, I., and Bork, P. (2019). Interactive tree of life (iTOL) v4: recent updates and new developments. *Nucleic Acids Res.* 47 (W1), W256–W259. doi: 10.1093/nar/gkz239

Li, D., Liu, C. M., Luo, R., Sadakane, K., and Lam, T. W. (2015). MEGAHIT: an ultra-fast single-node solution for large and complex metagenomics assembly *via* succinct de bruijn graph. *Bioinformatics* 31 (10), 1674–1676. doi: 10.1093/bioinformatics/btv033

Liu, X., Mao, B., Gu, J., Wu, J., Cui, S., Wang, G., et al. (2021). Blautia-a new functional genus with potential probiotic properties? *Gut Microbes* 13 (1), 1–21. doi: 10.1080/19490976.2021.1875796

Li, S., Wang, C., Zhang, C., Luo, Y., Cheng, Q., Yu, L., et al. (2021). Evaluation of the effects of different bacteroides vulgatus strains against DSS-induced colitis. *J. Immunol. Res.* 2021, 9117805. doi: 10.1155/2021/9117805

Lobo-Ruiz, A., and Tulla-Puche, J. (2018). "Synthetic approaches of naturally and rationally designed peptides and peptidomimetics," in *Peptide applications in biomedicine, biotechnology and bioengineering* (Elsevier). p. 23-49. doi: 10.1016/b978-0-08-100736-5.00002-8

Lv, L. J., Li, S. H., Li, S. C., Zhong, Z. C., Duan, H. L., Tian, C., et al. (2019). Early-onset preeclampsia is associated with gut microbial alterations in antepartum and postpartum women. *Front. Cell Infect. Microbiol* 9, 224. doi: 10.3389/fcimb.2019.00224

Miao, T., Yu, Y., Sun, J., Ma, A., Yu, J., Cui, M., et al. (2021). Decrease in abundance of bacteria of the genus bifidobacterium in gut microbiota may be related to pre-eclampsia progression in women from East China. *Food Nutr. Res.* 65, 5781. doi: 10.29219/fnr.v65.5781

Molvarec, A., Czegle, I., Szijarto, J., and Rigo, J.Jr. (2015). Increased circulating interleukin-17 levels in preeclampsia. *J. Reprod. Immunol.* 112, 53–57. doi: 10.1016/j.jri.2015.05.007

Nishino, K., Nishida, A., Inoue, R., Kawada, Y., Ohno, M., Sakai, S., et al. (2018). Analysis of endoscopic brush samples identified mucosa-associated dysbiosis in inflammatory bowel disease. *J. Gastroenterol.* 53 (1), 95–106. doi: 10.1007/s00535-017-1384-4

Olm, M. R., Brown, C. T., Brooks, B., and Banfield, J. F. (2017). dRep: a tool for fast and accurate genomic comparisons that enables improved genome recovery from metagenomes through de-replication. *ISME J.* 11 (12), 2864–2868. doi: 10.1038/ismej.2017.126

Parks, D. H., Chuvochina, M., Chaumeil, P. A., Rinke, C., Mussig, A. J., and Hugenholtz, P. (2020). A complete domain-to-species taxonomy for bacteria and archaea. *Nat. Biotechnol.* 38 (9), 1079–1086. doi: 10.1038/s41587-020-0501-8

Parks, D. H., Imelfort, M., Skennerton, C. T., Hugenholtz, P., and Tyson, G. W. (2015). CheckM: Assessing the quality of microbial genomes recovered from isolates, single cells, and metagenomes. *Genome Res.* 25 (7), 1043–1055. doi: 10.1101/gr.186072.114

Parks, D. H., Rinke, C., Chuvochina, M., Chaumeil, P. A., Woodcroft, B. J., Evans, P. N., et al. (2017). Recovery of nearly 8,000 metagenome-assembled genomes substantially expands the tree of life. *Nat. Microbiol.* 2 (11), 1533–1542. doi: 10.1038/s41564-017-0012-7

Petriz, B. A., Castro, A. P., Almeida, J. A., Gomes, C. P., Fernandes, G. R., Kruger, R. H., et al. (2014). Exercise induction of gut microbiota modifications in obese, non-obese and hypertensive rats. *BMC Genomics* 15, 511. doi: 10.1186/1471-2164-15-511

Piddock, L. J. V. (2006). Multidrug-resistance efflux pumps? *not just resistance. Nat. Rev. Microbiol.* 4 (8), 629–636. doi: 10.1038/nrmicro1464

Quinn, K. H., Lacoursiere, D. Y., Cui, L., Bui, J., and Parast, M. M. (2011). The unique pathophysiology of early-onset severe preeclampsia: role of decidual T regulatory cells. *J. Reprod. Immunol.* 91 (1-2), 76–82. doi: 10.1016/j.jri.2011.05.006

Rajilic-Stojanovic, M., Biagi, E., Heilig, H. G., Kajander, K., Kekkonen, R. A., Tims, S., et al. (2011). Global and deep molecular analysis of microbiota signatures in fecal samples from patients with irritable bowel syndrome. *Gastroenterology* 141 (5), 1792–1801. doi: 10.1053/j.gastro.2011.07.043

Redman, C. W. (1991). Current topic: pre-eclampsia and the placenta. *Placenta* 12 (4), 301–308. doi: 10.1016/0143-4004(91)90339-h

Riley, J. K., and Nelson, D. M. (2010). Toll-like receptors in pregnancy disorders and placental dysfunction. *Clin. Rev. Allergy Immunol.* 39 (3), 185–193. doi: 10.1007/s12016-009-8178-2

Round, J. L., and Mazmanian, S. K. (2009). The gut microbiota shapes intestinal immune responses during health and disease. *Nat. Rev. Immunol.* 9 (5), 313–323. doi: 10.1038/nri2515

Sanchez-Aranguren, L. C., Prada, C. E., Riano-Medina, C. E., and Lopez, M. (2014). Endothelial dysfunction and preeclampsia: Role of oxidative stress. *Front. Physiol.* 5. doi: 10.3389/fphys.2014.00372

Singh, M. D., Thomas, P., Owens, J., Hague, W., and Fenech, M. (2015). Potential role of folate in pre-eclampsia. *Nutr. Rev.* 73 (10), 694–722. doi: 10.1093/nutrit/nuv028

Strimmer, K. (2008). Fdrtool: A versatile r package for estimating local and tail area-based false discovery rates. *Bioinformatics* 24 (12), 1461–1462. doi: 10.1093/bioinformatics/btn209

Toldi, G., Vasarhelyi, Z. E., Rigo, J.Jr., Orban, C., Tamassy, Z., Bajnok, A., et al. (2015). Prevalence of regulatory T-cell subtypes in preeclampsia. *Am. J. Reprod. Immunol.* 74 (2), 110–115. doi: 10.1111/aji.12380

Toya, T., Corban, M. T., Marrietta, E., Horwath, I. E., Lerman, L. O., Murray, J. A., et al. (2020). Coronary artery disease is associated with an altered gut microbiome composition. *PloS One* 15 (1), e0227147. doi: 10.1371/journal.pone.0227147

Vargas-Rojas, M. I., Solleiro-Villavicencio, H., and Soto-Vega, E. (2016). Th1, Th2, Th17 and treg levels in umbilical cord blood in preeclampsia. *J. Matern Fetal Neonatal Med.* 29 (10), 1642–1645. doi: 10.3109/14767058.2015.1057811

Veraldi, S., Faraci, A. G., Valentini, D., and Bottini, S. (2021). Tropical ulcers: the first imported cases and review of the literature. *Eur. J. Dermatol.* 31 (1), 75–80. doi: 10.1684/ejd.2021.3968

Wacker, J., Fruhauf, J., Schulz, M., Chiwora, F. M., Volz, J., and Becker, K. (2000). Riboflavin deficiency and preeclampsia. *Obstet Gynecol* 96 (1), 38–44. doi: 10.1016/s0029-7844(00)00847-4

Wang, T., Du, X., Ji, L., Han, Y., Dang, J., Wen, J., et al. (2021). Pseudomonas aeruginosa T6SS-mediated molybdate transport contributes to bacterial competition during anaerobiosis. *Cell Rep.* 35 (2), 108957. doi: 10.1016/j.celrep.2021.108957

Wang, J., Gu, X., Yang, J., Wei, Y., and Zhao, Y. (2019). Gut microbiota dysbiosis and increased plasma LPS and TMAO levels in patients with preeclampsia. *Front. Cell Infect. Microbiol* 9, 409. doi: 10.3389/fcimb.2019.00409

Wang, C., Xiao, Y., Yu, L., Tian, F., Zhao, J., Zhang, H., et al. (2022). Protective effects of different bacteroides vulgatus strains against lipopolysaccharide-induced acute intestinal injury, and their underlying functional genes. *J. Adv. Res.* 36, 27–37. doi: 10.1016/j.jare.2021.06.012

Weiss, G. A., and Hennet, T. (2017). Mechanisms and consequences of intestinal dysbiosis. *Cell Mol. Life Sci.* 74 (16), 2959–2977. doi: 10.1007/s00018-017-2509-x

Willey, J. M., and van der Donk, W. A. (2007). Lantibiotics: peptides of diverse structure and function. *Annu. Rev. Microbiol.* 61, 477–501. doi: 10.1146/annurev.micro.61.080706.093501

Yazdanyar, A., Yeang, C., and Jiang, X. C. (2011). Role of phospholipid transfer protein in high-density lipoprotein- mediated reverse cholesterol transport. *Curr. Atheroscler Rep.* 13 (3), 242–248. doi: 10.1007/s11883-011-0172-5

Yonezawa, H., Motegi, M., Oishi, A., Hojo, F., Higashi, S., Nozaki, E., et al. (2021). Lantibiotics produced by oral inhabitants as a trigger for dysbiosis of human intestinal microbiota. *Int. J. Mol. Sci.* 22 (7), 3343. doi: 10.3390/ijms22073343

Zhang, Y., Liu, Z., Tian, M., Hu, X., Wang, L., Ji, J., et al. (2018). The altered PD-1/PD-L1 pathway delivers the 'one-two punch' effects to promote the Treg/Th17 imbalance in pre-eclampsia. *Cell Mol. Immunol.* 15 (7), 710–723. doi: 10.1038/cmi.2017.70

frontiers | Frontiers in Cellular and Infection Microbiology

TYPE Original Research
PUBLISHED 14 September 2022
DOI 10.3389/fcimb.2022.925444

OPEN ACCESS

EDITED BY
Jeyaprakash Rajendhran,
Madurai Kamaraj University, India

REVIEWED BY
Ameer Megahed,
University of Illinois at Urbana–Champaign, United States
Thevambiga Iyadorai,
University of Malaya, Malaysia

*CORRESPONDENCE
Riu Yamashita
riuyamas@east.ncc.go.jp

SPECIALTY SECTION
This article was submitted to Clinical Microbiology, a section of the journal Frontiers in Cellular and Infection Microbiology

RECEIVED 21 April 2022
ACCEPTED 29 August 2022
PUBLISHED 14 September 2022

CITATION
Sakai SA, Aoshima M, Sawada K, Horasawa S, Yoshikawa A, Fujisawa T, Kadowaki S, Denda T, Matsuhashi N, Yasui H, Goto M, Yamazaki K, Komatsu Y, Nakanishi R, Nakamura Y, Bando H, Hamaya Y, Kageyama S-I, Yoshino T, Tsuchihara K and Yamashita R (2022) Fecal microbiota in patients with a stoma decreases anaerobic bacteria and alters taxonomic and functional diversities. *Front. Cell. Infect. Microbiol.* 12:925444. doi: 10.3389/fcimb.2022.925444

Fecal microbiota in patients with a stoma decreases anaerobic bacteria and alters taxonomic and functional diversities

Shunsuke A. Sakai[1,2], Masato Aoshima[1,2], Kentaro Sawada[3], Satoshi Horasawa[4], Ayumu Yoshikawa[5], Takao Fujisawa[6], Shigenori Kadowaki[7], Tadamichi Denda[8], Nobuhisa Matsuhashi[9], Hisateru Yasui[10], Masahiro Goto[11], Kentaro Yamazaki[12], Yoshito Komatsu[13], Ryota Nakanishi[14], Yoshiaki Nakamura[4,5], Hideaki Bando[4,5], Yamato Hamaya[1,2], Shun-Ichiro Kageyama[15], Takayuki Yoshino[5], Katsuya Tsuchihara[1,2] and Riu Yamashita[2,16]*

[1]Graduate School of Frontier Science, Department of Integrated Biosciences, University of Tokyo, Kashiwa, Japan, [2]Division of Translational Informatics, Exploratory Oncology Research and Clinical Trial Center, National Cancer Center, Kashiwa, Japan, [3]Department of Medical Oncology, Kushiro Rosai Hospital, Kushiro, Japan, [4]Translational Research Support Section, National Cancer Center Hospital East, National Cancer Center Hospital East, Kashiwa, Japan, [5]Department of Gastroenterology and Gastrointestinal Oncology, National Cancer Center Hospital East, Kashiwa, Japan, [6]Department Head and Neck Medical Oncology, National Cancer Center Hospital East, Kashiwa, Japan, [7]Department of Clinical Oncology, Aichi Cancer Center Hospital, Nagoya, Japan, [8]Divisioin of Gastroenterology, Chiba Cancer Center, Chiba, Japan, [9]Department of Gastroenterological surgery Pediatric surgery, Gifu University Hospital, Gifu, Japan, [10]Department of Medical Oncology, Kobe City Medical Center General Hospital, Kobe, Japan, [11]Cancer Chemotherapy Center, Osaka Medical and Pharmaceutical University Hospital, Takatsuki, Japan, [12]Division of Gastrointestinal Oncology, Shizuoka Cancer Center, Shizuoka, Japan, [13]Department of Cancer Center, Hokkaido University Hospital, Hokkaido, Japan, [14]Department of Surgery and Science, Graduate School of Medical Sciences, Kyushu University, Fukuoka, Japan, [15]Department of Radiation Oncology and Particle Therapy, National Cancer Center Hospital East, Kashiwa, Japan, [16]Department of Computational Biology and Medical Sciences, Graduate School of Frontier Science, University of Tokyo, Kashiwa, Japan

Colorectal cancer (CRC) is one of the most common malignant diseases. Generally, stoma construction is performed following surgery for the resection of the primary tumor in patients with CRC. The association of CRC with the gut microbiota has been widely reported, and the gut microbiota is known to play an important role in the carcinogenesis, progression, and treatment of CRC. In this study, we compared the microbiota of patients with CRC between with and without a stoma using fecal metagenomic sequencing data from SCRUM-Japan MONSTAR-SCREEN, a joint industry-academia cancer research project in Japan. We found that the composition of anaerobes was reduced in patients with a stoma. In particular, the abundance of *Alistipes*, *Akkermansia*, *Intestinimonas*, and methane-producing archaea decreased. We also compared gene function (e.g., KEGG Orthology and

KEGG pathway) and found that gene function for methane and short-chain fatty acids (SCFAs) production was underrepresented in patients with a stoma. Furthermore, a stoma decreased Shannon diversity based on taxonomic composition but increased that of the KEGG pathway. These results suggest that the feces of patients with a stoma have a reduced abundance of favorable microbes for cancer immunotherapy. In conclusion, we showed that a stoma alters the taxonomic and functional profiles in feces and may be a confounding factor in fecal microbiota analysis.

KEYWORDS

gut microbiota, anaerobe, stoma, colostomy, colorectal cancer, 16S rRNA gene

1 Introduction

Recently, the relationship between the gut microbiome and cancer has been extensively studied (Ternes et al., 2020). Favorable gut microbiotas have been found to be associated with the efficacy of cancer treatment, and their therapeutic applications are also being developed. For example, several commensal bacteria (e.g., *Ruminococcaceae* family, *Akkermansia muciniphila*, *Bifidobacterium longum, Collinsella aerofaciens*, and *Enterococcus faecium*) and taxonomic diversity have been found to correlate with therapeutic efficacy with immune checkpoint inhibitors (ICI) against melanoma, renal cell carcinoma, and non-small cell lung cancer (Gopalakrishnan et al., 2018; Matson et al., 2018; Routy et al., 2018). In addition, studies on fecal microbiota transplantation from responders to ICI therapy to non-responders showed a significant response (Baruch et al., 2021; Davar et al., 2021).

Colorectal cancer (CRC) accounted for 10% of all cancers worldwide in 2020, and its incidence is expected to increase (Xi and Xu, 2021). In patients with CRC, several pathogenic bacteria, such as *Fusobacterium nucleatum* and *Peptostreptococcus anaerobius*, promote carcinogenesis by physically interacting with the tumor (Long et al., 2019; Ternes et al., 2020; Inamori et al., 2021). *Bacteroides fragilis* and *Escherichia coli* are involved in the carcinogenesis and progression of CRC, respectively, by releasing toxins (Haghi et al., 2019; Iyadorai et al., 2020). In contrast, several microbes (e.g., *Lactobacilli* and *Bifidobacteria*) suppress tumor progression as observed in a study using an animal model of CRC (Kim and Lee, 2022). In terms of treatment, *F. nucleatum* in the intestines of patients with CRC has been reported to inhibit the efficacy of 5-fluorouracil and oxaliplatin (Yu et al., 2017). CpG-oligonucleotide immunotherapy has also been used for several cancer types (Chuang et al., 2020). For example, CpG-oligonucleotide immunotherapy in a murine colon carcinoma model was associated with specific gut microbiota, such as *Alistipes* (Iida et al., 2013).

Stoma construction is a surgical procedure performed in patients with CRC and other cases, and it is performed for resection of the primary tumor and palliative stoma as a solution to gastrointestinal obstruction (Amersi et al., 2004; Pickard et al., 2018). In a study examining the quality of life of patients with CRC, 35% of patients with CRC underwent stoma construction (Verweij et al., 2016; Verweij et al., 2017). The number of patients with a stoma is estimated to be approximately 3 million worldwide, and stoma cases are increasing annually (Fortune Business Insights, 2020). Stoma construction opens the intestinal tract and prevents feces from entering the gastrointestinal tract downstream from the stoma. According to a study that examined the relationship between colonic transit time and fecal microbiota, microbial alpha diversity was higher when the fecal transit time through the descending colon was longer (Müller et al., 2020). A study also reported that the composition of the mucosal surface microbiota of the cecum, transverse colon, and sigmoid colon differs from each other (James et al., 2020). Therefore, the unavailability of the colorectal region downstream from stoma because of stoma may affect the analysis of the fecal microbiota. However, to the best of our knowledge, no study has reported the effect of stoma on the fecal microbiota.

In this study, we aimed to analyze the effect of a stoma on the fecal microbiota of patients with CRC. Here, we used 16S rRNA gene sequencing data and clinical data from MONSTAR-SCREEN, industry-academia collaborative cancer research project, to evaluate changes in fecal microbiota between patients with and without stoma. We compared various aspects of the microbiota, including taxonomy, bacteriological characteristics, gene functions, and diversity. Our study revealed

the characteristic fecal microbiota of patients with a stoma, and it was found that the stoma can significantly affect the results of fecal microbiota analysis.

2 Materials and methods

2.1 Study population and samples

SCRUM-Japan MONSTAR-SCREEN is a nationwide tissue and plasma genomic and fecal microbiome profiling study in Japan based on the SCRUM-Japan platform, in which 31 institutions participated. The key inclusion criteria were as follows: i) histopathologically confirmed unresectable or metastatic solid tumors, ii) age ≥20 years, and iii) life expectancy of at least 12 weeks (Nakamura et al., 2021). Fecal samples were collected from eligible patients between December 2019 and June 2021, and written informed consent was obtained. We used a commercial fecal sampling kit with a preservation solution (TechnoSuruga Laboratory Co., Ltd., Shizuoka, Japan). The samples were stored at room temperature for up to seven days and then frozen at -80°C until sample processing. In addition, information on patients' antibiotic use, proton-pump inhibitor (PPI) use, and the Bristol Scale was collected using a questionnaire.

This study was conducted in accordance with the Declaration of Helsinki and Japanese Ethical Guidelines for Medical and Health Research Involving Human Subjects. The study protocol was approved by the institutional review board of each participating institution and was registered at the University Hospital Medical Information Network (UMIN000036749). This study was conducted in July 2019.

2.2 Fecal microbiome analysis

2.2.1 DNA extraction and 16S ribosomal DNA sequencing

A stool suspension (150 µL) in a preservative solution was used for DNA extraction using a NucleoSpin 96 Soil (Macherey-Nagel GmbH & Co. KG, Düren, Germany) according to the manufacturer's instructions. The final volume of the extraction solution was 100 µL, and approximately 50 µL was obtained. Subsequently, the extracted DNA was purified using Agencourt AMPure XP (Beckman Coulter, Inc., Miami, FL, USA), and the concentration was quantified using the Picogreen dsDNA Assay Kit (Thermo Fisher Scientific, Inc., Waltham, MA, USA).

We used 1 ng of purified DNA (maximum amount for low-concentration samples) as a template for the first PCR using the 16S (V3-V4) Metagenomic Library Construction Kit for NGS (TaKaRa Bio, Inc., Shiga, Japan). PCR products were purified using Agencourt AMPure XP beads (Beckman Coulter, Inc.). The purified PCR product was used as a template for index PCR using a Nextera XT Index Kit (Illumina Inc., San Diego, CA, USA). The indexed PCR products were purified using Agencourt AMPure XP beads (Beckman Coulter, Inc.) and quantified using a Quant-it Picogreen dsDNA Assay Kit (Thermo Fisher Scientific, Inc.). Equimolar mixing of indexed PCR products was performed based on the concentration of each sample to obtain a library. The library size and concentration were calculated using a TapeStation (Agilent Technologies, Inc., Santa Clara, CA, USA). The library was sequenced with the MiSeq sequencer in a multiplex manner, using a 250 bp paired-end sequencing protocol with the MiSeq sequencing reagent kits v3 (Illumina Inc.) and approximately 40–50% of the PhiX Control (Illumina, Inc.).

2.2.2 16S rRNA gene sequencing processing

We employed QIIME2 (v2021.4), a microflora analysis pipeline (Bolyen et al., 2019), for FASTQ annotation. First, low-quality sequences in the FASTQ data were filtered out, and then the DADA2 algorithm was used to correct the error sequences, followed by the generation of a read count table of amplicon sequence variants (ASVs). The reads were rarefied to 42292 reads, which was the minimum number of reads in all samples. Then, a phylogenetic assignment was conducted using the SILVA database (v138) to obtain the number of reads by taxonomy. Next, the unweighted and weighted UniFrac distance matrices were obtained using the QIIME2 command. Finally, principal coordinate analysis (PCoA) was performed on these matrices. All of data are available in Supplementary Material 1.

2.2.3 Functional prediction and bacteriological characteristic annotation

We applied PICRUSt2 (v2.4.1) to predict taxonomic function at the gene level in ASV (Douglas et al., 2020). The relative abundance of gene families (KEGG Orthology [KO]) and metabolic pathways (KEGG pathway [pathway]) was determined. Predicted KO copy numbers per ASV were obtained from the PICRUSt2 output files. Subsequently, KOs and ASVs were averaged at the pathway and genus levels, respectively, to calculate the correlation between genus and pathway. The Genomes OnLine Database (GOLD) database (v8) was used to annotate bacteriological features regarding gram-stainability and oxygen requirements (Mukherjee et al., 2021). The microbial metadata in the database were added to the taxonomy in the order of species, genus, order, class, and phylum. The annotation was divided into 'Gram+' and 'Gram-' for Gram-stainability, and it was also divided into 'Anaerobe' and 'Non-anaerobe' based on oxygen requirement. If no single annotation could be determined even after referring to the species level, the annotation was classified as 'Various,' and if it did not exist in the database, it was classified as 'Unknown.'

2.2.4 Diversity analysis

Seven α-diversity indices from the relative abundance of ASV, KO, and pathway features per sample were calculated. First, the types of ASV, KO, and pathway features as an index based on richness were obtained, and we defined them as ASV observed, KO observed, and pathway observed, respectively. Shannon indices (ASV Shannon, KO Shannon, and Pathway Shannon) as the diversity of evenness and richness were calculated as follows:

$$H = -\sum_{i=1}^{S}(p_i log_2 p_i)$$

where $p_i$is defined as each feature ratio, and S is the number of features of the ASV, KO, and pathway. Finally, ASV Faith's PD, an index of the sum of phylogenetic distances between ASVs, was calculated. ASV observed, ASV Shannon, and ASV Faith's PD were defined as taxonomic diversity, and KO observed, KO Shannon, Pathway observed, and Pathway Shannon were defined as functional diversity.

2.3 Statistical analysis

In this study, the relative abundance of features (taxonomy, KO, and pathway), diversity (alpha and beta), and the ratio of taxonomic characteristics (gram stainability and oxygen requirement) were compared between patients with and without a stoma. We detected overrepresented KEGG pathway using Gene Set Enrichment Analysis (GSEA). The ALDEx2 algorithm (v1.24.0) was used to compare the taxonomy, KO, and pathway to determine significant features (Wilcoxon rank-sum test; Benjamini-Hochberg [BH] adjusted p-value< 0.3) (Fernandes et al., 2013; Fernandes et al., 2014). The DACOMP (v1.26) algorithm was also used to compare the ALDEx2 results (Brill et al., 2019). To compare the alpha diversity index, the Mann–Whitney U test was used to compare the two groups, and Cohen's d was used as the effect size. A permutation multivariate analysis of variance (PERMANOVA) was performed to test for differences in beta diversity. In a comparison of the gram stainability and oxygen requirement of the microflora, the compositional data were mapped onto the real number space by a centered log-ratio (clr) transformation of each bacteriological characteristic category (e.g., Gram+, Gram-, Anaerobe, and Non-anaerobe) ratio, followed by the Mann–Whitney U test between patients with and without a stoma. For the GSEA method, the effect sizes of KOs that were output by ALDEx2 were arranged in descending order, and ESs were calculated using the GESApy package (v0.10.5). In this case, the threshold for significant enrichment was set at a BH-adjusted p-value of< 0.05.

2.4 Visualization

Hierarchical fluctuation of taxonomy up to the family level was depicted using the R package Metacoder (v0.3.5) (Foster et al., 2017). Furthermore, a comprehensive graphic display of the KEGG pathway was generated using iPath (v3). The R package of pathview (v1.32.0) was used to illustrate the changes in KOs included in the KEGG pathway (Luo and Brouwer, 2013).

3 Results

3.1 Study population

The 16S rRNA gene sequence data of fecal samples from 220 patients with CRC before chemotherapy enrolled in MONSTAR-SCREEN were available. Of these 220 patients, we excluded 79 antibiotic users based on a questionnaire and 22 patients without information on stoma. Finally, pre-treatment fecal sample data from 119 patients (21 patients with a stoma [stoma group] and 98 patients without a stoma [non-stoma group]) were used in this study (Figure 1). In the stoma group, stomas were present in the small intestine, transverse colon, descending colon, and sigmoid colon (Supplementary Table 1). All patients in the analysis had stage IV CRC and an ECOG-PS<2. The clinical features of the patients are shown in Table 1. The age and BMI (mean ± [SD]) in the stoma group were 58 (± 17.2) and 20.9 (± 3.9), respectively. We also compared the frequency of consumption of fermented foods and drinking (Supplementary Table 2). We used the Bristol scale to evaluate fecal consistency, and the results showed that patients in the stoma group had soft stools (chi-square test: p< 0.001) (Supplementary Table 3). There were no other significant differences in any of the characteristics (e.g., gender, proton pump inhibitors, primary tumor resection, and primary tumor location).

3.2 Taxonomic composition of each sample and their characteristics

To confirm the change in bacterial composition in feces due to stoma, we obtained the number of ASV, a taxonomic unit classified by a single base change, after correcting for sequence errors. We observed that the number of ASV decreased in the stoma group (p = 0.001) (Figure 2A). We then analyzed the taxonomic composition and found that Archaea were present specifically in the non-stoma group (p = 0.04) (Supplementary Figure 1A). At the phylum level, *Firmicutes* (average relative

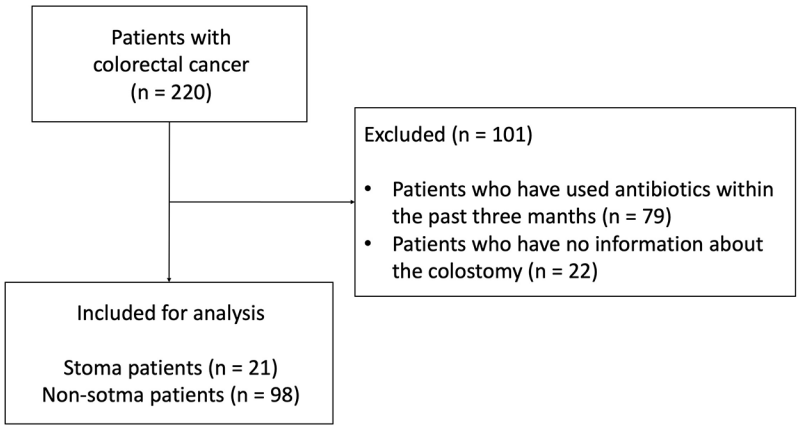

FIGURE 1
Consort diagram of this study.

abundance in the stoma group [S] = 56%, non-stoma group [N] = 54%), *Bacteroidota* (S = 22%, N = 28%), *Actinobacteriota* (S = 11%, N = 11%), and *Proteobacteria* (S = 11%, N = 4.2%) were predominant in both groups (Figure 2B). Comparing the two groups, *Firmicutes* (BH adjusted *p*-value = 0.04) and *Proteobacteria* (p = 0.1) were more abundant in the stoma group, whereas *Verrucomicrobiota* (p = 0.1) and *Desulfobacterota* (p = 0.06) were less abundant. These results showed that the phylum in feces was different in the stoma group than in patients without a stoma. In addition, focusing on the features of gram-stainability and anaerobicity, we used the Genomes OnLine Database (GOLD) to annotate these

TABLE 1 Patient characteristics.

	Stoma group	Non-stoma group	
Characteristics	**N = 21**[1]	**N = 98**[1]	***p*-value**[2]
Age (years)	58 (24–84)	63 (38–85)	0.2
BMI (kg/m^2)	21 (3.9)	23 (3.5)	0.07
Unknown	2	0	
Gender			1
Female	9 (43%)	44 (45%)	
Male	12 (57%)	54 (55%)	
PPI			0.3
User	16 (76%)	84 (86%)	
Non-user	5 (24%)	14 (14%)	
Primary tumor resection Yes	12 (57%)	67 (68%)	0.3
No	9 (43%)	31 (32%)	
Location of the primary tumor			0.2
Cecum	0 (0%)	7 (7.3%)	
Ascending colon	0 (0%)	10 (10%)	
Transverse colon	3 (15%)	15 (16%)	
Descending colon	2 (10%)	3 (3.1%)	
Sigmoid colon	5 (25 %)	31 (32%)	
Rectum	10 (50%)	30 (31%)	
No information	1	2	

[1]Mean (range); Mean (SD); n (%)
[2]Welch Two Sample t-test; Fisher's exact test; Pearson's Chi-squared
BMI, body mass index; PPI, proton-pump inhibitor.

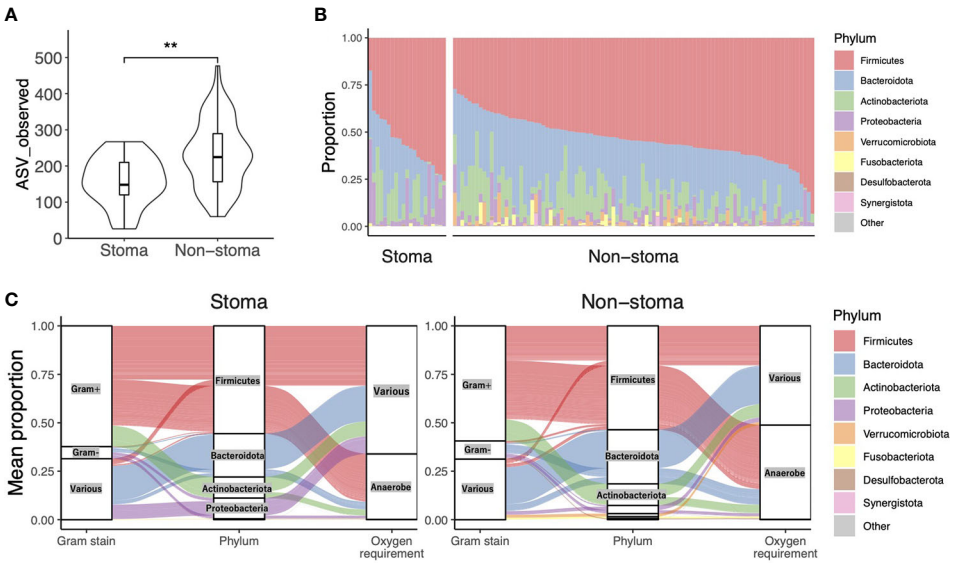

FIGURE 2
Taxonomic alpha diversity in patients with or without a stoma. **(A)** Violin plot of taxonomic richness (ASV observed). Significance differences between the two groups were tested using the Mann–Whitney U test. $^{**}p < 0.01$. **(B)** The composition of phylum-level bacteria. **(C)** The Sankey diagram shows the relationship between taxonomic composition at the phylum level, its Gram-stainability, and whether it is anaerobe or not. The vertical axis represents the average composition per stoma group or non-stoma group.

bacteriological features and compared their relative abundances between the two groups. There was no significant difference in the frequency of gram-positive (S = 62%, N = 59%; $p = 0.2$) and gram-negative (S = 6.3%, N = 9.4%; $p = 0.1$) bacteria between the two groups. In contrast, there was a significant decrease in the relative abundance of obligate anaerobes (S = 34%, N = 49%; $p < 0.001$) in the stoma group (Table 2, Supplementary Figure 1B). The Sankey diagram in Figure 2C shows the relationship between taxonomic composition at the phylum level, gram-stainability, and anaerobicity. Interestingly, although the results showed no large difference in the relative amounts of *Firmicutes*, which is generally considered anaerobic, the taxonomy annotated as anaerobic was greatly reduced in the stoma group. This result implied that a stoma was responsible for reducing obligate anaerobes in stools.

3.3 Stoma-induced variation in diversity and taxonomy

Next, we investigated the difference in beta-diversity between the stoma and non-stoma groups *via* principal coordinate analysis (PCoA) using unweighted and weighted UniFrac distances (Figure 3A, B). These results showed

TABLE 2 Comparison of Gram-stainability and oxygen requirement with and without a stoma.

Categories		Cohen's d^1	p-value^2	fdr^3
Gram-stainability	Gram+	0.23	0.2	0.2
	Gram-	-0.29	0.1	0.2
	Various	0.066	0.7	0.7
	Unknown	0.15	0.1	0.2
Oxygen requirement	Anaerobe	-0.86	**< 0.001**	**0.003**
	Non-anaerobe	0.51	**0.02**	**0.04**
	Various	-0.11	0.5	0.5
	Unknown	0.30	0.5	0.5

[1]Effect size (stoma group – non-stoma group); Criteria: d = 0.2 (small), d = 0.5 (medium), d = 0.8 (large)
[2]Mann–Whitney U-test
[3]p-value corrected using the Benjamini-Hochberg method
The p-value shown in bold indicate significant differences (p<0.05).

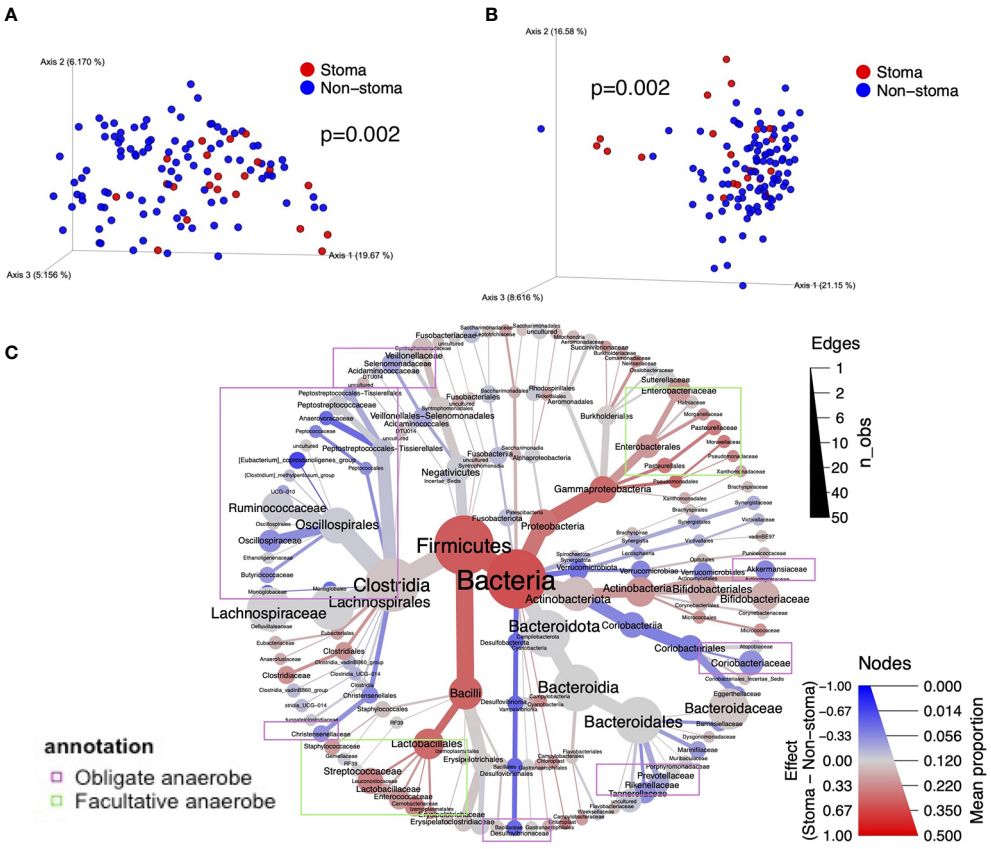

FIGURE 3
The difference in taxonomic beta diversity between the stoma group and non-stoma group. **(A)** PCoA plot of unweighted UniFrac distance. **(B)** PCoA plot of weighted UniFrac distance. **(C)** Heat tree with the effect size illustrates the hierarchical differences of bacteria. The color represents the effect size of the comparison in ALDEx2. The size of the nodes represents the average percentage of taxonomy, and the size of the edges represents the number of observations of genus-level bacteria belonging to the taxon of the parent node. Taxa surrounded by purple borders include obligate anaerobes, while taxa surrounded by light green borders include facultative anaerobes and aerobes. PCoA; Principal Coordinate Analysis.

significant taxonomic discrimination between the two groups. We subsequently performed permutation multivariate analysis of variance (PERMANOVA) with 999 permutations (unweighted UniFrac distance, F = 3.3, p = 0.002; weighted UniFrac distance, F = 4.5, p = 0.002). These results also showed significant quantitative and qualitative taxonomic discriminations between the two groups. The ALDEx2 algorithm was then used to examine the differences in the relative abundance of bacteria at each taxonomic level between the two groups, and a phylogenic heat map tree with the effect sizes is shown (Figure 3C and Supplementary Table 4). We found a tendency to decrease obligate anaerobes such as *Anaerovoracaceae, Oscillospiraceae, Desulfovibrionaceae, Rikenellaceae*, and *Akkermansiaceae* (BH adjusted p-value< 0.3, effect size< -0.17), at the family level in the stoma group. In contrast, facultative anaerobes and aerobes such as *Enterococcaceae, Pasteurellaceae, Pseudomonadaceae, Campylobacteraceae*, and *Morganellaceae* increased (BH adjusted p-value< 0.3, effect size > 0.17). We also observed that *Clostridiaceae* abundance was increased in the stoma group. At the genus level, *Monoglobus* (BH adjusted p = 0.1), *Akkermansia* (p = 0.3), *Alistipes* (p = 0.1), *Anaerotruncus* (p = 0.3), *Fusicatenibacter* (p = 0.3), *Intestinimonas* (p = 0.2), and *Dorea* (p = 0.2) were decreased in the stoma group. Meanwhile, *Acinetobacter* (p = 0.2), *Haemophilus* (p = 0.2), and *Enterococcus* (p = 0.2) increased (Supplementary Figure 2). The result was validated by another statistical tool, DACOMP, and we observed that 87% of the genera detected by ALDEx2 were also detected DACOMP (Supplementary Figure 3). These results also suggest that obligate anaerobes decreased, and other bacteria that could tolerate the oxygen environment increased in the stoma group. Comparing the number of ASVs between each stoma location (small intestine, right-side colon, and left-side colon) and the non-stoma group confirmed decreased fecal taxonomic diversity

in all stoma locations compared with the non-stoma group. The results also showed that the stoma of the small intestine had a lower number of ASVs than that of the right-side colon. (Supplementary Figure 4A). *Akkermansia* decreased in all stoma locations compared to that in the non-stoma group, while *Alistipes* decreased in the stoma of the small intestine and right-side colon (Supplementary Figure 4B).

3.4 Analysis of the difference in gene function inferred from bacteria between patients with and without a stoma

Next, we focused on the gene functions of patients with a stoma. We used PICRUSt2 to infer the gene functions of the microbiota and annotated KEGG Orthology (KO) against them. We applied the ALDEx2 algorithm to compare the relative abundance of KOs between the stoma and non-stoma groups. There was a significant reduction in the stoma group for glycolate oxidase FAD-binding subunit (K11472; BH adjusted p-value = 0.04), dimethyl sulfoxide reductase membrane subunit (K00185; p = 0.05), and acetate CoA/acetoacetate CoA-transferase alpha and beta subunits (K01034; p = 0.1, K01035; p = 0.1) (Supplementary Table 5). This result implies that the stoma reduced redox and SCFAs production. To evaluate which gene functions fluctuated at the metabolic pathway level, we subsequently performed Gene Set Enrichment Analysis (GSEA) to calculate the enrichment score (ES) of functional units in the KEGG pathway using all effect sizes of KOs (Supplementary Table 6). Figures 4A, B show the enriched pathways in the global metabolic maps. xylene degradation, benzoate degradation, glycerolipid metabolism, and photosynthesis were enriched in the stoma group (BH adjusted p< 0.05, ES > 0). In contrast, many pathways were decreased in the stoma group, such as methane metabolism, butanoate metabolism, and other amino acid metabolisms (BH adjusted p< 0.05, ES< 0). Focusing on the alteration of KOs belonging to methane metabolism, we found a decreasing tendency (BH adjusted p-value< 0.3, effect size< -0.17) for KOs such as heterodisulfide reductase subunits C2, B2, and A2 (1.8.7.3, 1.8.98.4, 1.8.98.5, 1.8.98.6), phosphosulfolactate synthase (4.4.1.19), and methanogen homocitrate synthase (2.3.3.-) in the stoma group (Figure 4C). These results suggest that a stoma increased the microbial pathway of xenobiotic biodegradation and metabolism but decreased that of anaerobic metabolism.

3.5 Investigation of taxonomic and their functional diversity index

To consider the changes in bacteria and their functions, we calculated various diversity indices and compared them between the stoma and the non-stoma groups. ASV, the output of QIIME2, is the unit that divides the taxonomy by a single nucleotide change after correcting for sequencing errors, KO is the gene set at the functional level inferred from the ASV using PICRUSt2, and the KEGG pathway is the sum of KOs belonging to each unit of the KEGG pathway. After obtaining the ASV, KO, KEGG pathway, we calculated Shannon diversity indices of those three categories and Faith's phylogenetic distance (Faith's PD) for ASVs. We found that the ASV observed, ASV Shannon, and ASV Faith's PD were significantly decreased in the stoma group (ASV observed, p = 0.001; ASV Shannon, p = 0.001; ASV Faith's PD, p = 0.02; Mann–Whitney U-test, BH adjusted p-value). In contrast, KO observed, KO Shannon, Pathway observed, and Pathway Shannon indices tended to increase in the stoma group (KO observed, p = 0.2; KO Shannon, p = 0.1; Pathway observed, p = 0.1; Pathway Shannon, p = 0.06) (Figure 5A). These results indicated that a stoma decreased taxonomic diversity but increased functional diversity.

Next, to elucidate the responsible genera and functions, we used effect size and presence per sample (p-value; Fisher's exact test) in the stoma and non-stoma cases (Figures 5B, C). We divided their features into three categories: >99% presence, 1–99% presence, and<1% presence, and defined them as "Common", "Uncommon", and "Rare", respectively. "Uncommon genera" and "Uncommon Pathway" showed significant differences of presence/absence ratio. Importantly, the effect size of "Uncommon genera" and "Uncommon Pathway" tended to coincide with the increase or decrease of the taxonomic and functional diversity in Figure 5A, respectively. These results suggested that "Uncommon genera" and "Uncommon Pathway" were responsible for increasing or decreasing diversity.

Notably, we observed contradictory tendencies between taxonomic and functional diversities (KO and pathway). We used PICRUSt2 to predict potential KOs and pathways, and the PICRUSt2 algorithm estimated the gene function of the microbiota by mapping ASVs onto a phylogenetic tree of taxa whose genomes have been sequenced. We examined the predicted KO copy numbers per ASV from the PICRUSt2 output. We identified the genus responsible for pathway richness among the features with a p-value of Fisher's exact test< 0.1. In Supplementary Figure 5, when the z-score was higher, there was a strong correlation between microbes and pathways. Most "Uncommon genera" did not influence the "Uncommon Pathway",and several "Uncommon genera" and "Rare genera" such as *Acinetobacter*, *Pseudomonas*, and *Campylobacter* related to xenobiotic degradation, one of the "Uncommon Pathway". These results illustrate that the stoma reduced many microbes with common functions but increased a few microbes with unique functions, which exemplified the conflicting changes in taxonomic and functional diversities.

10.3389

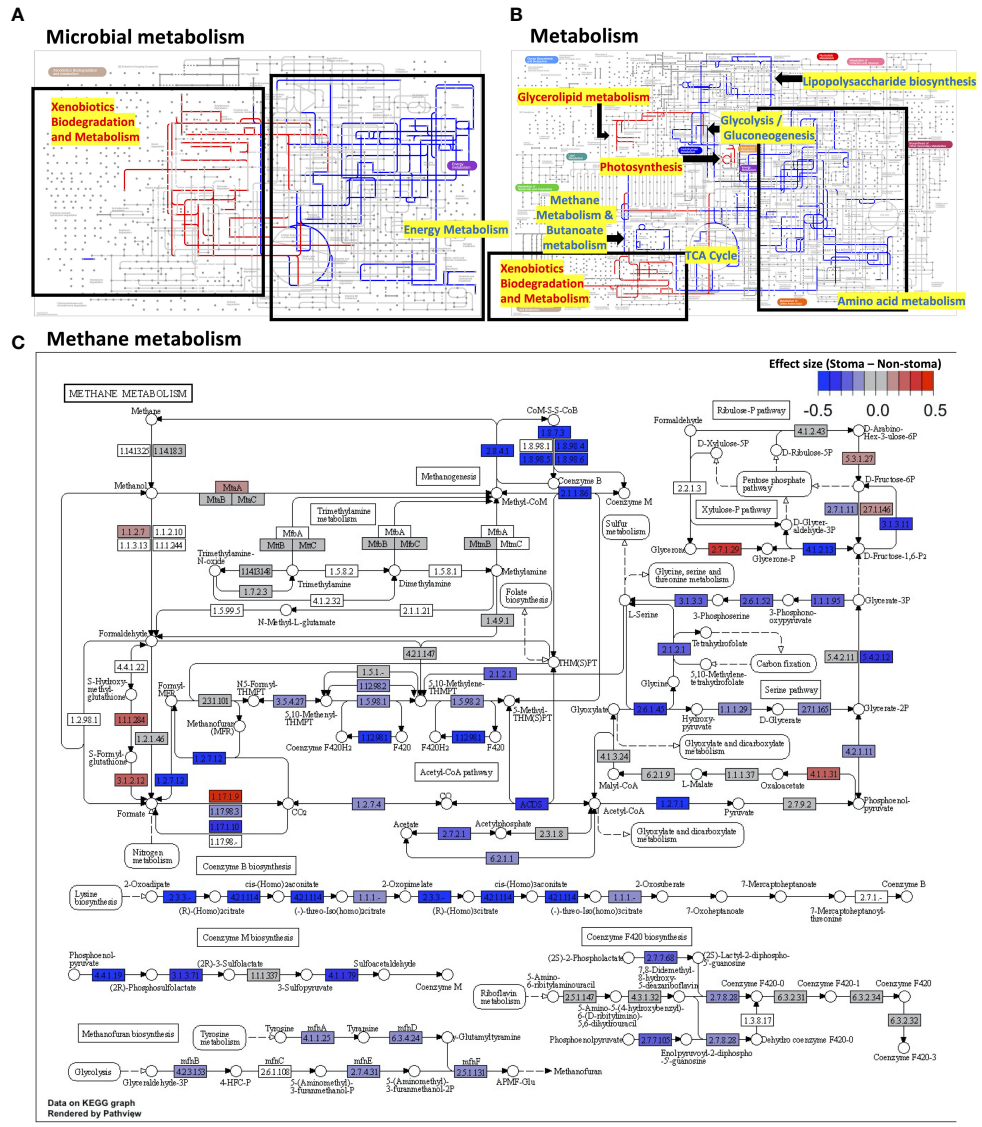

FIGURE 4
The difference in gene functions between the stoma group and non-stoma group. (**A**) Microbial pathway enrichment analysis results metabolism using Inath. The red edges indicate enrichment in patients with a stoma, the blue indicates enrichment in patients the light gray indicates no significant difference, and the gray indicates pathways do not present in both groups. Pathways with indicate that they were not covered by GSEA. (**B**) Overall metabolism pathway. (**C**) Methane metabolism. The color represents t the comparison (with a stoma vs. without a stoma) in ALDEx2_GSEA: Gene Set Enrichment Analysis.

4 Discussion

Stoma construction is a medical procedure performed in patients with colon cancer and is widely used worldwide (Amersi et al., 2004). However, there have been no reports analyzing changes in fecal microbiota in the presence or absence of a stoma. In this study, we used 16S rRNA gene sequencing analysis of 119 samples to infer fecal taxonomic composition and function and compared them between patients with and without a stoma.

Our metagenomic analysis revealed that a stoma decreased taxonomic diversity and obligate anaerobes, such as *Akkermansia*, *Intestinimonas*, and *Alistipes*. In addition, methane-producing archaea, such as *Methanobrevibacter* and *Methanosphaera*, were not detected in the stoma group, and the gene functions related to methane synthesis were consistently reduced in patients with a stoma. The taxonomic diversity (e.g., ASV observed, ASV Shannon, and ASV Faith's PD) of fecal microbiota increased as it transitioned through the descending colon (Müller et al., 2020). *Alistipes* and *Akkermansia* have been

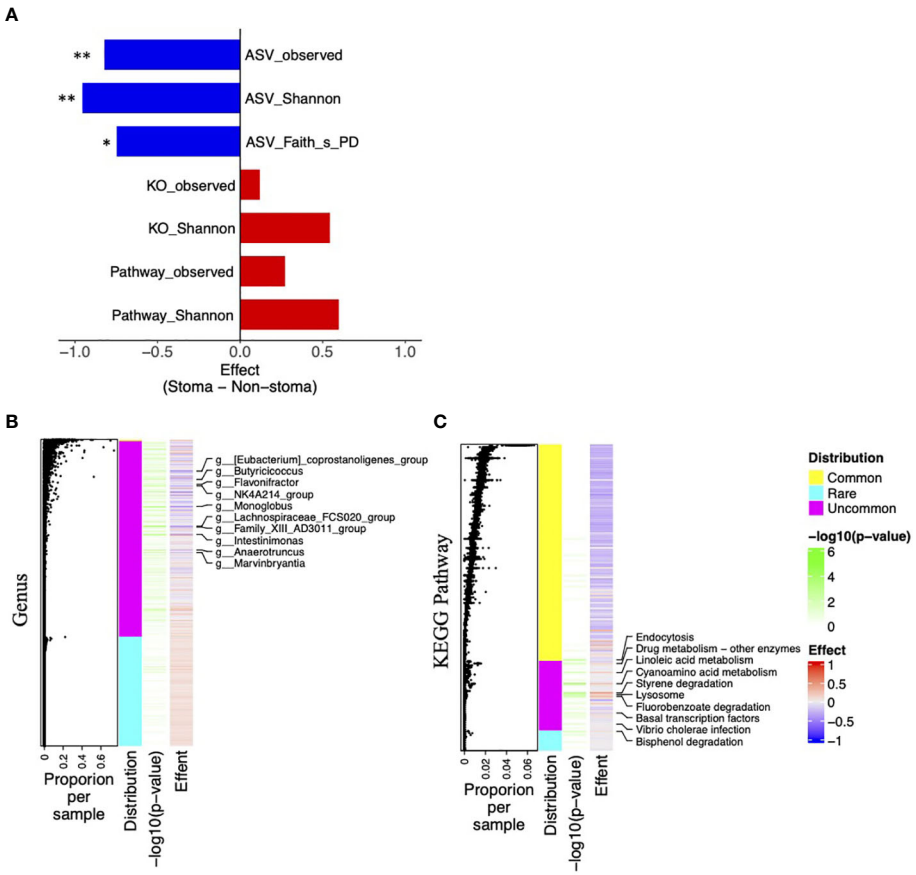

FIGURE 5
Difference of taxonomic and functional diversity indices between the stoma group and non-stoma group and distribution of features. **(A)** Bar plot of effect size when comparing taxonomic (ASV) and functional (KO and Pathway) diversity indices between two groups. Significance differences between the two groups were tested using the Mann–Whitney U test. * $p< 0.05$, ** $p< 0.01$. **(B)** Heatmap of taxonomic genus-level effect sizes, annotated with jitter plots representing average composition per sample of features. Significance differences between the two groups were tested using Fisher's exact test. The labels on the vertical axis indicate genera with p-values less than 0.05. **(C)** Pathway effect sizes.

reported to be preferentially present in the intestinal mucosa on the left side rather than on the right side (Flemer et al., 2017). Moreover, methanogens were more prevalent in the left-side colon than in the right-side (Macfarlane et al., 1992). Genes involved in methane production have also been reported to be overrepresented in the left colon (Nava et al., 2012). A stoma creates an opening of the ileum or colon; that is, patients with a stoma reduce fecal transit of the distal colorectum, where diversity of microbiota is high, and certain bacteria are present in higher abundance. Consistent with these findings, our results showed that fecal taxonomic diversity and *Alistipes* tended to decrease when the stoma was located in the proximal gastrointestinal tract compared with that in the distal region. Furthermore, a comparison based on the Bristol scale showed that stool form and hardness were strongly correlated with fecal bacterial richness, *Akkermansia*, and *Methanobrevibacter* (Vandeputte et al., 2016). We showed that most fecal samples from patients with a stoma had soft stools. Therefore, microbiota and taxonomic diversity changes in patients with a stoma may be attributed to low stool hardness and a decreased fecal transition period in the left-side colonic region. Notably, our observations also implied that the overall population of obligate anaerobes was lower in patients with a stoma. A study in mouse models showed that luminal oxygen partial pressure decreased from the proximal to the distal colon (He et al., 1999). As mentioned above, the feces of patients with a stoma transit less to the distal colon region. Altogether, it is suggested that the feces of patients with a stoma do not transit to the colonic region with the lowest partial oxygen pressure in the gut; therefore, we observed a decreasing population of obligate anaerobes. These previous reports and our observations imply that the changes in the microbiota of patients with a stoma are attributed to their intestinal environment rather than that of the stoma pouch.

Interestingly, functional diversity and many gene functions related to xenobiotics, such as styrene, xylene, and benzoate degradation, were enriched in patients with a stoma. We also

found an increase in aerobic bacteria such as *Enterococcus*, *Pseudomonas*, and *Acinetobacter* in patients with a stoma. These bacteria are responsible for the gene functions related to xenobiotics (Desouky, 2003; Fernández et al., 2009; Saffarian et al., 2017) and can cause wound and suppurative infections (Bryanti and Hammond, 1974; Mihu et al., 2010; Doughari et al., 2011; Kim et al., 2015). In addition, many patients (21%–70%) with a stoma have complications, including peristomal infection (Shabbir and Britton, 2010). According to a previous study on surgical site infections due to stoma reversal surgery, these patients might have been infected with *Enterococcus* and *Pseudomonas* (Liang et al., 2013). Combining these observations, a high abundance of *Pseudomonas*, *Acinetobacter*, and *Enterococcus* in feces was associated with peristomal infection.

Several reports have shown that fecal taxonomic diversity is positively correlated with the efficacy of immune checkpoint inhibitors (ICI) in patients with non-small cell lung cancer (NSCLC), renal cell carcinoma (RCC), and malignant melanoma (MMe) (Gopalakrishnan et al., 2018; Matson et al., 2018; Routy et al., 2018). At each taxon level, ICI responders with NSCLC and RCC had a higher abundance of *Akkermansia, Intestinimonas*, and *Alistipes* (Routy et al., 2018; Derosa et al., 2022), and the responders with MMe and NSCLC also had many methanogenic archaea and *Methanobrevibacter*, respectively (Simpson et al., 2020; Song et al., 2020). In addition, *Alistipes* positively affects the efficiency of CpG-oligonucleotide immunotherapy in CRC (Iida et al., 2013). Many of these bacteria are short-chain fatty acids (SCFAs) producers (Derrien et al., 2004; Bui et al., 2015; Venegas et al., 2019; Parker et al., 2020). In this study, SCFA-related gene function was also coherently decreased in stoma cases. SCFA-producing bacteria and methanogens are known to be involved in host immunomodulation (Bang et al., 2014; Chaudhary et al., 2018; Venegas et al., 2019), which may be a mechanism that influences tumor invasion immunity in cancer therapy (Nomura et al., 2020; Luu et al., 2021). This indicates that the relative abundance of the so-called favorable bacteria in cancer immunotherapy is reduced in the feces of patients with a stoma.

This study has several limitations. First, there may be a time gap between defecation and stool collection in patients with a stoma, and to our knowledge, no study has evaluated how fecal microbial composition changes when feces are left in a clean and enclosed space such as a stoma pouch. We have already discussed that the changes in the fecal microbiota were caused by a decrease in the fecal transit period in the left-side colonic region, low stool hardness, and peristomal infection. Therefore, these changes may not be due to the exposure time in the environment of the stoma pouch. Furthermore, in this study, the small sample size of patients with a stoma was not sufficient to detect stoma location-specific microbiota characteristics. A more detailed discussion may be possible if a larger sample size of patients with a stoma is available.

In conclusion, we investigated the fecal microbiota of patients with CRC and compared the stoma and non-stoma groups. These results showed a significant difference in the fecal microbiota of patients with stoma compared with those without a stoma, and observed differential microbiota was related to the efficacy of cancer immunotherapy. Thus, we caution against interpreting the results of the gut microbiota analysis in patients with a stoma.

Data availability statement

The datasets presented in this study can be found in online repositories. The names of the repository/repositories and accession number(s) can be found below: https://qindao.hgc.jp/cgi-bin/files/Sakai_et_al_readcount_table.xlsx.

Ethics statement

The studies involving human participants were reviewed and approved by University Hospital Medical Information Network (UMIN000036749). The patients/participants provided their written informed consent to participate in this study.

Author contributions

SS, MA, and RY designed the study, and performed the research, analyzed the data, and contributed equally. SS, MA, RY, YH, SK, KS, SH, AY, TF, YN, KN, HB, TY, and KT provided scientific insight into this study. SS wrote the manuscript. RY and KT supervised the study and revised the manuscript accordingly. All members have read the manuscript and approved the content.

Funding

This study was supported by the National Cancer Center Research and Development Fund (grant number 31-A-10). This study was also supported by AMED Seeds A (grant number CPOT, 21-A-33).

Acknowledgments

We thank all members of the SCRUM-Japan and MONSTAR teams. We also thank the lab members.

Conflict of interest

SK reports honoraria from Eli Lilly, Taiho, Ono, Bristol-Myers Squibb, Chugai, Bayer, Merck Serono, Daiichi Sankyo, Eisai; and research funding from Taiho, Eli Lilly, MSD, Chugai, Nobelpharma, Ono, Daiichi Sankyo, and Yansen.TD reports honoraria from Sawai Pharmaceutical; speakers' bureau from Sysmex; and research funding from MSD and Ono Pharmaceutical. HY reports honoraria from Taiho Pharmaceutical, Chugai, Bristol-Myers Squibb, Daiichi-Sankyo, Terumo, Eli Lilly Japan, Merck Biopharma, Yakult Honsha, and Bayer Yakuhin; and research funding from MSD, Daiichi-Sankyo, and Ono Pharmaceutical. MG reports honoraria from Yakult Honsha, Taiho Pharmaceutical, Daiichi-Sankyo, Eisai, and Ono Pharmaceutical; and research funding from Chugai, Taiho Pharmaceutical, Nippon Kayaku, Ono Pharmaceutical, and Eli Lilly. YK reports honoraria from Asahi Kasei Pharma, Bayer Yakuhin, Bristol-Myers Squibb., Chugai, Daiichi-Sankyo, Eli Lilly, Kyowa Kirin, Medical Review, Merck Biopharma, Mitsubishi Tanabe Pharma, Moroo, Nipro, Ono Pharmaceutical, Pfizer Japan, Sanofi, Shire Japan, and Taiho Pharmaceutical; and research funding from A2 Healthcare, Asahi Kasei Pharma, Astellas Pharma, Bayer Yakuhin, Daiichi-Sankyo, Sumitomo Dainippon Pharma, Eisai, Mediscience Planning, NanoCarrier, Ono Pharmaceutical, Parexel International, Sanofi-aventis, Shionogi & Co., Ltd., Taiho Pharmaceutical, Yakult Honsha, Incyte, IQVIA, MSD, Nippon Zoki Pharmaceutical, Syneos Health Clinical, and Sysmex. YN reports research grants from Taiho Pharmaceutical, Chugai Pharmaceutical, Guardant Health, Genomedia, Daiichi Sankyo, Seagen, and Roche Diagnostics. HB reports honoraria from Taiho Pharmaceutical, Lilly Japan, Takeda Pharmaceutical, Chugai, Sanofi, and Yakult Honsha: and research funding from AstraZeneca and Sysmex. TY reports honoraria from Taiho Pharmaceutical, Chugai Pharmaceutical, Eli Lilly, Merck Biopharma, Bayer Yakuhin, Ono Pharmaceutical, and MSD; and research funding from Ono Pharmaceutical, Sanofi, Daiichi Sankyo, PAREXEL International, Pfizer Japan, Taiho Pharmaceutical, MSD, Amgen, Genomedia, Sysmex, Chugai Pharmaceutical, and Nippon Boehringer Ingelheim KT reports honoraria from SRL Diagnostics, DNA Chip Research, Chugai, Novartis, Takeda, MSD, Sysmex, Nippon Kayaku, Illumina, Fujitsu, Varian Medical Systems, Miyarisan Pharmaceutical, Bristol-Myers Squibb, AstraZeneca, and Novartis. RY reports honoraria from Takeda Pharmaceutical.

The remaining authors declare that the research was conducted in the absence of any commercial or financial relationships that could be constructed as a potential conflict of interest.

Publisher's note

Supplementary material

The Supplementary Material for this article can be found online at: https://www.frontiersin.org/articles/10.3389/fcimb.2022.925444/full#supplementary-material

References

Amersi, F., Stamos, M. J., and Ko, C. Y. (2004). Palliative care for colorectal cancer. *Surg. Oncol. Clin. N. Am.* 13, 467–477. doi: 10.1016/j.soc.2004.03.002

Bang, C., Weidenbach, K., Gutsmann, T., Heine, H., and Schmitz, R. A. (2014). The intestinal archaea methanosphaera stadtmanae and methanobrevibacter smithii activate human dendritic cells. *PloS One* 9, e99411. doi: 10.1371/journal.pone.0099411

Baruch, E. N., Youngster, I., Ben-Betzalel, G., Ortenberg, R., Lahat, A., Katz, L., et al. (2021). Fecal microbiota transplant promotes response in immunotherapy-refractory melanoma patients. *Science* 371, 602–609. doi: 10.1126/science.abb5920

Bolyen, E., Rideout, J. R., Dillon, M. R., Bokulich, N. A., Abnet, C. C., Al-Ghalith, G. A., et al. (2019). Reproducible, interactive, scalable and extensible microbiome data science using QIIME 2. *Nat. Biotechnol.* 37, 850–852. doi: 10.1038/s41587-019-0190-3

Brill, B., Amir, A., and Heller, R. (2019). Testing for differential abundance in compositional counts data, with application to microbiome studies. *arXiv. preprint.* arXiv:1904.08937.

Bryanti, R. E., and Hammond, D. (1974). Interaction of purulent material with antibiotics used to treat pseudomonas infections. *Antimicrob. Agents Chemother.* 6, 702–707. doi: 10.1128/AAC.6.6.702

Bui, T. P. N., Ritari, J., Boeren, S., de Waard, P., Plugge, C. M., and de Vos, W. M. (2015). Production of butyrate from lysine and the amadori product fructoselysine by a human gut commensal. *Nat. Commun.* 6, 1–10. doi: 10.1038/ncomms10062

Chaudhary, P. P., Conway, P. L., and Schlundt, J. (2018). Methanogens in humans: potentially beneficial or harmful for health. *Appl. Microbiol. Biotechnol.* 102, 3095–3104. doi: 10.1007/s00253-018-8871-2

Chuang, Y. C., Tseng, J. C., Huang, L. R., Huang, C. M., Huang, C. Y. F., and Chuang, T. H. (2020). Adjuvant effect of toll-like receptor 9 activation on cancer immunotherapy using checkpoint blockade. *Front. Immunol.* 11. doi: 10.3389/fimmu.2020.01075

Davar, D., Dzutsev, A. K., McCulloch, J. A., Rodrigues, R. R., Chauvin, J.-M., Morrison, R. M., et al. (2021). Fecal microbiota transplant overcomes resistance to anti-PD-1 therapy in melanoma patients. *Science* 371, 595–602. doi: 10.1126/science.abf3363

Derosa, L., Routy, B., Thomas, A. M., Iebba, V., Zalcman, G., Friard, S., et al. (2022). Intestinal akkermansia muciniphila predicts clinical response to PD-1 blockade in patients with advanced non-small-cell lung cancer. *Nat. Med.* 28, 315–324. doi: 10.1038/s41591-021-01655-5

Derrien, M., Vaughan, E. E., Plugge, C. M., and de Vos, W. M. (2004). Akkermansia municiphila gen. nov., sp. nov., a human intestinal mucin-degrading bacterium. *Int. J. Syst. Evol. Microbiol.* 54, 1469–1476. doi: 10.1099/ijs.0.02873-0

Desouky, A.-E.-H. (2003). Acinetobacter: environmental and biotechnological applications. *Afr. J. Biotechnol.* 2, 71–74. doi: 10.5897/AJB2003.000-1014

Doughari, H. J., Ndakidemi, P. A., Human, I. S., and Benade, S. (2011). The ecology, biology and pathogenesis of acinetobacter spp.: An overview. *Microbes Environ.* 26, 101–112. doi: 10.1264/jsme2.ME10179

Douglas, G. M., Maffei, V. J., Zaneveld, J. R., Yurgel, S. N., Brown, J. R., Taylor, C. M., et al. (2020). PICRUSt2 for prediction of metagenome functions. *Nat. Biotechnol.* 38, 669–673. doi: 10.1038/s41587-020-0550-z

Fernandes, A. D., Macklaim, J. M., Linn, T. G., Reid, G., and Gloor, G. B. (2013). ANOVA-like differential expression (ALDEx) analysis for mixed population RNA-seq. *PloS One* 8(7):e67019. doi: 10.1371/journal.pone.0067019

Fernandes, A. D., Reid, J. N., Macklaim, J. M., Mcmurrough, T. A., Edgell, D. R., and Gloor, G. B. (2014). Unifying the analysis of high-throughput sequencing datasets: characterizing RNA-seq, 16S rRNA gene sequencing and selective growth experiments by compositional data analysis. *Microbiome* 2, 1–13. doi: 10.1186/2049-2618-2-15

Fernández, M., Duque, E., Pizarro-Tobías, P., van Dillewijn, P., Wittich, R. M., and Ramos, J. L. (2009). Microbial responses to xenobiotic compounds. identification of genes that allow pseudomonas putida KT2440 to cope with 2,4,6-trinitrotoluene. *Microb. Biotechnol.* 2, 287–294. doi: 10.1111/j.1751-7915.2009.00085.x

Flemer, B., Lynch, D. B., Brown, J. M. R., Jeffery, I. B., Ryan, F. J., Claesson, M. J., et al. (2017). Tumour-associated and non-tumour-associated microbiota in colorectal cancer. *Gut* 66, 633–643. doi: 10.1136/gutjnl-2015-309595

Fortune Business Insights (2020). Available at: https://www.fortunebusinessinsights.com/press-release/amp/ostomy-stoma-care-and-accessories-market-9658 (Accessed February 2, 2022).

Foster, Z. S. L., Sharpton, T. J., and Grünwald, N. J. (2017). Metacoder: An r package for visualization and manipulation of community taxonomic diversity data. *PloS Comput. Biol.* 13(2):1005404. doi: 10.1371/journal.pcbi.1005404

Gopalakrishnan, V., Spencer, C. N., Nezi, L., Reuben, A., Andrews, M. C., Karpinets, T., et al. (2018). Gut microbiome modulates response to anti-PD-1 immunotherapy in melanoma patients. *Science* 359, 97–103. doi: 10.1126/science.aan4236

Haghi, F., Goli, E., Mirzaei, B., and Zeighami, H. (2019). The association between fecal enterotoxigenic b. fragilis with colorectal cancer. *BMC Cancer.* 19, 879. doi: 10.1186/s12885-019-6115-1

He, G., Shankar, R. A., Chzhan, M., Samouilov, A., Kuppusamy, P., and Zweier, J. L. (1999). Noninvasive measurement of anatomic structure and intraluminal oxygenation in the gastrointestinal tract of living mice with spatial and spectral EPR imaging (oximetrymagnetic resonance imagingmetabolismactivated charcoalfree radical). *Proc. Natl. Acad. Sci.* 96, 4586–4591. doi: 10.1073/pnas.96.8.4586

Iida, N., Dzutsev, A., Stewart, C. A., Smith, L., Bouladoux, N., Weingarten, R. A., et al. (2013). Commensal bacteria control cancer response to therapy by modulating the tumor microenvironment. *Science* 342, 967–970. doi: 10.1126/science.1240527

Inamori, K., Togashi, Y., Fukuoka, S., Akagi, K., Ogasawara, K., Irie, T., et al. (2021). Importance of lymph node immune responses in MSI-H/dMMR colorectal cancer. *JCI Insight* 6(9):e137365. doi: 10.1172/jci.insight.137365

Iyadorai, T., Mariappan, V., Vellasamy, K. M., Wanyiri, J. W., Roslani, A. C., Lee, G. K., et al. (2020). Prevalence and association of pks+ escherichia coli with colorectal cancer in patients at the university Malaya medical centre, Malaysia. *PloS One* 15(1):e0228217. doi: 10.1371/journal.pone.0228217

James, K. R., Gomes, T., Elmentaite, R., Kumar, N., Gulliver, E. L., King, H. W., et al. (2020). Distinct microbial and immune niches of the human colon. *Nat. Immunol.* 21, 343–353. doi: 10.1038/s41590-020-0602-z

Kim, M., Christley, S., Khodarev, N. N., Fleming, I., Huang, Y., Chang, E., et al. (2015). Pseudomonas aeruginosa wound infection involves activation of its iron acquisition system in response to fascial contact. *J. Trauma Acute. Care Surg.* 78, 823–829. doi: 10.1097/TA.0000000000000574

Kim, J., and Lee, H. K. (2022). Potential role of the gut microbiome in colorectal cancer progression. *Front. Immunol.* 12. doi: 10.3389/fimmu.2021.807648

Liang, M. K., Li, L. T., Avellaneda, A., Moffett, J. M., Hicks, S. C., and Awad, S. S. (2013). Outcomes and predictors of incisional surgical site infection in stoma reversal. *JAMA Surg.* 148, 183–189. doi: 10.1001/jamasurgery.2013.411

Long, X., Wong, C. C., Tong, L., Chu, E. S. H., Ho Szeto, C., Go, M. Y. Y., et al. (2019). Peptostreptococcus anaerobius promotes colorectal carcinogenesis and modulates tumour immunity. *Nat. Microbiol.* 4, 2319–2330. doi: 10.1038/s41564-019-0541-3

Luo, W., and Brouwer, C. (2013). Pathview: An R/Bioconductor package for pathway-based data integration and visualization. *Bioinformatics* 29, 1830–1831. doi: 10.1093/bioinformatics/btt285

Luu, M., Riester, Z., Baldrich, A., Reichardt, N., Yuille, S., Busetti, A., et al. (2021). Microbial short-chain fatty acids modulate CD8+ T cell responses and improve adoptive immunotherapy for cancer. *Nat. Commun.* 12, 1–12. doi: 10.1038/s41467-021-24331-1

Macfarlane, G. T., Gibson, G. R., and Cummings, J. H. (1992). Comparison of fermentation reactions in different regions of the human colon. *J. Appl. Bacteriol.* 72, 57–64. doi: 10.1111/j.1365-2672.1992.tb04882.x

Matson, V., Fessler, J., Bao, R., Chongsuwat, T., Zha, Y., Alegre, M.-L., et al. (2018). The commensal microbiome is associated with anti-PD-1 efficacy in metastatic melanoma patients. *Science* 359, 104–108. doi: 10.1126/science.aao3290

Mihu, M. R., Sandkovsky, U., Han, G., Friedman, J. M., Nosanchuk, J. D., and Martinez, L. R. (2010). Nitric oxide releasing nanoparticles are therapeutic for acinetobacter baumannii wound infections. *Virulence* 1, 62–67. doi: 10.4161/viru.1.2.10038

Mukherjee, S., Stamatis, D., Bertsch, J., Ovchinnikova, G., Sundaramurthi, J. C., Lee, J., et al. (2021). Genomes OnLine database (GOLD) v.8: Overview and updates. *Nucleic Acids Res.* 49, D723–D733. doi: 10.1093/nar/gkaa983

Müller, M., Gerben, X., Hermes, D. A., Emanuel, X., Canfora, E., Smidt, X. H., et al. (2020). Distal colonic transit is linked to gut microbiota diversity and microbial fermentation in humans with slow colonic transit. *Am. J. Physiol. Gastrointest. Liver. Physiol.* 318, 361–369. doi: 10.1152/ajpgi.00283.2019.-Longer

Nakamura, Y., Fujisawa, T., Taniguchi, H., Bando, H., Okamoto, W., Tsuchihara, K., et al. (2021). SCRUM-Japan GI-SCREEN and MONSTAR-SCREEN: Path to the realization of biomarker-guided precision oncology in advanced solid tumors. *Cancer Sci.* 112, 4425–4432. doi: 10.1111/cas.15132

Nava, G. M., Carbonero, F., Croix, J. A., Greenberg, E., and Gaskins, H. R. (2012). Abundance and diversity of mucosa-associated hydrogenotrophic microbes in the healthy human colon. *ISME. J.* 6, 57–70. doi: 10.1038/ismej.2011.90

Nomura, M., Nagatomo, R., Doi, K., Shimizu, J., Baba, K., Saito, T., et al. (2020). Association of short-chain fatty acids in the gut microbiome with clinical response to treatment with nivolumab or pembrolizumab in patients with solid cancer tumors. *JAMA Netw. Open* 3, e202895. doi: 10.1001/jamanetworkopen.2020.2895

Parker, B. J., Wearsch, P. A., Veloo, A. C. M., and Rodriguez-Palacios, A. (2020). The genus alistipes: gut bacteria with emerging implications to inflammation, cancer, and mental health. *Front. Immunol.* 11. doi: 10.3389/fimmu.2020.00906

Pickard, C., Thomas, R., Robertson, I., and Macdonald, A. (2018). Ostomy creation for palliative care of patients with nonresectable colorectal cancer and bowel obstruction. *J. Wound Ostomy. Continence. Nurs.* 45, 239–241. doi: 10.1097/WON.0000000000000424

Routy, B., le Chatelier, E., Derosa, L., Duong, C. P. M., Alou, M. T., Daillère, R., et al. (2018). Gut microbiome influences efficacy of PD-1-based immunotherapy against epithelial tumors. *Science* 359, 91–97. doi: 10.1126/science.aan3706

Saffarian, A., Touchon, M., Mulet, C., Tournebize, R., Passet, V., Brisse, S., et al. (2017). Comparative genomic analysis of acinetobacter strains isolated from murine colonic crypts. *BMC Genom.* 18, 1–12. doi: 10.1186/s12864-017-3925-x

Shabbir, J., and Britton, D. C. (2010). Stoma complications: a literature overview. *Colorectal. Dis.* 12, 958–964. doi: 10.1111/j.1463-1318.2009.02006.x

Simpson, R., Batten, M., Shanahan, E., Read, M., Silva, I., Aangelatos, A., et al. (2020). Intestinal microbiota predict response and toxicities during anti-PD-1/anti-CTLA-4 immunotherapy. *Pathology* 52, S127. doi: 10.1016/j.pathol.2020.01.433

Song, P., Yang, D., Wang, H., Cui, X., Si, X., Zhang, X., et al. (2020). Relationship between intestinal flora structure and metabolite analysis and immunotherapy efficacy in Chinese NSCLC patients. *Thorac. Cancer.* 11, 1621–1632. doi: 10.1111/1759-7714.13442

Ternes, D., Karta, J., Tsenkova, M., Wilmes, P., Haan, S., and Letellier, E. (2020). Microbiome in colorectal cancer: how to get from meta-omics to mechanism? *Trends Microbiol.* 28, 401–423. doi: 10.1016/j.tim.2020.01.001

Vandeputte, D., Falony, G., Vieira-Silva, S., Tito, R. Y., Joossens, M., and Raes, J. (2016). Stool consistency is strongly associated with gut microbiota richness and composition, enterotypes and bacterial growth rates. *Gut* 65, 57–62. doi: 10.1136/gutjnl-2015-309618

Venegas, D. P., de la Fuente, M. K., Landskron, G., González, M. J., Quera, R., Dijkstra, G., et al. (2019). Short chain fatty acids (SCFAs)-mediated gut epithelial and immune regulation and its relevance for inflammatory bowel diseases. *Front. Immunol.* 10. doi: 10.3389/fimmu.2019.00277

Verweij, N. M., Hamaker, M. E., Zimmerman, D. D. E., van Loon, Y. T., van den Bos, F., Pronk, A., et al. (2017). The impact of an ostomy on older colorectal cancer

patients: a cross-sectional survey. *Int. J. Colorectal. Dis.* 32, 89–94. doi: 10.1007/s00384-016-2665-8

Verweij, N. M., Schiphorst, A. H. W., Maas, H. A., Zimmerman, D. D. E., van den Bos, F., Pronk, A., et al. (2016). Colorectal cancer resections in the oldest old between 2011 and 2012 in the Netherlands. *Ann. Surg. Oncol.* 23, 1875–1882. doi: 10.1245/s10434-015-5085-z

Xi, Y., and Xu, P. (2021). Global colorectal cancer burden in 2020 and projections to 2040. *Transl. Oncol.* 14, 101174. doi: 10.1016/j.tranon.2021.101174

Yu, T. C., Guo, F., Yu, Y., Sun, T., Ma, D., Han, J., et al. (2017). Fusobacterium nucleatum promotes chemoresistance to colorectal cancer by modulating autophagy. *Cell* 170, 548–563.e16. doi: 10.1016/j.cell.2017.07.008

frontiers | Frontiers in Cellular and Infection Microbiology

TYPE Original Research
PUBLISHED 20 September 2022
DOI 10.3389/fcimb.2022.943859

OPEN ACCESS

EDITED BY
Sathyavathi Sundararaju,
Sidra Medicine, Qatar

REVIEWED BY
Anju Sharma,
Sidra Medicine, Qatar
Sathiya Pandi Narayanan,
Sidra Medicine, Qatar

*CORRESPONDENCE
Hongzhi Wang
wanghz@hfcas.ac.cn
Hongcang Gu
gu_hongcang@cmpt.ac.cn

†These authors have contributed equally to this work

SPECIALTY SECTION
This article was submitted to Clinical Microbiology, a section of the journal Frontiers in Cellular and Infection Microbiology

RECEIVED 14 May 2022
ACCEPTED 22 August 2022
PUBLISHED 20 September 2022

CITATION
Deng Q, Cao Y, Wan X, Wang B, Sun A, Wang H, Wang Y, Wang H and Gu H (2022) Nanopore-based metagenomic sequencing for the rapid and precise detection of pathogens among immunocompromised cancer patients with suspected infections. *Front. Cell. Infect. Microbiol.* 12:943859. doi: 10.3389/fcimb.2022.943859

Nanopore-based metagenomic sequencing for the rapid and precise detection of pathogens among immunocompromised cancer patients with suspected infections

Qingmei Deng[1,2,3†], Yongqing Cao[4†], Xiaofeng Wan[1,3], Bin Wang[5], Aimin Sun[1,3], Huanzhong Wang[1,3], Yunfei Wang[5], Hongzhi Wang[1,2,3*] and Hongcang Gu[1,2,3*]

[1]Anhui Province Key Laboratory of Medical Physics and Technology, Institute of Health and Medical Technology, Hefei Institutes of Physical Science, Chinese Academy of Science, Hefei, China, [2]Science Island Branch, Graduate School of University of Science and Technology of China, Hefei, China, [3]Hefei Cancer Hospital, Chinese Academy of Sciences, Hefei, China, [4]The Cancer Hospital of the University of Chinese Academy of Sciences, Institute of Basic Medicine and Cancer, Chinese Academy of Sciences, Hangzhou, China., [5]Zhejiang ShengTing Biotechnology Company, Hangzhou, China

Cancer patients are at high risk of infections and infection-related mortality; thereby, prompt diagnosis and precise anti-infectives treatment are critical. This study aimed to evaluate the performance of nanopore amplicon sequencing in identifying microbial agents among immunocompromised cancer patients with suspected infections. This prospective study enlisted 56 immunocompromised cancer patients with suspected infections. Their body fluid samples such as sputum and blood were collected, and potential microbial agents were detected in parallel by nanopore amplicon sequencing and the conventional culture method. Among the 56 body fluid samples, 47 (83.9%) samples were identified to have at least one pathogen by nanopore amplicon sequencing, but only 25 (44.6%) samples exhibited a positive finding by culture. Among 31 culture-negative samples, nanopore amplicon sequencing successfully detected pathogens in 22 samples (71.0%). Nanopore amplicon sequencing showed a higher sensitivity in pathogen detection than that of the conventional culture method (83.9% vs. 44.6%, P<0.001), and this advantage both existed in blood samples (38.5% vs. 0%, P=0.039) and non-blood samples (97.7% vs. 58.1%, P<0.001). Compared with the culture method, nanopore amplicon sequencing illustrated more samples with bacterial infections (P<0.001), infections from fastidious pathogens (P=0.006), and co-infections (P<0.001). The mean turnaround time for nanopore amplicon sequencing was about 17.5 hours, which was shorter than that of the conventional culture assay. This study suggested nanopore amplicon sequencing as a rapid and precise method for detecting pathogens

among immunocompromised cancer patients with suspected infections. The novel and high-sensitive method will improve the outcomes of immunocompromised cancer patients by facilitating the prompt diagnosis of infections and precise anti-infectives treatment.

KEYWORDS

cancer, pathogen detection, infections, metagenomic sequencing, nanopore amplicon sequencing

Introduction

Cancer causes serious harm to human health worldwide and has long been a significant challenge in biomedical and clinical research (Siegel et al., 2021). Infections are common among cancer patients and are accountable for most noncancer causes of death (Zaorsky et al., 2017; Lehrnbecher et al., 2021). Some clinical observational studies revealed that cancer patients with common bacterial infections had a 2-fold increased risk of death than those without infections (Brand et al., 2016; Hjelholt et al., 2021). Anti-cancer therapies such as conventional chemotherapy, radiotherapy, and treatments using immune checkpoint inhibitors (ICIs) or targeted drugs can result in the immunocompromised status among cancer patients, increasing the risk of infections (Eilers et al., 2010; Weil et al., 2018; Malek et al., 2021). Because of the high prevalence and the adverse outcomes, infections represent a substantially challenging issue in the management of cancer patients, especially for those with immunocompromised status (Casto et al., 2021). Therefore, there is currently an urgent need to improve both the surveillance and treatments for infections among cancer patients.

Early diagnosis and effective therapy with precise anti-infectives are critical to improving the outcomes of patients suffering from infections (Van Cutsem et al., 2016; Garcia-Vidal et al., 2021). Conventional culture-based pathogen detection methods have defects such as lower sensitivity and longer turnaround time, thus having limited roles in rapidly and accurately detecting pathogens (Peri et al., 2022). Recently, multiple novel microbiological detection techniques have been developed, and some show great potential in the diagnosis of infections in terms of turnaround time, accuracy, and antimicrobial resistance (Henderson et al., 2021; Peri et al., 2021b). The nanopore-sequencing developed based on the Oxford Nanopore Technologies is one representative of the third-generation sequencing techniques, and its role in the identification of pathogens has gained increasing attention in recent years (Ferreira et al., 2021). Nanopore-sequencing presents many significant merits, such as higher sensitivity, better accuracy, and less turnaround time than the routine culture-based methods, thus enabling patients to receive earlier and more precise antimicrobial therapies (Dippenaar et al., 2021; Noone et al., 2021). However, the application of nanopore amplicon sequencing in detecting pathogens among immunocompromised cancer patients has not been evaluated. Cancer patients, especially those with immunocompromised status, are at high risk of infections. The early and accurate identification of pathogens by nanopore amplicon sequencing will undoubtedly benefit those patients. This study evaluated its performance in detecting pathogens among immunocompromised cancer patients with suspected infections, and a side-by-side comparison with the culture method was demonstrated.

Methods

Patient enrolment

This prospective study was designed to evaluate the performance of nanopore amplicon sequencing in detecting pathogens among immunocompromised cancer patients with suspected infections. The schematic workflow of pathogen detection by nanopore-sequencing was shown in Supplementary Figure 1. Hospitalized cancer patients with suspected infections were routinely screened in those two hospitals between January 2021 and July 2021. To be enrolled in this study, patients must meet the following inclusion criteria: 1) a precise diagnosis of cancer; 2) symptoms of infections during this hospital stay; 3) sufficient amount of body fluid samples such as sputum, blood and bronchoalveolar lavage fluid (BALF) for testing by nanopore-sequencing and the conventional culture-based method; 4) a written informed consent. Patients with the following conditions were excluded: 1) no evidence of infections; 2) the sample volume not enough for testing; 3) missing one test result; 4) no written informed consent. This study was approved by the Ethics Committee of the Hefei Cancer Hospital of Chinese Academy of Science and the Cancer Hospital of the University of Chinese Academy of

Sciences. This study followed guidelines established by the Helsinki Declaration (World Medical Association, 2013).

Sample collection

Body fluid samples including BALF, sputum, abscess, peritoneal fluid, pleural fluid, urine, blood, and other fluids were collected in sterile tubes from patients. All body fluid samples must meet the criteria for clinical examination. The culture assays for bacteria and fungi were performed routinely in-house at hospitals. Samples were processed immediately unless otherwise specified.

Conventional culture

Potential pathogens were detected routinely by the standard culture methods for detection of pathogens at the Laboratory Medicine Department. Generally, clinical specimens were cultured on blood agar media, MacConkey agar media, chocolate agar media, and Sabouraud agar media (Babio Biotechnology, China). For the cultivation of anaerobic and facultatively anaerobic bacteria, samples were incubated for 18-72 hours at 36.5 ± 0.5°C in 5%CO2. For the cultivation of anaerobic bacteria, samples were incubated in anaerobic bags for 18-72 hours at 36.5 ± 0.5°C. For fungi culture, samples were incubated for 7 days at 28 ± 0.5°C. For a blood culture, samples were incubated for 5 days at 35.5 ± 0.5°C. Pathogen identification was performed with BacT/ALERT 3D Automated Microbial Detection System (bioMérieux, Inc., France) and/or VITEK® 2 COMPACT Automated Microbial Identification System (bioMérieux, Inc., USA). Owing to the high requirements in specialized facilities and biosafety for virus culture and the lower sensitivity, culture-based virus detection was not routinely carried out in these two hospitals (Leland and Ginocchio, 2007; Cassedy et al., 2021).

DNA extraction and polymerase chain reaction amplification

DNA from samples was extracted using the QIAamp DNA Microbiome Kit (Cat. No. 51707, Qiagen, Hilden, Germany) per the manufacturer's instructions. Viral DNA was extracted from clinical samples with conventional DNA extraction protocols. The extracted DNA was used for PCR amplification of the 16S rDNA regions and fungal internal transcribed spacer (ITS) regions using a 16S rDNA PCR kit and a fungal ITS PCR kit. To reduce the complexity of library preparation and control time cost, PCR amplification of the 16S rDNA regions and fungal ITS regions was performed in one tube with an optimized primer mixture, in which the primer ratios of bacteria and fungi were set at 5:2. For the detection of possible DNA viruses in clinical specimens, PCR amplification of key genes of 10 common DNA viruses such as Epstein-Barr virus (EBV) and human cytomegalovirus (HCMV) was performed separately. The primers details used for PCR amplification were shown in the Supplementary Table 1. The PCR conditions were shown as follows: initiation denaturation step at 98°C for 3min, then six cycles of 95°C for 15s/66°C for 60s/72°C for 30s, then another 29 cycles of 95°C for 15s/61°C for 60s/72°C for 30s, and a final extension step of 72°C for 5min. All PCRs were performed on an ABI 2720 Thermal Cycler (Cat. No. 435659; ABI, California, USA).

Library preparation

Products from PCR experiments were then purified with 0.8× AMPure beads for Nanopore Barcode PCR step. The purified PCR products were used for Nanopore barcode PCR according to PCR Barcoding Expansion Pack 1-96 (EXP-PBC096). The Nanopore barcode PCR products were purified with 0.6× AMPure beads, and each purified barcode PCR product was pooled with equal amounts for nanopore library preparation. The purified PCR products were used for subsequent library preparation, and it was carried out using the DNA library preparation kit following the manufacturer's instructions (Cat. No. SQK-LSK109, Oxford Nanopore Technologies, Oxford, UK). The library was further eluted with 15μl TE buffer for quantified. For each sample, two parallel libraries were prepared and sequenced separately including one for detecting bacteria and fungi and one for detecting DNA viruses (Karamitros and Magiorkinis, 2018).

Nanopore sequencing

The purified libraries were loaded on a Nanopore flow cell (R9.4.1) on MinION platform after chip priming and were sequenced using GridION platform, and 80 fmol final library for each sample was loaded (Jain et al., 2015). Real-time data acquisition was performed with the MinKNOW software. Sequenced reads were then used for subsequent analyses of pathogen identification.

Identification of pathogens

Sequenced reads were analyzed by the What's In My Pot (WIMP) workflow *via* EPI2ME (Juul et al., 2015; Sakai et al., 2019). The reads less than 200 bp and greater than 2500 bp were filtered, reads derived from human DNA were removed by searching each read against the human genome using minimap2 (Li, 2018), and the remaining reads were aligned to

the pathogens databases in National Center for Biotechnology Information (NCBI). Pathogens were classified at the species level based on the percentage of coverage and identity. Generally, those microorganisms within the top 10 pathogens ranked by aligned reads and with at least 10 aligned reads or a relative abundance score >0.5% were classified as possible pathogens and were subjected to further evaluation. For some special pathogens such as *Mycobacterium tuberculosis*, specific criteria were adopted.

Limit of detection

To evaluate the limit of detection (LoD) of nanopore amplicon sequencing for bacteria and fungi in clinical body fluid, we spiked the two most common clinical pathogens, *Escherichia coli and Candida albicans*, into the negative sputum specimen of healthy donors, starting from 10^6 copies/ml in a series of 10-fold dilution gradient to 10^2 copies/ml. Pathogen detection for each concentration was performed with two replicates for accuracy and reproducibility. The positive threshold of effective reads for analysis were set to coverage ≥85% and identity ≥ 90%. The limit of detection was defined as the concentration at which the total valid reads of sequencing was ≥30,000, and the reads of the pathogens were ≥10 in both replicates.

Validation of identified pathogens

The presence of some clinically significant pathogens in clinical samples were further validated by quantitative reverse transcription PCR (RT-qPCR) assays or Sanger sequencing. Those validation experiments were performed with the residual DNA extracted from clinical samples. In general, pathogens such as *Mycobacterium tuberculosis* and fungi such as *Candida glabrata*, *Candida albicans*, *Candida tropicalis*, *Pneumocystis jirovecii* and *Aspergillus niger* would be confirmed with genus- or species-specific commercial RT-PCR diagnostic kits in accordance with the manufacturer's instructions. For DNA viruses, Sanger sequencing would be used to validate the presence of those DNA viruses in the clinical samples.

Statistical analyses

Normally distributed continuous data were shown as mean with standard deviation (SD), while those data with non-normal distribution were shown as median with interquartile range (IQR). For normally distributed data, differences between groups were calculated by t-test; while for data of non-normal distribution, differences between groups were calculated by Mann-Whitney U test. Count data were displayed as a number with percentage, and differences between groups were evaluated by Fisher's exact test or Chi-square test. The performance of those two methods in detecting pathogens was compared, and subgroups stratified by pathogen type and sample type were performed. Data were analyzed by R software (Version 3.6.1, R Foundation). A two-sided $P < 0.05$ was considered to be statistically significant.

Results

Characteristics of patients

A total of 56 immunocompromised cancer patients with suspected infections were enrolled in this study (Table 1). Among those patients, the most common cancer type was lung cancer (22 cases, 39.3%), followed by esophageal cancer (7 cases, 12.5%), cervical cancer (5 cases, 8.9%), and liver cancer (5 cases, 8.9%). The treatments for those patients were also diverse, including chemotherapy for 41 cases (73.2%), radiotherapy applied to 13 patients (23.2%), ICIs therapy among 18 cases (32.1%), and anti-cancer targeted therapy for 21 individuals (37.5%) (Table 1). The most common specimen types were BALF (16 cases, 28.6%), followed by blood (13 cases, 23.2%), sputum (13 cases, 23.2%), urine (7 cases, 12.5%), and peritoneal fluid (3 cases, 5.4%) (Table 1).

Pathogens identified in body fluid samples of immunocompromised cancer patients with suspected infections

Among the 56 body fluid samples collected from immunocompromised cancer patients with suspected infections, 47 (83.9%) samples were identified to have at least one pathogen by nanopore-based metagenomic sequencing or cultures, and no pathogen was detected in the remaining nine (16.1%) specimens (Supplementary Table 2). Only 25 (44.6%) samples were identified to have pathogens by culture, suggesting the poor performance of the conventional culture method in detecting pathogens (Supplementary Table 2). Remarkably, nanopore-sequencing successfully detected pathogens from 22 out of the 31 culture-negative samples (71.0%) (Supplementary Table 2).

All 43 non-blood samples, except one, contained at least one pathogen recognized by either nanopore-based metagenomic sequencing or the culture method (42 cases, 97.7%). Interestingly, among the 42 pathogen-carrying specimens, the culture method failed to find pathogens in approximately 40% of them (17 samples, 40.5%). As for the 13 blood samples, one or more than one type of pathogens was found among five (38.5%) samples by nanopore-based metagenomic sequencing. In contrast, the culture method did not detect pathogens in those

TABLE 1 Demographic and clinical characteristics of 56 cancer patients recruited in this study.

Items	Data
Age (Years, mean ± SD)	61.2 (13.5)
Male (n, %)	37 (66.1%)
Cancer types (n, %)	
Lung cancer	22 (39.3%)
Esophageal cancer	7 (12.5%)
Cervical cancer	5 (8.9%)
Liver cancer	5 (8.9%)
Colorectal cancer	4 (7.1%)
Bladder cancer	2 (3.6%)
Gastric cancer	2 (3.6%)
Lymphoma	2 (3.6%)
Ovarian cancer	2 (3.6%)
Other types[#]	5 (8.9%)
Treatments (n, %)	
Chemotherapy	41 (73.2%)
Radiotherapy	13 (23.2%)
ICIs	18 (32.1%)
Targeted therapy	21 (37.5%)
Sample types (n, %)	
BALF	16 (28.6%)
Blood	13 (23.2%)
Sputum	13 (23.2%)
Urine	7 (12.5%)
Peritoneal fluid	3 (5.4%)
Bile	2 (3.6%)
Pleural fluid	1 (1.8%)
Nasal secretions	1 (1.8%)
Antibiotic use (n, %)	47 (83.9%)
CRP (mg/L, median with IQR)	95.0 (133.9)
White blood cell count (10^9/L, mean ± SD)	9.5 (7.0)

([#]Other cancers included acute myeloid leukemia, mediastinal carcinoma, multiple myeloma, nasopharyngeal carcinoma, oral cancer, pancreatic cancer and prostate cancer, and there was one case for each of those cancers. SD, standard deviation; ICIs, immune checkpoint inhibitors; IQR, interquartile range; BALF, bronchoalveolar lavage fluid.)

samples, suggesting the extremely poor performance of the gold standard method for blood samples.

The pathogens identified by nanopore-sequencing among immunocompromised cancer patients with suspected infections were shown in Table 2. Nanopore-sequencing detected bacteria in 42 cases (75.0%), viruses in 10 cases (17.9%), fungi in 16 cases (28.6%), co-infections in 27 cases (48.2%), and fastidious pathogens in eight cases (14.3%) (Table 2). The most common pathogen detected was *Escherichia coli* (11 cases, 19.6%), followed by *Stenotrophomonas maltophilia* (9 cases, 16.1%), *Candida albicans* (9 cases, 16.1%), Human gammaherpesvirus 4 (Epstein-Barr virus; 5 cases, 8.9%), *Pseudomonas aeruginosa* (5 cases, 8.9%) and *Haemophilus influenzae* (5 cases, 8.9%), *Klebsiella pneumoniae* (4 cases, 7.1%) and *Pneumocystis jirovecii* (4 cases, 7.1%).

In the validation experiments, the presence of *Mycobacterium tuberculosis* in the clinical samples from three patients by nanopore-sequencing was all confirmed by commercial RT-PCR diagnostic kits. The presence of fungi (*Candida glabrata*, *Candida albicans*, *Candida tropicalis*, *Pneumocystis jirovecii* and *Aspergillus niger*) in the clinical samples from 16 patients by nanopore-sequencing was also all confirmed by commercial RT-PCR diagnostic kits. Ten DNA viruses included 5 EBV, 4 Human alphaherpesvirus 1 (Herpes simplex virus type 1, HSV1) and 2 HCMV were identified by nanopore-sequencing. The presence of those three DNA viruses including EBV, HSV1 and HCMV had been validated by Sanger sequencing in those clinical samples at the early stage of our study, and Sanger sequencing peak maps were shown in the Supplementary Figure 2.

For the false negative findings in culture, 22 out of 31 culture-negative samples were identified to have at least one pathogen by nanopore amplicon sequencing, which proved the high risk of false negative findings in culture. In two samples (No. 17 and No. 33), findings from culture showed the presence of *Candida krusei* and *Proteus mirabilis*. However, those two pathogens were not identified by nanopore amplicon sequencing, which may be caused by the false positive findings in culture or false negative findings in nanopore-sequencing.

Comparison of the performance of those two pathogen detection methods

Table 3 showed the comparison between nanopore amplicon sequencing and the conventional culture method in their performance of detecting pathogens among immunocompromised cancer patients with suspected infections. Nanopore amplicon sequencing exhibited a significantly high sensitivity than the conventional culture method (83.9% vs. 44.6%, P<0.001), and this advantage existed regardless sample types, blood samples (38.5% vs. 0%, P=0.039) vs. non-blood samples (97.7% vs. 58.1%, P<0.001) (Table 3, Figure 1). There were 24 cases from which one or more pathogens were detected by nanopore amplicon sequencing; however, no pathogen or an inconsistent finding was found from the cultured specimens (Supplementary Table 3).

Compared with the conventional culture method, nanopore amplicon sequencing revealed a significant number of patients with bacterial infections (75.0% vs. 33.9%, P<0.001) or co-infections with other types of pathogens (48.2% vs. 12.5%, P<0.001) (Table 3, Figure 1). Not surprisingly, nanopore amplicon sequencing detected three common fastidious pathogens (*Streptococcus pneumoniae, Haemophilus influenzae*, and *Moraxella catarrhalis*) from multiple patients, while the conventional culture method failed all cases (14.3% vs. 0.0%, P=0.006).

TABLE 2 Summary of pathogens identified by nanopore amplicon sequencing among immunocompromised cancer patients with suspected infections.

Pathogens	All samples (n, %)		Positive in culture (n, %)		Negative in culture (n, %)	
	Total	Positive	Total	Positive	Total	Positive
All pathogens	56	47 (83.9%)	25	25 (100%)	31	22 (71.0%)
Fastidious pathogens[#]	56	8 (14.3%)	0	–*	56	8 (14.3%)
Bacteria	56	42 (75.0%)	19	21 (100%)	37	23 (62.2%)
Viruses	56	10 (17.9%)	0	–*	56	10 (17.9%)
Fungi	56	16 (28.6%)	8	6 (75.0%)	48	10 (20.8%)
Co-infections	56	27 (48.2%)	7	7 (100%)	49	20 (40.8%)

([#]Fastidious pathogens included streptococcus pneumoniae, haemophilus influenzae, and moraxella catarrhalis. *Not applicable.)

Among 18 fungi-positive samples, nanopore amplicon sequencing successfully identified pathogens in 16 samples, but the conventional culture method only found pathogens from eight patients (88.9% vs 44.4%, P=0.012). Moreover, nanopore amplicon sequencing also detected viruses from 10 samples, which was difficult to be detected *via* the conventional culture method (17.9% vs. 0.0%, P=0.001).

The mean turnaround time (defined as the time from test initiation to the delivery of test results) for this nanopore amplicon sequencing was about 17.5 hours, which was far less than that of the conventional culture method (about 3-5 days).

Limit of detection

Negative sputum specimens of healthy donors without *Escherichia coli and Candida albicans* in PCR testing and mNGS was used for the LoD test. After trimming the low-quality reads and the reads derived from human DNA, the clean reads were analyzed. The results of sample spiked with *Escherichia coli* or *Candida albicans* indicated that as the amount of input decreased, the reads of the pathogen also decreased (Figure 2). The LoD was determined to be 10^3 copies/ml with two replicates ≥ 10 reads for *Escherichia coli* and 10^2 copies/ml with two replicates ≥ 10 reads for *Candida albicans*, respectively (Figure 2). The LoD of the *Candida albicans* was lower than that of *Escherichia coli* as the detection abundance of fungi was higher than that of bacteria in the same dilution gradient (Figure 2).

Discussion

Rapid and accurate diagnostics of pathogenic microorganisms can enable the early use of appropriate antibiotics and improve patients' prognosis. Conventional

TABLE 3 Comparison of the performance in detecting pathogens between nanopore amplicon sequencing and conventional culture.

Comparison	Number of patients	Nanopore-sequencing	Conventional culture	P values
All samples	56	47 (83.9%)	25 (44.6%)	<0.001
Subgroup by pathogens				
Fastidious pathogens*	56	8 (14.3%)	0 (0%)	0.006
Co-infections	56	27 (48.2%)	7 (12.5%)	<0.001
Bacteria	56	42 (75.0%)	19 (33.9%)	<0.001
Fungi	56	16 (28.6%)	8 (14.3%)	0.065
Viruses	56	10 (17.9%)	0 (0%)	0.001
Subgroup by sample types				
Non-blood samples	43	42 (97.7%)	25 (58.1%)	<0.001
BALF	16	16 (100%)	11 (68.8%)	0.043
Blood	13	5 (38.5%)	0 (0%)	0.039
Sputum	13	12 (92.3%)	6 (46.2%)	0.03
Urine	7	7 (100%)	4 (57.1%)	0.192
Other samples[#]	7	7 (100%)	4 (57.1%)	0.192

*Fastidious pathogens included streptococcus pneumoniae, haemophilus influenzae, and moraxellacatarrhalis. #Other samples included bile, pleural fluid, peritoneal fluid, and nasal secretions.

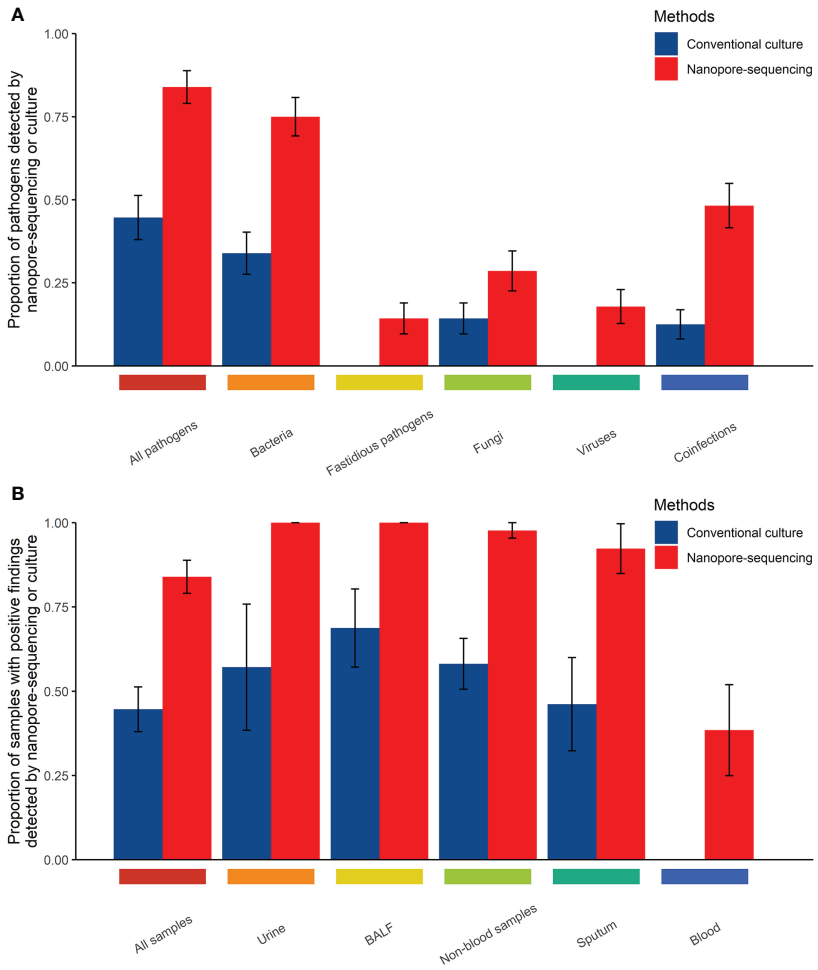

FIGURE 1
Comparison of the performance of those two methods in detecting pathogens in body fluid samples from immunocompromised cancer patients with suspected infections (**A**, Comparison of the performance of those two methods in detecting pathogens by types of pathogens; **B**, Comparison of the performance of those two methods in detecting pathogens by types of samples).

diagnostics of pathogenic microorganisms such as culture have obvious limitations in the management of infections such as long turnaround time and limited sensitivity (Buchan and Ledeboer, 2014; Peri et al., 2022). For RT-qPCR assays or some Sanger sequencing-based assays, a key premise for their successful use is the accurate prediction of suspicious pathogens, which is challenging and requires clinicians to have enough professional qualities (Buchan and Ledeboer, 2014; Church et al., 2020). Moreover, the application of RT-qPCR assays and/or Sanger sequencing-based assays is also limited by throughput and usually cannot cover all suspicious pathogens in clinical practice (Church et al., 2020). Therefore, there is an urgent need for the development of both quick and accurate detection methods of pathogenic microorganisms. In the past decade, metagenomic analyses such as metagenomic next-generation sequencing (mNGS) and nanopore sequencing have emerged as an efficient approach for pathogen detection for patients with infections, which can also detect pathogens in a comprehensive and unbiased way (Chiu and Miller, 2019; Gu et al., 2019). The performance of detecting pathogens under different clinical situations between nanopore sequencing and other methods have also been compared in some clinical studies (Ashikawa et al., 2018; Charalampous et al., 2019; Chan et al., 2020; Deng et al., 2020; Morrison et al., 2020; Fu et al., 2022). Through comparisons with other methods such as culture, RT-qPCR assays and Sanger sequencing-based diagnostics, those studies have confirmed that nanopore sequencing undoubtedly have several advantages such as significantly shorter turnaround time, accurate detection of causative pathogens, simultaneous detection of multiple types of pathogens and accurate detection of antibiotic resistance genes (Ashikawa et al., 2018; Charalampous et al., 2019; Chan et al., 2020; Deng et al., 2020;

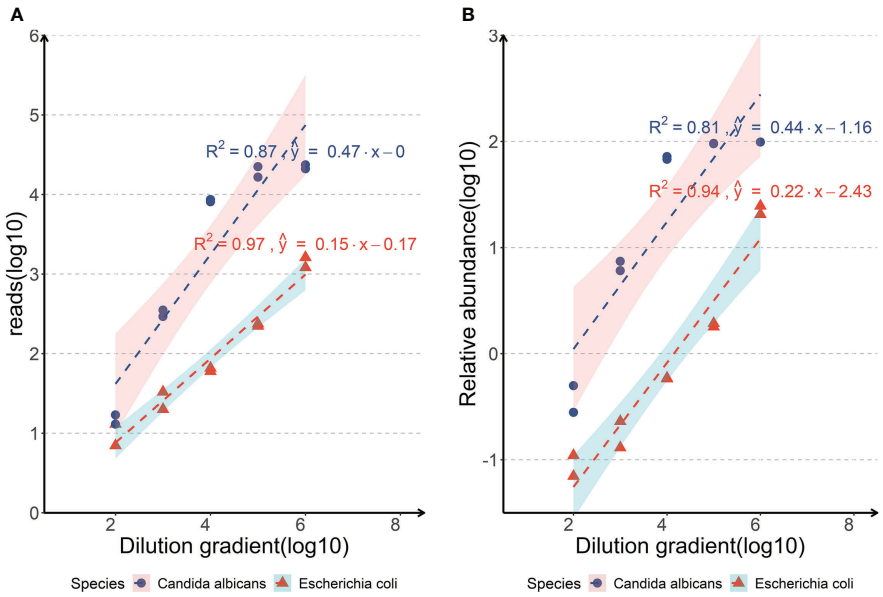

FIGURE 2
Analyses of the limits of detection of the nanopore amplicon sequencing assay in detecting *Escherichia coli* or *Candida albicans of* body fluid samples. (**A**, Correlations between the reads of the pathogen detected by nanopore amplicon sequencing and the dilution gradient of pathogens spiked in negative sputum; **B**, Correlations between the relative abundance of the pathogen detected by nanopore amplicon sequencing and the dilution gradient of pathogens spiked in negative sputum).

Morrison et al., 2020; Fu et al., 2022). Therefore, nanopore sequencing has several advantages in detecting causative pathogens compared with RT-qPCR assays or Sanger sequencing-based assays, and can provide more support for the adequate management of infections.

Cancer patients, especially those with immunocompromised status, are at high risk of infections, and there are unmet needs in the early and accurate diagnosis of infections for those patients in clinical practice. This study aimed to evaluate the role of nanopore amplicon sequencing in detecting pathogens among immunocompromised cancer patients with suspected infections. To the best of our knowledge, this is the first study designed to evaluate the role of nanopore amplicon sequencing in pathogen detection among immunocompromised cancer patients. The findings from this study illustrate nanopore amplicon sequencing as a rapid and precise method of pathogen detection. Its superior performance in detecting pathogens may help to improve the outcomes of immunocompromised cancer patients by facilitating the prompt diagnosis of infections and precise anti-infectives treatment.

Both chemotherapy and radiotherapy can significantly increase the risk of infections or infection-related mortality among cancer patients, primarily attributed to the impaired immunity because of the cytotoxic effects of chemotherapy or radiotherapy on hematopoietic stem cells and immune cells (Marchetti and Calandra, 2002; Verma et al., 2016; Wise, 2016; Weil et al., 2018). Prophylactic use of antibiotics before chemotherapy and radiotherapy is a possible infection-control intervention for cancer patients, but its application in the clinic is very limited (Schlesinger et al., 2009; Egan et al., 2019; Van Den Bosch et al., 2021). The adverse effects of antibiotic abuse on human health and the emergence of antibiotic resistance also discourage the prophylactic use of antibiotics as an infection-control intervention for cancer patients (Vento and Cainelli, 2003). Therefore, preventing infections among cancer patients is still a considerable challenge, and effective infection-control strategies are urgently needed.

Early and precise detection of the pathogens is critical to initiating anti-infectives therapy and improving the outcomes of patients with infections, which is difficult to achieve in clinical practice (Bloch and Bailin, 2019; Lamy et al., 2020). Emerging clinical studies in the last five years suggest that sequencing-based metagenomic analyses can detect pathogens earlier and quicker (Rodino et al., 2020; Gu et al., 2021; Piantadosi et al., 2021). Both mNGS and nanopore sequencing have been used to detect pathogens, and have proven to be more efficient than conventional diagnostics of pathogens (Chiu and Miller, 2019). Moreover, metagenomic sequencing-based approaches can also uncover critical information on antibiotic resistance, which is, of course, beneficial for treating patients with infections. Several recent studies further compare the performance of these metagenomic sequencing methods in detecting pathogenic microorganisms under different clinical situations (Schmidt et al., 2017; Votintseva et al., 2017; Gu et al., 2021).

Those studies reveal that nanopore sequencing has similar efficiency in detecting pathogens compared with mNGS, but has a shorter turnaround time (Schmidt et al., 2017; Votintseva et al., 2017; Gu et al., 2021). Besides, compared with nanopore sequencing, mNGS have several drawbacks such as longer sequencing time, bulky sequencers and the requirement of sequencing run to be completed before analysis, which impair its application in clinical practice (Rutanga et al., 2018; Chiu and Miller, 2019; Schuele et al., 2021). Therefore, compared with mNGS, nanopore-sequencing can achieve similar sensitivity and accuracy in microbial identification, but it generally requires a less turnaround time, thus making it a more appropriate solution for pathogen detection.

In this study, we evaluated the performance of nanopore amplicon sequencing in parallel with the traditional culture method for detecting pathogens among immunocompromised cancer patients. The results demonstrated that nanopore amplicon sequencing could detect common pathogens such as bacteria, viruses, and fungi. Our sequencing-based assay also uncovered fastidious pathogens and two or more types of pathogens caused co-infections, which generally posed significant challenges for the culture method. Lastly, from receiving samples to generating the test reports, the assay time for nanopore sequencing was approximately 17.5 hours compared to 3-5 days for the culture method, ensuring a rapid detection of pathogens for patients with suspected infections. Therefore, our study shows the feasibility of nanopore amplicon sequencing in rapidly and accurately diagnosing infections among immunocompromised cancer patients.

Improvement in the surveillance of infections may improve supportive care for cancer patients and reduce infection-related mortality. Besides the diagnostic role in suspected infections, metagenomic analyses using next-generation sequencing are also of great interest in infection surveillance. A recent pilot trial by Goggin et al. revealed that some pathogens in cancer patients could be identified by plasma microbial cell-free DNA sequencing (mcfDNA-seq) days before the onset of bloodstream infections, thus enabling early diagnosis and timely treatment (Goggin et al., 2020). However, the performance of nanopore-sequencing in detecting pathogens before the onset of bloodstream infections is still unclear, which should be explored in the future.

In recent years, the spectrum of infections in cancer patients has changed noticeably (El-Sharif et al., 2012; Nesher and Rolston, 2014; Del Castillo et al., 2016). Some studies have shown more invasive fungal infections (Del Castillo et al., 2016; Hardak et al., 2020). Elevated antibiotic resistance among cancer patients with infections has also been reported (Arega et al., 2018). Yet, the current spectrum of infections in cancer patients has not been defined by metagenomic sequencing. We attempt to fill the gap in this study by utilizing nanopore amplicon sequencing (Table 2). Our data showed that fungal infections and polymicrobial co-infections were found among 27.1% and 45.8% of cases, respectively. Therefore, the two circumstances should not be ignored when treating cancer patients with suspected infections.

The LoD of the nanopore amplicon sequencing assay was tested on sputum specimen to determine the minimum of bacterial and fungal abundance. We selected sputum specimens as the experimental object mainly because the background microorganisms in sputum specimens were relatively rich, and the content of human-derived host DNA was also considerable, which had a good representative significance. The LoD was determined to be 10^3 copies/ml with two replicates ≥ 10 reads for *Escherichia coli* and 10^2 copies/ml with two replicates ≥ 10 reads for *Candida albicans*, respectively (Figure 2). Although the LoD of *Escherichia coli* was set up to 10^3 copies/ml in our experiment, we were able to detect it with a considerable number of reads at 10^2 copies/ml (7 and 13, respectively). Compared with the detection limits of other nanopore-seq assays from published literatures (arranging from 10^2 from 10^4 copies/ml), this nanopore amplicon sequencing assay has at least a non-inferior performance (Imai et al., 2017; Lewandowski et al., 2019; Player et al., 2020; Stefan et al., 2022).

Our study had several limitations. Firstly, the nanopore amplicon sequencing assay had low sensitivity in detecting pathogens in blood samples though it outperformed the conventional culture method. Deep sequencing might improve the sensitivity but indeed with a high-test cost. Secondly, the sample size for immunocompromised cancer patients with suspected infections in this study was not only small but scattered among different types of cancer. Future studies in which more patients of one particular or closely related cancers are recruited need to be performed. Additionally, the sample size was not large enough for specific sample type such as peritoneal fluid. Testing more samples with a better representation is needed to validate the overall performance of nanopore-sequencing. Thirdly, false negative findings in nanopore-sequencing are possible though such possibility is low, and some studies have confirmed the existence of false negative findings in nanopore-sequencing (Charalampous et al., 2019; Gu et al., 2021). Therefore, to reduce the risk of false findings and expand their clinical utility in detecting pathogens, nanopore-sequencing assays still need optimization. Finally, the spectrum of pathogens stratified by sites of infections or types of cancer remains to be determined in future studies.

In conclusion, our study suggests that the nanopore amplicon sequencing assay is a reliable method that allows detecting pathogens among immunocompromised cancer patients with suspected infections rapidly and precisely. Its superior performance in detecting pathogens can help to improve the treatment outcomes for immunocompromised cancer patients. In addition, the utility of nanopore amplicon

sequencing in the surveillance or screening of infections among cancer patients should be explored in the future.

Data availability statement

The datasets presented in this study can be found in online repositories. The names of the repository/repositories and accession number(s) can be found below: Metagenomic sequencing data have been deposited in the NCBI Sequence Read Archive (SRA) (PRJNA854790).

Ethics statement

The studies involving human participants were reviewed and approved by the ethics committee of the Hefei Cancer Hospital of Chinese Academy of Science and the Cancer Hospital of the University of Chinese Academy of Sciences. The patients/participants provided their written informed consent to participate in this study.

Author contributions

QD, YC, HG, and HZW designed and supervised the study. QD, YC, XW, AS, and HW enrolled patients and assisted in collection of samples. QD, YW, and HG performed experiments and analyzed data. QD, YC, BW, and HG wrote and edited the manuscript. All authors contributed to the article and approved the submitted version.

Funding

This study was funded by Research and Development Funding for Medical and Health Institutions (Grant number: 2021YL007) and by the Medical Health Science and Technology Project of Zhejiang Provincial Health Commission (Grant number: 2017188812).

Conflict of interest

The authors declare that the research was conducted in the absence of any commercial or financial relationships that could be construed as a potential conflict of interest.

Publisher's note

All claims expressed in this article are solely those of the authors and do not necessarily represent those of their affiliated organizations, or those of the publisher, the editors and the reviewers. Any product that may be evaluated in this article, or claim that may be made by its manufacturer, is not guaranteed or endorsed by the publisher.

Supplementary material

The Supplementary Material for this article can be found online at: https://www.frontiersin.org/articles/10.3389/fcimb.2022.943859/full#supplementary-material

SUPPLEMENTARY TABLE 1
Primers details used for PCR amplification.

SUPPLEMENTARY TABLE 2
Summary of pathogens identified in body fluid samples of immunocompromised cancer patients with suspected infections (#Other samples included bile, pleural fluid, peritoneal fluid and nasal secretions.)

SUPPLEMENTARY TABLE 3
Case series of patients with positive findings in nanopore amplicon sequencing but negative or inconsistent findings in cultures. (BALF, bronchoalveolar lavage fluid.)

References

Arega, B., Woldeamanuel, Y., Adane, K., Sherif, A. A., and Asrat, D. (2018). Microbial spectrum and drug-resistance profile of isolates causing bloodstream infections in febrile cancer patients at a referral hospital in Addis Ababa, Ethiopia. *Infect. Drug Resist.* 11, 1511–1519. doi: 10.2147/IDR.S168867

Ashikawa, S., Tarumoto, N., Imai, K., Sakai, J., Kodana, M., Kawamura, T., et al. (2018). Rapid identification of pathogens from positive blood culture bottles with the MinION nanopore sequencer. *J. Med. Microbiol.* 67, 1589–1595. doi: 10.1099/jmm.0.000855

Bloch, K. C., and Bailin, S. S. (2019). Update on fungal infections of the central nervous system: emerging pathogens and emerging diagnostics. *Curr. Opin. Infect. Dis.* 32, 277–284. doi: 10.1097/QCO.0000000000000541

Brand, J. S., Colzani, E., Johansson, A. L. V., Giesecke, J., Clements, M., Bergh, J., et al. (2016). Infection-related hospitalizations in breast cancer patients: Risk and impact on prognosis. *J. Infect.* 72, 650–658. doi: 10.1016/j.jinf.2016.04.003

Buchan, B. W., and Ledeboer, N. A. (2014). Emerging technologies for the clinical microbiology laboratory. *Clin. Microbiol. Rev.* 27, 783–822. doi: 10.1128/CMR.00003-14

Cassedy, A., Parle-Mcdermott, A., and O'kennedy, R. (2021). Virus detection: A review of the current and emerging molecular and immunological methods. *Front. Mol. Biosci.* 8, 637559. doi: 10.3389/fmolb.2021.637559

Casto, A. M., Fredricks, D. N., and Hill, J. A. (2021). Diagnosis of infectious diseases in immunocompromised hosts using metagenomic next generation sequencing-based diagnostics. *Blood Rev.* 53, 100906. doi: 10.1016/j.blre.2021.100906

Chan, W. S., Au, C. H., Leung, S. M., Ho, D. N., Wong, E. Y. L., To, M. Y., et al. (2020). Potential utility of targeted nanopore sequencing for improving etiologic diagnosis of bacterial and fungal respiratory infection. *Diagn. Pathol.* 15, 41. doi: 10.1186/s13000-020-00960-w

Charalampous, T., Kay, G. L., Richardson, H., Aydin, A., Baldan, R., Jeanes, C., et al. (2019). Nanopore metagenomics enables rapid clinical diagnosis of bacterial lower respiratory infection. *Nat. Biotechnol.* 37, 783–792. doi: 10.1038/s41587-019-0156-5

Chiu, C. Y., and Miller, S. A. (2019). Clinical metagenomics. *Nat. Rev. Genet.* 20, 341–355. doi: 10.1038/s41576-019-0113-7

Church, D. L., Cerutti, L., Gurtler, A., Griener, T., Zelazny, A., and Emler, S. (2020). Performance and application of 16S rRNA gene cycle sequencing for routine identification of bacteria in the clinical microbiology laboratory. *Clin. Microbiol. Rev.* 33, e00053–19. doi: 10.1128/CMR.00053-19

Del Castillo, M., Romero, F. A., Arguello, E., Kyi, C., Postow, M. A., and Redelman-Sidi, G. (2016). The spectrum of serious infections among patients receiving immune checkpoint blockade for the treatment of melanoma. *Clin. Infect. Dis.* 63, 1490–1493. doi: 10.1093/cid/ciw539

Deng, X., Achari, A., Federman, S., Yu, G., Somasekar, S., Bartolo, I., et al. (2020). Metagenomic sequencing with spiked primer enrichment for viral diagnostics and genomic surveillance. *Nat. Microbiol.* 5, 443–454. doi: 10.1038/s41564-019-0637-9

Dippenaar, A., Goossens, S. N., Grobbelaar, M., Oostvogels, S., Cuypers, B., Laukens, K., et al. (2021). Nanopore sequencing for mycobacterium tuberculosis: A critical review of the literature, new developments and future opportunities. *J. Clin. Microbiol.* 60, e0064621. doi: 10.1128/JCM.00646-21

Egan, G., Robinson, P. D., Martinez, J. P. D., Alexander, S., Ammann, R. A., Dupuis, L. L., et al. (2019). Efficacy of antibiotic prophylaxis in patients with cancer and hematopoietic stem cell transplantation recipients: A systematic review of randomized trials. *Cancer Med.* 8, 4536–4546. doi: 10.1002/cam4.2395

Eilers, R. E. Jr., Gandhi, M., Patel, J. D., Mulcahy, M. F., Agulnik, M., Hensing, T., et al. (2010). Dermatologic infections in cancer patients treated with epidermal growth factor receptor inhibitor therapy. *J. Natl. Cancer Inst.* 102, 47–53. doi: 10.1093/jnci/djp439

El-Sharif, A., Elkhatib, W. F., and Ashour, H. M. (2012). Nosocomial infections in leukemic and solid-tumor cancer patients: distribution, outcome and microbial spectrum of anaerobes. *Future Microbiol.* 7, 1423–1429. doi: 10.2217/fmb.12.125

Ferreira, F. A., Helmersen, K., Visnovska, T., Jorgensen, S. B., and Aamot, H. V. (2021). Rapid nanopore-based DNA sequencing protocol of antibiotic-resistant bacteria for use in surveillance and outbreak investigation. *Microb. Genom.* 7, 000557. doi: 10.1099/mgen.0.000557

Fu, Y., Chen, Q., Xiong, M., Zhao, J., Shen, S., Chen, L., et al. (2022). Clinical performance of nanopore targeted sequencing for diagnosing infectious diseases. *Microbiol. Spectr.* 10, e0027022. doi: 10.1128/spectrum.00270-22

Garcia-Vidal, C., Stern, A., and Gudiol, C. (2021). Multidrug-resistant, gram-negative infections in high-risk haematologic patients: an update on epidemiology, diagnosis and treatment. *Curr. Opin. Infect. Dis.* 34, 314–322. doi: 10.1097/QCO.0000000000000745

Goggin, K. P., Gonzalez-Pena, V., Inaba, Y., Allison, K. J., Hong, D. K., Ahmed, A. A., et al. (2020). Evaluation of plasma microbial cell-free DNA sequencing to predict bloodstream infection in pediatric patients with relapsed or refractory cancer. *JAMA Oncol.* 6, 552–556. doi: 10.1001/jamaoncol.2019.4120

Gu, W., Deng, X., Lee, M., Sucu, Y. D., Arevalo, S., Stryke, D., et al. (2021). Rapid pathogen detection by metagenomic next-generation sequencing of infected body fluids. *Nat. Med.* 27, 115–124. doi: 10.1038/s41591-020-1105-z

Gu, W., Miller, S., and Chiu, C. Y. (2019). Clinical metagenomic next-generation sequencing for pathogen detection. *Annu. Rev. Pathol.* 14, 319–338. doi: 10.1146/annurev-pathmechdis-012418-012751

Hardak, E., Fuchs, E., Geffen, Y., Zuckerman, T., and Oren, I. (2020). Clinical spectrum, diagnosis and outcome of rare fungal infections in patients with hematological malignancies: Experience of 15-year period from a single tertiary medical center. *Mycopathologia* 185, 347–355. doi: 10.1007/s11046-020-00436-x

Henderson, A., Bursle, E., Stewart, A., Harris, P. N. A., Paterson, D., Chatfield, M. D., et al. (2021). A systematic review of antimicrobial susceptibility testing as a tool in clinical trials assessing antimicrobials against infections due to gram-negative pathogens. *Clin. Microbiol. Infect.* 27, 1746–1753. doi: 10.1016/j.cmi.2021.03.019

Hjelholt, T. J., Rasmussen, T. B., Seesaghur, A., Hernandez, R. K., Marongiu, A., Obel, N., et al. (2021). Risk of infections and mortality in Danish patients with cancer diagnosed with bone metastases: a population-based cohort study. *BMJ Open* 11, e049831. doi: 10.1136/bmjopen-2021-049831

Imai, K., Tarumoto, N., Misawa, K., Runtuwene, L. R., Sakai, J., Hayashida, K., et al. (2017). A novel diagnostic method for malaria using loop-mediated isothermal amplification (LAMP) and MinION nanopore sequencer. *BMC Infect. Dis.* 17, 621. doi: 10.1186/s12879-017-2718-9

Jain, M., Fiddes, I. T., Miga, K. H., Olsen, H. E., Paten, B., and Akeson, M. (2015). Improved data analysis for the MinION nanopore sequencer. *Nat. Methods* 12, 351–356. doi: 10.1038/nmeth.3290

Juul, S., Izquierdo, F., Hurst, A., Dai, X., Wright, A., Kulesha, E, et al. (2015). What's in my pot? real-time species identification on the MinION™. *bioRxiv*. doi: 10.1101/030742

Karamitros, T., and Magiorkinis, G. (2018). Multiplexed targeted sequencing for Oxford nanopore MinION: A detailed library preparation procedure. *Methods Mol. Biol.* 1712, 43–51. doi: 10.1007/978-1-4939-7514-3_4

Lamy, B., Sundqvist, M., Idelevich, E. A.Escmid Study Group for Bloodstream Infections, E., and Sepsis (2020). Bloodstream infections - standard and progress in pathogen diagnostics. *Clin. Microbiol. Infect.* 26, 142–150. doi: 10.1016/j.cmi.2019.11.017

Lehrnbecher, T., Averbuch, D., Castagnola, E., Cesaro, S., Ammann, R. A., Garcia-Vidal, C., et al. (2021). 8th European conference on infections in leukaemia: 2020 guidelines for the use of antibiotics in paediatric patients with cancer or post-haematopoietic cell transplantation. *Lancet Oncol.* 22, e270–e280. doi: 10.1016/S1470-2045(20)30725-7

Leland, D. S., and Ginocchio, C. C. (2007). Role of cell culture for virus detection in the age of technology. *Clin. Microbiol. Rev.* 20, 49–78. doi: 10.1128/CMR.00002-06

Lewandowski, K., Xu, Y., Pullan, S. T., Lumley, S. F., Foster, D., Sanderson, N., et al. (2019). Metagenomic nanopore sequencing of influenza virus direct from clinical respiratory samples. *J. Clin. Microbiol.* 58, e00963–19. doi: 10.1128/JCM.00963-19

Li, H. (2018). Minimap2: pairwise alignment for nucleotide sequences. *Bioinformatics* 34, 3094–3100. doi: 10.1093/bioinformatics/bty191

Malek, A. E., Khalil, M., Hachem, R., Chaftari, A. M., Fares, J., Jiang, Y., et al. (2021). Impact of checkpoint inhibitor immunotherapy, primarily pembrolizumab, on infection risk in patients with advanced lung cancer: A comparative retrospective cohort study. *Clin. Infect. Dis.* 73, e2697–e2704. doi: 10.1093/cid/ciaa802

Marchetti, O., and Calandra, T. (2002). Infections in neutropenic cancer patients. *Lancet* 359, 723–725. doi: 10.1016/S0140-6736(02)07900-X

Morrison, G. A., Fu, J., Lee, G. C., Wiederhold, N. P., Canete-Gibas, C. F., Bunnik, E. M., et al. (2020). Nanopore sequencing of the fungal intergenic spacer sequence as a potential rapid diagnostic assay. *J. Clin. Microbiol.* 58, e01972–20. doi: 10.1128/JCM.01972-20

Nesher, L., and Rolston, K. V. (2014). The current spectrum of infection in cancer patients with chemotherapy related neutropenia. *Infection* 42, 5–13. doi: 10.1007/s15010-013-0525-9

Noone, J. C., Helmersen, K., Leegaard, T. M., Skramm, I., and Aamot, H. V. (2021). Rapid diagnostics of orthopaedic-Implant-Associated infections using nanopore shotgun metagenomic sequencing on tissue biopsies. *Microorganisms* 9, 97. doi: 10.3390/microorganisms9010097

Peri, A. M., Harris, P. N. A., and Paterson, D. L. (2022). Culture-independent detection systems for bloodstream infection. *Clin. Microbiol. Infect.* 28, 195–201. doi: 10.1016/j.cmi.2021.09.039

Peri, A. M., Stewart, A., Hume, A., Irwin, A., and Harris, P. N. A. (2021b). New microbiological techniques for the diagnosis of bacterial infections and sepsis in ICU including point of care. *Curr. Infect. Dis. Rep.* 23, 12. doi: 10.1007/s11908-021-00755-0

Piantadosi, A., Mukerji, S. S., Ye, S., Leone, M. J., Freimark, L. M., Park, D., et al. (2021). Enhanced virus detection and metagenomic sequencing in patients with meningitis and encephalitis. *mBio* 12, e0114321. doi: 10.1128/mBio.01143-21

Player, R., Verratti, K., Staab, A., Bradburne, C., Grady, S., Goodwin, B., et al. (2020). Comparison of the performance of an amplicon sequencing assay based on Oxford nanopore technology to real-time PCR assays for detecting bacterial biodefense pathogens. *BMC Genomics* 21, 166. doi: 10.1186/s12864-020-6557-5

Rodino, K. G., Toledano, M., Norgan, A. P., Pritt, B. S., Binnicker, M. J., Yao, J. D., et al. (2020). Retrospective review of clinical utility of shotgun metagenomic sequencing testing of cerebrospinal fluid from a U.S. tertiary care medical center. *J. Clin. Microbiol.* 58, e01729–20. doi: 10.1128/JCM.01729-20

Rutanga, J. P., Van Puyvelde, S., Heroes, A. S., Muvunyi, C. M., Jacobs, J., and Deborggraeve, S. (2018). 16S metagenomics for diagnosis of bloodstream infections: opportunities and pitfalls. *Expert Rev. Mol. Diagn.* 18, 749–759. doi: 10.1080/14737159.2018.1498786

Sakai, J., Tarumoto, N., Kodana, M., Ashikawa, S., Imai, K., Kawamura, T., et al. (2019). An identification protocol for ESBL-producing gram-negative bacteria bloodstream infections using a MinION nanopore sequencer. *J. Med. Microbiol.* 68, 1219–1226. doi: 10.1099/jmm.0.001024

Schlesinger, A., Paul, M., Gafter-Gvili, A., Rubinovitch, B., and Leibovici, L. (2009). Infection-control interventions for cancer patients after chemotherapy: a systematic review and meta-analysis. *Lancet Infect. Dis.* 9, 97–107. doi: 10.1016/S1473-3099(08)70284-6

Schmidt, K., Mwaigwisya, S., Crossman, L. C., Doumith, M., Munroe, D., Pires, C., et al. (2017). Identification of bacterial pathogens and antimicrobial resistance directly from clinical urines by nanopore-based metagenomic sequencing. *J. Antimicrob. Chemother.* 72, 104–114. doi: 10.1093/jac/dkw397

Schuele, L., Cassidy, H., Peker, N., Rossen, J. W. A., and Couto, N. (2021). Future potential of metagenomics in microbiology laboratories. *Expert Rev. Mol. Diagn.* 21, 1273–1285. doi: 10.1080/14737159.2021.2001329

Siegel, R. L., Miller, K. D., Fuchs, H. E., and Jemal, A. (2021). Cancer statistic. *CA Cancer J. Clin.* 71, 7–33. doi: 10.3322/caac.21654

Stefan, C. P., Hall, A. T., Graham, A. S., and Minogue, T. D. (2022). Comparison of illumina and Oxford nanopore sequencing technologies for pathogen detection from clinical matrices using molecular inversion probes. *J. Mol. Diagn.* 24, 395–405. doi: 10.1016/j.jmoldx.2021.12.005

Van Cutsem, G., Isaakidis, P., Farley, J., Nardell, E., Volchenkov, G., and Cox, H. (2016). Infection control for drug-resistant tuberculosis: Early diagnosis and treatment is the key. *Clin. Infect. Dis.* 62 (Suppl 3), S238–S243. doi: 10.1093/cid/ciw012

Van Den Bosch, C., Van Woensel, J., and Van De Wetering, M. D. (2021). Prophylactic antibiotics for preventing gram-positive infections associated with long-term central venous catheters in adults and children receiving treatment for cancer. *Cochrane Database Syst. Rev.* 10, CD003295. doi: 10.1002/14651858.CD003295.pub4

Vento, S., and Cainelli, F. (2003). Infections in patients with cancer undergoing chemotherapy: aetiology, prevention, and treatment. *Lancet Oncol.* 4, 595–604. doi: 10.1016/S1470-2045(03)01218-X

Verma, R., Foster, R. E., Horgan, K., Mounsey, K., Nixon, H., Smalle, N., et al. (2016). Lymphocyte depletion and repopulation after chemotherapy for primary breast cancer. *Breast Cancer Res.* 18, 10. doi: 10.1186/s13058-015-0669-x

Votintseva, A. A., Bradley, P., Pankhurst, L., Del Ojo Elias, C., Loose, M., Nilgiriwala, K., et al. (2017). Same-day diagnostic and surveillance data for tuberculosis *via* whole-genome sequencing of direct respiratory samples. *J. Clin. Microbiol.* 55, 1285–1298. doi: 10.1128/JCM.02483-16

Weil, B. R., Madenci, A. L., Liu, Q., Howell, R. M., Gibson, T. M., Yasui, Y., et al. (2018). Late infection-related mortality in asplenic survivors of childhood cancer: A report from the childhood cancer survivor study. *J. Clin. Oncol.* 36, 1571–1578. doi: 10.1200/JCO.2017.76.1643

Wise, J. (2016). Chemotherapy could make breast cancer patients more vulnerable to common infections. *BMJ* 532, i407. doi: 10.1136/bmj.i407

World Medical Association (2013). World medical association declaration of Helsinki: ethical principles for medical research involving human subjects. *JAMA* 310, 2191–2194. doi: 10.1001/jama.2013.281053

Zaorsky, N. G., Churilla, T. M., Egleston, B. L., Fisher, S. G., Ridge, J. A., Horwitz, E. M., et al. (2017). Causes of death among cancer patients. *Ann. Oncol.* 28, 400–407. doi: 10.1093/annonc/mdw604

frontiers | Frontiers in Cellular and Infection Microbiology

TYPE Original Research
PUBLISHED 26 September 2022
DOI 10.3389/fcimb.2022.979086

OPEN ACCESS

EDITED BY
Pushpanathan Muthuirulan,
Harvard University, United States

REVIEWED BY
Yafeng Qiu,
Shanghai Veterinary Research Institute (CAAS), China
Chaitanya Tellapragada,
Karolinska Institutet (KI), Sweden

*CORRESPONDENCE
Xiaoling Ma
maxiaoling@ustc.edu.cn

†These authors have contributed equally to the work and share first authorship

SPECIALTY SECTION
This article was submitted to Clinical Microbiology, a section of the journal Frontiers in Cellular and Infection Microbiology

RECEIVED 27 June 2022
ACCEPTED 24 August 2022
PUBLISHED 26 September 2022

CITATION
Zhang S, Wu G, Shi Y, Liu T, Xu L, Dai Y, Chang W and Ma X (2022) Understanding etiology of community-acquired central nervous system infections using metagenomic next-generation sequencing. *Front. Cell. Infect. Microbiol.* 12:979086. doi: 10.3389/fcimb.2022.979086

Understanding etiology of community-acquired central nervous system infections using metagenomic next-generation sequencing

Shanshan Zhang[1†], Gang Wu[2†], Yuru Shi[2], Ting Liu[2], Liangfei Xu[2], Yuanyuan Dai[2], Wenjiao Chang[2] and Xiaoling Ma[2*]

[1]Department of Medical Oncology, The First Affiliated Hospital of University of Science and Technology of China (USTC), Division of Life Sciences and Medicine, University of Science and Technology of China, Hefei, China, [2]Department of Clinical Laboratory, The First Affiliated Hospital of University of Science and Technology of China (USTC), Division of Life Sciences and Medicine, University of Science and Technology of China, Hefei, China

Background: Community-acquired central nervous system infections (CA-CNS infections) have the characteristics of acute onset and rapid progression, and are associated with high levels of morbidity and mortality worldwide. However, there have been only limited studies on the etiology of this infections. Here, metagenomic next-generation sequencing (mNGS), a comprehensive diagnosis method, facilitated us to better understand the etiology of CA-CNS infections.

Methods: We conducted a single-center retrospective study between September 2018 and July 2021 in which 606 cerebrospinal fluid (CSF) samples were collected from suspected CNS infectious patients for mNGS testing, and all positive samples were included in this analysis

Results: After the exclusion criteria, a total of 131 mNGS-positive samples were finally enrolled. Bacterial, viral, fungal, parasitic, specific pathogen and mixed infections were accounted for 32.82% (43/131), 13.74% (18/131), 0.76% (1/131), 2.29% (3/131) and 6.87% (9/131), respectively. A total of 41 different pathogens were identified, including 16 bacteria, 12 viruses, 10 fungi, and 1 parasite and 3 specific pathogens. The most frequent infecting pathogens are *Epstein-Barr virus* (n = 14), *Herpes simplex virus 1* (n = 14), *Mycobacterium tuberculosis* (n = 13), *Streptococcus pneumoniae* (n = 13), and *Cryptococcus neoformans* (n = 8). Some difficult-to-diagnose pathogen infections were also detected by mNGS, such as *Streptococcus suis*, *Pseudorabies virus*, *Bunyavirus*, *Orientia tsutsugamushi* and *Toxoplasma gondii*.

Conclusion: In this study, mNGS identified a wide variety of pathogens of CA-CNS infections and many of which could not be detected by conventional methods. Our data provide a better understanding of the etiology of CA-CNS

infections and show that mNGS represents a comparative screening of CSF in an unbiased manner for a broad range of human pathogens.

KEYWORDS

community-acquired central nervous system infections, etiology, metagenomic next-generation sequencing, diagnosis, cerebrospinal fluid

Introduction

Central nervous system (CNS) infections are inflammations of the brain and spinal cord caused by pathogenic microbes. Various environmental or commensal microorganisms can migrate through the blood-brain barrier (BBB) into the CNS to cause inflammation, manifested as fever, headache, vomiting, neck stiffness, disturbance of consciousness, convulsions and focal neurological deficits (Granerod et al., 2010). Although the incidences of CNS infections have fallen to 0.9 per 100,000 population in high-income countries like the USA, the global number of reported cases has risen during the past decade, particularly in Africa, with incidences up to 1000 per 100,000 population (GBD 2016 Neurology Collaborators, 2018). Despite the existence of antibiotic therapies, CNS infections are devastating clinical conditions that cause substantial mortality and severe sequelae (Brouwer et al., 2010).

Pathogen detection is important for diagnosis and treatment of CNS infections. Conventional methods used in clinical microbiology laboratories include culture techniques, antigen tests and polymerase chain reaction (PCR) (Brand et al., 2016). Culture-dependent method is regarded as the gold standard for pathogen diagnosis of infectious diseases, but this approach may take several days, and the results may be negative if antimicrobials are administered empirically or if the infection is caused by fastidious or nonculturable microorganisms like viruses (Brand et al., 2016). Antigen tests have a limited variety of reagents and are used only for the diagnosis of a few pathogen infections, such as Cryptococcus (Antinori et al., 2005). Although multiplex PCR assays, such as FilmArray meningitis or encephalitis panel are considered sensitive methods that allow the rapid detection and identification of infectious agents, they are restricted to a partial number of suspected microorganisms, limiting their utility as a standalone test in CNS infections diagnostics (Leber et al., 2016).

Recently, metagenomic next-generation sequencing (mNGS) has emerged as an unbiased technology that allows the simultaneous identification of all microorganisms in a single clinical sample (Goldberg et al., 2015; Miao et al., 2018; Miller et al., 2019). This culture-independent application ensures a detailed sequencing of the total DNA or RNA content of the microbiome and can be used for universal pathogen detection regardless of the microbe type (e.g., bacteria, viruses, fungi or parasites) (Schlaberg et al., 2017). Owing to its sensitivity, speed, and cost-effectiveness considerations, mNGS has the potential to become a routine workup in infectious disease diagnosis and pathogen identification of unknown origin.

CNS infections can be acquired spontaneously in the community (community-acquired CNS infections [CA-CNS infections]) or in the hospital as a complication of invasive procedures or head trauma (hospital-acquired CNS infections [HA-CNS infections]) (van de Beek et al., 2006; van de Beek et al., 2010). Compared with HA-CNS infections, CA-CNS infections are caused by a wider variety of pathogens, including bacteria, viruses, fungi, parasites and other specific microbes (van de Beek et al., 2021). Because of the limitations of conventional diagnostic methods for CNS infections, most of the current data on epidemiology of CNS infectious syndromes were focused on specific types of pathogens (van Kassel et al., 2020; van de Beek et al., 2021). In addition, vaccination and epidemiology make the etiology of CA-CNS infections differ among different countries and regions, and there is still a lack of studies to facilitate our investigation on etiology of CA-CNS infections. Therefore, we performed a retrospective study of a large-scale cohort that was positive for CSF pathogen detection using mNGS, and attempted to provide a better understanding of etiology of CNS infection in community settings via one standalone detection method.

Materials and methods

Study design

All patients were admitted to the First Affiliated Hospital of University of Science and Technology of China, which is a large class IIIA general hospital with 5750 beds. From September 2018 to July 2021, suspected CNS infectious patients underwent lumbar puncture after signing informed consents. CSF samples were sent for routine testing, biochemical testing and culture for bacteria and fungi. If the patient was critically ill, the CSF sample was tested by mNGS synchronously; if not, further mNGS was conducted when the CSF culture was negative. Metagenomic transcriptome sequencing was performed when patients were

suspected of viral infection but negative for mNGS DNA sequencing. All mNGS-positive samples were included in this analysis, and the exclusion criteria were as follows: not consistent with clinical diagnosis; incomplete medical history; replicated specimens from one patient; hospital-acquired infections (samples from hospitalized patients undergoing brain surgery, organ or hematopoietic stem cell transplantation) and neonatal meningitis. Eligible patients included for analysis were categorized into six groups according to the mNGS results: bacterial infections, viral infections, fungal infections, parasitic infections, other specific pathogen infections and mixed infections. Figure 1 presents the flow chart of study enrolment.

DNA extraction, library preparation, and mNGS of CSF

1.5-3 ml CSF sample was collected from each patient by lumbar puncture in accordance with standard procedures. A 1.5 ml microcentrifuge tube with 0.6 ml sample and 250 μl, 0.5 mm glass bead were attached to a horizontal platform on a vortex mixer and agitated vigorously at 2800-3200 rpm for 30 min. Then 7.2 μl lysozyme was added for wall-breaking reaction. 0.3 ml sample was separated into a new 1.5 ml microcentrifuge tube and DNA was extracted using the TIANamp Micro DNA Kit (DP316, Tiangen Biotech) according to the manufacturer' s recommendation (Long et al., 2016).

Nucleic acids RNA extracted from the clinical samples using the TIANamp Micro RNA Kit (DP431, Tiangen Biotech, Beijing, China) in accordance with the manufacturer's standard protocols. The reverse transcription reaction was performed to generate single-strand cDNA, followed by the synthesis of double-strand cDNA using the PMseq™ RNA Infection Pathogen High-throughput Detection Kit according to the manufacturer's instructions.

Then, DNA libraries were constructed through DNA fragmentation, end repair, adapter ligation and PCR amplification. Agilent 2100 was used for quality control of the DNA libraries. Quality qualified libraries were pooled, DNA Nanoball (DNB) was made and sequenced by BGISEQ-50/MGISEQ-2000 platform. Negative control was set as quality control in each test.

Interpretation of mNGS data

Raw sequence data were first filtered by removing common background microorganisms and low-quality reads. Then the filtered sequences were mapped to the human reference database (hg38) using Burrows-Wheeler alignment to computationally subtract the human sequence (Li and Durbin, 2009). The remaining data were further classified by simultaneously alignment to Pathogens Metagenomics Database (Refseq). The classification reference databases were downloaded from the National Center Biotechnology Information (NCBI) (ftp://ftp.ncbi.nlm.nih.gov/genomes/). RefSeq contains 4945 whole genome sequence of viral taxa, 6350 bacterial genomes or scaffolds, 1064 fungi and 234 parasites related to human infections.

The criteria for positive results were as follows: 1) mNGS identified bacteria (mycobacteria and nocardia excluded), virus and parasites when the coverage rate was 10-fold greater than that of any other microorganisms. 2) mNGS identified

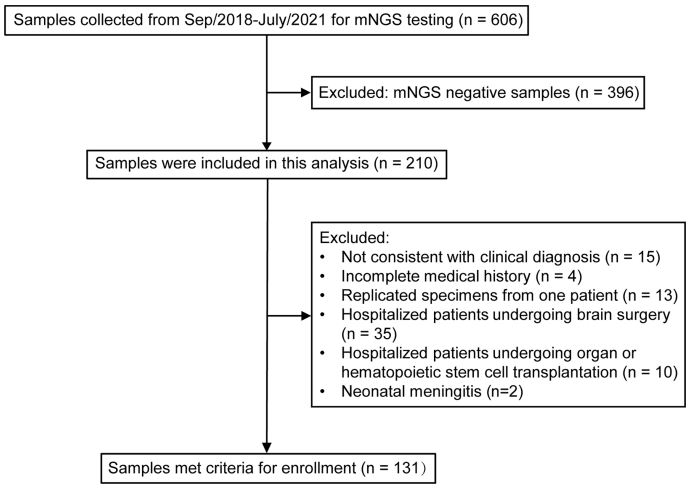

FIGURE 1
Flowchart of study enrollment.

Mycobacterium tuberculosis when the genus-specific read number ≥ 1. 3) mNGS identified nontuberculous mycobacteria and nocardia when the mapping read number (genus or species level) was in the top 10 in the bacteria list. 4) mNGS identified fungi when the coverage rate was 5-fold greater than that of any other microorganisms.

Statistical analysis

Differences across independent binomial variables were evaluated by Chi-square test and Fisher's exact test. Differences across continuous variables were evaluated by analysis of variance (ANOVA) when they conform to Gaussian distribution and by Mann-Whitney test or Kruskal Wallis test when not. Data analyses were performed using GraphPad Prism software (version 8.0). P values < 0.05 were considered significant, and all tests were two-tailed.

Standard protocol approvals, registrations, and patient consents

This study was approved by the Ethics Committee of the First Affiliated Hospital of University of Science and Technology of China (approval no. 2021-BE(H)-005). Written informed consent was obtained from all patients or their legal representatives.

Results

Clinical characteristics and CSF laboratory examinations of enrolled patients

Between September 2018 and July 2021, a total of 606 samples were collected for mNGS detection, of which 210 were positive. We next excluded 15 samples that not consistent with clinical diagnosis, 4 samples with incomplete medical history, 13 replicated specimens, 45 cases with hospital-acquired infections and 2 cases with neonatal meningitis, and 131 samples were finally enrolled as CA-CNS infections. Overall, males accounted for the majority of patients with bacterial (35/57 [61.40%]) and viral (33/43 [76.74%]) infections, but a minority in the fungal infection group (8/18 [44.44%]). The average age of total 131 patients was 42.37 ± 22.84 years, 18 patients were 12 years of age or younger and 36 patients were over 65 years of age. Bacteria caused more infections in children (11/57 [19.30%]) but fewer infections in the elderly (8/57 [14.03%]) than viruses (children, 9.30%; elderly, 34.89%) and fungi (children, 5.56%; elderly, 22.22%). Bacterial (33/57 [57.89%]) and fungal (12/18 [66.67%]) infections occurred more frequently in spring and summer, while viral (22/43 [51.16%]) infections were more common in fall and winter. The typical neurological manifestations of enrolled patients were headache (66/131 [51.16%]), disturbance of consciousness (47/131 [36.43%]), neck stiffness (30/131 [23.26%]) and convulsions (19/131 [14.73%]), with many patients also presenting systemic symptoms such as fever (94/131 [72.84%]), and vomiting (30/131 [23.26%]). Most patients were admitted to the infectious disease department (42/131 [32.06%]), neurology department (34/131 [25.95%]) or intensive care unit (ICU) (29/131 [22.14%]), followed by the pediatric department (18/131 [13.47%]) or hematology department (6/131 [4.58%]). Critically ill patients who were admitted to the ICU more commonly had bacterial (12/57 [21.05%]) and viral (13/43 [30.23%]) infections than fungal (1/18 [5.56%]) ones. CSF laboratory results in different CNS infections groups revealed that the bacterial subgroup had a significantly higher CSF white blood cell (WBC) count ($p < 0.0016$) and protein level ($p = 0.0053$) but a lower glucose level ($p = 0.0393$) than the viral and fungal subgroups. Besides, CSF chlorine level was significantly lower in fungal infections patients than in those with bacterial and viral infections ($p = 0.0037$). Thanks to the rapid mNGS diagnosis and timely antibiotic treatment, most infected patients eventually improved or recovered (107 [81.68%]). The clinical and laboratory data are summarized in Table 1.

Etiological diagnosis of CA-CNS infections using mNGS

In this study, etiological diagnosis showed that bacterial infections (57/131 [43.51%]) were the most common, while viral, fungal, parasitic and specific pathogen infections were accounted for 32.82% (43/131), 13.74% (18/131), 0.76% (1/131) and 2.29% (3/131) of all patients, respectively. In 9 (6.87%) patients, two causative agents were identified, including 3 with recorded mixed infections of Cryptococcus neoformans and Epstein-Barr virus (Figure 2A). In addition, we found the positive rate of was 7.63% (10/131) by culture, 21.37% (28/131) by antigen test and 3.05% (4/131) by PCR, including 4 were confirmed by two different methods (Supplementary Table). The read numbers of Mycobacterium tuberculosis were significantly lower than those of other types of microbes, while these cases were eventually confirmed as tubercular meningitis (TBM) through the medical history, other examination results and treatment outcomes (Figure 2B).

As shown in Figure 2C, we identified 140 pathogens of 41 different pathogens in the CSF from 131 patients. 16 different agents were detected from patients with bacterial infections, of which Mycobacterium tuberculosis (13 cases) and Streptococcus pneumoniae (13 cases) were the most frequent causative microbes, followed by Enterococcus faecium (6 cases), Acinetobacter baumannii (4 cases) and Klebsiella pneumoniae (4 cases). Among viral infections caused by 13 different agents,

TABLE 1 Clinial characteristics and CSF laboratory examinations of enrolled cases.

	mNGS-positive samples (n=131)	Bacterial infections (n=57) (a)	Viral infections (n=43) (b)	Fungal infections (n=18) (c)	p value among a-c
Gender no. (%)					0.0449*
Male	83 (63.36)	35 (61.40)	33 (76.74)	8 (44.44)	
Female	48 (36.64)	22 (38.60)	10 (23.26)	10 (55.56)	
Age no. (%)					0.0854
0-12 yr	18 (13.74)	11 (19.30)	4 (9.30)	1 (5.56)	
13-60 yr	77 (58.78)	38 (66.67)	24 (55.81)	13 (72.22)	
>60 yr	36 (27.48)	8 (14.03)	15 (34.89)	4 (22.22)	
Month no. (%)					0.4048
Mar.-Aug.	75 (57.25)	33 (57.89)	21 (48.84)	12 (66.67)	
Sept.-Feb.	56 (42.75)	24 (42.11)	22 (51.16)	6 (33.33)	
Clinical manifestation no. (%)					
Fever	94 (72.87)	42 (73.68)	31 (75.61)	11 (61.11)	0.5823
Headache	66 (51.16)	32 (56.14)	17 (41.46)	12 (66.67)	0.0996
Neck stiffness	30 (23.26)	19 (33.33)	8 (19.51)	2 (11.11)	0.0843
Vomiting	30 (23.26)	15 (26.32)	9 (21.95)	3 (16.67)	0.648
Disturbance of consciousness	47 (36.43)	19 (33.33)	20 (48.78)	4 (22.22)	0.1579
Convulsions	19 (14.73)	9 (15.79)	8 (19.51)	2 (11.11)	0.7651
Department no. (%)					0.0280*
Infectious disease department	42 (32.06)	21 (36.84)	10 (23.26)	7 (38.88)	
Intensive care unit	29 (22.14)	12 (21.05)	13 (30.23)	1 (5.56)	
Neurology department	34 (25.95)	11 (19.30)	14 (32.56)	5 (27.78)	
Pediatric department	18 (13.74)	11 (19.30)	4 (9.30)	2 (11.11)	
Hematology department	6 (4.58)	2 (3.51)	2 (4.65)	1 (5.56)	
Others	2 (1.53)	0	0	2 (11.11)	
CSF laboratory test, median (range)					
CSF WBC ($\times 10^6$/L)	121 (0.00-21229.00)	211 (1.00-21229.00)	57 (1.00-579.00)	20 (1.00-217.00)	< 0.0001*
CSF Protein (g/L)	1.03 (0.20-25.77)	1.38 (0.20-25.77)	0.94 (0.29-13.61)	0.49 (0.22-9.90)	0.0053*
CSF Glucose (mmol/L)	3.1 (0.05-14.13)	2.58 (0.15-7.19)	3.32 (0.83-7.61)	2.94 (1.32-4.42)	0.0393*
CSF Chlorine (mmol/L)	118.3 (94.70-137.70)	118.3 (94.70-137.70)	117.4 (106.4-132.20)	104.9 (116.00-132.80)	0.0037*
Outcome no. (%)					0.7245
Improvement	107 (81.68)	45 (78.95)	37 (86.05)	16 (88.89)	
Progression	21 (16.03)	10 (17.54)	6 (13.95)	2 (11.11)	
Death	3 (2.29)	2 (3.51)	0	0	

Statistics: Chi-square or Fisher's exact test for calculations of clinical characteristics. ANOVA or Kruskal Wallis test for calculations of CSF laboratory examinations. *P value < 0.05.

the top 5 most commonly detected pathogens were Epstein-Barr virus (EBV) (14 cases), Herpes simplex virus 1 (HSV1) (14 cases), Cytomegalovirus (CMV) (4 cases), Varicella zoster virus (VZV) (4 cases) and Pseudorabies virus (PRV) (3 cases), while 2 Bunyavirus infections were observed using RNA mNGS. The most frequently detected fungal infections were cryptococcal meningitis (8 cases), aspergillus meningitis (6 cases) and candidal meningitis (5 cases). In addition, 1 case was parasitic infection caused by Toxoplasma gondii and 3 cases were infected with other specific pathogens [Mycoplasma hominis (n = 1), Orientia tsutsugamushi (n = 1), Rickettsia (n = 1)].

Diagnosis of CA-CNS infections caused by specific pathogens using mNGS

mNGS of has already been widely used for identifying novel or unexpected pathogens in various infectious diseases, we

10.3389/fcimb.2022.979086

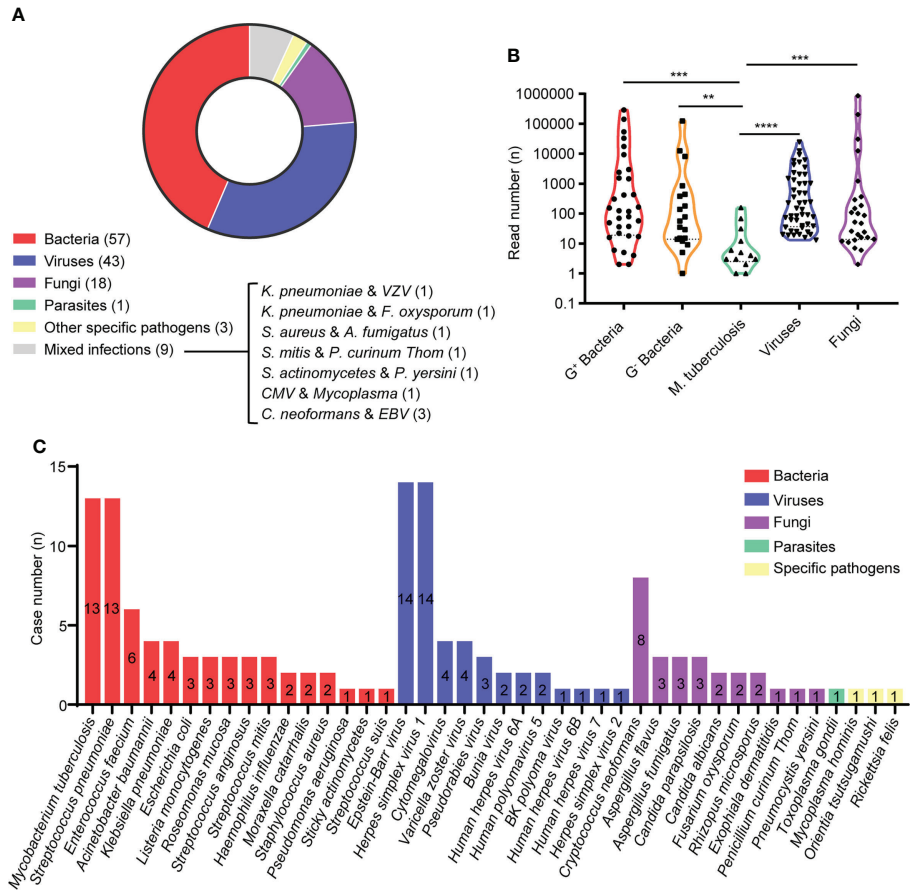

FIGURE 2
Etiolgy of CA-CNS infections identified by mNGS in the present study. **(A)** Pie charts demonstrated the distribution of different types of microbial infections. **(B)** Violin polot showed read numbrers of pathogen species. G^+ bacteria (n = 32); G^- bacteria (n = 19); *Mycobacterium tuberculosis* (n = 13); viruses (n = 49); fungi (n = 26). Data were analyzed by Mann-Whitney test. **(C)** A total of 40 different species of pathogens were detected in the different infectious groups with their corresponding frequencies plotted in histograms. ** $p < 0.01$, *** $p < 0.001$, **** $p < 0.0001$.

therefore report herein the utility of mNGS for identifying microbial pathogens in five challenging cases of CA-CNS infections in our study.

Streptococcus suis

This patient was a 59-year-old butcher. On September 2018, he hurt his left finger when dissecting dead swine. Two days later, he presented with vomiting, fever, weakness and somnolence, which rapidly progressed to coma and petechiae and was admitted to the ICU. His WBC count was 17.04 × 109/L with 88.7% neutrophils; prothrombin time (PT) was 48.8 s; D dimer (D-D) > 20.00 mg/L; procalcitonin (PCT) was 100 ng/ml and C-reactive protein (CRP) was 107.98 mg/L. CSF examination revealed a WBC count of 233 × 109/L comprising 62% neutrophils, a glucose level of 0.5 mmol/L, a total protein level of 2.6 g/L and a chlorine level of 120.0 mmol/L. Bacterial and fungal cultures of blood and CSF were negative, raising concern for an alternative diagnosis. His CSF mNGS data contained 289518 reads aligning to Streptococcus suis. After etiological diagnosis was achieved, he was treated with a high dose of penicillin for 16 days and repeated blood and CSF examination results improved to the baseline.

Pseudorabies virus

A previously healthy 44-year-old pork vender was admitted to our hospital on January 2019 with a 4-day history of headache and cough and a 1-day history of fever (41°C) and intermittent convulsions. Other symptoms included neck stiffness and disturbance of consciousness. Routine laboratory investigations revealed CRP was 18.40 mg/L; Creatine kinase (CK) was 16111 IU/L; CK-MB was 150 IU/L and Myoglobin (Mb) was 8770 ng/ml. The rest of the blood and CSF laboratory tests were all within the normal range. Magnetic resonance imaging (MRI) of the brain showed hyperintense signal distributed symmetrically in

the bilateral cerebral hemispheres (Figures 3–C), which was consistent with the characteristics of encephalitis. Etiology diagnoses including serum TORCH series, immune combination and PCR of EBV and CMV were all negative. We treated him with sodium valproate to prevent seizures and sent the CSF samples for analysis with mNGS. The results showed 83 reads specifically mapped to Pseudorabies virus. Then, the CSF specimen sent for PCR amplified PRV and the result of CSF PRV IgG antibody test was positive. After 2 months of treatment with acyclovir, ceftriaxone and sodium valproate, he showed mild clinical improvement and was transferred to the rehabilitation hospital.

Bunyavirus

On March 2021, a 40-year-old woman was bitten by insects when picking tea and then presented with diarrhea, fatigue and fever (39°C). She was admitted to the infectious disease department and laboratory tests showed WBC count was 1.99 × 109/L with 61.6% neutrophils; and platelet (PLT) count was 38 × 109/L. CSF routine and biochemistry tests were within the normal ranges. Serum TORCH series and antibody tests for EBV and tsutsugamushi disease were negative, while Hepatitis B virus (HBV) antigen test was positive. The patient was treated empirically with ribavirin, minocycline and levofloxacin. However, she developed worsening unconsciousness and coagulation disorders, with gradual decreases of blood pressure (67/26 mmHg) and oxygen saturation (SaO2) (78%). Then she was transferred to the ICU and CSF sample was immediately tested by mNGS. The sequencing detection identified 1321 RNA sequence reads uniquely corresponding to Bunyavirus. The patient was subsequently treated with continuous blood purification combined with antiviral therapy. Nevertheless, the disease rapidly progressed with aggravated shock and disseminated intravascular coagulation (DIC), and she was finally discharged voluntarily.

Orientia tsutsugamushi

On November 2020, a 71-year-old woman was admitted to the neurology department of our hospital because of fever and insanity without obvious predisposing factors for 5 days. She presented with intermittent convulsions, unable to recognize her family, raving and urinary incontinence. Upon admission, PLT count was 87 × 109/L and CRP was 298.6 mg/L. The rest of the blood laboratory tests were all within the normal range. The cytology of CSF demonstrated increased WBCs (23 × 106/L) and protein concentration (0.78 g/L). After admission, the patient's symptoms gradually deteriorated with progressive decrease of PLT count, myocardial damage and pulmonary infection. Bacterial cultures were negative while CSF mNGS returned 14 reads mapping to Orientia tsutsugamushi. After etiological diagnosis was identified, treatment with levofloxacin and mannitol was initiated. On the 20th day, her clinical condition was noticeably improved with recovered from fever and pulmonary infection. A repeat lumbar puncture revealed improved WBCs and protein. Thus, she was discharged on the 23rd day.

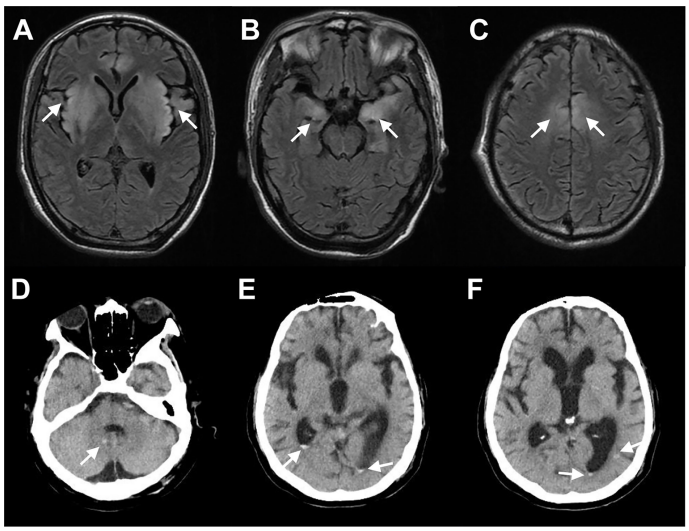

FIGURE 3
Selected Neuroimaging. **(A–C)** MRI of patient infected with *Porcine herpesvirus 1* showed hyperintense signal distributed symmetrically in the bilateral insula lobe, the basal ganglia, the hippocampus, and the frontal lobe on T2 fluid-attenuated inversion recovery (FLAIR). **(D–F)** CT of patient infected with *Toxoplasma gondii* showed multiple oval high-density shadows in the right cerebellar hemisphere, the posterior regions of bilateral ventricles, and the posterior corner of the left lateral ventricle. Arrows point to areas with enhanced signals.

Toxoplasma gondii

A 68-year-old male patient was admitted to our hospital on October 2019 due to fever (40°C) accompanied by diarrhea for 3 days. He had a history of coronary heart disease for 4 years and had received heart transplant 1 month previously. After the surgery, he had been taking immunosuppressive drugs including tacrolimus, motimecocuronol ester and hormone. Blood tests on admission showed WBC count of 13.4 × 109/L, neutrophil rate of 82.6%; CRP of 62.27 mg/L; CK of 564.0 IU/L; CK-MB of 249 IU/L; and brain natriuretic peptide (BNP) of 3734 pg/ml. Lumbar puncture was subsequently performed and CSF WBC count was 307 × 106/L, of which neutrophils accounted for 94%; proteins was 1.50 g/L; glucose was 14.13 mmol/L; chlorine was 119 mmol/L. Brian computed tomography (CT) revealed multiple oval high-density shadows in the right cerebellar hemisphere and the posterior regions of bilateral ventricles (Figure 3D–F). After empirical treatment with ceftizoxime, azithromycin and oseltamivir, his symptoms worsened with the developed oliguria, dyspnea and decreased SaO2. His CSF was collected for mNGS to determine the pathogen and the results showed a total of 8999 unique sequences of Toxoplasma gondii. CSF specimen that had been subsequently sent for PCR also amplified the Toxoplasma gene. After the diagnosis was confirmed, sulfonamides were replaced for anti-infection treatment. However, the patient's condition aggravated progressively and he eventually died.

Discussion

The clinical management of patients with CA-CNS infections is highly dependent on the underlying cause of infection or inflammation, making it necessary to obtain a specific etiological diagnosis whenever possible (Polage and Cohen, 2016; van de Beek et al., 2016). Culture remains the mainstay in diagnosing CNS infections, while in clinical laboratories, culture is only used for bacteria and fungi detection. Viruses can grow and reproduce only by obligate parasitism in living sensitive host cells, so the culture medium of viruses is demanding, highly specific, and the culture processes are too complex to be available in many clinical laboratories (Storch, 2000; Kelley and Caliendo, 2001). In our study, mNGS detected 56 cases (42.75% [56/131]) infected with viruses, parasites and other specific pathogens that cannot be cultured. Actually, owing to the use of antibiotics before lumbar puncture and the slow growth of some pathogens such as Mycobacterium tuberculosis and Cryptococcus neoformans, the yield of CSF cultures in suspected cases is low (Glaser et al., 2006). Zhang et al. reported that in 83 cases of mNGS positive CSF specimens, the culture positive rate was 18.07% (15/83) (Zhang et al., 2020). In our study, mNGS was selected only when the patient was critically ill or CSF culture was negative, so the positive rate of culture was only 7.63% (10/131) in the mNGS-positive population.

FilmArray meningitis/encephalitis panel is a multiplex PCR assay from BioFire Diagnostics to simultaneously detects 14 pathogens, including six bacteria (S. pneumoniae, N. meningitidis, H. influenzae, S. agalactiae, E. coli K1, and L. monocytogenes), seven viruses (enterovirus, HSV-1/2, VZV, CMV, HHV-6, and human parechovirus), and C. neoformans/C. gattii from ≤ 200 µl of CSF in about 1 h (Leber et al., 2018; Tansarli and Chapin, 2020). A total of 42 different species of pathogens were identified from 131 cases in this study and 32 of them from 55 cases were not included in FilmArray panel, indicating that this method is unable to detect all microbes in general and cannot meet the need for diagnosing CA-CNS infections.

Since Wilson et al. identified Leptospira santarosai in the CSF sample of a case with meningoencephalitis in 2014 (Wilson et al., 2014), there has been great interests in the use of mNGS for pathogen detection (Goldberg et al., 2015; Miao et al., 2018; Miller et al., 2019). Miao et al. reported that mNGS could yield a higher sensitivity for pathogen identification and is less affected by prior antibiotic exposure (Miao et al., 2018). In 2021, mNGS was recommended in an expert consensus to assist clinical decision making in cases with CNS infections (Chinese Society of Infectious Diseases and Cerebrospinal Fluid Cytology, 2021). Thus, we sought to define the performance of mNGS testing in CA-CNS infections, especially in the difficult-to-diagnose patient population.

Bacterial meningitis is a considerable burden worldwide. It has been reported that Streptococcus pneumoniae, Neisseria meningitidis, Haemophilus influenzae, and Listeria monocytogenes are the most common pathogens of community-acquired suppurative meningitis (Bijlsma et al., 2016). In our study, there were 13 cases of Streptococcus pneumoniae, 4 of Haemophilus influenzae and 3 of Listeria monocytogenes, while no Neisseria meningitidis was found, which may be related to the vaccination in China. Among the 13 cases of Streptococcus pneumoniae infection, 6 involved were children and 2 finally led to progression or death, demonstrating the importance of pneumococcal immunization (McGill et al., 2016). Listeria monocytogenes is an uncommon but important cause of severe CA-CNS infections. However, it is a challenge for clinicians to diagnose listeria encephalitis at an early stage because of the low positive rate by Gram staining and culture (Paul et al., 1994). In this study, we identified 3 cases of Listeria monocytogenes, highlighting the feasibility of mNGS as a diagnostic method for CNS listeria infections. In addition, we found TBM accounted for 9.92% (13/131) of CA-CNS infections. Xing et al. reported that among the 44 patients with presumed TBM, CSF culture were all negative and Xpert MTB/RIF positivity rate was 16.13% (5/31), while mNGS positivity rate was 27.27% (12/44) (read number ≥ 1),

indicating mNGS is extremely feasible for diagnosing TBM when at least one specific read is matched to the Mycobacterium tuberculosis complex (Xing et al., 2020).

We found that viruses are the second most common pathogens after bacteria, and 5 patients had mixed infections with bacteria or fungi. Actually, in clinical work, viral and/or mixed infections are easily ignored, but mNGS can diagnose them more effectively. EBV is the most frequent causative virus in our cohort and 3 cases were co-infected with Cryptococcus neoformances. The clinical significance of EBV in CSF is not completely understood. Kelly et al. reported that immunosuppressed patients have elevated concentrations of EBV antibodies in the blood due to large numbers of EBV-infected B lymphocytes, and high EBV viral load is a marker of poor outcome in individuals with co-infections (Kelly et al., 2012). In this study, we also observed RNA sequence reads corresponding to Bunyavirus in 2 cases. It is now possible to detect RNA viruses using mNGS, but the process is complex and expensive, so it is not used in all cases.

Our data showed that the pathogens of fungal infections are widely distributed and accounted for the largest proportion of co-infected patients, among which Cryptococcus neoformans is the most common. Cryptococcus neoformans is also the most common cause of adult meningitis in HIV-infected individuals. It is also found in an increasing number of patients with other types of natural and iatrogenic immunosuppression (Williamson et al., 2017). Among the 8 patients infected with Cryptococcus neoformans in this study, 4 had rheumatic autoimmune disease and 3 had mixed infection. In addition, only one Cryptococcus neoformans was detected by culture in all samples, indicating mNGS has advantages in diagnosis of fungal infections. A descriptive study also showed that mNGS was regarded as a useful tool for the identification of cryptococcal meningitis (Xing et al., 2019).

We further selected 5 challenging cases of CA-CNS infections caused respectively by Streptococcus suis, Pseudorabies virus, Bunyavirus, Orientia tsutsugamushi and Toxoplasma gondii that were confirmed using mNGS. Streptococcus suis and Porcine herpesvirus 1 are zoonotic pathogens that can cause cross-species transmission and induce human infections (Wang et al., 2018; Tan et al., 2021). Most patients have occupations related to pig farming or butchery and become infected via the invasion of wounds by pathogens. Bunyavirus and Orientia tsutsugamushi are insect-borne pathogens which are transmitted to humans through the bites of infected insects. Bunyavirus infection often occurs in environments inhabited by ticks between March and October. Most patients have a history of working in mountains and presented with multiorgan dysfunction (Hulswit et al., 2021). Oriental tsutsugamushi infection, also named as scrub typhus, has clear regional and seasonal characteristics, often occurring in southern China between May and November. Rodents are the main source of this infection, which is transmitted to humans through chigger bites. The toxin released after death of Orientia tsutsugamushi causes toxemia and multiorgan lesions (Lu et al., 2021). The patient who infected with Toxoplasma gondii in this study had received heart transplant and taken immunosuppressants for a long time, making him are susceptible to toxoplasma infection. Toxoplasmic encephalitis is an opportunistic CNS infectious disease caused by the zoonotic pathogens Toxoplasma gondii. It is more common to occur in patients with immunodeficiency or long-term immunosuppressive therapy. With the continuous renewal of immunosuppressive agents in recent years, the clinical incidence of toxoplasmic encephalitis has increased significantly (Kochanowsky and Koshy, 2018). Infections with these pathogens often cause acute symptoms and are difficult to be detected by conventional methods. Therefore, mNGS is an accurate and time-saving technology for the diagnosis of infectious diseases in these conditions.

There are some limitations in our study. Firstly, our data are from a single-center study and cannot fully reflect the etiology of CA-CNS infections. Furthermore, RNA library preparations were conducted in a limited number of patients suspected of viral infection but negative for mNGS DNA sequencing, which might let to neglection of some neuroinvasive RNA viruses like enterovirus. Finally, this is a retrospective study without a careful design in the early stage. Therefore, the detection methods used in different cases were not completely consistent. For example, mNGS and culture were conducted synchronously only when the patient was critically ill, while in other cases mNGS was conducted when the culture was negative so that the positivity rate of culture was extremely low in this study. In Conclusion, CA-CNS infections are caused by a wide variety of pathogens so that traditional methods cannot meet the diagnostic requirements. Our data provided a better understanding on the etiology of CA-CNS infections and showed that mNGS represents a comparative screening of CSF in an unbiased manner for a broad range of human pathogens.

Data availability statement

The raw sequence data reported in this paper have been deposited in the Genome Sequence Archive in National Genomics Data Center, China National Center for Bioinformation / Beijing Institute of Genomics, Chinese Academy of Sciences (GSA: CRA008203) that are publicly accessible at https://ngdc.cncb.ac.cn/gsa.

Ethics statement

The studies involving human participants were reviewed and approved by Ethics Committee of the First Affiliated Hospital of University of Science and Technology of China (USTC) (approval no. 2021-BE(H)-005). Written informed consent to participate in this study was provided by the participants' legal guardian/next of kin. Written informed consent was obtained

from the individual(s) for the publication of any potentially identifiable images or data included in this article.

Author contributions

SZ and GW were responsible for data interpretation, figure preparation, and manuscript drafting and editing; TYS and TL were responsible for next-generation sequencing analysis for this study. LX, YD and WC were responsible for acquisition of clinical data and manuscript editing. XM were responsible for overall project conception, study design, data interpretation and manuscript preparation and editing. All authors contributed to the article and approved the submitted version.

Acknowledgments

We thank the patients for cooperating with our investigation and acknowledge the professionalism and compassion demonstrated by all the healthcare workers involved in patients' care.

Conflict of interest

The authors declare that the research was conducted in the absence of any commercial or financial relationships that could be construed as a potential conflict of interest.

Publisher's note

All claims expressed in this article are solely those of the authors and do not necessarily represent those of their affiliated organizations, or those of the publisher, the editors and the reviewers. Any product that may be evaluated in this article, or claim that may be made by its manufacturer, is not guaranteed or endorsed by the publisher.

Supplementary material

The Supplementary Material for this article can be found online at: https://www.frontiersin.org/articles/10.3389/fcimb.2022.979086/full#supplementary-material

References

Antinori, S., Radice, A., Galimberti, L., Magni, C., Fasan, M., and Parravicini, C. (2005). The role of cryptococcal antigen assay in diagnosis and monitoring of cryptococcal meningitis. *J. Clin. Microbiol.* 43 (11), 5828–5829. doi: 10.1128/jcm.43.11.5828-5829.2005

Bijlsma, M. W., Brouwer, M. C., Kasanmoentalib, E. S., Kloek, A. T., Lucas, M. J., Tanck, M. W., et al. (2016). Community-acquired bacterial meningitis in adults in the netherland-14: a prospective cohort study. *Lancet Infect. Dis.* 16 (3), 339–347. doi: 10.1016/s1473-3099(15)00430-2

Brand, A., Singer, K., Koehl, G. E., Kolitzus, M., Schoenhammer, G., Thiel, A., et al. (2016). LDHA-associated lactic acid production blunts tumor immunosurveillance by T and NK cells. *Cell Metab.* 24 (5), 657–671. doi: 10.1016/j.cmet.2016.08.011

Brouwer, M. C., Tunkel, A. R., and van de Beek, D. (2010). Epidemiology, diagnosis, and antimicrobial treatment of acute bacterial meningitis. *Clin. Microbiol. Rev.* 23 (3), 467–492. doi: 10.1128/cmr.00070-09

Chinese Society of Infectious Diseases and Cerebrospinal Fluid Cytology (2021). Expert consensus on clinical application of metagenomic next−generation sequencing of cerebrospinal fluid in the diagnosis of infectious diseases of the central nervous system. *Chin. J. Neurol.* 54 (12), 1234–1240.

GBD 2016 Neurology Collaborators. (2018). Global, regional, and national burden of meningiti-2016: a systematic analysis for the global burden of disease study 2016. *Lancet Neurol.* 17 (12), 1061–1082. doi: 10.1016/s1474-4422(18)30387-9

Glaser, C. A., Honarmand, S., Anderson, L. J., Schnurr, D. P., Forghani, B., Cossen, C. K., et al. (2006). Beyond viruses: clinical profiles and etiologies associated with encephalitis. *Clin. Infect. Dis.* 43 (12), 1565–1577. doi: 10.1086/509330

Goldberg, B., Sichtig, H., Geyer, C., Ledeboer, N., and Weinstock, G. M. (2015). Making the leap from research laboratory to clinic: Challenges and opportunities for next-generation sequencing in infectious disease diagnostics. *mBio* 6 (6), e01888–e01815. doi: 10.1128/mBio.01888-15

Granerod, J., Ambrose, H. E., Davies, N. W., Clewley, J. P., Walsh, A. L., Morgan, D., et al. (2010). Causes of encephalitis and differences in their clinical presentations in England: a multicentre, population-based prospective study. *Lancet Infect. Dis.* 10 (12), 835–844. doi: 10.1016/s1473-3099(10)70222-x

Hulswit, R. J. G., Paesen, G. C., Bowden, T. A., and Shi, X. (2021). Recent advances in bunyavirus glycoprotein research: Precursor processing, receptor binding and structure. *Viruses* 13(2):353. doi: 10.3390/v13020353

Kelley, V. A., and Caliendo, A. M. (2001). Successful testing protocols in virology. *Clin. Chem.* 47 (8), 1559–1562. doi: 10.1093/clinchem/47.8.1559

Kelly, M. J., Benjamin, L. A., Cartwright, K., Ajdukiewicz, K. M., Cohen, D. B., Menyere, M., et al. (2012). Epstein-Barr virus coinfection in cerebrospinal fluid is associated with increased mortality in Malawian adults with bacterial meningitis. *J. Infect. Dis.* 205 (1), 106–110. doi: 10.1093/infdis/jir707

Kochanowsky, J. A., and Koshy, A. A. (2018). Toxoplasma gondii. *Curr. Biol.* 28 (14), R770–r771. doi: 10.1016/j.cub.2018.05.035

Leber, A. L., Everhart, K., Balada-Llasat, J. M., Cullison, J., Daly, J., Holt, S., et al. (2016). Multicenter evaluation of BioFire FilmArray Meningitis/Encephalitis panel for detection of bacteria, viruses, and yeast in cerebrospinal fluid specimens. *J. Clin. Microbiol.* 54 (9), 2251–2261. doi: 10.1128/jcm.00730-16

Leber, A. L., Everhart, K., Daly, J. A., Hopper, A., Harrington, A., Schreckenberger, P., et al. (2018). Multicenter evaluation of BioFire FilmArray respiratory panel 2 for detection of viruses and bacteria in nasopharyngeal swab samples. *J. Clin. Microbiol.* 56(6):e01945–17. doi: 10.1128/jcm.01945-17

Li, H., and Durbin, R. (2009). Fast and accurate short read alignment with burrows-wheeler transform. *Bioinformatics* 25 (14), 1754–1760. doi: 10.1093/bioinformatics/btp324

Long, Y., Zhang, Y., Gong, Y., Sun, R., Su, L., Lin, X., et al. (2016). Diagnosis of sepsis with cell-free DNA by next-generation sequencing technology in ICU patients. *Arch. Med. Res.* 47 (5), 365–371. doi: 10.1016/j.arcmed.2016.08.004

Lu, C. T., Wang, L. S., and Hsueh, P. R. (2021). Scrub typhus and antibiotic-resistant orientia tsutsugamushi. *Expert Rev. Anti Infect. Ther.* 19 (12), 1519–1527. doi: 10.1080/14787210.2021.1941869

McGill, F., Heyderman, R. S., Panagiotou, S., Tunkel, A. R., and Solomon, T. (2016). Acute bacterial meningitis in adults. *Lancet* 388 (10063), 3036–3047. doi: 10.1016/s0140-6736(16)30654-7

Miao, Q., Ma, Y., Wang, Q., Pan, J., Zhang, Y., Jin, W., et al. (2018). Microbiological diagnostic performance of metagenomic next-generation sequencing when applied to clinical practice. *Clin. Infect. Dis.* 67 (suppl_2), S231–s240. doi: 10.1093/cid/ciy693

Miller, S., Naccache, S. N., Samayoa, E., Messacar, K., Arevalo, S., Federman, S., et al. (2019). Laboratory validation of a clinical metagenomic sequencing assay for pathogen detection in cerebrospinal fluid. *Genome Res.* 29 (5), 831–842. doi: 10.1101/gr.238170.118

Paul, M. L., Dwyer, D. E., Chow, C., Robson, J., Chambers, I., Eagles, G., et al. (1994). Listeriosis–a review of eighty-four cases. *Med. J. Aust.* 160 (8), 489–493. doi: 10.5694/j.1326-5377.1994.tb138313.x

Polage, C. R., and Cohen, S. H. (2016). State-of-the-Art microbiologic testing for community-acquired meningitis and encephalitis. *J. Clin. Microbiol.* 54 (5), 1197–1202. doi: 10.1128/jcm.00289-16

Schlaberg, R., Chiu, C. Y., Miller, S., Procop, G. W., and Weinstock, G. (2017). Validation of metagenomic next-generation sequencing tests for universal pathogen detection. *Arch. Pathol. Lab. Med.* 141 (6), 776–786. doi: 10.5858/arpa.2016-0539-RA

Storch, G. A. (2000). Diagnostic virology. *Clin. Infect. Dis.* 31 (3), 739–751. doi: 10.1086/314015

Tansarli, G. S., and Chapin, K. C. (2020). Diagnostic test accuracy of the BioFire® FilmArray® meningitis/encephalitis panel: a systematic review and meta-analysis. *Clin. Microbiol. Infect.* 26 (3), 281–290. doi: 10.1016/j.cmi.2019.11.016

Tan, L., Yao, J., Yang, Y., Luo, W., Yuan, X., Yang, L., et al. (2021). Current status and challenge of pseudorabies virus infection in China. *Virol. Sin.* 36 (4), 588–607. doi: 10.1007/s12250-020-00340-0

van de Beek, D., Brouwer, M. C., Koedel, U., and Wall, E. C. (2021). Community-acquired bacterial meningitis. *Lancet* 398 (10306), 1171–1183. doi: 10.1016/s0140-6736(21)00883-7

van de Beek, D., Cabellos, C., Dzupova, O., Esposito, S., Klein, M., Kloek, A. T., et al. (2016). ESCMID guideline: diagnosis and treatment of acute bacterial meningitis. *Clin. Microbiol. Infect.* 22 (Suppl 3), S37–S62. doi: 10.1016/j.cmi.2016.01.007

van de Beek, D., de Gans, J., Tunkel, A. R., and Wijdicks, E. F. (2006). Community-acquired bacterial meningitis in adults. *N Engl. J. Med.* 354 (1), 44–53. doi: 10.1056/NEJMra052116

van de Beek, D., Drake, J. M., and Tunkel, A. R. (2010). Nosocomial bacterial meningitis. *N Engl. J. Med.* 362 (2), 146–154. doi: 10.1056/NEJMra0804573

van Kassel, M. N., van Haeringen, K. J., Brouwer, M. C., Bijlsma, M. W., and van de Beek, D. (2020). Community-acquired group b streptococcal meningitis in adults. *J. Infect.* 80 (3), 255–260. doi: 10.1016/j.jinf.2019.12.002

Wang, Y., Wang, Y., Sun, L., Grenier, D., and Yi, L. (2018). Streptococcus suis biofilm: regulation, drug-resistance mechanisms, and disinfection strategies. *Appl. Microbiol. Biotechnol.* 102 (21), 9121–9129. doi: 10.1007/s00253-018-9356-z

Williamson, P. R., Jarvis, J. N., Panackal, A. A., Fisher, M. C., Molloy, S. F., Loyse, A., et al. (2017). Cryptococcal meningitis: epidemiology, immunology, diagnosis and therapy. *Nat. Rev. Neurol.* 13 (1), 13–24. doi: 10.1038/nrneurol.2016.167

Wilson, M. R., Naccache, S. N., Samayoa, E., Biagtan, M., Bashir, H., Yu, G., et al. (2014). Actionable diagnosis of neuroleptospirosis by next-generation sequencing. *N Engl. J. Med.* 370 (25), 2408–2417. doi: 10.1056/NEJMoa1401268

Xing, X. W., Zhang, J. T., Ma, Y. B., He, M. W., Yao, G. E., Wang, W., et al. (2020). Metagenomic next-generation sequencing for diagnosis of infectious encephalitis and meningitis: A Large, prospective case series of 213 patients. *Front. Cell Infect. Microbiol.* 10. doi: 10.3389/fcimb.2020.00088

Xing, X. W., Zhang, J. T., Ma, Y. B., Zheng, N., Yang, F., and Yu, S. Y. (2019). Apparent performance of metagenomic next-generation sequencing in the diagnosis of cryptococcal meningitis: a descriptive study. *J. Med. Microbiol.* 68 (8), 1204–1210. doi: 10.1099/jmm.0.000994

Zhang, Y., Cui, P., Zhang, H. C., Wu, H. L., Ye, M. Z., Zhu, Y. M., et al. (2020). Clinical application and evaluation of metagenomic next-generation sequencing in suspected adult central nervous system infection. *J. Transl. Med.* 18 (1), 199. doi: 10.1186/s12967-020-02360-6

frontiers | Frontiers in Cellular and Infection Microbiology

TYPE Original Research
PUBLISHED 27 September 2022
DOI 10.3389/fcimb.2022.951703

OPEN ACCESS

EDITED BY
Liang Yang,
Southern University of Science and Technology, China

REVIEWED BY
Wang Ke,
Guangxi Medical University, China
Lanlan Wei,
Shenzhen Third People's Hospital, China

*CORRESPONDENCE
Hui Bu
Huibuneurology@126.com
Han Xia
xiahan@hugobiotech.com

†These authors have contributed equally to this work and share first authorship

SPECIALTY SECTION
This article was submitted to Clinical Microbiology, a section of the journal Frontiers in Cellular and Infection Microbiology

RECEIVED 24 May 2022
ACCEPTED 29 August 2022
PUBLISHED 27 September 2022

CITATION
Yu L, Zhang Y, Zhou J, Zhang Y, Qi X, Bai K, Lou Z, Li Y, Xia H and Bu H (2022) Metagenomic next-generation sequencing of cell-free and whole-cell DNA in diagnosing central nervous system infections.
Front. Cell. Infect. Microbiol. 12:951703.
doi: 10.3389/fcimb.2022.951703

Metagenomic next-generation sequencing of cell-free and whole-cell DNA in diagnosing central nervous system infections

Lili Yu[1†], Ye Zhang[2†], Jiemin Zhou[2], Yu Zhang[1], Xuejiao Qi[1], Kaixuan Bai[1], Zheng Lou[2], Yi Li[1], Han Xia[2*] and Hui Bu[1*]

[1]Department of Neurology, The Second Hospital of Hebei Medical University, Shijiazhuang, China, [2]Department of Scientific Affairs, Hugobiotech Co., Ltd., Beijing, China

Background: Central nervous system (CNS) infections pose a fatal risk to patients. However, the limited sample volumes of cerebrospinal fluid (CSF) and low detection efficiency seriously hinder the accurate detection of pathogens using conventional methods.

Methods: We evaluated the performance of metagenomics next-generation sequencing (mNGS) in diagnosing CNS infections. CSF samples from 390 patients clinically diagnosed with CNS infections were used for the mNGS of cell-free DNA (cfDNA) (n =394) and whole-cell DNA (wcDNA) (n =150).

Results: The sensitivity of mNGS using cfDNA was 60.2% (237/394, 95% confidence interval [CI] 55.1%–65.0%), higher than that of mNGS using wcDNA (32.0%, 95% [CI] 24.8%–40.2%, 48/150) and conventional methods (20.9%, 95% [CI] 16.2%–26.5%, 54/258) ($P < 0.01$, respectively). The accuracy of mNGS using cfDNA in positive samples was 82.6%. Most of viral (72.6%) and mycobacterial (68.8%) pathogens were only detected by the mNGS of cfDNA. Meningitis and encephalitis with *Streptococcus pneumoniae* infection might be more likely to result in critically ill diseases, while Human alphaherpesvirus 3 was prone to cause non-critically ill diseases.

Conclusions: This is the first report on evaluating and emphasizing the importance of mNGS using CSF cfDNA in diagnosing CNS infections, and its extensive application in diagnosing CNS infections could be expected, especially for viral and mycobacterial CNS infections.

KEYWORDS

CNS infection, critically ill patients, sensitivity, mNGS, cell-free DNA, whole-cell DNA

Introduction

Central nervous system (CNS) infections are mainly caused by bacteria, fungi, viruses, and parasites (Zhang et al., 2020). They can result in meningitis, encephalitis, abscess, and so on (Zhang et al., 2020) and lead to 100% mortality in some cases (Ma et al., 2015). Meningitis affected more than 1.2 million people each year (Cain et al., 2019) with a mortality of more than 26% (320,000 people died from meningitis) in 2016 (Cain et al., 2019; Zhang et al., 2020). Of the deaths from meningitis, approximately 40% were due to bacterial meningitis (approximately 120,000 deaths) (Cain et al., 2019; Zhang et al., 2020). Viral encephalitis and meningitis contributed to 34% of adult CNS infections, and 14% of meningitis was tuberculous meningitis (TBM) (Ho Dang Trung et al., 2012). However, it is difficult to distinguish TBM from cryptococcal meningitis (CM) and viral meningitis due to the lack of specificity in clinical presentation and cerebrospinal fluid (CSF) parameters of those patients (Abassi et al., 2015; Leonard, 2017; Ji et al., 2020). In addition to death, some unoptimistic prognoses may be generated if timely diagnosis and proper therapy were not provided, including neurological disability (Berhane et al., 2021). Accordingly, not only timely but also accurate diagnosis are needed to improve prognoses and decrease mortality.

The conventional CSF culture method, as the most commonly used diagnostic tool, can only identify approximately 30%–40% of CNS infections (Leber et al., 2016) whose detection rates are as low as 6% in developing countries (Zhang et al., 2020), while some pathogens take weeks to grow (Gu et al., 2021). Although hypothesis-based PCR (Gu et al., 2021), Xpert (Bahr et al., 2018), and BioFire FilmArray Panel (Leber et al., 2016) are more accurate and sensitivities for some pathogens can reach 100% (Leber et al., 2016), they either need a prior hypothesis of the causative pathogens (Gu et al., 2021) or are restricted to the detection of a limited number of pathogens (Zhang et al., 2020). Unbiased metagenomics next-generation sequencing (mNGS) has been extensively used in clinical infections (Wilson et al., 2019; Chen et al., 2021a; Gu et al., 2021; Chen et al., 2021b) after the first successful application in diagnosing CNS infections (Wilson et al., 2014). Most importantly, the mNGS of cell-free DNA (cfDNA) has been proven to be a promising tool for detecting and identifying pathogens in body fluids (Gu et al., 2021).

However, long-held conflict in the location of proliferation and infection between intracellular and extracellular pathogens (Casadevall and Fang, 2020) challenged whether the mNGS of cfDNA can accurately detect causative pathogens from CSF. Compared to the mNGS of cfDNA, although the mNGS of whole-cell DNA (wcDNA) obtained from the differential lysis method can detect more reads per million (RPM) of *Cryptococcus neoformans*, its detection of trace *Mycobacterium tuberculosis* was hindered (Ji et al., 2020). The differential lysis method can significantly improve the detection performance of dominant pathogens at the expense of trace pathogens (Thoendel et al., 2018; Gu et al., 2021). Furthermore, the detection rate (Zhang et al., 2020) of mNGS directly using the wcDNA of CSF samples without differential lysis was only approximately 50%. We hypothesized that the performance of mNGS using cfDNA is better than that of mNGS using wcDNA in CNS infections.

To verify our hypothesis, we retrospectively enrolled patients with CNS infections mainly diagnosed as bacterial, viral, mycobacterial, or cryptococcal infections by conventional methods. The remaining CSF samples from those patients were used to evaluate the accuracies of mNGS using cfDNA and wcDNA, including the positive rate and sensitivity, while the performance of the conventional methods and pathogen profiles in CNS infections were also summarized.

Materials and methods

Ethics statement

Study protocols were approved by the Ethical Review Committee of the Second Hospital of Hebei Medical University, Hebei, China (approval no. 2020-P027). All procedures were in accordance with the ethical standards of the responsible committee on human experimentation (institutional and national) and with the Helsinki Declaration of 1975, as revised in 2000. Informed consent was obtained from all patients enrolled in the study or their next kin/guardian.

Sample selection and patient division

For this retrospective study, a total of 478 consecutive patients admitted to the Second Hospital of Hebei Medical University of China from June 2018 to June 2021 and diagnosed as CNS infections were assessed for eligibility. The definition of suspected CNS infections was based on the diagnostic criteria of encephalitis, meningitis, meningoencephalitis, and meningomyelitis of a previous study (Schibler et al., 2019): a) patients with no alternative cause altered the mental status (decreased or altered level of consciousness, lethargy, or personality change) for ≥24 h and with at least two following symptoms, including fever ≥38.2°C within 72 h before or after admission, generalized or partial seizures not fully attributable to a preexisting seizure disorder, new onset of focal neurologic findings, CSF leukocyte count ≥5 M/L, abnormality of brain parenchyma on neuroimaging indicating encephalitis, and abnormality by electroencephalography consistent with encephalitis; b) patients with CSF leukocyte count ≥5 M/L and with at least two following symptoms, including headache, fever (≥38.2°C), photo- and/or phonophobia, and neck stiffness; and c)

patients with asymmetrical flaccid weakness combined with reduced/absent reflexes and sensory symptoms or with the hyperintensities of the spinal cord on T2-weighted magnetic resonance imaging.

For all patients with symptoms meeting the above definition, the clinical information, including epidemiology, clinical manifestations, laboratory test results, imaging results, conventional diagnostic results, outcomes after anti-infective treatments, and 2-month follow-ups, was assessed for the final diagnosis by two clinicians independently. Any discrepancies in the determination of etiology were resolved by direct communication with treating physicians or by a mutual consensus with a third clinician. Only patients with confirmed CNS infections were assessed for eligibility in this study.

The remaining CSF samples used for further mNGS tests from patients with CNS infections were screened using the following exclusion criteria: 1) the volume of CSF was not enough for mNGS detection; 2) the quality of CSF was too low to perform mNGS, such as hemolytic CSF; 3) the constructed DNA libraries of samples were unqualified and were not next sequenced; 4) final diagnoses were indefinite; and 5) the patients declined to participate. Given the low incidence rates of CNS infections and the limitation in funding, we retrospectively enrolled more patients using the limited funding without formal statistical considerations.

Clinical diagnostic tests included routine bacterial and fungal smears and cultures, India Ink, Alcian blue staining, acid-fast staining, serum antigen and antibody tests, interferon-γ release assays, tubercalin test, and PCR. The definition of encephalitis, meningitis, and meningoencephalitis was based on a previous study (Schibler et al., 2019). According to the modified Rankin Scale (mRS) (Sulter et al., 1999) and intensive care unit (ICU) admission, we divided patients into critically or non-critically ill patients.

The remaining 394 CSF samples from these 390 patients were transported to Hugobiotech (Hugobiotech, Beijing, China) on dry ice for mNGS tests. During the process from the wet lab to dry lab of mNGS, corresponding researchers were not informed with any clinical results, including laboratory tests, clinical information, and the final clinical diagnosis.

DNA extraction

CfDNA and wcDNA were extracted from CSF (~2 ml) using the QIAamp DNA Micro Kit (QIAGEN, Hilden, Germany) based on its manual. For cfDNA extraction, the cells in samples were removed by centrifugation and the supernatant was collected for the subsequent extraction, while the total CSF sample was directly used for wcDNA extraction without centrifugation. In this study, the extraction of cfDNA and wcDNA was performed in 394 and 150 samples, respectively. The simple random sampling method was used for the random selection of samples for wcDNA extraction.

Metagenomics next-generation sequencing detection

DNA libraries were constructed using the QIAseq™ Ultralow Input Library Kit (QIAGEN, Hilden, Germany) according to the instructions. The quality of constructed libraries was assessed by Qubit (Thermo Fisher, Waltham, USA) and Agilent 2100 Bioanalyzer (Agilent Technologies, Palo Alto, CA, USA). All qualified libraries were sequenced on the Nextseq 550 platform (Illumina, San Diego, CA, USA), with 75 bp single-end reads of approximately 20 million per library after sequencing. Adapters and short (<35 bp), low-quality (Q < 30), and low-complexity reads were removed to generate clean data using bowtie2, which were then mapped to the human reference database (hg38) to filter out human host DNA reads. The remaining reads were finally blasted against Microbial Genome Databases (http://ftp.ncbi.nlm.nih.gov/genomes/) using Burrows–Wheeler Aligner software, followed by species annotation analysis using the least common ancestor method. Negative controls (sterile deionized water) and positive controls (synthesized fragments with known quantities) were established for each batch of experiments using the same wet lab procedures and bioinformatics analysis as the clinical samples. The read number and RPM of each detected microbe were calculated. For detected microbes, including bacteria (*Mycobacterium* excluded), fungi (*Cryptococcus* excluded), and parasites, a positive mNGS result was given when its coverage ranked in the top 10 of similar microbial species (or genera) and was absent in the negative control ("No template" control, NTC) or when its ratio of RPM between the sample and NTC (RPM_{sample}/RPM_{NTC}) > 10 if $RPM_{NTC}\neq0$. For viruses, *Mycobacterium*, and *Cryptococcus*, a positive mNGS result was considered when at least one unique read was mapped to the species level and absent in NTC or RPM_{sample}/RPM_{NTC} > 5 when $RPM_{NTC}\neq0$.

Statistical analysis

Descriptive statistics were used for demographic information as mean ± SD. The proportion of the specified group was presented as percentage. The positive rate and sensitivity of mNGS using cfDNA, mNGS using wcDNA, and conventional methods were calculated (percentage with 95% confidence interval [CI]) and compared (chi-square test). According to the clinical manifestations, the patients were also divided into the critically ill group and non-critically ill group, as well as the meningitis group and encephalitis group, respectively. The pathogen spectrum characteristics between

different groups were compared (chi-square test). A *p*-value less than 0.05 was considered statistically significant.

Data availability

Sequencing data were deposited to the National Genomics Data Center (http://ngdc.cncb.ac.cn) under accession number PRJCA008673. The authors declare that the main data supporting the findings are available within this article. The other data generated and analyzed for this study are available from the corresponding author upon reasonable request.

Results

Patient baseline

A total of 478 consecutive patients diagnosed as CNS infections from June 2018 to June 2021 were assessed for eligibility, while, combined with exclusion criteria for samples, 394 CSF samples from 390 patients were enrolled for this study. There were 256 men and 134 women (Table 1). The average age was 43.6 ± 1.7 years (from 13 to 85 years old). The average length of hospital stay was 19.9 ± 1.2 days (from 2 to 96 days). A total of 100 patients (25.6%) experienced underlying diseases, including diabetes, hypertension, hepatitis B, the postoperation of diseases, skull defect, and sinusitis. A total of 38 patients (9.7%) had immunodeficiency, including systemic lupus erythematosus, nephrotic syndrome, postoperation of cancer, and HIV. Furthermore, 35 patients had other infections, such as pneumonia. The common symptoms of the 390 patients with CNS infections were fever (288), headache (277), nausea and vomiting (142), meningeal irritation (134), consciousness disorder (115), focal neurological deficit (83), epilepsy (74), and behavior change (38). The most common diseases caused by CNS infections were meningitis (168) and encephalitis (169), followed by meningoencephalitis (41), meningomyelitis (9), and brain abscess (3). The 109 patients (27.95%) with an MRS score of ≥4 admitted to ICU for treatment were defined as critically ill patients.

TABLE 1 The baseline of the patients enrolled in this study.

	Number of patients
Male (%)	256 (66.3%)
Age (year)	43.6 ± 1.7
Hospital stay (day)	19.9 ± 1.2
Underlying diseases	100
Immunosuppressed diseases	38
With critical illnesses	109
CNS infectious diseases	
Meningitis	168
Encephalitis	169
Meningoencephalitis	41
Encephalomyelitis	9
Brain abscess	3
Coinfections of other organs	35
Symptoms	
Fever	288
Headache	277
Nausea/vomiting	142
Meningeal irritation	134
Consciousness disorder	115
Focal neurological deficit	83
Epilepsy	74
Behavior change	38

Performance of metagenomics next-generation sequencing using cell-free DNA and whole-cell DNA

We randomly selected 150 CSF samples from the enrolled 390 patients to perform mNGS tests using both cfDNA and wcDNA simultaneously (Figure 1A). The positive rate of mNGS using cfDNA (66.7%, 95% [CI] 58.5%–74.0%, 100/150) was higher than that of mNGS using wcDNA (34.7%, 95% [CI] 27.2%–42.9%, 52/150) ($P<0.01$). The sensitivity of mNGS using cfDNA (64.0%, 95% [CI] 55.71%–71.55%, 96/150) was also higher than that of mNGS using wcDNA (32.0%, 95% [CI] 24.8%–40.2%, 48/150) ($P<0.001$) (Figure 1C). Furthermore, among those samples with mNGS results coincident with the final clinical diagnoses, only 1 out of 48 samples by the mNGS of wcDNA cannot be confirmed by the mNGS of cfDNA, while the mNGS of wcDNA did not identify causative pathogens from 51% of samples (49/96) successfully diagnosed by the mNGS of cfDNA. Interestingly, approximately 98% of the 49 samples were viral ($n = 36$) and mycobacterial infections ($n = 11$). Given the slight differences in mNGS detection between viral and mycobacterial infections, we further evaluated the performance of mNGS using both cfDNA and wcDNA at the pathogen level.

We found a significant difference in the detection of viruses and *Mycobacterium* (Figure 2A). In general, the number of detected RPMs using the mNGS of cfDNA was significantly higher than that using the mNGS of wcDNA (94,344 vs. 27,153, $P<0.05$) (Figure 2B). For *Mycobacterium* detection, only 5 positive results were found by the mNGS of both cfDNA and wcDNA, while 11 positive results were only detected by the mNGS of cfDNA. Furthermore, a higher performance of mNGS using cfDNA than that of mNGS using wcDNA can also be found in detecting viruses (82 vs. 31), including Human gammaherpesvirus 4 (EBV, 27 vs. 13), Human alphaherpesvirus 3 (VZV, 12 vs. 8), and Human alphaherpesvirus 1 (HSV, 9 vs. 4). The above results unravel that the accuracy of mNGS using CSF cfDNA is higher

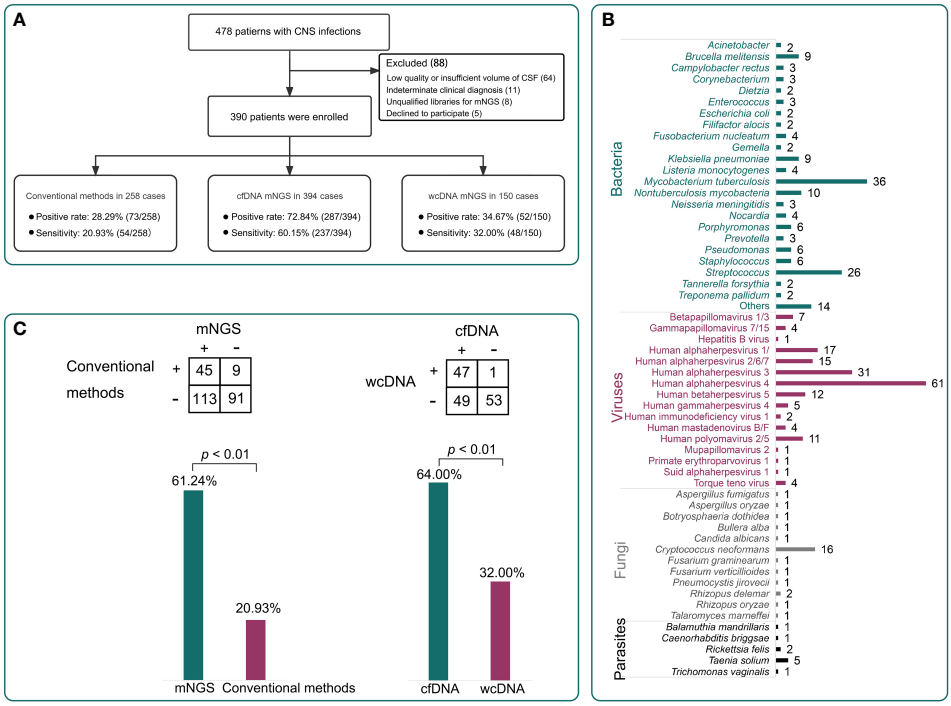

FIGURE 1
Patient enrollment and the performance of different methods. **(A)**, A total of 390 patients were enrolled in this study. The positive rates of conventional methods, metagenomics next-generation sequencing (mNGS) using cell-free DNA (cfDNA), and mNGS using whole-cell DNA (wcDNA) were 28.3%, 72.8%, and 34.7%, respectively. The sensitivities were 20.9%, 60.2%, and 32.0%, respectively. **(B)**, The pathogen profiles by the mNGS of cfDNA. **(C)**, Comparisons among different methods. The mNGS of cfDNA showed significantly higher sensitivity than the mNGS of wcDNA and conventional methods ($P < 0.01$).

than that of mNGS using CSF wcDNA in diagnosing CNS infections, especially for viral and mycobacterial CNS infections.

Performance of metagenomics next-generation sequencing using cell-free DNA and conventional methods

mNGS using cfDNA was performed in other CSF samples to assess its importance in diagnosing CNS infections, while conventional methods were previously conducted on 258 CSF samples to assist diagnosis (Figure 3A). Taking the final clinical diagnosis as a gold standard, the performance of mNGS using cfDNA was much better than that of conventional methods (Figure 1A). mNGS and conventional methods respectively detected causative pathogens from 287 (72.8%) out of 394 samples and 73 (28.3%) out of 258 samples. Furthermore, the sensitivity of mNGS (60.2%, 95% [CI] 55.1%–65.0%, 237/394) was significantly higher than that of conventional methods (20.9%, 95% [CI] 16.2%–26.5%, 54/258) (P<0.01). Among the 258 samples, mNGS can detect causative pathogens from 113 samples with negative results by conventional methods. The above results unravel that mNGS detection using CSF cfDNA should be considered as a preferred examination in diagnosing CNS infections.

Pathogen profiles detected by conventional methods and mNGS using cfDNA

Pathogens detected by conventional methods were limited to some species. The most commonly detected causative pathogens were *Cryptococcus* (n = 17), HSV (n = 15), Human betaherpesvirus 5 (CMV) (n = 18), *Klebsiella pneumoniae* (n = 4), *Brucella melitensis* (n = 4), and *M. tuberculosis* (n = 3) (Figure 3B). Conversely, mNGS identified a total of 65 bacteria, 23 viruses, 12 fungi, and 5 parasites (Figure 1B). Capturing more causative pathogens can provide a comprehensive reference for accurate infection diagnosis.

Based on mNGS detection, we further classified the patients into bacterial infection (n = 141), viral infection (n = 155), fungal infection (n = 28), and parasitic infection (n=9), while 44 patients were coinfected with different kinds of pathogens (Figure 3C). The most common bacterial causative pathogens were *M. tuberculosis* (n = 36), *Streptococcus pneumoniae* (n = 15), non-tuberculous mycobacteria (n = 10), *B. melitensis* (n =

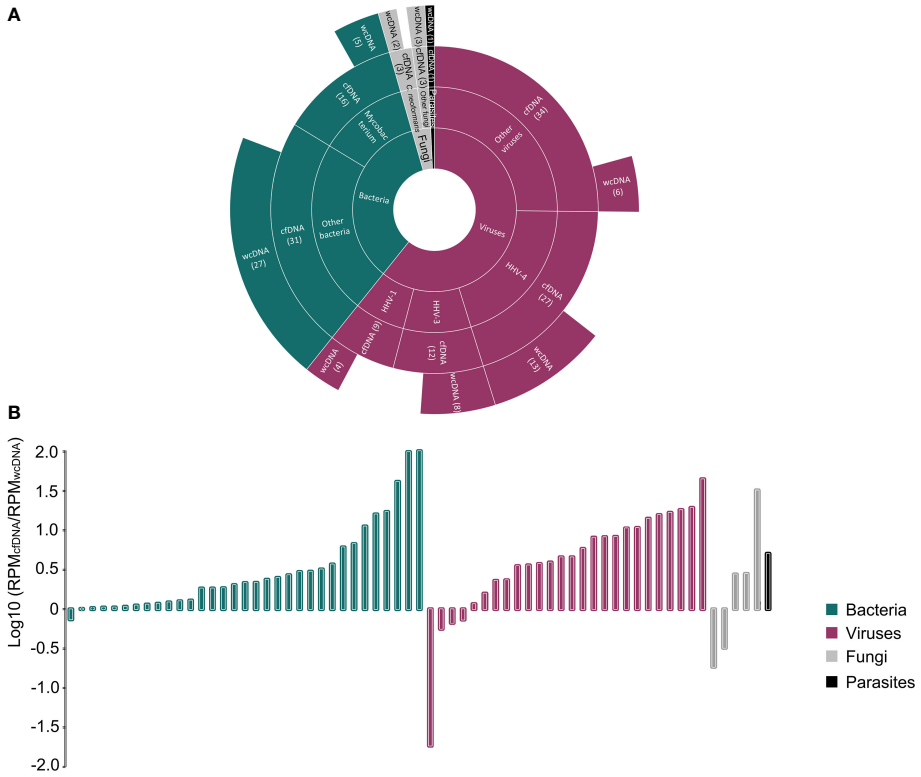

FIGURE 2
Comparison between the mNGS of cfDNA and wcDNA. **(A)**, Summaries of case numbers by detected pathogens, including bacteria, viruses, fungi, and parasites. The mNGS of cfDNA detected more viral and mycobacterial infections than the mNGS of wcDNA. **(B)**, Difference in the number of detected RPMs for the same pathogen between the mNGS of cfDNA and wcDNA. The value of >0 represents that the number of detected RPMs by the mNGS of cfDNA is higher than that by the mNGS of wcDNA.

9), and *K. pneumoniae* ($n = 9$). *C. neoformans* ($n = 16$) was the most common fungal causative pathogen, which was similar to the result of conventional methods. In addition, mNGS results showed that EBV ($n = 61$) contributed approximately 40% to the viral infection, which was only detected in three samples using conventional methods.

Performance of metagenomics next-generation sequencing using cell-free DNA in infection diagnosis of critically ill patients

Compared with non-critically ill patients, a better performance of mNGS in infection diagnosis was found for critically ill patients. After division, 110 and 284 CSF samples were respectively obtained from critical and non-critical ill patients. Positive results were found in 88 samples of critically ill patients and 199 samples of non-critically ill patients. Taking the final diagnoses as a gold standard, a high sensitivity of mNGS was found in both critically (65.5%, 95% [CI] 55.7%–74.1%, 72/110) and non-critically (58.1%, 95% [CI] 52.1%–63.9%, 165/284) ill patients. Our findings show that the application of mNGS using CSF cfDNA is beneficial to accurately identify the causative pathogens of CNS infections.

Furthermore, we found the difference in causative pathogens between critically and non-critically ill patients (Figure 4). More than 52% of critically ill patients (38/72) were attributed to bacterial infections, while the percentage of viral infections was only 25% (18/72). However, non-critically ill patients were much more susceptible to viral infection (49.1%, 81/165) rather than bacterial infection (28.5%, 47/165) (Figure 4A). The analysis of pathogen profiles (Figure 4B) showed that *M. tuberculosis* and EBV were commonly detected in both critically and non-critically ill patients, while high ratios of *S. pneumoniae* and VZV were respectively found in critically and non-critically ill patients. High ratios of bacterial (~58%) and viral (83%) infections were also found in meningitis and encephalitis patients, respectively. However, the ratios of meningitis were similar to those of encephalitis in both critically and non-critically ill patients. The above raises a question of which types of infection in meningitis or encephalitis are more likely to result in critically ill diseases.

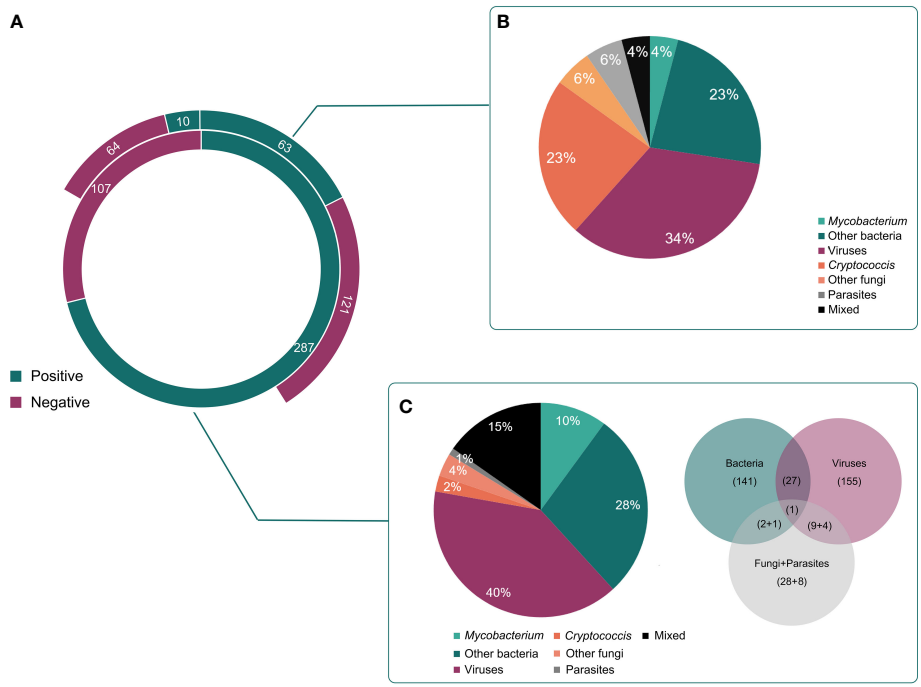

FIGURE 3
Different kinds of infections by mNGS and conventional methods. **(A)**, The detected results of mNGS and conventional methods in all enrolled patients. **(B)**, Different kinds of infections in positive cases detected by conventional methods. **(C)**, Different kinds of infections in positive cases detected by mNGS.

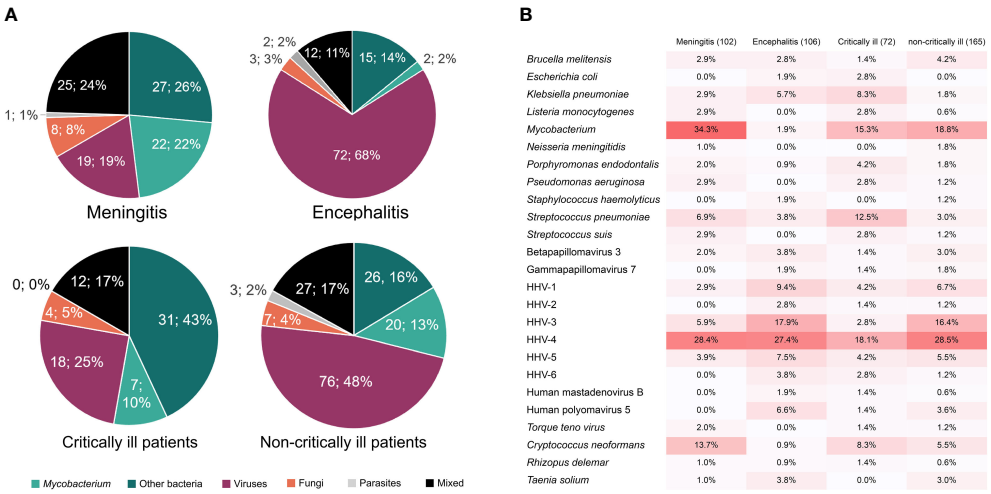

	Meningitis (102)	Encephalitis (106)	Critically ill (72)	non-critically ill (165)
Brucella melitensis	2.9%	2.8%	1.4%	4.2%
Escherichia coli	0.0%	1.9%	2.8%	0.0%
Klebsiella pneumoniae	2.9%	5.7%	8.3%	1.8%
Listeria monocytogenes	2.9%	0.0%	2.8%	0.6%
Mycobacterium	34.3%	1.9%	15.3%	18.8%
Neisseria meningitidis	1.0%	0.0%	0.0%	1.8%
Porphyromonas endodontalis	2.0%	0.9%	4.2%	1.8%
Pseudomonas aeruginosa	2.9%	0.0%	2.8%	1.2%
Staphylococcus haemolyticus	0.0%	1.9%	0.0%	1.2%
Streptococcus pneumoniae	6.9%	3.8%	12.5%	3.0%
Streptococcus suis	2.9%	0.0%	2.8%	1.2%
Betapapillomavirus 3	2.0%	3.8%	1.4%	3.0%
Gammapapillomavirus 7	0.0%	1.9%	1.4%	1.8%
HHV-1	2.9%	9.4%	4.2%	6.7%
HHV-2	0.0%	2.8%	1.4%	1.2%
HHV-3	5.9%	17.9%	2.8%	16.4%
HHV-4	28.4%	27.4%	18.1%	28.5%
HHV-5	3.9%	7.5%	4.2%	5.5%
HHV-6	0.0%	3.8%	2.8%	1.2%
Human mastadenovirus B	0.0%	1.9%	1.4%	0.6%
Human polyomavirus 5	0.0%	6.6%	1.4%	3.6%
Torque teno virus	2.0%	0.0%	1.4%	1.2%
Cryptococcus neoformans	13.7%	0.9%	8.3%	5.5%
Rhizopus delemar	1.0%	0.9%	1.4%	0.6%
Taenia solium	1.0%	3.8%	0.0%	3.0%

FIGURE 4
The percentages of causative pathogens in meningitis, encephalitis, critically ill, and non-critically ill patients by mNGS using cfDNA. **(A)**, Different kinds of infections in meningitis, encephalitis, critically ill, and non-critically ill patients. **(B)**, Main causative pathogens in meningitis, encephalitis, critically ill, and non-critically ill patients.

Causative pathogens of meningitis and encephalitis detected by modified next-generation sequencing using cell-free DNA

Different infection types were found in meningitis and encephalitis patients. Causative pathogens in 102 meningitis and 106 encephalitis patients were further confirmed by mNGS (Figure 4). We found that *Mycobacterium* was the dominant pathogen in meningitis patients (34.3%), which was detected in few encephalitis patients (1.9%). Combined with non-differential distribution between critically and non-critically ill patients, we proposed that *Mycobacterium* is more likely to cause meningitis. The low ratios of *S. pneumoniae* in both meningitis and encephalitis patients and high ratios in critically ill patients indicate that meningitis and encephalitis with *S. pneumoniae* infection might be more likely to result in critically ill diseases, whereas the high ratios of VZV in both encephalitis patients (17.9%) and non-critically ill patients (16.4%) suggest that CNS VZV infection might only result in non-critically ill diseases.

Discussion

This is the first report on evaluating the accuracies of mNGS using CSF cfDNA and CSF wcDNA and on emphasizing the advantage of mNGS using cfDNA in diagnosing CNS infections, especially for viral and mycobacterial CNS infections. The sensitivity of mNGS using cfDNA can reach up to 60.2%, with an accuracy of 82.6% among the patients with positive results. The pathogen profiles of mNGS using cfNDA were analyzed. *M. tuberculosis* and EBV were commonly detected in both critically and non-critically ill patients. Meningitis and encephalitis with *S. pneumoniae* infection might be more likely to result in critically ill diseases, while CNS infection with VZV might only result in non-critically ill diseases.

The mNGS of CSF cfDNA exhibited better performance in diagnosing CNS infections than the mNGS of wcDNA and conventional methods. The limited volumes of CSF samples (Ji et al., 2020) and low detection efficiency (Leber et al., 2016; Bahr et al., 2018; Ge et al., 2021) of conventional methods hindered the accurate detection of pathogens, while mNGS can achieve an unbiased detection of pathogens from different kinds of samples (Gu et al., 2021). The sensitivity of mNGS was determined by the pathogen DNA ratio in a sample (Ebinger et al., 2021). In our study, during wcDNA extraction, the differential lysis method was not included to filter human DNA from the CSF sample (Thoendel et al., 2018), while cfDNA was directly extracted from the low-cellularity supernatant of the CSF sample (Ji et al., 2020; Gu et al., 2021), resulting in the fact that the pathogen DNA ratio of cfDNA might be higher than that of wcDNA for the same CSF sample. This may be the reason why the sensitivity of mNGS using cfDNA is higher than that of mNGS using wcDNA not only in our study but also in the published study on CNS infection (Wilson et al., 2019). Accordingly, the detection of mNGS using CSF cfDNA should be considered as a preferred examination in diagnosing CNS infections.

Pathogens causing viral and mycobacterial CNS infections were susceptible to mNGS detection using cfDNA rather than using wcDNA. Given the low loads of viruses (Carbo et al., 2020) and *Mycobacterium* (Brown et al., 2016) in CSF, a better performance of mNGS using cfDNA in our study may be attributed to its advantage in DNA extraction and bioinformatics analysis for trace pathogens. First of all, wcDNA extraction involves the cell wall lysis of pathogens using an extraction kit (Wilson et al., 2019), increasing the risk of DNA degradation (Thoendel et al., 2018; Gu et al., 2021) and influencing the DNA recovery rate of pathogens with low loads. Furthermore, the DNA of intracellular pathogens can exist in body fluids in the form of cfDNA (Casadevall and Fang, 2020), and we have proven that the mNGS of cfDNA can successfully detect *Mycobacterium* and viruses from bronchoalveolar fluid samples (Chen et al., 2021a).

Furthermore, the difference in the pathogen DNA ratio can affect the denoising performance of the bioinformatics algorithm in the dry-lab pipeline of mNGS, influencing the subsequent identification of trace pathogens (Ji et al., 2020). We previously found that the bioinformatics algorithm used in this study can decode and identify two reads of a desired pathogen (Wu et al., 2020). A lower DNA recovery rate and worse denoising performance comprehensively reduce the accuracy of mNGS using wcDNA in detecting trace pathogens. Accordingly, the mNGS of cfDNA is much more suitable for diagnosing viral and mycobacterial CNS infections than the mNGS of wcDNA.

A high percentage of mycobacterial CNS infection was found in critically ill patients. In our study, most of the mycobacterial infections were meningitis (Figure 4). Mycobacterial meningitis can cause high morbidity (25%) and mortality (15%–40%) (Komorowski et al., 2021), whose manifestation is similar to bacterial or viral meningitis (Sethi and Davies, 2020). Furthermore, mycobacterial meningitis is subacute (Sethi and Davies, 2020; Komorowski et al., 2021) and the detection rates by conventional methods are low (Wang et al., 2019), resulting in delayed diagnosis and treatment. Accordingly, the use of conventional methods without mNGS for diagnosing mycobacterial meningitis may subsequently lead to infection progression, increasing the percentage of mycobacterial infection in critically ill patients. Based on our findings, an extensive application of mNGS using CSF cfDNA in diagnosing mycobacterial CNS infection could be expected.

mNGS using cfDNA can quickly and accurately unveil the prevalence of viral CNS infections and define their roles in causing

critical and non-critical illnesses, especially for EBV and VZV. EBV is responsible for 2%–5% of viral encephalitis and meningitis patients, and a review covering a 10-year period revealed that EBV was occasionally detected in CSF using PCR (Lee et al., 2021), which was consistent with our result of conventional methods (2/258). However, we detected EBV in 61 out of 394 samples using cfDNA mNGS. Latent infection in B lymphocytes is essential for the persistence and transmission of EBV, which is estimated to infect >90% of adults worldwide (Hong et al., 2021). Latency (Hong et al., 2021) and low load (Carbo et al., 2020) might allow EBV to escape from detection by PCR, further indicating that the limit of detection for mNGS is much lower than that for PCR. Furthermore, the high percentages of EBV in both critically and non-critically ill patients emphasize that more clinical attention should be paid to latent viral infection.

We found a high ratio of VZV in non-critically ill patients (median age: 48.5 years old), which was consistent with the long-held opinion that VZV preferentially affected elder patients (Mailles et al., 2009; Grahn and Studahl, 2015). With age, immunosenescence and treatment-related immunosuppression provide conditions for the reactivation and infection of latent VZV (Arruti et al., 2017). Theoretically, elder critically ill patients (median age: 63 years old) were much more susceptible to VZV infection than non-critically ill patients. However, VZV was only detected in three critically ill patients (37, 46, and 69 years old) using mNGS. The continuous use of antimicrobial drugs can significantly influence the pathogen detection of CNS infection using mNGS (Zhang et al., 2020). VZV might be sensitive to specific therapy for critically ill patients in ICU, leading to a low detection rate in critically ill patients. The above suggests that the timing for mNGS in CNS infection needs to be dug out to accurately identify pathogens.

Limitations

This is a single-center retrospective study; potential bias from participant recruitment and data collection cannot be ruled out, and more samples from multiple hospitals are needed to further evaluate the performance of mNGS, especially for the comparison between the mNGS of cfDNA and wcDNA. Negative controls from healthy cases and those with non-infectious CNS diseases should be included to detect the potential of mNGS in ruling out infection. In addition, the potential of mNGS to help with the timely adjustment of treatments should also be evaluated. The pathogenesis of viral CNS infections should be further explored.

Conclusions

Our findings highlight the importance of mNGS using CSF cfDNA in diagnosing CNS infections, especially for viral and mycobacterial CNS infections. The most commonly detected pathogens by mNGS were *M. tuberculosis* and EBV. Furthermore, more clinical attention should be paid to CNS infections with *S. pneumoniae* and latent viruses. Based on our findings, an extensive application of mNGS using CSF cfDNA in diagnosing CNS infection could be expected.

Data availability statement

The datasets presented in this study can be found in online repositories. The names of the repository/repositories and accession number(s) can be found below: https://ngdc.cncb.ac.cn/, PRJCA008673.

Ethics statement

Study protocols were approved by the Ethical Review Committee of the Second Hospital of Hebei Medical University, Hebei, China (approval no. 2020-P027). All procedures were in accordance with the ethical standards of the responsible committee on human experimentation (institutional and national) and with the Helsinki Declaration of 1975, as revised in 2000. Informed consent was obtained from all patients enrolled in the study or their next kin/guardian.

Author contributions

ZL and HB designed the paper. LY, YeZ, and JZ drafted the manuscript. LY, YuZ, XQ, KB, and YL carried out the clinical care and management of the patients. HX performed the mNGS tests and analyzed the data. YeZ and JZ revised the manuscript. All authors approved the final manuscript as submitted and agreed to be accountable for all aspects of the work.

Funding

This work was supported by the Science and Technology Program of Hebei (No.20377790D) and the Science and Technology Project of Xi'an (No. 21RGSF0013).

Conflict of interest

YeZ, JZ, ZL, and HX are employed by Hugobiotech Co., Ltd.

The remaining authors declare that the research was conducted in the absence of any commercial or financial relationships that could be construed as a potential conflict of interest.

Publisher's note

References

Abassi, M., Boulware, D. R., and Rhein, J. (2015). Cryptococcal meningitis: diagnosis and management update. *Curr. Trop. Med. Rep.* 2, 90–99. doi: 10.1007/s40475-015-0046-y

Arruti, M., Piñeiro, L., Salicio, Y., Cilla, G., Goenaga, M., and De Munain, A. L. (2017). Incidence of varicella zoster virus infections of the central nervous system in the elderly: a large tertiary hospital-based series, (2007–2014). *J. neurovirology* 23, 451–459. doi: 10.1007/s13365-017-0519-y

Bahr, N. C., Nuwagira, E., Evans, E. E., Cresswell, F. V., Bystrom, P. V., Byamukama, A., et al. (2018). Diagnostic accuracy of xpert MTB/RIF ultra for tuberculous meningitis in HIV-infected adults: a prospective cohort study. *Lancet Infect. Dis.* 18, 68–75. doi: 10.1016/S1473-3099(17)30474-7

Berhane, M., Gidi, N. W., Eshetu, B., Gashaw, M., Tesfaw, G., Wieser, A., et al. (2021). Clinical profile of neonates admitted with sepsis to neonatal intensive care unit of jimma medical center, a tertiary hospital in Ethiopia. *Ethiopian J. Health Sci.* 31, 485–494.

Brown, J., Clark, K., Smith, C., Hopwood, J., Lynard, O., Toolan, M., et al. (2016). Variation in c-reactive protein response according to host and mycobacterial characteristics in active tuberculosis. *BMC Infect. Dis.* 16, 1–8. doi: 10.1186/s12879-016-1612-1

Cain, M. D., Salimi, H., Diamond, M. S., and Klein, R. S. (2019). Mechanisms of pathogen invasion into the central nervous system. *Neuron* 103, 771–783. doi: 10.1016/j.neuron.2019.07.015

Carbo, E. C., Buddingh, E. P., Karelioti, E., Sidorov, I. A., Feltkamp, M. C., Peter, A., et al. (2020). Improved diagnosis of viral encephalitis in adult and pediatric hematological patients using viral metagenomics. *J. Clin. Virol.* 130, 104566. doi: 10.1016/j.jcv.2020.104566

Casadevall, A., and Fang, F. C. (2020). The intracellular pathogen concept. *Mol. Microbiol.* 113, 541–545. doi: 10.1111/mmi.14421

Chen, Z., Cheng, H., Cai, Z., Wei, Q., Li, J., Liang, J., et al. (2021b). Identification of microbiome etiology associated with drug resistance in pleural empyema. *Front. Cell. infection Microbiol.* 11, 637018. doi: 10.3389/fcimb.2021.637018

Chen, Y., Feng, W., Ye, K., Guo, L., Xia, H., Guan, Y., et al. (2021a). Application of metagenomic next-generation sequencing in the diagnosis of pulmonary infectious pathogens from bronchoalveolar lavage samples. *Front. Cell. infection Microbiol.* 11, 168. doi: 10.3389/fcimb.2021.541092

Ebinger, A., Fischer, S., and Höper, D. (2021). A theoretical and generalized approach for the assessment of the sample-specific limit of detection for clinical metagenomics. *Comput. Struct. Biotechnol. J.* 19, 732–742. doi: 10.1016/j.csbj.2020.12.040

Ge, M., Gan, M., Yan, K., Xiao, F., Yang, L., Wu, B., et al. (2021). Combining metagenomic sequencing with whole exome sequencing to optimize clinical strategies in neonates with a suspected central nervous system infection. *Front. Cell. infection Microbiol.* 11. doi: 10.3389/fcimb.2021.671109

Grahn, A., and Studahl, M. (2015). Varicella-zoster virus infections of the central nervous system-prognosis, diagnostics and treatment. *J. Infection* 71, 281–293. doi: 10.1016/j.jinf.2015.06.004

Gu, W., Deng, X., Lee, M., Sucu, Y. D., Arevalo, S., Stryke, D., et al. (2021). Rapid pathogen detection by metagenomic next-generation sequencing of infected body fluids. *Nat. Med.* 27, 115–124. doi: 10.1038/s41591-020-1105-z

Ho Dang Trung, N., Le Thi Phuong, T., Wolbers, M., Nguyen Van Minh, H., Nguyen Thanh, V., Van, M. P., et al. (2012). Aetiologies of central nervous system infection in Viet nam: a prospective provincial hospital-based descriptive surveillance study. *PloS One* 7, e37825. doi: 10.1371/journal.pone.0037825

Hong, J., Wei, D., Wu, Q., Zhong, L., Chen, K., Huang, Y., et al. (2021). Antibody generation and immunogenicity analysis of EBV gp42 n-terminal region. *Viruses* 13, 2380. doi: 10.3390/v13122380

Ji, X.-C., Zhou, L.-F., Li, C.-Y., Shi, Y.-J., Wu, M.-L., Zhang, Y., et al. (2020). Reduction of human DNA contamination in clinical cerebrospinal fluid specimens improves the sensitivity of metagenomic next-generation sequencing. *J. Mol. Neurosci.* 70, 659–666. doi: 10.1007/s12031-019-01472-z

Komorowski, A. S., Lo, C. K., Irfan, N., and Singhal, N. (2021). Meningitis caused by mycobacterium tuberculosis in a recent immigrant to Canada. *CMAJ* 193, E1807-E1810. doi: 10.1503/cmaj.210740

Leber, A. L., Everhart, K., Balada-Llasat, J.-M., Cullison, J., Daly, J., Holt, S., et al. (2016). Multicenter evaluation of BioFire FilmArray meningitis/encephalitis panel for detection of bacteria, viruses, and yeast in cerebrospinal fluid specimens. *J. Clin. Microbiol.* 54, 2251–2261. doi: 10.1128/JCM.00730-16

Lee, G.-H., Kim, J., Kim, H.-W., and Cho, J. W. (2021). Clinical significance of Epstein-Barr virus in the cerebrospinal fluid of immunocompetent patients. *Clin. Neurol. Neurosurg.* 202, 106507. doi: 10.1016/j.clineuro.2021.106507

Leonard, J. M. (2017). Central nervous system tuberculosis. *Microbiol. Spectr.* 5 (2). doi: 10.1128/microbiolspec.TNMI7-0044-2017

Mailles, A., Stahl, J.-P., Committee, B. O. T. S., and Group, T. I. (2009). Infectious encephalitis in France in 2007: a national prospective study. *Clin. Infect. Dis.* 49, 1838–1847. doi: 10.1086/648419

Ma, J., Jia, R., Li, J., Liu, Y., Li, Y., Lin, P., et al. (2015). Retrospective clinical study of eighty-one cases of intracranial mucormycosis. *J. Global Infect. Dis.* 7, 143–150. doi: 10.4103/0974-777X.170497

Schibler, M., Brito, F., Zanella, M.-C., Zdobnov, E. M., Laubscher, F., L'huillier, A. G., et al. (2019). Viral sequences detection by high-throughput sequencing in cerebrospinal fluid of individuals with and without central nervous system disease. *Genes* 10, 625. doi: 10.3390/genes10080625

Sethi, V., and Davies, N. W. (2020). Acute neurological infections. *Medicine* 485757–580. doi: 10.1016/j.mpmed.2020.06.005

Sulter, G., Steen, C., and De Keyser, J. (1999). Use of the barthel index and modified rankin scale in acute stroke trials. *Stroke* 30, 1538–1541. doi: 10.1161/01.str.30.8.1538

Thoendel, M. J., Jeraldo, P. R., Greenwood-Quaintance, K. E., Yao, J. Z., Chia, N., Hanssen, A. D., et al. (2018). Identification of prosthetic joint infection pathogens using a shotgun metagenomics approach. *Clin. Infect. Dis.* 67, 1333–1338. doi: 10.1093/cid/ciy303

Wang, S., Chen, Y., Wang, D., Wu, Y., Zhao, D., Zhang, J., et al. (2019). The feasibility of metagenomic next-generation sequencing to identify pathogens causing tuberculous meningitis in cerebrospinal fluid. *Front. In Microbiol.* 10, 1993. doi: 10.3389/fmicb.2019.01993

Wilson, M. R., Naccache, S. N., Samayoa, E., Biagtan, M., Bashir, H., Yu, G., et al. (2014). Actionable diagnosis of neuroleptospirosis by next-generation sequencing. *New Engl. J. Med.* 370, 2408–2417. doi: 10.1056/NEJMoa1401268

Wilson, M. R., Sample, H. A., Zorn, K. C., Arevalo, S., Yu, G., Neuhaus, J., et al. (2019). Clinical metagenomic sequencing for diagnosis of meningitis and encephalitis. *New Engl. J. Med.* 380, 2327–2340. doi: 10.1056/NEJMoa1803396

Wu, M., Chen, Y., Xia, H., Wang, C., Tan, C. Y., Cai, X., et al. (2020). Transcriptional and proteomic insights into the host response in fatal COVID-19 cases. *Proc. Natl. Acad. Sci.* 117, 28336–28343. doi: 10.1073/pnas.2018030117

Zhang, Y., Cui, P., Zhang, H.-C., Wu, H.-L., Ye, M.-Z., Zhu, Y.-M., et al. (2020). Clinical application and evaluation of metagenomic next-generation sequencing in suspected adult central nervous system infection. *J. Trans. Med.* 18, 1–13. doi: 10.1186/s12967-020-02360-6

frontiers | Frontiers in Cellular and Infection Microbiology

TYPE Original Research
PUBLISHED 07 October 2022
DOI 10.3389/fcimb.2022.977591

OPEN ACCESS

EDITED BY
Sathyavathi Sundararaju,
Sidra Medicine, Qatar

REVIEWED BY
Andrea Hahn,
Children's National Hospital,
United States
Francisco J. Medrano,
Virgen del Rocío University Hospital,
Spain
Anju Sharma,
Qatar University, Qatar

*CORRESPONDENCE
Qing Yang
lisaqing2004@126.com

†These authors have contributed equally to this work and share first authorship

SPECIALTY SECTION
This article was submitted to Clinical Microbiology, a section of the journal Frontiers in Cellular and Infection Microbiology

RECEIVED 24 June 2022
ACCEPTED 20 September 2022
PUBLISHED 07 October 2022

CITATION
Wu D, Wang W, Xun Q, Wang H, Liu J, Zhong Z, Ouyang C and Yang Q (2022) Metagenomic next-generation sequencing indicates more precise pathogens in patients with pulmonary infection: A retrospective study. *Front. Cell. Infect. Microbiol.* 12:977591. doi: 10.3389/fcimb.2022.977591

Metagenomic next-generation sequencing indicates more precise pathogens in patients with pulmonary infection: A retrospective study

Dengfeng Wu[1†], Wei Wang[1†], Qiufen Xun[1], Hongluan Wang[2], Jiarong Liu[3], Ziqing Zhong[1], Chao Ouyang[1] and Qing Yang[1*]

[1]Department of Respiratory and Critical Care Medicine, The Second Affiliated Hospital of Nanchang University, Nanchang, China, [2]Department of Respiratory and Critical Care Medicine, Jiangxi Provincial People's Hospital, Nanchang, China, [3]Department of Nephrology Medicine, The Second Affiliated Hospital of Nanchang University, Nanchang, China

Background: Timely identification of causative pathogens is important for the diagnosis and treatment of pulmonary infections. Metagenomic next-generation sequencing (mNGS), a novel approach to pathogen detection, can directly sequence nucleic acids of specimens, providing a wide range of microbial profile. The purpose of this study was to evaluate the diagnostic performance of mNGS in the bronchoalveolar lavage fluid (BALF) of patients with suspected pulmonary infection.

Methods: From April 2019 to September 2021, 502 patients with suspected pneumonia, who underwent both mNGS of BALF and conventional microbiological tests (CMTs), were classified into different groups based on comorbidities. The diagnostic performances of mNGS and CMTs were compared. Comprehensive clinical analysis was used as the reference standard.

Results: The diagnostic accuracy and sensitivity of mNGS were 74.9% (95% confidence interval [CI], 71.7-78.7%) and 72.5% (95% CI, 68.2-76.8%) respectively, outperformed those of CMTs (36.9% diagnostic accuracy, 25.4% sensitivity). For most pathogens, the detection rate of mNGS was higher than that of CMTs. Polymicrobial infections most often occurred in immunocompromised patients (22.1%). Only 2.3% patients without underlying diseases developed polymicrobial infections. Additionally, the spectrums of pathogens also varied among the different groups. We found the positive predictive values (PPV) to be dependent upon both the pathogen of interest as well as the immunologic status of the patient (e.g., the PPV of Mycobacterium tuberculosis was 94.9% while the PPV of Pneumocystis jirovecii in immunocompetent individuals was 12.8%). This information can help physicians interpret mNGS results.

Conclusion: mNGS of BALF can greatly enhance the accuracy and detection rate of pathogens in patients with pulmonary infections. Moreover, the comorbidities and types of pathogens should be taken consideration when interpreting the results of mNGS.

KEYWORDS

metagenomic next-generation sequencing, bronchoalveolar lavage fluid, pulmonary infection, etiology diagnosis, comorbidities

Introduction

Pulmonary infection remains one of the leading causes of morbidity and mortality worldwide (GBD 2016 Causes of Death Collaborators, 2017). Accurate antimicrobial treatment can improve the cure rate, reduce broad-spectrum antibiotic use, and decrease medical costs. Therefore, timely identification of causative pathogens is critical for improving the clinical prognosis (Metlay et al., 2019). Conventional cultures are routinely used to detect the pathogens in pulmonary infections. However, this method is time-consuming and exhibit a low detection rate. Culture-independent techniques (polymerase chain reaction[PCR] and serological testing) have been proven useful for broadening the scope of detectable pathogens and increasing the detection rate; however, they require clinicians to speculate the pathogenic species (Jain et al., 2015, Gadsby et al., 2016).Hence, a rapid and unbiased diagnostic approach is urgently required.

Metagenomic next-generation sequencing (mNGS), a nucleic acid sequencing technique, can detect nearly all pathogens in theory (Chiu and Miller, 2019; Gu et al., 2019). To date, mNGS has been increasingly applied to pulmonary infections and has shown better diagnostic performance than cultures, especially in immunocompromised patients and in patients with severe pneumonia (Dickson et al., 2017, Han et al., 2019, Xie et al., 2019). Optimal lower respiratory tract specimens are crucial for microbial diagnosis. Bronchoalveolar lavage fluid (BALF) is an easily available clinical specimen that can avoid contamination by oropharyngeal flora when compared with sputum, enabling higher sensitivity than blood (Dubourg et al., 2015, Chen et al., 2020). However, there are still numerous challenges when applying mNGS of BALF samples in pulmonary infection, because of the presence of commensal microbes in the respiratory tract and the complexity of pulmonary infections (Dickson et al., 2016, Dickson et al., 2017). Thus, further investigation on the application of mNGS for BALF samples is required for identifying pathogens contributing to pulmonary infections.

In the present study, we evaluated the value of mNGS in the diagnosis of patients suspected with pulmonary infection compared to that of conventional microbiological tests (CMTs). Moreover, we assessed the spectrum of pathogens in patients with different comorbidities. The positive predictive values (PPVs) of different pathogens were calculated to evaluate the reliability of positive results of mNGS.

Methods

Study design and population

Adult patients (aged > 18 years) with suspected pulmonary infection from The Second Affiliated Hospital of Nanchang University and Jiangxi Provincial People's Hospital between April 2019 and September 2021 were retrospectively reviewed. Age, sex, comorbidities, laboratory test results, lung images, antibiotic therapy, and patient outcomes were recorded. Patients suspected with pulmonary infection required new-onset shadows on chest images and at least one of the following symptoms: 1) cough, dyspnea, or other respiratory symptoms; 2) fever; and 3) leukocytosis or leukocytopenia. 502 patients were enrolled in the study. All patients underwent bronchoscopy to obtain BALF samples. Both CMTs and mNGS of BALF were performed to detect pathogens. Based on the comorbidities, 502 patients were classified into four groups: 1) immunocompromised group: patients were viewed as the immunosuppressed host; 2) bronchiectasis group: patients were diagnosed with bronchiectasis (destructive pneumonophthisis patients were also classified into this group because of the structural lesions in the lung); 3) other comorbidities group: patients with other comorbidities which can increase the risk of pulmonary infections (including diabetes, chronic obstructive pulmonary disease, interstitial lung disease, bronchial asthma, cerebrovascular disease, lung cancer treated with targeted therapy or surgery, and liver cirrhosis, apart from the above two groups) (Martino et al., 2005, Wu et al., 2016); and 4) simple pulmonary infection group: patients without previous underlying diseases. Immunosuppressed hosts were required to meet any of the following criteria: 1) long-term steroid therapy (> 20 mg/d prednisone-equivalent and cumulative dose≥600

mg), 2) autoimmune disease treated with immunosuppressive agents or cytotoxic drugs, 3) solid-organ transplantation, 4) recent chemotherapy during the last month, 5) hematological malignancy, 6) agranulocytosis, and 7) human immunodeficiency virus (HIV) infection (Ramirez et al., 2020, Peng et al., 2021). For bronchiectasis patients, computed tomography of the chest had to fulfil at least one of the following criteria: 1) the inner diameter of the bronchus/the diameter of the concomitant pulmonary artery > 1; 2) the bronchi do not become thinner from the center to the periphery; 3) the bronchioles could be seen in the range of 1 cm from the peripheral pleura (Bonavita and Naidich, 2012).

Conventional microbiological tests

Conventional microbiological tests (CMTs) included a smear and culture of bacteria and fungi, acid-fast stain, PCR, Grocott's methenamine silver stain, and *Cryptococcus* capsular polysaccharide test. Other methods, such as galactomannan antigen and (1,3)-β-D-glucans test for fungi, tuberculin skin test, and enzyme-linked immune spot for *Mycobacterium tuberculosis*, were not regarded as etiologically confirmed methods.

Clinical comprehensive analysis was regarded as the reference standard

Two experienced clinicians in the management of pulmonary infection independently reviewed the medical records of all patients along with the results of mNGS. First, clinicians judged whether the patients had infectious or non-infectious diseases. Second, the causative pathogens were determined by a comprehensive analysis based on clinical manifestations, test results, chest radiology, and treatment response. The determination of the causative pathogens should at least meet the following criteria: etiological examination (including conventional microbiological tests and mNGS) detected the pathogens. Characteristic medical imaging and clinical manifestations can be helpful in the diagnosis of causative pathogens.

Sample processing

Once acquired, 2mL BALF was placed in a ribozyme free centrifuge tube at -20°C and sent to BGI-Hua da (Wuhan, China) on dry ice for sequencing and bioinformatics analysis on the same day. A1.5mL microcentrifuge tube with 0.6mL BALF and 250μL 0.5mm glass bead were attached to a horizontal platform on a vortex mixer and agitated vigorously at 2800-3200 rpm for 30 min. 7.2μL lysozyme was then added for wall-breaking reaction. DNA was extracted using a TIANamp Micro DNA Kit (DP316, TIANGEN BIOTECH) according to the manufacturer's recommendations.

The remaining BALF was sent to a clinical microbiology laboratory. Bacterial cultures, fungal cultures, acid-fast bacteria (AFB) staining, PCRs of mycobacteria and gram staining were performed for every samples. Bacterial cultures were set up on MacConkey and blood agar plates. Fungal cultures were set up on liquid Sabouraud medium. AFB staining was performed using the Ziehl-Neelsen staining method. PCRs for virus, bacteria, and fungal were performed according to the clinician's discretion.

Sequencing and bioinformatic analysis

The extracted DNA was first fragmented to yield -150 bp fragments with enzymatic digestion (RM0434, BGI Wuhan Biotechnology, Wuhan, China). For the construction of DNA library, fragmented DNA was further end-repaired, ligated to adapters and amplified using PCR with the PMseqTM high throughput gene detection kit for infectious pathogens (combined probe anchored polymerization sequencing method, RM0438, BGI-Shenzhen, Shenzhen, China), according to the manufacturer's instructions. Based on the qualified double strand DNA library, single-stranded circular DNA library was then generated through DNA-denaturation and circularization. Then DNA nanoballs (DNBs) were formed by rolling circle amplification (RCA) using a universal kit for sequencing reaction (Combinatorial Probe-Anchor Synthesis, RM0170, BGI-Shenzhen, Shenzhen, China),. DNBs were qualified by Qubit® ssDNA Assay Kit (Thermo Fisher Scientific) and were further sequenced by MGISEQ-2000 platform (MGI, China). High quality sequencing data were generated by removing low-quality, adapter contamination, and short (length < 35 base pairs [bp]) reads. The total number of sequencing reads was at least 20 million per library. Human host sequences mapped to the human reference genome (hg19) were then excluded by computational subtraction using Burrows–Wheeler alignment (Li and Durbin, 2009). The remaining reads were classified into four microbial genome databases (bacteria, fungi, viruses, and parasites) by simultaneously aligning to the Pathogens Metagenomics Database (PMDB). The classification reference databases were acquired from NCBI (ncbi.nlm.nih.gov/genomes/). RefSeq contains the whole genome sequence of 4,945 viruses, 6,350 bacteria, 1064 fungi related to human infections, and 234 parasites associated with human diseases.

Criteria for a positive mNGS result

Given the lack of standards to interpret the reports of mNGS and the variety of different sequencing platforms, the following criteria were applied to define positive results: 1) possessing pulmonary pathogenicity reported in the literature; 2) bacteria:

>30% relative abundance at the genus level for opportunistic pathogenic bacteria, ≥3 stringently mapped reads at the species level for high pathogenicity bacteria, ≥1 stringently mapped read for *Mycobacterium tuberculosis complex* and non-tuberculous mycobacteria (Langelier et al., 2018, Chen et al., 2021); 3) fungi (*Candida* excluded): ≥1 stringently mapped read at the species level or ≥10 stringently mapped reads for mold at the species level (Peng et al., 2021); 4) mycoplasma, chlamydia: ≥1 stringently mapped reads at the species level; 5) oral commensals, *Candida*, viruses: evaluated by a physician based on clinical manifestations and examination results (Peng et al., 2021).

Statistical analysis

Continuous variables were reported as medians and interquartile ranges. Categorical variables were expressed as frequencies and percentages. The 95% confidence intervals of the proportions were calculated using Wilson's method. McNemar's test was used to compare the detection rates of CMTs and mNGS. Chi-square tests were used to evaluate the statistical difference between non-matched samples and odd radio. All statistical analyses were performed using SPSS25. All tests were two-tailed, and statistical significance was set at $P < 0.05$.

Results

Patient characteristics

The baseline characteristics of 502 patients recruited for this study were presented in Table 1. Two hundred and ninety-seven were males. The median age was 58.0 years. 104(20.7%) patients were classified into immunocompromised group. 93(18.5%) patients were classified into bronchiectasis group. 90 patients were classified into the other comorbidities group. 215(42.8%) patients were classified into simple pulmonary infection group. 306(61%) patients had already received therapy of antibiotics before hospitalization (the most common antibiotics were β-lactam and quinolones).

TABLE 1 Clinical characteristics of 502 patients.

Characteristics	Value
Age, years, median (Q1, Q3)	58.0(47.0, 68.0)
Gender, male, n (%)	297 (59.2%)
Antibiotic therapy before hospitalization	306 (61.0%)
Comorbidities	
Immunocompromised group, n (%)	104 (20.7%)
Autoimmune disease	30
Long-term therapy of steroids	25
Recent chemotherapy	21
Solid-organ transplantation	18
Hematological malignancy	7
Agranulocytosis	2
HIV	1
Bronchiectasis group, n (%)	93 (18.5%)
Bronchiectasis patients	91
Destructive pneumonophthisis	2
Other comorbidities group, n (%)	90 (17.9%)
Diabetes	37
Chronic obstructive pulmonary disease	30
Interstitial lung disease	6
Bronchial asthma	4
Cerebrovascular disease	6
Targeted therapy and surgical of lung cancer	4
Liver cirrhosis	3
Simple pulmonary infection group, n (%)	215 (42.8%)

Infection types

According to a comprehensive analysis of medical records and the results of mNGS, 84.1% (422/502) of patients were diagnosed with pulmonary infection and 15.9% of (80/502) patients were considered non-infectious diseases, including malignancies, organizing pneumonia, and vasculitis. Among the infectious patients, 355 patients were detected the causative pathogens (including 49 patients with polymicrobial infection and 306 patients with monomicrobial infection), whereas 67 patients were not confirmed the causative pathogen. It is worth noting that polymicrobial infections most often occurred in the immunocompromised group (22.1%, [95%CI, 14.0%-30.2%]), followed by the bronchiectasis group (9.7%, [95%CI, 3.6%-15.8%]) and other comorbidities (13.3% [95%CI, 6.2%-20.5%]). However, only 2.3% (95%CI, 0.3%-4.4%) of patients in the simple pulmonary infection group had polymicrobial infection (Table 2), and the proportion of polymicrobial infections in the immunocompromised group was much higher than that in the simple pulmonary infection group (OR= 11.9 [95%CI, 4.4-32.4%]). Similar results were also observed in the bronchiectasis (OR= 4.5 [95%CI, 1.5-13.8%]) and other comorbidities group (OR= 6.5 [95%CI, 2.2-18.9%]).

Pathogen spectrum in different groups

The spectrum of pathogens varied among patients with different comorbidities. In the immunocompromised group, the most common pathogens were *Pseudomonas jirovecii* (31.0%) and *Aspergillus* (17.2%). In the bronchiectasis group, the most common pathogens were *Pseudomonas aeruginosa* (24.1%) and non-*Mycobacterium tuberculosis* (24.1%). The most common pathogens in the other comorbidities group

10.3389/fcimb.2022.977591

TABLE 2 Infection types in different comorbidities.

	Pulmonary infection	Non-infection	Polymicrobial infection	Monomicrobial infections	Not confirmed pathogen
Total	422 (84.1%)	80 (15.9%)	49 (9.7%)	306 (61.0%)	67 (13.3%)
Immunocompromised group	98 (94.2%)	6 (5.8%)	23 (22.1%)	69 (66.3%)	6 (5.8%)
Bronchiectasis group	85 (91.4%)	8 (8.6%)	(9.7%)	60 (64.5%)	16 (17.2%)
Other comorbidities group	71 (78.8%)	19 (21.1%)	12 (13.3%)	45 (50.0%)	14 (15.6%)
Simple pulmonary infection group	168 (78.1%)	47 (21.9%)	5 (2.3%)	132 (61.4%)	31 (14.4%)

were *Mycobacterium tuberculosis* (20.3%), *Aspergillus* (14.5%), and anaerobes (11.6%). The most common pathogens in the simple pulmonary infection group were *Mycobacterium tuberculosis* (37.3%) and *Chlamydia psittaci* (12.7%) (Figure 1).

Comparison of mNGS and CMTs

In the present study, 306 infectious patients obtained accurate microbiological diagnosis by mNGS. However, only 107 infectious patients were detected the causative pathogens by CMTs. In 37 infectious patients with positive results of mNGS, the detection results were inconsistent with the causative pathogens determined by a comprehensive analysis of medical records (Figure 2). Diagnostic accuracy was defined as proportion of correctly diagnosed patients (both infectious and non-infectious) among all patients. Sensitivity was defined as the proportion of infectious patients with correct diagnosis among the total number of infectious patients. The diagnostic accuracy of mNGS was much higher than that of CMTs (74.9% *vs.* 36.9%,

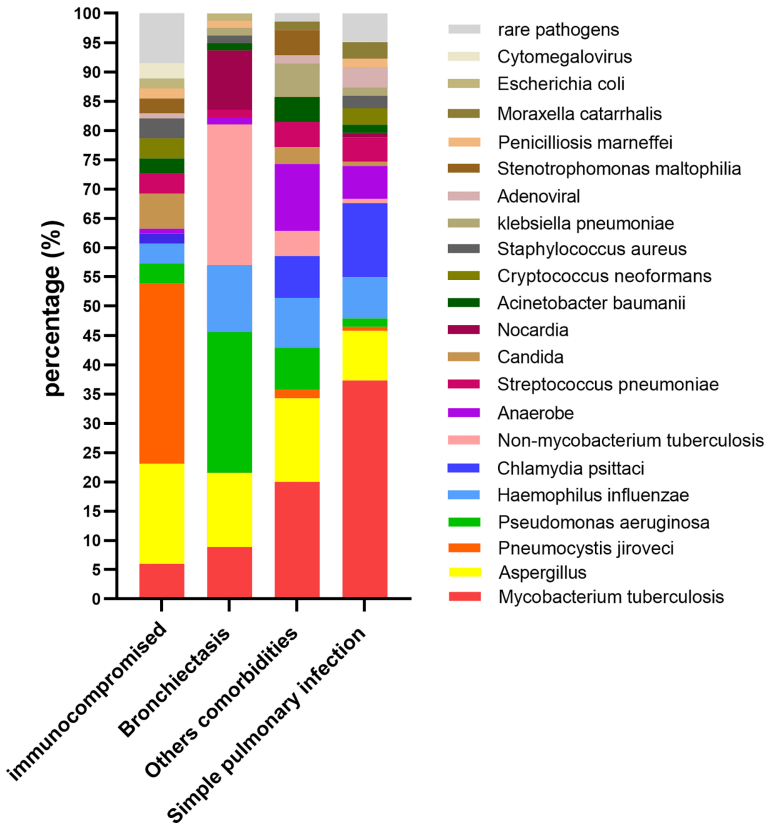

FIGURE 1
The percentage of different pathogens(y-axis) in patients with different comorbidities (x-axis).

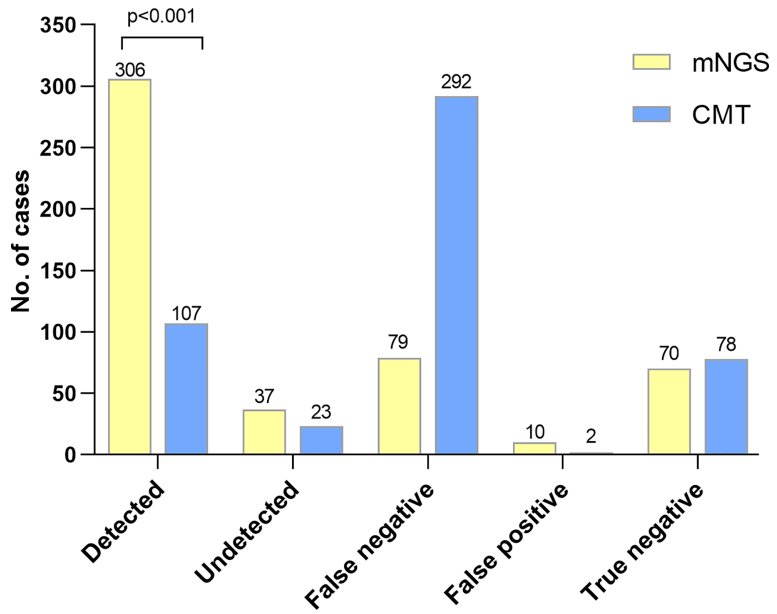

FIGURE 2
The diagnostic performance between mNGS and CMTs. Detection group: the causative pathogens were detected by mNGS or CMTs in infectious patients. Misdetection group: positive results by mNGS or CMTs were not corresponded with the reference standard in infectious patients. False negative: negative results but in non-infectious patients. False positive: positive results but in non-infectious patients. True negative: negative result by mNGS or CMTs in non-infectious patients. Patients were diagnosed with infectious or non-infectious diseases and the causative pathogens of infectious patients were determined according to comprehensive analysis of medical records. Causative pathogens detected by mNGS were more than by CMTs (p<0.001).

p<0.001). The sensitivity of mNGS was also higher than that of CMTs (72.5% *vs.* 25.4%, p< 0.001). In addition, 70 of 149 patients with negative mNGS results were diagnosed with non-infectious diseases, and the negative predictive value (NPV) of mNGS was 47% (95%CI, 38.9%-55.1%) (Table 3).

Among 355 patients with microbiologically confirmed infection, 406 pathogens were detected (some of the patients were diagnosed with polymicrobial infection). 120(29.6%) pathogens were detected by mNGS and CMTs simultaneously, 239(58.9%) pathogens were detected by mNGS separately, 12 (3.0%) pathogens were detected by CMTs separately, and 35 (8.6%) pathogens were confirmed by other methods. The pathogen detection rate of mNGS was much higher than that of CMTs (88.4% *vs.* 32.5%, p< 0.001). As shown in Figure 3, in most pathogens, mNGS also showed better diagnostic performance than CMTs, especially in *Mycoplasma, Chlamydia* and *viruses* which were exclusively detected by mNGS. For *Acinetobacter baumannii*, *Nocardia*, *Staphylococcus aureus*, *Escherichia coli* and *Legionella*, there was no statistical difference between the two methods because of the small sample size. However, these pathogens also showed at trend that mNGS was superior to CMTs.

The PPV of pathogens in mNGS reports

To evaluate the reliability of positive mNGS results, the PPV of mNGS was calculated for different pathogens. Bacteria were classified into different groups according to their pathogenicity and the possibility of colonizing the respiratory tract. *Haemophilus influenzae*, *Streptococcus pneumoniae*, and *Moraxella catarrhalis* are the most common pathogens causing community-acquired pneumonia, which can also colonize the nasopharynx (Teo et al., 2015). The summarized PPV was 71.9%

TABLE 3 The diagnostic performance between mNGS and CMTs.

	Diagnostic accuracy	Sensitivity	NPV
	(95% CI)	(95% CI)	(95%CI)
mNGS	74.9(71.7-78.7)	72.5(68.2-76.8)	47.0(38.9-55.1)
CMTs	36.9(32.6-41.1)	25.4(21.2-29.5)	21.1(16.9-25.3)

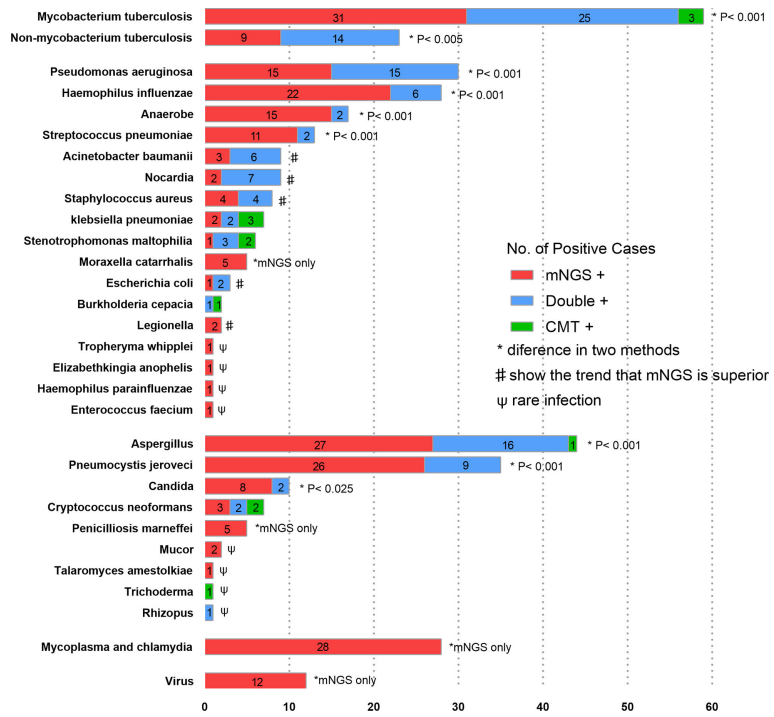

FIGURE 3
The overlap of positivity between mNGS and CMTs for different pathogens. Numbers in the histogram represents the corresponding cases of pathogens. In *Mycobacterium tuberculosis*, *Non-mycobacterium tuberculosis*, *Pseudomonas aeruginosa*, *Haemophilus influenzae*, *Anaerobe*, *Streptococcus pneumoniae*, *Aspergillus* and *Pneumocystis jirovecii*, the detection rates of mNGS were higher than those of CMTs. As for *Acinetobacter baumanii*, *Nocardia*, *Staphylococcus aureus* and *Escherichia coli*, there were no statistical differences, but mNGS tended to outperform CMTs.

(95%CI, 60.6-83.2%). *Nocardia, Staphylococcus aureus, Escherichia coli*, and *Legionella* are highly pathogenic to the respiratory tract. Their summarized PPV was 82.8% (95%CI, 68.1-97.4%). Unlike previous bacteria, *Pseudomonas aeruginosa, Acinetobacter baumannii, Klebsiella pneumoniae* and *Stenotrophomonas maltophilia* can colonize the lower respiratory tract. Their summarized PPV was 97.7% (95%CI, 93.7-100%). The PPVs of *Aspergillus* and *Pneumocystis jirovecii* were 86.0% and 67.3%, respectively. Among mycobacteria, the PPVs of *Mycobacterium tuberculosis* and *Non-mycobacterium tuberculosis* were 94.9% and 67.6%, respectively (Figure 4A). Notably, the immunocompromised group had a higher PPV of *Pneumocystis jirovecii* than the other three groups (80.5% *vs.* 12.8% p=0.006) (Figure 4B). Similarly, the PPV of non-*Mycobacterium tuberculosis* in the bronchiectasis group was higher than that in the other three groups (90.5% *vs.* 30.8%, p=0.001) (Figure 4C).

Discussion

In this study, 502 patients with suspected pulmonary infections were retrospectively analyzed. According to a comprehensive analysis of medical records, 422 (84.1%) patients were diagnosed with pulmonary infection and 80 (15.9%) were considered to have non-infectious diseases. Based on comorbidities, patients were classified into four groups. The spectrum of pathogens and proportion of polymicrobial infections varied among the different groups. Moreover, we systematically compared the diagnostic performance of mNGS of BALF and CMTs; the former was significantly superior to the latter. In addition, it can also be demonstrated that the PPVs of mNGS varied in different types of pathogens, which should be considered when interpreting the results of mNGS.

The diagnostic accuracy and sensitivity of mNGS were 74.9% (95%CI, 71.7-78.7%) and 72.5% (95%CI, 68.2-76.8%), respectively, which were much higher than those of CMTs. In a study of 235 patients with suspected pneumonia, the sensitivity of BALF mNGS reached up to 73.33% (Chen et al., 2021). In another study of 132 patients, compared to conventional testing, mNGS suggested potentially missed diagnoses in 22 patients involving 48 additional pathogenic microorganisms (Zhan et al., 2021). This study also demonstrated that the detection rate of mNGS was higher than that of CMTs in most of the pathogens. In a retrospective study of 72 patients, the detection rate of

10.3389/fcimb.2022.977591

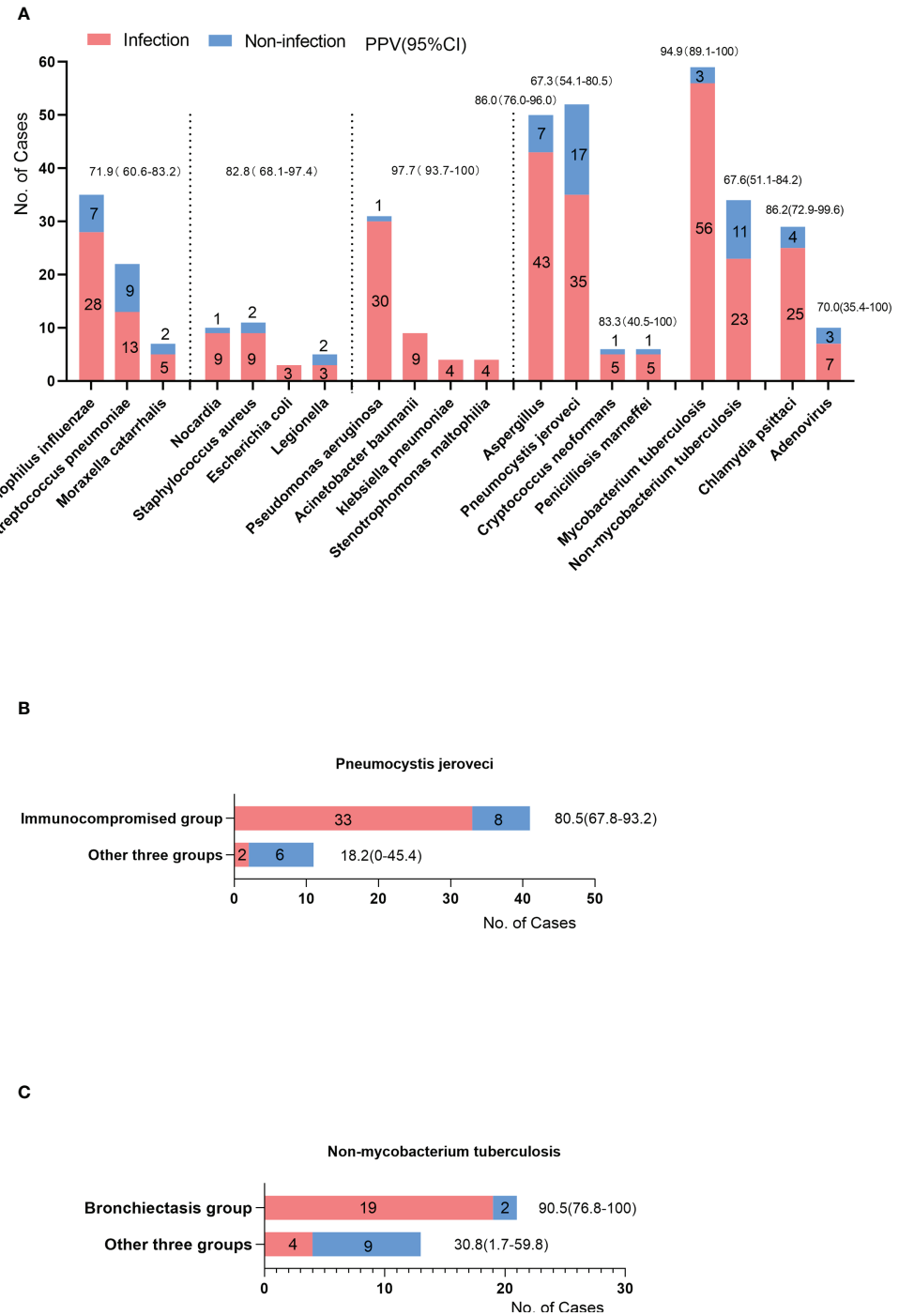

FIGURE 4
(A) The cases of positive results of mNGS (y-axis) in different pathogens (x-axis). Some were the causative pathogens (infection cases), others were considered environmental contaminants or colonized microbes (non-infection cases). The PPV was the proportion of infection cases among the cases of positive results. The PPVs and 95%CI were listed on the top of the bars. **(B)** The PPV of *Pneumocystis jirovecii* in immunocompromised group compared with other three groups. **(C)** The PPV of *Non-mycobacterium tuberculosis* in bronchiectasis group compared with other three groups.

bacteria by mNGS was also higher than conventional methods. As for fungi, the detection rate of mNGS is reported comparable to conventional tests because of the introduction of Galactomannan antigen and (1,3)-β-D-glucans (Fang et al., 2020). However, these two methods are not regarded as etiologically confirmed tests because they cannot indicate the specific species of pathogens. When the two methods were excluded, the detection rate of mNGS was higher than that of conventional tests for fungi (Miao et al., 2018).

Unlike previous studies (Chen et al., 2021; Peng et al., 2021), we did not observe a high NPV value (47.0%, 95%CI [38.9-55.1%]). For example, in a retrospective study, the NPV for different pathogens varied from 73.5% to 100% (Peng et al., 2021). Another study demonstrated that the NPV of mNGS of BALF was 85.88% (95%CI,76.25–92.18%) (Chen et al., 2021). There are explanations for these conflicting results. *Mycobacterium tuberculosis* was the most common pathogens in this study. The detection of *Mycobacterium tuberculosis* requires cell wall disruption to release nucleic acid (Simner et al., 2018). A low biomass in DNA extraction can also decrease the NPV. Moreover, rare pathogens (like *Kingella, Tropheryma whipplei*) and viruses (such as *Human herpes virus* and *Torque teno virus*) are usually not regarded as causative pathogens unless they are considered significant by the managing clinicians. To the best of our knowledge, this research is the largest sample size investigation to evaluate the diagnostic performance of mNGS for BALF in patients with pneumonia.

Immunocompromised patients have a more complex microbial etiology, with a higher detection rate of *Pneumocystis jirovecii* and *Aspergillus*. *Pseudomonas aeruginosa* and non-*Mycobacterium tuberculosis* were the dominant pathogens in patients with bronchiectasis. *Pseudomonas aeruginosa* was the most common pathogen isolated from the respiratory tract specimens of patients with bronchiectasis. Non-*Mycobacterium tuberculosis* has been increasingly detected globally (To et al., 2020). In this study, 40.0% (14/35) of the patients with positive acid-fast stains were diagnosed with non-*Mycobacterium tuberculosis* infection by mNGS. Since not all patients with positive acid-fast staining had *Mycobacterium tuberculosis* infection, and the culture of *Mycobacterium* takes one to three months, mNGS might be an efficient method to distinguish non-*Mycobacterium tuberculosis* infection (Shi et al., 2020). *Mycobacterium tuberculosis* was the most common pathogen in the patients without these comorbidities. The high detection rate of this bacterium is reasonable. First, there is a high prevalence of *Mycobacterium tuberculosis* infection in China (Organization, W.H., 2021). Moreover, most of the patients enrolled in our study received empirical anti-infective treatment. Interestingly, a significant number of patients in the simple pulmonary infection group were diagnosed with *Chlamydia psittaci* infection, which may be associated with universal poultry production in Jiangxi, China (Li et al., 2021).

Another strength of our study is that we strived to evaluate the PPVs of mNGS for different types of pathogens, which can help clinicians interpret the reports of mNGS. The summarized PPV of *Haemophilus influenzae*, *Streptococcus pneumoniae*, and *Moraxella catarrhalis* were 71.9% (95%CI, 60.6-83.2%). As the most common colonizing bacteria in the nasopharynx (Teo et al., 2015), these pathogens can be carried into the BALF during bronchoscopy. Thus, attention should be paid to distinguish between colonization and infection based on the positive results of these pathogens. The summarized PPV of *Pseudomonas aeruginosa, Acinetobacter baumannii, Klebsiella pneumoniae*, and *Stenotrophomonas maltophilia* were 97% (95%CI, 93.7-100%). This high value is mainly due to a stricter positive criterion in reports of mNGS; these bacteria were not considered a positive result of mNGS if their relative abundance at the genus level was less than 30%. A similar high PPV of these pathogens was observed in Peng et al.'s study (Peng et al., 2021). It should be noted that the PPV of *Pneumocystis jirovecii* in the immunocompromised group was much higher than that in the other three groups (80.5%–18.2%, p=0.006). The positive result for *Pneumocystis jirovecii* in immunocompromised patients is more likely to be the causative pathogen. In contrast, the positive result of *Pneumocystis jirovecii* in immunocompetent patients is more likely to be considered environmental contaminants. Similar features can be observed in non-*Mycobacterium tuberculosis*. Therefore, the commodities and types of pathogens should be considered when interpreting mNGS reports.

The potential for pathogen detection using mNGS has been confirmed in many studies and clinical contexts. However, there are still limitations to the application of mNGS in clinical settings. Multiple evidence suggested that the respiratory tract is not a sterile environment. Commensal microbes commonly exist in the respiratory tract of healthy individuals, indicating that microbes with many reads in mNGS reports are not always the causative pathogen (Dickson et al., 2017). In addition, the existence of environmental contaminants, opportunistic pathogens, and mismatch of DNA fragments also makes it difficult to interpret the reports of mNGS. Therefore, a reasonable and accurate interpretation is an important bottleneck (Han et al., 2019). The cost is another concern for the widespread use of mNGS. In China, the current cost is approximately $600 per sample, which is much higher than that of conventional tests (Miao, Ma et al., 2018, Fang, Mei et al., 2020). Currently, a vast proportion of the reads (>90%) sequenced by mNGS are host-derived, which means most of money is spent on these invalid sequences. Reducing the host reads prior to sequencing using host depletion methods can effectively reduce the total cost (Marotz et al., 2018). Increasing the number of test samples per run can also reduce the cost per sample, but it comes at the expense of turnaround time (Rutanga et al., 2018). In addition, encouraging more high-quality sequencing platforms to participate in the market can indirectly reduce costs.

This study has several limitations. First, it is a retrospective study of two center, which may lead to potential selection bias. Second, we failed to conduct cultures for *Mycobacterium tuberculosis* and non-*Mycobacterium tuberculosis*. Third, the patients classified into other comorbidity groups had different comorbidities (e.g. diabetes, chronic obstructive pulmonary disease, interstitial lung disease, cerebrovascular disease, lung cancer treated with targeted therapy or surgical, liver cirrhosis), which may be associated with the heterogeneity of the spectrum of pathogens. Forth, most patients enrolled in the present study have received anti-infective therapy before hospitalization, which might result in the underestimation of culture sensitivity and higher chance of infections caused by opportunistic pathogens. Finally, the interpretation of the mNGS results depends on the clinician's subjective judgment, which may lead to bias.

Overall, the application of mNGS to BALF can improve pathogen detection in patients with pulmonary infections. However, the interpretation of reports and the cost of mNGS remain concerns. This study demonstrated that the commodities and types of pathogens should be considered when interpreting mNGS reports. Further investigations are still needed for the extension of mNGS.

Data availability statement

The datasets presented in this study can be found in online repositories. The names of the repository/repositories and accession number(s) can be found below: https://db.cngb.org/search/project/CNP0002658/.

Ethics statement

The studies involving human participants were reviewed and approved by Ethics Committee of Second Affiliated Hospital of Nanchang University (No. 2019-013) Jiangxi Provincial People's Hospital (No.2021-076). The patients/participants provided their written informed consent to participate in this study.

Author contributions

DW and WW analyzed the data, drafted the first version of the manuscript, and submitted it to the publication; QX and HW collected data and helped to analyze data; JL, ZZ, and CO helped to collect data; QY was responsible for the entire project, designed the experiment, and revised the draft of the manuscript. All authors contributed to the article and approved the submitted version.

Funding

This work was supported by the National Natural Science Foundation of China (Grant no. 81860011).

Acknowledgments

We would like to acknowledge the patients for cooperating with our investigation.

Conflict of interest

The authors declare that the research was conducted in the absence of any commercial or financial relationships that could be construed as a potential conflict of interest.

Publisher's note

References

Bonavita, J., and Naidich, D. P. (2012). Imaging of bronchiectasis. *Clin. Chest Med.* 33 (2), 233–248. doi: 10.1016/j.ccm.2012.02.007

Chen, X., Ding, S., Lei, C., Qin, J., Guo, T., Yang, D., et al. (2020). Blood and bronchoalveolar lavage fluid metagenomic next-generation sequencing in pneumonia. *Can. J. Infect. Dis. Med. Microbiol.* 2020. doi: 10.1155/2020/6839103

Chen, Y., Feng, W., Ye, K., Guo, L., Xia, H., Guan, Y., et al. (2021). Application of metagenomic next-generation sequencing in the diagnosis of pulmonary infectious pathogens from bronchoalveolar lavage samples. *Front. Cell Infect. Microbiol.* 11, 541092. doi: 10.3389/fcimb.2021.541092

Chiu, C. Y., and Miller, S. A. (2019). Clinical metagenomics. *Nat. Rev. Genet.* 20 (6), 341–355. doi: 10.1038/s41576-019-0113-7

Dickson, R. P., Erb-Downward, J. R., Freeman, C. M., McCloskey, L., Falkowski, N. R., Huffnagle, G. B., et al. (2017). Bacterial topography of the healthy human lower respiratory tract. *mBio* 8 (1). doi: 10.1128/mBio.02287-16

Dickson, R. P., Erb-Downward, J. R., Martinez, F. J., and Huffnagle, G. B. (2016). The microbiome and the respiratory tract. *Annu. Rev. Physiol.* 78, 481–504. doi: 10.1146/annurev-physiol-021115-105238

Dubourg, G., Abat, C., Rolain, J. M., and Raoult, D. (2015). Correlation between sputum and bronchoalveolar lavage fluid cultures. *J. Clin. Microbiol.* 53 (3), 994–996. doi: 10.1128/JCM.02918-14

Fang, X., Mei, Q., Fan, X., Zhu, C., Yang, T., Zhang, L., et al. (2020). Diagnostic value of metagenomic next-generation sequencing for the detection of pathogens in

bronchoalveolar lavage fluid in ventilator-associated pneumonia patients. *Front. Microbiol.* 11, 599756. doi: 10.3389/fmicb.2020.599756

Gadsby, N. J., Russell, C. D., McHugh, M. P., Mark, H., Conway Morris, A., Laurenson, I. F., et al. (2016). Comprehensive molecular testing for respiratory pathogens in community-acquired pneumonia. *Clin. Infect. Dis.* 62 (7), 817–823. doi: 10.1093/cid/civ1214

GBD 2016 Causes of Death Collaborators (2017). Global, regional, and national age-sex specific mortality for 264 causes of death, 1980-2016: a systematic analysis for the Global Burden of Disease Study 2016. *Lancet.* 390 (10100), 1151–1210. doi: 10.1016/S0140-6736(17)32152-9

Gu, W., Miller, S., and Chiu, C. Y. (2019). Clinical metagenomic next-generation sequencing for pathogen detection. *Annu. Rev. Pathol.* 14, 319–338. doi: 10.1146/annurev-pathmechdis-012418-012751

Han, D., Li, Z., Li, R., Tan, P., Zhang, R., and Li, J. (2019). mNGS in clinical microbiology laboratories: on the road to maturity. *Crit. Rev. Microbiol.* 45 (5-6), 668–685. doi: 10.1080/1040841X.2019.1681933

Jain, S., Self, W. H., Wunderink, R. G., Fakhran, S., Balk, R., Bramley, A. M., et al. (2015). Community-acquired pneumonia requiring hospitalization among U.S. adults. *N Engl. J. Med.* 373 (5), 415–427. doi: 10.1056/NEJMoa1500245

Langelier, C., Zinter, M. S., Kalantar, K., Yanik, G. A., Christenson, S., O'Donovan, B., et al. (2018). Metagenomic sequencing detects respiratory pathogens in hematopoietic cellular transplant patients. *Am. J. Respir. Crit. Care Med.* 197 (4), 524–528. doi: 10.1164/rccm.201706-1097LE

Li, H., and Durbin, R. (2009). Fast and accurate short read alignment with burrows-wheeler transform. *Bioinformatics* 25 (14), 1754–1760. doi: 10.1093/bioinformatics/btp324

Li, H., Tan, M., Zhang, F., Ji, H., Zeng, Y., Yang, Q., et al. (2021). Diversity of avian leukosis virus subgroup J in local chickens, Jiangxi, China. *Sci. Rep.* 11 (1), 4797. doi: 10.1038/s41598-021-84189-7

Marotz, C. A., Sanders, J. G., Zuniga, C., Zaramela, L. S., Knight, R., and Zengler, K. (2018). Improving saliva shotgun metagenomics by chemical host DNA depletion. *Microbiome* 6 (1), 42. doi: 10.1186/s40168-018-0426-3

Martino, R., Foley, N., Bhogal, S., Diamant, N., Speechley, M., and Teasell, R. (2005). Dysphagia after stroke: incidence, diagnosis, and pulmonary complications. *Stroke* 36 (12), 2756–2763. doi: 10.1161/01.STR.0000190056.76543.eb

Metlay, J. P., Waterer, G. W., Long, A. C., Anzueto, A., Brozek, J., Crothers, K., et al. (2019). Diagnosis and treatment of adults with community-acquired pneumonia. an official clinical practice guideline of the American thoracic society and infectious diseases society of America. *Am. J. Respir. Crit. Care Med.* 200 (7), e45–e67. doi: 10.1164/rccm.201908-1581ST

Miao, Q., Ma, Y., Wang, Q., Pan, J., Zhang, Y., Jin, W., et al. (2018). Microbiological diagnostic performance of metagenomic next-generation sequencing when applied to clinical practice. *Clin. Infect. Dis.* 67 (suppl_2), S231–s240. doi: 10.1093/cid/ciy693

Organization, W. H (2021). Global tuberculosis report. Available at: https://www.who.int/publications/i/item/9789240037021

Peng, J. M., Du, B., Qin, H. Y., Wang, Q., and Shi, Y. (2021). Metagenomic next-generation sequencing for the diagnosis of suspected pneumonia in immunocompromised patients. *J. Infect.* 82 (4), 22–27. doi: 10.1016/j.jinf.2021.01.029

Ramirez, J. A., Musher, D. M., Evans, S. E., Dela Cruz, C., Crothers, K. A., Hage, C. A., et al. (2020). Treatment of community-acquired pneumonia in immunocompromised adults: A consensus statement regarding initial strategies. *Chest* 158 (5), 1896–1911. doi: 10.1016/j.chest.2020.05.598

Rutanga, J. P., Van Puyvelde, S., Heroes, A. S., Muvunyi, C. M., Jacobs, J., and Deborggraeve, S. (2018). 16S metagenomics for diagnosis of bloodstream infections: opportunities and pitfalls. *Expert Rev. Mol. Diagn.* 18 (8), 749–759. doi: 10.1080/14737159.2018.1498786

Shi, C. L., Han, P., Tang, P. J., Chen, M. M., Ye, Z. J., Wu, M. Y., et al. (2020). Clinical metagenomic sequencing for diagnosis of pulmonary tuberculosis. *J. Infect.* 81 (4), 567–574. doi: 10.1016/j.jinf.2020.08.004

Simner, P. J., Miller, S., and Carroll, K. C. (2018). Understanding the promises and hurdles of metagenomic next-generation sequencing as a diagnostic tool for infectious diseases. *Clin. Infect. Dis.* 66 (5), 778–788. doi: 10.1093/cid/cix881

Teo, S. M., Mok, D., Pham, K., Kusel, M., Serralha, M., Troy, N., et al. (2015). The infant nasopharyngeal microbiome impacts severity of lower respiratory infection and risk of asthma development. *Cell Host Microbe* 17 (5), 704–715. doi: 10.1016/j.chom.2015.03.008

To, K., Cao, R., Yegiazaryan, A., Owens, J., and Venketaraman, V. (2020). General overview of nontuberculous mycobacteria opportunistic pathogens: Mycobacterium avium and mycobacterium abscessus. *J. Clin. Med.* 9 (8). doi: 10.3390/jcm9082541

Wu, H. P., Chu, C. M., Lin, C. Y., Yu, C. C., Hua, C. C., Yu, T. J., et al. (2016). Liver cirrhosis and diabetes mellitus are risk factors for staphylococcus aureus infection in patients with healthcare-associated or hospital-acquired pneumonia. *Pulm Med.* 2016, 4706150. doi: 10.1155/2016/4706150

Xie, Y., Du, J., Jin, W., Teng, X., Cheng, R., Huang, P., et al. (2019). Next generation sequencing for diagnosis of severe pneumonia: Chin-2018. *J. Infect.* 78 (2), 158–169. doi: 10.1016/j.jinf.2018.09.004

Zhan, Y., Xu, T., He, F., Guan, W. J., Li, Z., Li, S., et al. (2021). Clinical evaluation of a metagenomics-based assay for pneumonia management. *Front. Microbiol.* 12, 751073. doi: 10.3389/fmicb.2021.751073

frontiers | Frontiers in Cellular and Infection Microbiology

TYPE Original Research
PUBLISHED 07 October 2022
DOI 10.3389/fcimb.2022.929701

OPEN ACCESS

EDITED BY
Arun Prasath Lakshmanan,
Sidra Medicine, Qatar

REVIEWED BY
Kushani Shah,
Dana–Farber Cancer Institute,
United States
William Bolosky,
Microsoft Research, United States

*CORRESPONDENCE
Hongdong Tan
doctortanhd427@163.com

SPECIALTY SECTION
This article was submitted to Clinical Microbiology, a section of the journal Frontiers in Cellular and Infection Microbiology

RECEIVED 27 April 2022
ACCEPTED 15 September 2022
PUBLISHED 07 October 2022

CITATION
Xu L, Zhou Z, Wang Y, Song C and Tan H (2022) Improved accuracy of etiological diagnosis of spinal infection by metagenomic next-generation sequencing.
Front. Cell. Infect. Microbiol. 12:929701.
doi: 10.3389/fcimb.2022.929701

Improved accuracy of etiological diagnosis of spinal infection by metagenomic next-generation sequencing

Liang Xu[1], Zheng Zhou[2], Yao Wang[3,4], Chao Song[3,4] and Hongdong Tan[1]*

[1]Department of Spinal Infection, Shandong Public Health Clinical Center, Jinan, China, [2]Katharine Hsu International Research Institute of Infectious Disease, Shandong Public Health Clinical Center, Jinan, China, [3]State Key Laboratory of Translational Medicine and Innovative Drug Development, Jiangsu Simcere Diagnostics Co., Ltd., Nanjing, China, [4]Department of Medicine, Nanjing Simcere Medical Laboratory Science Co., Ltd., Nanjing, China

Currently, the use of metagenomic next-generation sequencing (mNGS), a new approach to identify organisms in infectious diseases, is rarely reported in the diagnosis of spinal infection. This study aimed to evaluate the potential value of mNGS in etiological diagnosis of spinal infection. In this retrospective study, the clinical data of patients with suspected spinal infection were collected by electronic medical records. Specimens obtained from each patient were tested *via* mNGS assay and other conventional microbiological tests (CMTs). The sensitivity and specificity of mNGS and CMTs were calculated using the final clinical diagnosis as the golden standard. In total, 108 patients were eligible for the study, with the mean length of stay of 42.8 days. Regarding the overall identification of pathogens, mNGS exhibited a better performance than CMTs, and several nontuberculous mycobacteria, fungi, and bacteria were newly discovered. In the diagnosis of spinal infection, the sensitivity, specificity, and area under the curve of mNGS were 90.72%, 81.82%, and 0.89, respectively, which were all higher than 52.17%, 56.25%, and 0.72 of the CMTs. At hospital discharge, the C-reactive protein, erythrocyte sedimentation rate, and white blood cell count of patients significantly decreased compared with hospitalization (all $p < 0.05$), and 88.89% showed good outcomes. These findings may suggest that mNGS has a better diagnostic accuracy in pathogenic identification of patients with suspected spinal infection, and patients treated with NGS-guided antimicrobial therapy mostly seem to have good outcomes.

KEYWORDS

metagenomic next-generation sequencing, microbiological test, spinal infection, diagnostic accuracy, antimicrobial therapy

Introduction

Spinal infections, which commonly occur as vertebral osteomyelitis, discitis, and epidural abscesses, have the potential to cause significantly serious consequences even death if not treated promptly and precisely at early stage, although the overall incidence is not very high (approximately 2.2/100,000 per year) (Beronius et al., 2001; Grammatico et al., 2008; Duarte and Vaccaro, 2013). Because of aging population and the increased number of immunocompromised people in China, the incidence of spinal infections is increasing year by year. However, the onset of this disease is insidious, and the performance is not typical, causing a great trouble to the diagnosis (Zhang et al., 2019). A significant delay of approximately 2–6 months usually occurs until establishment of a final diagnosis and treatment because of the low specificity of signs and symptoms at clinical presentation (Lener et al., 2018).

As an innovative etiological diagnostic tool, metagenomic next-generation sequencing (mNGS) technology has been widely used in the diagnosis of various infectious diseases with advantages of rapidly and unbiasedly capturing pathogens as well as species identification in a single clinical sample (Simner et al., 2018). Notably, this non-targeted identification strategy is revolutionizing the field of microbial diagnostics away from conventional diagnostic strategies based on prior assumptions regarding some certain pathogens (Besser et al., 2018). Another benefit of mNGS is the shortened turnaround time of about 30 h, which overcomes the difficulty of long cultivation period for some microorganisms, such as mycobacteria, and provides more possibilities for early and effective treatment (Li et al., 2021). Consequently, clinicians of infectious department have used mNGS frequently for detection of pathogens in various clinical specimens, including blood, cerebrospinal fluid, and bronchoalveolar lavage fluid (Wilson et al., 2014; Parize et al., 2017; Wilson et al., 2018; Miller et al., 2019; Qian et al., 2021). Indeed, mNGS provides an alternative to diagnose patients with suspected infections for which the pathogenic cause is unknown despite prior comprehensive microbiological investigations.

Currently, there are few studies on the use of mNGS in the identification of pathogens within spinal infection-associated tissue specimens. Therefore, this study was performed to evaluate the potential value of mNGS in the etiological diagnosis of spinal infection.

Materials and methods

Patients

In this study, the patients with suspected spinal infection from Shandong Chest Hospital between March 2020 and August 2021 were retrospectively analyzed. Inclusion criteria included are as follows: (1) fever; (2) presence of chest pain not relieved by rest or analgesics; (3) abnormal magnetic resonance imaging; and (4) previous and current episodes of tuberculosis (TB). Patients with incomplete clinical information were excluded. Written consent forms were obtained from all the patients. This study was approved by the Institutional Review Board of Shandong Chest Hospital (approval number: 2021XKYYEC-44), a part of Shandong Public Health Clinical Center.

Clinical data collection

The clinical data of patients were collected by directly reviewing electronic medical records in hospital system, including gender, age, infectious sites, comorbidities, clinical symptoms, laboratory results, radiological features, and treatment regimens.

Specimen collection and conventional microbiological tests

When suspected spinal infection was diagnosed, blood specimens were obtained immediately and tested by four conventional methods, including blood culture, T-SPOT.TB test plus TB immunoglubin G (IgG) rapid test, G/GM assay, and serum agglutination test for brucellosis. Tissue specimens were achieved through surgical biopsy and submitted to clinical laboratories for pathogenic culture, smear and staining, and nucleic acid testing (X-pert and mNGS). The workflow of specimen collection and test methods possibly involved in the patients was presented in Figure 1.

Metagenomic next-generation sequencing

Tissue samples were processed for wall breaking through an in-house developed method. The tissue was first transferred into a lysis tube (MP Lysing Matri A), 400 µl of phosphate-buffered saline was added, and then the MP FastPrep-24^{TM} 5G instrument was used for shaking at 6 m/s for 120 s. After wall breaking, nucleic acid extraction was conducted using a micro-sample genomic DNA extraction kit (DP316, Tiangen), and the nucleic acid extracted was subjected to nucleic acid quantitative quality inspection using Qubit 4.0. The nucleic acid that passed the quality inspection participated in the process of library construction as follows: the DNA was first cut into about 200 bp by enzyme digestion; then, end-repair, a-tail adjunction,

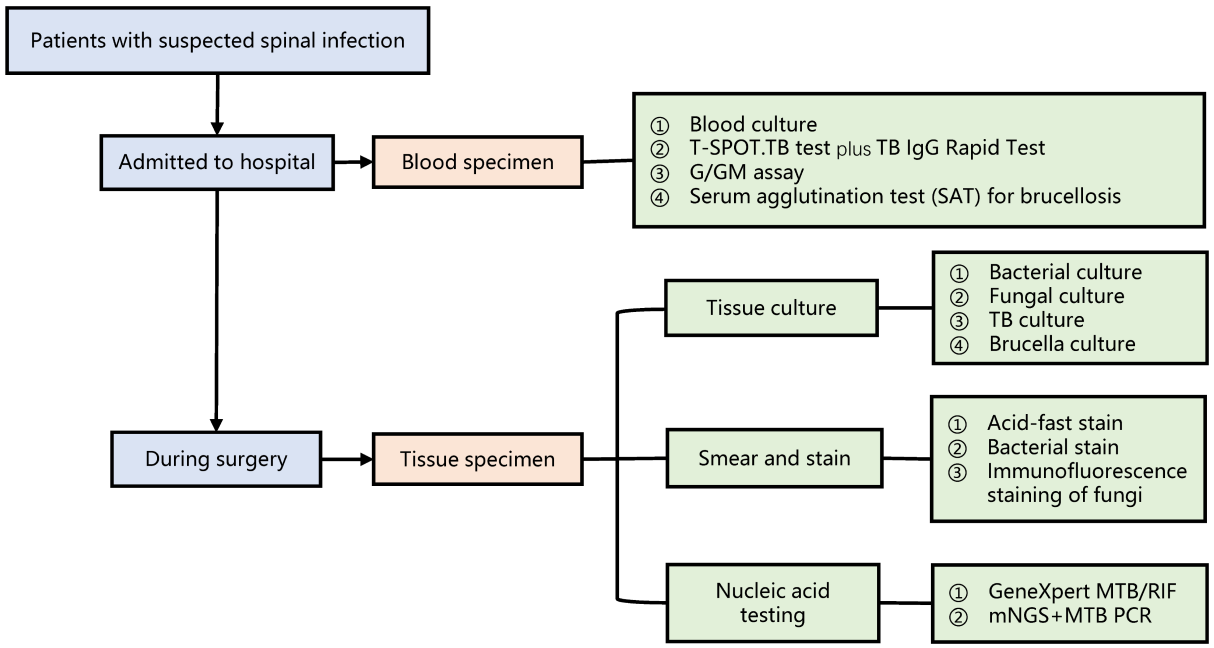

FIGURE 1
The workflow of specimen collection and test methods possibly involved in the patients.

adapter ligation, and labeling were performed; finally, polymerase chain reaction (PCR) was applied for enrichment, and Agilent 4200 was used to detect the fragments of the library. Subsequently, the library concentration quality was checked using Qubit 4.0. The library with qualified fragments and concentration was sequenced on an Illumina NextSeq 550 DX platform for single-end 75-bp sequencing.

Fastp was used for FASTQ file quality control. High-quality sequencing data were generated by removing low-quality reads, adapter contamination, short reads (50 bp), and duplicated reads. Human sequence data were excluded and mapped to a human reference (GRCh38) using a powerful alignment tool called Burrows–Wheeler Alignment (Li and Durbin, 2009). After removing human sequences, the remaining sequencing data were aligned to National Center for Biotechnology Information nucleotide (NCBI nt) database by Scalable Nucleotide Alignment Program (Zaharia et al., 2011). As described in a previous study (Chen et al., 2020), the mapped data were processed with in-house scripts, including taxonomy annotation, genome coverage/depth calculation, and abundance calculation. Kraken2 was used to perform microbial classification. Abundance of species within a sample was estimated with Braken. The results were further verified by BLAST.

Clinical golden standards and outcome assessment

In this study, the clinical golden standard was described as the final clinical diagnosis, which was decided by physicians based on the patient's clinical records, microbiological tests, imaging and histopathological analysis, past medication information, etc. The sensitivity and specificity were calculated on the basis of this.

Physicians adjusted the treatment strategy according to mNGS results. To evaluate the effect of the mNGS-guided treatment, three representative inflammatory indicators—white blood cell count (WBC), erythrocyte sedimentation rate (ESR), and C-reactive protein (CRP)—were recorded and compared at the time of hospitalization and hospital discharge. The clinical outcomes were described as complete recovery, improved symptoms, voluntary hospital discharge, and death.

Statistical analysis

All statistical analyses were performed using R package (version 3.6.3). The dichotomous variables were counted to evaluate the sensitivity and specificity of different detection

methods, and the results were presented with 95% confidence intervals (CIs). R package "pROC" (version 1.18) was employed to draw receiver operator characteristic (ROC) curves. The Wilcoxon rank sum test was used to compare the differences of three inflammatory indicators before and after treatment under the mNGS-guided therapy. The value of $p < 0.05$ was considered statistically significant.

Results

Patient characteristics

Between March 2020 and August 2021, 108 patients were eligible for the study, among whom 55 were male patients. Their mean age was 57.8 years, and the mean length of stay was 42.8 days. The infectious sites included lumbar spine (75.9%), thoracic spine (18.5%), lumbar and thoracic spine (4.6%), and cervical spine (0.9%). Among 108 cases, 103 (95.4%) experienced the pain at the infected sites, and 47 (43.5%) reported limb pain and numbness prior to the hospital admission. Fever or recurrent fever occurred in 34.3% of patients before or during hospitalization. In addition, 5.6% of patients experienced weight loss and another 3.7% had night sweats. The most frequent comorbidities were diabetes (20.4%) and hypoalbuminemia (20.4%). Table 1 describes the patient characteristics in detail.

TABLE 1 Characteristics of 108 patients enrolled in this study.

Characteristics	N (%)
Age, years, median (range)	57.8 (14.0–82.0)
Gender (male)	55 (58.5)
Length of stay, day, median (range)	42.8 (6.0–120.0)
Infectious sites	
Lumbar spine	82 (75.9)
Thoracic spine	20 (18.5)
Thoracic spine and lumbar spine	5 (4.6)
Cervical spine	1 (0.9)
Symptoms	
Pain	103 (95.4)
Limb pain and numbness	47 (43.5)
Fever	37 (34.3)
Weight loss	6 (5.6)
Night sweat	4 (3.7)
Laboratory parameters, median (range)	
WBC count, 10 × 9 cells/L	6.6 (2.7–12.5)
ESR, mm/H	51.7 (3.0–124.0)
CRP, mg/L	39.2 (0.1–165.5)
Comorbidities	
Diabetes	22 (20.4)
Hypertension	22 (20.4)
Liver and renal dysfunction	8 (7.4)
Immunosuppression	1 (0.9)
Others	36 (33.3)

WBC, white blood cell count; ESR, erythrocyte sedimentation rate; CRP, C-reactive protein.

Isolates of pathogens identified by the clinical golden standard

As shown in Figure 2, a total of 27 types of bacteria (including six types of mycobacteria) and four types of fungi were detected through the clinical golden standard. Among mycobacteria, *Mycobacterium tuberculosis* (MTB) was detected with the highest number of isolates (n = 21), and five non-tuberculous mycobacteria (NTM) were detected once each. Except for mycobacteria, the top five bacterial isolates were *Escherichia coli*, *Brucella melitensis*, *Staphylococcus aureus*, *Staphylococcus epidermidis*, and *Klebsiella pneumoniae*. The four fungi with one isolate included *Aspergillus flavus*, *Aspergillus candidus*, *Aspergillus fumigatus*, and *Candida parapsilosis*.

Concordance between CMTs and mNGS

For the identification of MTB, mNGS and conventional microbiological tests (CMTs) showed the same detection ability. The MTB was identified in 17 cases by both mNGS and CMTs, in four cases only by mNGS, and four cases only by CMTs. Brucella was detected in two cases using mNGS alone and three cases using CMTs alone. Except for the pathogens mentioned above, mNGS exhibited a better detection performance than CMTs in all other pathogens. *Escherichia coli* was detected in nine cases by mNGS but only in two cases by CMTs. Moreover, *Staphylococcus aureus* (n = 3), *Staphylococcus epidermidis* (n = 4), and *Klebsiella pneumoniae* (n = 4) were missed by CMTs but detected by mNGS. Notably, novel pathogens were discovered by mNGS, including NTM (n = 5), fungi (n = 4), and bacteria (n = 15) (Figure 3A).

Of all patients, the pathogens were identified in 44 cases using both CMTs and mNGS assays, in 44 cases using mNGS alone, and in 11 cases using CMTs alone; no pathogens were detected in nine cases by either CMTs or mNGS assays (Figure 3B). Analysis of the pathogens detected in 44 patients using both CMTs and mNGS assays showed that the pathogens were completely matched in 32 cases at the level of species and only matched in 11 cases at the genus level but totally unmatched in one case.

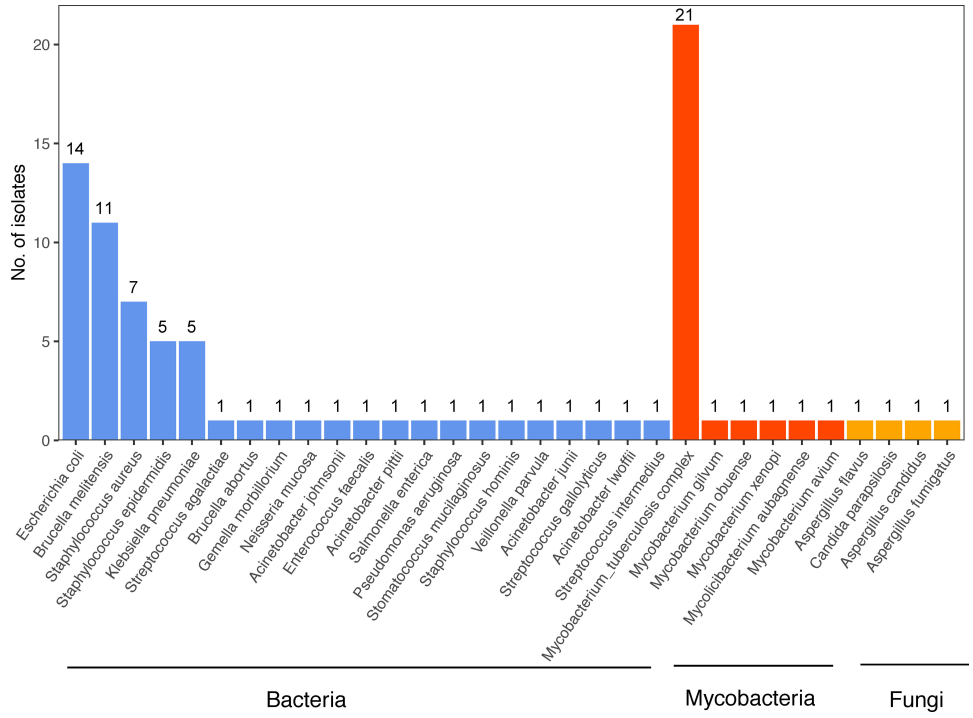

FIGURE 2
Isolates of pathogens detected by the clinical golden standard.

Diagnostic performance of mNGS

In the diagnosis of spinal infection, the overall sensitivity of mNGS came up to 90.72%, significantly higher than 52.17% of the CMTs ($p < 0.001$), and its overall specificity was also slightly higher than that of CMTs although no statistical significance (81.82% vs. 56.25%, $p = 0.231$). Regarding the identification of bacteria, mycobacteria, and fungi, the sensitivity of mNGS was all superior to that of CMTs (bacteria: 90.30% vs. 53.40%; mycobacteria: 83.90% vs. 67.74%; fungi: 100.00% vs. 25.00%; Table 2). In addition, the area under the curve (AUC) of mNGS was 0.89, significantly larger than 0.72 of CMTs, which further confirmed a better diagnostic performance of mNGS than CMTs in spinal infection (Figure 4).

Inconsistent analysis between mNGS and CMTs

Mycobacteria in nine patients were detected by mNGS but missed by CMTs. Meanwhile, mycobacteria in four patients were identified by CMTs but missed by mNGS (Figure 3A). Some of these negative mNGS results may be due to the low concentration of nucleic acid extraction caused by the difficulty in the cell wall breaking of mycobacteria. There were also some cases confirmed by mNGS but false positive by CMTs because of contamination (Table 3). The fungi in four patients were identified by mNGS at the level of species but missed by CMTs, among which higher G/GM test scores related to possible fungi infection were suggested in three cases (Table 4).

Outcomes under the mNGS-guided antimicrobial therapy

At the time of hospital discharge, the CRP, ESR, and WBC of patients all significantly decreased compared with hospital admission (all $p < 0.05$; Figure 5). Of the 108 patients, 17 (15.74%) were completely recovered, 79 (73.15%) had improved symptoms, 12 (11.11%) voluntarily discharged from hospital, and no deaths occurred, suggesting that the patients treated with the mNGS-guided antimicrobial therapy mostly showed good outcomes.

Discussion

As a novel diagnostic tool widely used in the field of infectious diseases, mNGS has been proven to be a powerful molecular technique over the CMTs in the field of bone and joint

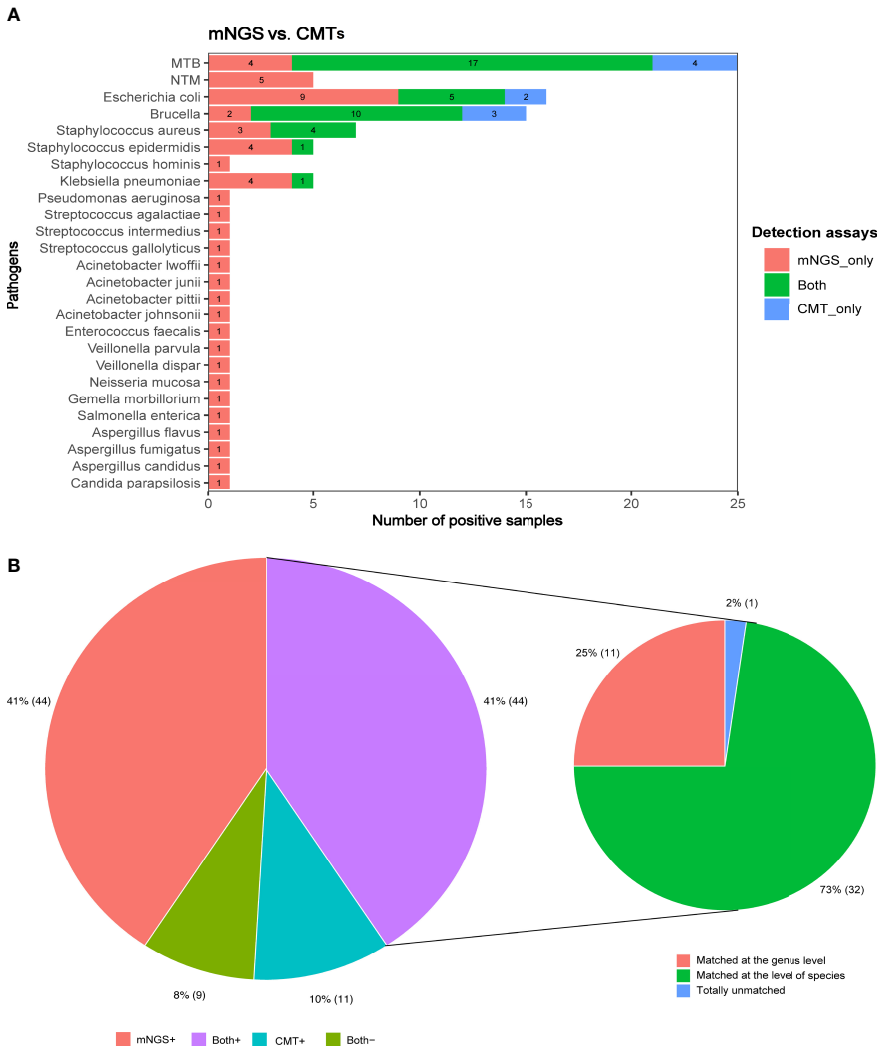

FIGURE 3
(A) The number of positive samples detected by CMTs and mNGS for each pathogen identified by the clinical golden standard. **(B)** The concordance between mNGS and CMTs in the detection of pathogens.

TABLE 2 Diagnostic performance of mNGS vs. CMTs in spinal infection.

Pathogens	Testing	Sensitivity (95% CI; n/N)	Specificity (95% CI; n/N)
All	mNGS	90.72% (0.827–0.954; 88/97)	81.82% (0.478–0.968; 9/11)
	CMTs	52.17% (0.416–0.626; 48/92)	56.25% (0.306–0.792; 9/16)
Bacteria	mNGS	90.30% (0.82–0.952; 84/93)	81.82% (0.478–0.968; 9/11)
	CMTs	53.40% (0.425–0.641; 47/88)	56.25% (0.306–0.792; 9/16)
Mycobacteria	mNGS	83.90% (0.655–0.939; 26/31)	90.00% (0.541–0.995; 9/10)
	CMTs	67.74% (0.485–0.826; 21/31)	90.00% (0.541–0.995; 9/10)
Fungi	mNGS	100.00% (0.396–1; 4/4)	100.00% (0.629–1; 9/9)
	CMTs	25.00% (0.013–0.78; 1/4)	100.00% (0.628–0.996; 9/9)

mNGS, metagenomic next-generation sequencing; CMTs, conventional microbiological tests.

10.3389/fcimb.2022.929701

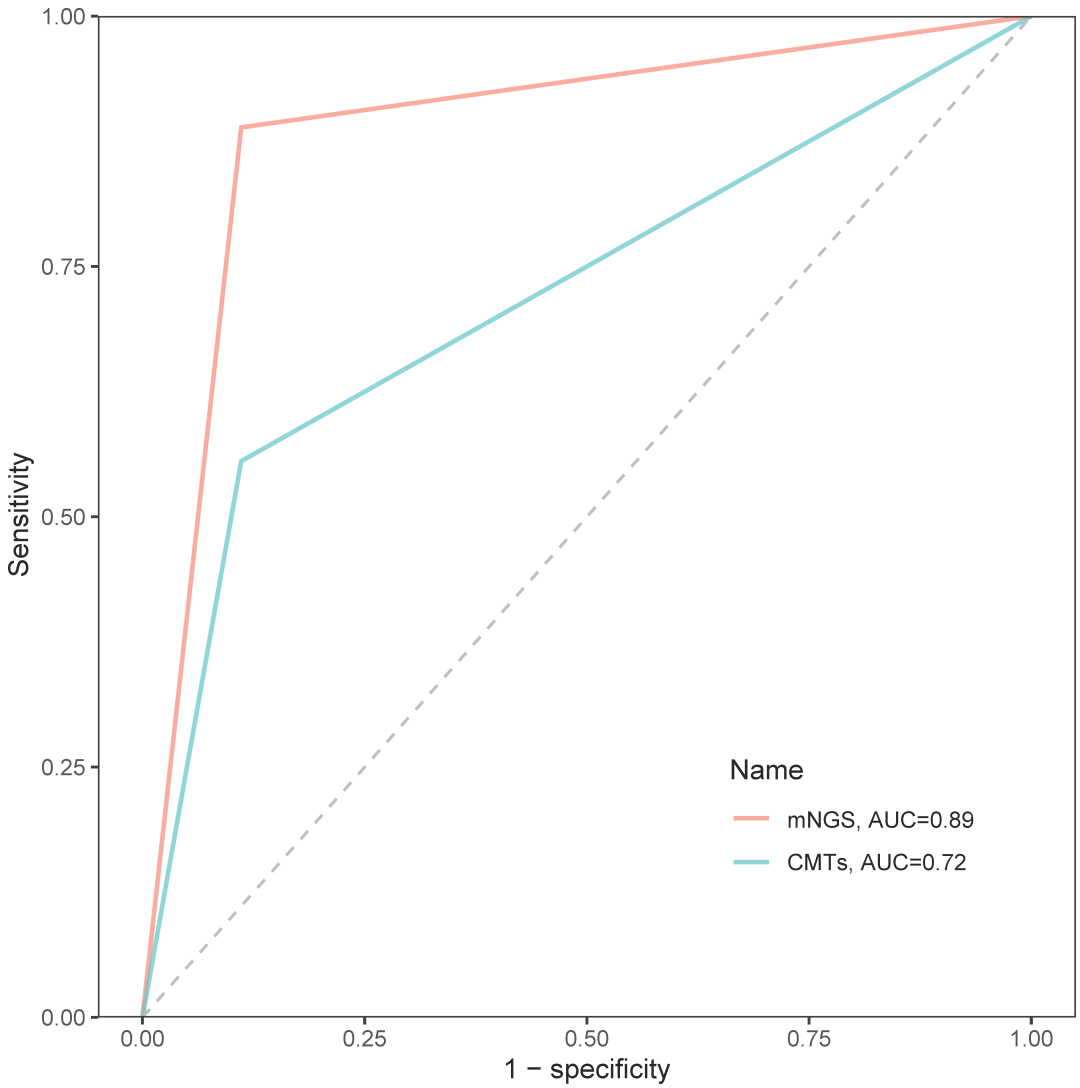

FIGURE 4
The receiver operator characteristic curves of mNGS and CMTs in the diagnosis of spinal infection.

TABLE 3 Inconsistent analysis between mNGS and CMTs in the bacterial subgroup.

Patient no.	mNGS	PCR for MTB	T-spot	Culture	X-pert	Clinical golden standard	Comments
4	–	NaN	–	–	+	MTB	MTB missed by mNGS
6	–	+	+	MTB	+	MTB	
11	*M. Aubagnense*	–	+	–	–	M. Aubagnense	T-spot unable to distinguish MTB and NTM
12	*M. luteum*	–	+	–	–	*M. luteum*	
34	*E. coli*	–	–	*E. faecalis*	–	*E. coli*	Culture contaminated
60	*E. coli*	–	–	*S. epidermidis*	–	*E. coli*	

mNGS, metagenomic next-generation sequencing; CMTs, conventional microbiological tests; PCR, polymerase chain reaction; MTB, mycobacterium tuberculosis; NTM, non-tuberculous mycobacteria.

TABLE 4 Analysis of inconsistent results between mNGS and CMTs in fungi subgroup.

Patient no.	mNGS	G/GM	Culture	Clinical golden standard	Comments
4	*Aspergillus flavus*	+	Aspergillus	*Aspergillus flavus*	CMTs and mNGS results matched at the genus level.
6	*Aspergillus fumigatus*	+		*Aspergillus fumigatus*	Possible fungal infection suggested by CMTs was verified by mNGS.
78	*Aspergillus luteus*	+		*Aspergillus luteus*	
51	*Candida parapsilosis*			*Candida parapsilosis*	Pathogens missed by CMTs were detected by mNGS.

mNGS, metagenomic next-generation sequencing; CMTs, conventional microbiological tests.

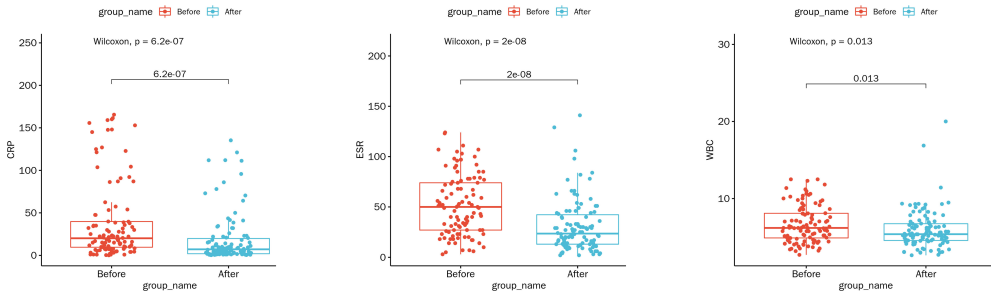

FIGURE 5
Comparison of laboratory indicators at the time of hospitalization and hospital discharge under the mNGS-guided treatment. Abbreviations: WBC, white blood cell count (10^9/L); ESR, erythrocyte sedimentation rate (mm/h); CRP, C-reactive protein (mg/L).

infections (Huang et al., 2020). However, research on the clinical value of mNGS technology in the field of spinal infection is still very rare. Recently, a study involving 30 cases of suspected spinal infection showed a higher sensitivity of mNGS but similar specificity than the culture method (Ma et al., 2022). Currently, there are various clinical tools for diagnosing spinal infection, far more than just culture, such as PCR, T-spot, and X-pert. Many of them have even been used conventionally for a long time. Therefore, in this study, we retrospectively analyzed the clinical data of 108 patients with suspected spinal infection to comprehensively explore the diagnostic value of mNGS technology. The results indicated a higher sensitivity and specificity, as well as a larger AUC of the mNGS than the CMTs in the overall identification of bacteria, mycobacteria, and fungi, suggesting a better diagnostic accuracy of mNGS in spinal infection. Moreover, the patients presented significantly decreased CRP, ESR, and WBC levels at hospital discharge, and most of them had good outcomes, further highlighting the potential value of the mNGS-guided antimicrobial therapy.

Nearly all known pathogens from clinical samples can be detected simultaneously using mNGS (Chiu and Miller, 2019; Gu et al., 2019; Gu et al., 2021). Our results further demonstrated the performance of mNGS in the detection of nearly all common pathogens that may cause spinal infection. In addition, novel pathogens including NTM (n = 5), fungi (n = 4), and bacteria (n = 15) were discovered by mNGS, suggesting a certain potential of mNGS in identifying novel pathogens associated with spinal infection. Gene Xpert, a rapid automated molecular test, is an efficient assay for the rapid diagnosis of spinal TB (Upadhyay et al., 2020; Karthek et al., 2021). A previous study showed that mNGS combined with Xpert had an overall superior advantage over conventional methods and significantly improved the etiological diagnosis of MTB (Zhou et al., 2019). In this study, however, Xpert was classified to the CMTs. Our results still showed comparable diagnostic abilities of mNGS with CMTs in the identification of MTB, including MTB identified in four cases using mNGS alone and that detected in four cases using CMTs alone. It has been acknowledged that mycobacteria require significant cell wall disruption to efficiently lyse the organisms for nucleic acid release (Simner et al., 2018). Therefore, it was speculated that the four cases of CMT-positive alone missed by mNGS might result from the low concentration of nucleic acid extraction. Two of the four cases were PCR-positive for MTB, suggesting that the minimum nucleic acid concentration required for a positive metagenomic test might be higher than that for a positive PCR test. In addition, mNGS was found to have huge advantages over the CMTs in the detection of NTM, which might be attributed to the inability of CMTs to distinguish between MTB and NTM. Generally, NTM is equally hard to culture successfully to MTB in clinical settings, and almost no specific immunological tests for NTM have been widely used yet; thus, accurate diagnosis of NTM becomes a big challenge. In our study, the NTM in five cases was identified by mNGS because of its

ability to identify pathogens at the level of species but all missed by the CMTs. Moreover, MTB and NTM were detected in only two cases through biopsy pathology but missed by both mNGS and CMTs, indicating that mNGS may have a breakthrough in the diagnosis of spinal infection caused by mycobacterium. It is recommended to combine mNGS and all the CMTs for routine detection if patients are highly suspected of mycobacterium infection.

A major strength of our study was that it preliminarily and comprehensively evaluated the diagnostic value of mNGS in patients with spinal infection caused by several dominant pathogens and the patients' outcomes under the mNGS-guided antimicrobial therapy. Although it was a retrospective study, the sample size was relatively larger compared with a previous study (Ma et al., 2022), leading to more reliability of our results. Nevertheless, there were several limitations that should be concerned. First, only four cases were ultimately diagnosed as fungal infection, leading to highly serendipitous diagnostic results. Second, a control group was not included for analysis of the outcomes; it only observed the difference before and after treatment in patients receiving mNGS-guided medication. In the future, more large-scale and well-designed studies should be performed to further explore the application value of mNGS technology in the field of spinal infection.

In conclusion, mNGS has a better diagnostic accuracy in pathogenic identification of patients with suspected spinal infection, and patients treated with NGS-guided antimicrobial therapy mostly seem to have good outcomes. In the future, more large-scale and well-designed studies should be performed to further validate our results.

Data availability statement

The data presented in the study are deposited in the NCBI GenBank repository (accession number 2627724).

Ethics statement

The studies involving human participants were reviewed and approved by The Institutional Review Board of Shandong Chest Hospital. Written informed consent to participate in this study was provided by the participants' legal guardian/next of kin.

Author contributions

LX contributed to study conception and study design and wrote the first draft of the manuscript. ZZ participated in writing "Materials and methods". YW and CS were responsible for data acquisition, analysis, and interpretation. HT contributed to editing and reviewing the manuscript. All authors approved the submitted version.

Acknowledgments

We thank Mrs. Furong Du, Mr. Xing Zhang, and Mr. Guanghua Lu (State Key Laboratory of Translational Medicine and Innovative Drug Development, Jiangsu Simcere Diagnostics Co., Ltd.) for their great contributions to the data collection, analysis, and interpretation of the manuscript.

Conflict of interest

Authors YW and CS is employed by Nanjing Simcere Medical Laboratory Science Co., Ltd and Jiangsu Simcere Diagnostics Co., Ltd.

The remaining authors declare that the research was conducted in the absence of any commercial or financial relationships that could be construed as a potential conflict of interest.

Publisher's note

References

Beronius, M., Bergman, B., and Andersson, R. (2001). Vertebral osteomyelitis in göteborg, Sweden: a retrospective study of patients during 1990-95. *Scand. J. Infect. Dis.* 33, 527–532. doi: 10.1080/00365540110026566

Besser, J., Carleton, H. A., Gerner-Smidt, P., Lindsey, R. L., and Trees, E. (2018). Next-generation sequencing technologies and their application to the study and control of bacterial infections. *Clin. Microbiol. Infect.* 24, 335–341. doi: 10.1016/j.cmi.2017.10.013

Chen, H., Yin, Y., Gao, H., Guo, Y., Dong, Z., Wang, X., et al. (2020). Clinical utility of in-house metagenomic next-generation sequencing for the diagnosis of lower respiratory tract infections and analysis of the host immune response. *Clin. Infect. Dis.* 71, S416–S426. doi: 10.1093/cid/ciaa1516

Chiu, C. Y., and Miller, S. A. (2019). Clinical metagenomics. *Nat. Rev. Genet.* 20, 341–355. doi: 10.1038/s41576-019-0113-7

Duarte, R. M., and Vaccaro, A. R. (2013). Spinal infection: state of the art and management algorithm. *Eur. Spine J.* 22, 2787–2799. doi: 10.1007/s00586-013-2850-1

Grammatico, L., Baron, S., Rusch, E., Lepage, B., Surer, N., Desenclos, J. C., et al. (2008). Epidemiology of vertebral osteomyelitis (VO) in France: analysis of

hospital-discharge data 2002-2003. *Epidemiol. Infect.* 136, 653–660. doi: 10.1017/S0950268807008850

Gu, W., Deng, X., Lee, M., Sucu, Y. D., Arevalo, S., Stryke, D., et al. (2021). Rapid pathogen detection by metagenomic next-generation sequencing of infected body fluids. *Nat. Med.* 27, 115–124. doi: 10.1038/s41591-020-1105-z

Gu, W., Miller, S., and Chiu, C. Y. (2019). Clinical metagenomic next-generation sequencing for pathogen detection. *Annu. Rev. Pathol.* 14, 319–338. doi: 10.1146/annurev-pathmechdis-012418-012751

Huang, Z. D., Zhang, Z. J., Yang, B., Li, W. B., Zhang, C. J., Fang, X. Y., et al. (2020). Pathogenic detection by metagenomic next-generation sequencing in osteoarticular infections. *Front. Cell Infect. Microbiol.* 10. doi: 10.3389/fcimb.2020.00471

Karthek, V., Bhilare, P., Hadgaonkar, S., Kothari, A., Shyam, A., Sancheti, P., et al. (2021). Gene Xpert/MTB RIF assay for spinal tuberculosis- sensitivity, specificity and clinical utility. *J. Clin. Orthop Trauma* 16, 233–238. doi: 10.1016/j.jcot.2021.02.006

Lener, S., Hartmann, S., Barbagallo, G. M. V., Certo, F., Thomé, C., and Tschugg, A. (2018). Management of spinal infection: a review of the literature. *Acta Neurochir (Wien)* 160, 487–496. doi: 10.1007/s00701-018-3467-2

Li, N., Cai, Q., Miao, Q., Song, Z., Fang, Y., and Hu, B. (2021). High-throughput metagenomics for identification of pathogens in the clinical settings. *Small Methods* 5, 2000792. doi: 10.1002/smtd.202000792

Li, H., and Durbin, R. (2009). Fast and accurate short read alignment with burrows-wheeler transform. *Bioinformatics* 25, 1754–1760. doi: 10.1093/bioinformatics/btp324

Ma, C., Wu, H., Chen, G., Liang, C., Wu, L., and Xiao, Y. (2022). The potential of metagenomic next-generation sequencing in diagnosis of spinal infection: a retrospective study. *Eur. Spine J.* 31, 442–447. doi: 10.1007/s00586-021-07026-5

Miller, S., Naccache, S. N., Samayoa, E., Messacar, K., Arevalo, S., Federman, S., et al. (2019). Laboratory validation of a clinical metagenomic sequencing assay for pathogen detection in cerebrospinal fluid. *Genome Res.* 29, 831–842. doi: 10.1101/gr.238170.118

Parize, P., Muth, E., Richaud, C., Gratigny, M., Pilmis, B., Lamamy, A., et al. (2017). Untargeted next-generation sequencing-based first-line diagnosis of infection in immunocompromised adults: a multicentre, blinded, prospective study. *Clin. Microbiol. Infect.* 23, 574.e1–574.e6. doi: 10.1016/j.cmi.2017.02.006

Qian, Y. Y., Wang, H. Y., Zhou, Y., Zhang, H. C., Zhu, Y. M., Zhou, X., et al. (2021). Improving pulmonary infection diagnosis with metagenomic next generation sequencing. *Front. Cell Infect. Microbiol.* 10. doi: 10.3389/fcimb.2020.567615

Simner, P. J., Miller, S., and Carroll, K. C. (2018). Understanding the promises and hurdles of metagenomic next-generation sequencing as a diagnostic tool for infectious diseases. *Clin. Infect. Dis.* 66, 778–788. doi: 10.1093/cid/cix881

Upadhyay, M., Patel, J., Kundnani, V., Ruparel, S., and Patel, A. (2020). Drug sensitivity patterns in xpert-positive spinal tuberculosis: an observational study of 252 patients. *Eur. Spine J.* 29, 1476–1482. doi: 10.1007/s00586-020-06305-x

Wilson, M. R., Naccache, S. N., Samayoa, E., Biagtan, M., Bashir, H., Yu, G., et al. (2014). Actionable diagnosis of neuroleptospirosis by next-generation sequencing. *N Engl. J. Med.* 370, 2408–2417. doi: 10.1056/NEJMoa1401268

Wilson, M. R., O'Donovan, B. D., Gelfand, J. M., Sample, H. A., Chow, F. C., Betjemann, J. P., et al. (2018). Chronic meningitis investigated *via* metagenomic next-generation sequencing. *JAMA Neurol.* 75, 947–955. doi: 10.1001/jamaneurol.2018.0463

Zaharia, M., Bolosky, W. J., Curtis, K., Fox, A., Patterson, D., Shenker, S., et al. (2011) *Faster and more accurate sequence alignment with SNAP.* Available at: https://ui.adsabs.harvard.edu/abs/2011arXiv1111.5572Z (Accessed 8 July 2022).

Zhang, N., Zeng, X., He, L. C., Liu, Z. L., Liu, J. M., Zhang, Z. H., et al. (2019). Present research situation of the MRI manifastations of spinal infection and its imitations. *Chin. J. Magn. Reson. Imaging* 10, 223–227. doi: 10.12015/issn.1674-8034.2019.03.013

Zhou, X., Wu, H., Ruan, Q., Jiang, N., Chen, X., Shen, Y., et al. (2019). Clinical evaluation of diagnosis efficacy of active mycobacterium tuberculosis complex infection *via* metagenomic next-generation sequencing of direct clinical samples. *Front. Cell Infect. Microbiol.* 9. doi: 10.3389/fcimb.2019.00351

frontiers | Frontiers in Cellular and Infection Microbiology

TYPE Original Research
PUBLISHED 27 October 2022
DOI 10.3389/fcimb.2022.967584

OPEN ACCESS

EDITED BY
Pushpanathan Muthuirulan,
Harvard University, United States

REVIEWED BY
Kapil Saharia,
University of Maryland, United States
Hua Gao,
Peking University People's Hospital, China

*CORRESPONDENCE
Xiaohua Chen
chenxiaohua2000@163.com
Xiaofeng Lian
xf909@126.com

†These authors have contributed equally to this work and share the first authorship

SPECIALTY SECTION
This article was submitted to Clinical Microbiology, a section of the journal Frontiers in Cellular and Infection Microbiology

RECEIVED 13 June 2022
ACCEPTED 03 October 2022
PUBLISHED 27 October 2022

CITATION
Zhang Y, Chen J, Yi X, Chen Z, Yao T, Tang Z, Zang G, Cao X, Lian X and Chen X (2022) Evaluation of the metagenomic next-generation sequencing performance in pathogenic detection in patients with spinal infection.
Front. Cell. Infect. Microbiol. 12:967584.
doi: 10.3389/fcimb.2022.967584

Evaluation of the metagenomic next-generation sequencing performance in pathogenic detection in patients with spinal infection

Yi Zhang[1†], Jinmei Chen[1†], Xiaoli Yi[2†], Zhiheng Chen[3], Ting Yao[1], Zhenghao Tang[1], Guoqing Zang[1], Xuejie Cao[2], Xiaofeng Lian[3*] and Xiaohua Chen[1*]

[1]Department of Infectious Diseases, Shanghai Jiao Tong University Affiliated Sixth People's Hospital, Shanghai, China, [2]Genoxor Medical Science and Technology Inc., Shanghai, China, [3]Department of Orthopedics, Shanghai Jiao Tong University Affiliated Sixth People's Hospital, Shanghai, China

Spinal infection is a rarely occurred pathology, whose diagnosis remains a major challenge due to the low sensitivity of culturing techniques. Metagenomic next-generation sequencing (mNGS) is a novel approach to identify the pathogenic organisms in infectious diseases. In this study, mNGS technology was adopted for pathogenic detection in spinal infection from the tissue and pus samples. Additionally, the diagnostic performance of mNGS for spinal infection was evaluated, by comparing it with that of the conventional microbial culture, with the histopathological results as the gold standard. Overall, 56 samples from 38 patients were enrolled for mNGS testing, and 69 samples were included for microbial culture. 30 patients (78.95%) were identified to be positive by the mNGS method, which was higher than that of microbial culture (17, 44.74%). The sensitivity and specificity of mNGS with pus samples were 84.2% and 100.0%, respectively, which outperformed those of microbial culture (42.1% and 100.0%). The pathogen identification results were applied to medication guidance, and all 38 patients experienced favorable outcomes at three months, followed-up post-treatment, without any adverse effects. These findings proved that mNGS was superior to microbial culture in pathogenic identification of the spinal infection, thereby showing great promise in guiding drug administration and improving clinical outcomes.

KEYWORDS

spinal infection, microbial culture, pathogenic detection, diagnosis, metagenomic next-generation sequencing (mNGS)

Introduction

Infections occurring in the vertebral bodies, intervertebral discs, and surrounding soft tissues are all classified as spinal infections (Lener et al., 2018). Pathogens can be directly inoculated during spinal surgery or contiguously spread by adjacent site infection (Tsantes et al., 2020). Spinal infection symptoms are generally nonspecific and range from back pain to fever, spinal deformation, instability, and even death (Cornett et al., 2016; Nagashima et al., 2018), which hampers the diagnosis of spinal infection. In the early stage of diagnosis, magnetic resonance imaging (MRI) is usually applied to exclude other non-infectious spinal diseases (Fucs et al., 2012). Generally, microbial culture is the primary method to distinguish the microorganisms in bone and joint infections; however, the positive rate is only around 40% to 70% due to antibiotic treatment, fastidious microorganisms, and biofilm formation (Huang et al., 2020).

Molecular-level analysis technologies, such as polymerase chain reaction (PCR), have also been employed in the etiological diagnosis of spinal infection (Merino et al., 2012). However, it requires empirical speculation of potential pathogens by clinical symptoms, which limits the detection scope, especially for rare pathogens and complex infections. Metagenomic next-generation sequencing (mNGS), as a culture-independent and unbiased analysis method, has attracted wide attention. Most studies have demonstrated that mNGS has a similar sensitivity to specific PCR assays (Miller and Chiu, 2021). Moreover, mNGS has been proven capable of identifying more potential pathogens than conventional methods, especially for rare, indistinguishable, and complex pathogens (Han et al., 2019).

The usability of mNGS for diagnosing osteoarticular infection has been evaluated by comparing it with other standard methods. As reported, mNGS improved the diagnosis of osteoarticular infection from abscess specimens, with a greater pathogen detection rate than conventional culture-based methods (Zhao et al., 2020). In the prosthetic joint infection, a higher positive rate has been observed by mNGS than microbial culture, with even higher sensitivity and specificity when the culture results were negative (Thoendel et al., 2018). In addition, mNGS has been proven to be more sensitive than broad-range PCR for detecting prosthetic joint infection in joint fluid and be capable of identifying more pathogens in polymicrobial and fungal infections (Wang et al., 2020). In spinal-related infection, disseminated tuberculosis has been successfully diagnosed using mNGS from the resected sample from spinal surgery (Ye et al., 2021).

Moreover, the potential of mNGS in the etiological diagnosis of spinal infection has been revealed, achieving a sensitivity and specificity of 70.3% and 75.0%, respectively (Ma et al., 2022). Therefore, this study was conducted to evaluate the diagnostic performance of mNGS in pathogenic detection involved in spinal infection, by comparing it with that of the traditional microbial culture. Furthermore, the potential clinical benefits of mNGS in medication guidance and improving clinical outcomes were also analyzed, as well as the choice of optimal sample types for mNGS testing.

Materials and methods

Patient enrollment, clinical assessment, and sample collection

From January 1st to December 31st, 2021, a cohort of patients with spinal infection was admitted to the Department of Infectious Diseases in Shanghai Jiao Tong University Affiliated Sixth People's Hospital. Spinal infection is an infectious disease affecting the vertebral body, the intervertebral disc, and the adjacent paraspinal tissue. All subjects with a suspected spinal infection underwent surgical treatment. The collected tissue and pus samples were histopathologically examined and sent for the mNGS and microbial culture for etiological examination. Only those finally diagnosed with spinal infection were enrolled and analyzed in this manuscript. Suspicion of spinal infection was based on the patients' complaints, clinical symptoms, laboratory examinations, and imaging findings, including MRI and computed tomography (CT). Diagnosis of spinal infection was based on the above results, combined with histopathological analysis of infected tissues. The most common complaints of patients with spinal infection are back or neck pain, depending on the location of the infection (Tsantes et al., 2020). Laboratory examinations include white blood cell (WBC) count and concentrations of inflammatory factors such as erythrocyte sedimentation rate (ESR) and C-reactive protein (CRP). MRI remains the most reliable method to diagnose spinal infection, and CT is devoted to precisely detecting bony changes and bone necrosis.

In case of doubt, surgical treatment should be considered. All patients in the present study underwent surgical intervention, percutaneous transforaminal endoscopic debridement and drainage (Chen et al., 2022). The generated tissue and pus samples were collected during surgery, and then pathological examinations were conducted with the infected tissues. At the same time, their samples were sent for pathogenic identification within two hours to identify the causative infectious organisms. Finally, 38 patients were diagnosed with spinal infection and had not received any antimicrobial therapy before sample collection. Clinical and demographic data of these patients were collected from the electronic patient dossiers of Shanghai Sixth People's Hospital.

Tissue and pus samples were analyzed with the mNGS technology, completed by a third company (Genoxor Medical Technology, Shanghai, China). Among the 38 subjects, single samples of tissue or pus were collected in 20 patients, and double samples, including tissue and pus, were obtained in 18 patients (Supplementary Table 1). Therefore, 56 samples from the 38

patients were tested for pathogenic identification by mNGS. Meanwhile, 32 blood and 37 pus samples from 38 patients (Supplementary Table 1) were applied to the clinical microbial culture in our hospital.

Sequencing and data analysis

In the mNGS analysis, DNA was extracted directly from tissue and (or) pus using the TIANamp Maxi DNA Kit (DP710, Tiangen Biotech, Beijing, China), following the manufacturer's standard protocols. The extracted DNA was fragmented ultrasonically to yield 200-300bp fragments. DNA libraries were constructed through an end-repaired adapter and amplified through PCR. Agilent 2100 system (Agilent Technologies, Santa Clara, USA) was used for quality control of the DNA libraries, which were sequenced on the Illumina NextSeq platform (Genoxor Medical Technology, Shanghai, China). All sequencing data were deposited in the database under the Sequence Read Archive (SRA) accession number PRJNA827921.

High-quality sequencing data were generated after filtering out low-quality, low-complexity, and shorter reads (<35 bp) by bcl2fastq2. To eliminate the effect of the human sequences, the data mapped to the human reference genome were excluded using a powerful alignment tool called Bowtie2. The remaining data were aligned to the Microbial Genome Databases, including viruses, bacteria, fungi, and parasites. The databases were downloaded from NCBI (ftp://ftp.ncbi.nlm.nih.gov/genomes/). It contains 13434 whole-genome sequences of viral taxa, 7982 bacterial genomes or scaffolds, 917 fungi related to human infection, 4411 viruses related to human infection, and 124 parasites associated with human diseases.

Interpretation of metagenomic data

The number of unique alignment reads was calculated and standardized to get the number of reads stringently mapped to pathogen species, standardized strictly mapped reads number (SDSMRN). In the report interpretation process, it needs to filter the blacklist and the negative control and analyze the specificity of the sequencing sequence. The blacklist is an in-house database. For different types of microbes, the thresholds were set as follows: Bacterial/Fungus: SDSMRN≥3, species was reported; Parasite: SDSMRN≥50; *Mycobacterium tuberculosis* complex (MTC)/ Brucella/Nocardia: SDSMRNG≥1, species were reported.

Statistical analyses

Histopathological results were accurate indications of infection or lack thereof and were regarded as the gold standard. Following the extracted data, 2×2 contingency tables were derived to determine sensitivity, specificity, positive predictive value (PPV), and negative predictive value (NPV). Sensitivity and specificity were calculated based on the formulas TP (true positive)/(TP+FN) (false negative) and TN (true negative)/(TN+FP) (false positive), respectively. PPV is expressed by the TP/(TP+FP) ratio, while NPV from the TN/(TN+FN). McNemar's test was used to compare the sensitivity, specificity, PPV, and NPV. Comparison between two groups was analyzed using Fisher's exact test, and a $P<0.05$ was defined as statistical significance. All statistical analyses were performed using SPSS 20.0 (IBM, Chicago, USA).

Results

Demographic characteristics and mNGS sequencing information

A total of 38 patients diagnosed with spinal infection were enrolled between January 1st, 2021 and December 31st, 2021, including 29 males and 9 females. The mean age was 57.4 ± 12.9 (ranges 23-71) years old. Patients with spinal infections commonly present with unspecific symptoms, such as back pain, fever, paresis, and contingent neurological deficits, which hinder early diagnosis. The laboratory test results are listed in Table 1. All the infectious patients underwent percutaneous transforaminal endoscopic debridement and drainage, and the histopathological analysis images were demonstrated in Supplementary Figure 1. The most common pathologic characteristics are bone necrosis, neutrophil infiltration, caseous necrosis, and tubercles. The culture result for mycobacteria was presented in Supplementary Figure 2. The information on the types of spinal infections was provided in Table 1, with one or more types in each patient. Vertebral osteomyelitis occurs in most cases, frequently combined with discitis, paravertebral infection, and epidural abscess. Statistically, Vertebral osteomyelitis was found in 35 (92.11%) cases, discitis in 20 (52.63%) cases, paravertebral infection in 11 (28.95%) cases, and epidural abscess in 2 (5.26%) cases. At the last follow-up (three months after surgery), all 38 patients recovered from the spinal infection.

Pathogenic microorganisms identified by mNGS

A single tissue sample was collected in 16 patients, and single pus was collected in 4 patients. 18 patients performed a double-sample examination, including tissue and pus samples. To summarize, 34 tissue and 22 pus samples, a total of 56 samples from the 38 participants, were analyzed by mNGS. Following the optimized procedures, we conducted the mNGS analysis on the 56 samples, and a total of 19,735,816 raw reads were generated from sequencing, ranging from 3,014,099 to 51,271,214 reads per specimen. Of the 38 patients, there were 30 patients (78.95%)

TABLE 1 Demographic characteristic of the patients with spinal infection.

Characteristics		
Total number	Cases	38
Age,	Years, mean (range)	57.4 ± 12.9 (23-71)
Sex	Male (%)	29 (76.32)
	Female (%)	9 (23.68)
Laboratory tests	Hemoglobin (g/L)	121.6 ± 17.7
	WBC ($\times10^9$/L)	7.05 ± 4.32
	ESR (mm/h)	67.24 ± 34.34
	CRP (mg/L)	38.99 ± 62.16
Types of procedures	Percutaneous transforaminal endoscopic debridement and drainage (n, %)	38 (100%)
Types of spinal infection	Vertebral osteomyelitis (n, %)	35 (92.11%)
	Discitis (n, %)	20 (52.63%)
	Paravertebral infection (n, %)	11 (28.95%)
	Epidural abscess (n, %)	2 (5.26%)
Follow-up time	Months after treatment	3
Outcomes	Recovery (n, %)	38 (100%)

WBC, white blood cell; ESR, erythrocyte sedimentation; CRP, C-reactive protein.

with positive mNGS results (Table 2), a single microorganism was detected in 24 (80%) patients, and multiple pathogens were found in 6 (20%) patients (Figure 1A). In the 56 samples, 43 (76.79%) were proven to be mNGS positive, including 26 tissue (60.47%) and 17 pus (39.53%) samples (Figure 1B).Pathogenic microorganism analyses revealed that 26 kinds of pathogenic microorganisms were identified by mNGS, among which 25 were classified into species. Still, *Brucella* in three samples was identified just at the genus level. 21 bacterial pathogens, one mycoplasma, and three viruses were recognized at the species level. *Human beta-herpesvirus 5*, *human herpesvirus 1*, and *human gammaherpesvirus 4* were separately identified in three samples. Statistically, 14 gram-positive and 7 gram-negative bacterial species were detected, adding *Brucella* as gram-negative. In the 34 tissue samples, the most frequent species detected through mNGS were *M. tuberculosis complex* (17.65%) and *S. aureus* (17.65%), followed by the *M. hominis* (5.88%) and *Brucella* (5.88%) (Figure 2A). Similarly, *S. aureus* (27.27%) was the top microorganism found in the 22 pus samples, and the second top was the *M. tuberculosis complex* (22.73%) (Figure 2B).

Comparison of mNGS versus microbial culture in pathogenic detection

In the present work, the microbial culture was the most used method for pathogenic identification in infectious diseases. Therefore, to evaluate the diagnostic performance of mNGS in spinal infection, the results of mNGS were compared to those of microbial culture. Among 38 patients, 32 blood and 37 pus samples were sent for microbial culture, once a positive result was yielded in either type of the sample, the patient would be judged as a positive result by microbial culture. However, culture-positive results were only found in 17 cases, with a positive rate of 44.74%. The most common microorganism identified by microbial culture was also the *S. aureus* (15.79%), followed by the *acid-fast bacillus* (10.53%) (Figure 3A).

When comparing results of mNGS with microbial culture, we compared the tissue and pus samples (for mNGS) with blood and pus samples (for microbial culture), and a significant difference was found between the positive rate by mNGS (78.95%) and by microbial culture (44.74%) (P=0.0042) (Table 2). In the 21 patients with pus samples for both mNGS and microbial culture, we evaluated the diagnostic performance of these two methods. As shown in Table 3, the sensitivity and specificity of mNGS were 84.2% and 100.0%, respectively, and these values of culture were 42.1% and 100.0%, separately.

Figure 3B indicated that the results of mNGS and microbial culture were both positive in 14 of 38 (36.84%) patients and both negative in 5 (13.16%) patients. 16 (42.11%) patients were determined to be single-positive by mNGS, and 3 (7.89%) were single-positive by microbial culture (Figure 3B). The information of the 14 double-positive cases was analyzed and presented in Figure 3C. Table 4 showed the detailed pathogenic

TABLE 2 Comparison of the positive rate of mNGS (with tissue and pus samples) and microbial culture (with blood and pus samples).

Methods	Cases	Positive cases	Negative cases	Positive rate	P value
mNGS	38	30	8	78.95%	
Microbial culture	38	17	21	44.74%	0.0042

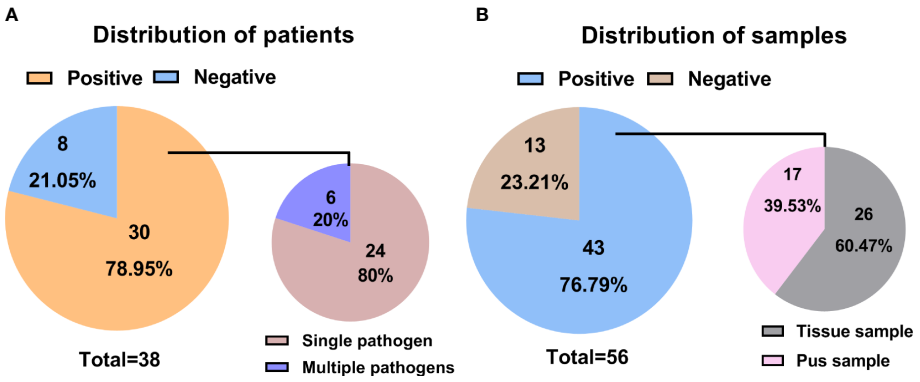

FIGURE 1
Statistical data on mNGS information in different patients and samples. **(A)** Distributions of positive and negative results in patients with spinal infection; **(B)** Distributions of positive and negative results in samples associated with a spinal infection.

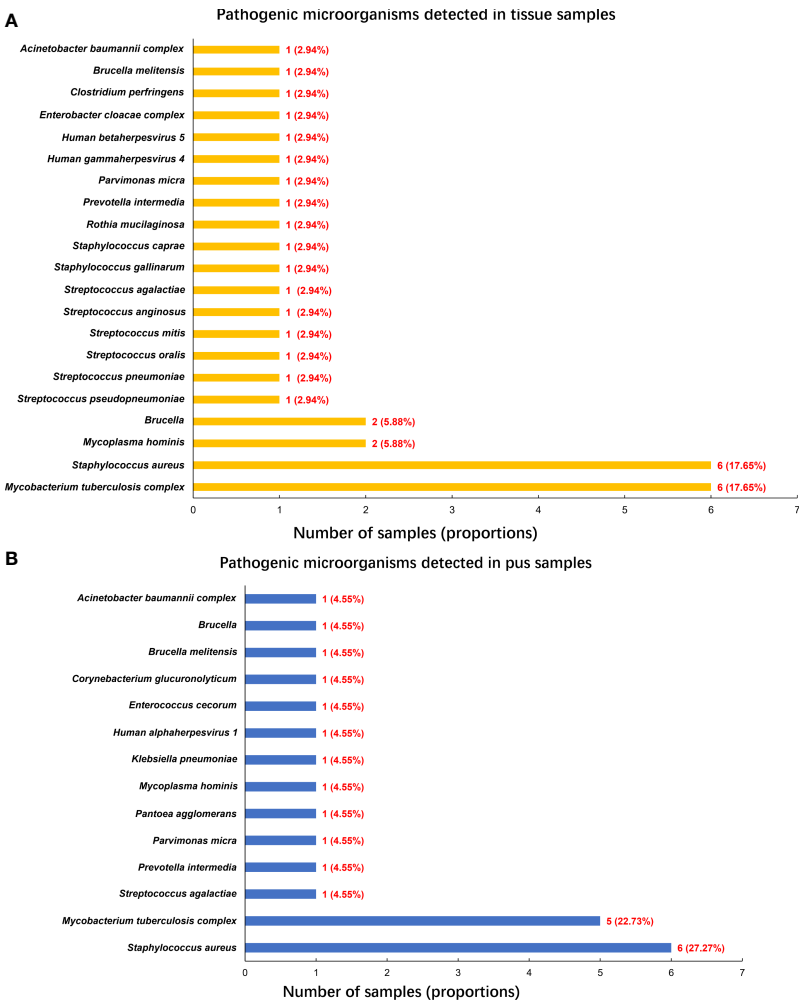

FIGURE 2
Pathogenic microorganisms detected by mNGS. **(A)** Pathogenic microorganisms detected in tissue samples; **(B)** Pathogenic microorganisms detected in pus samples.

10.3389/fcimb.2022.967584

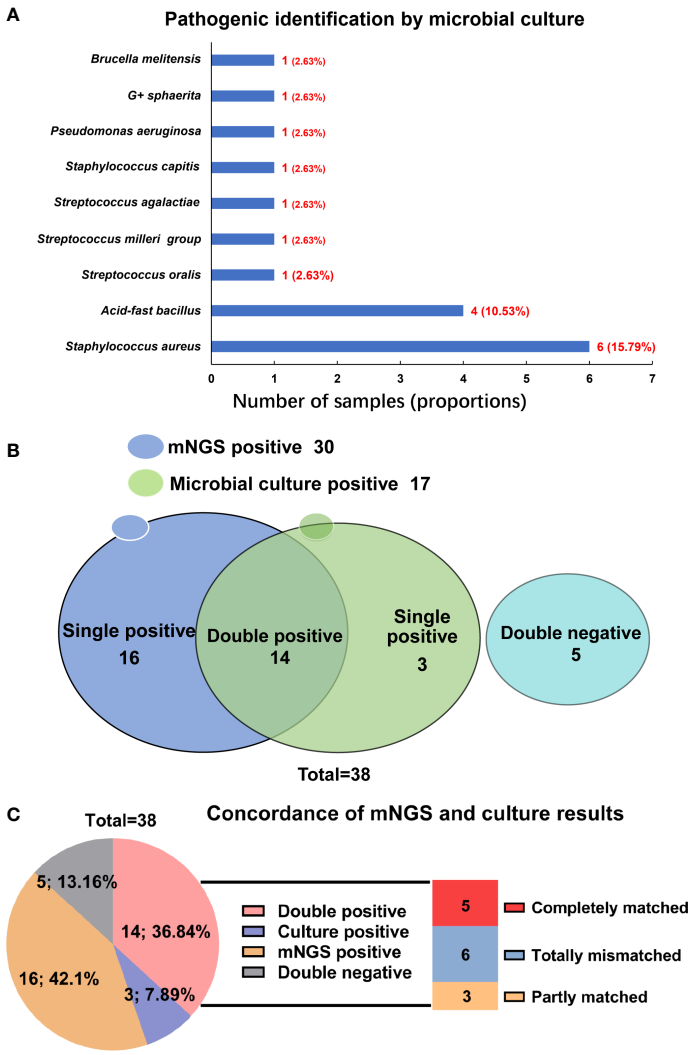

FIGURE 3
Comparison of mNGS and microbial culture in pathogenic identification in spinal infection. **(A)** Pathogenic microorganisms identified by microbial culture; **(B)** The detecting results of mNGS and microbial culture in different cases; **(C)** The concordance of mNGS and microbial culture in detecting pathogenic microorganisms.

TABLE 3 Comparison of diagnosis performance of mNGS and microbial culture in patients who had pus samples for both methods.

Methods	Cases	Sensitivity	Specificity	PPV	NPV
mNGS	21	84.2%	100.0%	100.0%	40%
Microbial culture	21	42.1%	100.0%	100.0%	15.38%

PPV, Positive predictive value; NPV, Negative predictive value.

microorganisms detected by the two methods and their causative agents. In detail, 5 cases were completely matched (patients 1-5), while 6 cases were totally mismatched (patients 6-11). The remaining three patients (patients 12-14) were found to be "partly matched" defined as at least one overlap of pathogens when polymicrobial results were observed (Figure 3C).

mNGS-guided antimicrobial therapy and clinical outcomes

According to the results of pathogenic identification, 33 patients were classified as infected, and 5 patients were considered aseptic. The pathogen identification results were applied to medication guidance.

TABLE 4 Matching of pathogenic microorganisms detected by mNGS and microbial culture.

Patients	mNGS	Microbial culture	Causative agent
Patient 1	*S. aureus*	*S. aureus*	*S. aureus*
Patient 2	*S. aureus*	*S. aureus*	*S. aureus*
Patient 3	*B. melitensis*	*B. melitensis*	*B. melitensis*
Patient 4	*S. aureus*	*S. aureus*	*S. aureus*
Patient 5	*S. agalactiae*	*S. agalactiae*	*S. agalactiae*
Patient 6	*M. tuberculosis complex*, *R. mucilaginosa*	*Acid-fast bacillus*	*M. tuberculosis*
Patient 7	*M. tuberculosis complex*	*Acid-fast bacillus*	*M. tuberculosis*
Patient 8	*S. caprae*	S. capitis	*S. caprae*, S. capitis
Patient 9	*M. tuberculosis complex*	*Acid-fast bacillus*	*M. tuberculosis*
Patient 10	*M. tuberculosis complex*	*Acid-fast bacillus*	*M. tuberculosis*
Patient 11	*S. mitis*, *S. oralis*, *S. pneumoniae*, *S. pseudopneumoniae*	*S. milleri group*	*Streptococcus*
Patient 12	*S. aureus*, *S. anginosus*	*S. aureus*	*S. aureus*
Patient 13	*S. aureus*, *H. betaherpesvirus 5*	*S. aureus*	*S. aureus*
Patient 14	*S. aureus*, *K. pneumoniae*, *E. cecorum*, *P. agglomerans*, *H. alphaherpesvirus 1*	*S. aureus*	*S. aureus*

The target pathogens were confirmed accordingly for patients with double-positive results by mNGS and culture (14 patients), and the corresponding antibiotics were administrated. Otherwise, in patients with single positive results by mNGS (16 patients) or microbial culture (3 patients), a suspected pathogenic microorganism was proposed according to the comprehensive consideration based on clinical symptoms, and empiric antibiotic therapy was applied. If the outcome were desirable after drug use, the suspected pathogen would be confirmed to be the causative microorganisms. Three months later, all 38 patients were followed-up, and they experienced favorable outcomes, and no adverse effect was noted, proving the success of the mNGS-guided antimicrobial therapy.

Evaluation of the optimal sample types for mNGS pathogenic detection

To find out the optimal sample types for mNGS pathogenic detection, we compared the diagnosis efficiency of tissue and pus samples. Table 5 showcased that 26 were found to be positive in 34 tissues, and the positive rate was 76.47%. In the 26 positive samples, the causative agent pathogen was identified in 25 tissues; hence the accordance rate was 96.15% (25/26). Further, the positive rate in the 22 pus samples was 77.27%, and the accordance rate was 100%. There was no significance in the positive rate and accordance rate between the two types of samples (P>0.05). Overall, no significant superiority was noted between tissue and pus as the pathogenic detection sample by mNGS.

Discussion

At present, mNGS provides the potential for fast pathogen identification without a prior target hypothesis. In the present study, we described the utility of mNGS in detecting the pathogenic organisms associated with spinal infection. A broad spectrum of pathogens in 25 species was seen, ranging from bacteria, viruses, to *M. hominis*. Meanwhile, the diagnostic performance of mNGS in spinal infection was compared with the traditional microbial culture pairwisely. It can be concluded that mNGS is superior to microbial culture, thereby emerging as a promising technique in the etiological examination of spinal infection.

Notably, *S. aureus* was our study's most frequent bacterial pathogen identified by mNGS in 6 tissues and 6 pus samples. As a common pathogenic bacterium for spinal infection, *S. aureus* can cause a range of diseases, which has been reported to reduce antibiotic and immune cell penetration, leading to persistent and refractory infection (Gurtman et al., 2019; Gordon et al., 2020). Additionally, *M. tuberculosis* was our cohort's second most frequent microorganism, which has been considered the world's leading infectious killer (Chin, 2019). Spinal tuberculosis accounts for approximately 1% to 3% of all tuberculosis cases and 50% of musculoskeletal infections (Wang et al., 2021). It is worth noting that the opportunistic pathogen *M. hominis*, which causes the potential infection in the human genitourinary tract (Saadat et al., 2020), has not been reported in spinal infection. Fortunately, with the extensive use of mNGS technology, the rapid diagnosis and effective treatment of spinal infection caused by these microorganisms will be achieved soon.

By assessing the positive rate, species diversity, sensitivity and specificity, and its benefit to antimicrobial therapy, our data fully demonstrated that mNGS performed better than microbial culture in several aspects. Primarily, mNGS provided a higher pathogen detection ratio than standard culture-based testing, with a sensitivity of 84.2% in the pus samples. Another recent

TABLE 5 Comparison of the diagnosis efficiency of tissue and pus samples by mNGS.

Sample types	Total number	Positive rate	Accordance rate
Tissue	34	76.47% (26, 8)	96.15% (25, 1)
Pus	22	77.27% (17, 5)	100% (17, 0)
P value		>0.05	>0.05

study has revealed 70.3% of sensitivity by mNGS in spinal infection tissue samples (Ma et al., 2022), which has been reported to range from 36% to 100% in diverse samples or under special status (Miao et al., 2018). Furthermore, our study proved that mNGS allowed a broader range of pathogen detection, and the underestimated polymicrobial infection might significantly benefit from it. Except for *M. tuberculosis*, its superior feasibility in identifying *Brucella* spp. has been demonstrated in the present study. In previous research, mNGS has been confirmed with a favorable effect in detecting *Brucella* spp. (Mongkolrattanothai et al., 2017). Given the high pathogenicity of these microorganisms, mNGS may contribute a lot in providing reference to clinical diagnosis. Nevertheless, the relatively high cost of mNGS is the main shortcoming that limits its sample size and hinders its wide use in clinical, a challenge that urgently needs to be addressed in the future.

Many may recognize the advantages of mNGS of shortened turnaround time (Gu et al., 2021). In addition, diverse clinical sample types allowed by mNGS are also essential for effective treatment. The analyses of the samples associated with spinal infection are more complicated than those from common lesion sites because of the thick pyogenic fluid specimens and fat-rich tissues (Di Martino et al., 2019). After analyses of the pathogens detected in tissue and pus samples by mNGS, no significant superiority was noted between them. The relatively small sample sizes could explain it, or the tissue and pus samples are all suitable candidates for mNGS testing in pathogen identification in spinal infection.

In summary, mNGS is certified to identify a broad spectrum of pathogenic microorganisms in patients with spinal infection. It performs better than the conventional microbial culture method in detection ratio, allowing for the identification of rare and vital pathogens and diverse samples. These findings highlight the critical role of mNGS in guiding drug administration and improving clinical outcomes for patients with a spinal infection. Moreover, the wide use of mNGS in pathogen detection can be expected soon.

Data availability statement

The datasets presented in this study can be found in online repositories. The names of the repository/repositories and accession number(s) can be found in the article/Supplementary Material.

Ethics statement

The studies involving human participants were reviewed and approved by the Ethics Committee of the Shanghai Jiao Tong University Affiliated Sixth People's Hospital (No. 2017-127). The patients/participants provided their written informed consent to participate in this study.

Author contributions

XL and XhC conceived of and designed the study, and provided data acquisition. YZ and JC collected the clinical data, analyzed and interpreted the data, and drafted the manuscript. XY contributed to the data analysis and interpretation, and the manuscript writing. ZC performed the study design, data collection, and manuscript drafting. TY and ZT contributed to the development of methodology and manuscript review and revision. GZ is a major contributor to data analyses and manuscript revision. XjC provided mNGS data acquisition and manuscript writing. All authors read and approved the final manuscript.

Funding

This work was supported by grants from the National Natural Science Foundation of China (No. 82070615).

Conflict of interest

XY and XjC are employed by the Genoxor Medical Science and Technology Inc.

The remaining authors declare that the research was conducted in the absence of any commercial or financial relationships that could be construed as a potential conflict of interest.

Publisher's note

All claims expressed in this article are solely those of the authors and do not necessarily represent those of their affiliated organizations, or those of the publisher, the editors and the reviewers. Any product that may be evaluated in this article, or

claim that may be made by its manufacturer, is not guaranteed or endorsed by the publisher.

Supplementary material

The Supplementary Material for this article can be found online at: https://www.frontiersin.org/articles/10.3389/fcimb.2022.967584/full#supplementary-material

SUPPLEMENTARY FIGURE 1
Images show the histopathological examination of spinal infection. **(A)** The blue circle indicates the tubercles, and the yellow arrows indicate the Langhans multinucleated giant cells; **(B)** The red circles indicate caseous necrosis; **(C)** The blue circles indicate the granulomatous tubercles; **(D)** The red circle indicates caseous necrosis, and the yellow arrows indicate the Langhans multinucleated giant cells.

SUPPLEMENTARY FIGURE 2
Image indicates the culture results for mycobacteria.

References

Chen, Z. H., Wang, X., Zhang, Y., Wu, S. T., Wu, Y. H., Shi, Q., et al. (2022). Percutaneous transforaminal endoscopic debridement and drainage with accurate pathogen detection for infectious spondylitis of the thoracolumbar and lumbar spine. *World Neurosurg.* 164, e1179–e1189. doi: 10.1016/j.wneu.2022.05.123

Chin, J. H. (2019). Neurotuberculosis: A clinical review. *Semin. Neurol.* 39, 456–461. doi: 10.1055/s-0039-1687840

Cornett, C. A., Vincent, S. A., Crow, J., and Hewlett, A. (2016). Bacterial spine infections in adults: Evaluation and management. *J. Am. Acad. Orthopaedic Surgeons* 24, 11–18. doi: 10.5435/JAAOS-D-13-00102

Di Martino, A., Papalia, R., Albo, E., Diaz, L., Denaro, L., and Denaro, V. (2019). Infection after spinal surgery and procedures. *Eur. Rev. Med. Pharmacol. Sci.* 23, 173–178. doi: 10.26355/eurrev_201904_17487

Fucs, P., Meves, R., and Yamada, H. H. (2012). Spinal infections in children: a review. *Int. Orthopaedics* 36, 387–395. doi: 10.1007/s00264-011-1388-2

Gordon, O., Miller, R. J., Thompson, J. M., Ordonez, A. A., Klunk, M. H., Dikeman, D. A., et al. (2020). Rabbit model of staphylococcus aureus implant-associated spinal infection. *Dis. Model. Mech.* 13, dmm045385. doi: 10.1242/dmm.045385

Gu, W., Deng, X., Lee, M., Sucu, Y. D., Arevalo, S., Stryke, D., et al. (2021). Rapid pathogen detection by metagenomic next-generation sequencing of infected body fluids. *Nat. Med.* 27, 115–124. doi: 10.1038/s41591-020-1105-z

Gurtman, A., Begier, E., Mohamed, N., Baber, J., Sabharwal, C., Haupt, R. M., et al. (2019). The development of a staphylococcus aureus four antigen vaccine for use prior to elective orthopedic surgery. *Hum. Vaccin Immunother.* 15, 358–370. doi: 10.1080/21645515.2018.1523093

Han, D., Li, Z., Li, R., Tan, P., Zhang, R., and Li, J. (2019). mNGS in clinical microbiology laboratories: on the road to maturity. *Crit. Rev. Microbiol.* 45, 1–18. doi: 10.1080/1040841X.2019.1681933

Huang, Z. D., Zhang, Z. J., Yang, B., Li, W. B., and Lin, J. H. (2020). Pathogenic detection by metagenomic next-generation sequencing in osteoarticular infections. *Front. Cell. Infect Microbiol.* 10, 471. doi: 10.3389/fcimb.2020.00471

Lener, S., Hartmann, S., Barbagallo, G. M. V., Certo, F., Thom, C., and Tschugg, A. (2018). Management of spinal infection: a review of the literature. *Acta Neurochirurgica* 160, 487–496. doi: 10.1007/s00701-018-3467-2

Ma, C., Wu, H., Chen, G., Liang, C., Wu, L., and Xiao, Y. (2022). The potential of metagenomic next-generation sequencing in diagnosis of spinal infection: a retrospective study. *Eur. Spine J.* 31, 442–447. doi: 10.1007/s00586-021-07026-5

Merino, P., Candel, F. J., Gestoso, I., Baos, E., and Picazo, J. (2012). Microbiological diagnosis of spinal tuberculosis. *Int. Orthopaedics* 36, 233–238. doi: 10.1007/s00264-011-1461-x

Miao, Q., Ma, Y., Wang, Q., Pan, J., Zhang, Y., Jin, W., et al. (2018). Microbiological diagnostic performance of metagenomic next-generation sequencing when applied to clinical practice. *Clin. Infect. Dis.* 67, S231–S240. doi: 10.1093/cid/ciy693

Miller, S., and Chiu, C. (2021). The role of metagenomics and next-generation sequencing in infectious disease diagnosis. *Clin. Chem.* 68, 115–124. doi: 10.1093/clinchem/hvab173

Mongkolrattanothai, K., Naccache, S. N., Bender, J. M., Samayoa, E., Pham, E., Yu, G., et al. (2017). Neurobrucellosis: Unexpected answer from metagenomic next-generation sequencing. *J. Pediatr. Infect. Dis. Soc.* 6, 393–398. doi: 10.1093/jpids/piw066

Nagashima, H., Tanishima, S., and Tanida, A. (2018). Diagnosis and management of spinal infections. *J. Orthop Sci.* 23, 8–13. doi: 10.1016/j.jos.2017.09.016

Saadat, S., Karami, P., Jafari, M., Kholoujini, M., Rikhtegaran Tehrani, Z., Mohammadi, Y., et al. (2020). The silent presence of mycoplasma hominis in patients with prostate cancer. *Pathog. Dis.* 78, ftaa037. doi: 10.1093/femspd/ftaa037

Thoendel, M. J., Jeraldo, P. R., Greenwood-Quaintance, K. E., Yao, J. Z., Nicholas, C., Hanssen, A. D., et al. (2018). Identification of prosthetic joint infection pathogens using a shotgun metagenomics approach. *Clin. Infect. Dis.* 67, 1333–8. doi: 10.1093/cid/ciy303

Tsantes, A. G., Papadopoulos, D. V., Vrioni, G., Sioutis, S., Sapkas, G., Benzakour, A., et al. (2020). Spinal infections: An update. *Microorganisms* 8, 476. doi: 10.3390/microorganisms8040476

Wang, C. X., Huang, Z., Fang, X., Li, W., Yang, B., and Zhang, W. (2020). Comparison of broad-range polymerase chain reaction and metagenomic next-generation sequencing for the diagnosis of prosthetic joint infection. *Int. J. Infect. Dis.* 95, 8–12. doi: 10.1016/j.ijid.2020.03.055

Wang, B., Wang, Y., and Hao, D. (2021). Current study of medicinal chemistry for treating spinal tuberculosis. *Curr. Med. Chem.* 28, 5201–5212. doi: 10.2174/0929867328666201222125225

Ye, Y., Yang, N., Zhou, J., Qian, G., and Chu, J. (2021). Case report: Metagenomic next-generation sequencing in diagnosis of disseminated tuberculosis of an immunocompetent patient. *Front. Med.* 8, 687984. doi: 10.3389/fmed.2021.687984

Zhao, M., Tang, K., Liu, F., Zhou, W., Fan, J., Yan, G., et al. (2020). Metagenomic next-generation sequencing improves diagnosis of osteoarticular infections from abscess specimens: A multicenter retrospective study. *Front. Microbiol.* 11, 2034. doi: 10.3389/fmicb.2020.02034

frontiers | Frontiers in Cellular and Infection Microbiology

TYPE Original Research
PUBLISHED 09 January 2023
DOI 10.3389/fcimb.2022.1001607

OPEN ACCESS

EDITED BY
Jeyaprakash Rajendhran,
Madurai Kamaraj University, India

REVIEWED BY
Rusung Tan,
University of British Columbia, Canada
Rubayet Hasan,
Liflabs Ontario, Canada

*CORRESPONDENCE
Qixing Chen
qixingchen@zju.edu.cn
Qiang Shu
shuqiang@zju.edu.cn

SPECIALTY SECTION
This article was submitted to Clinical Microbiology, a section of the journal Frontiers in Cellular and Infection Microbiology

RECEIVED 23 July 2022
ACCEPTED 19 December 2022
PUBLISHED 09 January 2023

CITATION
Chen Y, Mao L, Lai D, Xu W, Zhang Y, Wu S, Yang D, Zhao S, Liu Z, Xiao Y, Tang Y, Meng X, Wang M, Shi J, Chen Q and Shu Q (2023) Improved targeting of the 16S rDNA nanopore sequencing method enables rapid pathogen identification in bacterial pneumonia in children.
Front. Cell. Infect. Microbiol. 12:1001607.
doi: 10.3389/fcimb.2022.1001607

Improved targeting of the 16S rDNA nanopore sequencing method enables rapid pathogen identification in bacterial pneumonia in children

Yinghu Chen[1,2,3], Lingfeng Mao[3], Dengming Lai[1,2,3], Weize Xu[1,2,3], Yuebai Zhang[1,2], Sihao Wu[3], Di Yang[3], Shaobo Zhao[1,2], Zhicong Liu[1,2], Yi Xiao[1,2], Yi Tang[3], Xiaofang Meng[3], Min Wang[3], Jueliang Shi[3], Qixing Chen[1,2,3]* and Qiang Shu[1,2,3]*

[1]The Children's Hospital, Zhejiang University School of Medicine, Hangzhou, China, [2]National Clinical Research Center for Child Health, Hangzhou, China, [3]Joint Research Center for Molecular Diagnosis of Severe Infection in Children, Binjiang Institute of Zhejiang University, Hangzhou, China

Objectives: To develop a rapid and low-cost method for 16S rDNA nanopore sequencing.

Methods: This was a prospective study on a 16S rDNA nanopore sequencing method. We developed this nanopore barcoding 16S sequencing method by adding barcodes to the 16S primer to reduce the reagent cost and simplify the experimental procedure. Twenty-one common pulmonary bacteria (7 reference strains, 14 clinical isolates) and 94 samples of bronchoalveolar lavage fluid from children with severe pneumonia were tested. Results indicating low-abundance pathogenic bacteria were verified with the polymerase chain reaction (PCR). Further, the results were compared with those of culture or PCR.

Results: The turnaround time was shortened to 6~8 hours and the reagent cost of DNA preparation was reduced by employing a single reaction adding barcodes to the 16S primer in advance. The accuracy rate for the 21 common pulmonary pathogens with an abundance ≥ 99% was 100%. Applying the culture or PCR results as the gold standard, 71 (75.5%) of the 94 patients were positive, including 25 positive cultures (26.6%) and 52 positive quantitative PCRs (55.3%). The median abundance in the positive culture and qPCR samples were 29.9% and 6.7%, respectively. With an abundance threshold increase of 1%, 5%, 10%, 15% and 20%, the test sensitivity decreased gradually to 98.6%, 84.9%, 72.6%, 67.1% and 64.4%, respectively, and the test specificity increased gradually to 33.3%, 71.4%, 81.0%, 90.5% and 100.0%, respectively.

Conclusions: The nanopore barcoding 16S sequencing method can rapidly identify the pathogens causing bacterial pneumonia in children.

KEYWORDS

nanopore sequencing, 16S rDNA, bacterial pneumonia, BALF, prospective study

Introduction

Next-generation sequencing (NGS) was first reported for the diagnosis of neuroleptospirosis in 2014 (Wilson et al., 2014). Subsequently, the NGS has been tentatively applied in detecting pathogens causing infection, such as the coronavirus disease 2019 (COVID-19) and plague (Zhu et al., 2020; Stefan et al., 2016). However, due to the high cost and long turnaround time, NGS is usually applied to detect pathogens causing infections with treatment failure rather than early-stage severe infections in clinical setting (Consensus et al., 2020; Hutchins et al., 2019). For children with severe bacterial infection, rapid pathogen identification is important for the administration of appropriate antibiotics. Nanopore sequencing technology, with the advantages of long reads, and real-time sequencing and analysis, makes it possible to quickly detect and diagnose local pathogen (Sedlazeck et al., 2018; Shiota et al., 2018). Several studies on the application of nanopore sequencing in pathogen diagnosis have been reported (Charalampous et al., 2019; Leggett et al., 2020; Baldan et al., 2021; Zhao et al., 2021). Besides, nanopore sequencing may be used to screen for drug resistance mutations and virulence genes of pathogens (Zhou et al., 2021; Ferreira et al., 2021).

In this study, we developed a nanopore barcoding 16S rDNA sequencing (NB16S-seq) method, which was a 16S full-length gene amplification with barcoded primers prior to targeted third-generation sequencing (TGS). The amplification of full-length 16S rDNA improves the sensitivity and decreases the limit of detection. In addition, the barcode sequence is added to the primer in advance, and this optimization can detect the amplification of full-length 16S rDNA and the ligation of barcodes in one step. The above features not only reduce the reagents cost of end-repair and dA-tailing for all samples to one pooled sample but also avoid the aerosol contamination from the barcode addition step. This prospective study was carried out to ascertain the significance of the NB16S-seq in the identification of bacterial pneumonia pathogens.

Methods

Study design and participants

This was a prospective study on an improved 16S rDNA nanopore sequencing method. Before testing clinical samples, the 21 common pathogens of bacterial pneumonia (7 reference strains and 14 clinical isolates) were sequenced by the NB16S-seq to establish its accuracy.

Bronchoalveolar lavage fluid (BALF) (5 ml) from patients with pulmonary infection was collected in the respiratory endoscopy room between December 2021 and January 2022, and pulmonary infection was confirmed by either pulmonary X-ray or CT. The BALF was sent for culture, NB16S-seq test and *M. pneumonia* RNA detection. Pathogens with negative cultures and positive NB16S-seq (abundant ≥ 5.0%) were verified by quantitative polymerase chain reaction (qPCR). If only one pathogen was detected and its abundance was between 1% and 5%, the qPCR verification was also performed.

The gold standard of the BALF testing is either culture or qPCR. We collected the following data: age, sex, symptoms, diagnosis, antibiotics use, imaging, and duration from admission to sequencing, etc. Routine clinical microbiological investigation included the BALF culture and detection of routine respiratory virus (including respiratory syncytial virus, adenovirus, influenza A and B, and parainfluenza A, B and C) antigens from nasopharyngeal swabs with Rapid Antigen Detection Kits (Kaibili, Hangzhou Innovation Biotechnology Co., Ltd., Hangzhou, China).

Definitions

'Respiratory pathogens' or 'pathogens' were defined in this study as common causes of respiratory infection to differentiate them from commensal organisms. The respiratory pathogens identified in this study were *S. pneumoniae, H. influenzae, M. catarrhalis, M. pneumoniae, S. aureus, S. agalactiae, L. gormanii, B. pertussis, P. aeruginosa, S. marcescens*, and *A. baumannii*.

DNA extraction

Samples were processed in the genetic diagnostic center. The BALF was collected and stored at 4 °C before testing. The 7 reference strains and 13 clinically isolated strains were inoculated on Columbia blood plate culture medium for DNA extraction. These strains were identified by matrix-assisted laser desorption ionization time-of-flight mass spectrometry (MALDI-TOF MS; Bruker Daltoniks, Germany) before DNA extraction. The QIAamp® DNA Mini Kit (QIAGEN, Germany) was used for the purification of microbial DNA. BALF (300μL) was first centrifuged at 13,000 rpm for 5 min to remove the supernatant, and then, the precipitate was suspended in normal saline (200 μL). The mixture was added to buffer ATL (180 μL) and proteinase K (20 μL), mixed by vortexing and incubated at 56 °C for 30 min at 500 rpm in a thermomixer (Eppendorf, Germany). For the 21 bacterial strains, 200 μL of sample (1×10^8 CFU/ml), which was directly added to buffer ATL (180 μL) and proteinase K (20 μL), was incubated at 56 °C for 30 min at 500 rpm in a thermomixer after mixing well. The following experimental steps were carried out according to the manufacturer's instructions.

16S rDNA full-length gene amplification and nanopore sequencing

The concentration of isolated DNA from samples was measured with a Qubit dsDNA HS Assay Kit and a Qubit 4.0 Fluorometer (Thermo Fisher, USA) according to the instructions of the manufacturer. A total of 5~10 ng of DNA template (10 μL) was used for 16S rDNA full-length sequence amplification (primers: 5'-barcode-27F-AGAGTTTGATCMTGGCTCAG-3', 5'-barcode-1492R-CGGTTACCTTGTTACGACTT-3') with 25 μL of Q5 Hot Start High-Fidelity 2X Master Mix (M0494L, New England Biolabs, USA) and 14.5 μL of nuclease-free water (New England Biolabs, USA). PCR amplicons were visualized by 1% agarose gel electrophoresis, followed by purification using 1x AMPure XP beads (Beckman Coulter, USA), and the DNA concentration was measured with a Qubit 4.0 Fluorometer. 1~48 amplified DNA was pooled in equimolar amounts. The pooled DNA was end-repaired and dA-tailed with NEBNext FFPE DNA Repair Mix (New England Biolabs, USA) and NEBNext Ultra II End Repair/dA-Tailing Module (New England Biolabs, USA), followed by purification with AMPure XP beads (Beckman Coulter, USA). Then, the nanopore sequencing was performed using the ligation sequencing kit SQK-LSK110 (Oxford Nanopore Technologies, UK), and the DNA library was loaded into an R9.4.1 flow cell (Oxford Nanopore Technologies, UK) for sequencing for 1~3 hours in the GridION platform according to the sample number. In every sequencing process run, negative process controls were added to the DNA extraction and amplification steps with sterile nuclease-free water to monitor contamination from the environment.

Bioinformatics and pathogen identification

First, raw reads were demultiplexed with an in-house script to eliminate interference from error splitting. Porechop was used to trim the adapter and barcode on the end of the reads (Wick et al., 2018). Seqkit was used to filter reads, retaining those with a size range of 1.3–1.6 kb and qscore ≧ 12 (Shen et al., 2016). To identify the pathogen, clean reads were mapped to the 16S database collected from NCBI and GTDB using minimap2 v2.17 (Li H, 2018) with the parameter "-ax map-ont", and the program samtools v1.10 (Danecek et al., 2021) was used to remove unmapped, nonunique mapped and multiple-mapped reads with the parameter "view -F2308". The species abundance in the sample were incorporated into the biological classification according to the NCBI taxonomy tree. The pathogen identification was determined according to the matching between the species abundance in the sample and the guide for pathogens in the Manual of Clinical Microbiology, 12th edition. The thresholds used in this study for pathogen identification were defined as follows: the valid read number was greater than 5000, and the reliable species abundance for pathogen identification was 1%. To reduce the impact of similar homologous segments of the same species and miscellaneous bacteria in the environment on the analytical results, we tabulated bacterial species that were frequently cultured in the BALF samples into a table (for details, see Supplementary Table 1). If the test bacteria met the following conditions, they were considered "detected bacteria": ① the abundance of detected bacteria was more than 1% and the species was in the above mentioned high-frequency bacterial table; ② if not in the Supplementary Table 1, at most two species with abundance ≥5% were reported in the same genus; and ③ if there were more than ten species not in the Supplementary Table 1, they were classified according to their abundance, and only the first ten species were reported.

Statistical analysis

Stata 15 software was used for ROC analysis, and the sensitivity, specificity and area under the ROC curve were calculated under different cross-sections. Data are expressed as the median (interquartile range).

Results

Rapid NB16S-seq test method

The NB16S-seq workflow is shown in Figure 1. The report time was 8 hours after receiving the BALF sample and could be shortened to 6 hours. This was significantly shorter than the time of culture and NGS. Rapid diagnosis may enhance the early identification of pathogens and contribute to the successful treatment of severe infection.

Evaluating the NB16S-seq test with reference strains, clinical isolates and BALF specimens

The NB16S-seq results for these 21 bacterial strains are shown in Table 1. All bacterial species in Table 1 were correctly detected with an abundance of ≥ 99%, suggesting that the NB16S-seq is accurate in the detection of common pathogens of pulmonary infection.

Among the 110 eligible BALF samples, 94 met the criteria (Figure 2A). The demographic and clinical characteristics of the patients are shown in Table 2, including 88 cases of community acquired pneumonia, 6 cases of hospital acquired pneumonia (HAP), 15 cases of acute respiratory distress syndrome, 20 cases with ICU admission, 1 case of progression, 2 cases of death, and 91 cases of improvement or recovery. The NB16S-seq results regarding bacteria and their abundances are shown in a heatmap (Figure 2B, detail data seen in Supplementary Table 2). The heatmap shows many commensal organisms, fewer opportunistic pathogens, and various abundant common pathogens. This may be related to the following: ① opportunistic pathogens are often isolated in HAP, and only 6 HAP children (6.4%) were enrolled; ② commensal organisms exist in the oropharynx, which might contaminate BALF specimens; and ③ eighty-eight patients (93.6%) received antibiotics before sampling, potentially mitigating pathogen abundance.

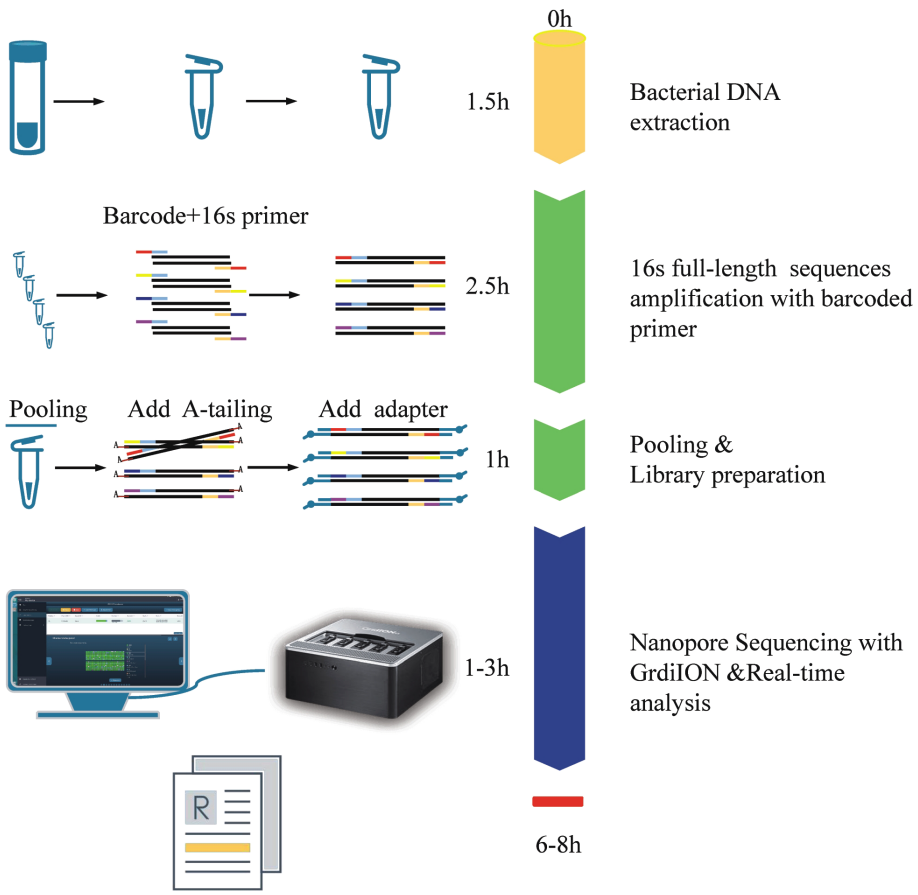

FIGURE 1
The process and schematic representation of NB16S-seq. The turnaround time was approximately 6~8 h from sample collection to results.

TABLE 1 Evaluating the NB16S-seq test with 21 common respiratory pathogens. Seven reference strains and 14 clinical isolates were used to verify the detection results of the NB16S-seq.

Species	Strain	Code	NB16S-seq results		
			Species	Reads (n)	Abundance (%)
S. pneumoniae	ATCC49619		S. pneumoniae	31628	99.82
H. influenzae	ATCC49247		H. influenzae	37192	99.96
M. catarrhalis	211227241		M. catarrhalis	35127	99.99
S. aureus	ATCC25923		S. aureus	30350	99.87
S. pyogenes	ATCC19615		S. pyogenes	35378	99.97
E. coli	ATCC25922		E. coli	33651	99.6
K. pneumoniae	211227130		K. pneumoniae	32330	99.5
K. aerogenes	21WJ8254	210919133	K.a aerogenes	32505	99.97
S. marcescens	21WJ8334	211223048	S. marcescens	36867	99.85
S. enterica	ATCC14028		S. enterica	28901	99.71
N. meningitidis	21WJ8288	211029149	N. meningitidis	42568	99
L.monocytogenes	21WJ8301	2111111189	L.monocytogenes	30327	99.98
P. aeruginosa	ATCC27853		P. aeruginosa	10402	99.88
S. maltophilia	21WJ8338	211223215	S. maltophilia	11331	99.81
A. baumannii	211226029		A. baumannii	13591	99.6
A. johnsonii	21WJ8155	210615244	A. johnsonii	8891	99.44
E. faecalis	21WJ8320	211206091	E. faecalis	46805	99.91
E. faecium	211227058		E. faecium	37730	99.91
S. mitis	21WJ8314	211124076	S. mitis	27988	99.43
M. osloensis	21WJ8171	210706090	M. osloensis	35673	99.96
B. cepacia	21WJ8247	210906065	B. cepacia	11921	99.83
The accuracy rate for bacterial species with an abundance ≥ 99% was 100%.					

Exploring the appropriate NB16S-seq threshold to identify pathogen

Applying the BALF culture or qPCR results as the gold standard, BALF NB16S-seq results were analyzed (details in Supplementary Table 3). Seventy-one (75.5%) of the 94 BALF specimens were positive according to the gold standard, 25 (26.6%) were culture positive, and 52 (55.3%) were qPCR positive. The number of samples containing 0, 1, 2, 3 and 5 pathogenic bacteria with detected abundance ≥ 1% for each bacterium were 7, 54, 28, 4 and 1, respectively. The relationship between NB16S-seq abundance and positive culture, positive PCR and negative PCR is shown in Figure 3A, and the median abundances were 29.9%, 6.7% and 4.2%, respectively. The abundance on bacterial NB16S-seq was closely related to the positive culture and qPCR results. The NB16S-seq abundance of three-quarters of the BALF with positive culture and positive qPCR was ≥5.2% and 2.7%, respectively.

With the increase in the specimens' NB16S-seq abundance threshold to 1%, 5%, 10%, 15% and 20%, the test sensitivity decreased gradually to 98.6%, 84.9%, 72.6%, 67.1% and 64.4%, respectively, and the test specificity increased progressively to 33.3%, 71.4%, 81.0%, 90.5% and 100.00%, respectively (see Figure 3B). If a low NB16S-seq abundance of common pathogens was detected in the BALF, the relationship between the bacteria and pulmonary infection was further evaluated, as these might have been colonizing bacteria. Therefore, for all common respiratory pathogens with an NB16S-seq abundance ≥ 1%, a cut-off value ≥ 5% was applied because at this cut-off the Youden Index (84.9% + 71.4% - 100% = 56.3%) was the largest.

According to the gold standard, *S. pneumonia* was detected 29 times, *M. pneumoniae* 23 times, *H. influenzae* 18 times, *P. aeruginosa* 4 times, *A. baumannii* thrice, both *S. aureus* and *B.*

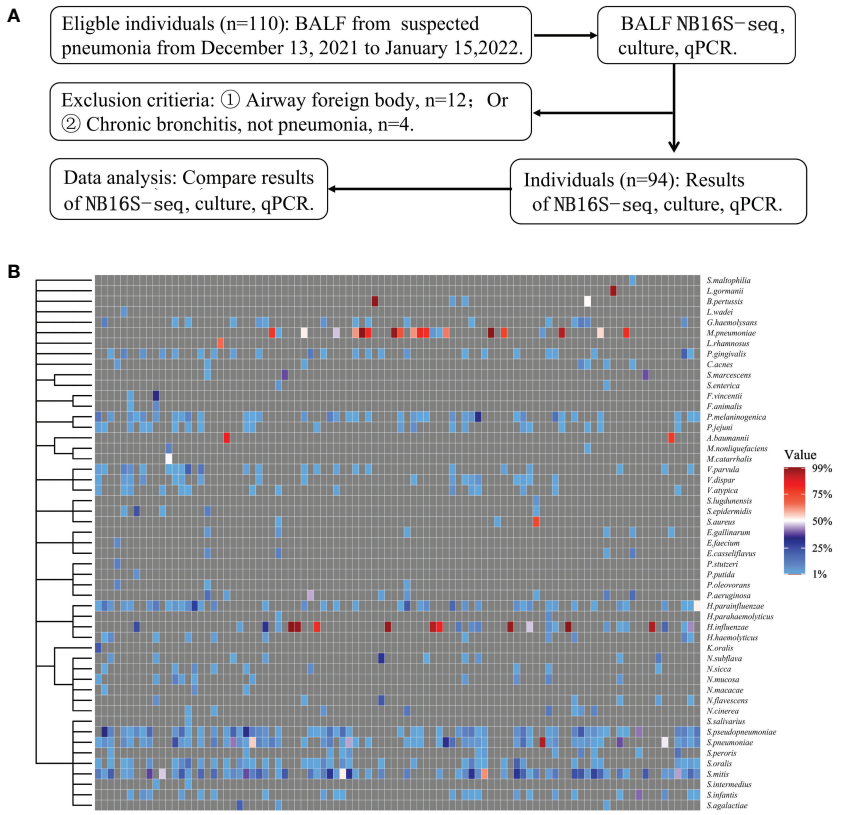

FIGURE 2
Evaluation of NB16S-seq in the etiological diagnosis of pediatric pneumonia **(A)**: BALF form pediatric pneumonia tested with NB16S-seq, culture or qPCR in our hospital between November 2021 and January 2022. **(B)**. Heatmap of bacteria abundance ≥1.0% in 94 BALF samples tested by NB16S-seq. Each column in the **(C)** indicates a sample. Formula of abundance = (number of sequences for a species/total number of sequences in the specimen) ×100%. The value indicates abundance, and different colors of the value bar represent the different NB16S-seq abundances.

pertussis twice, along with *M. catarrhalis*, *S. agalactiae*, *L. gormanii*, and *S. marcescens* being detected once in 94 BALF specimens (details in Supplementary Table 3). When the cut-off value of specimens' NB16S-seq abundance was the same, the sensitivity and specificity of each pathogen were different (Figure 3). The relationship between the NB16S-seq abundance threshold, together with the sensitivity and specificity of common strains was analyzed (Table 3). Accordingly, 4.5% was an appropriate cut-off for *S. pneumonia* (Figure 3C), 5.6% for *H. influenzae* (Figure 3D), 1.2% for *M. pneumonia* (Figure 3E) and *S. aureus* (Figure 3F), and 1.4% for *P. aeruginosa* (Figure 3G). The appropriate cutoff value of *S. pneumonia* and *H. influenzae* was higher than that of *M. pneumonia, S. aureus* and *P.aeruginosa*, which may be related to the oropharyngeal colonization of *H. influenzae* and *S. pneumonia*, while the possibility of colonization of the other three bacteria was low.

To optimize the interpretations of NB16S-seq results, an abundance cut-off of 1.0% might be appropriate for organisms that are not typical colonizers of upper respiratory tract (e.g., *M. pneumonia, S. aureus*, and *P. aeruginosa*), and 5.0% for the other eight bacteria that typically colonize the upper respiratory. NB16S-seq abundances were evaluated with these two different cut-off values, the true or false positive, and true or false negative results are shown in Table 4, the sensitivity, specificity, positive and negative predictive values were 85.9%, 73.6%, 83.9% and 76.5%, respectively, and after applying two different abundance cut-off values for two different group of bacteria, Youden Index (85.9%+73.6% -100%=59.5%) was higher than that (56.3%) of single 5.0% cutoff value.

Discussion

Pneumonia is one of the main causes of death in children under 5 years old (Liu et al., 2015). Timely and appropriate antibiotic treatment could significantly reduce mortality. However, diversity and antibiotic resistance complicates the pathogenic treatment (Yiang et al., 2021). Rapid and sensitive

TABLE 2 Demographic and clinical characteristics of the 94 pediatric pneumonia patients.

Variable	Pediatric pneumonia, n=94
Age, Median (Interquartile,IQR), month	49.02 (16.58-88.90)
Male, n (%)	45 (47.9%)
Diagnosis at admission, n (%)	
CAP	88 (93.6%)
HAP	6 (6.4%)
ARDS	15 (16.0%)
Symptoms	
Cough	94 (100%)
Fever	51 (54.3%)
Dyspnea	14 (14.9%)
Received antibiotic before sequencing, n (%)	88 (93.6%)
Underlying disease, n (%)	22 (23.4%)
Laboratory findings	
White blood cell, Median (IQR), $\times10^9$/L	10.17 (7.71-14.54)
Neutrophils, Median (IQR), $\times10^9$/L	5.78 (3.63-8.58)
CRP, Median (IQR), mg/L	11.47 (0.5775-50.7)
PCT, Median (IQR), ng/ml	0.123 (0.065-0.49)
Pneumonia confirmed by image, n (%)	94 (100%)
Chest X-ray, pneumonia, n (%)	64 (68.1%)
Pulmonary CT, n (%)	92 (97.9%)
Consolidation or atelectasis	14 (14.9%)
Lung abscess or cavity	2 (2.1%)
Pleural inflammation	11 (11.7%)
Airway malformation	13 (13.8%)
Duration from admission to sequencing, Median (IQR), days	3 (1-5)
Invasive mechanical ventilation, n (%)	7 (7.4%)
Length of hospital stay, Median (IQR), days	8 (6-11)
ICU admission, n (%)	19 (20.2%)
Length of ICU stay, Median (IQR),days	20 (8-44)
Outcome, n (%)	
Improvement or recovery	91 (96.8%)
Progress	1 (1.1%)
Death	2 (2.1%)

pathogen identification is important. Routine pathogen detection cannot meet clinical needs due to prolonged time period required or limited detection of single or few kinds of pathogens (Holter et al., 2015; Hassibi et al., 2018; Klein et al., 2021).

In recent years, the application of nanopore sequencing technology in pathogen detection has gained much attention. Compared with the NGS, nanopore sequencing technology has the following advantages (Goldberg et al., 2015; Sedlazeck et al., 2018): ① shorter time from sampling to results, ② simpler

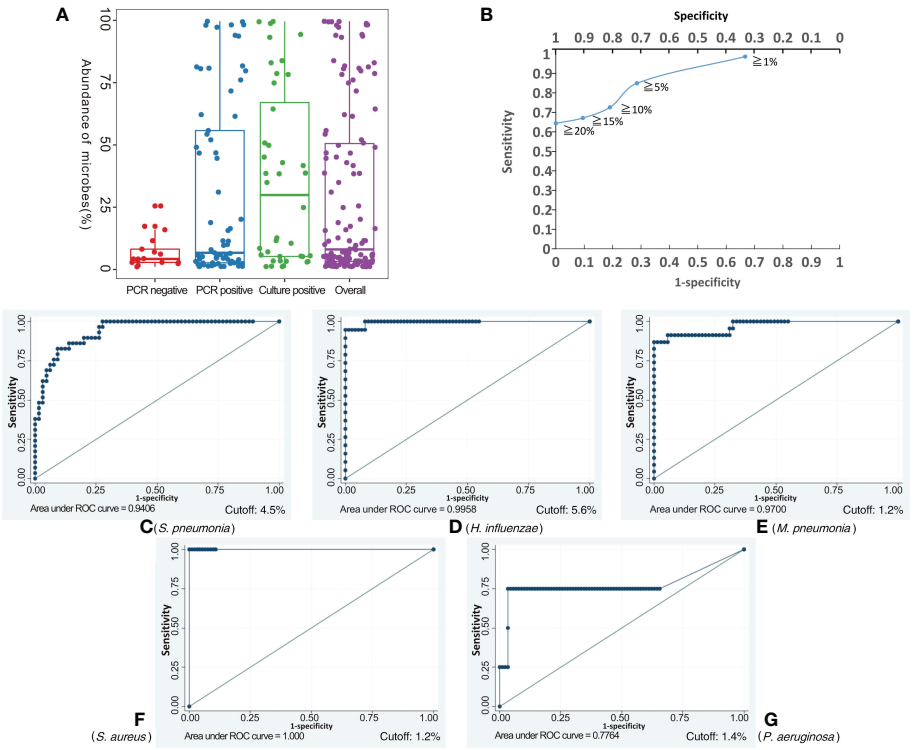

FIGURE 3
Exploring the appropriate NB16S-seq threshold to identify pathogenic bacteria. The relationship between BALF NB16S-seq abundance and positive culture, positive qPCR and negative qPCR results **(A)**. Correlation between NB16S-seq abundance threshold and sensitivity and specificity of BALF pathogen detection **(B)**. For common respiratory pathogens, an NB16S-seq abundance ≥ 5% is an appropriate criterion to designate a sample positive for a pathogen **(C–G)**. The relationship between the NB16S-seq abundance threshold and the sensitivity and specificity for different strains, *S. pneumonia* **(C)**, *H. influenza* **(D)**, *M. pneumonia* **(E)**, *S. aureus* **(F)**, and *P. aeruginosa* **(G)**. A value of 4.5% was an appropriate cutoff for *S. pneumonia* **(C)**, 5.6% for *H. influenzae* **(D)**, 1.2% for *M. pneumonia* **(E)** and *S. aureus* **(F)**, and 1.4% for *P. aeruginosa* **(G)**.

TABLE 3 The relationship between the NB16S-seq abundance threshold and the sensitivity and specificity for different strains according to the gold standard test (either culture or PCR) results.

	Cutoff (%)	Sensitivity (%)	Specificity (%)	AUC
S. pneumonia	1.3	100	60.0	0.9406
	4.5	82.7	90.8	
	10.0	44.8	98.5	
H. influenzae	1.2	94.7	92.0	0.9958
	5.6	94.7	98.7	
	10.5	84.2	100	
M. pneumonia	1.2	87.0	98.6	0.9700
	5.2	82.6	100.0	
S. aureus	1.2	100.0	98.9	1.000
	2.1	100.0	100.0	
	74.9	50.0	100.0	

(Continued)

TABLE 3 Continued

	Cutoff (%)	Sensitivity (%)	Specificity (%)	AUC
P. aeruginosa	1.4	75.0	94.4	0.7764
	5.2	50.0	96.7	
	11.4	25.0	96.7	

For common respiratory tract colonizers (such as S. pneumonia and H. influenzae), an NB16S-seq abundance ≥ 4.5% is an appropriate criterion to designate a sample positive for a pathogen; while for bacteria (such as M. pneumonia, S. aureus, and P. aeruginosa) that rarely colonize the respiratory tract, ≥1.2% is an appropriate criterion. AUC, area under the ROC curve.

sequencing library construction, ③ long sequence reading without assembly, and ④ real-time sequencing and analysis. Compared with the previous 16S rDNA nanopore sequencing method, the NB16S-seq has the following advantages: ① reduced the reagent cost for each sample, and ② optimized the experimental procedure.

The NB16S-seq method includes bacterial DNA extraction, 16S rDNA amplification, pooling and library preparation, nanopore sequencing and real-time analysis. The NB16S-seq was verified for 7 reference strains and 14 clinical isolates. The accuracy rate for species was 100%, and their abundance was ≥ 99%. In the process of 16S rDNA amplification and species database comparison, there was no error, and no other species appeared incorrectly. The 16S rDNA is a commonly used molecular clock in bacterial systematic classification. Bacterial universal primers can amplify the 16S rDNA fragments of all bacteria, and the difference in variable regions can be used to distinguish different bacteria. As an increasing number of bacterial 16S rDNA sequences are being determined and included in the NCBI and GTDB databases, it is faster and more convenient to identify species based on the 16S rDNA (Robeson et al., 2021). The similarity rate of 16S rDNA among some species (such as: *S. pneumoniae* and *S. mitis*) is greater than 99%, which intricates the difficulty of species identification (Church et al., 2020; Yatera et al., 2021). Interestingly, the NB16S-seq can effectively distinguish them.

Among the bacteria detected by the NB16S-seq, oropharyngeal-colonizing bacteria were the most common. In particular, the BALF culture reported them as colonizing bacteria, and the NB16S-seq listed them in the appendix results as detected bacteria. These bacteria can cause infective endocarditis, meningitis, and local tissue abscesses. The NGS showed that colonizing anaerobic bacteria in the oropharynx are closely related to lung abscesses (Mu et al., 2021).

Some pathogenic bacteria, such as *S. pneumoniae* and *H. influenzae* may colonize the oropharynx. Furthermore, differentiating commensal from pathogens is complex. However, our results showed the NB16S-seq abundance to be beneficial in distinguishing pathogens from commensals. When the NB16S-seq abundance was increased from 1% to 5%, the specificity also increased from 33.3% to 71.5%, and significantly reduced the false-positive rate. When the abundance extended to 20%, the specificity was 100%. Some pathogenic bacteria, such as *M. pneumoniae*, *S. aureus* and *P. aeruginosa* rarely colonize the

TABLE 4 Evaluating BALF NB16S-seq with the gold standard test (either culture or qPCR).

NB16S-seq Result	Gold Standard	No. of Samples	Definition	Category Description	Sensitivity	Specificity	PPV	NPV
Neg (51)	Neg (39)	37	TN	Culture Neg and qPCR ND	85.9%	73.6%	83.9%	76.5%
	Pos (12)	10	FN	Culture Neg, qPCR Pos				
		2	FN	Culture Pos				
Pos (87)	Neg (14)	11	FP	Culture Neg, qPCR Pos				
		2	FP	Culture Pos				
	Pos (73)	44	TP	Culture Neg, PCR Pos				
		24	TP	Culture Pos				

The strains with abundance ≥1% were compared with gold standard. The number of samples containing 0, 1, 2, 3 and 5 pathogenic bacteria with an abundance ≥ 1% was 7, 54, 28, 4 and 1, respectively. Pathogens with negative culture and positive NB16S-seq (abundance ≥5%) results were verified by qPCR. If only one pathogen was detected and its abundance was between 1% and 5%, qPCR verification was also performed. Formula of abundance = (number of sequences for a species/total number of sequences in the specimen) ×100%. To evaluate the NB16S-seq results, the abundance cut-off applied for different bacteria was either 5.0% or 1.0% (1.0% for M. pneumonia, S. aureus, and P. aeruginosa, 5% for the other 8 bacteria). Neg, negative; Pos, positive; TP, true positive; FP, false positive; FP, false positive; FN, false negative; PPV, positive predictive value; NPV, negative predictive value.Eleven species were considered as common respiratory pathogens in this study, *S. pneumoniae*, *H. influenzae*, *M. catarrhalis*, *M. pneumoniae*, *S. aureus*, *S. agalactiae*, *L. gormanii*, *B. pertussis*, *P. aeruginosa*, *S. marcescens*, and *A. baumannii*.

oropharynx. Interestingly, they had a high specificity when the abundance was ≥ 1%, implying that the bacteria exist in the BALF.

Conclusions

We report a rapid pathogen diagnostic method, the NB16S-seq, for use in bacterial pneumonia with an optimized experimental procedure and lower cost. Pathogens can be identified in 6~8 h. For oropharyngeal-colonizing pathogens, an NB16S-seq abundance of 5% is the best cutoff point, and 1% is the best cutoff for pathogens that rarely colonize.

Data availability statement

The datasets presented in this study can be found in online repositories. The names of the repository/repositories and accession number(s) can be found below: We have uploaded the sequencing to the GSA, Project Number is PRJCA011155, which can be visited in https://ngdc.cncb.ac.cn/bioproject/browse/PRJCA011155.

Ethics statement

The studies involving human participants were reviewed and approved by the ethics committee of The Children's Hospital of Zhejiang University of Medicine. Written informed consent to participate in this study was provided by the participants' legal guardian/next of kin. Written informed consent was obtained from the minor(s)' legal guardian/next of kin for the publication of any potentially identifiable images or data included in this article.

Author contributions

YC and LM contributed equally to this work and share first authorship. YC, DL, and WX collected and analyzed medical data of the patients, wrote and revised the manuscript. YZ, ZL, and SZ participated in the treatment of the patients and data collection. LM, SW, DY, YX, YT, XM, MW, and JS participated in the Improved targeting 16S rDNA nanopore sequencing and data analysis. QC and QS contributed to the treatment plan and made a critical revision of the manuscript. All authors contributed to the article and approved the submitted version.

Funding

This work was supported by the Fundamental Research Funds for the Central Universities (+226-2022-00060), "Pioneer" and "Leading Goose" R&D Program of Zhejiang Province (2023C03028), and the National Natural Science Foundation of China (82071812).

Acknowledgments

We thank Professor Kangchen Zhao from Jiangsu Provincial Center for Disease Control and Prevention for providing primers of the 7 common pathogenic bacteria.

Conflict of interest

The authors declare that the research was conducted in the absence of any commercial or financial relationships that could be construed as a potential conflict of interest.

Publisher's note

Supplementary material

The Supplementary Material for this article can be found online at: https://www.frontiersin.org/articles/10.3389/fcimb.2022.1001607/full#supplementary-material

References

Baldan, R., Cliff, P. R., Burns, S., Medina, A., Smith, G. C., Batra, R., et al. (2021). Development and evaluation of a nanopore 16S rRNA gene sequencing service for same day targeted treatment of bacterial respiratory infection in the intensive care unit. *J. Infect.* 83 (2), 167–174. doi: 10.1016/j.jinf.2021.06.014

Charalampous, T., Kay, G. L., Richardson, H., Aydin, A., Baldan, R., Jeanes, C., et al. (2019). Nanopore metagenomics enables rapid clinical diagnosis of bacterial lower respiratory infection. *Nat. Biotechnol.* 37 (7), 783–792. doi: 10.1038/s41587-019-0156-5

Church, D. L., Cerutti, L., Gürtler, A., Griener, T., Zelazny, A., and Emler, S. (2020). Performance and application of 16S rRNA gene cycle sequencing for routine identification of bacteria in the clinical microbiology laboratory. *Clin. Microbiol. Rev.* 33 (4), e00053–e00019. doi: 10.1128/CMR.00053-19

Consensus Group Of Experts On Application Of Metagenomic Next Generation Sequencing In The Pathogen Diagnosis In Clinical Moderate And Severe Infections, Professional Committee Of Sepsis And Shock Chinese Research Hospital Association, Professional Committee Of Microbial Toxins Chinese Society For Microbiology and Professional Committee Of Critical Care Medicine Shenzhen Medical Association (2020). Expert consensus for the application of metagenomic next generation sequencing in the pathogen diagnosis in clinical moderate and severe infections. *Zhonghua Wei Zhong Bing Ji Jiu Yi Xue* 32 (5), 531–536. doi: 10.3760/cma.j.cn121430-20200228-00095

Danecek, P., Bonfield, J. K., Liddle, J., Marshall, J., Ohan, V., Pollard, M. O., et al. (2021). Twelve years of SAMtools and BCFtools. *Gigascience* 10 (2), giab008. doi: 10.1093/gigascience/giab008

Ferreira, F. A., Helmersen, K., Visnovska, T., Jørgensen, S. B., and Aamot, H. V. (2021). Rapid nanopore-based DNA sequencing protocol of antibiotic-resistant bacteria for use in surveillance and outbreak investigation. *Microb. Genom.* 7 (4), 557. doi: 10.1099/mgen.0.000557

Goldberg, B., Sichtig, H., Geyer, C., Ledeboer, N., and Weinstock, G. M. (2015). Making the leap from research laboratory to clinic: Challenges and opportunities for next-generation sequencing in infectious disease diagnostics. *mBio* 6 (6), e01888–e01815. doi: 10.1128/mBio.01888-15

Hassibi, A., Manickam, A., Singh, R., Bolouki, S., Sinha, R., Jirage, K. B., et al. (2018). Multiplexed identification, quantification and genotyping of infectious agents using a semiconductor biochip. *Nat. Biotechnol.* 36 (8), 738–745. doi: 10.1038/nbt.4179

Holter, J. C., Müller, F., Bjørang, O., Samdal, H. H., Marthinsen, J. B., Jenum, P. A., et al. (2015). Etiology of community-acquired pneumonia and diagnostic yields of microbiological methods: a 3-year prospective study in Norway. *BMC Infect. Dis.* 15, 64. doi: 10.1186/s12879-015-0803-5

Hutchins, R. J., Phan, K. L., Saboor, A., Miller, J. D., Muehlenbachs, A.CDC NGS Quality Workgroup (2019). Practical guidance to implementing quality management systems in public health laboratories performing next-generation sequencing: Personnel, equipment, and process management (Phase 1). *J. Clin. Microbiol.* 57 (8), e00261–e00219. doi: 10.1128/JCM.00261-19

Klein, M., Bacher, J., Barth, S., Atrzadeh, F., Siebenhaller, K., Ferreira, I., et al. (2021). Multicenter evaluation of the unyvero platform for testing bronchoalveolar lavage fluid. *J. Clin. Microbiol.* 59 (3), e02497–e02420. doi: 10.1128/JCM.02497-20

Leggett, R. M., Alcon-Giner, C., Heavens, D., Caim, S., Brook, T. C., Kujawska, M., et al. (2020). Rapid MinION profiling of preterm microbiota and antimicrobial-resistant pathogens. *Nat. Microbiol.* 5 (3), 430–442. doi: 10.1038/s41564-019-0626-z

Li, H. (2018). Minimap2: pairwise alignment for nucleotide sequences. *Bioinformatics* 34 (18), 3094–3100. doi: 10.1093/bioinformatics/bty191

Liu, L., Oza, S., Hogan, D., Perin, J., Rudan, I., Lawn, J. E., et al. (2015). Global, regional, and national causes of child mortality in 2000-13, with projections to inform post-2015 priorities: an updated systematic analysis. *Lancet* 385 (9966), 430–440. doi: 10.1016/S0140-6736(14)61698-6

Mu, S., Hu, L., Zhang, Y., Liu, Y., Cui, X., Zou, X., et al. (2021). Prospective evaluation of a rapid clinical metagenomics test for bacterial pneumonia. *Front. Cell Infect. Microbiol.* 11. doi: 10.3389/fcimb.2021.684965

Robeson, M. S.2nd, O'Rourke, D. R., Kaehler, B. D., Ziemski, M., Dillon, M. R., Foster, J. T., et al. (2021). RESCRIPt: Reproducible sequence taxonomy reference database management. *PloS Comput. Biol.* 17 (11), e1009581. doi: 10.1371/journal.pcbi.1009581

Sedlazeck, F. J., Rescheneder, P., Smolka, M., Fang, H., Nattestad, M., von Haeseler, A., et al. (2018). Accurate detection of complex structural variations using single-molecule sequencing. *Nat. Methods* 15 (6), 461–468. doi: 10.1038/s41592-018-0001-7

Shen, W., Le, S., Li, Y., and Hu, F. (2016). SeqKit: A cross-platform and ultrafast toolkit for FASTA/Q file manipulation. *PloS One* 11 (10), e0163962. doi: 10.1371/journal.pone.0163962

Shiota, H., Barral, S., Buchou, T., Tan, M., Couté, Y., Charbonnier, G., et al. (2018). Nut directs p300-dependent, genome-wide H4 hyperacetylation in Male germ cells. *Cell Rep.* 24 (13), 3477–3487.e6. doi: 10.1016/j.celrep.2018.08.069

Stefan, C. P., Koehler, J. W., and Minogue, T. D. (2016). Targeted next-generation sequencing for the detection of ciprofloxacin resistance markers using molecular inversion probes. *Sci. Rep.* 6, 25904. doi: 10.1038/srep25904

Wick, R. R., Volkening, J. J., and Loman, N. (2018). *Porechop is a tool for finding and removing adapters from Oxford nanpore reads*. Available at: https://github.com/rrwick/Porechop.

Wilson, M. R., Naccache, S. N., Samayoa, E., Biagtan, M., Bashir, H., Yu, G., et al. (2014). Actionable diagnosis of neuroleptospirosis by next-generation sequencing. *N Engl. J. Med.* 370 (25), 2408–2417. doi: 10.1056/NEJMoa1401268

Yatera, K., Noguchi, S., and Mukae, H. (2021). Perspective on the clone library method for infectious diseases. *Respir. Investig.* 59 (6), 741–747. doi: 10.1016/j.resinv.2021.07.003

Yiang, G. T., Tzeng, I. S., Shui, H. A., Wu, M. Y., Peng, M. Y., Chan, C. Y., et al. (2021). Early screening of risk for multidrug-resistant organisms in the emergency department in patients with pneumonia and early septic shock: Single-center, retrospective cohort study. *Shock* 55 (2), 198–209. doi: 10.1097/SHK.0000000000001599

Zhao, N., Cao, J., Xu, J., Liu, B., Liu, B., Chen, D., et al. (2021). Targeting RNA with next- and third-generation sequencing improves pathogen identification in clinical samples. *Adv. Sci. (Weinh)* 8 (23), e2102593. doi: 10.1002/advs.202102593

Zhou, M., Wu, Y., Kudinha, T., Jia, P., Wang, L., Xu, Y., et al. (2021). Comprehensive pathogen identification, antibiotic resistance, and virulence genes prediction directly from simulated blood samples and positive blood cultures by nanopore metagenomic sequencing. *Front. Genet.* 12. doi: 10.3389/fgene.2021.620009

Zhu, N., Zhang, D., Wang, W., Li, X., Yang, B., Song, J., et al. (2020). A novel coronavirus from patients with pneumonia in China 2019. *N Engl. J. Med.* 382 (8), 727–733. doi: 10.1056/NEJMoa2001017

frontiers | Frontiers in Cellular and Infection Microbiology

TYPE Original Research
PUBLISHED 27 January 2023
DOI 10.3389/fcimb.2023.991011

OPEN ACCESS

EDITED BY
Sathyavathi Sundararaju,
Sidra Medicine, Qatar

REVIEWED BY
Arun Decano,
University of Oxford, United Kingdom
Marwan Osman,
Cornell University, United States

*CORRESPONDENCE
Liping Tang
1714189813@qq.com
Ying Cao
xymz339436@126.com

†These authors have contributed equally to this work

SPECIALTY SECTION
This article was submitted to Clinical Microbiology, a section of the journal Frontiers in Cellular and Infection Microbiology

RECEIVED 11 July 2022
ACCEPTED 13 January 2023
PUBLISHED 27 January 2023

CITATION
Huang R, Yuan Q, Gao J, Liu Y, Jin X, Tang L and Cao Y (2023) Application of metagenomic next-generation sequencing in the diagnosis of urinary tract infection in patients undergoing cutaneous ureterostomy.
Front. Cell. Infect. Microbiol. 13:991011.
doi: 10.3389/fcimb.2023.991011

Application of metagenomic next-generation sequencing in the diagnosis of urinary tract infection in patients undergoing cutaneous ureterostomy

Rong Huang[1†], Qian Yuan[1†], Jianpeng Gao[2†], Yang Liu[3], Xiaomeng Jin[4], Liping Tang[1*] and Ying Cao[1*]

[1]Nursing Department, The First Affiliated Hospital of Nanchang University, Nanchang, China, [2]Medical department, Genskey Medical Technology Co., Ltd, Beijing, China, [3]Clinical Laboratory, The First Affiliated Hospital of Nanchang University, Nanchang, China, [4]Thoracic Surgical ICU, Yantai Yuhuangding Hospital, Yantai, China

Objective: Urinary tract infection (UTI) is an inflammatory response of the urothelium to bacterial invasion and is a common complication in patients with cutaneous ureterostomy (CU). For such patients, accurate and efficient identification of pathogens remains a challenge. The aim of this study included exploring utility of metagenomic next-generation sequencing (mNGS) in assisting microbiological diagnosis of UTI among patients undergoing CU, identifying promising cytokine or microorganism biomarkers, revealing microbiome diversity change and compare virulence factors (VFs) and antibiotic resistance genes (ARGs) after infection.

Methods: We performed a case-control study of 50 consecutive CU patients from December 2020 to January 2021. According to the clinical diagnostic criteria, samples were divided into infected group and uninfected group and difference of urine culture, cytokines, microorganism, ARGs and VFs were compared between the two groups.

Results: Inflammatory responses were more serious in infected group, as evidenced by a significant increase in *IFN-α* (p=0.031), *IL-1β* (0.023) and *IL-6* (p=0.018). Clinical culture shows that there is higher positive rate in infected group for most clinical pathogens like *Escherichia coli, Klebsiella pneumoniae, Staphylococcus aureus, Candida auris etc.* and the top three pathogens with positive frequencies were *E. coli*, *K. pneumoniae*, and *Enterococcus faecalis.* Benchmarking clinical culture, the total sensitivity is 91.4% and specificity is 76.3% for mNGS. As for mNGS, there was no significant difference in microbiome α- diversity between infected and uninfected group. Three species biomarkers including *Citrobacter freundii, Klebsiella oxytoca*, and *Enterobacter cloacae* are enriched in infected group based on Lefse. *E. cloacae* were significantly correlated with IL-6 and IL-10. *K. oxytoca* were significantly

correlated with IL-1β. Besides, the unweighted gene number and weighted gene abundance of VFs or ARGs are significantly higher in infected group. Notablely, ARGs belonging to fluoroquinolones, betalatmas, fosfomycin, phenicol, phenolic compound abundance is significantly higher in infected group which may have bad effect on clinical treatment for patients.

Conclusion: mNGS, along with urine culture, will provide comprehensive and efficient reference for the diagnosis of UTI in patients with CU and allow us to monitor microbial changes in urine of these patients. Moreover, cytokines (*IL-6, IL-1β,* and *IFN-a*) or microorganisms like *C. freundii, K. oxytoca* or *E. cloacae* are promising biomarkers for building effective UTI diagnostic model of patients with CU and seriously the VFs and ARGs abundance increase in infected group may play bad effect on clinical treatment.

KEYWORDS

UTI, mNGS, cutaneous ureterostomy, biomarker, ARGs

Introduction

With estimated 573,000 new cases and 213,000 deaths in 2020, bladder cancer is the tenth most dominating cancer worldwide (Sung et al., 2021). Several factors, such as tobacco smoking and exposure to certain chemicals, have been regarded as main risk factors contributing to bladder cancer (Cumberbatch et al., 2018). Radical cystectomy (RC) with urinary diversion (UD) is the gold standard for the treatment of muscle invasive bladder cancer (MIBC) and high-risk non-muscle invasive bladder cancer (NMIBC) (Farber et al., 2018). Cutaneous ureterostomy (CU), a reliable choice for the older and frail population, has its advantage like relatively simple procedure and faster postoperative recovery time (Witjes et al., 2021).

Nowadays, Urinary tract infection (UTI) is the second most common infectious disease, caused by different type of microbial agents, which can stimulate innate and adaptive responses passing through the physical barriers. Among these responses, toll-like receptors (TLRs), which activate a range of different immune system components, including chemokines, interferons, interleukins, antimicrobial peptides, and proinflammatory cytokines, are critical component of the innate immune response to all types of infection (Behzadi and Behzadi, 2016). UTI is a common complication for patients undergoing RC with an incidence ranging from 19% to 43% (Mano et al., 2014; Ghoreifi et al., 2020; Gayarre Abril et al., 2021). In addition, patients with CU also need to be inserted with ureteral stents to drain urine, and research has shown that a bacterial biofilm can be formed on the surface of these stents in only a short space of time. Consequently, it is difficult for antibiotics to enter, thus leading to catheter-related UTI, drug resistance, and prolonged UTI (Bader et al., 2013). Recurrent UTI and increasing antimicrobial resistance lead to an increase in readmission rate and economic burden of patients, thus exerting serious effects on a patient's life quality (Flores-Mireles et al., 2015; Liu et al., 2016). Therefore, patients with CU need efficient and precise diagnosis in order to be treated effectively as early as possible and to avoid overtreatment.

However, diagnosis of UTI is generally based on traditional urinary culture tests and clinical manifestations; these strategies are associated with certain limitations. First, traditional urinary culture tests are suitable for fast-growing bacteria, whereas some organisms not suitable for standard culture conditions such as fastidious bacteria and fungi are involved in UTI (Siddiqui et al., 2011; Wolfe et al., 2012; Moustafa et al., 2018). Second, traditional urine culture and drug sensitivity tests take a long time to complete and cannot guide the selection of clinical antibiotics in a rapid manner. Third, bladder is not sterile, and studies of the urine of healthy subjects has provided evidence of bladder-associated microbial populations (Smelov et al., 2016). Moreover, patients undergoing CU whose bladder is removed, do not have typical symptoms of UTI such as frequent urination, urgency, and dysuria. In addition, indwelling ureteral stents can lead to a high incidence of bacteriuria. It has been reported that the incidence of chronic indwelling stent bacterial colonization and bacteriuria is 100% (Kaufman et al., 2009), which all complicate the diagnosis of UTI in these patients.

Metagenomic next-generation sequencing (mNGS) is an unbiased method to sequence all nucleic acids (DNA) of a specimen in parallel (Simner et al., 2018). It can be used to accurately detect a wide range of pathogens. This emerging approach is favored by clinical laboratories for pathogenic detection of infectious diseases and has been used to determine the etiological diagnosis of some infectious diseases (Simner et al., 2018). Formerly, a positive urine culture test was considered to be indicative of UTI or asymptomatic bacteriuria (Whiteside et al., 2015). As urinary tract of healthy subjects has its own unique flora structure, mNGS can provide more comprehensive data relating to the microenvironment change of a patient's urinary tract than traditional culture. This may help doctors locate organisms that cause disease more accurately and move towards a "precision medicine" model (Dixon et al., 2020). In addition, mNGS facilitates

mining VFs and ARGs so as to monitor the prevalence of highly virulent and drug-resistant microorganisms.

In the study, focusing on patients undergoing CU, we aimed to explore the performance of mNGS in helping diagnosis UTI, the significantly different biomarkers such as cytokines, microorganism structure and pathogenic microorganisms which would lay a foundation for future UTI diagnostic model construction.

Materials and methods

Patients and samples

We performed a case-control study of 50 patients with CU from December 2020 to January 2021. Skin swabs around the stoma, ureteral stents, urine and blood samples were collected according to the standard procedure (National Health Commission of the people's Republic of China, 2018). Urine, ureteral stents and skin swabs were collected for routine culture test and urine samples were frozen in the freezer at -80°C and sent to Genskey's laboratory for mNGS test. Additionally, cytokines detection and urinalysis were performed. All samples were submitted for inspection immediately after collection. According to the inclusion-exclusion criteria and clinical infection diagnostic criteria (Table 1) (Horan et al., 2008; National Health and Family Planning Commission of the people's Republic of China, 2016; Flaig et al., 2020), the included patients were classified into an infected group and an uninfected group.

Urinalysis

It was detected by AX4030 automatic urine dry chemical analyzer (Arkray Company of Japan). Urine bacterial count and white blood cell count were determined by UF1000i urine tangible component analyzer (Sysmex Company, Japan), and the operation was carried out strictly in accordance with the instrument instructions.

Urine culture and susceptibility testing

1μL clean midstream urine was inoculated on Columbia blood plate and McConkey medium plate (Oxoid company, UK). The isolated bacteria were counted after cultured at 37°C for 48 hours. Bacterial identification and drug sensitivity test were carried out by VITEK 2 Compact automatic identification drug sensitivity instrument (Bio Mérieux S.A.). According to the Clinical and Laboratory Standards Institute (CLSI) guidelines (Humphries et al., 2018), MICs were admeasured using frozen Trek Sensititre custom plates (Thermo Scientifific).

Cytokines detection

Detection of 12 cytokines by flow immunofluorescence photoluminescence with multiple microspheres. The kit was purchased from Qingdao Raiscare Biotechnology Co., Ltd., and the detection instrument was BD FACS Calibur flow cytometry.

DNA extraction, library preparation and mNGS

Urine samples (5mL) and the negative batch controls samples were collected using Sterile screw freezing tubes. 800uL was absorbed from the liquefied sample, transferred to centrifuge tube, and centrifuged at 13600g for 5min. the supernatant was discarded, and the precipitation was used for extraction. DNA was extracted with a

TABLE 1 Several criteria in our study.

Inclusion criteria	
1)	Patients who were diagnosed as bladder cancer and underwent CU according to the bladder cancer diagnosis and treatment guidelines of the National Comprehensive Cancer Network (NCCN) in 2020
2)	Patients who gave informed consent to participate in this study
Exclusion criteria	
1)	Patients who were complicated with infection besides urinary system
2)	Patients who were on long-term steroids and immunosuppressants
3)	Patients who received antibiotics treatment within 14 days prior to inclusion
Elimination criteria	
1)	The urine samples were sequenced by mNGS and suspected of contamination or had too few sequences
Clinical infection diagnostic criteria	
1)	A positive urine culture ($\geq 10^5$cfu/mL) with documented symptoms (fever, flank pain, changes in urine color, character or smell, etc.)
2)	A positive urine culture ($\geq 10^5$cfu/mL) that need to receive antibiotic treatment by practitioner discretion
3)	A negative/unavailable urine culture with documented symptoms consistent with a clinical diagnosis of UTI (including urinalysis suggestive of UTI)

Genskey Micro DNA Kit (1901, Genskey, Tianjin) and measured by Qubit dsDNA HS Assay Kits.

The DNA libraries were constructed by an NGS library construction kit(2012B, Genskey, Tianjin). The DNA libraries quality was assessed using an Agilent 2100 Bioanalyzer (Agilent Technologies, SantaClara, USA). The constructed DNA library concentration was determined by qPCR and, must be at least 1 Nmol/L.

Finally, all sample DNA libraries were mixed and sequenced with a single-stranded circular DNA was added by 2-3 quantitative sets to obtain DNA nanospheres. The DNA nanospheres were loaded on the sequencing chip and sequenced using the MGISEQ-2000 sequencing platform MGI, Shenzhen, China).

Bioinformatic analysis of mNGS

Data quality control.

For quality control like adapter contamination and low-quality, raw reads were filtered by fastp (v0.19.5) (Humphries et al., 2018). Reads that were mapped to human reference assembly GRCh38 were removed with bowtie2 v2.3.4.3 (Langmead and Salzberg, 2012).

Taxonomic assignment and comparation with culture

After that reads were aligned to the microorganism database consisted of about 12000 genomes (including bacteria, viruses, fungi, protozoa, homo sapiens and other multicellular eukaryotic pathogens) (Jing et al., 2021) with kraken2 (v2 2.1.2) (Lu et al., 2022) as previously described. Then, the abundance of the annotated taxa was corrected based on bracken (-r 50 -t 10) (Lu et al., 2017) and was further standardized to 20,000,000 (20M) sequencing data. In order to determine the positive detection rate of mNGS, we calculated the ratio of the abundance of each pathogen in the samples versus the controls in the same batch. If foldchange >10 or pathogens were not detected in the controls, positive mNGS was defined (Miller et al., 2019). Next, the sensitivity, specificity and accuracy of each pathogen were calculated in urine samples positive for the clinical culture. Sensitivity was defined as TP/(TP+FN). Specificity was defined as TN/(TN+FP). Accuracy was defined as (TP+TN)/(TP+FP+TN+FN).

Microbiome diversity comparation.

To assess the organism richness rarefaction analysis was performed with in-house R script on species level. We also calculated the within-sample (α) diversity using Shannon index and Simpson index on genus level to estimate the richness of samples using QIIME v1.9.1 (Hall and Beiko, 2018). Principal Coordinate Analysis (PCoA) ware performed using Bray-Curtis distance.Permutational analysis of variance (PERMANOVA) was applied to test group effection like “Gender”, “Chronic Underlying Diseases”, “Batch effect”, “Infected or Uninfected “ based on distance matrix using vegan package(distance = ‘bray’, permutations = 999) (Wang Z. et al., 2020). LefSe (Linear discriminant analysis Effect Size) (Segata et al., 2011) was used to test the difference in taxa abundance and function analyze. To evaluate their associations between microorganisms and inflammatory factors, we performed mantel test analyze to find the possible biomarker (Yang et al., 2017).

VFs comparation.

We analyzed bacterial virulence factors using Virulence factor database (VFDB) (Chen et al., 2005) by BLASTn v2.9.0+ (Chen et al., 2015) based method with 95% identity and 95% query coverage cutoffs, relatively strict than previous research (Jin et al., 2021). VFs abundance were calculated as follows (Zhao et al., 2020):

$$\text{Abundance}\ (coverage, /M\ read) = \frac{(N_{mapped\ reads} * L_{reads})/L_{VFs}}{S}$$

Where $N_{mapped\ reads}$ is the number of reads mapped to VF and L_{reads} is the sequence length of BGI reads (SE50). L_{VFs} is the length of VFs and S is the size of the data (M read)

Next, we conducted a comparison of the total gene number and abundance of the VF among the infected group, uninfected group and controls as presented in boxplot figure and heatmap. A differential VF analysis was performed among three groups *via* Lefse Then, we combined the differential VFs with the classification of VF and contribution of taxa accordint to VFDB database and showed the relationship by Sankey diagram. Box figure and heatmap were visualized through R pheatmap package. Sankey diagram were visualized through https://sankeymatic.com/.

ARGs comparation.

We performed read-based method to detect ARGs by RGI bwt model (Alcock et al., 2020) and calculated the ARG abundance in the same way as VFs. Total ARG gene number and ARG abundance were compared among the infected, uninfected and NC group with boxplot. Procrustes analysis (Wang et al., 2020) was performed to evaluate the correlation between ARG profiles and species community structure on the base of Bray-Curtis matrices. Drug class is from the output file of RGI with further manual integration.

Statistical analysis

Power Analysis was performed by pwr.t2n.test function in pwr (v1.2-2) package of R. Odds ratio analyze by R package epitools oddsratio function. The Wilcoxon test (Mann Whitney U-test) was used to analyze differences across subgroups which was performed by R ggpubr package. Data analysis was performed by GraphPad Prism 8 software and R. $P< 0.05$ was statistically significant in our study.

Code availability

The core software used is described in Materials and Methods. The scripts in this study are available on github: https://github.com/GoGoGao/UTI_mNGS_research.

Result

Subject characteristics and study design

Our study protocols were in compliance with the published research (Chen et al., 2020). In the group with underlying diseases, the incidence of infection was 77.8% (14/18) while in the group without underlying disease, the incidence of infection was only 65.5% (21/32) (Supplementary Figure 1A). The odds ratio of underlying disease to no underlying disease was 1.82 (95% CI = [0.42,9.41], P=0.39). Though we observed a ratio increase of the Infected and Uninfected, it was not statistically significant. As bladder cancer is more prevalent in males,[1] our study featured more male patients (42/50, 84%) than female patients (8/50, 16%). When all 42 male cases were considered, we found that 71.4% (30/42) had infection; this was higher than the rate of infection in females (5/8; 62.5%) (Supplementary Figure 1B). The odds ratio of male to female is 0.67 (95% CI = [0.11,5.01], P=0.63). There was no significant difference between the two groups with regards to age (P=0.24, Wilcoxon test).

When compared to the uninfected group by Wilcoxon, the serum levels of *IFN-α* (p=0.031), *IL-1β* (0.023), *IL-6* (p=0.018), *LE* (p=1.9e-05), along with *U_BACT* (p=0.00016) and *WBC count* (p=0.00016), were all significantly higher in infected group (Supplementary Figure 2). Although no statistical difference was evident, the levels of *IFN-γ*, *IL-17*, along with *red blood cell (RBC)*, in the infected group also showed a tendency to be higher in infected group (Table 2). Therefore, inflammatory responses were more serious in infected group, probably due to the presence of pro-inflammatory bacteria. Boxplot analysis of the 3 key significantly different cytokines between infected and uninfected revealed that their concentrations increased with disease exacerbation.

Urine samples obtained from the patients were sent for both clinical laboratory tests and mNGS testing. The mNGS test pipeline included cfDNA (cell-free DNA) extraction from urine, library preparation, sequencing, and comprehensive bioinformatics analysis relating to virulence genes, taxonomy and ARG profile (Figure 1).

The distribution of pathogens in patients undergoing CU

To investigate the important pathogens leading to UTI in patients with CU, we performed traditional cultures on samples of urine, skin swabs, and ureteral stents, from 50 patients. The detailed culture results from each sample are shown in the table below

TABLE 2 Characteristics of subjects.

Patients Characteristics	Uninfected (n=15)	Infected (n=35)	P	Normal Range	Characteristics type
Gender			–		**basic**
Male	12 (80%)	30 (86.0%)			
Female	3 (20%)	5 (14.0%)			
Age (years)	64 (47-80)	67 (57-82)	0.240		
IFN-a, pg/ml	1.43 (0.31-2.5)	1.83 (0.78-3.18)	**0.031**	0-8.5	**Cytokines detection**
IL-1β, pg/ml	1.77 (0-23.25)	8.97 (0-73.67)	**0.023**	0-12.4	
IL-6, pg/ml	4.00 (0.1-9.1)	8.30 (0.25-30.95)	**0.018***	0-5.4	
IFN-γ, pg/ml	6.10 (2.18-11.91)	6.50 (0.44-21.08)	0.920	0-23.1	
IL-10, pg/ml	0.83 (0.56-1.27)	0.91 (0.3-4.23)	0.700	0-12.9	
IL-12P70, pg/ml	0.21 (0-2.1)	0.06 (0-0.62)	0.550	0-3.4	
IL-17, pg/ml	1.57 (0.77-5.53)	2.08 (0.92-14.62)	0.120	0-21.4	
IL-2, pg/ml	0.61 (0-0.62)	0.77 (0-2.99)	0.480	0-7.5	
IL-4, pg/ml	0.64 (0.45-1.54)	0.63 (0-1.34)	0.140	0-8.56	
IL-5, pg/ml	1.98 (0.21-6.91)	2.14 (0-4.96)	0.380	0-3.1	
IL-8, pg/ml	8.72 (2.55-35.41)	9.31 (0-80.96)	0.320	0-20.6	
TNF-a, pg/ml	1.25 (0.04-4.35)	1.48 (0-7.36)	0.910	0-16.5	
Nitrite (NIT)	0 (0)	0.21 (0-1)	0.100	Negative (-)	**Urinalysis**
Leukocyte esterase (LE)	0.86 (0.5-2)	2.54 (1-4)	**0.000**	Negative (-)	
Bacteria count (U BACT), number/μl	179.82(0-881.8)	2613.64 (26.6-22218.4)	**0.000**	0-32.8	
Red blood cell count (RBC), number/μl	631.79(4.3-4729.7)	898.67 (0.1-9840.5)	0.750	0.2-13.8	
White blood cell count (WBC), number/μl	191.99(14.3-385.5)	2823.35 (7.5-36212.4)	0.000	0-7.1	

Data are presented as n (%) or means (range).
Bold and underlined number means P<0.05, Wilcoxon test.

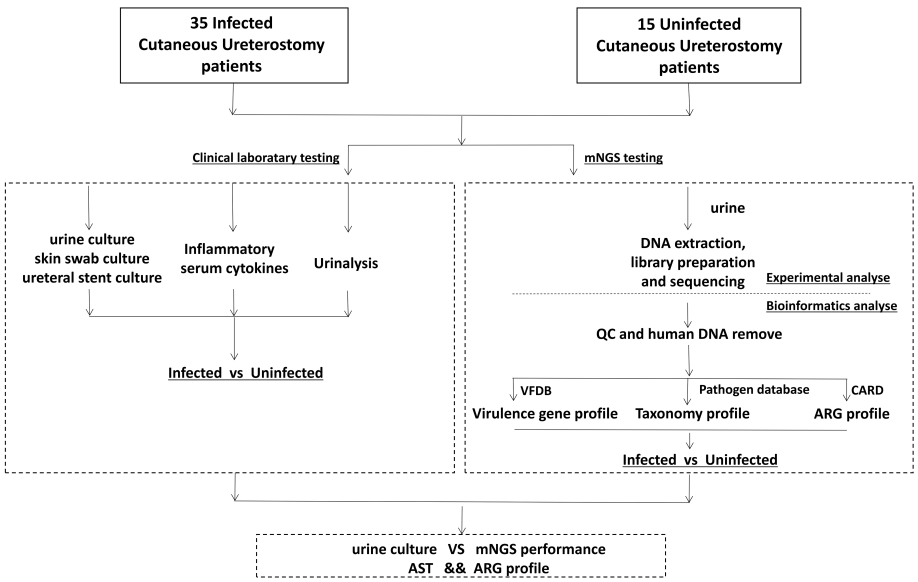

FIGURE 1
Schematic workflow of this study. Samples from 50 Cutaneous Ureterostomy patients were collected and sent for both conventional clinical laboratory testing and mNGS testing. We did Infected-vs-Uninfected difference analyse of urine culture, Inflammatory serum cytokines, virulence gene, taxonomy and ARG profile. Besides, comparation between urine culture and mNGS and association between ARG profile and Antibiotic Susceptible Test are performed.

(Supplementary Table S1). We also calculated the frequency of the positive microorganisms in all types of samples and ploted a column chart of 20 species which are culture positive at least in 2 samples in order to show differences between the two groups directly (Figure 2A). Analysis showed that the top three pathogens with positive frequencies in the three types of samples were *E. coli*, *K. pneumoniae*, and *E. faecalis* (Supplementary Table S2). Of these, the positive number of 17 species in the infected group was higher than that in the uninfected group, including *E. coli*, *K. pneumoniae*, *S. aureus*, *Proteus mirabilis*, and *Morganella morganii*. Six pathogens were positive only in the infected group: *P. mirabilis*, *E. cloacae complex*, *Neisseria mucosa*, *K. oxytoca*, *C. auri*, and *C. freundii* (Figure 2A). The presence of pathogens in uninfected group, including *E. coli*, *K. pneumoniae*, and *E. faecalis*, indicated that bacterial colonization also exists in normal urine. Therefore, we speculate that when the body's immune system is weakened, these pathogens can reproduce and cause infection. Interestingly, except for *Providencia rettger*, the other 19 microorganisms are all positive whether in urine, skin swabs or ureteral stents, which indicates that the pathogenic organisms in urine may easily originate from their surrounding environment for patients with CU.

mNGS performance comparing with clinical culture

DNA was extracted from urine samples and sequenced on the MGISEQ-2000 platform; 142.28 Gb of 50-bp single-end reads were generated in total, with an average of 45.17 ± 19.00 (standard deviation) million reads per sample. The data set for all samples was greater than 20M, which is a common data volume standard in mNGS research (Supplementary Table S3) (Liu et al., 2021). Based on foldchange >10 criteria for mNGS, mNGS exhibited high positive detection rate for pathogens in urine samples. Overall, the mNGS assay showed 91.4% sensitivity and 76.3% specificity compared to clinical culture (Supplementary Table S4, Figure 2B). The reason for the low specificity may be the negative results of clinical culture. In total 265 cases were classified as mNGS false-positive, and 78% of cases happen in the infected group (Supplementary Table S5; Figure 2B). There were four species with accuracy above 90%, *C. auris, Staphylococcus epidermidis, Staphylococcus haemolyticu* and *S. aureus*, and *C. auris* with the highest accuracy of 98%. The sensitivity, specificity and accuracy for each clinically culture positive pathogens are specifically shown in Figure 2C.

In a word, mNGS showed possibility to help clinician diagnose UTI but it is still a challenge to distinguish between colonizing bacteria and infectious bacteria whether for mNGS or culture.

Microbiome diversity change

First of all, rarefaction curve analysis was carried out to evaluate whether the sequence size or sample size was complete or incomplete. The curve in each group is near smooth when the sequencing data are great enough with few new species undetected (Figure 3A). To evaluate the diversity change and exclude the confounding factors like gender, batch effect, underlying disease, we performed PerMANOVA analyze and the variance explained by gender (P=0.02, Supplementary Table S6) were greater than by other potential cofounders and disease status (P=0.22 and 0.13,

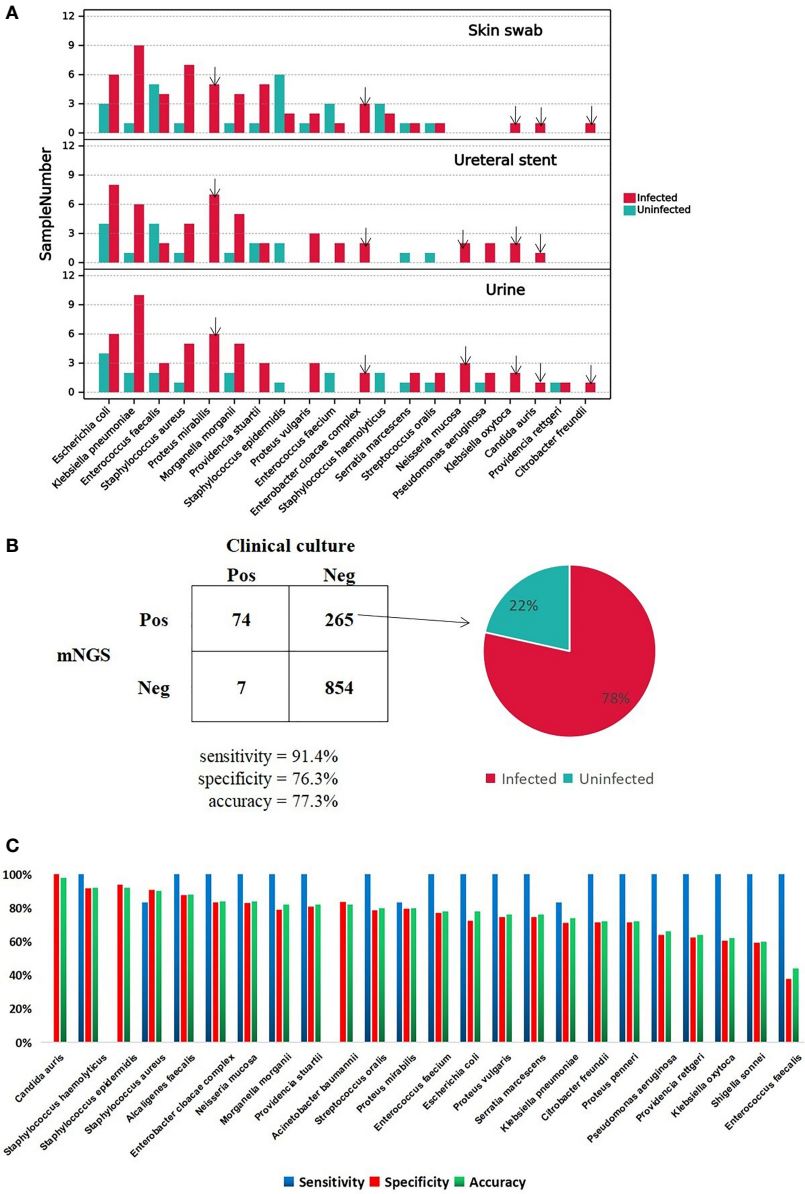

FIGURE 2
A Major positive microorganism of Clinical culture in Skin swab, Ureteral stent and Urine. The arrow marks the species detected only in Infected group. **B** The comparison of performance between Clinical culture and mNGS. The pie chart shows the proportion of false-positive microorganism identified by mNGS in Infected group versus uninfected group. **C**. The mNGS performance of each pathogen comparing with clinical culture.

respectively, Supplementary Table S6). Next, we conducted an analysis of microbial changes at the community level between infected group and uninfected group among 42 male samples (30 infected and 12 uninfected). The Chao1 index and Simpson index analyzes showed that there was no significance in infected group versus uninfected group at the genus level (PerMANOVA, P=0.073 and 0.86, respectively, Figures 3C, D). The Chao1 median index was higher in infected group which may indicate bacteria are more likely to increase in infected group. Beta diversity based on weighted principal coordinate analysis (PCoA) revealed that there was no different separation in infected group versus uninfected group (PerMANOVA, P=0.75, Figure 3B). Then, we performed a Lefse analysis to identify differentially enriched taxa in both groups. By LDA>3 cutoff, we got 65 significant biomarkers (Supplementary Table S7) in total and 22 were at species level presented in Figure 3E. Three were observed in the infected group (*E. clbacae, K. oxytoca* and *C. freundii*) and nineteen in uninfected group as follows: *C. acnes, Human polyomavirus 2, Ralstonia insidiosa, Staphylococcus hominis, Staphylococcus epidermidis, Ralstonia pickettii, Burkholderia multivorans, Staphylococcus warneri, Moraxella osloensis, Burkholderia cepacia, Gordonia bronchialis, Gordonia paraffiniivorans, Corynebacterium tuberculostearicum, Corynebacterium pseudogenitalium, Malassezia restricta, Methyotenera mobilis, Paraburkholderia fungorum* and *Burkholderia pyrrocinia*. Most of the uninfected enriched microorganisms were from environment.

We conducted a correlated analysis between the differentially taxa and clinical variables using Mantel test. As is shown in Figure 4 and

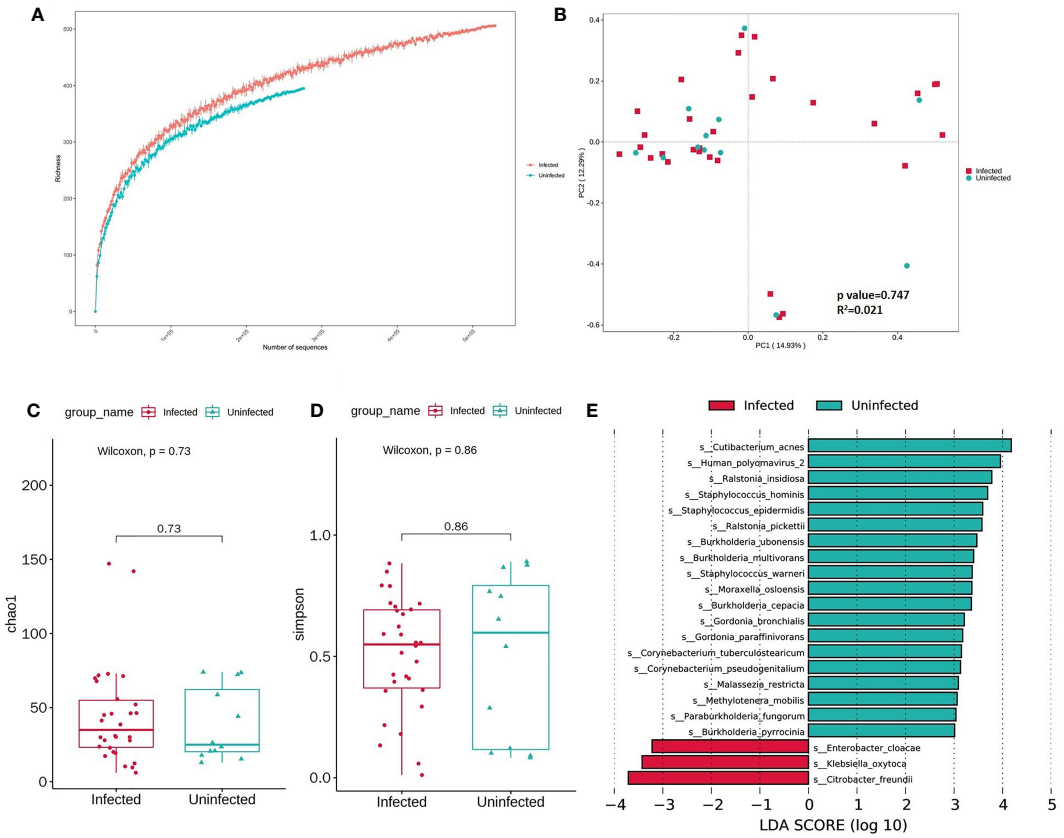

FIGURE 3
(A) Rarefaction curves for species number in Infected(n=35) and Uninfected (n = 15) after 100 random sampling. The curve in each group is near smooth when the sequencing data are great enough with few new species undetected. **(B)** Weighted Principal Coordinate Analysis (PCoA) using Bray-Curtis distance based on the relative abundance in 50 samples. Significant differences across groups are established at the first principal component (PC1) values and PC2, and shown in the box plots above. (Wilcoxon, P=0.747, R2 = 0.021). **(C, D)** Comparison of α diversity (as accessed by Chao1 index and Simpson index) based on the genus profile in two groups for Chao1 index, P=0.73; for Simpson, P=0.86. P values are from Wilcoxon test. **(E)** Boxplot of 22 differentially enriched species across Infected and Uninfected group based on Lefse.

Supplementary Table S8, Infected-enriched *E. cloacae* were significantly correlated with IL-6 and IL-10 (IL-10 = 0.16, P< 0.05, IL-6 = 0.18, P< 0.05). Besides, Infected-enriched *K. oxytoca* were significantly correlated with IL-1β (IL-1β=0.15, P<0.05). For Uninfected-enriched biomarkers, the Mantel test result are as follows: *G. bronchialis*: rIL-4 = 0.28, P<0.05; *G. paraffinivorans:* rIL-5 = 0.24, P< 0.05; *M. osloensis:* rIL-4 = 0.13, P<0.05; *R. pickettii:* rIL-8 = 0.09, P<0.05; *S. hominis:* IL-4 = 0.15, P<0.05; *S. warneri:* rIL-12P70 = 0.26, P<0.05). These findings suggested that the Lefse biomarkers were related to ILs level which may be associated with CU infection.

Virulence factors comparation

To survive in a hostile host environment, pathogenic bacteria tend to establish infections by deploying VFs (Ünal and Steinert, 2014). We compared the VFs among three groups. Through unweighted analysis, the VFs gene number were significantly increased in Infected group compared with Uninfected group (P=0.017, Figures 5A, C). Through weighted analysis, the abundance of VFs was increased in the Infected group compared with Uninfected group (P=0.12, Figure 5B). The abundance of VFs in both Infected group and Uninfected group were significantly more than controls (P<0.05, Figures 5B, D). We identified 39 significantly enriched VFs among three groups *via* LEFSE, including 30 VFs in Infected group, 5 VFs in Uninfected group and 4 VFs in controls (Figure 5E). In Infected group, most of the enriched VFs were assigned as *Capsule*, *Flagella*, *pyoverdine*, *TTSS* and so on. The main contributors to the enriched VFs were *P. aeruginosa, K. pneumoniae* and *E. faecalis*. In Uninfected group, the enriched VFs were assigned as *Flagella*, *Capsule I*, *Esp* and *Enterobactinthe*. The main contribution to the enriched VFs was *Burkholderia pseudomallei*. In controls, the enriched VFs were assigned as *Flagella*, *AcrAB* and *xcp secretion system*. The main contribution to the enriched VFs was *B. pseudomallei* (Supplementary Table S9). In a word, the more VFs the more serious infection.

ARGs comparation

When comparing to Uninfected group and controls, the numbers of ARGs were significantly increased in Infected group (Figures 6A, B). The total abundance of ARGs was also insignificantly increased in Infected group when compared to Uninfected group. The abundance of ARGs assigned to each drug class was also higher in Infected group than Uninfected group. Among them, the abundance of

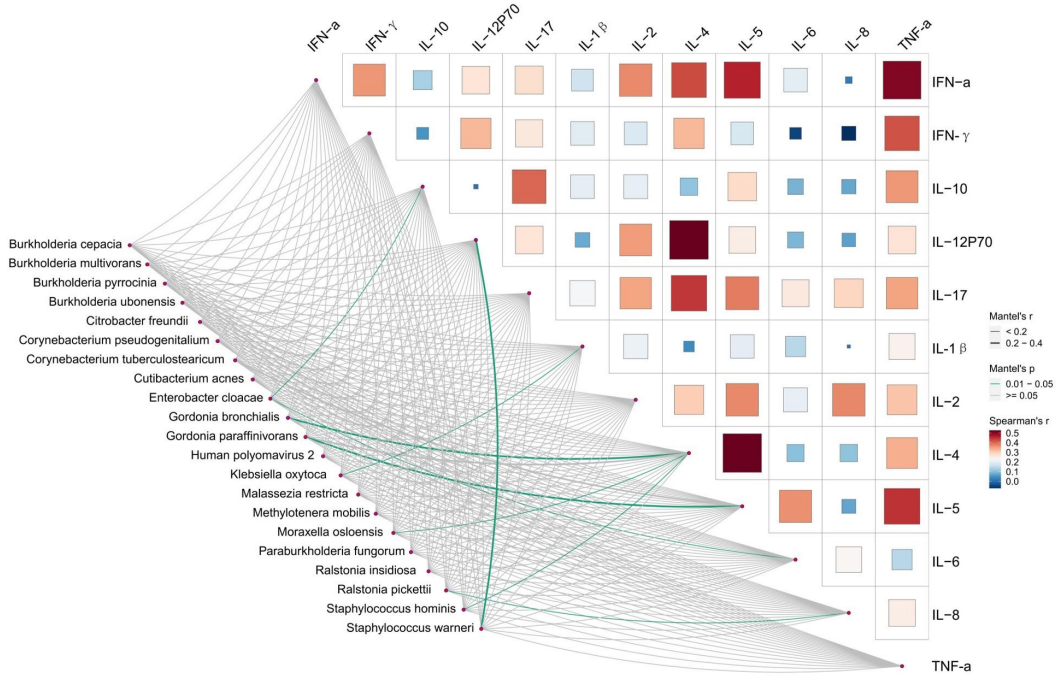

FIGURE 4
Relationships between Inflammatory factors and microbiome diversity. Pairwise comparisons of Inflammatory factors with a color gradient denoting Spearman's correlation coefficients. Taxonomic groups were related to each Inflammatory factors by mantel test. Green line indicates the significant relationship and gray line indicates the unsignificant relationship. Line width means the weight of regression coefficient.

Fluoroquinolones, betalatmas, Fosfomycin, Phenicol, Phenolic compound resistance were significant higher in Infected group (Figure 6C). We performed a Procrustes analysis in order to demonstrate the associations between ARGs and microbial composition. The analysis revealed a significant correlation (P = 0.001, 9999 permutations) between ARGs profiles and species-based microbial community composition, with the Procrustes sum of squares M2 = 0.5382 (Figure 6D).

Discussion

In this study, we aim to evaluate the mNSG performance comparing with traditional culture for infected or uninfected patients undergoing CU. Benchmarking clinical culture, the total sensitivity is 91.4% and specificity is 76.3% for mNGS. According to the intersection microorganism profile among urine, swabs and ureteral stent samples, pathogenic organisms in the urine may originate from their surrounding environment. Inflammatory factors like IL-6, IL-1β, and IFN-a or microorganisms biomarkers *C. freundii, K. oxytoca*, and *E. cloacae* need further research for indicating infection and constructing UTI diagnostic model of patients with CU. VFs and ARGs increase in infected group may have bad effect on clinical treatment for patients.

The incidence and risk factors of UTI

Some underlying host factors are known to exert influence on the etiology of UTI and may complicate UIT, including age, diabetes, spinal cord injury, and catheterization (Ronald, 2003). In our study patients undergoing CU with chronic underlying diseases have a higher risk of infection. There are few studies in existing literatures relating to the rate, risk factors and common pathogens of UTI in patients undergoing CU. Given the large differences in the incidence of UTI and the high rate of asymptomatic bacteriuria reported in the literature (Mano et al., 2014; Ghoreifi et al., 2020; Gayarre Abril et al., 2021), it follows that UTI needs to be clearly defined in order to better define the specific form of UTI in this unique patient population so that we can treat this condition appropriately. In terms of risk factors, it is not yet confirmed if coexisting diabetes increases the risk of UTI. A previous study of 1248 patients with different urinary diversion types showed that the presence of diabetes increased the risk of UTI after RC (Parker et al., 2016). However, another study, involving patients with an orthotopic neobladder (ONB), showed that age, gender, Charlson Comorbidity Index (CCI), perioperative chemotherapy, and diabetes are not associated with UTI (Mano et al., 2014). However, another study showed that none of these were risk factors except for CCI (Clifford et al., 2018). Generally, the incidence of UTI is higher in women. As bladder cancer is known to be more prevalent in males and our study sample size was limited, our results showed that males had a higher risk of infection.

The relationship between cytokines and UTI

As a family of cytokines, interleukins play a hugely significant part in the regulation of the immune system. Secreted by white blood cells and the epithelial cells of the urinary tract, IL-6 is a highly sensitive and specific biomarker for UTI and is a known response to

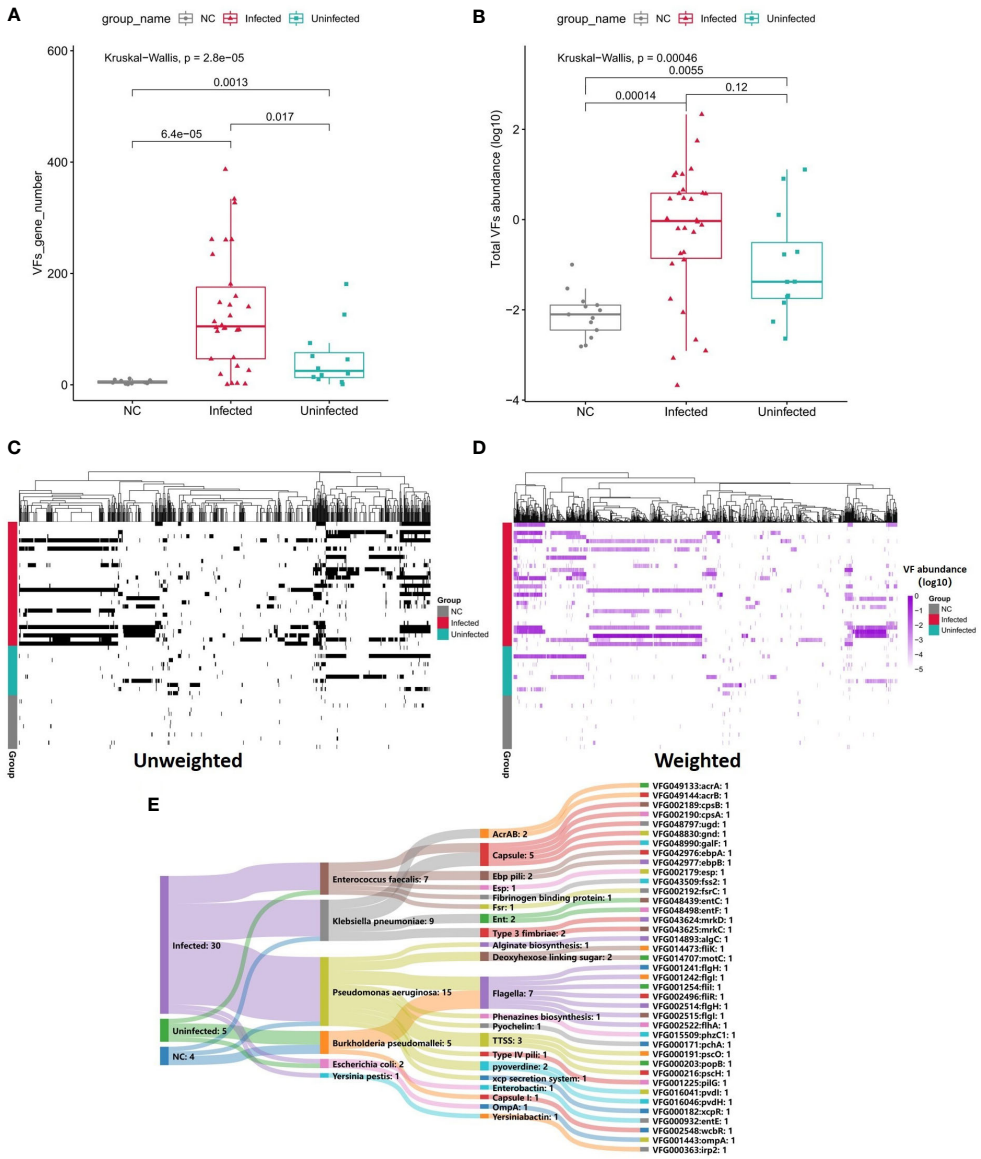

FIGURE 5
(A) Boxplot shows the number of VFs among three groups. P values are from Wilcoxon test. **(B)** Boxplot shows the LOG10-based abundance of VFs among three groups. P values are from Wilcoxon test. **(C)** Heatmap (unweighted) shows the association between VFs and samples. Black shows the identification of the VF while white shows no identification of the VF. **(D)** Heatmap (weighted, MaxAbs method) shows the association between VFs and samples. Shades of purple shows the abundance of the VF, the deeper the color, the higher the abundance. The normalization was through MaxAbs method. That is, the abundance of each gene is divided by the absolute value of the maximum VF abundance in all samples, and then log10 is further taken. VF even abundance=log (VF abundance/|Max VF abundance|). As for VF abundance=0, VF even abundance=-5. **(E)** Sankey map for differential VFs, Based on VF abundance profile, set LDA=3 to screen the enriched VFs in Infected group, Uninfected group and controls, and set VFs annotation information (VFs type, species attribution) in VFDB database.

inflammation (Yang et al., 2021). In the immune response to UTI, IL-6 and IL-8 are activated and released (Klarström Engström et al., 2019); both of these are associated with the severity of UTI (Sundén et al., 2017). Both Sheu (Sheu et al., 2006) and Gurgoze (Gürgöze et al., 2005) confirmed that the serum levels of IL-6 in patients with pyelonephritis were obviously higher than lower urinary tract infection (L-UTI) patients or healthy individuals. In another study. Olszyna reported that the concentrations of IL-8 in patients with positive urine cultures were significantly higher than those of healthy subjects (Olszyna et al., 2001). Another researcher confirmed that serum levels of IL-6 were more sensitive and specific than IL-8 for the diagnosis of pyelonephritis (Sheu et al., 2007). Conversely, Krzemien did not observe a discrepancy between urinary IL-6 and IL-8 concentrations between patients with pyelonephritis and L-UTI (Krzemień et al., 2004). Il-1 β, a sub-type of IL-1, which is found at high levels in various body fluids, such as the serum, urine, and synovial fluid, is known to be involved in the regulation of the immune system. IL-1β is considered as a candidate biomarker to distinguish upper urinary tract infection (U-UTI) from L-UTI (Masajtis-Zagajewska and Nowicki, 2017). Other research has shown that several cytokines (TNF-α, IL-8, IL-6, and IL1B) can significantly promote the growth of uropathogenic *E. coli* (UPEC) (Engelsöy et al., 2019; Demirel et al., 2020). The inhibition of NF-KB can lead to the long-term colonization of UPEC in the bladder;

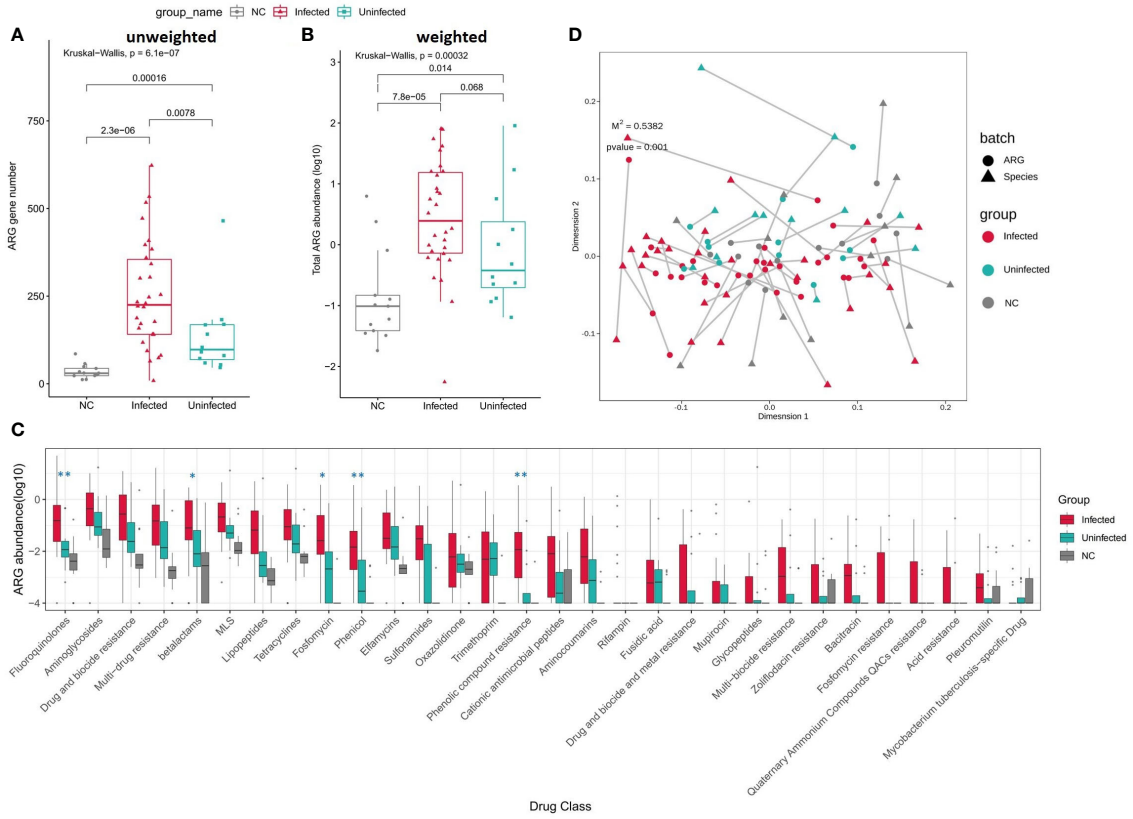

FIGURE 6
(A) Boxplot shows the number of ARGs among three groups. P values are from Wilcoxon test. **(B)** Boxplot shows the LOG10-based abundance of ARGs among three groups. P values are from Wilcoxon test. **(C)** Boxplot shows the LOG10-based abundance of ARGs of each drug class among three groups. (Wilcoxon,*: 0.01<p<0.05,** :p<0.01) **(D)** Procrustes analysis of the correlation between ARG profiles and species community structure on the base of Bray-Curtis matrices.

moreover, RELA and NFKB1 can be activated by UPEC colonization (Liu et al., 2015). Similar to these published findings, we found that the levels of IL-6, IL-1β, and IFN-α were significantly increased in the infected group. Further analysis should attempt to correlate these factors with other indicators or changes in the flora in order to better apply these promising biomarkers.

Statistical analysis of pathogenic detection by clinical culture

Bacteriological cultures of urine are usually positive for aerobic or fast-growing organisms, such as *E. coli* and *E. faecalis* (Foxman, 2014). UPEC utilize multiple chaperone–usher pathway pili tipped with adhesins with diverse receptor specificities to colonize various host tissues and habitats (Kalas et al., 2018). A retrospective analysis of 1133 patients after RC (Clifford et al., 2018) identified the same top three pathogens as we did in the present study; these pathogens also existed in the uninfected group. We therefore speculate that these organisms would multiply and cause infection when the body's immunity was low or when the balance of the flora was disrupted. In addition, we found that most of the bacteria cultured in urine also existed in skin swabs and ureteral stents, thus indicating that the pathogenic organisms in urine may originate from their surrounding environment. Therefore, on one hand, we need to focus on the skin around the stoma, as this can be colonized by a diverse milieu of organisms depending on the topographical location, endogenous host factors, and exogenous environmental factors relating to the ecology of the skin surface. Usually most of these organisms are harmless or even beneficial to their host unless common skin disorders or some external intervention occurs (Grice and Segre, 2011). If a patient presents with peristomal skin complications, the balance in the flora may be disrupted, thereby increasing the risk of UTI. On the other hand, patient health education should be enhanced; they should be instructed to pay more attention to hand hygiene when changing stoma bags daily. Furthermore, stoma bags should not be used for long periods of time. By performing these simple tasks, it is possible to reduce the risk of bacterial invasion and colonization.

Potential of mNGS for assisting UTI diagnose

Many reports have shown that mNGS has higher levels of sensitivity than traditional culture for certain sample types, such as blood, cerebrospinal fluid, and bronchoalveolar lavage fluid (Blauwkamp et al., 2019; Liu et al., 2019). However, few studies have attempted to use mNGS on urine samples and compared results

to traditional culture methods. In our study, the total sensitivity is 91.4% for mNGS while the specificity is just 76.3%.For example, *E. faecalis*, possibly colonized bacteria in urine, Top1 false positive species in our study (Table S5) which is positive just in 5 samples for culture, but in mNGS besides the 5sample, another 28 samples are positive and Infected: Uninfected is 20:8 which is possibly be explained by culture false negative. The other mNGS false positive microorganisms, like *Shigella sonnei*, just have the same phenomenon. Totally,78% false positive cases happen in infected group, and is accepted by clinician which suggests that mNGS could have a high potential for assisting UTI diagnose. What's more, mNGS can comprehensively provide a wide range of data on the status of the microenvironment in the urinary tract along with data relating to genotype drug resistance in the diagnosis of UTI (Dixon et al., 2020).

A comparison of virulence factors

The reason why pathogens can invade a host and reproduce is due to the complex coordination of VFs. Bacterial virulence factors are usually proteins that enable pathogens to parasitize a host, including gene products associated with adhesion, invasion, secretory systems, toxins, and iron uptake systems (Chen et al., 2012). These virulence factors play a role in bacterial adhesion, invasion, and escape from the host's immune defense, thus enabling them to survive, replicate, and even form and maintain biofilms in the host (Ruer et al., 2015; Mühlen and Dersch, 2016). In the infected group, we found the significant increase of VFs abundance and most of them belonging to *P. aeruginosa*, *E. faecalis*, *K. pneumoniae* including TTSS, HSI.I, Phenazines, and Pyochelin, and VFs in the infected group were mainly related to the secretion system and iron absorption. The secretory system is one of the secretory pathways for VFs and plays a significant role in bacterial pathogenicity. The specific proteins produced by these VFs can be directly introduced into host cells to cause infection. Iron is an indispensable element for the growth of most organisms. Studies have indicated that an increase in the efficiency of the bacterial iron intake system to obtain iron is the main factor responsible for an increase in bacterial virulence; the pathogenicity of bacteria is strongly related to the ability of bacteria to take up iron (Shon et al., 2013). The analysis revealed the enriched VFs in the infected group were mostly *P. aeruginosa* and *E. faecalis* in our study. A previous study demonstrated that the main mechanism responsible for the action of *P. aeruginosa* was intimately associated with the multitype secretion system it encodes, including the type II secretion system (T2SS), type III secretion system (T3SS), type VI secretion system (T6SS), and quorum sensing (QS) system (Golovkine et al., 2017). The 6.3 Mbp genome of *P. aeruginosa* also provides a richer gene pool, and greater virulence, than other pathogens; this is the reason why the virulence genes in the infected group belonged to *P. aeruginosa*. Generally, *E. faecalis* is related to polymicrobial infections of the urinary tract and surgical wound sites. Moreover, the secretion of L-ornithine by *E. faecalis* can stimulate *E. coli* biofilms to grow and survive. Furthermore, under iron limiting conditions, L-ornithine be used by *E. coli* to synthesize the enterobacterium siderophore, thus resulting in the growth of *E. faecalis* and the formation of biofilm (Keogh et al., 2016).

Drug resistance

Technologies such as NGS are expanding our abilities to detect and study antimicrobial resistance (Boolchandani et al., 2019). Whole-genome sequencing (WGS) studies of *E. coli*, *Enterococcus* spp., *K. pneumoniae*, and *Salmonella enterica serovar Typhimurium* have proved that it is possible to predict resistance phenotypes either by rule-based strategies or by machine learning (Kos et al., 2015; Khaledi et al., 2020). mNGS can improve the detection of pathogens that can easily be missed by clinicians or by traditional culture tests (Ramachandran and Wilson, 2020). Resistance phenotype could be mediated by protein homolog model features, like betalactams *KPC* conferring resistant to carbapenem, protein variant model features, like *P. aeruginosa oprD* variants conferring resistant to carbapenem and *gyrA* variants conferring resistance to quinolones, protein overexpression model features, like efflux pump complex *MexZ* conferring antibiotic resistance to erythromycin in *E. coli*. After infection, ARGs belonging to several drug-class are increased in infected group including those clinical concerned carbapenemase/ESBL genes among Gram-negative bacteria or mecA/C among *S. aureus* and in the future we could possibly use mNGS to monitor those in ARGs profile of CU patients so as to rationally guide the use of antibiotic.

Conclusion

mNGS, with high sensitivity, could provide a more accurate and fast evidence for helping UTI diagnosis in patients with CU and allow us to monitor the microbial, VFs and ARGs changes in the urine of these patients and improve treatment.

Limitation

We acknowledge the limitations of our research. First of all, the population of patients show a less diversity and representativeness owing to the subjects were obtained from one hospital. Secondly, there is a lack of unified definition of UTI, especially for complex situations or special populations, such as Cu patients. UTI needs to be clearly defined to better describe the actual UTI rate and treat it in time. The study population have a recurrent UTI with a high incidence, but we didn't perform a longitudinal study, which is one of the directions that can be studied in the future.

Data availability statement

The datasets presented in this study can be found in NCBI Sequence Read Archive (SRA), and the accession number is PRJNA779226.

Ethics statement

The studies involving human participants were reviewed and approved by Ethics Committee of the First Affiliated Hospital of

Nanchang University. The patients/participants provided their written informed consent to participate in this study.

Author contributions

RH wrote the manuscript, and RH and QY both performed and completed the whole experiment, and they were also responsible for data collection. JG analyzed the data and participated in the discussion of drug resistance genes. YL, XJ, LT, and YC contributed to conception and design of the study. YL, LT, and YC directed and supervised all of the research. All authors contributed to the article and approved the submitted version.

Funding

Science and Technology Department Foundation of Jiangxi Province (No: 20202BBGL73090).

Acknowledgments

The authors would like thank all the subjects, their families, and collaborating clinicians for their participation. The biospecimens used in this study were provided by The First Affiliated Hospital of Nanchang University. RH, QY, and JG contributed equally to this study. Besides, we thank Guanhua Rao, Lijuan Yuan, Ming Wu for helpful discussions on this work.

Conflict of interest

JG was employed by Genskey Medical Technology Co., Ltd.

The remaining authors declare that the research was conducted in the absence of any commercial or financial relationships that could be construed as a potential conflict of interest.

Publisher's note

Supplementary material

The Supplementary Material for this article can be found online at: https://www.frontiersin.org/articles/10.3389/fcimb.2023.991011/full#supplementary-material

SUPPLEMENTARY FIG 1

A, B, Composition ratio of the infected and uninfected samples considering underlying diseases influence (A) and gender (B).

SUPPLEMENTARY FIG 2

Boxplot of 6 significantly different Urinalysis and cytokines in serum (Wilcoxon, *: 0.01<p<0.05, ** :0.001<p<0.01, ***:0.0001<p<0.0001).

References

Alcock, B. P., Raphenya, A. R., Lau, T. T. Y., Tsang, K. K., Bouchard, M., Edalatmand, A., et al. (2020). CARD 2020: antibiotic resistome surveillance with the comprehensive antibiotic resistance database. *Nucleic Acids Res.* 48 (D1), D517–d525. doi: 10.1093/nar/gkz935

Bader, M. J., Zilinberg, K., Weidlich, P., Waidelich, R., Püls, M., Gratzke, C., et al. (2013). Encrustation of urologic double pigtail catheters-an ex vivo optical coherence tomography (OCT) study. *Lasers Med. Sci.* 28 (3), 919–924. doi: 10.1007/s10103-012-1177-1

Behzadi, E., and Behzadi, P. (2016). The role of toll-like receptors (TLRs) in urinary tract infections (UTIs). *Cent Eur. J. Urol* 69 (4), 404–410. doi: 10.5173/ceju.2016.871

Blauwkamp, T. A., Thair, S., Rosen, M. J., Blair, L., Lindner, M. S., Vilfan, I. D., et al. (2019). Analytical and clinical validation of a microbial cell-free DNA sequencing test for infectious disease. *Nat. Microbiol.* 4 (4), 663–674. doi: 10.1038/s41564-018-0349-6

Boolchandani, M., D'Souza, A. W., and Dantas, G. (2019). Sequencing-based methods and resources to study antimicrobial resistance. *Nat. Rev. Genet.* 20 (6), 356–370. doi: 10.1038/s41576-019-0108-4

Chen, L., Xiong, Z., Sun, L., Yang, J., and Jin, Q. (2012). VFDB 2012 update: toward the genetic diversity and molecular evolution of bacterial virulence factors. *Nucleic Acids Res.* 40 (Database issue), D641–D645. doi: 10.1093/nar/gkr989

Chen, L., Yang, J., Yu, J., Yao, Z., Sun, L., Shen, Y., et al. (2005). VFDB: a reference database for bacterial virulence factors. *Nucleic Acids Res.* 33 (Database issue), D325–D328. doi: 10.1093/nar/gki008

Chen, Y., Ye, W., Zhang, Y., and Xu, Y. (2015). High speed BLASTN: an accelerated MegaBLAST search tool. *Nucleic Acids Res.* 43 (16), 7762–7768. doi: 10.1093/nar/gkv784

Chen, H., Yin, Y., Gao, H., Guo, Y., Dong, Z., Wang, X., et al. (2020). Clinical utility of in-house metagenomic next-generation sequencing for the diagnosis of lower respiratory tract infections and analysis of the host immune response. *Clin. Infect. Dis.* 71 (Suppl 4), S416–s426. doi: 10.1093/cid/ciaa1516

Clifford, T. G., Katebian, B., Van Horn, C. M., Bazargani, S. T., Cai, J., Miranda, G., et al. (2018). Urinary tract infections following radical cystectomy and urinary diversion: a review of 1133 patients. *World J. Urol* 36 (5), 775–781. doi: 10.1007/s00345-018-2181-2

Cumberbatch, M. G. K., Jubber, I., Black, P. C., Esperto, F., Figueroa, J. D., Kamat, A. M., et al. (2018). Epidemiology of bladder cancer: A systematic review and contemporary update of risk factors in 2018. *Eur. Urol* 74 (6), 784–795. doi: 10.1016/j.eururo.2018.09.001

Demirel, I., Persson, A., Brauner, A., Särndahl, E., Kruse, R., and Persson, K. (2020). Activation of NLRP3 by uropathogenic escherichia coli is associated with IL-1β release and regulation of antimicrobial properties in human neutrophils. *Sci. Rep.* 10 (1), 21837. doi: 10.1038/s41598-020-78651-1

Dixon, M., Stefil, M., McDonald, M., Bjerklund-Johansen, T. E., Naber, K., Wagenlehner, F., et al. (2020). Metagenomics in diagnosis and improved targeted treatment of UTI. *World J. Urol* 38 (1), 35–43. doi: 10.1007/s00345-019-02731-9

Engelsöy, U., Rangel, I., and Demirel, I. (2019). Impact of proinflammatory cytokines on the virulence of uropathogenic escherichia coli. *Front. Microbiol.* 10. doi: 10.3389/fmicb.2019.01051

Farber, N. J., Faiena, I., Dombrovskiy, V., Tabakin, A. L., Shinder, B., Patel, R., et al. (2018). Disparities in the use of continent urinary diversions after radical cystectomy for bladder cancer. *Bladder Cancer* 4 (1), 113–120. doi: 10.3233/blc-170162

Flaig, T. W., Spiess, P. E., Agarwal, N., Bangs, R., Boorjian, S. A., Buyyounouski, M. K., et al. (2020). Bladder cancer, version 3.2020, NCCN clinical practice guidelines in oncology. *J. Natl. Compr. Canc Netw.* 18 (3), 329–354. doi: 10.6004/jnccn.2020.0011

Flores-Mireles, A. L., Walker, J. N., Caparon, M., and Hultgren, S. J. (2015). Urinary tract infections: epidemiology, mechanisms of infection and treatment options. *Nat. Rev. Microbiol.* 13 (5), 269–284. doi: 10.1038/nrmicro3432

Foxman, B. (2014). Urinary tract infection syndromes: occurrence, recurrence, bacteriology, risk factors, and disease burden. *Infect. Dis. Clin. North Am.* 28 (1), 1–13. doi: 10.1016/j.idc.2013.09.003

Gayarre Abril, P., Subirá Ríos, J., Muñiz Suárez, L., Murillo Pérez, C., Ramírez Fabián, M., Hijazo Conejos, J. I., et al. (2021). Urinary tract infection as the main cause of admission in cystectomized patients. *Actas Urol Esp (Engl Ed)* 45 (4), 247–256. doi: 10.1016/j.acuro.2020.10.001

Ghoreifi, A., Van Horn, C. M., Xu, W., Cai, J., Miranda, G., Bhanvadia, S., et al. (2020). Urinary tract infections following radical cystectomy with enhanced recovery protocol: A prospective study. *Urol Oncol.* 38 (3), 75.e79–75.e14. doi: 10.1016/j.urolonc.2019.12.021

Golovkine, G., Reboud, E., and Huber, P. (2017). Pseudomonas aeruginosa takes a multi-target approach to achieve junction breach. *Front. Cell Infect. Microbiol.* 7. doi: 10.3389/fcimb.2017.00532

Grice, E. A., and Segre, J. A. (2011). The skin microbiome. *Nat. Rev. Microbiol.* 9 (4), 244–253. doi: 10.1038/nrmicro2537

Gürgöze, M. K., Akarsu, S., Yilmaz, E., Gödekmerdan, A., Akça, Z., Ciftçi, I., et al. (2005). Proinflammatory cytokines and procalcitonin in children with acute pyelonephritis. *Pediatr. Nephrol.* 20 (10), 1445–1448. doi: 10.1007/s00467-005-1941-6

Hall, M., and Beiko, R. G. (2018). 16S rRNA gene analysis with QIIME2. *Methods Mol. Biol.* 1849, 113–129. doi: 10.1007/978-1-4939-8728-38

Horan, T. C., Andrus, M., and Dudeck, M. A. (2008). CDC/NHSN surveillance definition of health care-associated infection and criteria for specific types of infections in the acute care setting. *Am. J. Infect. Control* 36 (5), 309–332. doi: 10.1016/j.ajic.2008.03.002

Humphries, R. M., Kircher, S., Ferrell, A., Krause, K. M., Malherbe, R., Hsiung, A., et al. (2018). The continued value of disk diffusion for assessing antimicrobial susceptibility in clinical laboratories: Report from the clinical and laboratory standards institute methods development and standardization working group. *J. Clin. Microbiol.* 56 (8), e00437-18. doi: 10.1128/jcm.00437-18

Jing, C., Chen, H., Liang, Y., Zhong, Y., Wang, Q., Li, L., et al. (2021). Clinical evaluation of an improved metagenomic next-generation sequencing test for the diagnosis of bloodstream infections. *Clin. Chem.* 67 (8), 1133–1143. doi: 10.1093/clinchem/hvab061

Jin, Y., Zhou, W., Zhan, Q., Zheng, B., Chen, Y., Luo, Q., et al. (2021). Genomic epidemiology and characterization of methicillin-resistant staphylococcus aureus from bloodstream infections in China. *mSystems* 6 (6), e0083721. doi: 10.1128/mSystems.00837-21

Kalas, V., Hibbing, M. E., Maddirala, A. R., Chugani, R., Pinkner, J. S., Mydock-McGrane, L. K., et al. (2018). Structure-based discovery of glycomimetic FmlH ligands as inhibitors of bacterial adhesion during urinary tract infection. *Proc. Natl. Acad. Sci. U.S.A.* 115 (12), E2819–e2828. doi: 10.1073/pnas.1720140115

Kaufman, D. S., Shipley, W. U., and Feldman, A. S. (2009). Bladder cancer. *Lancet* 374 (9685), 239–249. doi: 10.1016/s0140-6736(09)60491-8

Keogh, D., Tay, W. H., Ho, Y. Y., Dale, J. L., Chen, S., Umashankar, S., et al. (2016). Enterococcal metabolite cues facilitate interspecies niche modulation and polymicrobial infection. *Cell Host Microbe* 20 (4), 493–503. doi: 10.1016/j.chom.2016.09.004

Khaledi, A., Weimann, A., Schniederjans, M., Asgari, E., Kuo, T. H., Oliver, A., et al. (2020). Predicting antimicrobial resistance in pseudomonas aeruginosa with machine learning-enabled molecular diagnostics. *EMBO Mol. Med.* 12 (3), e10264. doi: 10.15252/emmm.201910264

Klarström Engström, K., Zhang, B., and Demirel, I. (2019). Human renal fibroblasts are strong immunomobilizers during a urinary tract infection mediated by uropathogenic escherichia coli. *Sci. Rep.* 9 (1), 2296. doi: 10.1038/s41598-019-38691-8

Kos, V. N., Déraspe, M., McLaughlin, R. E., Whiteaker, J. D., Roy, P. H., Alm, R. A., et al. (2015). The resistome of pseudomonas aeruginosa in relationship to phenotypic susceptibility. *Antimicrob. Agents Chemother.* 59 (1), 427–436. doi: 10.1128/aac.03954-14

Krzemień, G., Roszkowska-Blaim, M., Kostro, I., Szmigielska, A., Karpińska, M., Sieniawska, M., et al. (2004). Urinary levels of interleukin-6 and interleukin-8 in children with urinary tract infections to age 2. *Med. Sci. Monit* 10 (11), Cr593–Cr597.

Langmead, B., and Salzberg, S. L. (2012). Fast gapped-read alignment with bowtie 2. *Nat. Methods* 9 (4), 357–359. doi: 10.1038/nmeth.1923

Liu, N., Kan, J., Cao, W., Cao, J., Jiang, E., Zhou, Y., et al. (2019). Metagenomic next-generation sequencing diagnosis of peripheral pulmonary infectious lesions through virtual navigation, radial EBUS, ultrathin bronchoscopy, and ROSE. *J. Int. Med. Res.* 47 (10), 4878–4885. doi: 10.1177/0300060519866953

Liu, Y., Mémet, S., Saban, R., Kong, X., Aprikian, P., Sokurenko, E., et al. (2015). Dual ligand/receptor interactions activate urothelial defenses against uropathogenic e. coli. *Sci. Rep.* 5, 16234. doi: 10.1038/srep16234

Liu, Z., Tian, Q., Xia, S., Yin, H., Yao, D., and Xiu, Y. (2016). Evaluation of the improved tubeless cutaneous ureterostomy technique following radical cystectomy in cases of invasive bladder cancer complicated by peritoneal metastasis. *Oncol. Lett.* 11 (2), 1401–1405. doi: 10.3892/ol.2015.4045

Liu, D., Zhou, H., Xu, T., Yang, Q., Mo, X., Shi, D., et al. (2021). Multicenter assessment of shotgun metagenomics for pathogen detection. *EBioMedicine* 74, 103649. doi: 10.1016/j.ebiom.2021.103649

Lu, J., Breitwieser, F. P., Thielen, P., and Salzberg, S. L. (2017). Bracken: estimating species abundance in metagenomics data. *PeerJ Comput. Sci.* 3, e104. doi: 10.7717/peerj-cs.104

Lu, J., Rincon, N., Wood, D. E., Breitwieser, F. P., Pockrandt, C., Langmead, B., et al. (2022). Metagenome analysis using the kraken software suite. *Nat. Protoc* 17 (12), 2815-2839. doi: 10.1038/s41596-022-00738-y

Mano, R., Baniel, J., Goldberg, H., Stabholz, Y., Kedar, D., and Yossepowitch, O. (2014). Urinary tract infections in patients with orthotopic neobladder. *Urol Oncol.* 32 (1), 50.e59–50.e14. doi: 10.1016/j.urolonc.2013.07.017

Masajtis-Zagajewska, A., and Nowicki, M. (2017). New markers of urinary tract infection. *Clin. Chim. Acta* 471, 286–291. doi: 10.1016/j.cca.2017.06.003

Miller, S., Naccache, S. N., Samayoa, E., Messacar, K., Arevalo, S., Federman, S., et al. (2019). Laboratory validation of a clinical metagenomic sequencing assay for pathogen detection in cerebrospinal fluid. *Genome Res.* 29 (5), 831–842. doi: 10.1101/gr.238170.118

Moustafa, A., Li, W., Singh, H., Moncera, K. J., Torralba, M. G., Yu, Y., et al. (2018). Microbial metagenome of urinary tract infection. *Sci. Rep.* 8 (1), 4333. doi: 10.1038/s41598-018-22660-8

Mühlen, S., and Dersch, P. (2016). Anti-virulence strategies to target bacterial infections. *Curr. Top. Microbiol. Immunol.* 398, 147–183. doi: 10.1007/82_2015_490

National Health and Family Planning Commission of the people's Republic of China (2016). *Laboratory diagnosis of urinary tract infections* (Beijing: National Health and Family Planning Commission of the people's Republic of China), WS/T 489-2016.

National Health Commission of the people's Republic of China, (2018). Specimen collection and transport for clinical microbiology testing, Beijing, WS/T 640–2018

Olszyna, D. P., Vermeulen, H., Baan, A. H., Speelman, P., van Deventer, S. J., Gouma, D. J., et al. (2001). Urine interleukin-8 is a marker for urinary tract infection in postoperative patients. *Infection* 29 (5), 274–277. doi: 10.1007/s15010-001-1157-z

Parker, W. P., Toussi, A., Tollefson, M. K., Frank, I., Thompson, R. H., Zaid, H. B., et al. (2016). Risk factors and microbial distribution of urinary tract infections following radical cystectomy. *Urology* 94, 96–101. doi: 10.1016/j.urology.2016.03.049

Ramachandran, P. S., and Wilson, M. R. (2020). Metagenomics for neurological infections - expanding our imagination. *Nat. Rev. Neurol.* 16 (10), 547–556. doi: 10.1038/s41582-020-0374-y

Ronald, A. (2003). The etiology of urinary tract infection: traditional and emerging pathogens. *Dis. Mon* 49 (2), 71–82. doi: 10.1067/mda.2003.8

Ruer, S., Pinotsis, N., Steadman, D., Waksman, G., and Remaut, H. (2015). Virulence-targeted antibacterials: Concept, promise, and susceptibility to resistance mechanisms. *Chem. Biol. Drug Des.* 86 (4), 379–399. doi: 10.1111/cbdd.12517

Segata, N., Izard, J., Waldron, L., Gevers, D., Miropolsky, L., Garrett, W. S., et al. (2011). Metagenomic biomarker discovery and explanation. *Genome Biol.* 12 (6), R60. doi: 10.1186/gb-2011-12-6-r60

Sheu, J. N., Chen, M. C., Cheng, S. L., Lee, I. C., Chen, S. M., and Tsay, G. J. (2007). Urine interleukin-1beta in children with acute pyelonephritis and renal scarring. *Nephrol. (Carlton)* 12 (5), 487–493. doi: 10.1111/j.1440-1797.2007.00819.x

Sheu, J. N., Chen, M. C., Lue, K. H., Cheng, S. L., Lee, I. C., Chen, S. M., et al. (2006). Serum and urine levels of interleukin-6 and interleukin-8 in children with acute pyelonephritis. *Cytokine* 36 (5-6), 276–282. doi: 10.1016/j.cyto.2007.02.006

Shon, A. S., Bajwa, R. P., and Russo, T. A. (2013). Hypervirulent (hypermucoviscous) klebsiella pneumoniae: a new and dangerous breed. *Virulence* 4 (2), 107–118. doi: 10.4161/viru.22718

Siddiqui, H., Nederbragt, A. J., Lagesen, K., Jeansson, S. L., and Jakobsen, K. S. (2011). Assessing diversity of the female urine microbiota by high throughput sequencing of 16S rDNA amplicons. *BMC Microbiol.* 11, 244. doi: 10.1186/1471-2180-11-244

Simner, P. J., Miller, S., and Carroll, K. C. (2018). Understanding the promises and hurdles of metagenomic next-generation sequencing as a diagnostic tool for infectious diseases. *Clin. Infect. Dis.* 66 (5), 778–788. doi: 10.1093/cid/cix881

Smelov, V., Naber, K., and Bjerklund Johansen, T. E. (2016). Letter to the Editor: Diagnostic criteria in urological diseases do not always match with findings by extended culture techniques and metagenomic sequencing of 16S rDNA. *Open Microbiol. J.* 10, 23–26. doi: 10.2174/1874285801610010023

Sundén, F., Butler, D., and Wullt, B. (2017). Triggered urine interleukin-6 correlates to severity of symptoms in nonfebrile lower urinary tract infections. *J. Urol* 198 (1), 107–115. doi: 10.1016/j.juro.2017.01.070

Sung, H., Ferlay, J., Siegel, R. L., Laversanne, M., Soerjomataram, I., Jemal, A., et al. (2021). Global cancer statistics 2020: GLOBOCAN estimates of incidence and mortality worldwide for 36 cancers in 185 countries. *CA Cancer J. Clin.* 71 (3), 209–249. doi: 10.3322/caac.21660

Ünal, C. M., and Steinert, M. (2014). Microbial peptidyl-prolyl cis/trans isomerases (PPIases): virulence factors and potential alternative drug targets. *Microbiol. Mol. Biol. Rev.* 78 (3), 544–571. doi: 10.1128/mmbr.00015-14

Wang, J., Qin, X., Guo, J., Jia, W., Wang, Q., Zhang, M., et al. (2020). Evidence of selective enrichment of bacterial assemblages and antibiotic resistant genes by microplastics in urban rivers. *Water Res.* 183, 116113. doi: 10.1016/j.watres.2020.116113

Wang, Z., Yang, Y., Yan, Z., Liu, H., Chen, B., Liang, Z., et al. (2020). Multi-omic meta-analysis identifies functional signatures of airway microbiome in chronic obstructive pulmonary disease. *Isme J.* 14 (11), 2748–2765. doi: 10.1038/s41396-020-0727-y

Whiteside, S. A., Razvi, H., Dave, S., Reid, G., and Burton, J. P. (2015). The microbiome of the urinary tract–a role beyond infection. *Nat. Rev. Urol* 12 (2), 81–90. doi: 10.1038/nrurol.2014.361

Witjes, J. A., Bruins, H. M., Cathomas, R., Compérat, E. M., Cowan, N. C., Gakis, G., et al. (2021). European Association of urology guidelines on muscle-invasive and

metastatic bladder cancer: Summary of the 2020 guidelines. *Eur. Urol* 79 (1), 82–104. doi: 10.1016/j.eururo.2020.03.055

Wolfe, A. J., Toh, E., Shibata, N., Rong, R., Kenton, K., Fitzgerald, M., et al. (2012). Evidence of uncultivated bacteria in the adult female bladder. *J. Clin. Microbiol.* 50 (4), 1376–1383. doi: 10.1128/jcm.05852-11

Yang, W., Liu, P., Zheng, Y., Wang, Z., Huang, W., Jiang, H., et al. (2021). Transcriptomic analyses and experimental verification reveal potential biomarkers and biological pathways of urinary tract infection. *Bioengineered* 12 (1), 8529–8539. doi: 10.1080/21655979.2021.1987081

Yang, J., Zhang, X., Xie, Y., Song, C., Sun, J., Zhang, Y., et al. (2017). Ecogenomics of zooplankton community reveals ecological threshold of ammonia nitrogen. *Environ. Sci. Technol.* 51 (5), 3057–3064. doi: 10.1021/acs.est.6b05606

Zhao, R., Yu, K., Zhang, J., Zhang, G., Huang, J., Ma, L., et al. (2020). Deciphering the mobility and bacterial hosts of antibiotic resistance genes under antibiotic selection pressure by metagenomic assembly and binning approaches. *Water Res.* 186, 116318. doi: 10.1016/j.watres.2020.116318

frontiers | Frontiers in Cellular and Infection Microbiology

TYPE Case Report
PUBLISHED 02 February 2023
DOI 10.3389/fcimb.2023.1115268

OPEN ACCESS

EDITED BY
Pushpanathan Muthuirulan,
Harvard University, United States

REVIEWED BY
Kin-Ming (Clement) Tsui,
University of British Columbia, Canada
Çağrı Ergin,
Pamukkale University, Türkiye

*CORRESPONDENCE
Jian Xu
xujianqu@163.com

†These authors have contributed equally to this work

SPECIALTY SECTION
This article was submitted to Clinical Microbiology, a section of the journal Frontiers in Cellular and Infection Microbiology

RECEIVED 03 December 2022
ACCEPTED 23 January 2023
PUBLISHED 02 February 2023

CITATION
Xu L, Chen X, Yang X, Jiang H, Wang J, Chen S and Xu J (2023) Disseminated *Talaromyces marneffei* infection after renal transplantation: A case report and literature review.
Front. Cell. Infect. Microbiol. 13:1115268.
doi: 10.3389/fcimb.2023.1115268

Disseminated *Talaromyces marneffei* infection after renal transplantation: A case report and literature review

Liang Xu[1†], Xiuxiu Chen[2†], Xuying Yang[3†], Hongtao Jiang[1], Jianli Wang[1], Shaowen Chen[4] and Jian Xu[1*]

[1]Department of Organ Transplantation, The Second Affiliated Hospital of Hainan Medical University, Haikou, China, [2]The Department of Breast and Thyroid Surgery, The Second Affiliated Hospital of Hainan Medical University, Haikou, China, [3]Department of Scientific Affairs, Hugobiotech Co., Ltd., Beijing, China, [4]Department of Clinical Laboratory, The Second Affiliated Hospital of Hainan Medical University, Haikou, China

We reported a 31-year-old man who received renal transplantation for more than 2 years. He was admitted to our hospital on 9 March 2022 due to intermittent diarrhea accompanied by leukopenia for more than 1 month. The patient successively developed high fever, cough, anemia, weight loss, gastrointestinal bleeding, and liver function impairment. Computed tomography (CT) revealed a slight inflammation in the lower lobes of both lungs, enlargement of the lymph nodes in the retroperitoneal and the root of mesenteric areas, and hepatosplenomegaly. *Talaromyces marneffei* was detected by metagenomics next-generation sequencing (mNGS) in blood and bronchoalveolar lavage fluid, and the pathogen was subsequently verified by blood culture. After endoscopic hemostatic therapy and antifungal therapy with voriconazole and amphotericin B cholesteryl sulfate complex, the patient was successfully discharged. Oral voriconazole was given regularly after discharge. Diarrhea, fever, enlargement of the lymph nodes, and endoscopic evidence of erosion may indicate intestinal *T. marneffei* infection. Although the mortality of *T. marneffei* infection after renal transplantation is very high, timely and effective antifungal therapy with amphotericin B cholesteryl sulfate complex is still expected to improve its prognosis.

KEYWORDS

***Talaromyces marneffei*, renal transplantation, clinical characteristics, antifungal drug, prognosis**

Introduction

Talaromyces marneffei (*T. marneffei*), formerly known as *Penicillium marneffei*, is the third most common opportunistic pathogen and the only temperature-dependent dimorphic fungus in the genus *Talaromyces*. This pathogen grows in the filamentous form at 25°C and in the yeast form at 37°C. It is mainly prevalent in Southeast Asia and South China

(Yinget al., 2020; Sun et al., 2021; Li et al., 2022; Shi et al., 2022), with a mortality rate of up to one-third (Narayanasamy et al., 2021). In recent years, along with an increase in the frequency of organ transplantation, *T. marneffei* infections have been increasingly reported, and the affected area has a tendency to expand (He et al., 2021; Shen et al., 2022). *T. marneffei* mainly invades *via* the respiratory tract and then spreads to other tissues and organs of the body, including the reticuloendothelial system, skin, and gastrointestinal tract. Cases of *T. marneffei* infection with the digestive tract as original infection site are rare (Zhou et al., 2021). To the best of our knowledge, this is the first case report of *T. marneffei* caused by intestinal infection as the first symptom after renal transplantation. In this paper, we retrospectively analyzed the successful treatment experience of disseminated *T. marneffei* infection *via* digestive tract after renal transplantation. Furthermore, we summarized the clinical characteristics and treatment of *T. marneffei* infection in combination with the relevant literatures.

Case description

A 31-year-old man living in Hainan, China was admitted to the Second Affiliated Hospital of Hainan Medical University on 9 March 2022 due to low back pain with intermittent diarrhea for more than 1 month. He previously underwent renal transplantation in our hospital on 10 September 2021 due to uremia and was chronically treated with tacrolimus and mycophenolate enteric-coated tablets combined with methylprednisolone for maintenance of immune suppression therapy after surgery. His baseline serum creatinine (Cr) was 300 μmol/L. He had no history of AIDS, and time-zero biopsy of the transplanted kidney revealed no infection. On admission, no lesions were observed in the patient's skin, and blood routine showed the following results: white blood cell (WBC), 0.71×10^9/L; hemoglobin (Hb), 88 g/L; blood Cr, 435 μmol/L; procalcitonin (PCT), 17.49 ng/ml; and C-reactive protein (CRP), 463.2 mg/L. Magnetic resonance imaging (MRI) of lumbar vertebra showed Schmorl's node formation at the upper edge of the L3–5 vertebral body; multiple enlarged lymph nodes were found in the retroperitoneum. On admission, the patient was immediately empirically given piperacillin tazobactam sodium (4.5 g thrice daily) combined with caspofungin (50 mg once daily) for anti-infection treatment, as well as antidiarrheal, leukocyte-elevating treatment, suspension of mycophenolate enteric-coated tablets, and other treatments. The patient's diarrhea symptoms were relieved, WBC gradually returned to normal, PCT and CRP were decreased within 4 days after hospitalization, but he still had low back pain.

Bone marrow aspiration biopsy (right ilium and sternum) on 14 March 2022 revealed active hyperplasia of the myelogram with significant hyperplasia of the granulocytic lineages, left shift of nuclei, both erythroid lineages and megakaryocytic hyperplasia, and visible platelets. On 16 March 2022, the patient presented with a sudden onset of high fever (39.2°C) accompanied by a small amount of melena. Blood biochemical tests on 9 March 2022 revealed the following results: alanine aminotransferase (ALT), 37 U/L; aspartate aminotransferase (AST), 124 U/L; blood Cr, 469 μmol/L; PCT, 4.7 ng/ml; and CRP, 106 mg/L. The 1,3-β-glucan test revealed negative results (55.51 pg/ml). CD4+ T-cell count was 48/μl. Fecal occult blood test was weakly positive. CT on 17 March 2022 showed a little inflammation in the lower lobes of both lungs, lymphadenopathy in the retroperitoneum and mesenteric root, and hepatosplenomegaly (Figures 1A, B). The antibiotic regimen was changed to meropenem (1 g thrice daily), caspofungin (50 mg once daily), and ganciclovir (0.25 g twice daily). The patient still had irregular fever, and the low back pain was aggravated than before. The liver and kidney function were further deteriorated, with an ALT level of 310 U/L, an AST level of 1686 U/L, a blood Cr level of 613 μmol/L, a PCT level of 17.45 ng/ml, and a CRP level of 463.2 mg/L. On 21 March 2022, simultaneous mNGS (Hugobiotech, Beijing) using blood and bronchoalveolar lavage fluid (BALF) was performed: DNA was extracted using QIAamp DNA Micro Kit (QIAGEN, Hilden), and DNA libraries were built using QIAseq™ Ultralow Input Library Kit (QIAGEN, Hilden) according to the manufacturer's instructions. Qubit (Thermo Fisher, MA) and Agilent 2100 Bioanalyzer (Agilent Technologies, Palo Alto) were applied for quality evaluation of the libraries. Nextseq 550Dx platform (Illumina, San Diego) was used for mNGS detection (~10 M 75-bp single-end reads after sequencing). After removing short, low-quality, low-complexity, and human host reads, the remaining reads were aligned to Microbial Genome Databases (http://ftp.ncbi.nlm.nih.gov/genomes/) using BWA. *T. marneffei* was detected in both blood and BALF samples, and the number of unique sequences of *T. marneffei* in blood and BALF was 15,499 and 4373, respectively. The coverage of *T. marneffei* in blood and BALF detected by mNGS was 3.63% and 1.07%, respectively. The pathogen was subsequently confirmed by blood culture on 28 March 2022 (Figures 2A–C). Considering the compromised liver and kidney function of the patient, the anti-infective regimen was adjusted to

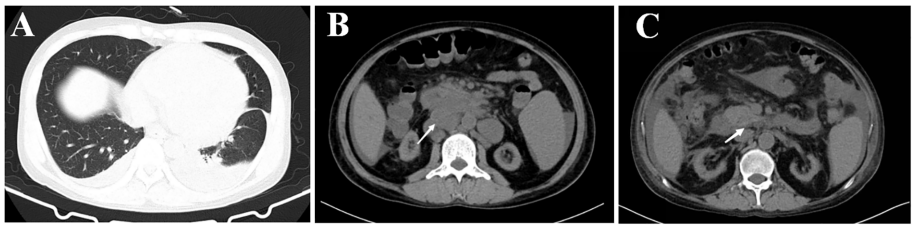

FIGURE 1
CT image results in lung and abdomen of the patient. **(A)** CT image of lung infection with *Talaromyces marneffei*. **(B)** CT image of abdomen, lymphadenopathy in the retroperitoneum and mesenteric root, and hepatosplenomegaly, the largest of which is 31×25 mm (white arrow). **(C)** CT image of abdomen, lymphadenopathy in the retroperitoneum and mesenteric root, and hepatosplenomegaly are improved, the largest of which becomes normal (white arrow).

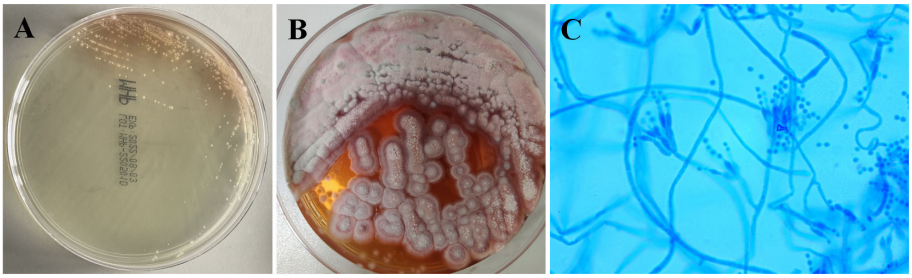

FIGURE 2
Culture results of this patient. **(A)** Blood culture on Sabouraud's agar medium plate at 37°C showed yeast phase. **(B)** Blood culture of *Talaromyces marneffei* in the mold phase at 25°C, characteristic red pigment production was observed. **(C)** Lactophenol cotton blue staining from fungal blood culture demonstrating septate hyphae and smooth conidia aloft phialides, which are borne to metulae.

voriconazole (200 mg twice daily) and meropenem (1 g thrice daily) on 21 March 2022, accompanied by methylprednisolone (80 mg/day) for immune maintenance treatment; anti-rejection drugs was stopped. The blood concentration of voriconazole was maintained at 2–5 μg/ml. After antifungal therapy, liver and kidney function and infection indicators of the patient were gradually improved, but diarrhea symptoms were aggravated than before, with watery stools about 500 ml/day.

On 11 April 2022, the patient had a shock after a sudden red bloody stool of 800 ml. Emergency endoscopic hemostasis and blood transfusion therapy were performed immediately. Gastroscopy revealed chronic non-atrophic gastritis. Colonoscopy revealed multiple ulcers in the colon, including bleeding from an ulcer surface in the ileocecal junction, which was stopped after cauterization and titanium clip hemostasis. Therefore, we excluded gastrointestinal bleeding caused by glucocorticoids, and the bleeding was considered associated with *T. marneffei* infection. On 21 April 2022, the patient received enteroscopy again due to red bloody stool of 600 ml; the bleeding point was still located in the ileocecal region, the same as the first bleeding. After blood transfusion, endoscopic hemostasis, and other treatment measures, the patient's gastrointestinal bleeding temporarily stopped. Unfortunately, repeated bleeding with 600 ml of red bloody stool occurred on 4 May 2022. Blood transfusion, endoscopic hemostasis, and other treatment measures were once more taken. Given that repeated endoscopic hemostasis was ineffective, voriconazole could only control parts of symptoms, and his liver function returned to normal, amphotericin B cholesteryl sulfate complex (4 mg/kg) was given for anti-infection on 2 May 2022. Gratifyingly, the patient's fever, diarrhea, gastrointestinal bleeding, and other clinical symptoms were gradually improved, and the infection indicators also gradually returned to normal.

After 3 weeks of antifungal therapy with amphotericin B cholesteryl sulfate complex, the patient was discharged on 27 May 2022, with serum creatinine maintained at 250 μmol/L. The patient continued maintenance therapy with voriconazole 200 mg twice daily. Methylprednisolone (4 mg) was maintained for anti-rejection therapy after discharge for 3 months, and tacrolimus was then added with a concentration of about 3 ng/ml; the blood Cr fluctuated between 280 and 327 μmol/L. After 7 months of follow-up, repeat abdominal CT showed resolution of the retroperitoneum and mesenteric root lymphadenopathy (Figure 1C), and no adverse events have been found. Important clinical information and treatment timelines for this patient during hospitalization are presented in Figure 3.

Discussion

T. marneffei was first isolated by Capponi et al. (1956) at the Pasteur Institute in 1956 from the liver of the Vietnamese bamboo mouse, but no formal description has been published. In 1959, laboratory personnel inoculated *T. marneffei* when the finger was pricked, causing local nodular lesions and ipsilateral axillary lymph node enlargement, and the fungus was named *Penicillium marneffei*. The first natural human infection of *T. marneffei* was reported in 1973 in an American patient with Hodgkin's disease who was living in

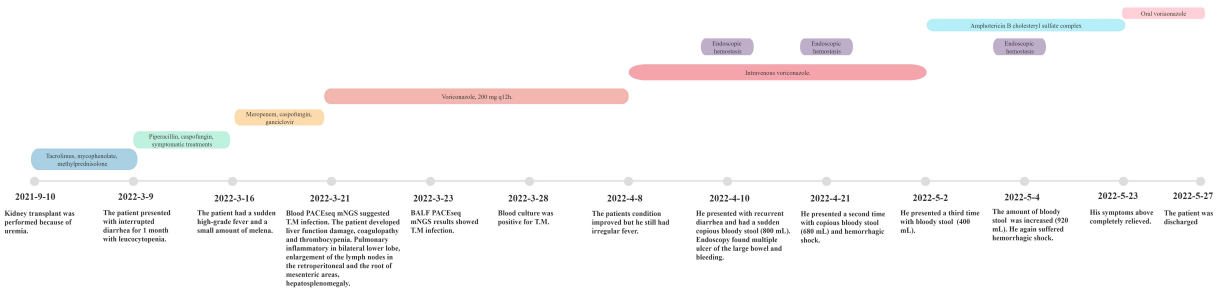

FIGURE 3
Important clinical information of the recipient and treatment timeline after renal transplantation.

Southeast Asia (Cao et al., 2019). In 2011, the RNA polymerase II largest subunit gene was sequenced and the phylogenetic relationship was analyzed; it was renamed *T. marneffei*, and the deep mycoses caused by *T. marneffei* were referred to as talaromycosis (Samson et al., 2011). *T. marneffei* infection can involve multiple organ systems, such as lung, skin, bone marrow, digestive system, and disseminated infections (Ding et al., 2021); the vast majority of the patients presented with fever, respiratory symptoms, anemia, skin lesions, hepatosplenomegaly, weight loss, and lymphadenopathy (He et al., 2021). The mortality rate of disseminated talaromycosis is high, reaching 80%–100% in patients without timely diagnosis and antifungal treatment; despite receiving antifungal treatment, its mortality rate is still as high as 30% (Li et al., 2021). At present, most scholars usually believe that yeast phase conidia of *T. marneffei* are first inhaled into the lungs, and then phagocytosed by macrophages and spread throughout the body *via* the blood circulation (Castro-Lainez et al., 2018); disseminated *T. marneffei* infection with the digestive tract as the first infection site in renal transplant recipients has not been reported.

In our case, the patient is living in Hainan for a long time and had no history of contact with bamboo mouse. The zero time biopsy of transplant kidney showed uninfected with *T. marneffei*, and the donor-derived infection could be excluded completely. The patient presented with low back pain with diarrhea as the first symptom and gradually developed pneumonia (mild pulmonary imaging changes) and gastrointestinal bleeding, which eventually improved after antifungal therapy. Imaging findings suggested retroperitoneal lymphadenopathy, and endoscopy also revealed multiple ulcers and bleeding in the colon. Therefore, we suspect that the patient had digestive tract bleeding caused by *T. marneffei* infection. Previous studies have shown that the clinical characteristics of intestinal *T. marneffei* infection included CD4 T cells < 50/μl, fever, abdominal pain, diarrhea, abdominal distension chronic gastrointestinal symptoms, abdominal lymphadenopathy (considered as indirect evidence of enterogenous infection), endoscopically confirmed erosions or ulcers, and biopsy of colonic tissue samples (Xie et al., 2022). Combined with this patient's condition, we suspect that the route of infection in this patient was digestive tract. Negative stool cultures alone cannot exclude enteric infection with *T. marneffei* due to the low load of fungi in the intestinal lumen (Pan et al., 2020). Fortunately, the early diagnosis and prompt treatment of this patient are due to mNGS technology (Zhang et al., 2020), which provides strong support for clinicians in the diagnosis of rare pathogen infections (Wilson Michael et al., 2014), even as an indication to determine whether to discontinue antifungal drugs (Xu et al., 2022). It should be noted that we have no direct evidence that the route of dissemination was *via* the digestive tract; the intestinal wall biopsy was not taken for this patient due to concerns that it might aggravate gastrointestinal bleeding.

Currently, there are rare cases of *T. marneffei* infection after kidney transplantation. We searched literatures in the Web of Science and PubMed databases based on "*Talaromyces marneffei*", "*Penicillium marneffei*", "kidney transplantation", and "renal transplantation", which had been published up to October 2022. A total of 10 officially published papers reporting 11 cases of *T. marneffei* infection after kidney transplantation were retrieved (Wang et al., 2003; Chan et al., 2004; Lin et al., 2010; Hart et al., 2012; Peng et al., 2017; Lang et al., 2020; Vergidis et al., 2021; Gupta et al., 2022; Li et al., 2022; Xing et al., 2022) (Table 1). The above 11 recipients were summarized in order to enhance the cognition of *T. marneffei* infection after renal transplantation and improve the prognosis. Of the 11 recipients, 7 were men and 4 were women; the age ranged from 34 to 67 years, with a median age of 47 years. Time from kidney transplantation to discovery of *T. marneffei* infection varied from 3 months to 11 years, with a median of 48 months. Six of the 11 patients had fever as the first symptom, 4 had cough with sputum, and only 1 had dry cough as the main symptom. Two patients had abdominal pain and one of them was complicated with diarrhea. One patient each had symptoms including subcutaneous nodules, scalp swelling, bone pain, and bladder irritation. At the same time, we found that the organs that were affected the most were the lungs (five cases), followed by skin (two cases), bone (two cases), and kidney (two cases). One of two patients with abdominal cavity involvement presented with mesenteric lymphadenopathy. Respiratory tract infection was identified in only 5 of 11 patients, and no gastrointestinal infection was reported. Among the 11 patients, 7 had positive blood cultures for *T. marneffei*, 2 had positive tissue cultures, and 2 were diagnosed by mNGS. Almost all patients were treated with reduced anti-rejection drugs, mainly because antifungal drugs (amphotericin B, liposomal amphotericin B, voriconazole, posaconazole, and fluconazole) had a side effect of increasing the concentration of tacrolimus. Two of the 11 patients died after treatment with voriconazole, including one due to resuscitation (as a result of rapid atrial fibrillation) failure and the other due to deterioration of the disease and abandonment of treatment after discharge. Six patients were cured with amphotericin B or liposomal amphotericin B combined with itraconazole. One patient each was cured with itraconazole, voriconazole, or posaconazole. The duration of treatment varied from 1 to 12 months, with a median of 9 months. Combined with our case, we found that fever was the most common initial symptoms of *T. marneffei* infection, whereas the specific clinical symptoms varied, which is mainly related to the infection sites. Hart et al. (2012) also reported a case of disseminated *T. marneffei* infection with diarrhea as the initial symptom in 2012. However, the patient was finally diagnosed with cytomegalovirus enteritis causing sigmoid perforation; fungal infection in digestive tract was not considered.

The therapeutic efficacy of voriconazole was unsatisfactory, and amphotericin B or liposomal amphotericin B remains the first choice. Xing et al. (2022) concluded that high-dose glucocorticoids should be used with caution in patients with *T. marneffei* infection in the transplant state. In our case, we believe that early antifungal therapy is critical. Based on the fact that glucocorticoids not only control fever symptoms but also maintain immunosuppression, we believe that the rational use of glucocorticoids does not affect prognosis, at least in our case.

Reducing the dose of anti-rejection drugs was mentioned in 9 of the 11 patients, but no specific rationale was detailed. In this case, we also reduced the dose of tacrolimus and MMF drugs. One reason is that both tacrolimus and MMF can inhibit T-cell activity or proliferation (Ferreira et al., 2020; Chen et al., 2021). Previous studies indicated that the incidence of *T. marneffei* infection was lower in patients with higher CD4+ T-cell lymphocyte counts. The probability of *T. marneffei* infection was 1.65% when the CD4+ T-cell

TABLE 1 Clinical information of *Talaromyces marneffei* infection after kidney transplantation.

Author	Region	Gender/ age	Onset time (days)	Clinical presentation	Radiological imaging/ Endoscopy	Infection route	Infection site	Diagnostic methods	The use of immunosuppressive agents	Treatment	Disease duration (months)	Prognosis
Wang et al. (2003)	Taiwan, China	M/47	33	Fever, dry cough, poor appetite, weight loss, skin lesions, subcutaneous masses.	Osteomyelitis	NA	Skin, bone	Cultures of the blood and debrided specimens	Reduced Tac dosage	L-AmB (2 mg/kg, 28 days), itraconazole (400 mg/day).	12	Survival
Chan et al. (2004)	Hong Kong, China	M/38	9	Fever, chills and rigor, central abdominal pain, cough for 1 week.	Pulmonary infiltrates, enlarged mesenteric lymph nodes	NA	Lung, bone, lymph nodes	Blood and bone marrow cultures, lymph node biopsy	Reduced Tac dosage, withheld MMF	AmB (30 days, cumulative dose of 0.75 g), itraconazole (200 mg/day).	9	Survival
Lin et al. (2010)	Taiwan, China	F/42	9	Pain in her left hip.	Osteolytic lesion on the left pelvic brim near acetabulum	NA	Bone	0 mg	NA	L-AmB (2 mg/kg, 21 days), oral itraconazole (200 mg per day, 8 months)	8	Survival
Hart et al. (2012)	Australian	M/67	48	Abdominal pain and diarrhea.	Normal	NA	Abdominal	Blood and peritoneal fluid cultures	Reduced Tac dosage	L-AmB (3 mg/kg) for 14 days, oral itraconazole.	8	Survival
Peng et al. (2017)	China	M/51	13	Fever and worsening renal functions.	Increased renal volume, hyperechoic and hypoechoic lesions in renal allograft	Respiratory tract	Kidney	Blood and biopsy of renal allograft	Withheld Tac and MP, change to CSA, continued MMF	L-AmB (0.4 mg/ kg/day, 14 days), followed by itraconazole.	1	Survival
Vergidis (Vergidis et al., 2021)	England	F/53	132	Cough with expectoration, night sweats, chills, decreased exercise.	Chest x-ray: left upper lobe mass; CT: mediastinal lymphadenopathy	Respiratory tract	Lung	Fine needle aspiration of the involved lymph nodes and lung mass	Reduced Tac dosage, withheld MMF	AmB (2 weeks), followed by itraconazole (12 months)	12	Survival
Lang et al. (2020)	China	M/34	48	A 4-month history of weakness and poor appetite, occasional nonproductive cough with hemoptysis.	CT: new patchy consolidation	Respiratory tract	Lung	NGS of BALF, fungal culture of BALF and blood	Reduced Tac and MMF dosage	Oral posaconazole at the dose of 10 ml (400 mg) bid.	6	Survival
Gupta et al. (2022)	India	F/41	84	Swelling on the right side of the scalp, pain and blurring of vision in the right eye.	CT: right-sided subcutaneous nodule; MRI: lytic lesion in right calvarium	NA	Subcutaneous infection	Fine-needle aspiration of the scalp lesion	NA	Itraconazole 200 mg twice daily.	10	Survival
Li et al. (2022)	China	F/47	132	Fever, frequent urination, and discomfort.	Ultrasonography: 5 mm separation of the transplanted	Respiratory tract	Kidney	Cultures of peripheral blood	Reduced Tac, MMF, MP	Voriconazole (0.2 g, every 12 h),	NA	Survival

(Continued)

10.3389/fcimb.2023.1115268

TABLE 1 Continued

Author	Region	Gender/age	Onset time (days)	Clinical presentation	Radiological imaging/Endoscopy	Infection route	Infection site	Diagnostic methods	The use of immunosuppressive agents	Treatment	Disease duration (months)	Prognosis
					kidney collecting system			and clean midstream urine		itraconazole capsules (200 mg/day).		
Xing et al. (2022)	China	M/61	4	A repeated cough, expectoration, intermittent fever.	CT: multiple nodules, patchy high-density shadows, and highdensity glass	NA	Lung	NGS of BALF	Reduced Tac	Voriconazole (0.2 g, every 12 h).	8	Died
Xing et al. (2022)	China	M/55	3	A repeated fever and shortness of breath after activity.	CT: ground glass-like shadows, a nodule in right lung	NA	Lung	NGS of peripheral blood	Tac and MMF discontinued, changed to MP 80 mg/day	Voriconazole	NA	Died

L-AMB, liposomal amphotericin B; AmB, amphotericin B; MMF, mycophenolate mofetil; NA, not available; CSA, cyclosporine; Tac, tacrolimus; MP, methylprednisolone; Itra, itraconazole; NGS, next-generation sequencing; Pred, methylpred; CT, computed tomography; BALF, bronchoalveolar lavage fluid; MRI, magnetic resonance imaging.

count ≥ 200 cells/μl, 14.89% when the CD4+ T-cell count < 200 cells/μl, and 28.06% when the CD4+ T-cell count < 50 cells/μl (Chen et al., 2017). Thus, the reduction or depletion of CD4+ T cells in recipients with *T. marneffei* infection is considered not conducive to infection control. Macrophages are unable to activate and kill bacteria (immune escape) if CD4+ T cells are reduced or depleted, resulting in massive macropinocytosis and massive fungal reproduction, systemic disseminated infection caused by macrophages through lymphatic and blood circulation may happen. Significant macrophage increase occurs in the reticuloendothelial system, manifesting as enlargement of the liver, spleen, and lymph nodes, resulting in focal necrosis of organs (Dong et al., 2019). Based on the clinical symptoms and the prognosis of this patient, a regimen of complete discontinuation of anti-rejection drugs and maintenance of immunosuppression with only steroids turned out to be safe and feasible in recipients with serious disseminated *T. marneffei* infections. However, clinicians still need to carefully decide whether such serious infection will endanger the patient's life, or whether it is controlled effectively without the use of immunosuppressive agents.

The mortality rate of gastrointestinal bleeding caused by *T. marneffei* infection in HIV patients is extremely high, and the successful management experience is not much (Cui et al., 2022). Due to the lack of guidelines for *T. marneffei* infection in organ transplant patients, as well as the concurrent severe impairment of liver and kidney function in our patient, voriconazole was used for induction therapy as recommended by the Centers for Disease Control and Prevention (Masur et al., 2014). However, symptoms of the patient were only partially resolved, and gastrointestinal bleeding persisted. In this case, when the recipient suffered from hemorrhagic shock caused by repeated gastrointestinal bleeding, the recipient was treated with two massive blood transfusions and two endoscopic hemostatic treatments with temporary success. Our team believes that surgical treatment alone is difficult to achieve effective therapeutic effects for recurrent gastrointestinal bleeding caused by *T. marneffei*, because it may still lead to postoperative intestinal anastomoses or bleeding anywhere in the intestine. Therefore, after his liver and kidney function improved, we decided to use antifungal therapy with amphotericin B cholesteryl sulfate complex (Thompson et al., 2021). Since there was no itraconazole in our center, consolidation therapy with voriconazole was still performed after induction therapy with amphotericin B cholesteryl sulfate complex and the treatment was successful.

Conclusions

In summary, recipients who have received immunosuppressive agents for a long time after renal transplantation, especially those who have lived or traveled in *T. marneffei*-endemic areas, should be alert to *T. marneffei* infection for unexplained symptoms, such as high fever, cough and expectoration, hepatosplenomegaly, lymphadenopathy, osteolytic damage, and even gastrointestinal bleeding. As shown in our case, hemorrhagic shock due to gastrointestinal bleeding is often fatal, and how to treat patients to the greatest extent through measures such as hemostasis, blood transfusion, and antifungal therapy requires clinicians to develop a more individualized treatment strategy based on available resources.

Data availability statement

The datasets presented in this study can be found in online repositories. The names of the repository/repositories and accession number(s) can be found in the article/supplementary material.

Ethics statement

Written informed consent was obtained from the individual(s) for the publication of any potentially identifiable images or data included in this article.

Author contributions

JW designed the paper. LX, XC, and XY drafted and revised the manuscript. LX, HJ, and JX carried out the clinical care and management of the patient. SC did the fungal identification tests. All authors contributed to the article and approved the submitted version.

Funding

This work was supported by the Hainan Provincial Natural Science Foundation of China (No. 820QN404) and the Hainan Province Health and Family Planning Industry Scientific Research Project (No. 20A200360).

Acknowledgments

The authors would like to thank the patient involved in this article.

Conflict of interest

Author XY was employed by Hugobiotech Co., Ltd.

The remaining authors declare that the research was conducted in the absence of any commercial or financial relationships that could be construed as a potential conflict of interest.

Publisher's note

References

Cao, C., Xi, L., and Chaturvedi, V. (2019). Talaromycosis (Penicilliosis) due to talaromyces (Penicillium) marneffei: Insights into the clinical trends of a major fungal disease 60 years after the discovery of the pathogen. *Mycopathologia* 184 (6), 709–720. doi: 10.1007/s11046-019-00410-2

Capponi, M., Segretain, G., and Sureau, P. (1956). Pénicillose de rhizomys sinensis [Penicillosis from rhizomys sinensis]. *Bull. Soc. Pathol. Exot Filiales* 49 (3), 418–421.

Castro-Lainez, M. T., Sierra-Hoffman, M., LLompart-Zeno, J., Adams, R., Howell, A., Hoffman-Roberts, H., et al. (2018). Talaromyces marneffei infection in a non-HIV non-endemic population. *IDCases* 12, 21–24. doi: 10.1016/j.idcr.2018.02.013

Chan, Y. H., Wong, K. M., Lee, K. C., Kwok, P. C., Chak, W. L., Choi, K. S., et al. (2004). Pneumonia and mesenteric lymphadenopathy caused by disseminated penicillium marneffei infection in a cadaveric renal transplant recipient. *Transpl Infect. Dis.* 6 (1), 28–32. doi: 10.1111/j.1399-3062.2004.00038.x

Chen, L., Peng, Y., Ji, C., Yuan, M., and Yin, Q. (2021). Network pharmacology-based analysis of the role of tacrolimus in liver transplantation. *Saudi J. Biol. Sci.* 28 (3), 1569–1575. doi: 10.1016/j.sjbs.2020.12.050

Chen, J., Zhang, R., Shen, Y., Liu, L., Qi, T., Wang, Z., et al. (2017). Clinical characteristics and prognosis of penicilliosis among human immunodeficiency virus-infected patients in Eastern China. *Am. J. Trop. Med. Hyg* 96 (6), 1350–1354. doi: 10.4269/ajtmh.16-0521

Cui, X., Su, F., Ye, H., Jiang, Y., and Guo, X. (2022). Disseminated talaromycosis complicated by recurrent gastrointestinal bleeding and hemorrhagic shock: A case report. *BMC Infect. Dis.* 22 (1), 238. doi: 10.1186/s12879-022-07230-8

Ding, X., Huang, H., Zhong, L., Chen, M., Peng, F., Zhang, B., et al. (2021). Disseminated talaromyces marneffei infection in a non-HIV infant with a homozygous private variant of RELB. *Front. Cell Infect. Microbiol.* 11. doi: 10.3389/fcimb.2021.605589

Dong, R. J., Zhang, Y. G., Zhu, L., Liu, H. L., Liu, J., Kuang, Y. Q., et al. (2019). Innate immunity acts as the major regulator in talaromyces marneffei coinfected AIDS patients: Cytokine profile surveillance during initial 6-month antifungal therapy. *Open Forum Infect. Dis.* 6 (6), ofz205. doi: 10.1093/ofid/ofz205

Ferreira, P. C. L., Thiesen, F. V., Pereira, A. G., Zimmer, A. R., and Fröehlich, P. E. (2020). A short overview on mycophenolic acid pharmacology and pharmacokinetics. *Clin. Transplant.* 34 (8), e13997. doi: 10.1111/ctr.13997

Gupta, P., Kaur, H., Kenwar, D. B., Gupta, P., Agnihotri, S., and Rudramurthy, S. M. (2022). First case of subcutaneous infection by talaromyces marneffei in a renal transplant recipient from India and review of literature. *J. Mycol Med.* 32 (1), 101207. doi: 10.1016/j.mycmed.2021.101207

Hart, J., Dyer, J. R., Clark, B. M., McLellan, D. G., Perera, S., and Ferrari, P. (2012). Travel-related disseminated penicillium marneffei infection in a renal transplant patient. *Transpl Infect. Dis.* 14 (4), 434–439. doi: 10.1111/j.1399-3062.2011.00700.x

He, L., Mei, X., Lu, S., Ma, J., Hu, Y., Mo, D., et al. (2021). Talaromyces marneffei infection in non-HIV-infected patients in mainland China. *Mycoses* 64 (10), 1170–1176. doi: 10.1111/myc.13295

Lang, Q., Pasheed Chughtai, A., Kong, W. F., and Yan, H. Y. (2020). Case report: Successful treatment of pulmonary talaromyces marneffei infection with posaconazole in a renal transplant recipient. *Am. J. Trop. Med. Hyg* 104 (2), 744–747. doi: 10.4269/ajtmh.20-0909

Li, D., Liang, H., Zhu, Y., Chang, Q., Pan, P., and Zhang, Y. (2022). Clinical characteristics, laboratory findings, and prognosis in patients with talaromyces marneffei infection across various immune statuses. *Front. Med.* 9. doi: 10.3389/fmed.2022.841674

Lin, J. N., Lin, H. H., Lai, C. H., Wang, J. L., and Yu, T. J. (2010). Renal transplant recipient infected with penicillium marneffei. *Lancet Infect. Dis.* 10 (2), 138. doi: 10.1016/S1473-3099(10)70005-0

Li, Y., Tang, M., Sun, S., Hu, Q., and Deng, S. (2022). Successful treatment of talaromyces marneffei infection in a kidney transplant recipient with voriconazole followed by itraconazole for the first time. *J. Mycol Med.* 32 (1), 101214. doi: 10.1016/j.mycmed.2021.101214

Li, Y., Wei, W., An, S., Jiang, J., He, J., Zhang, H., et al. (2021). Identification and analysis of lncRNA, microRNA and mRNA expression profiles and construction of ceRNA network in talaromyces marneffei-infected THP-1 macrophage. *PeerJ* 9, e10529. doi: 10.7717/peerj.10529

Masur, H., Brooks, J. T., Benson, C. A., Holmes, K. K., Pau, A. K., Kaplan, J. E., et al. (2014). Prevention and treatment of opportunistic infections in HIV-infected adults and adolescents: Updated guidelines from the centers for disease control and prevention, national institutes of health, and HIV medicine association of the infectious diseases society of America. *Clin. Infect. Dis.* 58 (9), 1308–1311. doi: 10.1093/cid/ciu094

Narayanasamy, S., Dat, V. Q., Thanh, N. T., Ly, V. T., Chan, J. F., Yuen, K. Y., et al. (2021). A global call for talaromycosis to be recognised as a neglected tropical disease. *Lancet Glob Health* 9 (11), e1618–e1e22. doi: 10.1016/S2214-109X(21)00350-8

Pan, M., Huang, J., Qiu, Y., Zeng, W., Li, Z., Tang, S., et al. (2020). Assessment of talaromyces marneffei infection of the intestine in three patients and a systematic review of case reports. *Open Forum Infect. Dis.* 7 (6), ofaa128. doi: 10.1093/ofid/ofaa128

Peng, J., Chen, Z., Cai, R., Huang, X., Lin, L., Liang, W., et al. (2017). Recovery from talaromyces marneffei involving the kidney in a renal transplant recipient: A case report and literature review. *Transpl Infect. Dis.* 19 (4), e12710. doi: 10.1111/tid.12710

Samson, R. A., Yilmaz, N., Houbraken, J., Spierenburg, H., Seifert, K. A., Peterson, S. W., et al. (2011). Phylogeny and nomenclature of the genus talaromyces and taxa accommodated in penicillium subgenus biverticillium. *Stud. Mycol* 70 (1), 159–183. doi: 10.3114/sim.2011.70.04

Shen, Q., Sheng, L., Zhang, J., Ye, J., and Zhou, J. (2022). Analysis of clinical characteristics and prognosis of talaromycosis (with or without human immunodeficiency virus) from a non-endemic area: a retrospective study. *Infection* 50 (1), 169–178. doi: 10.1007/s15010-021-01679-6

Shi, M., Lin, J., Wei, W., Qin, Y., Meng, S., Chen, X., et al. (2022). Machine learning-based in-hospital mortality prediction of HIV/AIDS patients with talaromyces marneffei infection in guangxi, China. *PloS Negl. Trop. Dis.* 16 (5), e0010388. doi: 10.1371/journal.pntd.0010388

Sun, J., Sun, W., Tang, Y., Zhang, R., Liu, L., Shen, Y., et al. (2021). Clinical characteristics and risk factors for poor prognosis among HIV patients with talaromyces marneffei bloodstream infection. *BMC Infect. Dis.* 21 (1), 514. doi: 10.1186/s12879-021-06232-2

Thompson, G. R.3rd, Le, T., Chindamporn, A., Kauffman, C. A., Alastruey-Izquierdo, A., Ampel, N. M., et al. (2021). Global guideline for the diagnosis and management of the endemic mycoses: an initiative of the European confederation of medical mycology in cooperation with the international society for human and animal mycology. *Lancet Infect. Dis.* 21 (12), e364–e74. doi: 10.1016/S1473-3099(21)00191-2

Vergidis, P., Rao, A., Moore, C. B., Rautemaa-Richardson, R., Sweeney, L. C., Morton, M., et al. (2021). Talaromycosis in a renal transplant recipient returning from south China. *Transpl Infect. Dis.* 23 (1), e13447. doi: 10.1111/tid.13447

Wang, J. L., Hung, C. C., Chang, S. C., Chueh, S. C., and La, M. K. (2003). Disseminated penicillium marneffei infection in a renal-transplant recipient successfully treated with liposomal amphotericin b. *Transplantation* 76 (7), 1136–1137. doi: 10.1097/01.TP.0000088667.02294.E7

Wilson Michael, R., Naccache Samia, N., Samayoa, E., Biagtan, M., Bashir, H., Yu, G., et al. (2014). Actionable diagnosis of neuroleptospirosis by next-generation sequencing. *New Engl. J. Med.* 370 (25), 2408–2417.

Xie, Z., Lai, J., Peng, R., Mou, M., Liang, H., and Ning, C. (2022). Clinical characteristics of HIV-associated talaromyces marneffei infection of intestine in southern China. *Int. J. Infect. Dis.* 120, 48–50. doi: 10.1016/j.ijid.2022.03.057

Xing, S., Zhang, H., Qiu, Y., Pan, M., Zeng, W., and Zhang, J. (2022). Clinical characteristics of transplant recipients infected with talaromyces marneffei: 2 case reports and a literature review. *Infect. Drug Resistance* 15, 2879–2890. doi: 10.2147/IDR.S363362

Xu, L., Xu, J., Zeng, F., Wu, Z., Gan, H., and Jiang, H. (2022). Invasive aspergillosis infection in the central nervous system after liver transplantation: a case report and literature review. *Chin. J. Organ Transplant.* 43 (7), 400–405. doi: 10.3760/cma.j.cn421203-20220312-00041

Ying, R. S., Le, T., Cai, W. P., Li, Y. R., Luo, C. B., Cao, Y., et al. (2020). Clinical epidemiology and outcome of HIV-associated talaromycosis in guangdong, China, during 2011-2017. *HIV Med.* 21 (11), 729–738. doi: 10.1111/hiv.13024

Zhang, W., Ye, J., Qiu, C., Wang, L., Jin, W., Jiang, C., et al. (2020). Rapid and precise diagnosis of t. marneffei pulmonary infection in a HIV-negative patient with autosomal-dominant STAT3 mutation: a case report. *Ther. Adv. Respir. Dis.* 14, 1753466620929225. doi: 10.1177/1753466620929225

Zhou, Y., Liu, Y., and Wen, Y. (2021). Gastrointestinal manifestations of talaromyces marneffei infection in an HIV-infected patient rapidly verified by metagenomic next-generation sequencing: A case report. *BMC Infect. Dis.* 21 (1), 376. doi: 10.1186/s12879-021-06063-1

frontiers | Frontiers in Cellular and Infection Microbiology

TYPE Original Research
PUBLISHED 11 May 2023
DOI 10.3389/fcimb.2023.1144625

OPEN ACCESS

EDITED BY
Sathyavathi Sundararaju,
Sidra Medicine, Qatar

REVIEWED BY
Selvasankar Murugesan,
Sidra Medicine, Qatar
Preeti Arivaradarajan,
Thiagarajar College, India

*CORRESPONDENCE
Yanjun Li
18611182875@163.com
Peng Li
jiekenlee@126.com
Hongbin Song
hongbinsong@263.net

†These authors have contributed equally to this work and share first authorship

RECEIVED 14 January 2023
ACCEPTED 18 April 2023
PUBLISHED 11 May 2023

CITATION
Cao Y, Jiang T, Lin Y, Fang X, Ding P, Song H, Li P and Li Y (2023) Time-series prediction and detection of potential pathogens in bloodstream infection using mcfDNA sequencing.
Front. Cell. Infect. Microbiol. 13:1144625.
doi: 10.3389/fcimb.2023.1144625

Time-series prediction and detection of potential pathogens in bloodstream infection using mcfDNA sequencing

Yinghao Cao[1,2†], Tingting Jiang[3,4†], Yanfeng Lin[4], Xiaofeng Fang[1,2], Peipei Ding[2], Hongbin Song[3,4*], Peng Li[4*] and Yanjun Li[1,2,5*]

[1]Department of Clinical Laboratory Medicine, School of Medicine, South China University of Technology, Guangzhou, China, [2]Department of Clinical Laboratory Medicine, The Sixth Medical Center of People's Liberation Army (PLA) General Hospital of Beijing, Beijing, China, [3]Department of Epidemiology and Biostatistics, School of Public Health, An Hui Medical University, Hefei, China, [4]Biosecurity Department, Chinese People's Liberation Army (PLA) Center for Disease Control and Prevention, Beijing, China, [5]School of Laboratory Medicine and Biotechnology, Southern Medical University, Guangzhou, China

Introduction: Next-generation sequencing of microbial cell free DNA (mcfDNA-seq) has emerged as a promising diagnostic method for blood stream infection (BSI) and offers the potential to detect pathogens before blood culture. However, its application is limited by a lack of clinical validation.

Methods: We conducted sequential mcfDNA-seq on blood samples from ICU participants at high risk of BSI due to pneumonia, or intravascular catheterization; and explored whether mcfDNA-seq could diagnose and detect pathogens in advance of blood culture positivity. Blood culture results were used as evaluation criteria.

Results: A total of 111 blood samples were collected during the seven days preceding and on the day of onset of 16 BSI episodes from 13 participants. The diagnostic and total predictive sensitivity of mcfDNA-seq were 90% and 87.5%, respectively. The proportion of pathogenic bacteria was relatively high in terms of both diagnosis and prediction. The reads per million of etiologic agents trended upwards in the days approaching the onset of BSI.

Discussion: Our work found that mcfDNA-seq has high diagnostic sensitivity and could be used to identify pathogens before the onset of BSI, which could help expand the clinical application of mcfDNA-seq.

KEYWORDS

microbial cell free DNA, next-generation sequencing, blood stream infection, pathogens, microbiology

1 Introduction

Infectious diseases remain among the major threats to humanity (Casadevall, 2017). Bloodstream infection (BSI) is one of the most lethal infections. Undetermined or delayed etiologic diagnoses often result in inadequate treatment, prolonged hospitalizations, readmissions, and increased mortality and morbidity (Ewig et al., 2002; Bleeker-Rovers et al., 2007). Furthermore, BSI mortality rates rise with delays of appropriate antibiotic therapy (Lodise et al., 2007; Zimlichman et al., 2013; Sterling et al., 2015). Rapid etiologic diagnosis and the prompt initiation of pathogen-directed therapy are crucial to improving clinical outcomes (Evans et al., 2021).

Blood culture is currently regarded as the gold standard for diagnosing BSI. However, blood culture sensitivity relies to a large degree on sample volume, requiring 40-80 mL blood to diagnose the majority of BSI, which is extremely damaging to the participant (Cockerill et al., 2004; Riedel et al., 2008). Although a predictive test to enable preemptive, pathogen-directed therapy could reduce morbidity and mortality, no such reliable method has been developed. In this context, the development of a blood-sparing and predictive etiologic diagnostic test is an unmet medical need.

Plasma microbial cell-free DNA sequencing (mcfDNA-seq) has emerged as a diagnostic tool and predictive test that may meet such a need. McfDNA-seq could detect a wide range of pathogens. The first diagnostic assay using mcfDNA-seq identified pathogens in lung transplant recipients in 2015 (De Vlaminck et al., 2015). Subsequent studies have reported that plasma mcfDNA-seq may identify the etiologic agents of BSI (Grumaz et al., 2016; Long et al., 2016; Jing et al., 2021; Wang et al., 2021).

Moreover, increased plasma cfDNA may indicate the onset of sepsis (Martins et al., 2000; Rhodes et al., 2006; Grumaz et al., 2016). The incidence rates of hospital-acquired BSI were 75% and 25% before and after transfer to ICU, respectively (Tabah et al., 2012; Timsit et al., 2020). ICU-acquired BSI was caused by catheter-related infections (21%), nosocomial pneumonia (21%), intra-abdominal infections (12%) or no definite source (24%) (Tabah et al., 2012). BSI may be predictive and mcfDNA-seq has the potential to predict BSI. However, its possible clinical role of BSI prediction has rarely been explored (Goggin et al., 2020).

In this study, we conducted sequential mcfDNA-seq on blood samples from participants hospitalized in ICU and at high risk of BSI, with the goal of evaluating the diagnostic performance of mcfDNA-seq and exploring whether it could identify etiologic agents before BSI develops.

2 Materials and methods

2.1 Participants and ethics

Participants in ICU receiving treatment were enrolled from October 2021 to June 2022 at the sixth medical center of PLAGH. The enrollment criteria were (1) participants with high risks for BSI (with pneumonia or receiving intravascular catheterization); (2) participants getting definitive diagnosis of BSI and having blood culture as a criterion; (3) mcfDNA-seq samples available for three or more days within the seven days prior to the time of collection of the positive blood culture. In total, we enrolled 13 participants for our research (Figure 1). Information of participants were collected from the electronic medical record. This study was approved by the ethics committee of the sixth medical center of PLAGH (Ethical acceptance number: H2KY2022-41). Informed consent was not required because no additional processes were done to participants and participant information was anonymized.

2.2 Specimen collection and processing

Blood samples were collected using standard aseptic technique and used for blood culture and mcfDNA-seq. Samples that were injected into blood culture bottles were processed in BacT/ALERT® 3D (bioMerieux, Inc.). Blood from positive-alarm culture bottles was extracted and inoculated into medium and incubated at 35°C for more than 24h in MCO-15AC (SANYO). Species-level identification was performed using Microflex LH/SH(Bruker).

Residual blood specimens obtained after blood routine tests were subjected to mcfDNA-seq. Only samples that otherwise would have been discarded were used; no samples were collected specifically for this study. After blood routine tests, approximately 500 to 600μL plasma would remain. The residual blood samples

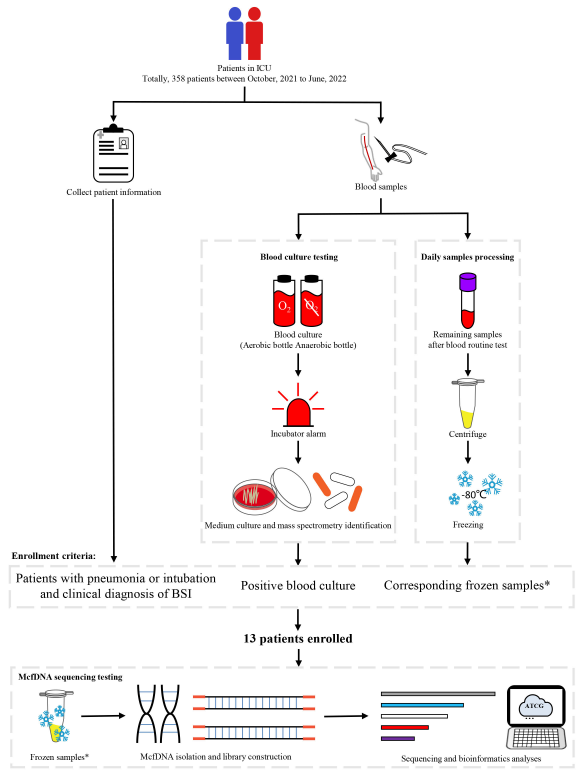

FIGURE 1
Study workflow. *Residual samples were used for mcfDNA-seq after participants were enrolled. Sequencing samples needed to be obtained during three or more days within the seven days prior to the collection time of the positive blood culture.

were aspirated without mixing and centrifuged at 1600g for 10mins at 4°C, and the supernatant would be centrifuged again at 16000g for 10 min at 4°C. Finally. 350μL supernatants containing plasma and cell-free DNA were then transferred into a new tube and frozen at -80°C for further experiments.

2.3 mcfDNA sequencing and bioinformatic analysis

500μL sample (350μL supernatants plus 150μL ultraclean water) was taken for nucleic acid extraction using QIAamp MinElute ccfDNA Mini Kit (50) according to the manufacture's instruction. The extracted mcfDNA were quantified by Qubit 3.0 fluorometer with Qubit dsDNA HS Assay Kit (ThermoFisher). The initial amount of each sample was 2.5ng. DNA libraries were constructed using MGIEasy Cell-free DNA Library Prep Kit. The constructed libraries were qualified using Qsep100 (Guangding Biotechnology, Taiwan, China). Sequencing was performed on MGISEQ-2000 with PE100 strategy. The raw reads were aligned using Centrifuge1.0.4 with the p+h+v database and the value of min-hitlen was set as 30 (Kim et al., 2016). The p+h+v database which consists of prokaryotic, human and viral genomes helped to obtain the reads of microorganism. In the data generated by Centrifuge 1.0.4, some reads which were aligned to specific species also were aligned to a group or complex. Only the reads aligned to a specific species represent reads that belong to a specific species. For estimating sensitivity, quantitative results of detected organisms were documented as positive or negative. Samples with pathogens identified by mcfDNA-seq (if mcfDNA-seq and blood culture results were concordant) were considered positive. For blood cultures yielding multiple isolates, samples with all of the isolates identified by mcfDNA-seq were considered positive.

2.4 Data definitions

The time of collection of a positive blood culture was defined as the onset of a BSI episode. Samples collected on the day of BSI onset were defined as the diagnostic sample and used to evaluate the performance of mcfDNA-seq, while samples collected during the seven days prior to the onset of BSI were defined as predictive samples and used to explored whether mcfDNA-seq could identify etiologic agents in advance.

Daily detective sensitivity was defined as the proportion of positive sequencing samples in all sequencing samples on a same day. Depending on the sampling time, daily detective sensitivity could be divided into diagnostic sensitivity estimated from samples collected on onset of BSI and daily predictive sensitivity estimated from samples collected prior to onset of BSI. Total predictive sensitivity was defined as the proportion of BSIs in which pre-onset mcfDNA-seq identified the same pathogen as blood culture on onset (Goggin et al., 2020).

For inter-sample comparison, reads per million (RPM) was used to normalize the effect of different numbers of raw reads as described in a previous study (Gu et al., 2021). RPM was defined as the number of species reads divided by the number of raw reads of a sample, and then multiplied by one million.

3 Results

3.1 Participant characteristics and sample distribution

Between October 2021 and June 2022, a total of 3099 blood samples from 358 participants in ICU were obtained during daily collections for clinical laboratory testing. Thirteen participants met our inclusion criteria (Table 1). The median participant age was 76 years (range: 32-94 years) and 84.6% (11 participants) were male. Ten participants had both pneumonia and intravascular catheterization, while two participants were diagnosed with pneumonia but did not have vascular catheters, and one participant had received intravascular catheter but had no other BSI risk factor. Seven participants had received antibiotic therapy for at least one day during the week before BSI onset. Participants were enrolled at a nearly constant rate throughout the research period (Figure 2A). Sixteen BSI episodes occurred among the thirteen participants. Except for participants P5 and P13, who had developed three and two BSI episodes, respectively, other participants experienced only one BSI episode.

The sample distribution by day was shown in Figure 2B. A total of 111 samples were collected. However, samples were not obtained every day from every participant. Twenty-two samples were used for both blood culture and mcfDNA-seq, while 11 samples were used only for blood culture and 78 samples were subjected only to mcfDNA-seq (Figure 2B). All participants had positive blood cultures on the day of BSI onset (BSI case definition), while blood cultures were obtained from only nine participants before BSI onset. An average of 6.9 (range: 4-8) samples were collected per BSI episode and an average of 6.25 (range: 3-8) samples were subjected to mcfDNA-seq.

TABLE 1 Participant characteristics.

Characteristic	Number
Total participants	13
Age	76 (32-94)
Sex	
Male	11
Female	2
Risk factors*	
Pneumonia	12
Intravascular catheterization	11
Empiric antibiotic therapy	7
Mortality#	6

*Getting more than seven days prior to positive blood culture.
#Deaths due to septic shock.

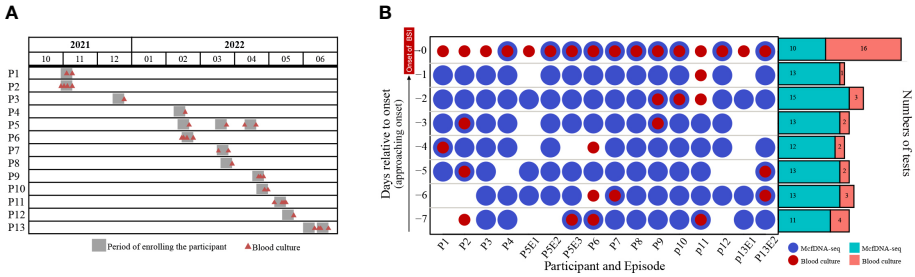

FIGURE 2
(A) The timeline of participant enrollment and **(B)** sample distribution. P and E indicate participant and episode, respectively. For example, P5E1 indicates the first BSI of Participant 5. Day -7 indicates the seventh day before the onset of BSI, while Day 0 indicates the day of BSI diagnosis.

3.2 Pathogens identified by blood culture

Thirty-three samples were cultured, of which seventeen obtained prior to the onset of BSI from nine participants were negative and the sixteen samples obtained on the onset of BSI were positive. Six different pathogens were identified, including *Klebsiella pneumoniae* (9/16), *Acinetobacter baumannii* (2/16), *Enterococcus faecium* (2/16), *Escherichia coli* (2/16), *Pseudomonas aeruginosa* (2/16) and *Staphylococcus hominis* (1/16) (Figure 3). Participant P1 was co-infected with *A. baumannii*, *E. faecium* and *K. pneumoniae*, while other BSIs were monobacterial. Participants P5 and P13 had recurrent BSI episodes caused by the same pathogen, *K. pneumoniae* and *P. aeruginosa*, respectively.

3.3 Diagnostic and predictive performance of mcfDNA-seq

Of 100 samples subjected to mcfDNA-seq, 87 were positive (Figure 4A). Nine of the ten samples submitted to mcfDNA at the onset of BSI were concordant with culture results except the sample of P6. Blood culture of P6 yielded *S. hominis*, while the top five species identified by mcfDNA-seq on Day 0 were *A. baumannii*, *P. aeruginosa*, *K. pneumoniae*, *S. epidermidis* and *Corynebacterium simulans*; *S. hominis* was not identified (Supplementary Table 1). Before the onset of BSI, 78 sequencing samples from 14 BSIs were positive; pathogens were identified by mcfDNA-seq in 14 of 16 sequential sets of samples of BSIs. Sequential mcfDNA-seq samples taken before the onset of BSI of P3 and P6 yielded discordant results with blood culture. The sequential mcfDNA-seq samples of P3 identified mainly *A. baumannii*, *K. pneumoniae* and *E. coli*, but not *E. faecium* (Supplementary Table 1). Sequential mcfDNA-seq samples from P6 including a sample taken at the onset of BSI identified mainly *K. pneumoniae*, *A. baumannii*, *Xanthomonas campestris*, but not *S. hominis* (Supplementary Table 1).

At the onset of BSI, we detected five cultured pathogens in nine sequenced samples, the proportion of which ranked highest in P4, P7, P8, P9, P10 and P13E2 and ranked second in P5E3 and P12 (Supplementary Table 1). Pathogenic bacteria accounted for the majority of the top ten bacteria (Figure 4B). Samples of P7, P8, P9 and P10 were collected daily and underwent sequential mcfDNA-seq. The composition and percentage of the top ten bacteria fluctuated between days (Figures 4C–F), respectively. Time-series analysis showed an increased proportion of *K. pneumoniae* identification within the three days prior to the onset of BSI. However, the percentage of *K. pneumoniae* identification during the early samples varied greatly.

The diagnostic sensitivity of mcfDNA-seq was 90% (9/10), while total predictive sensitivity was 87.5% (14/16). Daily predictive sensitivity of mcfDNA-seq ranged from 81.82% to 92.31%, which were all greater than 80% (Figure 4G).

RPM typically increased in the days approaching BSI onset (Figure 4H). However, there was a large RPM range between pathogens, and the RPM of the same bacterium also varied greatly (Figure 4I). *P. aeruginosa* displayed the highest RPM, ranging from 8.6×10^{-1} to 4.1×10^{3}. The most frequently identified

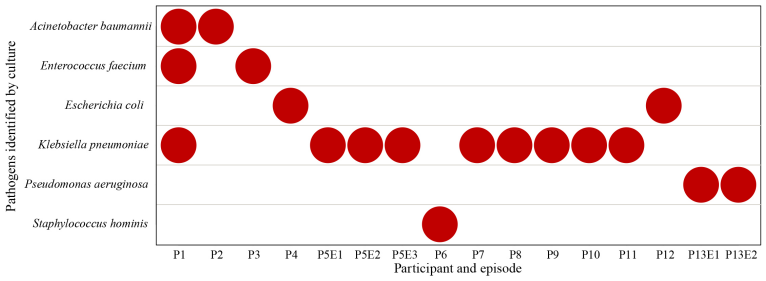

FIGURE 3
Pathogens identified at onset of BSI by culture.

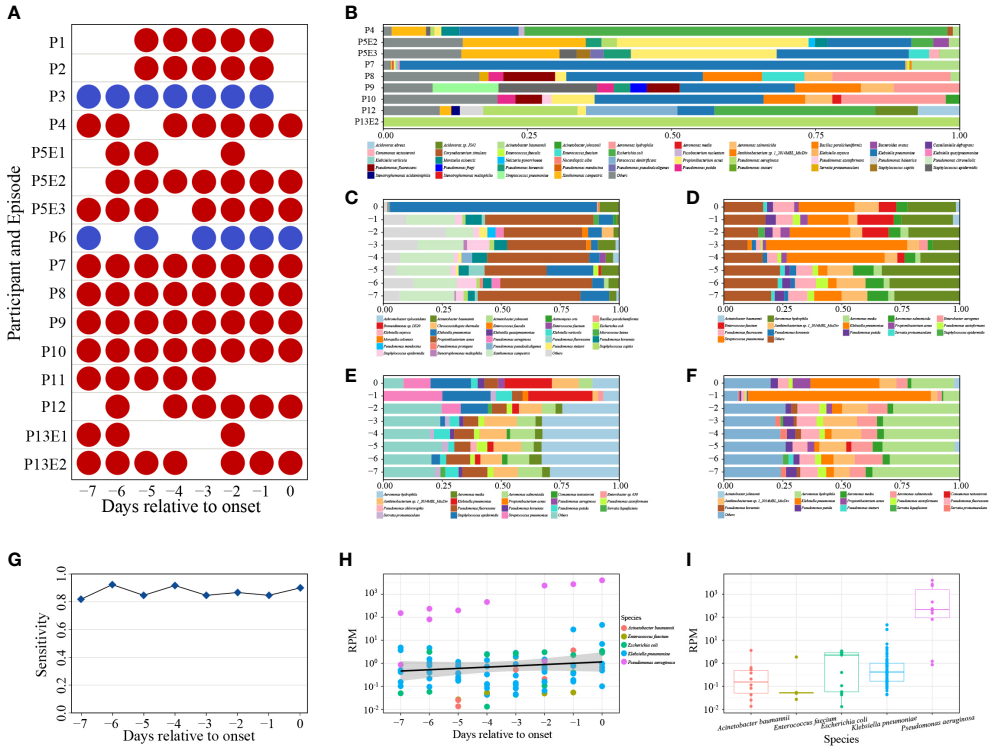

FIGURE 4
(A) Positive (red) and negative (blue) mcfDNA-seq results. **(B)** The percentages of the top ten bacteria of positive mcfDNA-seq samples on day of BSI onset. Species were sorted by name. **(C–F)** Variable percentages of the top ten bacteria of P7, P8, P9, P10. Species were sorted by name. **(G)** Sensitivity of mcfDNA-seq by days. **(H)** Variety of BSI pathogen-specific RPM by days. Circles represent RPM values of specific pathogens. Different colored circles represent different species. Black line indicates fitting curve of RPM. **(I)** RPM of pathogens. Circles represent RPM values of specific pathogens.

pathogen, *K. pneumoniae*, exhibited an RPM range from 4.3×10^{-2} to 4.6×10^{1}. The RPM of the other three pathogens ranged from 1.3×10^{-2} to 3.7×10^{0}.

4 Discussion

Metagenomic next-generation sequencing (mNGS) has received increasing attention as a clinical tool for pathogen detection. Multiple reports have demonstrated the advantages of mNGS to identify etiologic agents in diverse infections (Click et al., 2018; Hong et al., 2018; Fernandez-Carballo et al., 2019; Langelier et al., 2020; Chen et al., 2021). In addition, plasma mcfDNA may be an indicator of the onset of sepsis (Martins et al., 2000; Rhodes et al., 2006; Grumaz et al., 2016). Furthermore, mcfDNA-seq can not only be used for etiologic diagnosis, but may potentially predict BSI and thereby inform preemptive antimicrobial treatment.

The high diagnostic sensitivity and predictive value observed in our study suggests that mcfDNA-seq can facilitate BSI diagnosis and predict pathogens before BSI develops. The percentage of pathogenic bacteria was relatively high both in diagnostic and predictive samples. Furthermore, the RPMs of specific pathogens trended upward during the days approaching BSI onset, which could be related to the increasing microbial load in samples, as positive blood culture requires a significant inoculum of circulating bacteria. Blood culture requires 40-80 mL blood, which is a great burden on the participants. In the early stages of bacteremia, blood cultures may be negative. McfDNA-seq may have served as a “liquid biopsy” to diagnose occult focal infections before the onset of bacteremia, or may have detected early bacteremia below the threshold of detection of blood cultures, and requires much less blood than culture. Unfortunately, six participants died of BSI in our study. Thus, it is necessary to develop new pathogen detection methods to enable pre-emptive antibiotic therapy.

Despite these advantages of mcfDNA-seq, some limitations must be noted. In two of our participants, mcfDNA-seq did not detect pathogens identified by blood culture. This finding might have several explanations. First, the low microbial load in early samples requires deeper sequencing, and the sensitivity of mcfDNA-seq is highly dependent on the depth of sequencing. Second, mcfDNA is a remnant of microorganisms killed by anti-infective drugs and immune response (Gutierrez et al., 2019; Han et al., 2020) and has a very short half-life (Elshimali et al., 2013; Grumaz et al., 2016). The low content of mcfDNA or degraded mcfDNA further increased the difficulty of pathogen detection. In addition, mcfDNA analysis may be not suitable to detect intracellular pathogens (Chiu and Miller, 2019); consequently, the real-world clinical impact of plasma mNGS is still controversial (Hogan et al., 2021). In our study, it would be better to sample directly from participants instead of using residual blood samples.

And our work lacked healthy volunteer's specimens. The specificity of mcfDNA-seq remains to be further evaluated. Prospective clinical studies in larger cohorts including clinicians and healthy subjects are necessary to further evaluate mcfDNA as a tool for early or pre-emptive diagnosis.

Above all, our study demonstrated that mcfDNA-seq, a hypothesis-free diagnostic approach, may identify and predict pathogens causing BSI. Our findings may further assist the determination of the possible clinical utility of mcfDNA-seq.

Data availability statement

The data presented in the study are deposited in the China National GeneBank DataBase (CNGBdb) repository, accession number CNP0004130.

Ethics statement

The studies involving human participants were reviewed and approved by the ethics committee of the sixth medical center of PLAGH. Written informed consent for participation was not required for this study in accordance with the national legislation and the institutional requirements.

Author contributions

YL, PL, HS and YC conceived and designed the experiments. YC, XF and PD collected relative samples. TJ, YL performed the experiments. YC, TJ, YL, and HS participated in data analysis. YC, TJ and YL contributed reagents and materials. YC and PL wrote and revised the manuscript. All authors agree to be accountable for the content of the work. All authors contributed to the article and approved the submitted version.

Funding

This work was supported by a grant from National Key R&D Program of China (2021YFC2301002), the National science and technology Major project (2018ZX10305410), and Subproject of National science and technology Major Project (2018ZX10101003-001-006).

Acknowledgments

The authors thank the laboratory staff for obtaining and processing samples.

Conflict of interest

The authors declare that the research was conducted in the absence of any commercial or financial relationships that could be construed as a potential conflict of interest.

Publisher's note

Supplementary material

The Supplementary Material for this article can be found online at: https://www.frontiersin.org/articles/10.3389/fcimb.2023.1144625/full#supplementary-material

References

Bleeker-Rovers, C. P., Vos, F. J., de Kleijn, E., Mudde, A. H., Dofferhoff, T. S. M., Richter, C., et al. (2007). A prospective multicenter study on fever of unknown origin: the yield of a structured diagnostic protocol. *Med. (Baltimore)* 86 (1), 26–38. doi: 10.1097/MD.0b013e31802fe858

Casadevall, A. (2017). Crisis in infectious diseases: 2 decades later. *Clin. Infect. Dis.* 64 (7), 823–828. doi: 10.1093/cid/cix067

Chen, J., Zhao, Y., Shang, Y., Lin, Z., Xu, G., Bai, B., et al. (2021). The clinical significance of simultaneous detection of pathogens from bronchoalveolar lavage fluid and blood samples by metagenomic next-generation sequencing in patients with severe pneumonia. *J. Med. Microbiol.* 70 (1). doi: 10.1099/jmm.0.001259

Chiu, C. Y., and Miller, S. A. (2019). Clinical metagenomics. *Nat. Rev. Genet.* 20 (6), 341–355. doi: 10.1038/s41576-019-0113-7

Click, E. S., Murithi, W., Ouma, G. S., McCarthy, K., Willby, M., Musau, S., et al. (2018). Detection of apparent cell-free m. tuberculosis DNA from plasma. *Sci. Rep.* 8 (1), 645. doi: 10.1038/s41598-017-17683-6

Cockerill, F. R., Wilson, J. W., Vetter, E. A., Goodman, K. M., Torgerson, C. A., Harmsen, W. S., et al. (2004). Optimal testing parameters for blood cultures. *Clin. Infect. Dis.* 38 (12), 1724–1730. doi: 10.1086/421087

De Vlaminck, I., Martin, L., Kertesz, M., Patel, K., Kowarsky, M., Strehl, C., et al. (2015). Noninvasive monitoring of infection and rejection after lung transplantation. *Proc. Natl. Acad. Sci. U.S.A.* 112 (43), 13336–13341. doi: 10.1073/pnas.1517494112

Elshimali, Y. I., Khaddour, H., Sarkissyan, M., Wu, Y., and Vadgama, J. V. (2013). The clinical utilization of circulating cell free DNA (CCFDNA) in blood of cancer patients. *Int. J. Mol. Sci.* 14 (9), 18925–18958. doi: 10.3390/ijms140918925

Evans, L., Rhodes, A., Alhazzani, W., Antonelli, M., Coopersmith, C. M., French, C., et al. (2021). Surviving sepsis campaign: international guidelines for management of sepsis and septic shock 2021. *Intensive Care Med.* 47 (11), 1181–1247. doi: 10.1007/s00134-021-06506-y

Ewig, S., Torres, A., Angeles Marcos, M., Angrill, J., Rano, A., de Roux, A., et al. (2002). Factors associated with unknown aetiology in patients with community-acquired pneumonia. *Eur. Respir. J.* 20 (5), 1254–1262. doi: 10.1183/09031936.02.01942001

Fernandez-Carballo, B. L., Broger, T., Wyss, R., Banaei, N., and Denkinger, C. M. (2019). Toward the development of a circulating free DNA-based *In Vitro* diagnostic test for infectious diseases: a review of evidence for tuberculosis. *J. Clin. Microbiol.* 57 (4). doi: 10.1128/JCM.01234-18

Goggin, K. P., Gonzalez-Pena, V., Inaba, Y., Allison, K. J., Hong, D. K., Ahmed, A. A., et al. (2020). Evaluation of plasma microbial cell-free DNA sequencing to predict bloodstream infection in pediatric patients with relapsed or refractory cancer. *JAMA Oncol.* 6 (4), 552–556. doi: 10.1001/jamaoncol.2019.4120

Grumaz, S., Stevens, P., Grumaz, C., Decker, S. O., Weigand, M. A., Hofer, S., et al. (2016). Next-generation sequencing diagnostics of bacteremia in septic patients. *Genome Med.* 8 (1), 73. doi: 10.1186/s13073-016-0326-8

Gu, W., Deng, X., Lee, M., Sucu, Y. D., Arevalo, S., Stryke, D., et al. (2021). Rapid pathogen detection by metagenomic next-generation sequencing of infected body fluids. *Nat. Med.* 27 (1), 115–124. doi: 10.1038/s41591-020-1105-z

Gutierrez, J., Guimaraes, A. O., Lewin-Koh, N., Berhanu, A., Xu, M., Cao, Y., et al. (2019). Sustained circulating bacterial deoxyribonucleic acid is associated with complicated bacteremia. *Open Forum Infect. Dis.* 6 (4), ofz090. doi: 10.1093/ofid/ofz090

Han, D., Li, R., Shi, J., Tan, P., Zhang, R., and Li, J. (2020). Liquid biopsy for infectious diseases: a focus on microbial cell-free DNA sequencing. *Theranostics* 10 (12), 5501–5513. doi: 10.7150/thno.45554

Hogan, C. A., Yang, S., Garner, O. B., Green, D. A., Gomez, C. A., Dien Bard, J., et al. (2021). Clinical impact of metagenomic next-generation sequencing of plasma cell-free DNA for the diagnosis of infectious diseases: a multicenter retrospective cohort study. *Clin. Infect. Dis.* 72 (2), 239–245. doi: 10.1093/cid/ciaa035

Hong, D. K., Blauwkamp, T. A., Kertesz, M., Bercovici, S., Truong, C., and Banaei, N. (2018). Liquid biopsy for infectious diseases: sequencing of cell-free plasma to detect pathogen DNA in patients with invasive fungal disease. *Diagn. Microbiol. Infect. Dis.* 92 (3), 210–213. doi: 10.1016/j.diagmicrobio.2018.06.009

Jing, C., Chen, H., Liang, Y., Zhong, Y., Wang, Q., Li, L., et al. (2021). Clinical evaluation of an improved metagenomic next-generation sequencing test for the diagnosis of bloodstream infections. *Clin. Chem.* 67 (8), 1133–1143. doi: 10.1093/clinchem/hvab061

Kim, D., Song, L., Breitwieser, F. P., and Salzberg, S. L. (2016). Centrifuge: rapid and sensitive classification of metagenomic sequences. *Genome Res.* 26 (12), 1721–1729. doi: 10.1101/gr.210641.116

Langelier, C., Fung, M., Caldera, S., Deiss, T., Lyden, A., Prince, B. C., et al. (2020). Detection of pneumonia pathogens from plasma cell-free DNA. *Am. J. Respir. Crit. Care Med.* 201 (4), 491–495. doi: 10.1164/rccm.201904-0905LE

Lodise, T. P., Patel, N., Kwa, A., Graves, J., Furuno, J. P., Graffunder, E., et al. (2007). Predictors of 30-day mortality among patients with pseudomonas aeruginosa bloodstream infections: impact of delayed appropriate antibiotic selection. *Antimicrobial. Agents Chemother.* 51 (10), 3510–3515. doi: 10.1128/AAC.00338-07

Long, Y., Zhang, Y., Gong, Y., Sun, R., Su, L., Lin, X., et al. (2016). Diagnosis of sepsis with cell-free DNA by next-generation sequencing technology in ICU patients. *Arch. Med. Res.* 47 (5), 365–371. doi: 10.1016/j.arcmed.2016.08.004

Martins, G. A., Kawamura, M. T., and Carvalho, M. (2000). Detection of DNA in the plasma of septic patients. *Ann. New York Acad. Sci.* 906, 134–140. doi: 10.1111/j.1749-6632.2000.tb06603.x

Rhodes, A., Wort, S. J., Thomas, H., Collinson, P., and Bennett, E. D. (2006). Plasma DNA concentration as a predictor of mortality and sepsis in critically ill patients. *Crit. Care (London England)* 10 (2), R60. doi: 10.1186/cc4894

Riedel, S., Bourbeau, P., Swartz, B., Brecher, S., Carroll, K. C., Stamper, P. D., et al. (2008). Timing of specimen collection for blood cultures from febrile patients with bacteremia. *J. Clin. Microbiol.* 46 (4), 1381–1385. doi: 10.1128/JCM.02033-07

Sterling, S. A., Miller, W. R., Pryor, J., Puskarich, M. A., and Jones, A. E. (2015). The impact of timing of antibiotics on outcomes in severe sepsis and septic shock: a systematic review and meta-analysis. *Crit. Care Med.* 43 (9), 1907–1915. doi: 10.1097/CCM.0000000000001142

Tabah, A., Koulenti, D., Laupland, K., Misset, B., Valles, J., Bruzzi de Carvalho, F., et al. (2012). Characteristics and determinants of outcome of hospital-acquired bloodstream infections in intensive care units: the EUROBACT international cohort study. *Intensive Care Med.* 38 (12), 1930–1945. doi: 10.1007/s00134-012-2695-9

Timsit, J. F., Ruppe, E., Barbier, F., Tabah, A., and Bassetti, M. (2020). Bloodstream infections in critically ill patients: an expert statement. *Intensive Care Med.* 46 (2), 266–284. doi: 10.1007/s00134-020-05950-6

Wang, L., Guo, W., Shen, H., Guo, J., Wen, D., Yu, Y., et al. (2021). Plasma microbial cell-free DNA sequencing technology for the diagnosis of sepsis in the ICU. *Front. In Mol. Biosci.* 8. doi: 10.3389/fmolb.2021.659390

Zimlichman, E., Henderson, D., Tamir, O., Franz, C., Song, P., Yamin, C. K., et al. (2013). Health care-associated infections: a meta-analysis of costs and financial impact on the US health care system. *JAMA Internal Med.* 173 (22), 2039–2046. doi: 10.1001/jamainternmed.2013.9763

frontiers | Frontiers in Cellular and Infection Microbiology

TYPE Original Research
PUBLISHED 16 June 2023
DOI 10.3389/fcimb.2023.1135460

OPEN ACCESS

EDITED BY
Pushpanathan Muthuirulan,
Harvard University, United States

REVIEWED BY
Ashok Ayyappa,
University of Madras, India
Meena Subbarayan,
Gladstone Institutes, United States

*CORRESPONDENCE
Jifeng Yu
yujifengzzu@163.com
Zhongxing Jiang
jiangzx@zzu.edu.cn

RECEIVED 31 December 2022
ACCEPTED 01 June 2023
PUBLISHED 16 June 2023

CITATION
Zhang X, Wang F, Yu J and Jiang Z (2023) Clinical application value of metagenomic second-generation sequencing technology in hematologic diseases with and without transplantation.
Front. Cell. Infect. Microbiol. 13:1135460.
doi: 10.3389/fcimb.2023.1135460

Clinical application value of metagenomic second-generation sequencing technology in hematologic diseases with and without transplantation

Xia Zhang, Fang Wang, Jifeng Yu* and Zhongxing Jiang*

Department of Hematology, First Affiliated Hospital of Zhengzhou University, Zhengzhou, Henan, China

Introduction: Hematological patients are at risk of infections. It is unknown whether the pathogenic microbial spectrum differs between HSCT and non-HSCT patients, and whether metagenomic next-generation sequencing (mNGS) of peripheral blood can be used as a substitute test specimen such as alveolar lavage.

Methods: A retrospective study was conducted to evaluate the clinical application value of mNGS in hematological patients with and without HSCT.

Results: Viruses were prevalent pathogens in both non-HSCT (44%) and HSCT (45%) patients, chiefly human cytomegalovirus and Epstein–Barr virus. In non-HSCT patients, Gram-negative bacilli accounted for 33% (predominantly Klebsiella pneumonia), and Gram-positive cocci accounted for 7% (predominantly Enterococcus faecium) of pathogens. However, in HSCT patients, Gram-negative bacilli accounted for 13% (predominantly Stenotrophomonas maltophilia), and Gram-positive cocci accounted for 24% (predominantly Streptococcus pneumonia) of pathogens. Mucor was the most common fungu s in two groups. The positive rate of pathogens by mNGS was 85.82%, higher than conventional detection (20.47%, $P < 0.05$). Mixed infection accounted for 67.00%, among which the mixed infection of bacteria and virus (25.99%) was the most common. 78 cases had pulmonary infection, the positive rate of traditional laboratory tests was 42.31% (33/78), and of mNGS in peripheral blood was 73.08% (57/78), showing a statistical difference ($P = 0.000$). The non-HSCT patients had a higher frequency of Klebsiella pneumonia (OR=0.777, 95% CI, 0.697-0.866, $P = 0.01$) and Torque teno virus (OR=0.883, 95% CI, 0.820-0.950, $P = 0.031$) infections than HSCT patients, while the rates of Streptococcus pneumonia (OR=12.828, 95% CI, 1.378-119.367, $P = 0.016$), Candida pseudosmooth (OR=1.100, 95% CI, 0.987-1.225, $P = 0.016$), human betaherpesvirus 6B (OR=6.345, 95% CI, 1.105-36.437, $P = 0.039$) and human polyomavirus 1 (OR=1.100, 95% CI, 0.987-1.225, $P = 0.016$) infections were lower. Leishmania could be detected by mNGS.

Conclusion: mNGS of peripheral blood can be used as a substitute test method for hematological patients with pulmonary infection, the detection rate of mixed infections by mNGS was high, and mNGS has high clinical recognition rate and sensitivity in pathogen detection, and provides a basis for guiding the anti-infective treatment in hematological diseases with symptoms such as fever.

KEYWORDS

hematological diseases, infection, pathogen, metagenomic next-generation sequencing, hematopoietic stem cell transplant

Introduction

Patients with hematological diseases and recipients of hematopoietic stem cell transplantation (HSCT) are more prone to the development of infections due to immune reconstruction, the use of immunosuppressants, and other factors that cause damage to the immune system (Maschmeyer et al., 2019). Consequently, patients with hematopoietic malignancies are more vulnerable to infection caused by microbial organisms such as bacteria, viruses, and fungi due to immunocompromise. Infection is one of the main causes of death in patients with severe hematological diseases. In recent years, with the emergence of new pathogenic microorganisms, the increase in drug-resistant pathogenic microorganisms and the increase in immunosuppressed hosts, the morbidity and mortality of infection remain high, with a fatality rate among patients with sepsis reaching 50% (Chiu and Legrand, 2021). Severe acute bacterial infections are an enormous and growing health care burden, and they typically lack a timely diagnosis and thus adequate therapy in approximately 40% of clinical cases (Chao et al., 2020). In a study of 17, 990 patients with sepsis, Ricard Ferrer et al. (Ferrer et al., 2014) found that delayed antibiotic use led to sepsis and increased mortality. Invasive fungal infections are associated with unacceptably high mortality rates, killing approximately one and a half million people every year (Brown et al., 2012). Thus, it is of great importance to identify the pathogenic microorganisms as rapidly as possible in order to guide treatment. However, blood culture has a low sensitivity in probing many microorganisms, which can detect bacterial/fungal culture and the culture cycle is long (Hasanuzzaman et al., 2021). Quantitative real-time polymerase chain reaction (qRT–PCR) is quick and convenient, but it can only detect specific, suspected pathogens. Serum procalcitonin (PCT), C-reactive protein (CRP), erythrocyte sedimentation rate (ESR), (1,3)-β-D-glucan test (G test), and galactomannan test (GM test) have certain value in the diagnosis of infection. However, these indicators are affected by a variety of factors, and the specific pathogen cannot be identified (Cantey and Lee, 2021). There are also numerous pathogens that are difficult to detect, such as *Mycoplasma pneumoniae*, *Chlamydia pneumoniae*, *Cryptococcus neoformans*, *Pneumocystis carinii*, *Mycobacterium tuberculosis*, and common microorganisms. Despite these efforts, the etiology remains unknown in approximately 60% of cases, which results in delayed or ineffective treatments, increased mortality, and excessive health care costs (Schlaberg et al., 2017).

Metagenomic next-generation sequencing (mNGS) technology, as a diagnostic tool, is not susceptible to environmental interference, rapid, accurate and high positive rate, which can fulfill such a need. It overcomes the shortcomings of the traditional detection methods such as harsh culture conditions, long culture time and low positive rate. Through gene sequencing and database comparison, it can comprehensively analyze all possible pathogenic microorganisms in samples, with the characteristics of a short detection period and comprehensive detection (Gu et al., 2019).

It is also unknown whether the pathogenic microbial spectrum differs between HSCT and non-HSCT patients. Patients with hematologic diseases are also prone to concurrent thrombocytopenia and infection. Therefore, due to the risk of bleeding, the inability to obtain alveolar lavage solution through bronchoscopy presented great difficulties in the diagnosis and treatment of pathogenic microorganisms in patients with hematologic diseases. We will investigate whether mNGS of peripheral blood can be used as a substitute test specimen, when alveolar lavage is difficult to obtain. Consequently, we speculate that mNGS technology could improve clinical management methods of hematology patients with fever. This study retrospectively analyzed the pathogenic microorganism detection results and prognosis of hematological patients with fever from May 2021 to March 2022. It is expected to provide guidance for the treatment of patients and the prediction of the clinical prognosis.

Methods

Patient enrollment and clinical data collection

This retrospective study was approved by the Ethics Review Committee of the First Affiliated Hospital of Zhengzhou University, and written informed consent was obtained from all subjects or their guardians. Clinical samples of hospitalized patients were collected from May 2021 to March 2022. The inclusion criteria

were as follows: patients with obvious symptoms of infection, including (1) hematologic diseases; (2) any of the following symptoms or signs: fever (>38 °C), coughing, expectoration, pleural effusion, seroperitoneum, urinary tract infections, diarrhea, cardiac effusion, deep abscess, chest CT showing lung infection, etc. The clinical data of the patients were recorded, and blood, urine, excrement, and sputum samples were collected depending on their clinical condition. The clinical samples were used to perform bacterial culture, qRT–PCR or deoxyribonucleic acid (DNA) extraction followed by high-throughput sequencing.

Specimen collection

Clinical specimens, such as blood samples, bone marrow liquid, sputum, pus, nasopharyngeal/oropharyngeal/perianal swabs, pleural effusion, ascites, mid-stream urine samples, stool, pericardial effusion, and secretion, were obtained from patients as soon as possible after presentation and were collected before antimicrobial therapy began. Samples were stored at −80°C until transferred to the central laboratory.

Pathogen detection

The samples were placed in anaerobic and aerobic culture bottles and immediately sent to the bacterial room of our hospital for pathogen culture. Epstein–Barr virus (EBV), human cytomegalovirus (CMV) and BK virus were detected by PCR in patients with virus infection. The samples were placed in EDTA tubes and special virus transfer tubes and sent to Genskey Co., Ltd., Beijing, for mNGS detection of pathogenic microorganisms (Jing et al., 2021), which is known as shotgun sequencing with the following advantages: high sequencing throughput, high sensitivity, early identification of pathogens, and detection of special pathogens.

Sampling and mNGS sequencing

The metagenomic next-generation sequencing method was used as described in the reference (Jing et al., 2021; Zhang et al., 2021). Samples were collected by BCT tubes, centrifuged at 1600g for 10 min, and cfDNA was extracted from plasma supernatant. In the experiment, both internal control and external negative control were used in QC. DNA was extracted using the TIANamp Micro DNA Kit (TIANGEN, China) and quantified by fluorometry (ThermoFisher Scientific, USA) according to the manufacturer's recommendation.

DNA library was constructed according to the protocol of the BGISEQ-200 sequencing platform by DNA fragmentation, end-repair, adapter-ligation, and PCR amplification, which was qualified by Agilent 2100 (Agilent Technologies, USA) and Qubit 4.0 (Thermo Fisher, USA). Qualified double-stranded DNA libraries became single-stranded DNA by denaturation and cyclization. By rolling circle amplification (RCA), single-stranded circular DNA was transformed into DNA nanoballs (DNBs). The DNBs were carried out quality control by Qubit 4.0. Qualified DNBs were loaded into the flow cell and sequenced (50 bp, single-end) on the BGISEQ-200 platform (Zhang et al., 2021). Up to 20 libraries per batch were pooled to be sequenced on Illumina NextSeq 550 sequencers using a 75-cycle single-end sequencing strategy.

Bioinformatics pipeline

Adapters and low quality and short (<35bp) of reads were removed to obtain clean reads by using fastp software (Chen et al., 2018). Human host sequences were excluded by mapping to the human reference genome (hg38) by using STAR alignment (Dobin et al., 2013). Low complexity and duplicated reads were removed by using PRINSEQ algorithms (Schmieder and Edwards, 2011). The remaining clean reads were blasted against in-house microbial genome databases, which were mainly downloaded from NCBI (ftp://ftp.ncbi.nlm.nih.gov/genomes/) using Kraken2 software (Wood et al., 2019). In terms of species-specific read number, reads per million and genome coverage, the sequencing data list was analyzed.

Statistical analysis

Data were analyzed using SPSS 22.0 software (SPSS, Chicago, IL, US). Quantitative data were compared between the two groups using a t-test (for a normal distribution) or a nonparametric test (Mann–Whitney Test, not a normal distribution). For comparisons of the categorical data, the chi-squared ($\chi 2$) test was used. Data analysis was performed using GraphPad Prism 9 software (GraphPad Software, La Jolla, California). $P < 0.05$ was considered statistically significant.

Results

Patient characteristics and clinical samples

The characteristics of the 103 patients are summarized in Table 1. The median age was 39.3 years old, with 72 male and 31 female patients. There were 28 patients underwent HSCT and 75 patients with hematologic diseases who did not undergo HSCT. The underlying diseases included acute myeloid leukemia (n=34), acute lymphoblastic leukemia (n=12), acute mixed lineage leukemia (n=2), myelodysplastic syndromes (n=10), malignant lymphoma (n=5), chronic myeloid leukemia (n=2), chronic lymphocytic leukemia (n=2), multiple myeloma (n=7), hemophagocytic lymphohistiocytosis (n=5), aplastic anemia (n=8) and others (incldluing paroxysmal nocturnal hemoglobinuria, Henoch-Schonlein purpura, immune thrombocytopenia, and fever of undetermined origin (FUO), (n= 16). mNGS was performed 127 person-times. Clinical samples revealed 109 cases with clear pathogens and 18 with no pathogens. We analyzed the samples of pulmonary infection, 78 cases had pulmonary infection, the positive

TABLE 1 Patient characteristics.

Variables	cases	ratio (%)	P
Age, year, median (range)	39.3 (14~67)		
Gender (male/female)	72/31		
Underlying disease			
Leukemia			
acute myeloid leukemia	34	33.01	
acute lymphoblastic leukemia	12	11.65	
acute mixed lineage leukemia	2	1.94	
chronic myeloid leukemia	2	1.94	
chronic lymphocytic leukemia	2	1.94	
Myelodysplastic syndromes	10	9.71	
Malignant lymphoma	5	4.85	
Multiple myeloma	7	6.80	
Hemophagocytic lymphohistiocytosis	5	4.85	
Aplastic anemia	8	7.77	
Others (ITP, etc.)	16	15.53	
Status at transplant			
HSCT	28	27.18	
Non-HSCT	75	72.82	
Pathogens			
clear pathogens	109	85.83	
no pathogens	18	14.17	
Pulmonary infection	78		0.000
conventional testing		42.31	
mNGS		73.08	

ITP, immune thrombocytopenia; allo-HSCT, allogeneic hematopoietic stem cell transplantation; auto-HSCT, autologous hematopoietic stem cell transplantation.

rate of traditional laboratory tests such as sputum culture and blood culture was 42.31% (33/78), and the positive rate of mNGS in peripheral blood was 73.08% (57/78), showing a statistical difference (P = 0.000).

Clinical assessment

The results of mNGS were assessed clinically by physicians. To determine whether the pathogenic microorganism was the pathogen causing the patient's symptoms, the physicians evaluated the results in combination with the patient's clinical symptoms and other examinations, such as PCT, CRP, ESR, G test and GM test, blood culture, features of lung imaging, and fibreoptic bronchoscopy. It was considered a component of the etiology if the index patient met the clinical criteria of infection, whether confirmed by conventional tests or not.

Treatment regimens were adjusted according to the results of pathogenic microorganisms. Escalation of the antibiotics avoided empirical combinations, while de-escalation, with initial broad-spectrum antibiotic combinations, could minimize the collateral damage associated with antibiotic overuse. However, based on the clinical manifestations and test results, some results of the mNGS were considered meaningless, and the original treatment was continued (Table 2). Antifungal prophylaxis should not be used routinely in all patients with neutropenia. The rationale for antifungal prophylaxis is to prevent fungal infections in a specific group of high-risk patients, especially those with longer durations of neutropenia or with GVHD after allogeneic HSCT. Antifungal agents include azoles, amphotericin B products, and echinocandins and its selection is determined by the disease and therapy strategy. Therefore, the physician's clinical judgment is pivotal in the evaluation and modification in the antimicrobial regimen.

The coverage of sequencing results in hematologic diseases with and without transplantation

The mNGS results from our study revealed that viruses were the predominant pathogenic microorganisms in both non-HSCT (44%) and HSCT (45%) patients. Gram-negative bacilli accounted for 33%, and Gram-positive cocci accounted for 7% of pathogens in non-HSCT patients. However, Gram-negative bacilli accounted for 13% and Gram-positive cocci accounted for 24% of pathogens in HSCT patients. The percentage of fungi in non-HSCT patients

TABLE 2 Direction of clinical treatment by mNGS.

Clinical benefit of mNGS	mNGS guidance for patient management
Initiation therapy of antimicrobial agents	mNGS detected pathogens and directed application of antimicrobial agents.
De-escalation therapy of antimicrobial agents	According to the results of mNGS and traditional test, the pathogenic microorganisms were identified and the empirical anti-infective drugs were adjusted.
Upgradation therapy of antimicrobial agents	According to the results of mNGS and traditional test, the pathogenic microorganisms were identified and appropriate antimicrobial agents were selected.
Identification of pathogenic micro-organisms	mNGS detected pathogens and directed application of antibiotics.
No clinical significance	Combined with clinical symptoms and traditional test, it was ascertained that some pathogenic microorganisms had no clinical significance.

10.3389/fcimb.2023.1135460

(13%) was higher than that in HSCT patients (8%). Tubercle bacillus (8%) was detected by mNGS in HSCT patients but not in non-HSCT patients. Other pathogens (3%), such as *Mycobacterium tuberculosis* and Leishmania, were detected in FUO patients (Figures 1A, B). In the non-HSCT group, *Klebsiella pneumonia*, *Pseudomonas aeruginosa* and *Acinetobacter baumannii* were the top 3 bacteria. Whereas, *Stenotrophomonas maltophilia*, *Streptococcus pneumonia*, *Enterobacter cloacae* complex and *Enterococcus faecium* were bacteria that were commonly found in the HSCT group. In both the non-HSCT and HSCT patient groups,

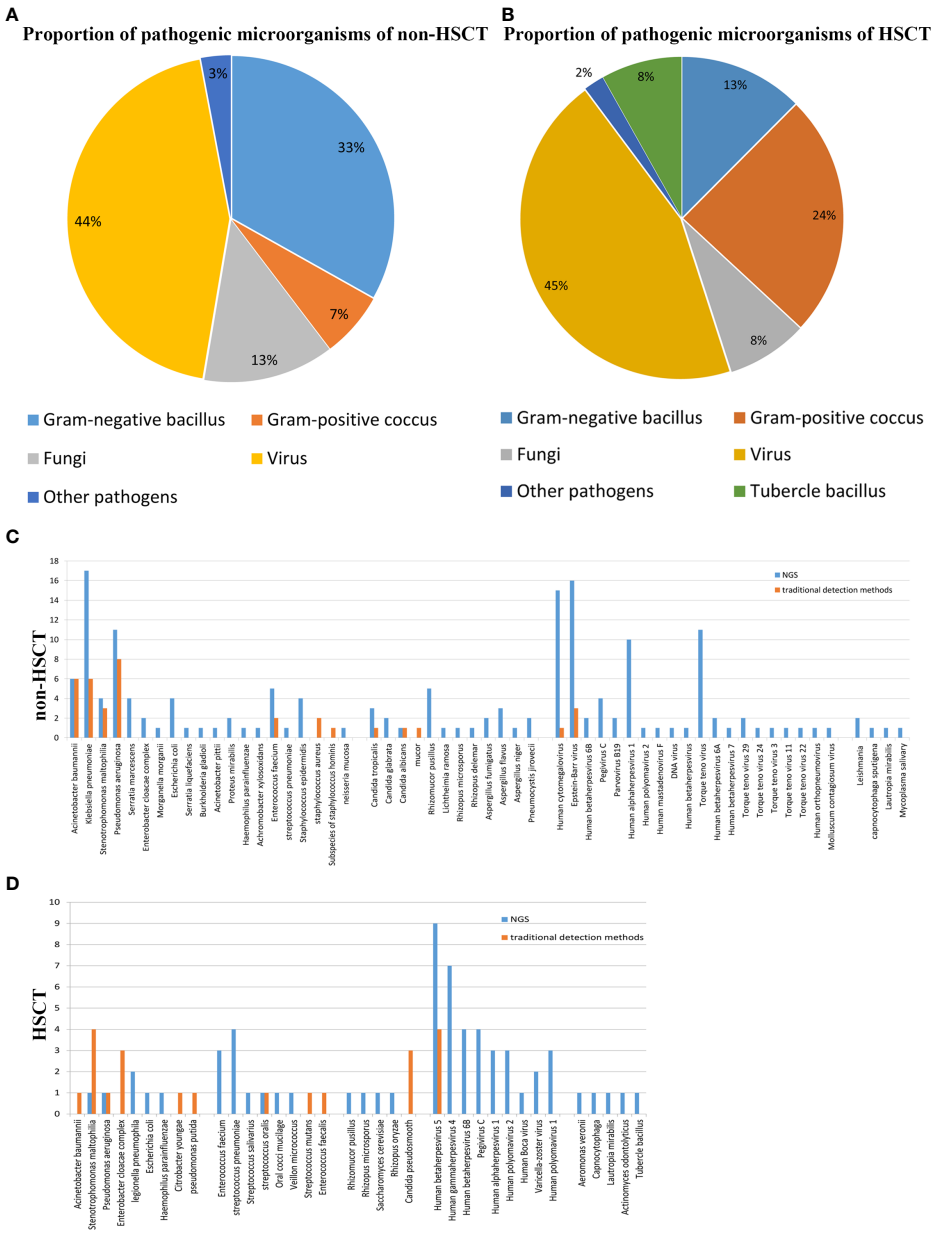

FIGURE 1
Patient characteristics and clinical samples. **(A)** The mNGS results revealed that bacteria occupied the bulk of pathogenic microorganisms in patients with hematological disease but not those with HSCT. Gram-negative bacillus accounted for a greater proportion of the bacteria. The proportion of virus was high in both the transplantation and nontransplantation groups. **(B)** In the nontransplantation group, *Klebsiella pneumonia*, *Pseudomonas aeruginosa* and *Acinetobacter baumannii* were the top 3 bacteria. However, *Stenotrophomonas maltophilia* and *Streptococcus pneumonia* were commonly found in the HSCT group. Mucor was the most common fungus, and human cytomegalovirus and Epstein–Barr virus were commonly found both in the transplantation and nontransplantation groups. **(C)** The detection rates of *Acinetobacter baumannii*, *Klebsiella pneumonia*, *Stenotrophomonas maltophilia*, *Pseudomonas aeruginosa*, *Enterococcus faecium* and *Staphylococcus aureus* in non-HSCT patients were higher than those of other bacteria. **(D)** EBV and CMV were the most common pathogenic microorganisms. Non-HSCT, non-hematopoietic stem cell transplant; HSCT, hematopoietic stem cell transplant.

Mucor was the most common fungus, and CMV and EBV were commonly found. The detection rate by mNGS method was higher than traditional detecting methods (Figures 1C, D).

Higher detection rate of pathogens by mNGS

The positive rates of pathogens in clinical samples detected by mNGS and conventional testing were compared. The positive rate of pathogenic microorganisms detected by mNGS was 85.82%, which was higher than conventional detection (20.47%, $P < 0.05$) (Figure 2A). The number of cases using mNGS and traditional methods to detect pathogens were quite different. Fifty cases of bacteria were detected by mNGS, and 40 cases were detected by traditional methods. Seventy-seven cases of viruses were detected by mNGS, 9 cases were detected by the traditional method, 19 cases of fungi were detected by mNGS, and 6 cases were detected by the traditional method (Figure 2B).

Spectra of pathogens and consistency of detection revealed by mNGS and conventional testing in hematological patients with and without transplantation

mNGS and conventional testing were performed in a total of 127 clinical samples. In the HSCT patient group, there were 12 cases of bacteria, 22 cases of viruses, 1 case of fungus detected by mNGS, 15 cases of bacteria, 4 cases of viruses, and 3 cases of fungi detected by conventional testing, such as PCR and/or culture. In the non-HSCT hematology patient group, there were 38 cases of bacteria, 55 cases of viruses, 18 cases of fungi detected by mNGS and 25 cases of bacteria, 5 cases of viruses, and 3 cases of fungi detected by conventional testing, such as PCR and/or culture. A total of 146 potential pathogens were identified by mNGS; 9 cases of viruses were detected by PCR, and 46 cases were detected by culture. The detection positive rate of mNGS was the highest among the three detection methods (Figure 3A).

The positive rate of viruses detected by mNGS was higher than that of traditional detection methods (66.7% *vs.* 12.12%), while for bacteria it was 36.6% *vs.* 45.45%, and for fungi it was 3.03% *vs.* 9.09% in the HSCT patient group. In the non-HSCT patient group, the positive rate of viruses detected by mNGS (58.51%) was higher than that of traditional detection methods (5.32%), for bacteria it was 40.43% *vs.* 26.59%, and for fungi it was 19.15% *vs.* 3.19%. The pathogens identified by mNGS and conventional testing were cross-validated by using either another assay or other samples collected from the same patient. There were significant differences in bacteria, fungi and viruses between non-HSCT and HSCT patients ($P < 0.05$) (Figures 3B, C). Among bacterium, fungus and virus groups, the detection rate of bacteria by culture was the highest while the detection rate of fungi was the lowest. There were no significant differences in bacteria, fungi and viruses detection rates between non-HSCT and HSCT patients ($P > 0.05$) (Figure 3C). The infection spectrum indicated that the detection rate of pathogenic microorganisms was higher in patients without hematopoietic stem cell transplantation (Figure 3D).

Consistency of detection was revealed by mNGS and conventional testings in hematological patients. Samples of 44 patients underwent mNGS, PCR, G and GM tests and culture testings simultaneously. EBV and/or CMV were detected as positive by mNGS but negative by PCR in 9 contemporaneous samples of the patients. However, the detection results were consistent in 35 of the patients. The consistency ratio between mNGS and traditional detection methods was 79.55%. Pathogens were identified in 28 patients by mNGS in combination with another laboratory testing (Table 3).

Different microbial etiologies in hematological patients with and without transplantation

To further evaluate the microbial etiology of infection in hematological diseases, the potential pathogens between the HSCT and non-HSCT patient groups were compared. Combined with mNGS and conventional testing, pathogenic microorganisms

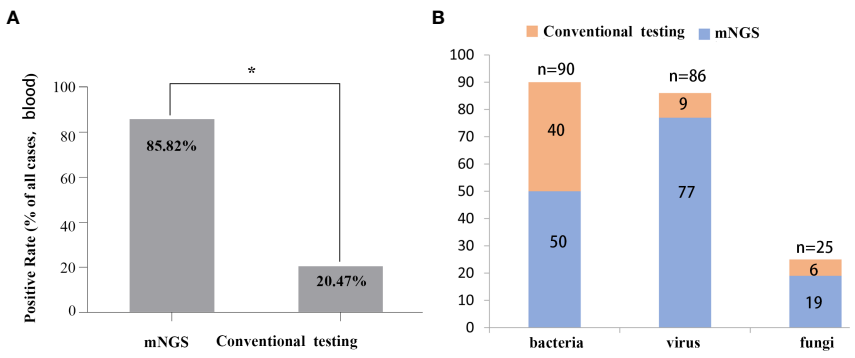

FIGURE 2
Comparison between mNGS and conventional testing for detecting pathogens in clinical samples. **(A)** Differences in rates of positivity by cases, $P < 0.05$. **(B)** Differences in the number of cases for pathogens detected by mNGS and the conventional method.

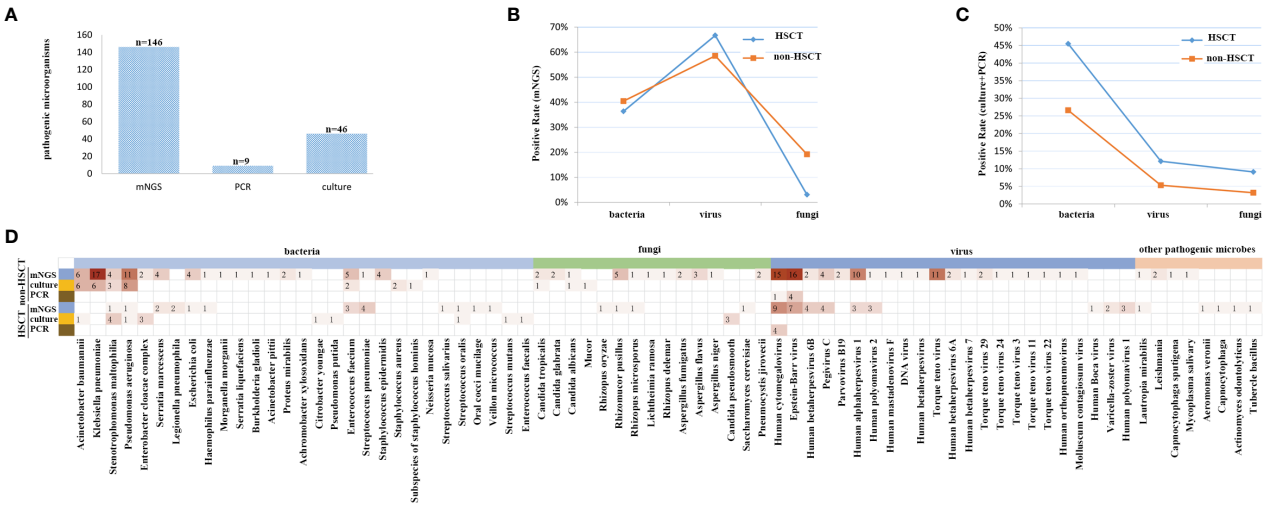

FIGURE 3
The coverage of sequencing results, focusing on all samples, and its high sensitivity for special pathogens. **(A)** The detection rate of mNGS was the highest among the three methods. **(B)** The detection rate of viruses was higher by mNGS, and after standardization of the rate, there were significant differences in bacteria, fungi and viruses between non-HSCT and HSCT patients, $P < 0.05$. **(C)** The detection rate of bacteria was the highest, and the detection rate of fungi was the lowest. There were no significant differences in bacteria, fungi and viruses between non-HSCT and HSCT patients, $P > 0.05$. **(D)** The infection spectrum indicated that the detection rate of pathogenic microorganisms was higher in patients without HSCT.

in clinical samples were detected in all of the HSCT patients. There were no pathogens detected in 16 non-HSCT patients. Bacteria were detected in the HSCT group (17 cases) and non-HSCT group (52 cases), while viruses were detected in the HSCT group (23 cases) and non-HSCT group (55 cases), and fungi were detected in the HSCT group (4 cases) and non-HSCT group (20 cases) (Figure 4A). There were 3 patients infected by bacteria, viruses and fungi simultaneously in the HSCT patient group, whereas 7 patients in the non-HSCT group. The odd ratio (OR) (95% confidence interval, CI) between the non-HSCT patient group and HSCT group was 1.243 (0.302-5.115). Viruses and fungi coexisted in 12 non-HSCT patients and 4 HSCT patients. The OR (95% CI) between them was 0.943 (0.282-3.155). Both bacteria and fungi were present in 11 non-HSCT patients and 3 HSCT patients. The OR (95% CI) between them was 0.755 (0.197-2.891). Both bacteria and viruses were present in 27 non-HSCT patients and 6 HSCT patients. The OR (95% CI) between them was 0.551 (0.205-1.486). There were no significant differences between any of the above groups (P> 0.05). Patients with mixed infection accounted for 67.00%. Among them, the mixed infection of bacteria and virus (25.99%) was the most common (Figure 4B). However, we found statistically significant differences in pathogens between the non-HSCT patient group and HSCT group (Figure 4C). The non-HSCT patients had a higher frequency of *Klebsiella pneumonia* (OR=0.777, 95% CI, 0.697-0.866, P = 0.01) and *Torque teno* virus (OR=0.883, 95% CI, 0.820-0.950, P = 0.031) infections than HSCT patients, while the rates of *Streptococcus pneumonia* (OR=12.828, 95% CI, 1.378-119.367, P = 0.016), *Candida pseudosmooth* (OR=1.100, 95% CI, 0.987-1.225, P = 0.016), human betaherpesvirus 6B (OR=6.345, 95% CI, 1.105-36.437, P = 0.039) and human polyomavirus 1 (OR=1.100, 95% CI, 0.987-1.225, P = 0.016) infections were lower in non-HSCT patients (Table 4).

Evaluation of the application of mNGS in hematological patients with and without transplantation in the real world

Clinical samples from patients were tested by mNGS and conventional methods. The application of mNGS in the real world was evaluated. 45 cases (48%) of pathogens were detected by mNGS only in non-HSCT group and 12 cases (36%) in HSCT group. Conventional testing detected pathogenic organisms in 6 cases (6%) of non-HSCT patients and 4 cases (12%) of HSCT patients which were negative by mNGS method. Pathogens identified by both mNGS and conventional testing were 27 (29%) cases in the non-HSCT group and 17 (52%) cases in the HSCT group. Pathogenic organisms identified by combining mNGS, the conventional testing results and clinical signs and symptoms included 16 (17%) cases in the non-HSCT group (Figure 5A). Figure 5B shows clinically determined pathogens detected only by mNGS rather than conventional methods in patients with hematological diseases, and 25 pathogens cannot be detected by conventional detection.

The clinical impact of mNGS in hematological patients was evaluated. mNGS had an overall beneficial impact on treatment in 61.70% of the non-HSCT patients and 75.8% of the HSCT patients. The beneficial impacts included initiation of antibiotic therapy (n=33 in non-HSCT, n=17 in HSCT), treatment de-escalation (n=10 in non-HSCT, n=2 in HSCT) and upgrading of anti-infection drugs (n=15 in non-HSCT, n=16 in HSCT). mNGS also identified pathogenic microorganisms in 18 cases (19%) in the non-HSCT group and 3 cases (9%) in the HSCT group. However, mNGS had no beneficial impact on treatment in 18 cases (19%) in the non-HSCT group and 5 cases (15%) in the HSCT group, because it could not direct the treatment or diagnosis of diseases (Figure 5C).

10.3389/fcimb.2023.1135460

TABLE 3 Pathogens identified by mNGS in combination with other laboratory testing.

Number	Diagnosis	Type of clinical sample	Pathogenic microorganism	Validation method
2	AML	blood, sputum	Candida tropicalis	culture, G test
14	AML	blood, sputum, perianal swab	Rhizomucor pusillus	G test
15	AML	blood, sputum, perianal swab	Rhizomucor pusillus	G test
16	AML	blood, stool	Rhizomucor pusillus	G test
36	MM	blood,sputum,mid-stream urine	Candida albicans	culture, G test
38	AMLL	blood	Klebsiella pneumoniae	culture
40	ALL	blood,secretion	Pseudomonas aeruginosa	culture
41	AML	blood,secretion	Pseudomonas aeruginosa	culture
43	AML	blood,sputum,perianal swab	Klebsiella pneumoniae	culture
47	MDS	blood	Candida tropicalis	G test
48	HLH	blood, mid-stream urine, oropharyngeal swab	EBV	PCR
53	HLH	blood	EBV	PCR
54	AA	blood	Lichtheimia ramosa	G test, mNGS dynamic monitoring
58	AML	blood, sputum, mid-stream urine	Pseudomonas aeruginosa	culture
70	Other	blood,pleural effusion	EBV	PCR
77	AML	blood,stool	Klebsiella pneumoniae	culture
79	ALL	blood	Pseudomonas aeruginosa	culture
82	AML	blood	CMV	PCR
84	HLH	blood,sputum,pleural effusion	Klebsiella pneumoniae	culture
88	MDS	blood,sputum	Pseudomonas aeruginosa	culture
94	MDS	blood	Pseudomonas aeruginosa	culture
96	AMLL, HSCT	blood, perianal swab	Escherichia coli	culture
98	PNH, HSCT	blood, perianal swab	CMV	PCR
104	MDS, HSCT	blood,stool	Stenotrophomonas maltophilia	culture
107	AA, HSCT	blood, perianal swab	EBV, CMV	PCR
113	AA, HSCT	blood, perianal swab	EBV, CMV	PCR
117	MDS, HSCT	blood, perianal swab	Rhizomucor pusillus	G test
118	AA, HSCT	blood	CMV	PCR

AML, acute myeloid leukemia; ALL, acute lymphoblastic leukemia; MM, multiple myeloma; AMLL, acute mixed lineage leukemia; MDS, myelodysplastic syndromes; HLH, hemophagocytic lymphohistiocytosis; AA, aplastic anemia; PNH, paroxysmal nocturnal hemoglobinuria; HSCT, hematopoietic stem cell transplantation; EBV, Epstein-barr virus; CMV, Human cytomegalovirus; PCR, polymerase chain reaction; G test, (1,3)-β-D-glucan test.

Discussion

Hematological diseases, especially hematological malignancies, require intensive treatment with chemotherapy, hormones and immunotherapeutic and molecular targeted agents (Maschmeyer et al., 2019). Refractory or relapsed leukemia/lymphoma/multiple myeloma patients after multiple chemotherapy regimens usually undergo HSCT, so these patients are more prone to the development of bloodstream infections due to immune reconstruction, the use of immunosuppressants and other factors that damage the overall immune system. Opportunistic infections that do not cause disease in people with normal immunity may have serious clinical consequences in patients with hematological diseases and post-transplantation patients. As this article notes that infection is common complication and one of the main causes of death in patients with hematological diseases (Hardak et al., 2016). Consequently, it is very important to find pathogenic microorganisms in time. However, standard testing fails to identify pathogens in most patients with hematological disease. Due to the lack of specific diagnostic basis for fungal, viral and Mycobacterium tuberculosis infections, infections may be classified as bacterial related infections. This also reflects that the traditional detection methods cannot comprehensively detect all possible pathogens of hematological diseases, and it is difficult to

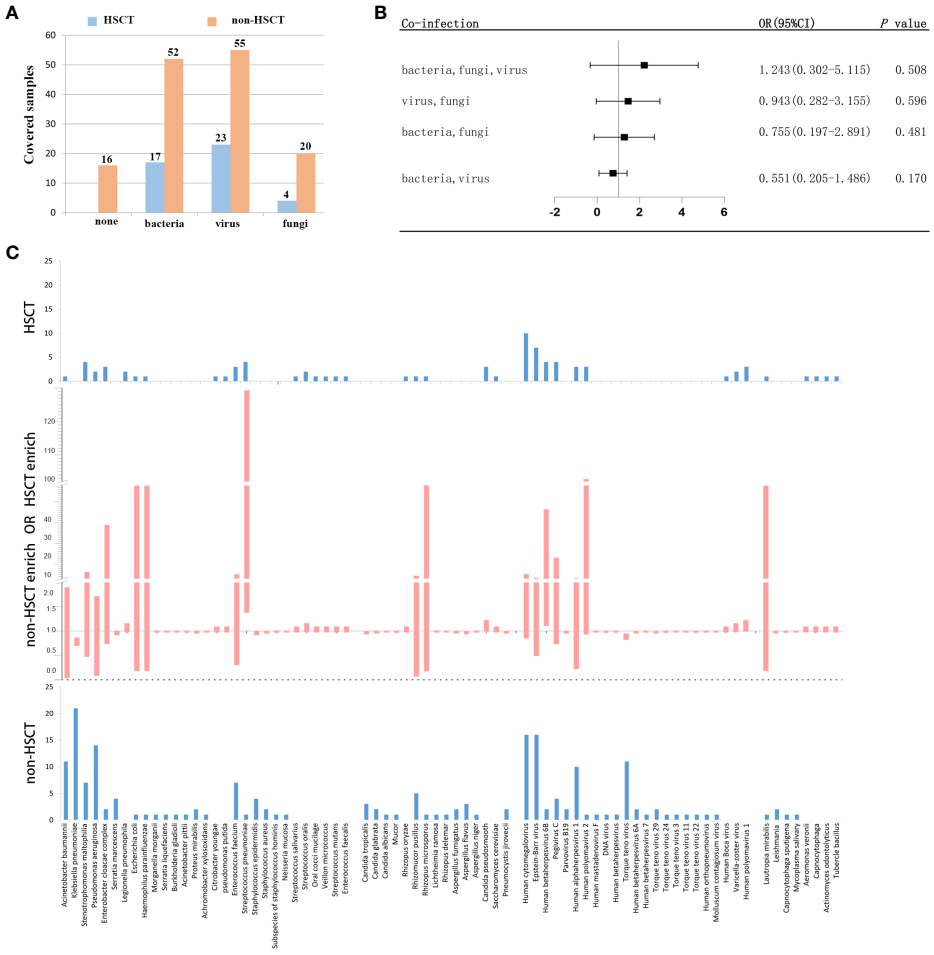

FIGURE 4
Different microbial etiologies in HSCT and non-HSCT patients. **(A)** Distribution of different types of microbial etiologies. **(B)** Potential coinfections in non-HSCT and HSCT patients. **(C)** Spectra of pathogenic microorganisms in HSCT and non-HSCT patients. The middle chart shows pathogenic microorganisms that were statistically significant ($P < 0.05$).

understand the characteristics of infection spectrum in the real-world.

One study showed that Gram-positive cocci were the most commonly isolated (75.8%), while Gram-negative bacilli infections occurred in 12.1% of patients undergoing chemotherapy for acute myeloid leukemia (Madani, 2000). However, another study performed by Rima Moghnieh et al. showed that 57.3% of the 75 bacteremic cases were due to Gram-negative organisms, and the remaining 42.7% were Gram-positive in febrile neutropenia adult cancer patients. *Escherichia coli* and *Klebsiella pneumonia* were the most prevalent Gram-negative organisms, representing 22.7% and 13.3% of the total cases, respectively (Moghnieh et al., 2015). However, in our study, it showed that the proportion of Gram-negative bacilli was higher than that of Gram-positive cocci (28% *vs.* 10%). We speculated that the reason for inconsistent results in different studies might be related to the different bacterial spectra in different regions, hospitals and different inclusion conditions of the patients. In our study for non-HSCT patients, the proportion of Gram-negative bacilli was higher than that of Gram-positive cocci (33% *vs.* 7%), while Gram-positive cocci were predominant in HSCT patients (Gram-negative bacilli *vs.* Gram-positive cocci, 13% *vs.* 24%). We hypothesize that the cause of the large difference in pathogenic bacteria between HSCT and non-HSCT patients is that HSCT recipients undergoing intensive myelosuppressive, immunosuppressive treatment and immune reconstruction are at high risk for severe, life-threatening bacterial infections. Our study showed that *Klebsiella pneumonia* accounted for the highest proportion, followed by *Pseudomonas aeruginosa* and *Acinetobacter baumannii*. *Stenotrophomonas maltophilia* accounted for the largest number of Gram-negative bacilli in HSCT patients, followed by *Enterobacter cloacae* complex. However, other studies suggested that *Escherichia coli* was the most common Gram-negative bacillus (Moghnieh et al., 2015). There were significant differences between the above studies. The reason may be that the patients included in other studies were infected due to neutropenia after HSCT, while the patients in our study had different infection conditions.

Hematological patients, especially HSCT recipients, are immunosuppressed and have received multiple courses of antibiotics in the past, and infections are more likely to occur in these patients with poor immunity. Vancomycin-resistant Enterococcus has increasingly become a major nosocomial

10.3389/fcimb.2023.1135460

TABLE 4 Spectra of pathogenic organisms between non-HSCT and HSCT patients.

Pathogens	Organisms	non-HSCT (94)	HSCT (33)	*P* value	Odds ratio (95% CI)
Acinetobacter baumannii	bacterium	11	1	0.128	0.236 (0.029-1.901)
Klebsiella pneumoniae	bacterium	21	0	0.010	0.777 (0.697-0.866)
Stenotrophomonas maltophilia	bacterium	7	4	0.309	1.714 (0.468-6.280)
Pseudomonas aeruginosa	bacterium	14	2	0.156	0.369 (0.079-1.717)
Enterobacter cloacae complex	bacterium	2	3	0.110	4.600 (0.733-28.849)
Serratia marcescens	bacterium	4	0	0.295	0.957 (0.917-0.999)
Legionella pneumophila	bacterium	0	2	0.066	1.065 (0.976-1.161)
Escherichia coli	bacterium	1	1	0.454	2.906 (0.177-47.829)
Haemophilus parainfluenzae	bacterium	1	1	0.454	2.906 (0.177-47.829)
Morganella morganii	bacterium	1	0	0.740	0.989 (0.969-1.010)
Serratia liquefaciens	bacterium	1	0	0.740	0.989 (0.969-1.010)
Burkholderia gladioli	bacterium	1	0	0.740	0.989 (0.969-1.010)
Acinetobacter pittii	bacterium	1	0	0.740	0.989 (0.969-1.010)
Proteus mirabilis	bacterium	2	0	0.546	0.979 (0.950-1.008)
Achromobacter xylosoxidans	bacterium	1	0	0.740	0.989 (0.969-1.010)
Citrobacter youngae	bacterium	0	1	0.260	1.031 (0.971-1.095)
Pseudomonas putida	bacterium	0	1	0.260	1.031 (0.971-1.095)
Enterococcus faecium	bacterium	7	3	0.508	1.243 (0.302-5.115)
Streptococcus pneumoniae	bacterium	1	4	0.016	12.828 (1.378-119.367)
Staphylococcus epidermidis	bacterium	4	0	0.295	0.957 (0.917-0.999)
Staphylococcus aureus	bacterium	2	0	0.546	0.979 (0.950-1.008)
Subspecies of staphylococcus hominis	bacterium	1	0	0.740	0.989 (0.969-1.010)
Neisseria mucosa	bacterium	1	0	0.740	0.989 (0.969-1.010)
Streptococcus salivarius	bacterium	0	1	0.260	1.031 (0.971-1.095)
Streptococcus oralis	bacterium	0	2	0.066	1.065 (0.976-1.161)
Oral cocci mucilage	bacterium	0	1	0.260	1.031 (0.971-1.095)
Veillon micrococcus	bacterium	0	1	0.260	1.031 (0.971-1.095)
Streptococcus mutans	bacterium	0	1	0.260	1.031 (0.971-1.095)
Enterococcus faecalis	bacterium	0	1	0.260	1.031 (0.971-1.095)
Candida tropicalis	fungus	3	0	0.402	0.968 (0.933-1.004)
Candida glabrata	fungus	2	0	0.546	0.979 (0.950-1.008)
Candida albicans	fungus	1	0	0.740	0.989 (0.969-1.010)
Mucor	fungus	1	0	0.740	0.989 (0.969-1.010)
Rhizopus oryzae	fungus	0	1	0.260	1.031 (0.971-1.095)
Rhizomucor pusillus	fungus	5	1	0.508	0.556 (0.063-4.494)
Rhizopus microsporus	fungus	1	1	0.454	2.906 (0.177-47.829)
Lichtheimia ramosa	fungus	1	0	0.740	0.989 (0.969-1.010)
Rhizopus delemar	fungus	1	0	0.740	0.989 (0.969-1.010)
Aspergillus fumigatus	fungus	2	0	0.546	0.979 (0.950-1.008)

(Continued)

10.3389/fcimb.2023.1135460

TABLE 4 Continued

Pathogens	Organisms	non-HSCT (94)	HSCT (33)	*P* value	Odds ratio (95% CI)
Aspergillus flavus	fungus	3	0	0.402	0.968 (0.933-1.004)
Aspergillus niger	fungus	1	0	0.740	0.989 (0.969-1.010)
Candida pseudosmooth	fungus	0	3	0.016	1.100 (0.987-1.225)
Saccharomyces cerevisiae	fungus	0	1	0.260	1.031 (0.971-1.095)
Pneumocystis jirovecii	fungus	2	0	0.546	0.979 (0.95-1.008)
Human cytomegalovirus	virus	16	10	0.087	2.12 (0.847-5.302)
Epstein-barr virus	virus	16	7	0.382	1.312 (0.486-3.543)
Human betaherpesvirus 6B	virus	2	4	0.039	6.345 (1.105-36.437)
Pegivirus C	virus	4	4	0.121	3.103 (0.730-13.200)
Parvovirus B19	virus	2	0	0.546	0.979 (0.950-1.008)
Human alphaherpesvirus 1	virus	10	3	0.550	0.840 (0.216-3.259)
Human polyomavirus 2	virus	1	3	0.054	9.300 (0.932-92.788)
Human mastadenovirus F	virus	1	0	0.740	0.989 (0.969-1.010)
DNA virus	virus	1	0	0.740	0.989 (0.969-1.010)
Human betaherpesvirus	virus	1	0	0.740	0.989 (0.969-1.010)
Torque teno virus	virus	11	0	0.031	0.883 (0.820-0.950)
Human betaherpesvirus 6A	virus	2	0	0.546	0.979 (0.950-1.008)
Human betaherpesvirus 7	virus	1	0	0.740	0.989 (0.969-1.010)
Torque teno virus 29	virus	2	0	0.546	0.979 (0.950-1.008)
Torque teno virus 24	virus	1	0	0.740	0.989 (0.969-1.010)
Torque teno virus 3	virus	1	0	0.740	0.989 (0.969-1.010)
Torque teno virus 11	virus	1	0	0.740	0.989 (0.969-1.010)
Torque teno virus 22	virus	1	0	0.740	0.989 (0.969-1.010)
Human orthopneumovirus	virus	1	0	0.740	0.989 (0.969-1.010)
Molluscum contagiosum virus	virus	1	0	0.740	0.989 (0.969-1.010)
Human Boca virus	virus	0	1	0.260	1.031 (0.971-1.095)
Varicella-zoster virus	virus	0	2	0.066	1.065 (0.976-1.161)
Human polyomavirus 1	virus	0	3	0.016	1.100 (0.987-1.225)
other	other	5	5	0.121	2.619 (0.742-9.240)

HSCT, hematopoietic stem cell transplant.

pathogen worldwide since its discovery in England and France in 1986 (O'Driscoll and Crank, 2015). Therefore, the possibility of vancomycin-resistant *Enterococcus faecium* should be considered during clinical treatment for patients with poor immunity if an empiric application of vancomycin is ineffective. Staphylococcus is the most common pyogenic coccus and is an important source of nosocomial cross-infection. Most staphylococci are nonpathogenic bacteria. When the patients are immunocompromised, some of the nonpathogenic Staphylococcus can proliferate and cause symptoms of infection. One study suggested that methicillin-resistant coagulase negative staphylococci (MRCNS) were the most common Gram-positive bacteria, representing 66% of Gram-positive bacteremias and 28% of total bacteremias in febrile neutropenia adult cancer patients (Moghnieh et al., 2015). In our study, it showed that *Enterococcus faecium* made up a relatively high proportion followed by *Staphylococcus epidermidis* of the Gram-positive cocci in non-HSCT patients. Another study showed the incidence of *Streptococcus pneumoniae* in HSCT recipients was 40.4 per 100 000 patients per year, which is 30-fold higher than that in patients without HSCT (van Veen et al., 2016), which was consistent with our research. The differences in the above results may be due to the different underlying diseases and antibiotics used by the patients. Therefore, when patients with hematologic diseases show symptoms of infection and staphylococci are detected, it was

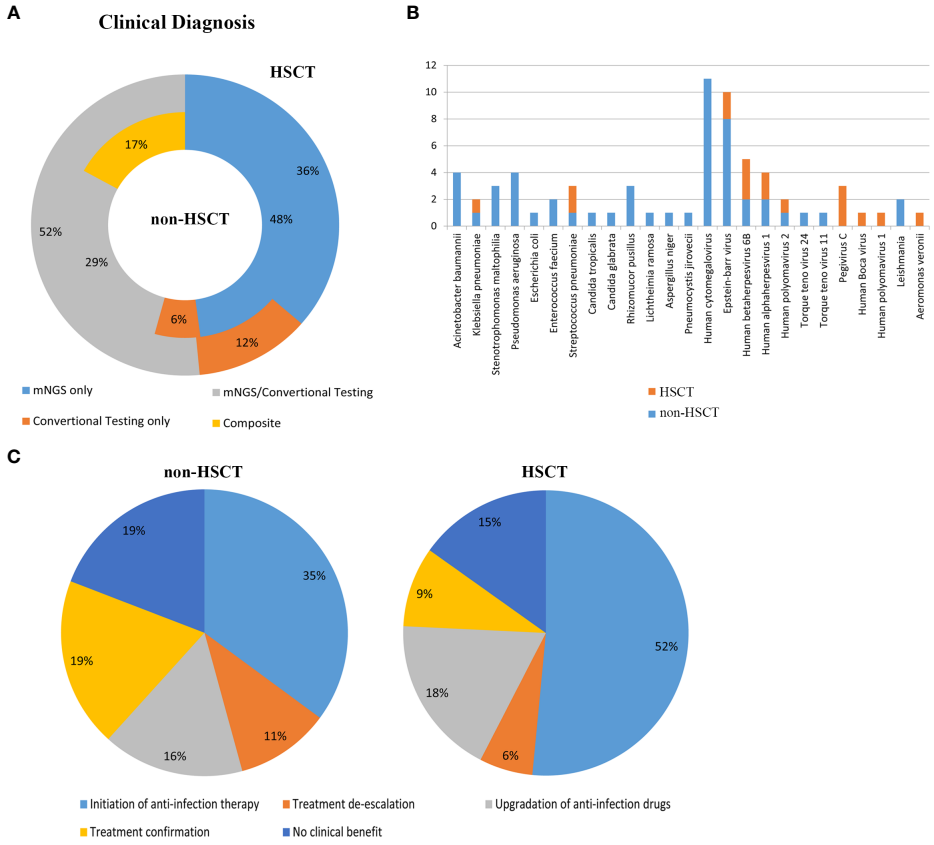

FIGURE 5
Evaluation of the application of mNGS in the real world. **(A)** Clinical diagnosis in the non-HSCT and HSCT groups. mNGS/conventional, pathogens identified by both methods; composite, pathogens identified by combining mNGS, the conventional testing results and clinical signs and symptoms; mNGS only and conventional testing only, pathogens identified by only a single method. Inner circle, non-HSCT; Outer circle, HSCT. **(B)** Clinically determined pathogens only detected by mNGS, not by conventional methods in hematological patients. **(C)** Evaluation of the clinical impact of mNGS in non-HSCT and HSCT patients.

still necessary to carefully determine whether it is a pathogen based on the clinical conditions.

High doses of steroids, irradiation, and the application of immunosuppressive agents are all risk factors for CMV activation (Hebart et al., 1997). During the post-transplant period, CMV reactivation occurs in up to 41% of patients, and CMV infection is an important cause of death (Marchesi et al., 2018). Our study showed that the incidence of CMV-activated infection was the highest among the viral infections. A meta-analysis showed that CMV infection was significantly associated with an increased risk of overall mortality (OM) and non-relapse mortality (NRM) after allo-HSCT. However, preemptive antiviral therapy does not benefit patients; in contrast, it results in a twofold increased risk of OM and NRM (Giménez et al., 2019). Therefore, the long-term application of anti-CMV drugs needs to be evaluated based on the specific situation of each patient. EBV, an identified oncogenic virus, causes more than 7 different types of malignancies, usually in immunocompromised individuals. Furthermore, some individuals with primary immunodeficiencies exhibit extreme susceptibility to EBV-induced diseases, such as severe and often fatal infectious mononucleosis, hemophagocytic lymphohistiocytosis, lymphoproliferative disease, and/or EBV+ B-cell lymphoma (Tangye and Latour, 2020). EBV activation is a common complication after allogeneic hematopoietic stem cell transplantation (allo-HSCT). EBV-related posttransplantation lymphoproliferative disorders (EBV-PTLDs) are rare but potentially fatal complications associated with T-cell depletion of grafts, HLA mismatch, severe graft-versus-host disease (GVHD) (Liu et al., 2018). Our mNGS results revealed that viruses were common pathogenic microorganisms in both non-HSCT (44%) and HSCT (45%) patients. The serological positive detection rate of CMV was the highest, followed by EBV. Therefore, the possibility of CMV and EBV infection should be first considered if fever occurs in hematological patients with or without transplant. The *Torque teno* virus (TTV), a highly prevalent nonpathogenic anellovirus, is a potential novel candidate for monitoring immunosuppression (Studenic et al., 2021). TTV is associated with many autoimmune diseases, such as idiopathic hepatitis and systemic lupus erythematosus. The incidence of autoimmune diseases after HSCT is between 2.1% and 5.5% (Daikeler et al., 2013; Faraci et al., 2014), and TTV infection may be an important contributing factor (Maximova et al., 2015). Our study showed that TTV was detected in non-HSCT patients, which suggested attention should be paid to the relationship between TTV infection and autoimmune disease in the treatment of hematological patients, and relevant examinations should be conducted.

With the application of immunosuppressive drugs, the morbidity due to fungal infection has gradually increased. A minority of these fungal infections cause life-threatening infections (Strickland and Shi, 2021). Köhler et al. showed that common fungi include *Cryptococcus neoformans*, *Aspergillus fumigatus* and *Candida albicans* (Köhler et al., 2014). Mucormycosis, which is difficult to diagnose, is an angioinvasive fungal infection with high morbidity and mortality. Diagnosis is often delayed, and the disease tends to progress rapidly. Patients with hematological malignancies or transplantation are more vulnerable to mucormycosis. The increased detection rate of mucormycosis may be due to the application of immunosuppressants and modern diagnostic tools identifying previously uncommon genera/species. Corticosteroids and other immunosuppressive agents are risk factors for mucormycosis (Cornely et al., 2019). In our study, the detection rate of fungi in nontransplant patients (13%) was higher than that in transplant patients (8%). However, the detection rate of Mucor was the highest, followed by Candida and Aspergillus. The reason for the high incidence of mucormycosis in our study may be that the enrolled patients were patients with hematological malignancies or transplantation, and mNGS could detect this pathogen early.

Immunosuppressed patients were more prone to mixed infections (Dropulic and Lederman, 2016). In our study, 76.7% patients suffered malignant hematologic diseases and 23.3% patients with non-malignant hematologic diseases had immunosuppression or used immunosuppressants. Our study showed patients with mixed infection accounted for 67.00%. Among them, the mixed infection of bacteria and virus (25.99%) was the most common, which indicated that mNGS had certain advantages in detecting mixed infection of pathogenic microorganisms.

Our study showed the pathogen detection rate of mNGS is higher than that of traditional detection methods, such as PCR and blood culture. The proportion of pathogens detected by mNGS was 85.82% and by conventional testing was 20.47%. The detection rate of mNGS for bacteria, fungi and viruses was higher than that of conventional testing, and even special pathogens, such as mycoplasma, *Mycobacterium tuberculosis* and Leishmania, which are difficult to cultivate, were detected. In the published literature (EORTC International Antimicrobial Therapy Cooperative Group, 1990; Madani, 2000; Collin et al., 2001; Moghnieh et al., 2015; Al-Otaibi et al., 2016; van Veen et al., 2016; Marchesi et al., 2018; Alonso-Álvarez et al., 2021), the majority of etiological analyses of hematological diseases have focused on bacterial and viral infections, while the analysis of fungal infections and special pathogen infections is relatively rare. In addition to the rarity of these pathogen infections, the detection technology is still not perfect, and the infection may be mistakenly attributed to bacterial infection. We hypothesize that the reasons for these phenomena are not only that the pathogenicity of these pathogens is low but also that identification of the etiological agents remains challenging because only a small proportion of pathogens are identifiable by the current diagnostic methods. Hence, mNGS has become an attractive strategy and is an objective, unbiased, and comprehensive method for the detection and taxonomic characterization of microorganisms (Li et al., 2021).

The application of mNGS in the real world was evaluated in this study. In the non-HSCT group, 48% of pathogens were identified by mNGS only, and it was 36% in the HSCT group. Conventional testing detected pathogenic organisms in 6% of non-HSCT patients and 12% of HSCT patients. Pathogens identified by both mNGS and conventional testing were 29% of cases in the non-HSCT group and 52% of cases in the HSCT group. Pathogenic organisms identified by combining mNGS, the conventional testing results and clinical signs and symptoms were 17% of cases in the non-HSCT group. There were 25 pathogens, such as Leishmania, which could only be detected by mNGS. Therefore, mNGS plays an important role in identifying pathogens for a clinical diagnosis, as well as having an overall beneficial impact on treatment, such as the rapid initiation of appropriate antibiotic therapy, treatment de-escalation and upgradation of anti-infection drugs. Meanwhile, mNGS also identified pathogenic microorganisms and directed the application of antibiotics. Consistent with the results of a previous study (Zhan et al., 2021), our study showed that mNGS has a significant role in guiding physicians to make personalized treatment plans for patients.

Although the success of mNGS in improving the diagnosis, treatment, and tracking of infectious diseases was confirmed compared with other traditional methods, the limitations of mNGS are worthy of our attention. First, the human host background and extraneous sources of nucleic acids may influence the testing results (Marotz et al., 2018). Second, infective pathogens cannot be differentiated from colonizing pathogens. Because the human microbiome is complex and certain parts of the human body are naturally colonized by many bacteria, fungi, and viruses, primarily within the respiratory and gastrointestinal tracts, skin, and vagina, while most areas within healthy individuals are physiologically sterile, with microorganisms present only under certain conditions. Interpretation of mNGS report is therefore quite difficult and requires experience in clinical, laboratory and microbiology research. Therefore, in determining the clinical significance of the detected microbe, the whole clinical situation must in all cases be taken into account (Li et al., 2021). Third, the high cost of mNGS detracts from the advantages of its high sensitivity and a short detection cycle, which limits the clinical application of mNGS (Li et al., 2021). Consequently, this technology should be further optimized, which could make mNGS more accurate and cost-effective and improve its universality.

As our study is a retrospective study, we just analyzed the pathogens of HSCT and non-HSCT group in hematological diseases and we just made summary and analysis of our existing data. However, since hematological diseases included many subtypes, the sample size of each subtype was relatively small, which is the shortcoming of our paper. Continuous studies will focus on the presence of specific pathogen associated with certain type of malignancies.

Conclusions

Our retrospective and monocentric study clinically showed mNGS has high clinical recognition rate and sensitivity in

pathogen detection and provides a basis for guiding the anti-infective treatment in hematological diseases with symptoms such as fever. Simultaneously, the detection rate of mixed infections by mNGS was high. But mNGS still could not replace the traditional detection methods. mNGS of peripheral blood can be used as an important supplementary detection method when traditional tests are negative, or specimens are difficult to obtain. mNGS is rapidly transforming from the laboratory to the clinic with its advantages, but the timing of its clinical use needs to be further explored.

Data availability statement

The original contributions presented in the study are included in the article/supplementary material. Further inquiries can be directed to the corresponding authors.

Ethics statement

The studies involving human participants were reviewed and approved by Ethics Committee of the First Affiliated Hospital of Zhengzhou University.

Author contributions

JY and ZJ conceived and designed the experiments. XZ and FW collected clinical samples and data. XZ wrote the manuscript. All authors contributed to the article and approved the submitted version.

Funding

This work was supported by the Joint Construction Project of the Henan Province Medical Science and Technology Research Plan (Grant NO. LHGJ 2018020048).

Conflict of interest

The authors declare that the research was conducted in the absence of any commercial or financial relationships that could be construed as a potential conflict of interest.

Publisher's note

References

Alonso-Álvarez, S., Colado, E., Moro-García, M. A., and Alonso-Arias, R. (2021). Cytomegalovirus in haematological tumours. *Front. Immunol.* 12. doi: 10.3389/fimmu.2021.703256

Al-Otaibi, F. E., Bukhari, E. E., Badr, M., and Alrabiaa, A. A. (2016). Prevalence and risk factors of gram-negative bacilli causing blood stream infection in patients with malignancy. *Saudi Med. J.* 37 (9), 979–984. doi: 10.15537/smj.2016.9.14211

Brown, G. D., Denning, D. W., Gow, N. A., Levitz, S. M., Netea, M. G., and White, T. C. (2012). Hidden killers: human fungal infections. *Sci. Transl. Med.* 4 (165), 165rv113. doi: 10.1126/scitranslmed.3004404

Cantey, J. B., and Lee, J. H. (2021). Biomarkers for the diagnosis of neonatal sepsis. *Clin. Perinatol* 48 (2), 215–227. doi: 10.1016/j.clp.2021.03.012

Chao, L., Li, J., Zhang, Y., Pu, H., and Yan, X. (2020). Application of next generation sequencing-based rapid detection platform for microbiological diagnosis and drug resistance prediction in acute lower respiratory infection. *Ann. Transl. Med.* 8 (24), 1644. doi: 10.21037/atm-20-7081

Chen, S., Zhou, Y., Chen, Y., and Gu, J. (2018). Fastp: an ultra-fast all-in-one FASTQ preprocessor. *Bioinformatics* 34 (17), i884–i890. doi: 10.1093/bioinformatics/bty560

Chiu, C., and Legrand, M. (2021). Epidemiology of sepsis and septic shock. *Curr. Opin. Anaesthesiol* 34 (2), 71–76. doi: 10.1097/aco.0000000000000958

Collin, B. A., Leather, H. L., Wingard, J. R., and Ramphal, R. (2001). Evolution, incidence, and susceptibility of bacterial bloodstream isolates from 519 bone marrow transplant patients. *Clin. Infect. Dis.* 33 (7), 947–953. doi: 10.1086/322604

Cornely, O. A., Alastruey-Izquierdo, A., Arenz, D., Chen, S. C. A., Dannaoui, E., Hochhegger, B., et al. (2019). Global guideline for the diagnosis and management of mucormycosis: an initiative of the European confederation of medical mycology in cooperation with the mycoses study group education and research consortium. *Lancet Infect. Dis.* 19 (12), e405–e421. doi: 10.1016/s1473-3099(19)30312-3

Daikeler, T., Labopin, M., Ruggeri, A., Crotta, A., Abinun, M., Hussein, A. A., et al. (2013). New autoimmune diseases after cord blood transplantation: a retrospective study of EUROCORD and the autoimmune disease working party of the European group for blood and marrow transplantation. *Blood* 121 (6), 1059–1064. doi: 10.1182/blood-2012-07-445965

Dobin, A., Davis, C. A., Schlesinger, F., Drenkow, J., Zaleski, C., Jha, S., et al. (2013). STAR: ultrafast universal RNA-seq aligner. *Bioinformatics* 29 (1), 15–21. doi: 10.1093/bioinformatics/bts635

Dropulic, L. K., and Lederman, H. M. (2016). Overview of infections in the immunocompromised host. *Microbiol. Spectr.* 4 (4), 10. doi: 10.1128/microbiolspec.DMIH2-0026-2016

EORTC International Antimicrobial Therapy Cooperative Group. (1990). Gram-positive bacteraemia in granulocytopenic cancer patients. *Eur. J. Cancer* 26 (5), 569–574. doi: 10.1016/0277-5379(90)90079-9

Faraci, M., Zecca, M., Pillon, M., Rovelli, A., Menconi, M. C., Ripaldi, M., et al. (2014). Autoimmune hematological diseases after allogeneic hematopoietic stem cell transplantation in children: an Italian multicenter experience. *Biol. Blood Marrow Transplant.* 20 (2), 272–278. doi: 10.1016/j.bbmt.2013.11.014

Ferrer, R., Martin-Loeches, I., Phillips, G., Osborn, T. M., Townsend, S., Dellinger, R. P., et al. (2014). Empiric antibiotic treatment reduces mortality in severe sepsis and septic shock from the first hour: results from a guideline-based performance improvement program. *Crit. Care Med.* 42 (8), 1749–1755. doi: 10.1097/ccm.0000000000000330

Giménez, E., Torres, I., Albert, E., Piñana, J. L., Hernández-Boluda, J. C., Solano, C., et al. (2019). Cytomegalovirus (CMV) infection and risk of mortality in allogeneic hematopoietic stem cell transplantation (Allo-HSCT): a systematic review, meta-analysis, and meta-regression analysis. *Am. J. Transplant.* 19 (9), 2479–2494. doi: 10.1111/ajt.15515

Gu, W., Miller, S., and Chiu, C. Y. (2019). Clinical metagenomic next-generation sequencing for pathogen detection. *Annu. Rev. Pathol.* 14, 319–338. doi: 10.1146/annurev-pathmechdis-012418-012751

Hardak, E., Avivi, I., Berkun, L., Raz-Pasteur, A., Lavi, N., Geffen, Y., et al. (2016). Polymicrobial pulmonary infection in patients with hematological malignancies:

prevalence, co-pathogens, course and outcome. *Infection* 44 (4), 491–497. doi: 10.1007/s15010-016-0873-3

Hasanuzzaman, M., Saha, S., Malaker, R., Rahman, H., Sajib, M. S. I., Das, R. C., et al. (2021). Comparison of culture, antigen test, and polymerase chain reaction for pneumococcal detection in cerebrospinal fluid of children. *J. Infect. Dis.* 224 (12 Suppl 2), S209–s217. doi: 10.1093/infdis/jiab073

Hebart, H., Schröder, A., Löffler, J., Klingebiel, T., Martin, H., Wassmann, B., et al. (1997). Cytomegalovirus monitoring by polymerase chain reaction of whole blood samples from patients undergoing autologous bone marrow or peripheral blood progenitor cell transplantation. *J. Infect. Dis.* 175 (6), 1490–1493. doi: 10.1086/516484

Jing, C., Chen, H., Liang, Y., Zhong, Y., Wang, Q., Li, L., et al. (2021). Clinical evaluation of an improved metagenomic next-generation sequencing test for the diagnosis of bloodstream infections. *Clin. Chem.* 67 (8), 1133–1143. doi: 10.1093/clinchem/hvab061

Köhler, J. R., Casadevall, A., and Perfect, J. (2014). The spectrum of fungi that infects humans. *Cold Spring Harb. Perspect. Med.* 5 (1), a019273. doi: 10.1101/cshperspect.a019273

Li, N., Cai, Q., Miao, Q., Song, Z., Fang, Y., and Hu, B. (2021). High-throughput metagenomics for identification of pathogens in the clinical settings. *Small Methods* 5 (1), 2000792. doi: 10.1002/smtd.202000792

Liu, L., Zhang, X., and Feng, S. (2018). Epstein-Barr Virus-related post-transplantation lymphoproliferative disorders after allogeneic hematopoietic stem cell transplantation. *Biol. Blood Marrow Transplant.* 24 (7), 1341–1349. doi: 10.1016/j.bbmt.2018.02.026

Madani, T. A. (2000). Clinical infections and bloodstream isolates associated with fever in patients undergoing chemotherapy for acute myeloid leukemia. *Infection* 28 (6), 367–373. doi: 10.1007/s150100070007

Marchesi, F., Pimpinelli, F., Ensoli, F., and Mengarelli, A. (2018). Cytomegalovirus infection in hematologic malignancy settings other than the allogeneic transplant. *Hematol. Oncol.* 36 (2), 381–391. doi: 10.1002/hon.2453

Marotz, C. A., Sanders, J. G., Zuniga, C., Zaramela, L. S., Knight, R., and Zengler, K. (2018). Improving saliva shotgun metagenomics by chemical host DNA depletion. *Microbiome* 6 (1), 42. doi: 10.1186/s40168-018-0426-3

Maschmeyer, G., De Greef, J., Mellinghoff, S. C., Nosari, A., Thiebaut-Bertrand, A., Bergeron, A., et al. (2019). Infections associated with immunotherapeutic and molecular targeted agents in hematology and oncology. a position paper by the European conference on infections in leukemia (ECIL). *Leukemia* 33 (4), 844–862. doi: 10.1038/s41375-019-0388-x

Maximova, N., Pizzol, A., Ferrara, G., Maestro, A., and Tamaro, P. (2015). Does teno torque virus induce autoimmunity after hematopoietic stem cell transplantation? a case report. *J. Pediatr. Hematol. Oncol.* 37 (3), e194–e197. doi: 10.1097/mph.0000000000000194

Moghnieh, R., Estaitieh, N., Mugharbil, A., Jisr, T., Abdallah, D. I., Ziade, F., et al. (2015). Third generation cephalosporin resistant enterobacteriaceae and multidrug resistant gram-negative bacteria causing bacteremia in febrile neutropenia adult cancer patients in Lebanon, broad spectrum antibiotics use as a major risk factor, and correlation with poor prognosis. *Front. Cell Infect. Microbiol.* 5. doi: 10.3389/fcimb.2015.00011

O'Driscoll, T., and Crank, C. W. (2015). Vancomycin-resistant enterococcal infections: epidemiology, clinical manifestations, and optimal management. *Infect. Drug Resist.* 8, 217–230. doi: 10.2147/idr.S54125

Schlaberg, R., Chiu, C. Y., Miller, S., Procop, G. W., and Weinstock, G. (2017). Validation of metagenomic next-generation sequencing tests for universal pathogen detection. *Arch. Pathol. Lab. Med.* 141 (6), 776–786. doi: 10.5858/arpa.2016-0539-RA

Schmieder, R., and Edwards, R. (2011). Quality control and preprocessing of metagenomic datasets. *Bioinformatics* 27 (6), 863–864. doi: 10.1093/bioinformatics/btr026

Strickland, A. B., and Shi, M. (2021). Mechanisms of fungal dissemination. *Cell Mol. Life Sci.* 78 (7), 3219–3238. doi: 10.1007/s00018-020-03736-z

Studenic, P., Bond, G., Kerschbaumer, A., Bécède, M., Pavelka, K., Karateev, D., et al. (2021). Torque teno virus quantification for monitoring of immunomodulation with biological compounds in the treatment of rheumatoid arthritis. *Rheumatol. (Oxford)* 61 (7), 2815–2825. doi: 10.1093/rheumatology/keab839

Tangye, S. G., and Latour, S. (2020). Primary immunodeficiencies reveal the molecular requirements for effective host defense against EBV infection. *Blood* 135 (9), 644–655. doi: 10.1182/blood.2019000928

van Veen, K. E., Brouwer, M. C., van der Ende, A., and van de Beek, D. (2016). Bacterial meningitis in hematopoietic stem cell transplant recipients: a population-based prospective study. *Bone Marrow Transplant.* 51 (11), 1490–1495. doi: 10.1038/bmt.2016.181

Wood, D. E., Lu, J., and Langmead, B. (2019). Improved metagenomic analysis with kraken 2. *Genome Biol.* 20 (1), 257. doi: 10.1186/s13059-019-1891-0

Zhan, Y., Xu, T., He, F., Guan, W. J., Li, Z., Li, S., et al. (2021). Clinical evaluation of a metagenomics-based assay for pneumonia management. *Front. Microbiol.* 12. doi: 10.3389/fmicb.2021.751073

Zhang, B., Zhou, J., Gui, R., Li, Z., Zu, Y., Wang, J., et al. (2021). Metagenomic next generation sequencing in the detection of pathogens in cerebrospinal fluid of patients after alternative donor transplantation: a feasibility analysis. *Front. Cell Infect. Microbiol.* 11. doi: 10.3389/fcimb.2021.720132

frontiers | Frontiers in Cellular and Infection Microbiology

TYPE Original Research
PUBLISHED 26 June 2023
DOI 10.3389/fcimb.2023.1192931

OPEN ACCESS

EDITED BY
Pushpanathan Muthuirulan,
Harvard University, United States

REVIEWED BY
Liang-jun Chen,
Wuhan University, China
Chaitanya Tellapragada,
Karolinska Institutet (KI), Sweden

*CORRESPONDENCE
Qilong Liu
13676936391@126.com

†These authors have contributed equally to this work and share first authorship

RECEIVED 24 March 2023
ACCEPTED 09 June 2023
PUBLISHED 26 June 2023

CITATION
Liu Q, Liu X, Hu B, Xu H, Sun R, Li P, Zhang Y, Yang H, Ma N and Sun X (2023) Diagnostic performance and clinical impact of blood metagenomic next-generation sequencing in ICU patients suspected monomicrobial and polymicrobial bloodstream infections.
Front. Cell. Infect. Microbiol. 13:1192931.
doi: 10.3389/fcimb.2023.1192931

Diagnostic performance and clinical impact of blood metagenomic next-generation sequencing in ICU patients suspected monomicrobial and polymicrobial bloodstream infections

Qilong Liu[1*†], Xiaojing Liu[2†], Bingxue Hu[3], Huan Xu[3], Rongqing Sun[1], Pengfei Li[1], Yunwei Zhang[1], Hongfu Yang[1], Ning Ma[1] and Xiaoge Sun[1]

[1]Intensive Care Unit, The First Affiliated Hospital of Zhengzhou University, Zhengzhou, Henan Province, China, [2]Department of Neurology, The First Affiliated Hospital of Zhengzhou University, Zhengzhou, Henan Province, China, [3]Department of Scientific Affairs, Vision Medicals for Infectious Diseases, Guangzhou, Guangdong Province, China

Introduction: Early and effective application of antimicrobial medication has been evidenced to improve outcomes of patients with bloodstream infection (BSI). However, conventional microbiological tests (CMTs) have a number of limitations that hamper a rapid diagnosis.

Methods: We retrospectively collected 162 cases suspected BSI from intensive care unit with blood metagenomics next-generation sequencing (mNGS) results, to comparatively evaluate the diagnostic performance and the clinical impact on antibiotics usage of mNGS.

Results and discussion: Results showed that compared with blood culture, mNGS detected a greater number of pathogens, especially for *Aspergillus spp*, and yielded a significantly higher positive rate. With the final clinical diagnosis as the standard, the sensitivity of mNGS (excluding viruses) was 58.06%, significantly higher than that of blood culture (34.68%, $P<0.001$). Combing blood mNGS and culture results, the sensitivity improved to 72.58%. Forty-six patients had infected by mixed pathogens, among which *Klebsiella pneumoniae* and *Acinetobacter baumannii* contributed most. Compared to monomicrobial, cases with polymicrobial BSI exhibited dramatically higher level of SOFA, AST, hospitalized mortality and 90-day mortality ($P<0.05$). A total of 101 patients underwent antibiotics adjustment, among which 85 were adjusted according to microbiological results, including 45 cases based on the mNGS results (40 cases escalation and 5 cases de-escalation) and 32 cases on blood culture. Collectively, for patients suspected BSI in critical condition, mNGS results can provide valuable diagnostic information and contribute to the optimizing of antibiotic treatment. Combining conventional tests with mNGS may significantly improve the detection rate for pathogens and optimize antibiotic treatment in critically ill patients with BSI.

KEYWORDS

bloodstream infection, intensive care unit, blood culture, metagenomics next generation sequencing, polymicrobial infection

1 Introduction

The bloodstream infection (BSI) is a potentially lethal complication that frequently results in multi-organ failure, septic shock, and disseminated intravascular coagulation. It also has a high mortality rate and large socioeconomic costs. The annual incidence of BSI can be as high as 204/100, 000 and the fatality rate 20.6%, accounting for about 10% intensive care unit (ICU) inpatients (Goto and Al-Hasan, 2013; Martinez and Wolk, 2016). It is widely accepted that the length of stay in patients of BSI is long, and any delay in the treatment may result in increased mortality (Ferrer et al., 2014). Therefore, the rapid and appropriate antibiotics treatment is now recognized as a key measure in the care of patients suspected BSI.

Blood culture is currently the standard method for diagnosing BSI. Other conventional microbiological tests (CMTs), such as direct microscopic examination (DME), nucleic acid amplification tests (NAAT), and serological tests, can also be applied in detecting pathogens. However, the practical use of culture and DME is constrained by time-consuming and low detection rates (Li et al., 2019). And NAAT and serological tests can only detect a few suspected pathogens. Recently, metagenomic next-generation sequencing (mNGS) have shown great potential in pathogen detection for patients suspected BSI (Geng et al., 2021; Hu et al., 2021; Jing et al., 2021). Thousands of pathogens are known to infect humans, but only a fraction of them can be identified using current clinical microbiology methods. The newly developed mNGS technology enables the rapid diagnosis of unexplained infections (Yan et al., 2021). Due to its nearly full coverage of causative pathogens and short turnaround time, mNGS has become a reliable method for the early identification of BSI. However, only a few studies have focused on the application of mNGS in ICU patients with BSI, and the clinical impact of mNGS is unclear (Geng et al., 2021; Hu et al., 2021; Yan et al., 2021; He et al., 2022). Therefore, this study retrospectively analyzed the clinical data of 162 critically BSI patients who received blood mNGS diagnoses to explore the clinical value and applicability.

2 Materials and methods

2.1 Study design

From July 1, 2019 to August 31, 2022, 219 patients suspected BSI were admitted to the ICU of the First Affiliated Hospital of Zhengzhou University. This single-center study retrospectively analyzed the clinical data of these patients, including general demographic information, clinical characteristics and outcomes. The inclusion criteria included: (1) age ≥ 18 years, (2) met the diagnostic criteria of sepsis 3.0 (Singer et al., 2016) and suspected BSI, (3) expected ICU hospitalization time ≥ 24 hours. Exclusion criteria included: (1) only received blood culture or mNGS test; (2) died before the results of blood culture or mNGS were returned; (3) repeated tests during 14 days after the first mNGS test. This study was approved by the Ethics Committee of the First Affiliated Hospital of Zhengzhou University (approval number: 2023-KY-0069).

2.2 Blood sample preparation

Disposable sterile needles were used to collect 25ml of whole blood samples within 24 hours of inclusion, among which, 20ml for blood culture (two bottles of aerobic and anaerobic), and 5ml for mNGS detection within 8 hours.

2.3 Blood culture

The BACT/ALERT 3D automatic bacterial culture instrument was applied for testing the blood samples. After incubating the samples for 5-7 days, the positive results were judged by at least two professional physicians to make sure the report is accurate. The final clinical positive result was concluded when any blood culture reported positive results, and environmental microbial contamination was excluded. If common bacteria found on the skin (such *Staphylococcus epidermidis*, *Propionibacterium acnes*, *Clostridium*, and *Corynebacterium diphtheriae*) or in the environment (like *Acinetobacter.spp*, *Bacillus.spp)* thrive in the oxygen bottle, the majority of these bacteria are considered contamination, however they may be considered as pathogenic in the following conditions: a) The same microorganism was cultured from blood samples collected from different body parts; b) The same microorganism has been isolated multiple times, and the results of drug susceptibility are the same.

2.4 Blood mNGS test and data analysis

Patients' blood samples of 3-4 mL were collected, put in EDTA tubes, and kept at room temperature for 3-5 minutes before the plasma was separated and centrifuged for 10 min at 1,600 g at 4°C within 8 hours after collection. Using the TIANamp Micro DNA Kit (DP316, TIANGEN BIOTECH, Beijing, China), DNA was extracted from 300μL plasma according to the manufacturer's instructions. Human DNA was removed using Benzonase (Qiagen) and Tween20 (Sigma) (Amar et al., 2021). The extracted DNA specimens were used for the constructing DNA libraries through DNA fragmentation, end repair, adapter ligation and PCR amplification. Subsequently, using single reads of 75 bp on the Illumina NextSeq 550 (Illumina, San Diego, California, USA) technology, libraries with proven quality were sequenced (Ren et al., 2018). For negative controls, PBMC samples with 10^5 cells/mL from healthy donors in parallel with each batch were also prepared (Deng et al., 2022; Tao et al., 2022), using the same protocol, and sterile deionized water was extracted alongside the specimens to serve as non-template controls (NTC) (Miller et al., 2019).

For bioinformatics analyses, trimmomatic (Bolger et al., 2014) was used to remove low quality reads, adapter contamination, and duplicate reads, as well as those shorter than 50 bp. Low complexity reads were removed by Kcomplexity with default parameters

(Bolger et al., 2014). Human sequence data were identified and excluded by mapping to a human reference genome (hg38) using Burrows-Wheeler Aligner software (Li and Durbin, 2009). The remaining sequencing information was aligned to the most recent databases for bacteria, viruses, fungi, and protozoa (NCBI; ftp://ftp.ncbi.nlm.nih.gov/genomes). Reads that met the criteria for being considered unique were those with alignment lengths greater than 80%, sequence identities greater than 90%, and suboptimal to optimal alignment score ratios lower than 0.8. The reads per million (RPM) ratio, or RPM-r, was defined as the RPM_{sample}/RPM_{NTC} (the RPM corresponding to a specific species or genus in the clinical sample divided by the RPM in the NTC), and a positive detection was reported for a certain species or genus if the RPM-r was ≥10.

2.5 Criteria for a positive mNGS result

The specifically mapped read number (SMRN) of each microbial taxonomy was normalized to SMRN per 20 million (M) of total sequencing reads (SDSMRN, standardized SMRN). The criteria for reporting mNGS result as followings (Qin et al., 2021):

i. SDSMRN ≥3 (mycobacteria excluded) for bacteria
ii. SDSMRN ≥3 for fungi/DNA virus
iii. SDSMRN ≥1 for RNA virus
iv. SDSMRN ≥100 for parasites
v. SDSMRN ≥3 for *Mycoplasma/Chlamydia* spp.
vi. SDSMRN ≥1 (or SDSMRNG ≥1 at genus level) for *Mycobacterium tuberculosis* (MTB) complex
vii. Reported Nocardia spp. by mNGS all considered positive

2.6 The diagnostic performance analysis

To compare diagnostic performance between mNGS and blood culture, a composite final diagnosis was retrospectively made by comprehensively considering the results of various examinations (laboratory findings, mNGS results and imagological findings), the patient's clinical manifestations and response to treatment. Then, the final clinical diagnosis was applied as reference standard, and the sensitivity, specificity, positive predictive value (PPV) and negative predictive value (NPV) were calculated (Blauwkamp et al., 2019).

2.7 Statistical analysis

SPSS 25.0 (IBM) and GraphPad Prism 9.3 (GraphPad Software) were utilized for statistical analysis and figures drawing. Continuous variables were presented as medians and interquartile value (IQR, P25, P75), categorical variables were expressed as counts and percentages. Comparison of categorical variables was done with chi-square test. The Mann-Whitney U test was employed for comparing the differences in the continuous variables. $P < 0.05$ was considered to indicate statistical significance.

3 Results

3.1 Patient characteristics

A total of 162 patients suspected BSI were finally included in this study (Figure 1). As shown in Table 1, 57.41% (93/162) patients had underlying diseases, such as hypertension (29.63%), diabetes (15.43%), and cerebrovascular disease (11.11%). The vast majority of patients (91.36%) had complications during hospitalization, mainly including respiratory system disease (55.56%), cardiovascular disease (48.77%) and renal insufficiency (25.31%). The most common source of infection was the lung (37.04%), followed by the abdomen (17.9%). A total of 124 (76.5%) patients were finally diagnosed as BSI, among them 78 were infected with single pathogens and the remaining 46 were co-infection. Table 2 demonstrated the clinical data of the patients. The median APACH II and SOFA were 17 and 10, respectively. A total of 45.68% and 58.64% cases died at 28-day and 90-day admission, respectively.

3.2 Comparison of mNGS and blood culture for pathogen detection

Firstly, we analyzed the ability of blood culture and blood mNGS for pathogens detection. As shown in Figure 2, a total of 66 pathogenic species were detected in 124 patients by blood culture and mNGS, including Gram-positive bacteria, Gram-negative bacteria, fungi, and viruses. Generally, blood mNGS detected a greater variety of microbes than culture. *Klebsiella pneumoniae*, *Acinetobacter baumannii*, and *Enterococcus faecium* were the most common bacteria. In terms of fungal detection by mNGS, *Aspergillus flavus*, *Aspergillus fumigatus*, and *Aspergillus oryzae* were most frequently detected and they were only detected by mNGS. Compared with blood culture, mNGS could detect a greater number of pathogens (253 vs 34, $P<0.0001$). Among them, the detection ability of mNGS for *Klebsiella pneumoniae*, *Enterococcus faecium*, *Aspergillus flavus* and *Aspergillus fumigatus* was significantly stronger than blood culture ($P<0.05$, Figures 2A-C). In 127 cases with prior antibiotics administration, mNGS had a significantly higher detection rate on *Klebsiella pneumoniae* and *Enterococcus faecium* than blood culture; but in 35 cases without prior antibiotics, no significant difference was observed between mNGS and blood culture in detecting *Klebsiella pneumoniae* (Supplementary Figure 1).

Moreover, the main viruses detected by mNGS were *Human betaherpes virus 5* (CMV), *Human gamaherpesvirus 4* (EBV) and *Torque teno virus* (TTV). mNGS made up for the shortcomings of the inability to detect viruses in blood culture (Figure 2D).

3.3 Comparison of clinical diagnostic value in BSI between mNGS and blood culture

Among 162 patients, mNGS showed positive result in 111 cases, with a positive rate of 68.5%, which was significantly higher than blood culture (26.5%, 43/162, $P<0.0001$, Figure 3A). After virus

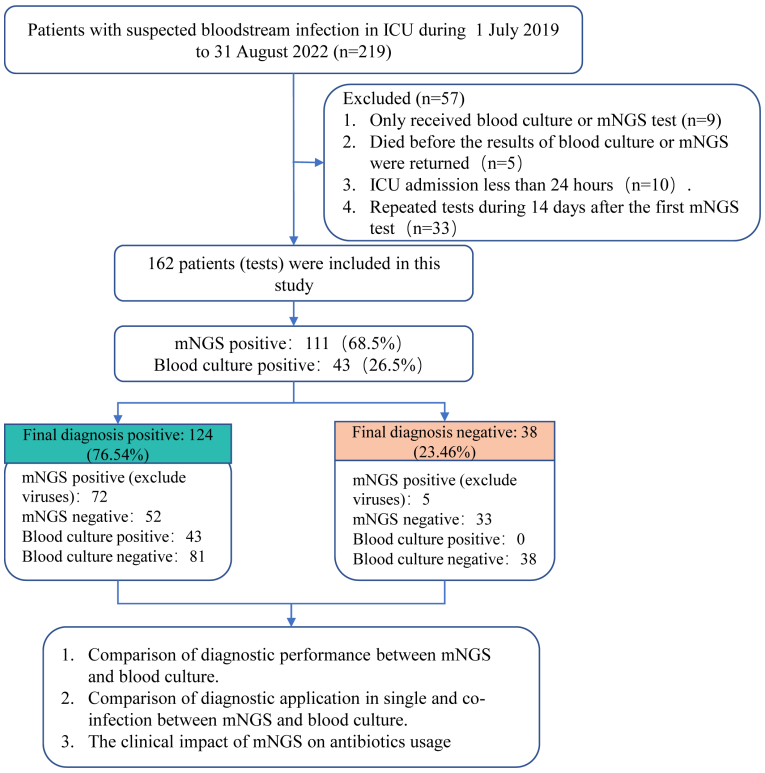

FIGURE 1
A schematic of the study profile.

TABLE 1 Demographic characteristic of patients.

Clinical features	n=162
Gender, male	99 (61.1)
Age, years	55 (44, 67)
Underlying diseases, n (%)	94 (58.02)
Hypertension	48 (29.63)
Diabetes mellitus	25 (15.43)
Cerebrovascular disease	18 (11.11)
Chronic cardiac disease	17 (10.49)
Chronic respiratory diseases	7 (4.32)
Chronic liver disease	7 (4.32)
Malignancy	5 (3.09)
Chronic kidney disease	4 (2.47)
Other	13 (8.02)
Comorbidity, n (%)	150 (92.59)
Disease of respiratory system	90 (55.56)
Disease of cardiovascular system	79 (48.77)
Renal insufficiency	41 (25.31)
Nervous system disease	19 (11.73)
Disease of digestive system	10 (6.17)
Immunosuppression	9 (5.56)
Hypohepatia	7 (4.32)
Anemia	3 (1.85)
Other	12 (7.41)
Infectious sources, n (%)	n=162
Lung	60 (37.04)
Abdomen	29 (17.9)
Gastrointestinal tract	13 (8.02)
Urinary tract	13 (8.02)
Catheter-related	12 (7.41)
Skin and soft tissue	10 (6.17)
Biliary tract	9 (5.56)
Primary	6 (3.7)
Central Nervous System	4 (2.47)
Other	6 (3.7)
Infectious type, n (%)	125 (77.16)
single infection	78 (62.9)
coinfection	46 (37.1)

(Continued)

TABLE 1 Continued

TABLE 2 Clinical characteristic of patients.

Clinical features	Number
APACHE II	17 (12, 22)
SOFA	10 (7, 15)
Time to progress to sepsis (days)	3 (2, 6)
WBC ($\times10^9$/L)	12.58 (8.25, 19.71)
Neutrophil (%)	87.55 (81.65, 92.5)
Platelet ($\times10^9$/L)	101 (42, 196.75)
ALT (U/L)	39.5 (17, 88.25)
AST (U/L)	44 (20, 95.5)
Total bilirubin(μmol/L)	18.52 (9.7, 35.28)
DBil (μmol/L)	9.65 (5.42, 25)
Serum albumin (g/L)	30.05 (25.53, 34.53)
D-dimer (mg/L)	2.74 (1.07, 5.94)
Prothrombin time (s)	13.8 (12.5, 16.33)
CRP (mg/L)	102.13 (44.2, 172)
PCT (ng/mL)	5.06 (0.96, 24)
Urea nitrogen (mmol/L)	12.25 (7.5, 19)
Creatinine (μmol/L)	94 (61, 170.25)
Mortality (28 days)	74 (45.68)
Mortality (hospitalization)	7 (4.32)
Mortality (90 days)	95 (58.64)
Duration of ICU stay (days)	12.5 (6, 22.25)
Total hospitalization time (days)	17.5 (10, 37.25)
Mechanical ventilation time (hours)	68.5 (0, 230.5)
Vasoactive drug use time (hours)	45.5 (0, 135.15)
Total hospitalization cost (CNY)	199246.92 (92737.73, 402597.59)

removal, the positive rate for mNGS was 47.5% (77/162), which was still significantly higher than that for blood culture (P<0.0001, Figure 3B). Blood culture and mNGS showed double positive results in 31 (19.14%) patients, among which the positive pathogens were partly matched in 32.26% (10/31) case and completely matched in 9.68% (3/31) cases (Figure 3C).

Under the circumstances of excluding viruses and using blood culture as standard, the sensitivity, specificity, PPV and NPV of mNGS were 58.14%, 56.3%, 32.47% and 78.82%, respectively, (Table 3). Still, using final clinical diagnosis as standard (Table 4), the sensitivity of mNGS was 58.06%, significantly higher than that of blood culture (34.68%, P<0.001). The specificity, PPV and NPV between mNGS and blood culture showed no statistical difference. And combining the results of blood mNGS and culture, the sensitivity, specificity, PPV and NPV were 72.58%, 86.84%, 94.74% and 49.25%, respectively. Additionally, the AUC for mNGS, blood culture, and blood mNGS plus culture, were 0.7245 (95% CI: 0.589 to 0.758), 0.6734 (95% CI: 0.639 to 0.810) and 0.7971 (0.719 to 0.876), respectively (Figure 4A).

3.4 Comparison of diagnostic application in single and mixed infections between mNGS and blood culture

According to the microbiological results (Figure 4B), 38 cases (23.46%) were regarded as non-infection, 75 cases (46.30%) as single bacterial infection in which 3 patients (1.85%) were identified as single fungi infection, and the remaining 46 cases (28.40%) mixed pathogens (≥2 organisms) infection. Among these 46 patients with co-infection (Figure 4B), 25 cases (54.35%) were infected with multiple bacteria, 16 cases (34.78%) with bacteria and fungi, and 2 cases with multiple fungi (one infected with *Candida tropicalis*, *Aspergillus flavus* and *Rhizopus oryzae*, the other infected with *Aspergillus flavus* and *Aspergillus fumigatus*), and 3 cases with bacteria and virus. In terms of specific microorganism species, *Klebsiella pneumoniae* and *Acinetobacter baumannii* contributed to the majority cases of co-infection, followed by *Enterococcus faecium* and *Aspergillus flavus* (Figure 4C). Meanwhile, BSI caused by *Aspergillus* spp. and *Candida* spp. were more likely to be associated with polymicrobial infections (Figure 4C). Comparison of clinical characteristics between mixed and single infections showed that cases with mixed infections exhibited significantly higher level of SOFA, AST, hospitalized mortality and 90-day mortality (P<0.05, Table 5 & Supplementary Figure 2).

Klebsiella pneumoniae contributed to 19 and 29 cases of single infection and co-infection, respectively (Supplementary Table 1). The majority of the infectious sources for single and mixed *Klebsiella pneumoniae* infection was lung. Except higher SOFA in mixed infection group (P=0.031), none other significant differences were observed in demographic and clinical characteristics between single and mixed *Klebsiella pneumoniae* infection group. A total of 17 and 16 patients were infected with single and mixed *Acinetobacter baumannii*, respectively. Compared with *Acinetobacter baumannii* single infection, co-infected patients exhibited lower serum albumin and urea nitrogen (P=0.04, Table 6).

3.5 The clinical impact of mNGS on antibiotics usage

The initial empirical treatment completely covered all identified pathogens in 48.76% (79/162) cases, partially covered in 43.21% (70/162) cases, and not covered any pathogen in 8.02% (13/162) cases (Figure 5A). The adjustment of empirical treatment strategy is made by summarizing microbiological results, laboratory findings and the response to the initial treatment. In this study, 101 patients underwent adjustment of antibiotics usage, including 18 cases [11 cases escalation and 7 cases de-escalation (antibiotics were discontinued or changed to a narrower spectrum)] in the complete coverage group, 70 cases (67 cases escalation and 3 cases de-escalation) in the partly coverage group, and 13 cases (12 cases escalation and 1 case de-escalation) in the uncovered group (Figure 5B). The adjustment basis of antibiotics usage was illustrated in Figure 5C. Antibiotics were adjusted based on clinical experience in 15 patients (15/101, 14.85%), including 11 cases escalation and 4 cases de-escalation.

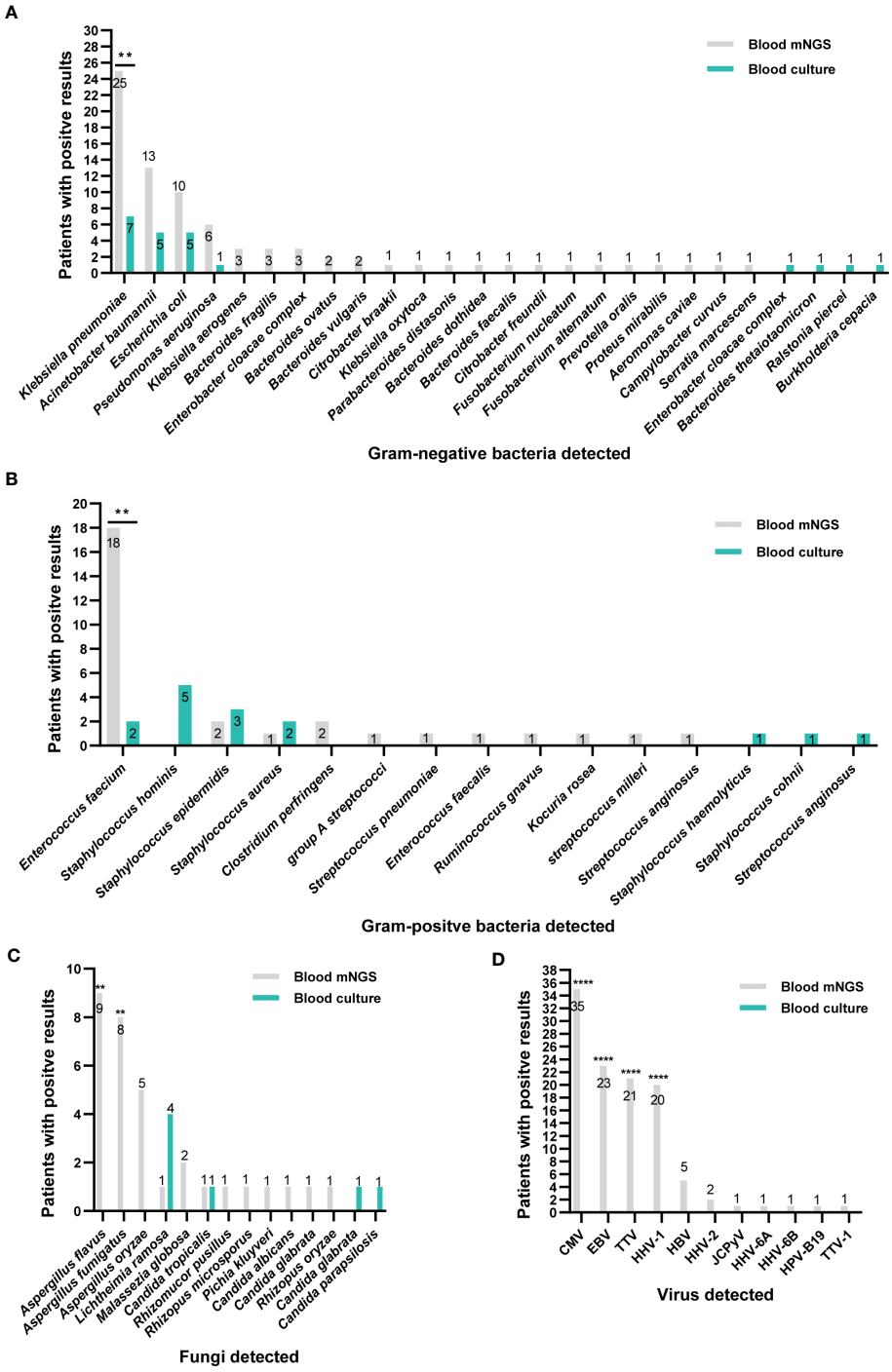

FIGURE 2
Distribution of pathogens identified by blood mNGS and blood culture. **(A)** Gram-negative bacteria. **(B)** Gram-positive bacteria. **(C)** fungi. **(D)** Viruses. **P<0.01 and ****P<0.0001. CMV, Cytomegalovirus; EBV, Epstein-Barr virus; TTV, Torque Teno virus; HHV, human herpes virus; HBV, Hepatitis B virus; JCPyV, JC polyomavirus.

According to microbiological results, 86 patients (86/101, 85.15%) received antibiotics adjustment. Among them, 14 cases were adjusted based only on the blood culture results (13 cases escalation and 1 case de-escalation), 16 patients were adjusted according to blood mNGS plus culture results (14 cases escalation and 2 cases de-escalation), and 8 cases were adjusted based on blood mNGS plus other CMT results (6 cases escalation and 2 cases de-escalation). Moreover, among 21 cases whose adjustment basis was only on blood mNGS, 20 cases resulted in an escalation of treatment and 1 case de-escalation of treatment. Totally, the antibiotics usage of 45 and 32 cases were adjusted according to mNGS and blood culture results, respectively (Figure 5C). In addition, mNGS and blood culture results contributed to the confirmation of empirical treatment in 21 cases and 6 cases, respectively (Figure 5C). Totally, among 101 patients received antibiotics adjustment, mNGS played a role in 45 patients, and the remaining 56 patients were adjusted according to other microbiological results; there was no statistical

10.3389/fcimb.2023.1192931

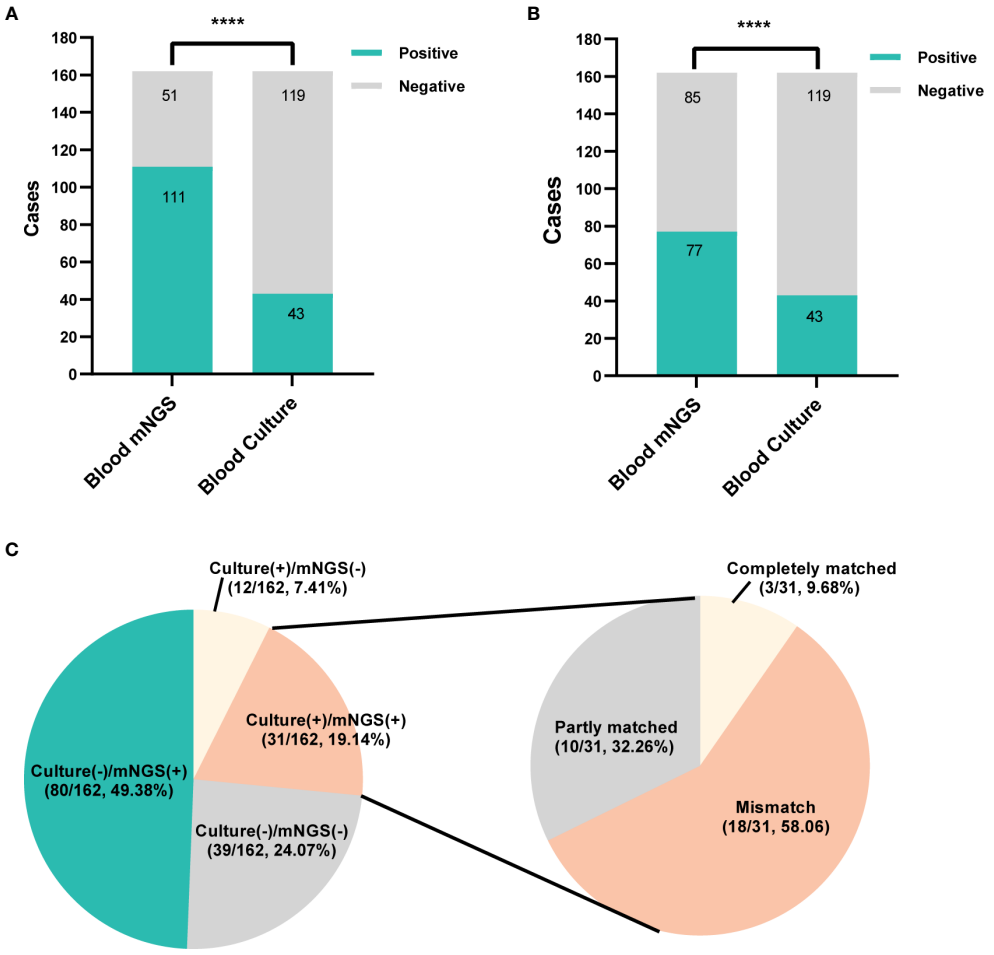

FIGURE 3
The positivity distribution of blood mNGS and blood culture. **(A)** The positive rates of mNGS and blood culture for all cases (n=162). ****P<0.0001. **(B)** The positive rates of mNGS and blood culture for all cases (n=162) after viruses detected by mNGS were excluded. ****P<0.0001. **(C)** Pie chart demonstrating the positivity distribution of mNGS and blood culture for all tests. The double-positive samples were further categorized as completely matched, partly matched (at least one overlap of pathogens was observed) and mismatched.

TABLE 3 The diagnostic performance of mNGS in ICU patients with BSI as compared to blood culture.

	Blood culture positive	Blood culture negative	Sensitivity (%)	Specificity (%)	PPV (%)	NPV (%)	AUC	Youden index (%)
mNGS positive	25	52	58.14	56.3	32.47	78.82	0.57	14.44
mNGS negative	18	67						

difference in mortality (28 days, hospitalization, 90 days), duration of ICU stay, total hospitalization time, mechanical ventilation time, vasoactive drug use time, and total hospitalization cost between the two groups (P>0.05, Supplementary Table 3).

3.6 Antibiotics de-escalation according to mNGS result

A total of 5 cases received antibiotics de-escalation based on mNGS result (Table 6). The infectious sources of 2 cases were lung, and the other 2 catheter, the remaining 1 urinary tract. mNGS detected at least 1 pathogen for all 5 cases, whereas only 2 cases were shown to be pathogens positive by blood culture (Case 3 *Candida glabrata*, Case 5 *Acinetobacter baumannii*). The final definite diagnosis of all 5 cases were made depending on mNGS results with CMTs. Among them, the confirmation of causative pathogen and the antibiotics adjustment of Case 1 was made only based on mNGS result. Case 1 was complicated with uremia, renal insufficiency, and high fever. Blood PCT was 100 ng/ml and CRP 199 mg/L, indicating critical infection. First, Meropenem and vancomycin were empirical prescribed. Then, according to

TABLE 4 Comparison of diagnostic performance between mNGS and blood culture in ICU patients with BSI.

	Final clinical diagnosis positive	Final clinical diagnosis negative	Sensitivity (%)	Specificity (%)	PPV (%)	NPV (%)	AUC (95% CI)	Youden index (%)
mNGS positive	72	5	58.06	86.84	93.51	38.82	0.7245 (0.639-0.810)	44.9
mNGS negative	52	33						
Blood culture positive	43	0	34.68	100	100	31.93	0.6734 (0.589-0.758)	34.68
Blood culture negative	81	38						
mNGS+blood culture positive	90	5	72.58	86.84	94.74	49.25	0.7971 (0.719-0.876)	59.42
mNGS+blood culture negative	35	32						

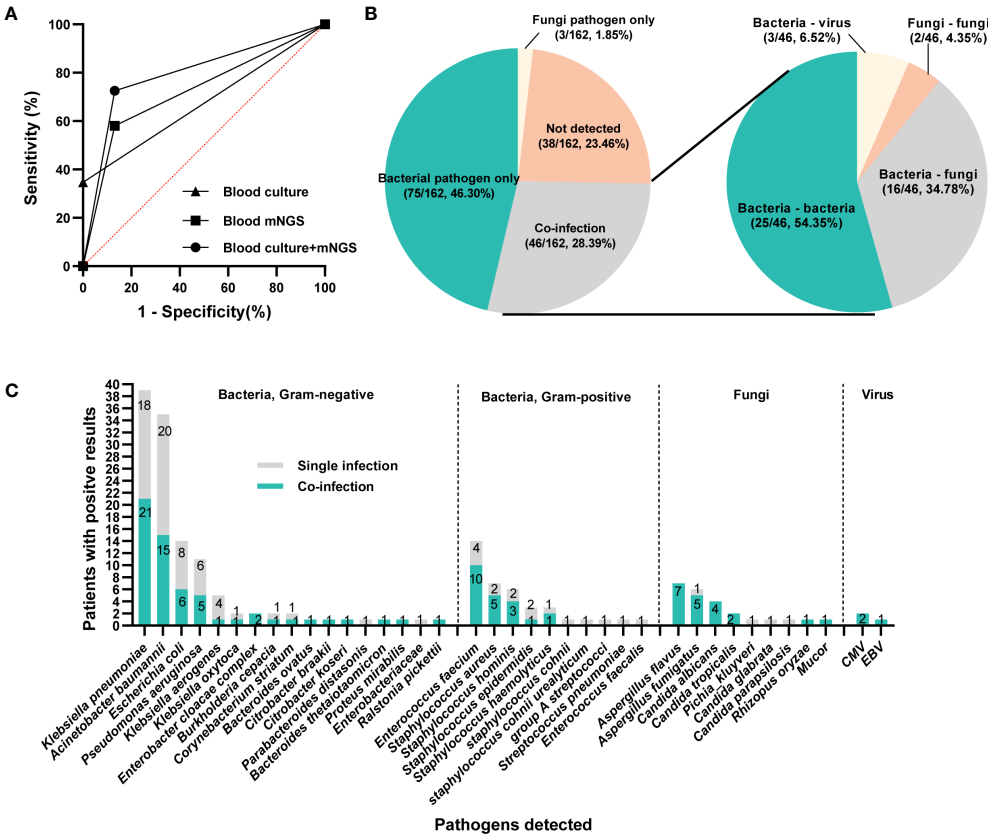

FIGURE 4
The infection types and responsible pathogens. **(A)** ROC curve of mNGS, blood culture and mNGS+culture with reference to final clinical diagnosis. **(B)** Pie chart demonstrating the infectious type, and the co-infection was further categorized as bacteria-bacteria, bacteria-fungi, bacteria-virus and fungi-fungi. **(C)** the distribution of microbial species that involving in single infection and co-infection.

Escherichia coli reported by mNGS, vancomycin was stopped and meropenem continued for anti-infection. Finally, case 1 discharged with recovered condition. Case 2-5 were also diagnosed as single pathogen infection. Case 3 was diagnosed as the infection of *Candida glabrata* based on the results of blood mNGS and culture, cefepime and tigacycline was replaced by voriconazole. Similarly, in Case 2, 4 and 5, empirical antibiotics were discontinued or changed to a narrower spectrum according to the results of blood mNGS and culture. Except Case 5, 4 cases achieved clinical cure or improvement. Case 5 was diagnosed as catheter-related *Acinetobacter baumannii* infection depending on the results of blood mNGS and culture, meropenem + tegacycline + teicolanin was replaced by meropenem + polymyxin. Although his initial disease severity was relative mild (APACHE II 10, SOFA 6), he developed acute cerebral infarction and died after abandoning treatments.

TABLE 5 Comparison of clinical characteristics between mixed and single infections.

Characteristics	Single infection (n=78)	Mixed infection (n=46)	*P* value
Gender, male,	47 (60.26)	32 (69.57)	0.298
Age, years	57 (46, 69.25)	51 (38.5, 60.75)	0.041
With underlying diseases	41 (52.56)	25 (54.35)	0.848
Presenting comorbidity	69 (88.46)	44 (95.65)	0.174
APACHE II	15.5 (11, 21)	17 (11.75, 24.5)	0.211
SOFA	9 (7, 13)	13 (8.75, 17.25)	0.013
Time to progress to sepsis (days)	3 (2, 6.25)	3 (1.75, 5.25)	0.486
WBC ($\times10^9$/L)	12.14 (7.75, 18.82)	14.15 (9.83, 21.55)	0.218
Neutrophil (%)	87.45 (81.95, 92.55)	89.5 (79.53, 92.83)	0.822
Platelet ($\times10^9$/L)	92.5 (42.75, 232.75)	103 (33.5, 174.75)	0.485
ALT (U/L)	30 (15.75, 73.75)	51.5 (22.5, 98.75)	0.076
AST (U/L)	34.5 (18, 80)	71 (28.5, 148)	0.003
Total bilirubin (μmol/L)	16.72 (8.95, 30.9)	21.6 (14.37, 42.3)	0.057
DBil (μmol/L)	8.8 (5.05, 18.9)	11.37 (7.85, 30.63)	0.067
Serum albumin (g/L)	30.05 (24.85, 35.45)	29.9 (25.33, 33.48)	0.578
D-dimer (mg/L)	2.74 (1.01, 5.74)	2.1 (1.11, 4.34)	0.508
Prothrombin time (s)	13.75 (12.2, 15.73)	13.9 (12.88, 19.43)	0.090
CRP (mg/L)	105.5 (48.95, 196.22)	111.3 (44.06, 172.17)	0.727
PCT (ng/mL)	4.35 (1.14, 28)	8.48 (0.83, 28.53)	0.798
Urea nitrogen (mmol/L)	13.15 (8.08, 18.93)	11.7 (6.23, 25.28)	0.741
Creatinine (μmol/L)	94 (59.85, 148.75)	103.5 (61, 251.5)	0.687
Mortality (28 days)	33 (42.31)	23 (50)	0.406
Mortality (hospitalization)	1 (1.28)	5 (10.87)	0.016
Mortality (90 days)	41 (52.56)	33 (71.74)	0.035
Duration of ICU stay (days)	14 (6, 25.75)	12.5 (6, 24.25)	0.444
Total hospitalization time (d)	22.5 (11, 44.75)	15.5 (8, 39.25)	0.266
Mechanical ventilation time (h)	54.5 (0, 238)	128.5 (14.25, 275.5)	0.142
Vasoactive drug use time (h)	36.6 (0, 123.5)	46.5 (3, 144)	0.750
Total hospitalization cost (CNY)	208799 (72110.99, 448181.77)	206138.14 (132801.84, 432240.25)	0.690

4 Discussion

The present study retrospectively compared the diagnostic performance of blood mNGS and culture in ICU patients suspected BSI, and results indicated that mNGS exhibited stronger potential in diagnosing BSI than blood culture, as evidenced by detecting a larger number of pathogens and yielding a higher sensitivity. In addition, mNGS could provide effective etiological basis for the adjustment of antibiotics usage.

BSI is a serious systemic infectious disease caused by the invasion of pathogenic microorganisms, which is a frequent complication in the ICU, predisposing patients to septic shock and death. According to studies conducted on septic patients within the first six hours of recorded hypotension, every hour delay in effective antibiotics usage resulted in an average 7.6% drop in survival rates, and if appropriate therapy was not administered within 24 hours, the survival probability for severe sepsis dropped from 80 to 10% (Kumar et al., 2006; Ferrer et al., 2014). Therefore, timely and accurate detection of pathogenic microorganisms is crucial. Blood culture is considered the gold standard for diagnosing BSI, but it is time-consuming and lower sensitivity (10% to 30%) (Previsdomini et al., 2012; Yealy et al., 2014). Serum immunological tests and PCR techniques can only detect a few specific pathogens and require specialized kits and primers.

In recent years, mNGS, as high-throughput sequencing, has been continually improved and popularized, providing a new and

10.3389/fcimb.2023.1192931

TABLE 6 The characteristics of cases received antibiotics de-escalation according to mNGS result.

Case No.	1	2	3	4	5
Gender	Female	Male	Female	Male	Male
Age (years)	48	35	67	50	41
Underlying diseases	Hypertension, Chronic kidney disease	/	Cerebrovascular disease, Chronic cardiac disease	Chronic liver disease	Hypertension
Comorbidity	/	Disease of respiratory system, Disease of cardiovascular system	/	Disease of respiratory system	Acute cerebral infarction
Infectious sources	Catheter-related	Lung	Urinary tract	Lung	Catheter-related
Blood Culture	Negative	Negative	*Candida glabrata*	Negative	*Acinetobacter baumannii*
Other CMTs	Sputum culture (negative)	Smear (negative), sputum culture (*Klebsiella pneumoniae*, *Pseudomonas aeruginosa*)	None	BALF culture (*Klebsiella pneumoniae*)	None
mNGS	*Escherichia coli*	*Pseudomonas aeruginosa*	*Human gamaherpesvirus 4 (EBV), Candida glabrata*	*Klebsiella pneumoniae, Human betaherpesvirus 5 (CMV), Human alphaherpesvirus 1, Torque teno virus, Torque teno virus 1, Human gamaherpesvirus 4 (EBV)*	*Acinetobacter baumannii, Human betaherpesvirus 5 (CMV), Torque teno virus 5, Lichtheimia ramosa*
Final confirmed pathogens	*Escherichia coli*	*Pseudomonas aeruginosa*	*Candida glabrata*	*Klebsiella pneumoniae*	*Acinetobacter baumannii*
Disease severity					
APACHE II	10	21	6	16	10
SOFA	8	10	8	9	6
Time to progress to sepsis (days)	2	3	2	5	11
Mechanical ventilation time (hours)	0	308	0	168	159
Vasoactive drug use time (hours)	0	258	70	202	13
Duration of ICU stay (days)	8	56	32	14	22
Total hospitalization time (days)	28	93	45	48	22
Laboratory findings					
WBC ($\times 10^9$/L)	3.11	2.99	5.97	7.27	10.62
Neutrophil (%)	87.2	61.62	82.0	93.1	96.4
CRP (mg/L)	199	137.2	122	150	202
PCT (ng/mL)	100	0.32	0.933	8.33	16
Treatments					
Empirical treatment	Meropenem, Vancomycin	Rifamycin, Biapenem, Polymyxin	Cefepime, Tigacycline	Imipenem, Carpofungin, Tiraconine	Meropenem, Tegacycline, Teicolanin

(Continued)

TABLE 6 Continued

Case No.	1	2	3	4	5
Treatment after Final confirmed pathogen diagnosis	Meropenem	Rifamycin, Amtriannan	Voriconazole	Ceftazidime avibactam, Carpofungin, Tiraconine	Meropenem, Polymyxin
The basis for antibiotics adjustment	mNGS	mNGS + sputum culture	mNGS + blood culture	mNGS + BALF culture	mNGS + blood culture
Outcomes					
28 days death	Survival	Survival	Survival	Survival	Death
Hospital death	Survival	Survival	Survival	Survival	Survival
90 days death	Survival	Survival	Survival	Survival	Death

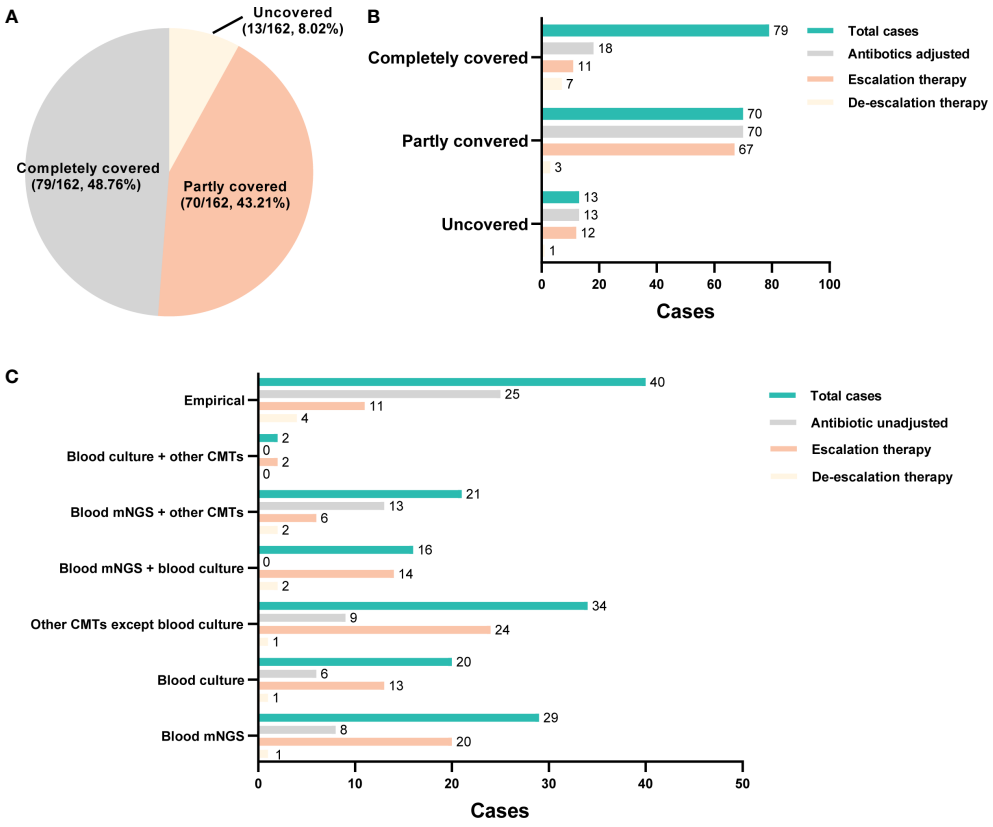

FIGURE 5
The adjustment of empirical antimicrobial treatment. **(A)** Pie chart illustrating the coverage of initial empirical antibiotics usage. **(B)** the adjustment of empirical antibiotics usage in each group. **(C)** the basis for the adjustment of empirical antibiotics usage.

powerful means for pathogen diagnosis. mNGS offers rapid and unbiased testing, characterized by broad-range pathogen detection, which can fulfil the limitations of culture. It has been widely accepted that mNGS has obvious advantages in detecting a broad-spectrum of pathogens, especially for the diagnosis of *Mycobacterium tuberculosis*, virus, anaerobic bacteria and fungi (Gu et al., 2019; Duan et al., 2021). In this study, we showed that blood mNGS not only detected a greater variety of microbes than culture, but also exhibited advantage in detecting common pathogens including *Klebsiella pneumoniae* and *Enterococcus faecium*. Notably, *Aspergillus flavus*, *Aspergillus fumigatus*, and *Aspergillus oryzae* were only detected by mNGS. Therefore, mNGS provided a good complementary to blood culture to maximize the overall detection of *Aspergillus* spp. Furthermore, in 18 cases, both culture and mNGS were positive but their results were not always consistent, this may be due to a number of variables, including the type of pathogen, the usage of antibiotics, and the mNGS reporting threshold. The prior application of

antibiotics will significantly reduce the detection sensitivity of blood culture, but has less impact on the sensitivity of mNGS (Miao et al., 2018), so mNGS will additionally detect the virus in situations where it is difficult to culture the virus. For example, in this study, the *Klebsiella pneumoniae* detection rate of mNGS was superior to that of culture (16.54% vs 3.15%, P <0.001) in cases with, but not without, antibiotic exposure. Besides, false negative results for mNGS may occur for samples with positive blood cultures because the pathogen load is below the mNGS detection limit or because the sample has a high host load, which impairs the detection.

mNGS has shown great potential in the diagnosis of clinical infectious diseases such as respiratory tract infections (Zheng et al., 2021; Diao et al., 2022), BSI (Eichenberger et al., 2022) and central nervous system infections (Frémond et al., 2015; Chiu et al., 2017). Emerging studies have demonstrated that mNGS exhibited superiority than culture test in identifying infectious diseases (Miao et al., 2018; Qian et al., 2020; Chen et al., 2021). Herein, mNGS exerted a positive rate of 68.5%, and reduced positive rate of 47.5% after virus removal, both were significantly higher than culture (26.5%, P<0.0001). The research of XIE et al (Xie et al., 2021) reported that for patients with pulmonary infection, the positive rate of pathogen detection by mNGS was 82.14%, which was significantly better than the 35.71% of conventional methods. In terms of ability for differentiating infection from non-infection, a study by TAO et al (Tao et al., 2022) found that for the diagnosis of infectious diseases, the sensitivity of mNGS was 74.32%, while the sensitivity of conventional detection was 38.2%. Similar results were also reflected in another study, which reported that the sensitivity of mNGS in diagnosing infectious diseases was 67.40%, which was better than culture (23.60%) (Duan et al., 2021). Consistently, our results showed that the sensitivity of mNGS was superior to that of culture (58.06% vs 34.68%, P<0.001), similar to a previous study performed on patients with suspected infectious disease (52.5% vs 34.2%; P < 0.01) (Miao et al., 2018). The high sensitivity of mNGS may be due to the longer survival time of pathogenic DNA and the little effect of antibiotics on mNGS results. Combined with previous studies, the results of this study further confirmed that the sensitivity of mNGS in diagnosing infectious diseases is significantly higher than traditional etiological detection. In this study, the PPV and NPV of mNGS in diagnosing BSI were 93.51% and 38.82%, respectively. The lower NPV than previous studies (88.6% (Jing et al., 2021), 83.87% (Chen et al., 2021)) may be due to the fact that the final diagnosis of certain mNGS-negative cases was made based on the positive CMT results from bronchoalveolar lavage fluid (BALF), sputum and drainage fluid. Also, the majority of patients had antibiotic treatment before the mNGS test, which could have affected the NPV of the mNGS.

According to the largest series reported, polymicrobial BSI accounts for 6%-34% of BSIs (Kiani et al., 1979; Lin et al., 2010). In this study, 37.1% (46/124) BSI cases were polymicrobial infections. The relatively high rate may be explained by the critical conditions of ICU patients we enrolled. Moreover, mNGS showed superiority in contributing to the identification of co-infection than blood culture. mNGS contributed to the identification of co-infection in 32 cases, while blood culture played a role in 16 cases' co-infection diagnosis. Mixed infections can hardly be identified by traditional culture methods, because various microorganisms interact with, and inhibit, each other (Semenec et al., 2023). Polymicrobial BSI is generally associated with a higher morbidity and more severe prognosis than monomicrobial BSI (Bouza et al., 2013). It was reported that mortality rate of hospitalized patients with polymicrobial BSI ranged from 21% to 63%, approximately twice the rate of those with monomicrobial infections (Cooper et al., 1990; Lin et al., 2010). Consistently, our results indicated that cases with mixed infection not only exhibited more serious condition (higher SOFA) but also showed a significant higher hospitalization mortality and 90-day mortality.

According to current recommendations, broad-spectrum antibiotic medication should be started as soon as feasible, ideally within one hour of the diagnosis of sepsis or septic shock, for the best therapeutic effectiveness (Evans et al., 2021). In actual clinical practice, however, it was discovered that roughly 46% of empirical antibiotic treatments were ineffective, increasing mortality rates by 35%, and roughly 50% of empirical antibiotic treatments were either unnecessary or broad-spectrum antibiotics, increasing the risk of antibiotic resistance and toxicity (Campion and Scully, 2018). Consequently, early antimicrobial therapy guidance, greater antibiotic stewardship, and improved clinical outcomes are all made possible by rapid and precise pathogens diagnosis for BSI. In the current study, initial empirical treatment completely covered all identified pathogens in 48.76% cases, and 62.35% cases underwent adjustment of antibiotics usage after diagnosis, among which, more cases were adjusted according to mNGS results than blood culture. For example, a patient who had previous pulmonary tuberculosis and presented with high fever, was diagnosed as septic shock on admission, with APACHE II 24 and PCT 7.1ng/ml. Prior to the return of microbiological results, empirical anti-infection treatment of imipenem was prescribed. Although the results of sputum culture and blood culture were negative, mNGS results suggested *Acinetobacter baumannii* infection, thus polymyxin combined with anti-infective therapy was added. Thereafter, the patient's infection was controlled and was successfully transferred out of the ICU. The proportion of antibiotics adjusted based only on mNGS results was 21 cases, including 20 cases of escalation and 1 case of de-escalation adjustment. mNGS results guided the de-escalated antibiotics management in a total of 5 cases through helping to exclude active infection which allowed for antibiotic de-escalation. Furthermore, in 21 cases where broad-spectrum antibiotics are empirically used before detection, mNGS result can be used alone or as an effective supplement to CMTs for continuing the empirical treatment.

There were some deficiencies in this study. First, this research is a retrospective study, lacking the support of data from multi-center and large number of samples. Second, the majority of microorganisms discovered by mNGS have not been verified by molecular tests. Finally, the majority of patients underwent treatment prior to the mNGS or culture test, which may have impacted the sensitivity of culture and mNGS.

Taken together, our findings indicated that mNGS has great potential in the precise diagnosis and anti-infection treatment of

clinical infectious diseases. Although it cannot replace blood culture detection technology, it can be used as a supplement to provide stronger diagnostic capabilities for BSI and optimize treatment.

Data availability statement

The data presented in the study are deposited in the Genome Warehouse in the National Genomics Data Center (https://ngdc.cncb.ac.cn) repository, accession number PRJCA016199.

Ethics statement

The studies involving human participants were reviewed and approved by Ethics Committee of the First Affiliated Hospital of Zhengzhou University (approval number: 2023-KY-0069). Written informed consent for participation was not required for this study in accordance with the national legislation and the institutional requirements.

Author contributions

QL and XJ contributed to research design and paper writing. RS, PL, YZ, HY, NM and XS contributed to data collection. HX, BX, QL and XJ performed data analysis. QL and XJ revised the manuscript. All authors contributed to the article and approved the submitted version.

Conflict of interest

The authors declare that the research was conducted in the absence of any commercial or financial relationships that could be construed as a potential conflict of interest.

Publisher's note

All claims expressed in this article are solely those of the authors and do not necessarily represent those of their affiliated organizations, or those of the publisher, the editors and the reviewers. Any product that may be evaluated in this article, or claim that may be made by its manufacturer, is not guaranteed or endorsed by the publisher.

Supplementary material

The Supplementary Material for this article can be found online at: https://www.frontiersin.org/articles/10.3389/fcimb.2023.1192931/full#supplementary-material

References

Amar, Y., Lagkouvardos, I., Silva, R. L., Ishola, O. A., Foesel, B. U., Kublik, S., et al. (2021). Pre-digest of unprotected DNA by benzonase improves the representation of living skin bacteria and efficiently depletes host DNA. *Microbiome* 9 (1), 123. doi: 10.1186/s40168-021-01067-0

Blauwkamp, T. A., Thair, S., Rosen, M. J., Blair, L., Lindner, M. S., Vilfan, I. D., et al. (2019). Analytical and clinical validation of a microbial cell-free DNA sequencing test for infectious disease. *Nat. Microbiol.* 4 (4), 663–674. doi: 10.1038/s41564-018-0349-6

Bolger, A. M., Lohse, M., and Usadel, B. (2014). Trimmomatic: a flexible trimmer for illumina sequence data. *Bioinformatics* 30 (15), 2114–2120. doi: 10.1093/bioinformatics/btu170

Bouza, E., Burillo, A., Muñoz, P., Guinea, J., Marín, M., and Rodríguez-Créixems, M. (2013). Mixed bloodstream infections involving bacteria and candida spp. *J. Antimicrob. Chemother.* 68 (8), 1881–1888. doi: 10.1093/jac/dkt099

Campion, M., and Scully, G. (2018). Antibiotic use in the intensive care unit: optimization and de-escalation. *J. Intensive Care Med.* 33 (12), 647–655. doi: 10.1177/0885066618762747

Chen, Y., Feng, W., Ye, K., Guo, L., Xia, H., Guan, Y., et al. (2021). Application of metagenomic next-generation sequencing in the diagnosis of pulmonary infectious pathogens from bronchoalveolar lavage samples. *Front. Cell Infect. Microbiol.* 11. doi: 10.3389/fcimb.2021.541092

Chiu, C. Y., Coffey, L. L., Murkey, J., Symmes, K., Sample, H. A., Wilson, M. R., et al. (2017). Diagnosis of fatal human case of st. Louis encephalitis virus infection by metagenomic sequencing, California, 2016. *Emerg. Infect. Dis.* 23 (10), 1964–1968. doi: 10.3201/eid2310.161986

Cooper, G. S., Havlir, D. S., Shlaes, D. M., and Salata, R. A. (1990). Polymicrobial bacteremia in the late 1980s: predictors of outcome and review of the literature. *Med. (Baltimore)* 69 (2), 114–123. doi: 10.1097/00005792-199069020-00005

Deng, W., Xu, H., Wu, Y., and Li, J. (2022). Diagnostic value of bronchoalveolar lavage fluid metagenomic next-generation sequencing in pediatric pneumonia. *Front. Cell Infect. Microbiol.* 12. doi: 10.3389/fcimb.2022.950531

Diao, Z., Han, D., Zhang, R., and Li, J. (2022). Metagenomics next-generation sequencing tests take the stage in the diagnosis of lower respiratory tract infections. *J. Adv. Res.* 38, 201–212. doi: 10.1016/j.jare.2021.09.012

Duan, H., Li, X., Mei, A., Li, P., Liu, Y., Li, X., et al. (2021). The diagnostic value of metagenomic next-generation sequencing in infectious diseases. *BMC Infect. Dis.* 21 (1), 62. doi: 10.1186/s12879-020-05746-5

Eichenberger, E. M., de Vries, C. R., Ruffin, F., Sharma-Kuinkel, B., Park, L., Hong, D., et al. (2022). Microbial cell-free DNA identifies etiology of bloodstream infections, persists longer than conventional blood cultures, and its duration of detection is associated with metastatic infection in patients with staphylococcus aureus and gram-negative bacteremia. *Clin. Infect. Dis.* 74 (11), 2020–2027. doi: 10.1093/cid/ciab742

Evans, L., Rhodes, A., Alhazzani, W., Antonelli, M., Coopersmith, C. M., French, C., et al. (2021). Surviving sepsis campaign: international guidelines for management of sepsis and septic shock 2021. *Intensive Care Med.* 47 (11), 1181–1247. doi: 10.1007/s00134-021-06506-y

Ferrer, R., Martin-Loeches, I., Phillips, G., Osborn, T. M., Townsend, S., Dellinger, R. P., et al. (2014). Empiric antibiotic treatment reduces mortality in severe sepsis and septic shock from the first hour: results from a guideline-based performance improvement program. *Crit. Care Med.* 42 (8), 1749–1755. doi: 10.1097/ccm.0000000000000330

Frémond, M. L., Pérot, P., Muth, E., Cros, G., Dumarest, M., Mahlaoui, N., et al. (2015). Next-generation sequencing for diagnosis and tailored therapy: a case report of astrovirus-associated progressive encephalitis. *J. Pediatr. Infect. Dis. Soc.* 4 (3), e53–e57. doi: 10.1093/jpids/piv040

Geng, S., Mei, Q., Zhu, C., Fang, X., Yang, T., Zhang, L., et al. (2021). Metagenomic next-generation sequencing technology for detection of pathogens in blood of critically ill patients. *Int. J. Infect. Dis.* 103, 81–87. doi: 10.1016/j.ijid.2020.11.166

Goto, M., and Al-Hasan, M. N. (2013). Overall burden of bloodstream infection and nosocomial bloodstream infection in north America and Europe. *Clin. Microbiol. Infect.* 19 (6), 501–509. doi: 10.1111/1469-0691.12195

Gu, W., Miller, S., and Chiu, C. Y. (2019). Clinical metagenomic next-generation sequencing for pathogen detection. *Annu. Rev. Pathol.* 14, 319–338. doi: 10.1146/annurev-pathmechdis-012418-012751

He, D., Liu, M., Chen, Q., Liu, Y., Tang, Y., Shen, F., et al. (2022). Clinical characteristics and the effect of timing for metagenomic next-generation sequencing in critically ill patients with sepsis. *Infect. Drug Resist.* 15, 7377–7387. doi: 10.2147/idr.S390256

Hu, B., Tao, Y., Shao, Z., Zheng, Y., Zhang, R., Yang, X., et al. (2021). A comparison of blood pathogen detection among droplet digital PCR, metagenomic next-generation sequencing, and blood culture in critically ill patients with suspected bloodstream infections. *Front. Microbiol.* 12. doi: 10.3389/fmicb.2021.641202

Jing, C., Chen, H., Liang, Y., Zhong, Y., Wang, Q., Li, L., et al. (2021). Clinical evaluation of an improved metagenomic next-generation sequencing test for the diagnosis of bloodstream infections. *Clin. Chem.* 67 (8), 1133–1143. doi: 10.1093/clinchem/hvab061

Kiani, D., Quinn, E. L., Burch, K. H., Madhavan, T., Saravolatz, L. D., and Neblett, T. R. (1979). The increasing importance of polymicrobial bacteremia. *Jama* 242 (10), 1044–1047. doi: 10.1001/jama.1979.03300100022015

Kumar, A., Roberts, D., Wood, K. E., Light, B., Parrillo, J. E., Sharma, S., et al. (2006). Duration of hypotension before initiation of effective antimicrobial therapy is the critical determinant of survival in human septic shock. *Crit. Care Med.* 34 (6), 1589–1596. doi: 10.1097/01.Ccm.0000217961.75225.E9

Li, H., and Durbin, R. (2009). Fast and accurate short read alignment with burrows-wheeler transform. *Bioinformatics* 25 (14), 1754–1760. doi: 10.1093/bioinformatics/btp324

Li, G., Sun, J., Pan, S., Li, W., Zhang, S., Wang, Y., et al. (2019). Comparison of the performance of three blood culture systems in a Chinese tertiary-care hospital. *Front. Cell Infect. Microbiol.* 9. doi: 10.3389/fcimb.2019.00285

Lin, J. N., Lai, C. H., Chen, Y. H., Chang, L. L., Lu, P. L., Tsai, S. S., et al. (2010). Characteristics and outcomes of polymicrobial bloodstream infections in the emergency department: a matched case-control study. *Acad. Emerg. Med.* 17 (10), 1072–1079. doi: 10.1111/j.1553-2712.2010.00871.x

Martinez, R. M., and Wolk, D. M. (2016). Bloodstream infections. *Microbiol. Spectr.* 4 (4), 4.4.42. doi: 10.1128/microbiolspec.DMIH2-0031-2016

Miao, Q., Ma, Y., Wang, Q., Pan, J., Zhang, Y., Jin, W., et al. (2018). Microbiological diagnostic performance of metagenomic next-generation sequencing when applied to clinical practice. *Clin. Infect. Dis.* 67 (suppl_2), S231–s240. doi: 10.1093/cid/ciy693

Miller, S., Naccache, S. N., Samayoa, E., Messacar, K., Arevalo, S., Federman, S., et al. (2019). Laboratory validation of a clinical metagenomic sequencing assay for pathogen detection in cerebrospinal fluid. *Genome Res.* 29 (5), 831–842. doi: 10.1101/gr.238170.118

Previsdomini, M., Gini, M., Cerutti, B., Dolina, M., and Perren, A. (2012). Predictors of positive blood cultures in critically ill patients: a retrospective evaluation. *Croat Med. J.* 53 (1), 30–39. doi: 10.3325/cmj.2012.53.30

Qian, Y. Y., Wang, H. Y., Zhou, Y., Zhang, H. C., Zhu, Y. M., Zhou, X., et al. (2020). Improving pulmonary infection diagnosis with metagenomic next generation sequencing. *Front. Cell Infect. Microbiol.* 10. doi: 10.3389/fcimb.2020.567615

Qin, H., Peng, J., Liu, L., Wu, J., Pan, L., Huang, X., et al. (2021). A retrospective paired comparison between untargeted next generation sequencing and conventional microbiology tests with wisely chosen metagenomic sequencing positive criteria. *Front. Med. (Lausanne)* 8. doi: 10.3389/fmed.2021.686247

Ren, L., Zhang, R., Rao, J., Xiao, Y., Zhang, Z., Yang, B., et al. (2018). Transcriptionally active lung microbiome and its association with bacterial biomass and host inflammatory status. *mSystems* 3 (5), 00199–18. doi: 10.1128/mSystems.00199-18

Semenec, L., Cain, A. K., Dawson, C. J., Liu, Q., Dinh, H., Lott, H., et al. (2023). Cross-protection and cross-feeding between klebsiella pneumoniae and acinetobacter baumannii promotes their co-existence. *Nat. Commun.* 14 (1), 702. doi: 10.1038/s41467-023-36252-2

Singer, M., Deutschman, C. S., Seymour, C. W., Shankar-Hari, M., Annane, D., Bauer, M., et al. (2016). The third international consensus definitions for sepsis and septic shock (Sepsis-3). *Jama* 315 (8), 801–810. doi: 10.1001/jama.2016.0287

Tao, Y., Yan, H., Liu, Y., Zhang, F., Luo, L., Zhou, Y., et al. (2022). Diagnostic performance of metagenomic next-generation sequencing in pediatric patients: a retrospective study in a Large children's medical center. *Clin. Chem.* 68 (8), 1031–1041. doi: 10.1093/clinchem/hvac067

Xie, G., Zhao, B., Wang, X., Bao, L., Xu, Y., Ren, X., et al. (2021). Exploring the clinical utility of metagenomic next-generation sequencing in the diagnosis of pulmonary infection. *Infect. Dis. Ther.* 10 (3), 1419–1435. doi: 10.1007/s40121-021-00476-w

Yan, G., Liu, J., Chen, W., Chen, Y., Cheng, Y., Tao, J., et al. (2021). Metagenomic next-generation sequencing of bloodstream microbial cell-free nucleic acid in children with suspected sepsis in pediatric intensive care unit. *Front. Cell Infect. Microbiol.* 11. doi: 10.3389/fcimb.2021.665226

Yealy, D. M., Kellum, J. A., Huang, D. T., Barnato, A. E., Weissfeld, L. A., Pike, F., et al. (2014). A randomized trial of protocol-based care for early septic shock. *N Engl. J. Med.* 370 (18), 1683–1693. doi: 10.1056/NEJMoa1401602

Zheng, Y., Qiu, X., Wang, T., and Zhang, J. (2021). The diagnostic value of metagenomic next-generation sequencing in lower respiratory tract infection. *Front. Cell Infect. Microbiol.* 11. doi: 10.3389/fcimb.2021.694756

frontiers | Frontiers in Cellular and Infection Microbiology

TYPE Original Research
PUBLISHED 26 June 2023
DOI 10.3389/fcimb.2023.1157540

OPEN ACCESS

EDITED BY
Jeyaprakash Rajendhran,
Madurai Kamaraj University, India

REVIEWED BY
Mathieu Garand,
Washington University in St. Louis, United States
Ashok Ayyappa,
University of Madras, India

*CORRESPONDENCE
Ruotong Ren
ruorabbit@163.com
Yanchun Li
1425649618@qq.com

†These authors have contributed equally to this work and share first authorship

RECEIVED 02 February 2023
ACCEPTED 29 May 2023
PUBLISHED 26 June 2023

CITATION
Xie G, Hu Q, Cao X, Wu W, Dai P, Guo W, Wang O, Wei L, Ren R and Li Y (2023) Clinical identification and microbiota analysis of *Chlamydia psittaci*- and *Chlamydia abortus*- pneumonia by metagenomic next-generation sequencing. *Front. Cell. Infect. Microbiol.* 13:1157540. doi: 10.3389/fcimb.2023.1157540

Clinical identification and microbiota analysis of *Chlamydia psittaci*- and *Chlamydia abortus*- pneumonia by metagenomic next-generation sequencing

Gongxun Xie[1†], Qing Hu[1†], Xuefang Cao[2†], Wenjie Wu[2†], Penghui Dai[1], Wei Guo[1], Ouxi Wang[2], Liang Wei[2], Ruotong Ren[2,3*] and Yanchun Li[1*]

[1]Department of Pathology, Hunan Provincial People's Hospital, The First Affiliated Hospital of Hunan Normal University, Changsha, Hunan, China, [2]Institute of Innovative Applications, MatriDx Biotechnology Co., Ltd, Hangzhou, Zhejiang, China, [3]Foshan Branch, Institute of Biophysics, Chinese Academy of Sciences, Beijing, China

Introduction: Recently, the incidence of chlamydial pneumonia caused by rare pathogens such as *C. psittaci* or *C. abortus* has shown a significant upward trend. The non-specific clinical manifestations and the limitations of traditional pathogen identification methods determine that chlamydial pneumonia is likely to be poorly diagnosed or even misdiagnosed, and may further result in delayed treatment or unnecessary antibiotic use. mNGS's non-preference and high sensitivity give us the opportunity to obtain more sensitive detection results than traditional methods for rare pathogens such as *C. psittaci* or *C. abortus*.

Methods: In the present study, we investigated both the pathogenic profile characteristics and the lower respiratory tract microbiota of pneumonia patients with different chlamydial infection patterns using mNGS.

Results: More co-infecting pathogens were found to be detectable in clinical samples from patients infected with *C. psittaci* compared to *C. abortus*, suggesting that patients infected with *C. psittaci* may have a higher risk of mixed infection, which in turn leads to more severe clinical symptoms and a longer disease course cycle. Further, we also used mNGS data to analyze for the first time the characteristic differences in the lower respiratory tract microbiota of patients with and without chlamydial pneumonia, the impact of the pattern of *Chlamydia* infection on the lower respiratory tract microbiota, and the clinical relevance of these characteristics. Significantly different profiles of lower respiratory tract microbiota and microecological diversity were found among different clinical subgroups, and in particular, mixed infections with *C. psittaci* and *C. abortus* resulted in lower lung microbiota diversity, suggesting that chlamydial infections shape the unique lung microbiota pathology, while

mixed infections with different *Chlamydia* may have important effects on the composition and diversity of the lung microbiota.

Discussion: The present study provides possible evidences supporting the close correlation between chlamydial infection, altered microbial diversity in patients' lungs and clinical parameters associated with infection or inflammation in patients, which also provides a new research direction to better understand the pathogenic mechanisms of pulmonary infections caused by *Chlamydia*.

KEYWORDS

***Chlamydia psittaci*, *Chlamydia abortus*, Metagenomic next-generation sequencing, Pulmonary microbiome, Chlamydial pneumonia**

Introduction

Chlamydia is a family of obligate intracellular Gram-negative bacteria with a unique biphasic life cycle in which a small extracellular infectious basic body (EB) and a metabolically active reticulum (RB) play a special role (Cheong et al., 2019; Marti and Jelocnik, 2022). Taxonomically, *Chlamydia* belongs to the order Chlamydiales and the family Chlamydiaceae and are currently subdivided into more than 10 species (Sachse et al., 2015; Zaręba-Marchewka et al., 2020). They are widely distributed worldwide and infect a variety of hosts, including amoebae, insects, aquatic animals, reptiles, birds and mammals. *C. trachomatis* and *C. pneumoniae* have been described as causative agents of female genital tract infections or trachoma and respiratory tract infections, respectively. In addition, other species such as *C. abortus, C. psittaci, C. pecorum and C. suis* are also thought to play a major role in animal infections (Cheong et al., 2019).

C. psittaci and *C. abortus* are known for their zoonotic potential and are often thought to be responsible for nautilus disease and human abortion, respectively (Pospischil et al., 2002; Wu et al., 2021). Human infection with *C. psittaci* is mainly through inhalation of dust containing respiratory secretions or dried faeces, or through direct contact with fresh faeces from infected birds or poultry (Harkinezhad et al., 2007; Shaw et al., 2019; Qin et al., 2022). There have also been some reports of possible human-to-human transmission of *C. psittaci* (Wallensten et al., 2014; Zhang et al., 2022c). Notably, as a newly discovered chlamydial species, *C. abortus* is closely related to the well-known *C. psittaci* in terms of genetics, host relatedness and associated disease pathological features (Joseph et al., 2015). However, to date, only sporadic cases of pneumonia caused by *C. abortus* have been reported worldwide (Ortega et al., 2015; Imkamp et al., 2022; Zhu et al., 2022a). *C. abortus* can be transmitted to humans *via* urine, faeces, milk, amniotic fluid, placenta, aborted foetuses and other excretion routes in sick animals (Zhu et al., 2022a).

Patients with chlamydial pneumonia usually present with non-specific clinical signs such as fever and weakness, with occasional loss of appetite, cough, myalgia and headache (Tang et al., 2022). Currently, the taxonomic identification of *Chlamydia* is based on isolation and culture of the pathogen, serological testing and further molecular typing (e.g. polymerase chain reaction and 16S rRNA gene sequencing) (Corsaro and Greub, 2006). *Chlamydia* culture usually requires the rigour of an experienced professional in a Class C3 laboratory. There are commercially available antigen or antibody test kits for *Chlamydia*, but the common cross-contamination of serological tests can also lead to false positive results (Corsaro and Venditti, 2004). Relative to culture and serological assays, PCR or PCR-based molecular typing techniques have better efficacy for *Chlamydia* detection or species identification, but require pre-assumptions and primer design specific to the chlamydial genome (Barati et al., 2017). In summary, the non-specific clinical presentation and the many limitations of pathogen identification methods dictate that chlamydial pneumonia due to *C. psittaci* and *C. abortus* is likely to be poorly diagnosed or even misdiagnosed, and may further result in delayed treatment or unnecessary antibiotic use.

Recently, metagenomic next-generation sequencing (mNGS) has emerged as a novel and promising method for the detection of infectious agents. Based on non-preference and high sensitivity, mNGS provides more sensitive pathogen detection results than conventional culture, especially for rare pathogen detection involved in clinically challenging cases (Miao et al., 2018; Li et al., 2021a; Wang et al., 2021; Yin et al., 2022). However, existing studies are mainly focus on the applicability of mNGS for the detection of *Chlamydia* infection in case reports or diagnostic performance assessments (Chen et al., 2020b; Duan et al., 2022; Liu et al., 2022b; Tang et al., 2022; Yang et al., 2022; Yin et al., 2022; Zhang et al., 2022c; Zhu et al., 2022b), but not on the microbiome characteristics of the lower respiratory tract in patients with

Abbreviations: mNGS, metagenomic next-generation sequencing; BALF, bronchoalveolar lavage fluid; RPM, reads per million; AUC, the area under the ROC curve; WBC, white blood cell; NE, neutrophil; CRP, C-reactive protein; PCT, procalcitonin; IL-6, interleukin-6; ESR, erythrocyte sedimentation rate; D-D, D-Dimer; BNP, brain natriuretic peptide; K, potassium ions; Na, sodium ion; Cl, chloride ion; Ca, calcium ion; LDH, lactic dehydrogenase; CK, creatine kinase; MYO, Myoglobin; CTnl, cardiac troponin I; ALT, alanine transaminase; AST, aspartate transferase; BUN, blood urea nitrogen; CREA, creatinine.

chlamydial pneumonia. In the present study, we first investigated the pathogenic profile of pneumonia patients with different chlamydial infection patterns, and subsequently compared the microbiota differences in the lower respiratory of patients with and without chlamydial pneumonia, and also analyzed the impact of chlamydial infection patterns on the microbiota dynamics of lower respiratory tract and finally we explored the correlation between the characteristics and the clinical parameters of patient care. Our results may answer to some extent the relevance of the lower respiratory microbiota to the signs and course of chlamydial pneumonia and also provide new insights into the pathogenesis of infectious pneumonia due to *Chlamydia*.

Materials and methods

Patient enrollment

The present study retrospectively enrolled patients with suspected pulmonary infection from January to December 2021 at Hunan Provincial People's Hospital, The First Affiliated Hospital of Hunan Normal University. Demographic information, clinical symptoms, laboratory test results, imaging examination results, diagnosis and treatment history, clinical course of the disease and outcomes were collected from electronic medical records.

This study was approved by the Ethics Committee of the Hunan Provincial People's Hospital and conducted in accordance with Declaration of Helsinki principles and relevant ethical and legal requirements.

Clinical sample collection and DNA extraction

Bronchoalveolar lavage fluid (BALF), sputum or peripheral blood samples were collected from each patient with the consent of themselves or their surrogates. The BALF samples were collected by experienced bronchoscopists after anesthesia with midazolam. The peripheral blood was centrifuged at 1600 ×*g* for 10 min and the collected supernatant was further centrifuged at 16000 ×*g* for 10 min to separate plasma. DNA extraction and library preparation from clinical samples were performed by using an NGS Automatic Library Preparation System (MatriDx Biotech Corp. Hangzhou). The quality of DNAs was assessed using a BioAnalyzer 2100 (Agilent Technologies; Santa Clara, CA, United States) combined with quantitative PCR to measure the adapters before sequencing.

Metagenomic next-generation sequencing

Qualified DNA libraries were pooled together and subsequently sequenced on Illumina NextSeq500 system (50 bp single-end; San Diego, CA, United States). To control the quality of each sequencing run, a negative control and a positive control were conducted in parallel. A total of 10 - 20 million reads were generated for each sample. The raw sequenced reads were first processed with quality control to remove short (length < 35 bp), low quality and low complexity reads, as well as those corresponding to adapters. Host sequences were filtered out based on the alignment to the human-secific database in NCBI using Bowtie2 (version 2.3.5.1). The clean reads were thus aligned to a manual-curated microbial database using Kraken2 (version 2.1.2; confidence = 0.5) for quick taxonomic classification. The classified reads of interested microorganisms were further validated through a second alignment to the microbial database using Bowtie2. The classification of candidate reads might also be conducted by BLAST (version 2.9.0) whenever the results of Kraken2 and Bowtie2 were inconsistent.

Before data analysis, microbes detected in clinical samples were first compared with those detected in the parallel NTC (no template control). Microorganisms with a reads per million (RPM) above 10 or if the organism was not detected in the parallel NTC were maintained and defined as microbiota for further analysis. Substantially, all species of microbiota were looked up in PubMed to determine whether the organisms cause pneumonia and the positive pathogenic microorganisms were defined as pathogens.

Statistical analysis

Categorical variables, shown as frequencies and percentages, were compared using Fisher's exact test. Continuous measurement data following normal distribution were shown as mean ± standard deviation (x ± s), and non-normal distribution was shown by median (range). Differences and significance were calculated using the Wilcoxon test or Kruskal-Wallis test (for non-normal distribution data). SPSS 26.0 (IBM Corporation) was used for statistical analysis. Data visualization was performed in R (Version 4.2.1). Specifically, bivariate or multivariate difference analysis was performed using unsupervised clustering methods with reference to the core steps of limma, voom, fit, eBays, etc. The final similarities (or differences) between groups were demonstrated using plotMDS in the limma package and the results were output using the topTable method sorted by *P*-value. RPKM values of microbes were log2 transformed before their relative abundance was analyzed. Variations in composition and abundance of microbes between groups were analyzed using the limma package. In this study, two-sided P values < 0.05 were considered statistically significant. Particularly, for multiple comparisons, FDR method was used to correct the primary *P*-value.

Results

Demographic and clinical characteristics of the cohort

A total of 43 samples from 41 patients, i.e. 23 (53.5%) females and 20 (46.5%) males, were included according to the sample entry

exclusion criteria for this study, with a median age of 55 years (range 30 - 74 years) and a median length of hospital stay of 12 days (range 4 - 47 days) (Table 1). Among these enrolled samples, a total of 25 (58.2%) had underlying diseases (Table 1). These clinical samples were first divided into the chlamydial pneumonia group (n=15) and the non-chlamydial pneumonia group (n=28) based on whether the pathogenic microorganism identified by mNGS contained *Chlamydia*. The two groups mentioned above were further divided into 5 subgroups according to clinical diagnosis. In details, the chlamydial pneumonia group was subdivided into the *C. psittaci* mono-infection subgroup (CP, n=7), the *C. abortus* mono-infection subgroup (CA, n=2) and the *C. psittaci*-*C. abortus* co-infection subgroup (PA, n=6). The non-chlamydial pneumonia group was subdivided into the infectious subgroup of other pathogens (O, n=16) and the non-infectious subgroup (N, n=12) (Figure 1A).

The majority of clinical symptoms in the enrolled patients were fever (65.1%), cough (69.8%), sputum (53.5%) and other non-specific symptoms (Table 1). The incidence of various clinical symptoms was significantly different across subgroups and patients with chlamydial infection displayed a relatively higher percentage, including fever (P = 0.009), chills (P = 0.009), weakness (P < 0.001), muscle aches (P = 0.039), urinary incontinence (P = 0.039), poor mental status (P = 0.011), loss of appetite (P = 0.001), anhelation (P = 0.007), dizziness (P = 0.019) and impaired consciousness (P = 0.043). Clinical test data were also significantly different among subgroups, such as WBC (P = 0.044), CRP (P = 0.006) and K^+ (P = 0.016) as listed in Table 1. After clinical treatment, most cases (81.4%) were found to be improved. However, complications occurred in seven patients during hospitalization and four of them were from the PA subgroup. Notably, based on previous clinical and public health management experience, the primary risk factor for chlamydial pneumonia is exposure to chickens or domestic animals, but in this study, only four patients with chlamydial pneumonia had a clear history of poultry or domestic animal contact, indicating that there might have other source of infection which is responsible for the occurrence of chlamydial pneumonia in this region. As shown in Table 1, these four patients were assigned to the CP group (2 patients), CA group (1 patient) and PA group (1 patient), while the risk factor exposure was not included as a grouping parameter in the subsequent microbiome difference analysis due to the small subset of these patients.

mNGS can effectively assist in the clinical diagnosis of chlamydial pneumonia

The methodological performance of mNGS in the diagnosis of chlamydial pneumonia was assessed by the receiver operating characteristic (ROC) curve and the final clinical diagnosis was included as the assessment criterion. In this study, the overall performance of mNGS in the detection of pathogens in the total enrolled samples obtained a sensitivity of 100%, an accuracy of 100% and a positive predictive value of 100% (Figure 1B). Meanwhile, the sensitivity, specificity, accuracy, positive predictive value and negative predictive value of mNGS for detecting *Chlamydia* infection were all 100% (Figure 1C). For both *C. abortus* and *C. psittaci*, the area under the ROC curve (AUC) for mNGS was 1. The cut-off values calculated from the Youden index for *C. abortus* and *C. psittaci* were 0.115 and 0.080, respectively (Supplementary Figure 1).

Spectrum analysis of responsible pathogens in different subgroups of *Chlamydia* infection

In this study, clinical samples identified as chlamydial infection using mNGS included 13 cases of BALF, 1 case of sputum, and 1 case of peripheral blood. A total of 15 responsible pathogens were detected and more than one pathogen was detected in each clinical sample (Figure 2A; Supplementary Table 1). We found that different subgroups of *Chlamydia* infection had different responsible pathogen profiles, with 11, 6, and 11 responsible pathogens detected in the CP, CA, and PA groups, respectively (Figure 2A; Supplementary Table 1). The relative abundance of the responsible pathogens also differed significantly among different chlamydial pneumonia subgroups. As shown in Figure 2B, the CP and PA groups have different spectrum of responsible pathogens. Combined with Bubble matrix analysis (Figure 2C), we can find that the main responsible pathogens identified in the CP group were *C. psittaci* (Frequency: 100% (7/7), Relative abundance: 41.0%) and *Candida glabrata* (28.6% (2/7), 15.7%). As expected, *C. psittaci* (100% (5/5), 36.5%) and *C. abortus* (100% (5/5), 25.9%) were the most enriched species in the PA group. In addition, the relative abundance of the following two responsible pathogens was significantly different (P < 0.05) among the two subgroups: *C. abortus* (0.0%, 25.9%) and *C. psittaci* (41.0%, 36.5%) (Supplementary Table 2).

Correlation analysis between responsible pathogens and clinical indices of *Chlamydia*-infection patients

To explore the correlation between clinical characteristics and responsible pathogens in chlamydial infection, spearman test was performed on responsible pathogens mentioned above (Figure 2D). The results showed that the abundance of *C. abortus* was significantly and positively correlated with the dynamics of clinical indicators such as white blood cell count (R = 0.73, P = 0.007), C-reactive protein (CRP) (R = 0.85, P = 0.001) and potassium ion content (K^+) (R = 0.81, P = 0.001), but negatively correlated with sodium ion content (Na^+) (R = -0.58, P = 0.064) (Figure 2D; Supplementary Figures 2E–H). *C. psittaci* was significantly and positively correlated with white blood cell count (R = 0.62, P = 0.032), CRP (R = 0.69, P = 0.013) and K^+ (R = 0.83, P = 0.001) and significantly negatively correlated with sodium ion content (Na^+) (R = -0.6, P = 0.05) (Figure 2D; Supplementary Figures 2A–D).

10.3389/fcimb.2023.1157540

TABLE 1 Demographic and clinical characteristics of patients and samples.

Characteristics	Overall (n=43)	CP (n=7)	CA (n=2)	PA (n=6)	N (n=12)	O (n=16)	*P*-value
Demographics							
Age, median (range, years)	55 (30-74)	53 (30-68)	59.5 (55-64)	57.5 (36-74)	52.5 (32-73)	59 (30-71)	0.655
Gender, (n, %) **							0.004
Female	23 (53.5)	7 (100.0)	0	5 (83.3)	6 (50)	5 (31.3)	
Male	20 (46.5)	0	2 (100.0)	1 (16.7)	6 (50)	11 (68.7)	
Temperature, median (range, °C) **	37.5 (36.0-41.0)	39.5 (39.0-40.0)	39.5 (39.0-40.0)	39.8 (38.5-41.0)	36.6 (36.2-39.0)	36.5 (36.0-39.0)	<0.001
Contact history (n, %) *	4 (9.3)	2 (28.6)	1 (50.0)	1 (16.7)	0	0	0.016
Underlying disease (n, %)	25 (58.2)	5 (71.4)	2 (100.0)	4 (66.7)	4 (33.3)	10 (62.5)	0.304
Clinical manifestations (n, %)							
Fever **	28 (65.1)	7 (100.0)	2 (100.0)	6 (100.0)	6 (50.0)	7 (43.8)	0.009
Cough	30 (69.8)	7 (100.0)	2 (100.0)	5 (83.3)	8 (66.7)	8 (50)	0.123
Expectoration	23 (53.5)	5 (71.4)	2 (100.0)	3 (50.0)	6 (50.0)	7 (43.8)	0.613
Chills **	9 (20.9)	3 (42.8)	2 (100.0)	2 (33.3)	1 (8.3)	1 (6.3)	0.009
Weakness **	15 (34.9)	7 (100.0)	1 (50.0)	5 (83.3)	0	2 (12.5)	<0.001
Myalgia *	3 (7.0)	2 (28.6)	0	1 (16.7)	0	0	0.039
Diarrhea	2 (4.7)	0	0	1 (16.7)	0	1 (6.3)	0.53
Urinary and fecal incontinence *	3 (7.0)	2 (28.6)	0	1 (16.7)	0	0	0.039
Poor mental state *	19 (44.2)	5 (71.4)	2 (100.0)	5 (83.3)	3 (25.0)	4 (25.0)	0.011
Poor appetite **	19 (44.2)	6 (85.7)	2 (100.0)	5 (83.3)	3 (25.0)	3 (18.8)	0.001
Poor sleep	10 (23.3)	2 (28.6)	0	4 (66.7)	2 (16.7)	2 (12.5)	0.106
Anhelation **	7 (16.3)	4 (57.1)	1 (50.0)	0	0	2 (12.5)	0.007
Headache	4 (9.3)	1 (14.3)	0	2 (33.3)	0	1 (6.3)	0.199
Dizzy *	4 (9.3)	2 (28.6)	0	2 (33.3)	0	0	0.019
Nausea and vomiting	3 (7.0)	2 (28.6)	0	0	0	1 (6.3)	0.228
Painful throat	2 (4.7)	1 (14.3)	0	1 (16.7)	0	0	0.178
Conscious disorders *	6 (14.0)	3 (42.8)	0	2 (33.3)	0	1 (6.3)	0.043
Chest tightness	2 (4.7)	1 (14.3)	0	1 (16.7)	0	0	0.178
Palpitations	2 (4.7)	1 (14.3)	0	1 (16.7)	0	0	0.178
Complications (n, %) **	7 (16.3)	0	1 (50.0)	4 (66.7)	0	2 (12.5)	0.002
Laboratory examination, mean (range)							
WBC (3.5–9.5 × 10^9/L) *	9.5 (2.7-21.0)	5.2 (4.2-6.5)	11.8 (9.5-14.2)	9.2 (6.4-12.4)	10.5 (4.2-21.0)	11.3 (2.7-19.0)	0.044
NE% (45–75%)	82.0 (0.8-96.1)	87.3 (0.8-88.4)	83.1 (82.4-83.7)	91.5 (0.9-96.1)	76.6 (40.1-94.7)	87.7 (1.7-93.7)	0.247
CRP (<10mg/L) **	139.3 (4.0-249.0)	139.3 (67.1-164.0)	159.2 (93.3-225.0)	203.3 (190.9-249.0)	41.6 (12.5-169.8)	109.1 (4.0-236.9)	0.006
PCT (0.02–0.05ng/mL)	0.32 (0.02-44.0)	0.54 (0.14-13.00)	0.39 (0.12-0.66)	0.44 (0.20-2.23)	0.36 (0.03-9.37)	0.24 (0.02-44.00)	0.845
IL-6 (0-7pg/mL)	65.6 (8.0-518.1)	92.0 (8.6-108.1)	N.A.	75.2 (8.0-518.1)	53.7 (11.7-68.4)	178.1 (21.4-373.8)	0.67
ESR (0-20mm/h)	60.0 (6.0-119.0)	62.0 (49.0-98.0)	65.5 (60.0-71.0)	38.0 (25.1-92.0)	30.0 (23.0-99.0)	64.0 (6.0-119.0)	0.532

(Continued)

TABLE 1 Continued

Characteristics	Overall (n=43)	CP (n=7)	CA (n=2)	PA (n=6)	N (n=12)	O (n=16)	*P*-value
D-D (0-0.55mg/L) *	2.8 (0.3-325.0)	4.4 (2.8-7.5)	1.9 (1.7-2.1)	2.4 (1.0-6.7)	1.5 (0.7-3.2)	5.2 (0.3-325.0)	0.025
BNP (0-125pg/mL)	508.6 (28.9-6430.0)	804.3 (273.2-6430.0)	498.6 (498.6-498.6)	590.8 (141.9-1028.1)	431.1 (28.9-785.0)	440.4 (77.0-2295.9)	0.72
K (3.5-5.3mmol/L) *	3.3 (2.9-4.4)	3.1 (3.0-3.2)	3.9 (3.3-4.4)	3.4 (3.1-4.3)	3.3 (3.2-4.1)	3.6 (2.9-4.4)	0.016
Na (137-147mmol/L)	137.5 (116.0-159.0)	138.0 (136.0-141.0)	124.0 (116.0-132.0)	130.0 (124.6-138.0)	138.0 (129.0-145.0)	141.0 (129.7-159.0)	0.058
Cl (99-110mmol/L)	101.0 (78.0-122.0)	106 (96.0-109.0)	84.5 (78.0-91.0)	97.2 (85.9-106.0)	101.0 (95.0-102.0)	105.0 (93.0-122.0)	0.059
Ca(2.10-2.90mmol/L)	1.99 (1.04-2.47)	1.99 (1.75-2.47)	2.18 (2.08-2.27)	1.88 (1.70-2.07)	1.99 (1.95-2.02)	1.57 (1.04-2.08)	0.228
LDH (100-240U/L)	317.4 (121.9-561.5)	336.0 (296.6-561.5)	357.0 (232.9-481.0)	384.0 (261.9-461.0)	287.4 (121.9-339.5)	306.8 (256.0-392.3)	0.427
CK (10-175U/L)	159.0 (11.0-2472.8)	327.9 (56.3-2472.8)	151.6 (111.5-191.6)	159.0 (47.2-1218.9)	303.4 (32.0-1464.3)	88.0 (11.0-1254.0)	0.871
MYO (0-85ng/mL)	88.1 (24.4-1395.7)	60.4 (24.4-523.3)	130.7 (82.1-179.2)	99.0 (61.0-111.2)	347.2 (24.6-1079.5)	88.1 (47.2-1395.7)	0.71
CTnl (0-0.034ng/mL)	0.025 (0.003-0.097)	0.025 (0.003-0.039)	0.031 (0.024-0.037)	0.009 (0.005-0.019)	0.095 (0.092-0.097)	0.025 (0.005-0.071)	0.134
ALT (9-50U/L)	56.9 (10.4-619.9)	64.3 (21.8-97.3)	77.5 (34.7-120.3)	94.0 (27.3-177.0)	27.6 (10.4-619.9)	34.1 (17.3-272.0)	0.728
AST (15-40U/L)	68.6 (12.0-857.3)	55.4 (22.2-206.3)	123.3 (29.2-217.4)	91.7 (33.6-217.0)	16.3 (12.9-857.3)	14.1 (12.0-171.8)	0.262
BUN (1.7-8.3mmol/L)	6.4 (1.7-19.4)	3.2 (2.2-6.4)	4.87 (3.1-6.6)	4.4 (1.7-7.6)	6.4 (4.6-8.4)	10.7 (2.8-19.4)	0.122
CREA (40-100μmol/L)	66.5 (15.0-143.0)	66.5 (52.0-69.4)	73.0 (57.0-89.0)	60.1 (35.2-76.1)	88.0 (15.0-132.4)	64.0 (25.8-143.0)	0.882
Hospitalized days, median (range)	12 (4-47)	11 (6-29)	12.5 (12-13)	9.5 (8-13)	12 (4-29)	14.5 (7-47)	0.811
Outcome (n, %)							0.636
Improved	35 (81.4)	5 (71.4)	2 (100.0)	4 (66.7)	11 (91.7)	13 (81.3)	
Not improved	8 (18.6)	2 (28.6)	0	2 (33.3)	1 (8.3)	3 (18.8)	

P.S., Significant differences among groups are indicated by asterisks, with * represents p<0.05 and ** represents p<0.01. N.A., Not applicable.

Characterization of pulmonary microbial communities in different subgroups of *Chlamydia* infection

As a respiratory organ, the lungs perform important gas exchange functions and also act as a vehicle to maintain the dynamic balance of microbial communities between the organism and the external environment, as well as between the upper and lower airways. A series of previous studies have shown that imbalance of microbiota in the lung may be closely associated with the development of pulmonary (infectious) diseases. Therefore, while we clarified the characteristics of the responsible pathogen spectrum in different subgroups of *Chlamydia* infection, we also wished to further investigate the effects of *Chlamydia* infection on the microbiota of the lower respiratory tract by analyzing the characteristics of the lung microbial communities detected by mNGS and their differences between different subgroups of *Chlamydia* infection. Figure 3 shows the distribution status (species level) of microbial communities in different *Chlamydia* infection subgroups and clinical controls, and provides overall information on the lung microbiota in patients with and without chlamydial infections. Using mNGS, we detected a total of 466 microbial species in all samples, most of which were bacteria (n=436), with a small number of fungi (n=23) and viruses (n=7). Figure 3A serves as a heatmap of the relative abundance of microbial species, showing the top 70 bacteria and all fungi and viruses in the 43 samples involved in this study.

To further investigate the effect of *Chlamydia* infection on the lung microbiota, we performed a comparative analysis of the microbial communities of 40 BALF samples from different *Chlamydia* infection subgroups (CP and PA groups) and clinical control groups (O and N groups). Compared to the control group N, the diversity of fungal and viral species was significantly reduced in the *Chlamydia*-infected groups (CP and PA groups) (Figure 3B; Supplementary Table 3). Additionally, the dominant microbial species in different chlamydial infection subgroups were not consistent, with the enriched species in the CP group being *Acinetobacter nosocomialis* (8.6%), *Aci. seifertii* (8.5%) and *Aci.*

10.3389/fcimb.2023.1157540

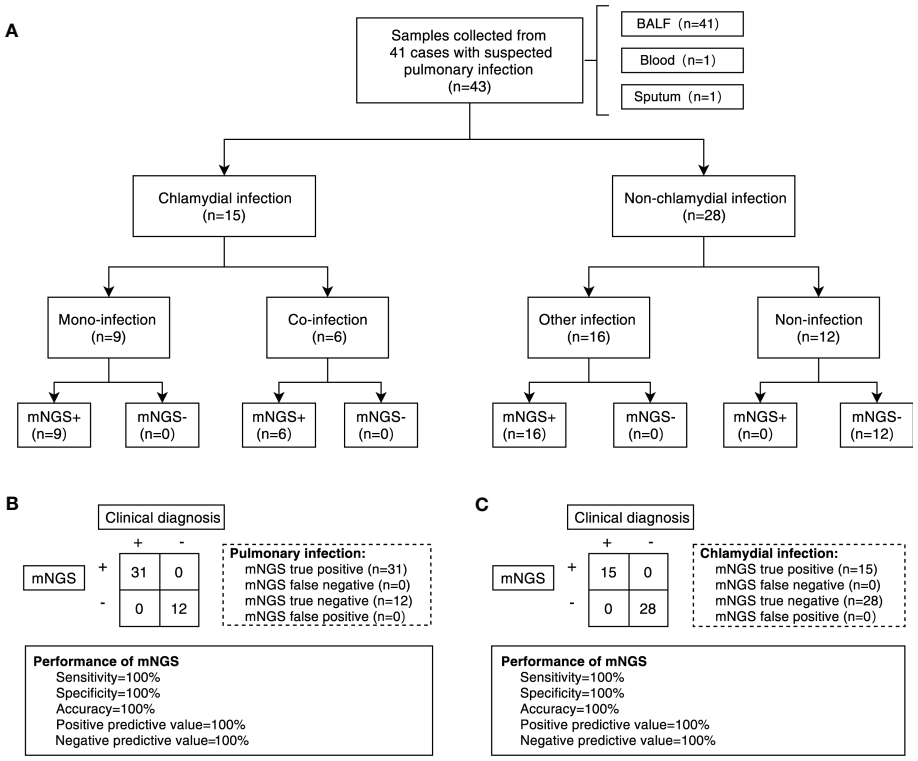

FIGURE 1
Overall design of the study and diagnostic performance of mNGS test. **(A)** Flowchart of patients and samples classification. A total of 43 samples were obtained from 41 patients for our study. Samples were divided into chlamydial infection and non-chlamydial infection groups. Samples in chlamydial infection were further divided into chlamydial mono-infection (CP group and CA group) and co-infection (PA group) subgroups, and samples in non-chlamydial infection group were further divided into other infection (O group) and non-infection (N group) subgroups. **(B)** The performance of mNGS in diagnosing pulmonary infection based on clinical diagnosis. **(C)** The performance of mNGS in diagnosing chlamydial infection based on clinical diagnosis. BALF, bronchoalveolar lavage fluid. mNGS, metagenomic next-generation sequencing.

lwoffii (8.1%), whereas the superior species in the PA group were *Abiotrophia defectiva* (13.0%), *A. para-adiacens* (10.9%) and *Aci. seifertii* (11.0%).

Based on the classical Alpha-diversity Shannon and Simpson index analysis shown in Figure 3C, there was no statistical difference of the lung microbial community detected between the CP and N groups. However, the lung microbial community diversity of the PA group ($P = 0.0039$ and $P = 0.0039$) and the O group ($P = 0.033$ and $P = 0.037$) (Shannon and Simpson) were both significantly lower than that of the N group. Notably, the PA group had the lowest level of Alpha-diversity in the lung microbial community, suggesting that co-infection with *C. psittaci* and *C. abortus* might have important effects on the composition and diversity of the lung microbiome.

In addition, with two parameters of relative abundance and frequency, we performed a collaborative analysis of the top 50 microorganisms (including the top 30 bacteria, top 15 fungi, and top 5 viruses) to identify the specific microorganisms in the different clinical subgroups (Figure 3D). The results showed that the overall relative abundance and frequencies of microorganisms in the *Chlamydia*-infected group were lower than those in the N and O groups. Also, we identified some microbial species that were specifically enriched in different chlamydial infection subgroups and clinical control groups, such as *Actinomyces timonensis* (P = 2.7e-04), *Act. johnsonii* (P = 3.8e-02) and *Aci. johnsonii* (P = 3.5e-02) in the O group, *Aci. lwoffii* (P = 1.3e-02) and *Act. mediterranea* (P = 2.1e-02) were enriched in group N, *Act. oris* (P = 3.7e-02) in group PA, and *Aci. pittii* (P = 4.7e-02) in both groups PA and N.

Correlation analysis between lung microbiome and clinical indices of *Chlamydia*-infection patients

We further wanted to understand whether the effect of *Chlamydia* infection on the microbiota diversity of the patient's lower respiratory tract correlated with clinical status. After mentioned-above screening for microorganisms specifically enriched in each clinical subgroup, we performed a correlation analysis based on the spearman test using the relative abundance of these differential microorganisms and the infection-related clinical parameters of the corresponding patients (Figure 3E). The results showed that *Act. timonensis*, which was enriched in group O, was significantly and positively correlated with WBC (R = 0.36, P = 0.033) and negatively correlated with calcium ions (Ca^{2+}) (R = -0.48, P = 0.044). *Aci. lwoffii* that enriched in group N was significantly negatively correlated with WBC (R = -0.41, P = 0.014), NE (R = -0.50, P = 0.002) and K^+ (R = -0.53, P = 0.005). *Act. mediterranea* enriched in group N was significantly positively

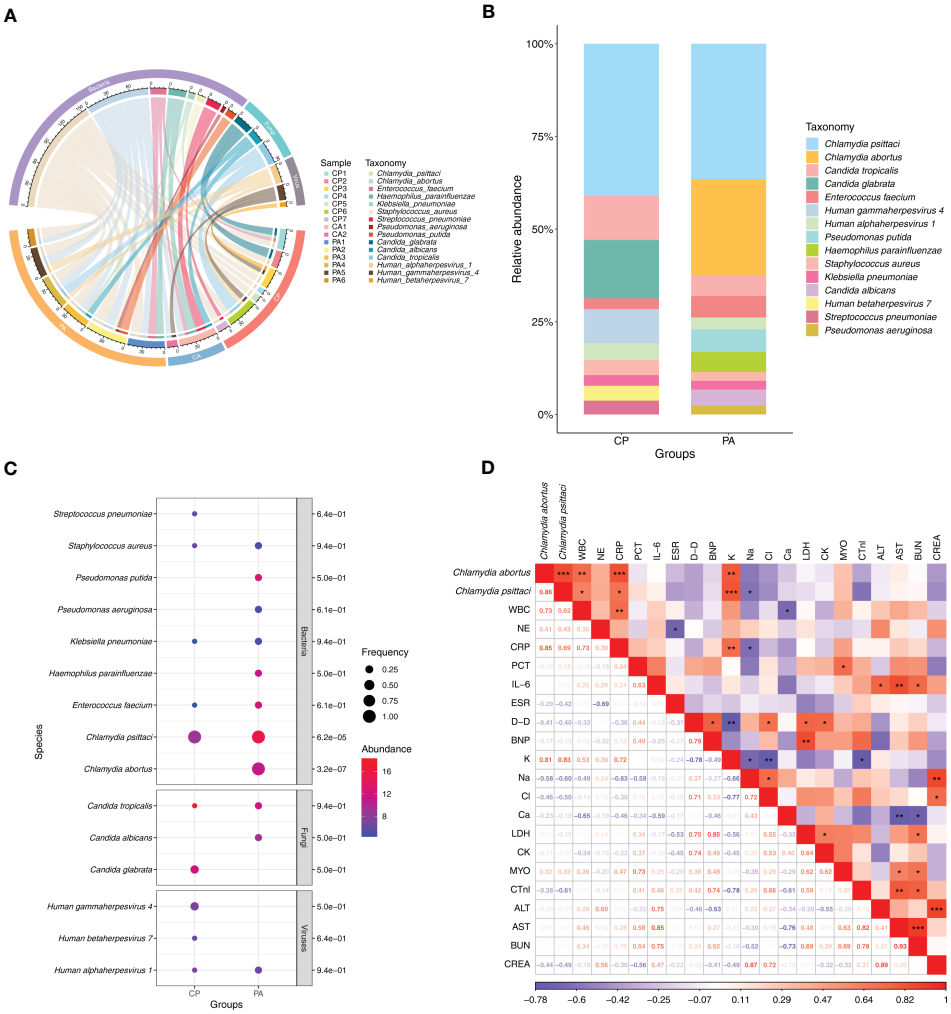

FIGURE 2
Distribution of responsible pathogens in patients with chlamydial pneumonia and analysis of the association between responsible pathogens and clinical indicators. **(A)** Composition of responsible pathogens in the different samples. **(B)** Relative abundance of responsible pathogens between different chlamydial pneumonia subgroups. **(C)** Differences in relative abundance and detection frequency of responsible pathogens between chlamydial pneumonia subgroups. *P* value were listed on the right of the bubble plot. Red and blue indicate high and low abundance respectively, and the bubble size reflects the frequency of microbes detected. **(D)** Spearman correlation analysis between responsible pathogens with clinical data. Red values indicate species were positively correlated with clinical data, while blue ones indicate the species were negatively correlated with clinical data. Significant associations ($P<0.05$) are indicated by asterisks, with * represents $P<0.05$, ** represents $P<0.01$ and *** represents $P<0.001$. WBC, white blood cell; NE, neutrophil; CRP, C-reactive protein; PCT, procalcitonin; IL-6, interleukin-6; ESR, erythrocyte sedimentation rate; D-D, D-Dimer; BNP, brain natriuretic peptide; K, potassium ions; Na, sodium ion; Cl, chloride ion; Ca, calcium ion; LDH, lactic dehydrogenase; CK, creatine kinase; MYO, Myoglobin; CTnI, cardiac troponin I; ALT, alanine transaminase; AST, aspartate transferase; BUN, blood urea nitrogen; CREA, creatinine.

correlated with WBC (R = 0.37, $P = 0.024$) and creatinine (CREA) (R = 0.52, $P = 0.022$). *Aci. johnsonii* enriched in the O group showed a significantly positive correlation with K^+ (R = 0.40, $P = 0.036$) and a significantly negative correlation with creatine kinase (CK) (R = -0.64, $P = 0.008$). *Act. oris* enriched in the PA group showed a significantly negative correlation with Ca^{2+} (R = -0.48, $P = 0.044$). *Aci. pittii* enriched in PA and N groups showed a significantly positive correlation with WBC (R = 0.39, $P = 0.018$) and a significantly negative correlation with LDH (R = -0.49, $P = 0.023$). These findings suggested that the dynamics of the pulmonary microbiota were closely related to the clinical parameters of patients after *Chlamydia* infection.

In order to understand the impact of chlamydial pneumonia-related pathogens on the composition and diversity of the patient's lung microbiota more precisely, we thus performed a spearman test-based correlation analysis of the three representative responsible pathogens in the chlamydial infection group and the key commensal microorganisms specifically enriched in different clinical subgroups described above (Supplementary Figure 3A). It was interestingly to note that the abundance of *C. psittaci* were significantly and negatively correlated with that of *Act. mediterranea* (R= - 0.34, $P = 0.033$; Supplementary Figures 3A, B), *Aci. johnsonii* (R = -0.43, $P = 0.006$; Supplementary Figures 3A, C), *Act. oris* (R = -0.32, $P = 0.044$; Supplementary Figures 3A, D) and *Act. johnsonii* (R = -0.46, $P = 0.003$; Supplementary Figures 3A, E). Given these facts, we hypothesized that after infection, *C. psittaci* might alter the composition and diversity of the pulmonary microbiota by decreasing the relative abundance of certain pulmonary commensal

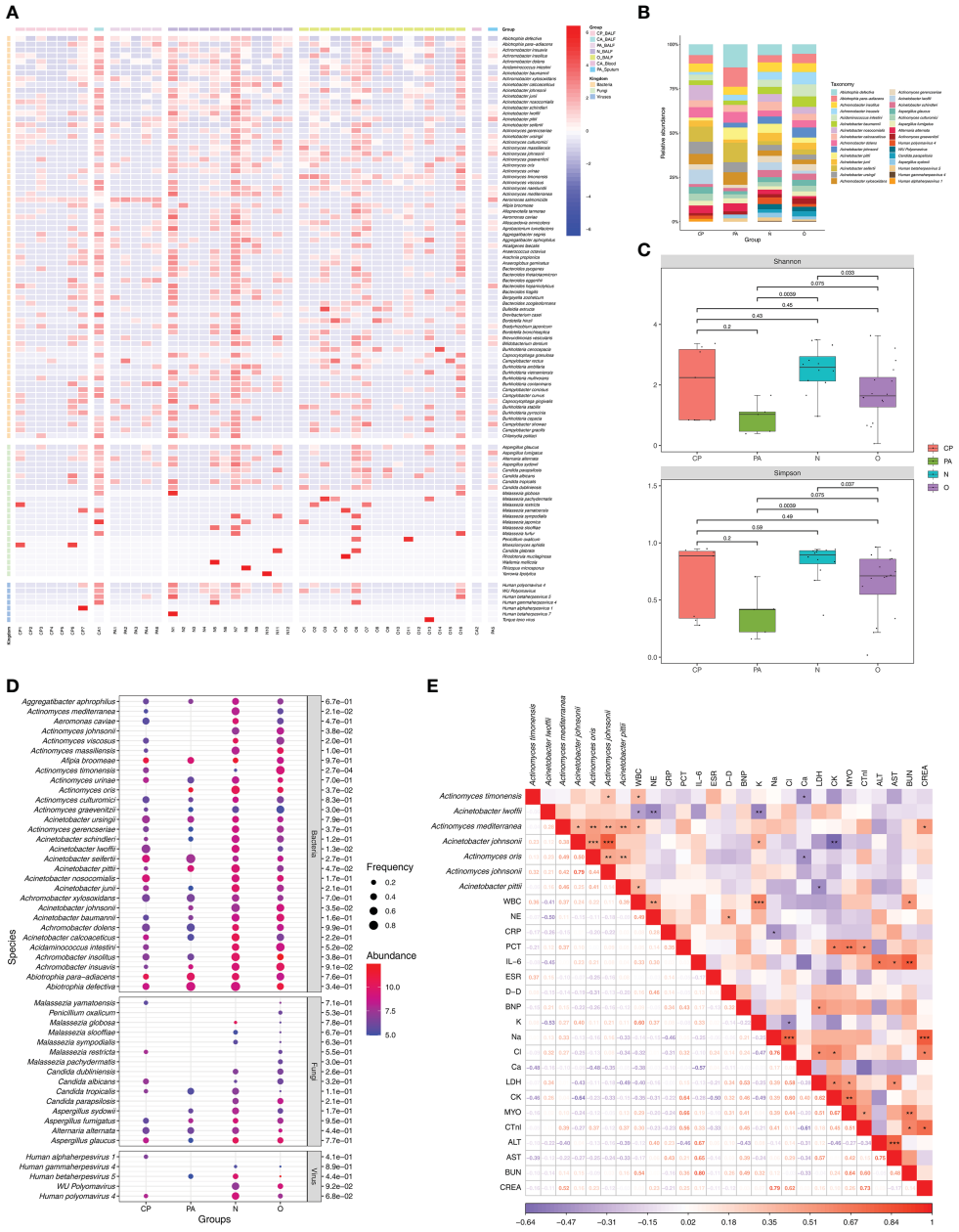

FIGURE 3
Microbiota communities at species level between different groups and analysis of the association between lung microbiota species and clinical data. **(A)** Composition of microbiome in the different samples. The heatmap exhibited the top 100 frequent species of the top 70 bacteria and all fungi and viruses. Group names and microbial kingdom are indicated by color bars on the right of map. **(B)** Relative abundance of frequency ranking top 30 microbes (consisted of the top 20 bacteria, the top 5 fungi and the top 5 viruses) in 40 BALF from different groups. **(C)** Alpha diversity differences of lung microbiota communities at species level between groups. Each dot represents one sample from each group. **(D)** Differences in relative abundance and detection frequency of frequency ranking top 50 microbes (consisted of the top 30 bacteria, the top 15 fungi and the top 5 viruses) in 40 BALF from different groups. *P* value were listed on the right of the bubble plot. Red and blue indicate high and low abundance respectively, and the bubble size reflects the frequency of microbes detected. **(E)** Spearman correlation analysis between microbial species with clinical data. Red values indicate species were positively correlated with clinical data, while blue ones indicate the species were negatively correlated with clinical data. Significant associations ($P<0.05$) are indicated by asterisks, with * represents $P<0.05$, ** represents $P<0.01$ and *** represents $P<0.001$. WBC, white blood cell; NE, neutrophil; CRP, C-reactive protein; PCT, procalcitonin; IL-6, interleukin-6; ESR, erythrocyte sedimentation rate; D-D, D-Dimer; BNP, brain natriuretic peptide; K, potassium ions; Na, sodium ion; Cl, chloride ion; Ca, calcium ion; LDH, lactic dehydrogenase; CK, creatine kinase; MYO, Myoglobin; CTnI, cardiac troponin I; ALT, alanine transaminase; AST, aspartate transferase; BUN, blood urea nitrogen; CREA, creatinine.

microorganisms, which in turn directly affect the clinical status of the patient and the course of pulmonary infection.

Discussion

In this study, we performed a comprehensive statistical analysis of the clinical characteristics of patients with suspected chlamydial pneumonia and classified these patients into different clinical subgroups. Pneumonia caused by *C. psittaci* infection is often misdiagnosed due to atypical clinical features and other diagnostic challenges. (Tang et al., 2022; Yang et al., 2022). Our study also found that most patients with suspected chlamydial pneumonia had no history of exposure to poultry, pets, or other farm animals, and they all had non-specific manifestations of pulmonary infection, such as fever, cough, and expectoration. These problems somehow pose a great challenge for rapid clinical confirmation of chlamydial infection. Previous studies have found that patients with pulmonary infection with *Chlamydia* have significantly elevated levels of inflammation-related markers in their peripheral blood, followed by a dramatic decrease to near normal levels after effective drug treatment (Li et al., 2021b). In our study, patients from different subgroups showed significant differences in clinical symptoms, peripheral blood inflammatory indicators and electrolyte levels. Specifically, patients with co-infection of *C. psittaci* and *C. abortus* had the highest peripheral blood CRP levels compared to other *Chlamydia* infection subgroups, indicating that co-infection might lead to severer pulmonary infections and a pan-systemic inflammatory state (Zhang et al., 2022b; Calderwood et al., 2023). Thus, the analysis of the responsible pathogen profile and the lung microbiota characteristics performed in this study for different patterns of *Chlamydia* infection and their correlation with the clinical status of the patients seems to be essential.

While the genomes of *C. psittaci* and *C. abortus* are highly homologous (Stephens et al., 2009; Wheelhouse and Longbottom, 2012), according to the Supplementary Table 1, the three infection groups, *C. psittaci* mono-infection, *C. abortus* mono-infection and mixed *C. psittaci* and *C. abortus* infections, did clearly showed unique spectrum of causative pathogens, which makes the etiological identification of *Chlamydia* pneumonia more complex and brings a great challenge to the pathogenic diagnosis in patients with *Chlamydia* pneumonia. Although there was only one BALF sample included in the CA group, it still showed a primary tendency. Of course, for a more solid conclusion, further researches are needed in the future. In recent years, as a high-throughput sequencing-based assay, mNGS has demonstrated good diagnostic performance for clinical infection pathogens, i.e., it can identify different types of pathogens, such as bacteria, fungi, viruses and parasites, in a single run, which is valuable for rapid and accurate diagnosis of mixed infections (Liang et al., 2022). However, previous studies have shown that there are some limitations to mNGS's use in the detection of virus, e.g. mNGS may not be able to detect low-level viral infections due to insufficient sequencing depth and coverage to identify low-abundance viral reads within a complex sample, mNGS may be prone to contamination, leading to the detection of false-positive viral sequences, mNGS may have difficulty detecting viruses with highly variable genomes due to bad alignment with the reference genomes, human genes in clinical samples also greatly influence the sensitivity of mNGS to detect viral pathogens. Therefore, all of the above shortcomings in viral detection raise concerns about the ability of mNGS to effectively detect low-abundance rare and unusual pathogens in clinical samples (Deng et al., 2020; Wang et al., 2020; Gu et al., 2021; Li et al., 2022). Our results showed that mNGS can effectively distinguish different species of *Chlamydia* from clinical samples and identify co-infections with other pathogenic microorganisms, such as *C. tropicalis*, *S. pneumoniae*, *H. influenzae*, *Enterococcus faecalis* and EBV. Furthermore, although due to the limited amounts of samples included in the CA group, it seemed difficult to statistically compare the pathogenic abundance between CA and CP groups. However, for the BALF sample of CA (i.e. CA1), there were five causative pathogens identified, which was much less than that in the CP group (10 in total), according to Supplementary Table 1. Moreover, based on clinical observations, patients in the CP group did show severer symptoms than that in the CA group. Therefore, we draw a primary conclusion here that there are more co-infecting pathogens identified in patients infected with *C. psittaci* compared to those infected with *C. abortus*, suggesting that *C. psittaci* infection might cause a potentially higher risk of co-infection, which in turn leads to severer clinical symptoms and a longer disease course, and this observation was also in accordance with the results of previous study (Liang et al., 2022). Interestingly, despite having a lower risk of co-infection, we observed unique *C. albicans* and *S. pneumoniae* co-infections in *C. abortus*-infected patients. Previous studies have found that *C. albicans* and *S. pneumoniae* co-infection was frequently observed in cases of acute mixed polymicrobial infections, and its presence may lead to worsening clinical symptoms (Eichelberger and Cassat, 2021). Although *C. abortus*-caused severe symptoms of infection have not been detected in this study, clinicians should still pay more attention on cases of mixed infections involving *C. abortus* and try to avoid the development of severe symptoms.

The microbiota of the lower respiratory tract contains specific ecological niches of commensal and pathogenic microorganisms, which play an important role in determining the onset and progression of disease (Man et al., 2017; Xia et al., 2022). The homeostatic state of microecological diversity in the lung may be influenced by various biotic or abiotic conditions (Liu et al., 2022a). Clinical studies based on infectious pneumonia have shown that increased colonization by opportunistic pathogens may lead to imbalance in the lower respiratory microecology and trigger symptoms of infection in the lower respiratory tract (De Pascale et al., 2021; Narendrakumar and Ray, 2022). Changes in the microbiota have been reported during lower respiratory tract infections and such changes are strongly associated with the course or prognosis of pneumonia (Hanada et al., 2018). Thus, it is evident that a clearer elucidation of the compositional changes in the lower respiratory microbiome would help to understand the pathogenic process and mechanisms of infectious pneumonia. A previous series of studies revealed the pulmonary microbial compositions by non-targeted pathogen metagenomics or 16S

rRNA sequencing, that the microbiomes of children with bacterial meningitis (Liao et al., 2021), patients with refractory *Mycoplasma pneumoniae* pneumonia (Zhou et al., 2022), patients with tuberculosis (Ding et al., 2021; Xiao et al., 2022), and patients with invasive pulmonary aspergillosis (Hérivaux et al., 2022). Unlike mNGS that can support high-resolution species-level microbial identification, 16S rRNA sequencing can only achieve precise identification and annotation at the bacterial genus level, which can neither distinguish between microbial species of the same genus with very high homology nor provide comprehensive microbial information (bacteria, fungi, viruses, *Mycoplasma*/*Chlamydia*, etc.) (Man et al., 2019). Therefore, in this study, we investigated the characteristics of the pulmonary microbiota of patients with and without *Chlamydia* infection by mNGS. BALF samples are widely used for pathogen detection in infectious diseases of the lower respiratory tract because they carry less oral microbial contamination and can yield accurate and representative lung microbial information (Bingula et al., 2020; Fenn et al., 2022; Jin et al., 2022; Zhang et al., 2022a). In this study, we characterized the lung microbiota using 40 BALF samples from patients with different *Chlamydia* infections and non-*Chlamydia* infections. The results showed that the lower respiratory microecological diversity was significantly lower in patients with *Chlamydia* infection than those with non-*Chlamydia* infection, similar to previous observations in patients with tuberculosis or ventilator-associated pneumonia (Hu et al., 2020; Fenn et al., 2022). Proximally, patients with invasive pulmonary aspergillosis also experienced reduced pulmonary microecological diversity, in particular, a significant reduction in the relative abundance of bacterial genera (Hérivaux et al., 2022). In our study, a significant reduction in the relative abundance of some bacterial species, such as *Aci. lwoffii* and *Act. mediterranea*, was also observed in patients with *Chlamydia* infection. Despite a series of clinical case reports showing that *Aci. lwoffii* can cause peritonitis, liver abscesses and even severe pneumonia (Toyoshima et al., 2010; Singh et al., 2016; Dammak et al., 2022), studies have shown that *Aci. lwoffii* has positive effects. For example, *Aci. lwoffii* can participate in the activation of macrophages in the lung, regulating the shift of M2a and M2c macrophages to M2b macrophages, thereby inhibiting the type 2 response that causes asthma (Kang et al., 2022). On the other hand, although no direct association of *Act. mediterranea* with human disease has been reported, *Actinomyces spp.* have been implicated in different processes of human physiology and pathology. For example, a study based on sequencing of the 16S ribosomal RNA gene V3-V4 region found that, compared to COVID-19 patients with common type, the abundance of commersal bacteria such as *Actinomycetes* was significantly lower in samples from patients with severe disease (Chen et al., 2022). Considering the pathogenic mechanisms, the reduction in microecological diversity may lead to a significant colonization of the lower respiratory tract by the dominant pathogens (Natalini et al., 2022), which in turn may have a negative impact on the infection process. Furthermore, our study found that although reduced pulmonary microecological diversity occurred in both *Chlamydia*-infected and non-*Chlamydia*-infected patients, the microbial species with altered relative abundance in the lower respiratory tract were significantly different in these two patient groups, suggesting that *Chlamydia* infection shapes the characteristics of the pulmonary microbiota in unique disease states.

Although there are few studies on the correlation between clinical parameters and microbiota characteristics in patients with pulmonary infections, we can still find some clues, for example, changes in various clinical indicators in patients with *Pneumocystis* pneumonia are closely associated with changes in the relative abundance of their low respiratory tract microbiota (Zhu et al., 2022b). In the present study, we observed significant differences between patients with and without *Chlamydia* infection in terms of clinical characteristics, key responsible pathogens and representative lower respiratory tract commensal microorganisms. Therefore, we attempted to correlate the above differential data at different levels to further explore the possible mechanisms by which *Chlamydia* and its commensal microorganisms influence the course of pulmonary infections in patients. We found that infection with *C. psittaci* significantly decreased the relative abundance of commensal microorganisms in the lower respiratory tract, such as *Actinomyces mediterraneae*, *Actinomyces johnsonii, Actinomyces ori, Actinomyces timonensis* and *Acinetobacter johnsonii*, and that changes in the relative abundance of these microorganisms in turn showed significant correlations with changes in clinical indicators related to infection or inflammation, for example, *Actinomyces timonensis* was positively correlated with white blood cell count, but negatively correlated with Ca^{+}, while *Actinomyces mediterraneae* positively correlated with both white blood cell count and CREA.

On the other hand, an increase in the relative abundance of *Chlamydia* was accompanied by a significant increase in the levels of white blood cell count, CRP, and K^{+}, while levels of Na^{+} decreased. Thus, the present study provides, to some extent, possible evidence supporting a close correlation among *Chlamydia* infection, altered microecological diversity of the patient's lungs and clinical parameters related to infection or inflammation, which also provides a possible research direction for unveiling the pathogenic mechanisms of pulmonary infections caused by *Chlamydia*.

Indeed, we are aware of the limitations of the present study. First, this study included a limited population of patients with chlamydial pneumonia, especially in the single infection group of *C. abortus*. Because of this, we were unable to obtain sufficient BALF samples to explore the characteristics of the pulmonary microbiome of patients with *C. abortus* infection. Therefore, increased amounts of clinical samples might be required in future studies to draw more accurate conclusions about the microecological diversity of the lower respiratory tract and its clinical relevance in patients with chlamydial pneumonia. Second, although we found that *Chlamydia* infection can remodel the microbiome of the lower respiratory tract, it remains unclear what changes occur in the pulmonary microbiome and their clinical relevance during treatment and even after cure in patients with *Chlamydia* pneumonia. Furthermore, some studies have reported that microbial imbalance can induce systemic metabolic alterations (Devaraj et al., 2013; Nieuwdorp et al., 2014) and host immune responses (Xia et al., 2022). Meanwhile, microorganisms such as *Bacillus* spp., *Actinomyces* spp. and even *Chlamydia psittaci* or *Chlamydia abortus* can directly or indirectly regulate the expression of host pro-inflammatory factors or important disease-related genes such as METTLE3, thus affecting

the physiological and pathological processes of the host (Pan et al., 2017; Chen et al., 2020a; Gómez-García et al., 2022; Wang et al., 2022; Xu et al., 2022; Zhang et al., 2022b). These previous studies will help us to conduct future research on the direction of microbial-host immune interactions in terms of how microbes and their metabolites regulate pro-inflammatory signaling pathways, and how microbes and their metabolites are involved in the regulation of signaling pathways and expression of key targets related to important diseases such as inflammation or tumours.

In summary, we detected and analyzed in this study the responsible pathogen profile, infection patterns, lung microbiota characteristics and their correlation with the clinical characteristics of patients with and without *Chlamydia* infection by mNGS. Our results suggest that *Chlamydia* infection disrupts the dynamic balance of the pulmonary microbiome, which may impact disease severity. The effects of *Chlamydia* infection on the clinical symptoms and the course of the disease in patients warrant further studies. Our findings help to deepen our understanding of the pathogenesis of chlamydial pneumonia, especially mixed *Chlamydia* infections.

Data availability statement

The datasets presented in this study can be found in online repositories. The names of the repository/repositories and accession number(s) can be found below: NCBI, SRA: PRJNA924534.

Ethics statement

The studies involving human participants were reviewed and approved by The Ethics Commitee of the Hunan Provincial People's Hospital, The First Affiliated Hospital of Hunan Normal University. The patients/participants provided their written informed consent to participate in this study.

Author contributions

GX, QH and YL are the primary physicians who provided diagnosis and treatment of the patients. GX, QH, XC, WW, LW and RR collected and analyzed clinical and sequencing data. PD, WG and OW prepared some paragraphs of the manuscript in Chinese. GX, QH, XC, WW, RR and YL wrote the manuscript. All authors contributed to the article and approved the submitted version.

Funding

This work was supported by grants from The Science Foundation for the State Key Laboratory for Infectious Disease Prevention and Control of China (Grant No. 2022SKLID308).

Conflict of interest

Authors XC, WW, OW, LW and RR are employed by MatriDx Biotechnology Co., Ltd.

The remaining authors declare that the research was conducted in the absence of any commercial or financial relationships that could be constructed as a potential conflict of interest.

Publisher's note

Supplementary material

The Supplementary Material for this article can be found online at: https://www.frontiersin.org/articles/10.3389/fcimb.2023.1157540/full#supplementary-material

SUPPLEMENTARY FIGURE 1
Receiver operating characteristic (ROC) curve of mNGS test for *Chlamydia abortus* **(A)** and *Chlamydia psittaci* **(B)** when clinical diagnosis was regarded as the gold standard.

SUPPLEMENTARY FIGURE 2
Spearman's test showed that *Chlamydia psittaci* was significantly positively correlated with WBC **(A)**, CRP **(B)**, K^+ **(C)** and significantly negatively correlated with Na^+ **(D)**, and *Chlamydia abortus* was was significantly positively correlated with WBC **(E)**, CRP **(F)**, K^+ **(G)** and negatively correlated with Na^+ **(H)**.

SUPPLEMENTARY FIGURE 3
Spearman correlation analysis between responsible pathogens with microbial species showed that *Chlamydia psittaci* was negatively correlated with micrbiobial species of *Actinomyces mediterranea* **(A, B)**, *Acinetobacter johnsonii* **(A, C)**, *Actinomyces oris* **(A, D)** and *Actinomyces johnsonii* **(A, E)**.

References

Barati, S., Moori-Bakhtiari, N., Najafabadi, M. G., Momtaz, H., and Shokuhizadeh, L. (2017). The role of zoonotic chlamydial agents in ruminants abortion. *Iran. J. Microbiol.* 9, 288–294.

Bingula, R., Filaire, E., Molnar, I., Delmas, E., Berthon, J.-Y., Vasson, M.-P., et al. (2020). Characterisation of microbiota in saliva, bronchoalveolar lavage fluid, non-malignant, peritumoural and tumour tissue in non-small cell lung cancer patients: a cross-sectional clinical trial. *Respir. Res.* 21, 129. doi: 10.1186/s12931-020-01392-2

Calderwood, C. J., Reeve, B. W., Mann, T., Palmer, Z., Nyawo, G., Mishra, H., et al. (2023). Clinical utility of c-reactive protein-based triage for presumptive pulmonary tuberculosis in south African adults. *J. Infect.* 86, 24–32. doi: 10.1016/j.jinf.2022.10.041

Chen, X., Cao, K., Wei, Y., Qian, Y., Liang, J., Dong, D., et al. (2020b). Metagenomic next-generation sequencing in the diagnosis of severe pneumonias caused by chlamydia psittaci. *Infection* 48, 535–542. doi: 10.1007/s15010-020-01429-0

Chen, Q., Li, Y., Yan, X., Sun, Z., Wang, C., Liu, S., et al. (2020a). Chlamydia psittaci plasmid-encoded CPSIT_P7 elicits inflammatory response in human monocytes *via* TLR4/Mal/MyD88/NF-κB signaling pathway. *Front. Microbiol.* 11. doi: 10.3389/fmicb.2020.578009

Chen, J., Liu, X., Liu, W., Yang, C., Jia, R., Ke, Y., et al. (2022). Comparison of the respiratory tract microbiome in hospitalized COVID-19 patients with different disease severity. *J. Med. Virol.* 94, 5284–5293. doi: 10.1002/jmv.28002

Cheong, H. C., Lee, C. Y. Q., Cheok, Y. Y., Tan, G. M. Y., Looi, C. Y., and Wong, W. F. (2019). Chlamydiaceae: diseases in primary hosts and zoonosis. *Microorganisms* 7, 146. doi: 10.3390/microorganisms7050146

Corsaro, D., and Greub, G. (2006). Pathogenic potential of novel chlamydiae and diagnostic approaches to infections due to these obligate intracellular bacteria. *Clin. Microbiol. Rev.* 19, 283–297. doi: 10.1128/CMR.19.2.283-297.2006

Corsaro, D., and Venditti, D. (2004). Emerging chlamydial infections. *Crit. Rev. Microbiol.* 30, 75–106. doi: 10.1080/10408410490435106

Dammak, N., Chaker, H., Agrebi, I., Toumi, S., Mseddi, F., Kammoun, K., et al. (2022). Acinetobacter lwoffi peritonitis in peritoneal dialysis: two cases report. *Tunis. Med.* 100, 481–484.

Deng, X., Achari, A., Federman, S., Yu, G., Somasekar, S., Bártolo, I., et al. (2020). Metagenomic sequencing with spiked primer enrichment for viral diagnostics and genomic surveillance. *Nat. Microbiol.* 5, 443–454. doi: 10.1038/s41564-019-0637-9

De Pascale, G., De Maio, F., Carelli, S., De Angelis, G., Cacaci, M., Montini, L., et al. (2021). Staphylococcus aureus ventilator-associated pneumonia in patients with COVID-19: clinical features and potential inference with lung dysbiosis. *Crit. Care* 25, 197. doi: 10.1186/s13054-021-03623-4

Devaraj, S., Hemarajata, P., and Versalovic, J. (2013). The human gut microbiome and body metabolism: implications for obesity and diabetes. *Clin. Chem.* 59, 617–628. doi: 10.1373/clinchem.2012.187617

Ding, L., Liu, Y., Wu, X., Wu, M., Luo, X., Ouyang, H., et al. (2021). Pathogen metagenomics reveals distinct lung microbiota signatures between bacteriologically confirmed and negative tuberculosis patients. *Front. Cell. Infect. Microbiol.* 11. doi: 10.3389/fcimb.2021.708827

Duan, Z., Gao, Y., Liu, B., Sun, B., Li, S., Wang, C., et al. (2022). The application value of metagenomic and whole-genome capture next-generation sequencing in the diagnosis and epidemiological analysis of psittacosis. *Front. Cell. Infect. Microbiol.* 12. doi: 10.3389/fcimb.2022.872899

Eichelberger, K. R., and Cassat, J. E. (2021). Metabolic adaptations during staphylococcus aureus and candida albicans Co-infection. *Front. Immunol.* 12. doi: 10.3389/fimmu.2021.797550

Fenn, D., Abdel-Aziz, M. I., van Oort, P. M. P., Brinkman, P., Ahmed, W. M., Felton, T., et al. (2022). Composition and diversity analysis of the lung microbiome in patients with suspected ventilator-associated pneumonia. *Crit. Care* 26, 203. doi: 10.1186/s13054-022-04068-z

Gómez-García, A. P., López-Vidal, Y., Pinto-Cardoso, S., and Aguirre-García, M. M. (2022). Overexpression of proinflammatory cytokines in dental pulp tissue and distinct bacterial microbiota in carious teeth of Mexican individuals. *Front. Cell. Infect. Microbiol.* 12. doi: 10.3389/fcimb.2022.958722

Gu, W., Deng, X., Lee, M., Sucu, Y. D., Arevalo, S., Stryke, D., et al. (2021). Rapid pathogen detection by metagenomic next-generation sequencing of infected body fluids. *Nat. Med.* 27, 115–124. doi: 10.1038/s41591-020-1105-z

Hanada, S., Pirzadeh, M., Carver, K. Y., and Deng, J. C. (2018). Respiratory viral infection-induced microbiome alterations and secondary bacterial pneumonia. *Front. Immunol.* 9. doi: 10.3389/fimmu.2018.02640

Harkinezhad, T., Verminnen, K., Van Droogenbroeck, C., and Vanrompay, D. (2007). Chlamydophila psittaci genotype E/B transmission from African grey parrots to humans. *J. Med. Microbiol.* 56, 1097–1100. doi: 10.1099/jmm.0.47157-0

Hérivaux, A., Willis, J. R., Mercier, T., Lagrou, K., Gonçalves, S. M., Gonçales, R. A., et al. (2022). Lung microbiota predict invasive pulmonary aspergillosis and its outcome in immunocompromised patients. *Thorax* 77, 283–291. doi: 10.1136/thoraxjnl-2020-216179

Hu, Y., Cheng, M., Liu, B., Dong, J., Sun, L., Yang, J., et al. (2020). Metagenomic analysis of the lung microbiome in pulmonary tuberculosis - a pilot study. *Emerg. Microbes Infect.* 9, 1444–1452. doi: 10.1080/22221751.2020.1783188

Imkamp, F., Albini, S., Karbach, M., Kimmich, N., Spinelli, C., Herren, S., et al. (2022). Zoonotic chlamydiae as rare causes of severe pneumonia. *Swiss Med. Wkly.* 152, w30102. doi: 10.4414/SMW.2022.w30102

Jin, X., Li, J., Shao, M., Lv, X., Ji, N., Zhu, Y., et al. (2022). Improving suspected pulmonary infection diagnosis by bronchoalveolar lavage fluid metagenomic next-generation sequencing: a multicenter retrospective study. *Microbiol. Spectr.* 10, e02473–e02421. doi: 10.1128/spectrum.02473-21

Joseph, S. J., Marti, H., Didelot, X., Castillo-Ramirez, S., Read, T. D., and Dean, D. (2015). *Chlamydiaceae* genomics reveals interspecies admixture and the recent evolution of *Chlamydia abortus* infecting lower mammalian species and humans. *Genome Biol. Evol.* 7, 3070–3084. doi: 10.1093/gbe/evv201

Kang, H., Bang, J.-Y., Mo, Y., Shin, J. W., Bae, B., Cho, S.-H., et al. (2022). Effect of acinetobacter lwoffii on the modulation of macrophage activation and asthmatic inflammation. *Clin. Exp. Allergy J. Br. Soc. Allergy Clin. Immunol.* 52, 518–529. doi: 10.1111/cea.14077

Li, N., Cai, Q., Miao, Q., Song, Z., Fang, Y., and Hu, B. (2021a). High-throughput metagenomics for identification of pathogens in the clinical settings. *Small Methods* 5, 2000792. doi: 10.1002/smtd.202000792

Li, N., Li, S., Tan, W., Wang, H., Xu, H., and Wang, D. (2021b). Metagenomic next-generation sequencing in the family outbreak of psittacosis: the first reported family outbreak of psittacosis in China under COVID-19. *Emerg. Microbes Infect.* 10, 1418–1428. doi: 10.1080/22221751.2021.1948358

Li, S., Tong, J., Liu, Y., Shen, W., and Hu, P. (2022). Targeted next generation sequencing is comparable with metagenomic next generation sequencing in adults with pneumonia for pathogenic microorganism detection. *J. Infect.* 85, e127–e129. doi: 10.1016/j.jinf.2022.08.022

Liang, Y., Dong, T., Li, M., Zhang, P., Wei, X., Chen, H., et al. (2022). Clinical diagnosis and etiology of patients with chlamydia psittaci pneumonia based on metagenomic next-generation sequencing. *Front. Cell. Infect. Microbiol.* 12. doi: 10.3389/fcimb.2022.1006117

Liao, H., Zhang, Y., Guo, W., Wang, X., Wang, H., Ye, H., et al. (2021). Characterization of the blood and cerebrospinal fluid microbiome in children with bacterial meningitis and its potential correlation with inflammation. *mSystems* 6, e00049–e00021. doi: 10.1128/mSystems.00049-21

Liu, M., Wen, Y., Ding, H., and Zeng, H. (2022b). Septic shock with chlamydia abortus infection. *Lancet Infect. Dis.* 22, 912. doi: 10.1016/S1473-3099(21)00756-8

Liu, C., Wu, K., Sun, T., Chen, B., Yi, Y., Ren, R., et al. (2022a). Effect of invasive mechanical ventilation on the diversity of the pulmonary microbiota. *Crit. Care* 26, 252. doi: 10.1186/s13054-022-04126-6

Man, W. H., de Steenhuijsen Piters, W. A. A., and Bogaert, D. (2017). The microbiota of the respiratory tract: gatekeeper to respiratory health. *Nat. Rev. Microbiol.* 15, 259–270. doi: 10.1038/nrmicro.2017.14

Man, W. H., van Houten, M. A., Mérelle, M. E., Vlieger, A. M., Chu, M. L. J. N., Jansen, N. J. G., et al. (2019). Bacterial and viral respiratory tract microbiota and host characteristics in children with lower respiratory tract infections: a matched case-control study. *Lancet Respir. Med.* 7, 417–426. doi: 10.1016/S2213-2600(18)30449-1

Marti, H., and Jelocnik, M. (2022). Animal chlamydiae: a concern for human and veterinary medicine. *Pathogens* 11, 364. doi: 10.3390/pathogens11030364

Miao, Q., Ma, Y., Wang, Q., Pan, J., Zhang, Y., Jin, W., et al. (2018). Microbiological diagnostic performance of metagenomic next-generation sequencing when applied to clinical practice. *Clin. Infect. Dis.* 67, S231–S240. doi: 10.1093/cid/ciy693

Narendrakumar, L., and Ray, A. (2022). "Respiratory tract microbiome and pneumonia," in *Progress in molecular biology and translational science* (Elsevier), 97–124. doi: 10.1016/bs.pmbts.2022.07.002

Natalini, J. G., Singh, S., and Segal, L. N. (2022). The dynamic lung microbiome in health and disease. *Nat. Rev. Microbiol.* 21, 222–235 doi: 10.1038/s41579-022-00821-x

Nieuwdorp, M., Gilijamse, P. W., Pai, N., and Kaplan, L. M. (2014). Role of the microbiome in energy regulation and metabolism. *Gastroenterology* 146, 1525–1533. doi: 10.1053/j.gastro.2014.02.008

Ortega, N., Caro, M. R., Gallego, M. C., Murcia-Belmonte, A., Álvarez, D., del Río, L., et al. (2015). Isolation of chlamydia abortus from a laboratory worker diagnosed with atypical pneumonia. *Ir. Vet. J.* 69, 8. doi: 10.1186/s13620-016-0067-4

Pan, Q., Zhang, Q., Chu, J., Pais, R., Liu, S., He, C., et al. (2017). Chlamydia abortus Pmp18.1 induces IL-1β secretion by TLR4 activation through the MyD88, NF-κB, and caspase-1 signaling pathways. *Front. Cell. Infect. Microbiol.* 7. doi: 10.3389/fcimb.2017.00514

Pospischil, A., Thoma, R., Hilbe, M., Grest, P., Zimmermann, D., and Gebbers, J.-O. (2002). Abort beim menschen durch chlamydophila abortus (Chlamydia psittaci serovar 1). *Schweiz. Arch. Für Tierheilkd.* 144, 463–466. doi: 10.1024/0036-7281.144.9.463

Qin, X.-C., Huang, J., Yang, Z., Sun, X., Wang, W., Gong, E., et al. (2022). Severe community-acquired pneumonia caused by *Chlamydia psittaci* genotype E/B strain circulating among geese in lishui city, zhejiang province, China. *Emerg. Microbes Infect.* 11, 2715–2723. doi: 10.1080/22221751.2022.2140606

Sachse, K., Bavoil, P. M., Kaltenboeck, B., Stephens, R. S., Kuo, C.-C., Rosselló-Móra, R., et al. (2015). Emendation of the family chlamydiaceae: proposal of a single genus, chlamydia, to include all currently recognized species. *Syst. Appl. Microbiol.* 38, 99–103. doi: 10.1016/j.syapm.2014.12.004

Shaw, K. A., Szablewski, C. M., Kellner, S., Kornegay, L., Bair, P., Brennan, S., et al. (2019). Psittacosis outbreak among workers at chicken slaughter plants, Virginia and Georgia, USA 2018. *Emerg. Infect. Dis.* 25, 2143–2145. doi: 10.3201/eid2511.190703

Singh, N. P., Sagar, T., Nirmal, K., and Kaur, I. R. (2016). Pyogenic liver abscess caused by acinetobacter lwoffii: a case report. *J. Clin. Diagn. Res. JCDR* 10, DD01–DD02. doi: 10.7860/JCDR/2016/18256.7943

Stephens, R. S., Myers, G., Eppinger, M., and Bavoil, P. M. (2009). Divergence without difference: phylogenetics and taxonomy of *Chlamydia* resolved. *FEMS Immunol. Med. Microbiol.* 55, 115–119. doi: 10.1111/j.1574-695X.2008.00516.x

Tang, J., Tan, W., Luo, L., Xu, H., and Li, N. (2022). Application of metagenomic next-generation sequencing in the diagnosis of pneumonia caused by chlamydia psittaci. *Microbiol. Spectr.* 10, e02384–e02321. doi: 10.1128/spectrum.02384-21

Toyoshima, M., Chida, K., and Suda, T. (2010). Fulminant community-acquired pneumonia probably caused by acinetobacter lwoffii. *Respirol. Carlton Vic* 15, 867–868. doi: 10.1111/j.1440-1843.2010.01780.x

Wallensten, A., Fredlund, H., and Runehagen, A. (2014). Multiple human-to-human transmission from a severe case of psittacosis, Sweden, January–February 2013. *Euro Surveill.* 19(42): 20937. doi: 10.2807/1560-7917.ES2014.19.42.20937

Wang, M., Li, M., Ren, R., Li, L., Chen, E.-Q., Li, W., et al. (2020). International expansion of a novel SARS-CoV-2 mutant. *J. Virol.* 94, e00567–e00520. doi: 10.1128/JVI.00567-20

Wang, C., Li, A., Shi, Q., and Yu, Z. (2021). Metagenomic next-generation sequencing clinches diagnosis of leishmaniasis. *Lancet* 397, 1213. doi: 10.1016/S0140-6736(21)00352-4

Wang, H., Wang, Q., Chen, J., and Chen, C. (2022). Association among the gut microbiome, the serum metabolomic profile and RNA m6A methylation in sepsis-associated encephalopathy. *Front. Genet.* 13. doi: 10.3389/fgene.2022.859727

Wheelhouse, N., and Longbottom, D. (2012). Endemic and emerging chlamydial infections of animals and their zoonotic implications: emerging chlamydial infections. *Transbound Emerg. Dis.* 59, 283–291. doi: 10.1111/j.1865-1682.2011.01274.x

Wu, H., Feng, L., and Fang, S. (2021). Application of metagenomic next-generation sequencing in the diagnosis of severe pneumonia caused by chlamydia psittaci. *BMC Pulm. Med.* 21, 300. doi: 10.1186/s12890-021-01673-6

Xia, X., Chen, J., Cheng, Y., Chen, F., Lu, H., Liu, J., et al. (2022). Comparative analysis of the lung microbiota in patients with respiratory infections, tuberculosis, and lung cancer: a preliminary study. *Front. Cell. Infect. Microbiol.* 12. doi: 10.3389/fcimb.2022.1024867

Xiao, G., Cai, Z., Guo, Q., Ye, T., Tang, Y., Guan, P., et al. (2022). Insights into the unique lung microbiota profile of pulmonary tuberculosis patients using metagenomic next-generation sequencing. *Microbiol. Spectr.* 10, e01901–e01921. doi: 10.1128/spectrum.01901-21

Xu, L., Zhao, Z., Mai, H., Tan, X., Du, Y., and Fang, C. (2022). Clinical and chest computed tomography features associated with severe chlamydia psittaci pneumonia diagnosed by metagenomic next-generation sequencing: a multicenter, retrospective, observational study. *Med. (Baltimore)* 101, e32117. doi: 10.1097/MD.0000000000032117

Yang, M., Yang, D.-H., Yang, H., Ding, S.-Z., Liu, C.-H., Yin, H.-M., et al. (2022). Clinical characteristics of chlamydia psittaci pneumonia infection in central south China. *Infect. Dis. Ther*. doi: 10.1007/s40121-022-00662-4

Yin, Q., Li, Y., Pan, H., Hui, T., Yu, Z., Wu, H., et al. (2022). Atypical pneumonia caused by chlamydia psittaci during the COVID-19 pandemic. *Int. J. Infect. Dis.* 122, 622–627. doi: 10.1016/j.ijid.2022.07.027

Zaręba-Marchewka, K., Szymańska-Czerwińska, M., and Niemczuk, K. (2020). Chlamydiae – what's new? *J. Vet. Res.* 64, 461–467. doi: 10.2478/jvetres-2020-0077

Zhang, J., Gao, L., Zhu, C., Jin, J., Song, C., Dong, H., et al. (2022a). Clinical value of metagenomic next-generation sequencing by illumina and nanopore for the detection of pathogens in bronchoalveolar lavage fluid in suspected community-acquired pneumonia patients. *Front. Cell. Infect. Microbiol.* 12. doi: 10.3389/fcimb.2022.1021320

Zhang, Z., Wang, P., Ma, C., Wang, J., Li, W., Quan, C., et al. (2022b). Host inflammatory response is the major factor in the progression of chlamydia psittaci pneumonia. *Front. Immunol.* 13. doi: 10.3389/fimmu.2022.929213

Zhang, Z., Zhou, H., Cao, H., Ji, J., Zhang, R., Li, W., et al. (2022c). Human-to-human transmission of chlamydia psittaci in China 2020: an epidemiological and aetiological investigation. *Lancet Microbe* 3, e512–e520. doi: 10.1016/S2666-5247(22)00064-7

Zhou, W., Chen, J., Xi, Z., Shi, Y., Wang, L., and Lu, A. (2022). Characteristics of lung microbiota in children's refractory mycoplasma pneumoniae pneumonia coinfected with human adenovirus b. *Can. J. Infect. Dis. Med. Microbiol.* 2022, 1–8. doi: 10.1155/2022/7065890

Zhu, M., Liu, S., Zhao, C., Shi, J., Li, C., Ling, S., et al. (2022b). Alterations in the gut microbiota of AIDS patients with pneumocystis pneumonia and correlations with the lung microbiota. *Front. Cell. Infect. Microbiol.* 12. doi: 10.3389/fcimb.2022.1033427

Zhu, C., Lv, M., Huang, J., Zhang, C., Xie, L., Gao, T., et al. (2022a). Bloodstream infection and pneumonia caused by chlamydia abortus infection in China: a case report. *BMC Infect. Dis.* 22, 181. doi: 10.1186/s12879-022-07158-zAbbreviations

frontiers | Frontiers in Cellular and Infection Microbiology

TYPE Case Report
PUBLISHED 04 July 2023
DOI 10.3389/fcimb.2023.1163846

OPEN ACCESS

EDITED BY
Jeyaprakash Rajendhran,
Madurai Kamaraj University, India

REVIEWED BY
Suchi Goel,
Indian Institute of Science Education and Research, Tirupati, India
Jia Hou,
Fudan University, China

*CORRESPONDENCE
Hui Mao
merrymh@yeah.net

RECEIVED 11 February 2023
ACCEPTED 19 June 2023
PUBLISHED 04 July 2023

CITATION
Du R, Feng Y and Mao H (2023) Case report: Diagnosis of *Talaromyces marneffei* infection in an HIV-negative patient with septic shock and high-titer anti-interferon gamma autoantibodies by metagenomic next-generation sequencing. *Front. Cell. Infect. Microbiol.* 13:1163846. doi: 10.3389/fcimb.2023.1163846

Case report: Diagnosis of *Talaromyces marneffei* infection in an HIV-negative patient with septic shock and high-titer anti-interferon gamma autoantibodies by metagenomic next-generation sequencing

Rao Du[1], Yinhe Feng[2] and Hui Mao[1]*

[1]Department of Pulmonary and Critical Care Medicine, West China Hospital, Sichuan University, Chengdu, Sichuan, [2]Department of Respiratory and Critical Care Medicine, People's Hospital of Deyang City, Affiliated Hospital of Chengdu College of Medicine, Deyang, Sichuan, China

Background: Sepsis is a life-threatening condition caused by a dysfunctional response to infection from the host. Septic shock, a subset of sepsis, caused by *Talaromyces marneffei* infection (talaromycosis) has rarely been reported. Owing to its slow culture and low yield, talaromycosis is typically misdiagnosed in HIV-negative patients as other infections, such as tuberculosis, bacterial pneumonia, and lung cancer, especially in non-endemic regions. Early and accurate diagnosis as well as efficient treatment options are required to improve prognosis.

Method: A 30-year-old HIV-negative Chinese woman from a non-endemic area of *T. marneffei* was initially misdiagnosed with tuberculosis. She had a poor response to anti-tuberculosis treatment. On July 16, 2022, she was admitted to our hospital; the patient developed septic shock on the third day after hospitalization and was ultimately diagnosed with talaromycosis *via* metagenomic next-generation sequencing (mNGS).

Result: The condition of the patient improved after appropriate treatment with amphotericin B. Furthermore, enzyme-linked immunosorbent assay results confirmed that the patient had a high-titer of anti-interferon gamma (IFN-γ) autoantibodies.

Conclusion: HIV-negative individuals with anti-IFN-γ autoantibodies typically have relapsing, refractory, and fatal infections, such as talaromycosis, which is typically misdiagnosed in the initial course of the disease. This can lead to septic shock. Clinicians should be aware that they may encounter HIV-negative patients with *T. marneffei* infection in non-endemic areas. Thus, mNGS is an effective technology for detecting *T. marneffei* infection. Additionally, the detection of anti-IFN-γ autoantibodies in these patients would aid in knowing their susceptibility to fatal infections.

KEYWORDS

***Talaromyces marneffei*, septic shock, HIV-negative patient, anti-interferon gamma autoantibodies, metagenomic next-generation sequencing**

1 Introduction

Sepsis is a major cause of death in critical patients and affects more than 30 million people worldwide annually (Huang et al., 2019). *Talaromyces marneffei* is a dimorphic fungus endemic to Southeast Asia, including Thailand, Vietnam, and China (Hu et al., 2013), that can cause severe infection. Occurrence of *T. marneffei* infections have been predominantly reported in HIV-positive patients. However, an increasing number of cases have recently been reported in non-HIV-infected patients. Culturing *T. marneffei* is essential for its diagnosis. Nonetheless, owing to the critical condition of *T. marneffei* infections, long time required for culturing, and low yield, clinical demands cannot be met (Ning et al., 2018). Accurate pathogen identification is crucial for the early initiation of appropriate antimicrobial treatment and sepsis management (Cecconi et al., 2018a). Thus, new methods are required to identify pathogens quickly and accurately, particularly in patients with septic shock. Herein, we report the case of a 30-year-old HIV-negative Chinese woman presenting recurrent fever, cough, and chest and back pain, who was eventually diagnosed with talarmycosis. She experienced a septic shock and was ultimately diagnosed with talaromycosis *via* metagenomic next-generation sequencing (mNGS) at our hospital. Upon fluid resuscitation and timely antifungal therapy, her condition improved. Through enzyme-linked immunosorbent assay (ELISA), we confirmed that the patient had a high level of anti-interferon gamma (IFN-γ) autoantibodies.

2 Case description

A 30-year-old Chinese female was admitted to our hospital with persistent fever and cough as well as and chest and back pain (lasting for 8 and 3 months, respectively). The maximum body temperature was 39.4°C, the fever was irregular. No other symptoms or signs of organ involvement was present. She had been initially admitted and treated at a local hospital. An examination at the local hospital showed an erythrocyte sedimentation rate of 59 mm/h. The HIV test yielded negative results; the results of the purified protein derivative test and interferon-γ release assay, which used the ELISA, were normal. The results of the acid-fast bacillus (AFB) test, smear, and cultures of the sputum and bronchoalveolar lavage fluid did not reflect any abnormalities. Even after 21-day antibiotic therapy (cefoperazone sulbactam), the patient showed no improvement. Considering her symptoms and the imaging features (Figure 1A) observed in her chest CT, she was prescribed anti-tuberculosis treatment comprising isoniazid, rifampicin, pyrazinamide, and ethambutol on December 15, 2021. She was non-responsive to the medications for up to six months. Meanwhile, her condition deteriorated, and she started experiencing chest and back pain. 2-deoxy-2-[fluorine-18] fluoro-D-glucose positron emission tomography/X-ray computed tomography (^{18}F-FDG PET/CT) indicated that the thoracic (T-6) vertebral body showed low metabolism (Figure 2A), and the left upper lobe of the lung indicated high metabolism (Figure 2B). Chest CT scans showed some osteolytic damage in the vertebrae (Figure 2C). The patient was then transferred to our hospital for further diagnosis and treatment. The patient had no history of unprotected sex or blood transfusions. In addition, there was no history of other personal or hereditary diseases. She also denied traveling to any area except her hometown over the past 10 years. The vital signs during the initial examination were as follows: body temperature, 37.3°C; blood pressure, 107/74 mmHg; heart rate, 107 beats/min; and respiratory rate: 20 breaths/min. Physical examination was normal, except for tenderness at the 5/6 thoracic spine level. Initial laboratory examinations reported the following: white blood cell count, 13.83 × 10^9/L; red blood cell count, 3.03 × 10^{12}/L; hemoglobin level, 77 g/L; neutrophil percentage, 95.4%; lymphocyte percentage, 2.8%; and albumin level, 35.9 g/L. C-reactive protein (112.00 mg/L), procalcitonin (17.70 ng/mL), and interleukin-6 (26.40 pg/mL) levels and erythrocyte sedimentation rate (110.00 mm/h) showed significant elevation. Multiple peripheral blood cultures yielded normal results. The possibility of bacterial infection was first considered based on the clinical characteristics and auxiliary examinations. The physician intravenously administered piperacillin-sulbactam and levofloxacin to the patient. However, the patient was feverish, with a maximum temperature of approximately 39°C.

3 Diagnostic assessment

Owing to the poor response of the patient to antibiotic and anti-tuberculosis therapy, we further searched for potential evidence of any other kind of infection. The β-1,3-D-glucan test, *Aspergillus* galactomannan test, *Cryptococcus* antigen test, *Pneumocystis japonicum* DNA test, repeated purified protein derivative test, interferon-γ release assay (using the ELISPOT assay), and acid-fast staining and sputum culture were all negative for their associated infections. Table 1 presents immunological reports of the patient under investigation. Chest CT scans showed scattered patches, nodules, and ground-glass shadows in the left upper lobe with ill-defined borders and thickening of some interlobular septa (Figure 1B). White blood cell count and C-reactive protein levels continuously increased, while hemoglobin and plasma albumin levels progressively decreased. Upon testing for them, we did not find any of the following antibodies in the patient: antinuclear antibodies, anti-double stranded DNA antibodies, anti-cyclic citrullinated peptide antibody, anti-keratin antibody, anti-neutrophil cytoplasmic antibodies, and HLA-B27. In conclusion, the diagnosis remained unclear. On the fifth day after admission to our hospital, the patient's blood pressure decreased to 70/42 mmHg, and she developed asthenia. A large amount of fluid was administered for rehydration; and the blood pressure was not raised significantly with fluid resuscitation. Vasoactive drug (m-hydroxyamine 50mg) was used to raise blood pressure, her blood pressure then increased to 90/60 mmHg, and we adjusted her treatment to intravenous meropenem and levofloxacin. A

Abbreviations: AFB, acid-fast bacillus; AIGA, anti-IFN-γ autoantibody; ELISA, enzyme-linked immunosorbent assay; IFN-γ, interferon gamma; mNGS, metagenomic next-generation sequencing; OD, optical density.

10.3389/fcimb.2023.1163846

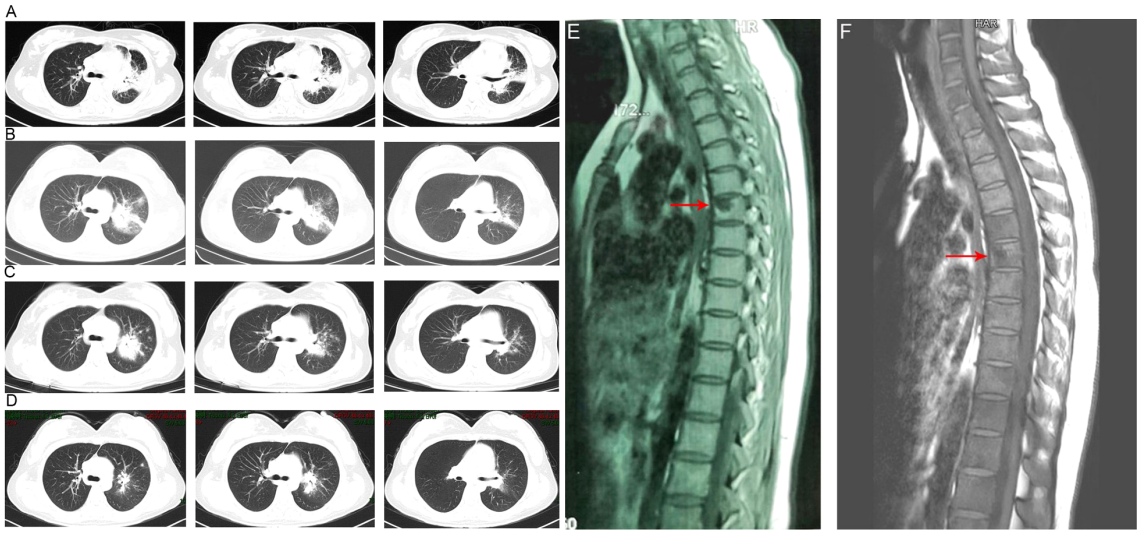

FIGURE 1
Chest computed tomography imaging results of the patient. **(A)** The chest CT before anti-tuberculosis treatment. **(B)** The chest CT before anti-*Talaromyces marneffei* treatment. Chest CT scans showed scattered patches, nodules, and ground-glass shadows in the left upper lobe with ill-defined borders and thickening of some interlobular septa. **(C)** The chest CT after 2 weeks of cumulative treatment with amphotericin B. The lesions in the left upper lobe of the lung were absorbed after two weeks of treatment with amphotericin B. **(D)** Chest CT scans of the local hospital after discharging from hospital 5 months. The lesions in the left upper lobe of the lung had been absorbed furthermore. **(E)**. The MRI of spine showed the lesions of thoracic vertebra. **(F)**. The MRI of spine showed the lesions of thoracic vertebra were absorbed after anti-fungal treatment.

percutaneous lung biopsy was performed after the patient's condition had slightly improved, which showed granulomatous inflammation. Some pathogens were observed in the macrophages and interstitium suspiciously. Hexamine silver (Figure 3A) and periodic acid-Schiff (PAS) staining (Figure 3B) were positive suspiciously, whereas AFB, mucous card red staining, and TB-qPCR were negative. Tumors were not detected. Due to scarce availability of lung tissue and denial by the patient's family, biopsy specimens were not sent for culturing. Eventually, we performed mNGS, which detected 1655 reads of *Talaromyces* spp. (Illumina NextSeq 550, Chengdu, China), including 1160 reads of *T. marneffei*, 435 reads of Human gamma herpesvirus 4 (EBV), no

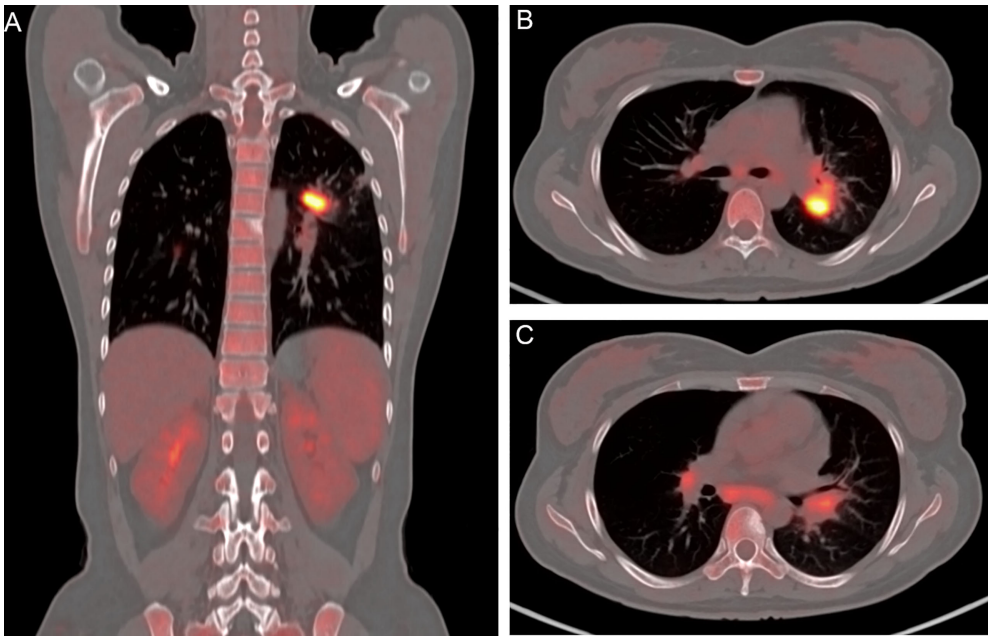

FIGURE 2
Positron emission tomography/X-ray computed tomography imaging results of the patient. **(A)** Thoracic (T-6) vertebral body showing low metabolism. **(B)** Left upper lobe of the lung showing high metabolism. **(C)** Osteolytic damage found in the vertebrae.

10.3389/fcimb.2023.1163846

TABLE 1 Immunological details of the reported patient.

Laboratory investigations	Results		Normal range
	Initial results	Recovery phase	
Lymphocyte subset			
$CD3^+T$ (%)	58.46	71.46	66.90–83.10
$CD4^+T$ (%)	41.95	47.62	33.19–47.85
$CD8^+T$ (%)	15.23	22.00	20.40–34.70
CD4/CD8	2.75	2.16	0.97-2.31
$CD3^+T$-cell (cell/μL)	105.00	2581	941.00–2226.00
$CD4^+T$-cell (cell/μL)	75.00	1720	471.00–1220.00
$CD8^+T$-cell (cell/μL)	27.00	795	303.00–1003.00
B-cell (%)	14.26	13.18	3.91–8.59
NK-cell (%)	24.04	14.22	9.26–23.92
B-cell (cells/μL)	26.00	476	175.00–332.00
NK-cell (cells/μL)	43.00	514	154.00–768.00
Immunoglobulin profile			
IgG (g/L)	21.90	16.9	8.00–15.50
IgA (mg/L)	4030.00	4800	836–2900
IgM (mg/L)	691.00	933	700.00–2200.00
IgE (IU/mL)	184.00	NA	5.00–150.00

NA, not available.

other bacteria and parasite had been detected. The MRI of spine showed the lesions of thoracic vertebra (Figure 1E). Thoracic cone biopsy was also performed to identify any thoracic vertebral lesions. mNGS of bone tissue revealed no pathogens. Pathological examination of the bone and bone marrow showed focal granuloma formation, and AFB smear, silver hexamine, PAS staining, and TB-qPCR results were negative. We could finally confirm *T. marneffei* infection *via* PCR amplification targeting the rDNA internal transcribed spacer region followed by a BLAST sequence comparison (https://blast.ncbi.nlm.nih.gov/Blast.cgi; GenBank accession no. MN700106.1, coverage 97%, identity 99.23%) (Figure 4A). These results showed that the patient was infected with *T. marneffei*. Anti-fungal therapy with amphotericin B was immediately initiated. She was treated with intravenous amphotericin B (0.6–1.0 mg/kg.d, ivgtt) as standard initial therapy. After 3 days of the antifungal treatment, the patient's body temperature normalized, and the talarmycosis-associated clinical symptoms were relieved. ELISA confirmed that the patient had a high titer of anti-IFN-γ autoantibodies (1:2500), the value of optical density (OD) was 1.149, which was much higher than negative control (Figure 4B). During the antifungal treatment, the patient's renal function was impaired. After discussing it with her family, we adjusted the antifungal therapy to liposomal amphotericin B (30 mg/d, ivgtt). Chest CT scans showed that the

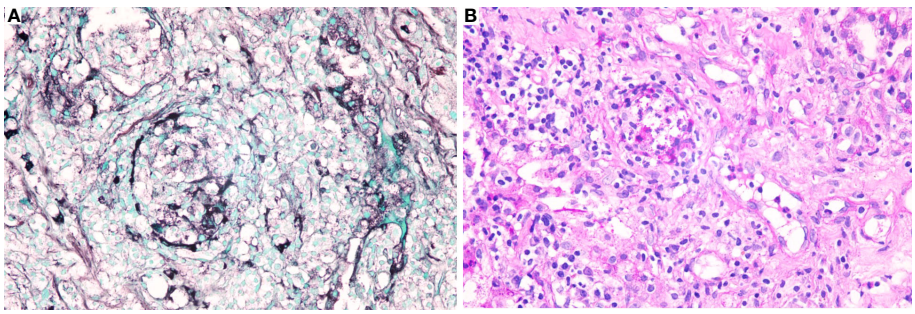

FIGURE 3
Specific stains of lung tissues. **(A)**. Hexamine silver staining of lung tissues was positive suspiciously; **(B)**. Periodic acid-Schiff (PAS) of lung tissues was positive suspiciously.

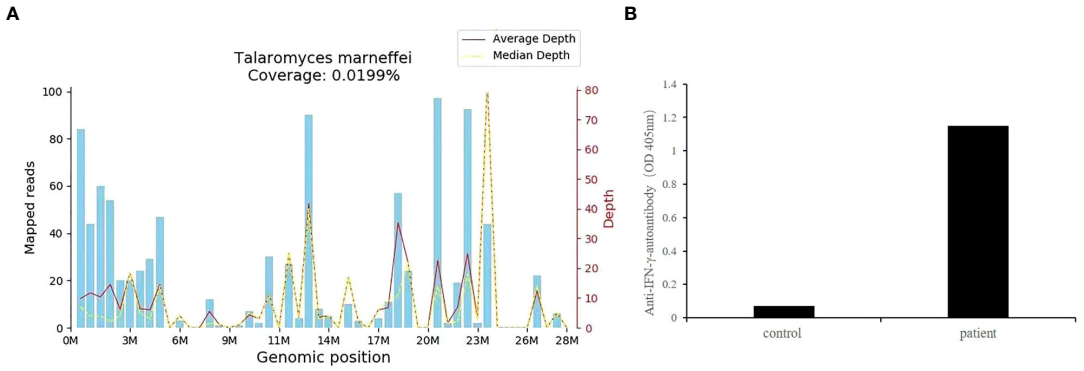

FIGURE 4
(A) *T. marneffei* coverage map. The identified reads were mapped to the *T. marneffei* reference genome (GenBank accession no. MN700106.1). The abscissa is the genome position of the *T. marneffei* reference genome. The left-side scale shows the number of matched mNGS sequences in the alignment. The right-side scale shows the sequencing depth (i.e., the number of times the base pair site has been sequenced). The blue bars show the number of matched mNGS sequences corresponding to various positions in the genome of the fungus. The red line represents the average sequence depth distribution at different positions in the fungal genome. The yellow line represents the median sequence depth distribution at different positions in the fungal genome. M, position in the genome in millions of base pairs (x-axis scale); **(B)** The OD of anti-IFN-γ-autoantibodies of this patient.

lesions in the left upper lobe of the lung had been absorbed after 2 weeks of cumulative treatment with amphotericin B (Figure 1C). The MRI of spine showed the lesions of thoracic vertebra were absorbed (Figure 1F). The main clinical diagnosis was severe *T. marneffei* pneumonia, spine *T. marneffei* infection, septic shock. Oral itraconazole was administered successively. Five months after discharge, there was no recurrence, which was confirmed *via* a telephonic follow-up, and Chest CT scans of the local hospital showed that the lesions in the left upper lobe of the lung had been absorbed furthermore (Figure 1D). A timeline of the patient with relevant data on the episodes and interventions is presented in Figure 5.

4 Discussion

Sepsis is a dysregulated host response to infection and is associated with acute organ dysfunction. Its incidence is high, and it remains a leading cause of death globally (Cecconi et al., 2018a). Depending on the patient's underlying circulatory, cellular, and metabolic abnormalities, the risk of mortality from septic shock can substantially increase (Cecconi et al., 2018a). The most common site of infection that can lead to sepsis in the intensive care unit is the lung (Vincent et al., 2009). In addition to gram-positive and gram-negative bacteria, fungal organisms can also lead to sepsis, and its incidences are rapidly increasing recently (Martin, 2012). Early initiation of appropriate antimicrobial therapy and restoration of tissue perfusion *via* fluid resuscitation are important for the initial management of sepsis.

T. marneffei, previously named *Penicillium marneffei*, is a dimorphic fungus that exhibits mycelial and yeast forms at 25 and 37°C, respectively (Andrianopoulos, 2020). In China, it is primarily distributed in southern regions such as Guangdong and Guangxi (Hu et al., 2013). The first case of infection in humans was reported in 1973 (DiSalvo et al., 1973). However, the mechanism through which *T. marneffei* infects humans remains unknown.

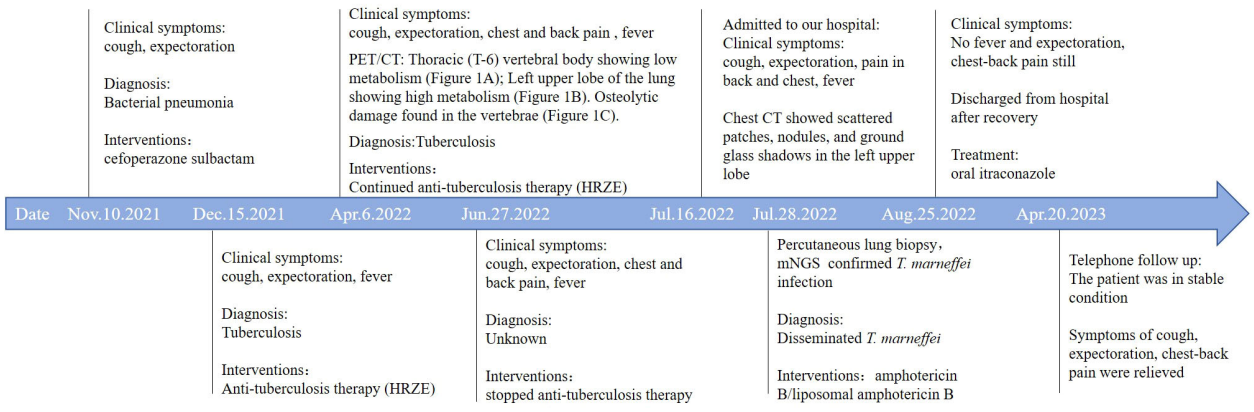

FIGURE 5
Timeline of the patient with relevant data on the episodes and interventions.

Reportedly, some subspecies of bamboo rats are mammalian reservoirs of this pathogen; nonetheless, the source of human infection is unclear (Deng et al., 1988). A key risk factor is contact with the endemic region of *T. marneffei* (Zeng et al., 2015). The longest incubation period is 10 years; however, most patients present their first symptoms in 6–12 months after leaving the endemic areas (Zheng et al., 2015). Nevertheless, our patient was from Guizhou and resided there all her life. She denied traveling to any talaromycosis-endemic area in the past 10 years. Therefore, we could not trace the site of infection in her case.

T. marneffei infection is typically found in patients with acquired immunodeficiency syndrome (AIDS), and it is the third most common opportunistic infection following tuberculosis and cryptococcosis in patients with AIDS, in tropical Southeast Asia (Vanittanakom et al., 2006). However, an increasing number of cases have been reported in HIV-negative patients with primary or secondary immunodeficiency, such as inborn errors of immunity (IEIs), autoimmune diseases, cancer, undergoing immunosuppressive therapy, and anti-IFN-γ autoantibody syndrome (Chan et al., 2016). IEIs includes STAT1 gain-of-function, IL-2 receptor common gamma chain deficiency, adenosine deaminase deficiency, CD40 ligand deficiency, and STAT3 deficiency, CARD9 deficiency, IFN-γ receptor 1 deficiency, RelB deficiency, and NFKB2 deficiency (Liu et al., 2022; Wang et al., 2022).

Anti-IFN-γ autoantibody (AIGA) syndrome is an emerging adult-onset immunodeficiency syndrome that was first described in 2004, characterized by high anti-IFN-γ autoantibody levels (Höflich et al., 2004). This association was first described in eight Chinese patients (Chan et al., 2016) and is primarily related to genetic variation (Guo et al., 2020). HLA class II alleles DRB1*16:02–DQB1*05:02 and HLA-DRB1*15:02–DQB1*05:01 are strongly associated with it (Guo et al., 2020). These patients are susceptible to infection by intracellular pathogens including *T. marneffei*, non-tuberculosis mycobacteria, and *Cryptococcus neoformans*. This syndrome has a considerably high mortality rate of 32%, and patients die at a median time of 25 months after diagnosis (Wipasa et al., 2018). AIGA-positive patients have a predisposition to the occurrence of multiple opportunistic infections (Shih et al., 2021) and disseminated infections and poor prognosis after standard antifungal treatment (Chen et al., 2021). Studies have revealed that 20.41% of HIV-negative adult patients with *T. marneffei* infection was AIGA-positive (Qiu et al., 2021). Compared to AIGA-negative patients, AIGA-positive patients with *T. marneffei* infection have fewer complications with underlying respiratory diseases but are more likely to be associated with the bone (Chen et al., 2021). Anti-IFN-γ autoantibodies significantly suppress the $CD4^+$ Th1-cell immune response, leading to the failure of pathogen clearance by the host. Even with a normal lymphocyte count, the activation and proliferation of $CD4^+$ T cells are impaired (Hu et al., 2021). Similarly, patients with autoantibody titers >2000 ng/mL showed strong inhibition of their $CD8^+$ T cells (Chen et al., 2022). The titer significantly increases as the condition worsens during the disease course (Qiu et al., 2022). In our case, the titer of IFN-γ autoantibodies was 2500 ng/mL, and the counts of CD4 T and CD8 T cells were 75 and 27 cells/μL, respectively, which are considerably lower than the normal range, indicating strong inhibition of $CD8^+$ T cells.

According to the immunoglobulin profile, the patient's IgG, IgA, IgE increased, while IgM decreased slightly, which was consistent with the study of Chen et al. (Chen et al., 2020). From the literature review, we can see that the immunoglobulin profile was not the same, some patients showed high IgM, some showed low IgM (You et al., 2021; Li et al., 2023). The reported trend of IgA, IgE and IgM in HIV-Negative patients with disseminated *Talaromyces marneffei* infection with high-titer anti-interferon gamma autoantibodies is not completely consistent, indicating that patients are heterogeneous. Keragala et al. guessed the initial low CD4, CD3, CD8 counts would have been due ongoing sepsis and after the infection is controlled the counts improved (Keragala et al., 2020). On the recovery stage, the blood routine data showed the neutrophil percentage, 53.6%; lymphocyte percentage, 36.0%. NK cells, B cells, CD3, CD4 and CD8 T cells were 514 cell/μL, 476 cell/μL, 2581 cell/μL, 1720 cell/μL, and 795 cell/μL respectively. The IgG was 16.90g/L, IgM and IgA was 933.00mg/L,4800.0mg/L respectively (Table 1). Based on those, we suspected the changes of the immune function was secondary to the severe infection or due to the anti- IFN-γ-autoantibodies. The immune deficiency mechanism of anti-IFN-γ autoantibodies may include inhibition of the CD4 + T cells' IFN-γ/pSTAT-1/Th1 pathway, ultimately leading to a severely compromised Th1 response. (Qiu et al., 2022). Regrettably, due to the refuse of patients' family, the patient didn't do genetic testing, we cannot know if the patient had STAT1 gain-of-function (GOF) mutations.

The clinical manifestations of *T. marneffei* infection are nonspecific and diverse and can present with fever, cough, expectoration, weight loss, skin lesions, generalized lymphadenopathy, and hepatomegaly (Zhou et al., 2014), which are generally atypical and may be confounded by the manifestations of other infectious diseases, such as tuberculosis. Both can cause fever, cough, expectoration, and bone damage. Owing to the smear staining microscopy, low positive rates of clinical samples, and long culture times, no single method can conclusively diagnose all tuberculosis cases (Jain et al., 2020). Thus, clinical examination, imaging, AFB smear, tuberculosis culture, molecular methods, histologic findings, and therapeutic approaches are needed. Purified protein derivative tests and TB-interferon-γ release assays can lead to the identification of false-negative patients with insufficient numbers or poor T-cell function (Diel et al., 2012). In our patient, the $CD4^+$ T cells count was 75 cells/μL, and she was immunodeficient. That could be one reason why she was infected with *M. tuberculosis* and/or *T. marneffei*. Considering the chest CT manifestations and bone destruction, tuberculosis could not be ruled out as there was no evidence of other pathogens. However, the symptoms did not resolve after 6 months of anti-tuberculosis treatment, indicating the need for improved pathogen diagnostic technologies.

The diagnosis of *T. marneffei* has traditionally been confirmed by isolating the fungus from clinical specimens. Owing to the prolonged incubation time, prompt diagnosis is challenging. Although several antigen and antibody detection assays have recently been developed, they do not meet clinical demands (Wong et al., 2001). mNGS is a newly developed nucleic acid

detection technology that can assist in the detection of infectious pathogens, particularly fastidious bacteria, slow-growing bacteria, and pathogens that cannot be isolated and cultured (Gu et al., 2019). The target-free detection strategy makes relying on any other prior test results unnecessary, which is more advantageous than broad-spectrum PCR. In terms of the time required to obtain results, using mNGS is considerably faster than culturing. For pathogens that cannot be cultured routinely, mNGS can quickly detect them in samples within 30 h (Zuo et al., 2023). In our case, the results of the routine pathogen detections were negative. When the pathologist could not diagnose the pathogen by microscopic morphology alone, the physician obtained a positive result for the presence of *T. marneffei* within 48 h using mNGS. After treatment with amphotericin B and amphotericin B liposomes, the patient's lung and thoracic cone lesions diminished, and she was discharged. This reflects the advantages of mNGS in the detection of rare pathogens.

Amphotericin B is the first-line treatment for talaromycosis-affected patients; however, itraconazole and voriconazole are also effective (He et al., 2021). Considering the patient's economic conditions, oral itraconazole (cheaper than voriconazole) was administered successively after 2 weeks of cumulative treatment with amphotericin B. The results were satisfactory.

In conclusion, for patients with recurrent fever, lung mass, and bone damage, in addition to tuberculosis and tumors, the possibility of *T. marneffei* infection and other rare pathogenic infections should be considered. mNGS could be an effective technology for *T. marneffei* detection in cases with septic shock. This case report aims to raise the awareness of physicians regarding the possibility of talaromycosis in non-endemic areas and HIV-negative patients. Anti-IFN-γ autoantibodies should be tested, particularly in patients with curtained recurrent infections like talaromycosis. Awareness of this disease among HIV-negative patients may promote prompt diagnosis, timely treatment, and better health outcomes.

Data availability statement

The data presented in the study are deposited in the online repository, the names of the repository/repositories and accession number(s) can be found below: https://www.ncbi.nlm.nih.gov/ and PRJNA987339.

Ethics statement

Ethical review and approval was not required for the study on human participants in accordance with the local legislation and institutional requirements. The patients/participants provided their written informed consent to participate in this study. Written informed consent was obtained from the individual(s) for the publication of any potentially identifiable images or data included in this article.

Author contributions

RD and YF collected and interpreted the data. RD drafted the manuscript. HM revised and edited the manuscript. All authors contributed to the article and approved the submitted version.

Funding

This work was supported by the Sichuan Science and Technology Project (Grant No. 2022YFS0105).

Acknowledgments

We would like to thank Vision Medicals Co., Ltd. for providing the mNGS methods and helping in interpreting the mNGS results.

Conflict of interest

The authors declare that the research was conducted in the absence of any commercial or financial relationships that could be construed as a potential conflict of interest.

Publisher's note

References

Andrianopoulos, A. (2020). Laboratory maintenance and growth of *Talaromyces marneffei*. *Curr. Protoc. Microbiol.* 56 (1), e97. doi: 10.1002/cpmc.97

Cecconi, M., Evans, L., Levy, M., and Rhodes, A. (2018a). Sepsis and septic shock. *Lancet* 392 (10141), 75–87. doi: 10.1016/S0140-6736(18)30696-2

Chan, J. F. W., Lau, S. K. P., Yuen, K. Y., and Woo, P. C. Y. (2016). *Talaromyces (Penicillium) marneffei* infection in non-HIV-infected patients. *Emerg Microbes Infections* 5 (3), e19. doi: 10.1038/emi.2016.18

Chen, Z. M., Li, Z. T., Li, S. Q., Guan, W. J., Qiu, Y., Lei, Z. Y., et al. (2021). Clinical findings of *Talaromyces marneffei* infection among patients with anti-interferon-γ immunodeficiency: a prospective cohort study. *BMC Infect. Dis.* 21 (1), 587. doi: 10.1186/s12879-021-06255-9

Chen, X., Xu, Q., Li, X., Wang, L., Yang, L., Chen, Z., et al. (2020). Molecular and phenotypic characterization of nine patients with STAT1 GOF mutations in China. *J. Clin. Immunol.* 40 (1), 82–95. doi: 10.1007/s10875-019-00688-3

Chen, Z. M., Yang, X. Y., Li, Z. T., Guan, W. J., Qiu, Y., Li, S. Q., et al. (2022). Anti-interferon-γ autoantibodies impair T-lymphocyte responses in patients with infections. *Infection Drug Resistance* 15, 3381–3393. doi: 10.2147/IDR.S364388

Deng, Z., Ribas, J. L., Gibson, D. W., and Connor, D. H. (1988). Infections caused by *Penicillium marneffei* in China and southeast Asia: review of eighteen published cases and report of four more Chinese cases. *Rev. Infect. Dis.* 10 (3), 640–652. doi: 10.1093/clinids/10.3.640

Diel, R., Loddenkemper, R., and Nienhaus, A. (2012). Predictive value of interferon-γ release assays and tuberculin skin testing for progression from latent TB infection to disease state: a meta-analysis. *Chest* 142 (1), 63–75. doi: 10.1378/chest.11-3157

DiSalvo, A. F., Fickling, A. M., and Ajello, L. (1973). Infection caused by *Penicillium marneffei*: description of first natural infection in man. *Am. J. Clin. Pathol.* 60 (2), 259–263. doi: 10.1093/ajcp/60.2.259

Gu, W., Miller, S., and Chiu, C. Y. (2019). Clinical metagenomic next-generation sequencing for pathogen detection. *Annu. Rev. Pathol.* 14, 319–338. doi: 10.1146/annurev-pathmechdis-012418-012751

Guo, J., Ning, X. Q., Ding, J. Y., Zheng, Y. Q., Shi, N. N., Wu, F. Y., et al. (2020). Anti-IFN-γ autoantibodies underlie disseminated *Talaromyces marneffei* infections. *J. Exp. Med.* 217 (12), e20190502. doi: 10.1084/jem.20190502

He, L., Mei, X., Lu, S., Ma, J., Hu, Y., Mo, D., et al. (2021). *Talaromyces marneffei* infection in non-HIV-infected patients in mainland China. *Mycoses* 64 (10), 1170–1176. doi: 10.1111/myc.13295

Höflich, C., Sabat, R., Rosseau, S., Temmesfeld, B., Slevogt, H., Döcke, W. D., et al. (2004). Naturally occurring anti-IFN-gamma autoantibody and severe infections with *Mycobacterium cheloneae* and *Burkholderia cocovenenans*. *Blood* 103 (2), 673–675. doi: 10.1182/blood-2003-04-1065

Hu, F., Liu, S., Liu, Y., Li, X., Pang, R., and Wang, F. (2021). The decreased number and function of lymphocytes is associated with *Penicillium marneffei* infection in HIV-negative patients. *J. MicrobioL Immunol Infection = Wei Mian Yu Gan Ran Za Zhi* 54 (3), 457–465. doi: 10.1016/j.jmii.2020.02.007

Hu, Y., Zhang, J., Li, X., Yang, Y., Zhang, Y., Ma, J., et al. (2013). *Penicillium marneffei* infection: an emerging disease in mainland China. *Mycopathologia* 175 (1-2), 57–67. doi: 10.1007/s11046-012-9577-0

Huang, M., Cai, S., and Su, J. (2019). The pathogenesis of sepsis and potential therapeutic targets. *Int. J. Mol. Sci.* 20 (21), 5376. doi: 10.3390/ijms20215376

Jain, A. K., Rajasekaran, S., Jaggi, K. R., and Myneedu, V. P. (2020). Tuberculosis of the spine. *J. Bone Joint Surgery. Am. Volume* 102 (7), 617–628. doi: 10.2106/JBJS.19.00001

Keragala, B., Gunasekera, C. N., Yesudian, P. D., Guruge, C., Dissanayaka, B. S., Liyanagama, D. P., et al. (2020). Disseminated *Mycobacterium simiae* infection in a patient with adult-onset immunodeficiency due to anti-interferon-gamma antibodies - a case report. *BMC Infect. Dis.* 20 (1), 258. doi: 10.1186/s12879-020-04984-x

Li, Z., Yang, J., Qiu, Y., Yang, F., Tang, M., Li, S., et al. (2023). Disseminated *Talaromyces marneffei* infection with STAT3-Hyper-IgE syndrome: a case series and literature review. *Open Forum Infect. Dis.* 10 (4). doi: 10.1093/ofid/ofac614

Liu, L., Sun, B., Ying, W., Liu, D., Wang, Y., Sun, J., et al. (2022). Rapid diagnosis of *Talaromyces marneffei* infection by metagenomic next-generation sequencing technology in a Chinese cohort of inborn errors of immunity. *Front. Cell Infect. Microbiol.* 12. doi: 10.3389/fcimb.2022.987692

Martin, G. S. (2012). Sepsis, severe sepsis and septic shock: changes in incidence, pathogens and outcomes. *Expert Rev. Anti-Infective Ther.* 10 (6), 701–706. doi: 10.1586/eri.12.50

Ning, C., Lai, J., Wei, W., Zhou, B., Huang, J., Jiang, J., et al. (2018). Accuracy of rapid diagnosis of *Talaromyces marneffei*: a systematic review and meta-analysis. *PloS One* 13 (4), e0195569. doi: 10.1371/journal.pone.0195569

Qiu, Y., Feng, X., Zeng, W., Zhang, H., and Zhang, J. (2021). Immunodeficiency disease spectrum in HIV-negative individuals with talaromycosis. *J. Clin. Immunol.* 41 (1), 221–223. doi: 10.1007/s10875-020-00869-5

Qiu, Y., Pan, M., Yang, Z., Zeng, W., Zhang, H., Li, Z., et al. (2022). *Talaromyces marneffei* and mycobacterium tuberculosis co-infection in a patient with high titer anti-interferon-γ autoantibodies: a case report. *BMC Infect. Dis.* 22 (1), 98. doi: 10.1186/s12879-021-07015-5

Shih, H. P., Ding, J. Y., Yeh, C. F., Chi, C. Y., and Ku, C. L. (2021). Anti-interferon-γ autoantibody-associated immunodeficiency. *Curr. Opin. Immunol.* 72, 206–214. doi: 10.1016/j.coi.2021.05.007

Vanittanakom, N., Cooper, C. R., Fisher, M. C., and Sirisanthana, T. (2006). *Penicillium marneffei* infection and recent advances in the epidemiology and molecular biology aspects. *Clin. Microbiol. Rev.* 19 (1), 95–110. doi: 10.1128/CMR.19.1.95-110.2006

Vincent, J. L., Rello, J., Marshall, J., Silva, E., Anzueto, A., Martin, C. D., et al. (2009). International study of the prevalence and outcomes of infection in intensive care units. *JAMA* 302 (21), 2323–2329. doi: 10.1001/jama.2009.1754

Wang, L., Luo, Y., Li, X., Li, Y., Xia, Y., He, T., et al. (2022). *Talaromyces marneffei* infections in 8 Chinese children with inborn errors of immunity. *Mycopathologia* 187 (5-6), 455–467. doi: 10.1007/s11046-022-00659-0

Wipasa, J., Chaiwarith, R., Chawansuntati, K., Praparattanapan, J., Rattanathammethee, K., and Supparatpinyo, K. (2018). Characterization of anti-interferon-γ antibodies in HIV-negative immunodeficient patients infected with unusual intracellular microorganisms. *Exp. Biol. Med.* 243 (7), 621–626. doi: 10.1177/1535370218764086

Wong, S. S., Wong, K. H., Hui, W. T., Lee, S. S., Lo, J. Y., Cao, L., et al. (2001). Differences in clinical and laboratory diagnostic characteristics of *penicilliosis marneffei* in human immunodeficiency virus (HIV)- and non-HIV-infected patients. *J. Clin. Microbiol.* 39 (12), 4535–4540. doi: 10.1128/JCM.39.12.4535-4540.2001

You, C. Y., Hu, F., Lu, S. W., Pi, D. D., Xu, F., Liu, C. J., et al. (2021). *Talaromyces marneffei* infection in an HIV-negative child with a CARD9 mutation in China: a case report and review of the literature. *Mycopathologia* 186 (4), 553–561. doi: 10.1007/s11046-021-00576-8

Zeng, W., Qiu, Y., Lu, D., Zhang, J., Zhong, X., and Liu, G. (2015). A retrospective analysis of 7 human immunodeficiency virus-negative infants infected by *Penicillium marneffei*. *Medicine* 94 (34), e1439. doi: 10.1097/MD.0000000000001439

Zheng, J., Gui, X., Cao, Q., Yang, R., Yan, Y., Deng, L., et al. (2015). A clinical study of acquired immunodeficiency syndrome associated *Penicillium marneffei* infection from a non-endemic area in China. *PloS One* 10 (6), e0130376. doi: 10.1371/journal.pone.0130376

Zhou, F., Bi, X., Zou, X., Xu, Z., and Zhang, T. (2014). Retrospective analysis of 15 cases of *Penicilliosis marneffei* in a southern China hospital. *Mycopathologia* 177 (5-6), 271–279. doi: 10.1007/s11046-014-9737-5

Zuo, Y. H., Wu, Y. X., Hu, W. P., Chen, Y., Li, Y. P., Song, Z. J., et al. (2023). The clinical impact of metagenomic next-generation sequencing (mNGS) test in hospitalized patients with suspected sepsis: a multicenter prospective study. *Diagnostics* 13 (2), 323. doi: 10.3390/diagnostics13020323

frontiers | Frontiers in Cellular and Infection Microbiology

TYPE Original Research
PUBLISHED 31 July 2023
DOI 10.3389/fcimb.2023.1184245

OPEN ACCESS

EDITED BY
Costas C. Papagiannitsis,
University of Thessaly, Greece

REVIEWED BY
Ganesh Babu Malli Mohan,
SASTRA University, India
Jie Liu,
Zunyi Medical University, China

*CORRESPONDENCE
Yubao Wang
yubaowang2020@hotmail.com
Jing Feng
zyyhxkfj@126.com

†These authors have contributed equally to this work

RECEIVED 11 March 2023
ACCEPTED 11 July 2023
PUBLISHED 31 July 2023

CITATION
Zhao Z, Chen X, Wang Y and Feng J (2023) Comparison of quality/quantity mNGS and usual mNGS for pathogen detection in suspected pulmonary infections. *Front. Cell. Infect. Microbiol.* 13:1184245. doi: 10.3389/fcimb.2023.1184245

Comparison of quality/quantity mNGS and usual mNGS for pathogen detection in suspected pulmonary infections

Zhan Zhao[1†], Xuefen Chen[1,2†], Yubao Wang[1*] and Jing Feng[1*]

[1]Respiratory Department, Tianjin Medical University General Hospital, Tianjin, China, [2]Department of Respiratory Medicine, Characteristic Medical Center of the Chinese People's Armed Police Force, Tianjin, China

Improved metagenomic next-generation sequencing (mNGS), for example, quality/quantity mNGS (QmNGS), is being used in the diagnosis of pulmonary pathogens. There are differences between QmNGS and the usual mNGS (UmNGS), but reports that compare their detection performances are rare. In this prospective study of patients enrolled between December 2021 and March 2022, the bronchoalveolar lavage fluid of thirty-six patients with suspected pulmonary infection was assessed using UmNGS and QmNGS. The sensitivity of QmNGS was similar to that of UmNGS. The specificity of QmNGS was higher than that of UmNGS; however, the difference was not statistically significant. The positive likelihood ratios (+LR) of QmNGS and UmNGS were 3.956 and 1.394, respectively, and the negative likelihood ratios (-LR) were 0.342 and 0.527, respectively. For the co-detection of pathogens, the depth and coverage of the QmNGS sequencing were lower than those of UmNGS, while for the detection of pathogens isolated from patients with pulmonary infection, the concordance rate was 77.2%. In the eleven patients with nonpulmonary infection, only viruses were detected using QmNGS, while UmNGS detected not only viruses but also bacteria and fungi. This study provides a basis for the selection of mNGS for the diagnosis of suspected pulmonary infection.

KEYWORDS

usual metagenomic next-generation sequencing, quality/quantity metagenomic next-generation sequencing, pulmonary infection, pathogen detection, pulmonary pathogens

1 Introduction

A pulmonary infection is a common respiratory disease that remains prevalent worldwide, with substantial mortality and morbidity (Wunderink and Waterer, 2017). It is estimated that approximately 5.6 million people acquire pulmonary infections each year in USA. The annual cost associated with pulmonary infections is approximately over $12 billion (Colice et al., 2004). This not only brings a burden on the economy, but also puts a

tremendous stress on public health. Numerous pathogens can cause pneumonia, making diagnosis challenging. Furthermore, early and effective antibacterial therapy is crucial for the prognosis of immunocompromised individuals and older individuals susceptible to pneumonia. Therefore, the clinical requirements for a rapid and accurate etiological diagnosis to improve patient outcomes are increasing. Typically, cultures, which are the gold standard for microbial identification, have long turnaround times, low sensitivity, and are limited to certain pathogens. Culture-independent pathogen detection methods such as immunological assays and nucleic acid amplification tests target only a fraction of the currently known pathogens (Murdoch et al., 2012). This often leads to delay clinical treatment. Metagenomic next-generation sequencing (mNGS) as a promising culture-independent technique demonstrates advantages such as rapidity for the pathogenic diagnosis of pulmonary infections.

mNGS, which combines high-throughput sequencing and bioinformatic analysis to detect microbial species and their abundances based on the BLAST database, is an unbiased detection method with high efficiency and a short turnaround time. mNGS shows good performance for pathogen diagnosis in both single and mixed pulmonary infections (Zhao et al., 2021). Although this detection technology has obvious advantages, it also faces significant challenges regarding sensitivity, interpretation, turnaround time, and laboratory workflow. In a pulmonary infection, since the content of human-derived DNA varies greatly in different samples and the diagnostic sensitivity of mNGS is affected by the content of human-derived DNA (Schlaberg et al., 2017), the ability to distinguish true pathogens from respiratory colonization and environmental contamination is hindered (Chen et al., 2020). Thus, it is important to know how to balance the human-derived DNA depletion techniques that are currently used to increase the sensitivity of mNGS, as using these techniques can lead to nonspecific clearance of pathogens (Charalampous et al., 2019). The process of an mNGS experiment is complex, and it is relatively difficult to verify the entire workflow and establish a stable quality control system. In addition, different sequencing platforms and bioinformatics pipelines applied by mNGS may affect the accuracy and reproducibility of the detection results. Currently, a few studies have attempted to compensate for the shortcomings of the current mNGS technology, among which quality/quantity mNGS (QmNGS) is the most representative. QmNGS is based on using selective human-derived DNA, a polymerase chain reaction (PCR)-free library preparation, and the spiking of constant concentrations of a nucleic acid internal control (IC) into all specimens to detect microbial abundance and cellularity. A wet laboratory workflow of QmNGS has been performed using an automated device (NGSmaster) (Luan et al., 2021). Although QmNGS claims have been said to reduce false negatives, its efficacy in the diagnosis of clinical pulmonary infection pathogens is unknown.

In this study, our aim was to compare the differences in etiological diagnoses such as diagnostic accuracy, concordance rate and sequencing depth and coverage for the co-detection of pathogens between QmNGS and usual mNGS (UmNGS). UmNGS is currently the most common mNGS technology. It is based on indiscriminate preparation of human-derived DNA and PCR-based library preparation. By comparing the effects of the different mNGS detection methods on the detection of clinical pulmonary infection pathogens, we further aimed to provide a more theoretical basis for clinical selection.

2 Materials and methods

2.1 Patients and specimen collection

Our prospective study included patients with a high suspicion of pulmonary infections who were admitted to the Tianjin Medical University General Hospital between November 2021 and March 2022. Patients were excluded based on poor coagulation, the presence of cardiac disease not allowing bronchoscopy, or refusal to participate in the study, and thirty-six patients were ultimately enrolled in this study. CT scans, sputum smear microscopy and culture, galactomannan test, (1,3)-β-D-glucan test, and other etiological tests according to their condition were performed on all patients. Furthermore, all patients underwent bronchoscopy and BALF was collected from lung lesions. A portion of the BALF was used for pathogen identification using cultures, smears, and Xpert. The remaining BALF was divided equally into two aliquots, each containing 4 ml, and stored at 4°C for mNGS detection. The demographic characteristics and related underlying diseases of the patients were collected from their medical records. Three or more professional physicians comprehensively determined the final clinical diagnosis of the patient according to the patient's clinical symptoms, signs, imaging, microbiology, and etiology results. The study was in accordance with the Ethics Review Board requirements of the Tianjin Medical University General Hospital (ChiCTR1900023727). Informed consent was obtained prior to the start of the examinations.

2.2 UmNGS and analysis

The mNGS detection process includes an experimental operation and a bioinformatic analysis. The experimental procedure includes sample pretreatment, nucleic acid extraction, library preparation, and sequencing. Data quality control of bioinformatics analysis, human sequence removal, and alignment and identification of microbial species. First, we collected BALF (0.5 ml) and added 1 g of glass beads (0.5 mm) to a 1.5 ml tube. We performed the DNA extraction according to the manufacturer's instructions for the TIANAMP Micro DNA Kit from TIANGEN BIOTECH (Beijing, China). The extracted nucleic acids were fragmented using the NextEra XT DNA Library Prep Kit (Illumina, San Diego, CA, United States) (Gu et al., 2019), followed by an end modification and primer addition. Finally, a library that met the sequencing requirements was obtained using PCR amplification. High-throughput sequencing was performed on the Illumina NextSeq sequencing platform. After obtaining the DNA sequence of the sample, quality control was performed, including adaper-trimming, low-complexity read filtering, and the

removal of substandard reads. The remaining reads were compared to GRCh38, which was the human genome reference sequence, and the human-related reads were removed using Bowtie2 (BWA). The data were then classified into bacteria, fungi, viruses, and parasites using microbial reference genomes (ftp://ftp.ncbi.nlm.nih.gov/genomes/). From the identified microorganisms, colonization bacteria and sample-contaminating bacteria were excluded based on the baseline detection and background microorganism database (Chiu and Miller, 2019).

2.2.1 UmNGS reporting criteria

The standard of interpretation of pathogen pathogenicity for the UmNGS report is: the threshold is generally at or above 8 RPM (reads per million), and for intracellular bacteria, a threshold of ≥1 RPM was considered meaningful.

2.3 QmNGS and analysis

2.3.1 IC spiked into all specimens

Double-stranded DNA was synthesized using PCR and shared no significant homology to genomes of any known organisms, serving as a spiked-in IC (spike below instead), according to previous nucleotide sequences (Zhang et al., 2022; Zhou et al., 2022). The spikes were amplified and then mixed with magnetic beads for purification (Matridx, Cat# MD012). The amplification concentration was measured using a Qubit 4 fluorometer (Thermo Fisher Scientific). For the extraction of nucleic acids, spikes (0.02 ng/μl) were included in each sample.

2.3.2 PCR-free library preparation and sequencing

400 μl of BALF was pipetted into a cartridge. The QmNGS wet lab workflow, including nucleic acid extraction, PCR-free library preparation, and purification, was performed automatically using the NGS master. The libraries were quantified using real-time PCR (chain) and pooled. Shotgun sequencing was performed using Illumina NextSeq. During each sequencing run, a negative control (NC, from healthy individuals, including human genomic DNA) and a positive control (a mixture of pathogen particles) were included for quality control, followed by trimming unnecessary adapter sequences and low-quality bases in the pipeline. Like UmNGS, sequences of human origin were identified using BWA (human reference genome) (Zhang et al., 2022). The host index was obtained by quantifying the number of human sequences on the molecular scale. If the host index was greater than 80% of similar samples, the human sequences were retained; otherwise, they were abandoned. The processed reads were mapped to NCBI GenBank to identify the microbial species, and the background microorganisms and contaminating bacteria were identified simultaneously.

2.3.3 QmNGS reporting criteria

An identified microbial species was considered pathogenic when: (i) NC in the same sequencing run did not find the species or RPM (sample) was five times or more than RPM (NC); and (ii) for intracellular bacteria, RPM ≥ 1 was considered pathogen (Zhang et al., 2022; Zhou et al., 2022).

2.4 Data analyses

The final clinical diagnoses in this study were obtained by three experienced clinicians through a comprehensive evaluation of the clinical manifestations, traditional pathogen tests, CT imaging, BALF culture, and mNGS results of the patients. Microbial species detected by mNGS were considered pathogens only if they were consistent with the final clinical diagnosis.

2.5 Statistical analyses

A t-test, Wilcoxon signed rank test, or chi-square test was used to compare differences between UmNGS and QmNGS. All statistical results were analyzed using SPSS 22.0 software, and results with *P*-values < 0.05 were defined as statistically significant.

3 Results

3.1 Patient characteristics

This prospective study included thirty-six patients, including nineteen men (52.8%) and seventeen women (47.2%), with an average age of 45 years. We found that 94.4% (n = 34) of the patients were immunocompromised, while only 5.6% (n = 2) had normal immune function. The immunocompromised patients suffered from hematological disorders or malignant tumors, and 67.6% (n=23) of them were diagnosed with a pulmonary infection. The final clinical diagnosis depended on clinical manifestations, imaging, traditional etiology tests, UmNGS and QmNGS, which included twenty-five (25/36, 69.4%) patients with a pulmonary infection and eleven (11/36 = 30.6%) patients with a nonpulmonary infection. Among the twenty-five patients with pulmonary infection, nineteen had non-mixed infections, and the rest (n = 6) had mixed infections. In the non-mixed infection group, ten patients had a single bacterial infection, seven had a single fungal infection, and two had a single viral infection. In the co-infection group, 33.3% (n = 2) of the patients were co-infected with one type of bacteria and one type of virus, 33.3% (n = 2) of the patients were co-infected with one type of fungus and a single bacterium, 16.7% (n = 1) of the patients were co-infected with one type of fungus and two types of bacteria, and 16.7% (n = 1) of the patients were co-infected with one type of fungus, three types of bacteria, and one type of virus (Table 1). In this study, thirty-five pulmonary pathogen infections were diagnosed in twenty-five patients with pulmonary infection, of which nineteen were diagnosed with bacterial pneumonia and eleven and five with fungal and viral pneumonia, respectively (Figure 1). After pathogen diagnosis, 84% of patients with pulmonary infection achieved relief in clinical symptoms through rational anti-infection treatment.

10.3389/fcimb.2023.1184245

TABLE 1 Characteristics of the enrolled cases.

Age	45 ± 14.3
Sex	
Male	19 (52.8%)
Female	17 (47.2%)
Immune function	
Normal	2 (5.6%)
Defective	34 (94.4%)
Nonpulmonary infection	11
Pulmonary infection	25
Non-mixed infection	19
Single bacterial infection	10
Single fungal infection	7
Single viral infection	2
Mixed infection	6
Bacterial with one viral co-infections	2
Fungal with one bacterial co-infection	2
Fungal with two bacterial co-infections	1
Fungal with three bacterial and one viral co-infections	1

3.2 Pathogen species in patients with pulmonary infection

In patients with bacterial infections diagnosed by mNGSs and conventional laboratory-based diagnostic testing, twelve species of bacteria were identified from nineteen isolated strains. The bacteria most commonly observed were *Mycobacterium tuberculosis*, which accounted for 4/19 infections (21.1%), followed by *Pseudomonas aeruginosa* accounted for 3/19 infection (15.8%), *Nocardia cyriacigeogica*, and *Nontuberculous mycobacteria*, all of which were observed in two cases (10.5%). The less common strains identified mostly belonged to gram-negative bacteria, including *Haemophilus influenzae*, *Actinobacillus urea*, *Legionella pneumophila*, *Stenotrophomonas maltophilia*, *Klebsiella pneumoniae*, *and Escherichia coli*, and only *Enterococcus faecium* and *Staphylococcus aureus* are gram-positive bacteria. Among the eleven patients with fungal infections, five species of fungi were detected based on mNGS and conventional diagnostic methods. The fungus most frequently detected was *Aspergillus* (n = 5, 45.5%), similar to a previous study (Yang et al., 2021). *Pneumocystis* and *Mucor* appeared with the same frequency (2, 18.2%). The relatively few isolated fungal species were *Botryotinia* and *Rhizopus* spp. For the five patients with viral infections, the strain most identified was *cytomegalovirus* (3, 60%), followed by *Epstein-Barr virus* and *human herpes simplex virus type 1* (Figure 2).

3.3 Detection performances of UmNGS and QmNGS in bronchoscopy and bronchoalveolar lavage fluid (BALF)

The comparison of UmNGS and QmNGS in the thirty-six patients with a suspected pulmonary infection is presented in Table 2. The sensitivity of UmNGS for diagnosing pulmonary infection was 76% (95% CI:54–90%), and the use of QmNGS was 72% (95% CI:50–87%). We did not find a significant difference in sensitivity between the two mNGS methods (P > 0.05). QmNGS was more specific (81.8%) than UmNGS (45.5%), with a difference of 36.3% (*P* = 0.219). Furthermore, we compare the difference in the LR for the two mNGS methods. The +LR values of QmNGS and UmNGS were 3.956 and 1.394, respectively, and the -LR values of

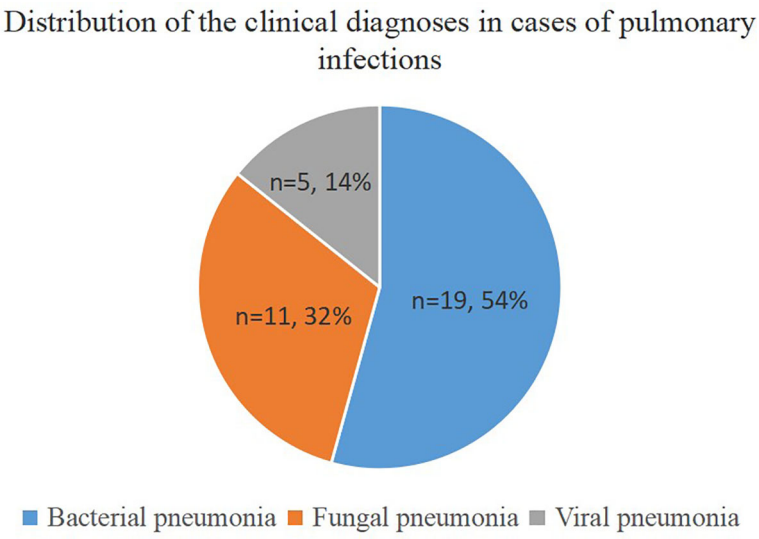

FIGURE 1
Distribution of clinical diagnoses in cases of pulmonary infections. The pie chart demonstrates the distribution of clinical diagnoses in 25 cases of pulmonary infection.

10.3389/fcimb.2023.1184245

QmNGS and UmNGS were 0.342 and 0.527, respectively. We did not find any difference in the LR between the two methods ($P > 0.05$).

The above study identified nineteen cases of bacterial infection, eleven cases of fungal infection, and five cases of viral infection in patients with pulmonary infection. We compared the detection rates of QmNGS and UmNGS for the different pathogen species (Table 3). For bacterial infections, UmNGS and QmNGS detected seventeen cases (17/19, 89.5%) and sixteen cases (16/19, 84.2%), respectively. In eleven cases of fungal infection, the detection rates of the two methods were the same (7/11, 63.6%). In this study, five cases of viral infection were detected, all detected by QmNGS, while the results for UmNGS were positive in four cases (4/5, 80%).

TABLE 2 The detection performance of QmNGS and UmNGS in pulmonary infections.

	Sensitivity % (95% CI)	Specificity % (95% CI[a])	+LR[b]	-LR[c]
QmNGS	72 (0.50-0.87)	81.8 (0.48-0.97)	3.956	0.342
UmNGS	76 (0.54-0.90)	45.5 (0.18-0.75)	1.394	0.527

[a]CI, confidence interval;
[b]+LR, positive likelihood ratio;
[c]-LR, negative likelihood ratio.

3.4 Comparison of UmNGS and QmNGS analysis for co-detected pathogens

As shown in Figure 3 and Supplementary Table 1, 68.6% (n = 24) of the pathogens were detected using both detection methods. This study further explored whether there were differences in unique reads, relative abundance ranking, coverage, and sequencing depth of pathogens detected simultaneously using UmNGS and QmNGS. The number of unique reads of pathogens using UmNGS ranged from two to 104,564, and most were mapped to > 6000 (7/24, 29%). For QmNGS, the unique reads ranged from one to 149107, and 42% of the co-detected pathogens had fewer than fifty reads (10/24), while UmNGS accounted for 13% (Figure 3A). In other words, the number of unique reads of QmNGS pathogens was smaller than that of UmNGS; however, no significant differences were observed in the unique reads between QmNGS and UmNGS ($P > 0.05$). To further compare the differences between the two mNGS methods in unique readings, we performed a sample-to-sample comparison based on the data shown Supplementary Table 1. After statistical analysis, there was still no difference with $P > 0.05$. At the same time, we compared the differences in the relative abundance ranking of the co-detected pathogens between the two mNGS methods. The results also did not show significant differences ($P = 0.638 > 0.05$) (Figure 3B). Similarly, the difference of the relative abundance rankings between the two mNGS methods for each sample was compared, and no significant difference was found after the paired samples test ($P > 0.05$). Further comparisons of the genome coverage of 24 co-detected pathogens showed that the genome coverage of UmNGS was significantly higher than that of QmNGS ($P < 0.05$) (Figure 3C). In addition, a comparison of the differences in the average sequencing depth of the two methods for the same pathogen indicated that the average sequencing depth of the detected pathogen by QmNGS was significantly shallower than that by UmNGS, and the difference was statistically significant ($P < 0.001$) (Figure 3D).

3.5 Concordance between UmNGS and QmNGS assay in patients with pulmonary infection

Supplementary Table 2 showed the thirty-five pathogen strains isolated from twenty-five patients with pulmonary infections and the detection performances of UmNGS and QmNGS for the strains level. We compared the consistency of UmNGS and QmNGS in the detection of these pathogens. The UmNGS and QmNGS assays

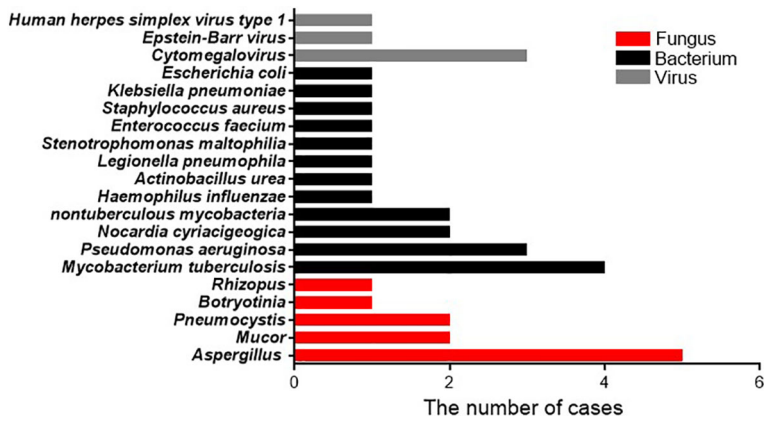

FIGURE 2
Pathogen occurrence in pathogen-infected patients. The X-axis shows the number of isolated pathogens in patients with clinically diagnosed pathogen-infected pneumonia.

TABLE 3 Comparison of the detection of pulmonary pathogens using the two different mNGS methods.

	Bacterial pneumonia	Fungal pneumonia	Viral pneumonia
QmNGS	16 (84.2%)	7 (63.6%)	5 (100%)
UmNGS	17 (89.5%)	7 (63.6%)	4 (80%)

were positive for 24/35 strains (68.6%) and negative for 3/35 strains (8.6%), while four strains (11.4%) were positive with QmNGS only, and four strains (11.4%) were positive with UmNGS only. The overall concordance rate between the two mNGS methods for pathogens detected in patients with pulmonary infection was 77.2%. To further describe the performance of the UmNGS and QmNGS concordance rate in different species of pathogens, we calculated the concordance rates of the two methods against bacteria, fungi, and viruses. The results showed that the concordance rates of different species of pathogens were different. The highest was for bacteria, up to 84.2%, followed by viruses, which was 80%, while the lowest concordance rate was for fungi at 63.7% (Figure 4).

3.6 The diagnostic performance of UmNGS and QmNGS in nonpulmonary infections

In this study, eleven cases of nonpulmonary infections were diagnosed based on relevant examinations. For nonpulmonary infections, the detection error rates for UmNGS and QmNGS were 54.5% (6/11) and 18.2% (2/11), respectively. However, the difference was not statistically significant ($P = 0.219$). Of the eleven patients with nonpulmonary infection, four cases were detected using QmNGS and UmNGS, and one case was incorrectly detected, as shown in Table 4 and Figure 5. Nonspecific pathogens detected by the two mNGSs included bacteria, fungi, and viruses. The highest proportion was bacteria, which accounted for five out of ten, all detected using UmNGS, followed by viruses (4/10), using both UmNGS and QmNGS, while the least detected species was fungus (1/10) using only UmNGS (Table 4). Overall, the species of nonspecific pathogens detected using QmNGS were relatively uniform, while that using UmNGS was relatively diverse, in patients with a nonpulmonary infection. Furthermore, the diagnostic accuracy rate of QmNGS was higher than that of UmNGS, but the difference was not statistically significant.

4 Discussion

Although mNGS has become a promising method for the diagnosis of infectious diseases, the limitations of mNGS testing, along with an increase in its clinical applications, have been highlighted. Institutions continue to optimize sequencing processes, database construction, and bioinformatics analyses to make mNGS more accurate and universal. Several optimized mNGSs are currently in the market. However, research on their performance in the clinical detection of pathogens is rare.

In this prospective study, we investigated the different performances of the two different mNGS methods with almost same costs, UmNGS and QmNGS, in the detection of infectious pathogens in BALF samples. We found that 54% of patients with

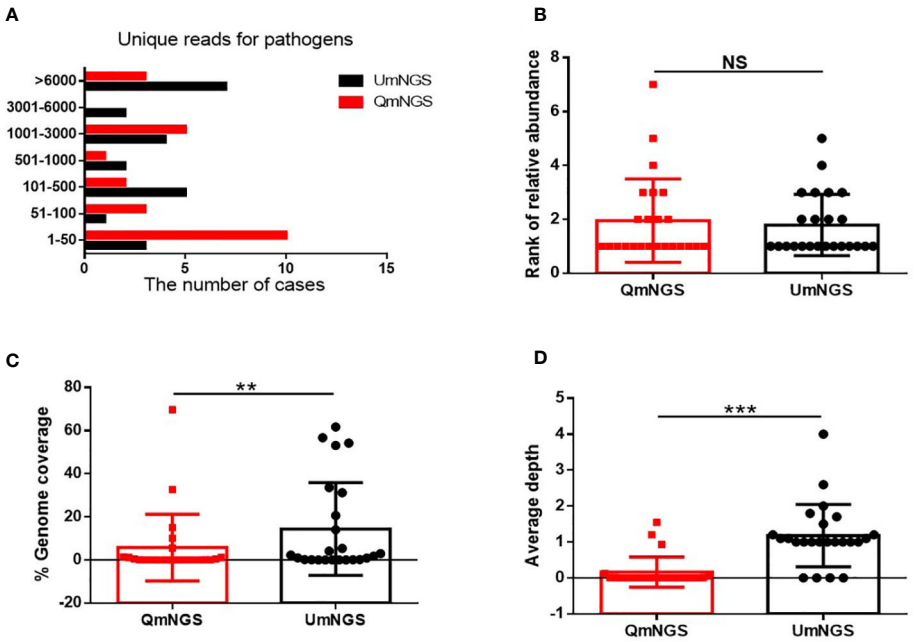

FIGURE 3
Comparison of UmNGS and QmNGS analysis for co-detected pathogens. The differences in the unique reads **(A)**, relative abundance ranking **(B)**, coverage **(C)**, and sequencing depth **(D)** of UmNGS and QmNGS for co-detected pathogens were compared, respectively. NS, no significant; $^{**}P < 0.05$; $^{***}P < 0.001$.

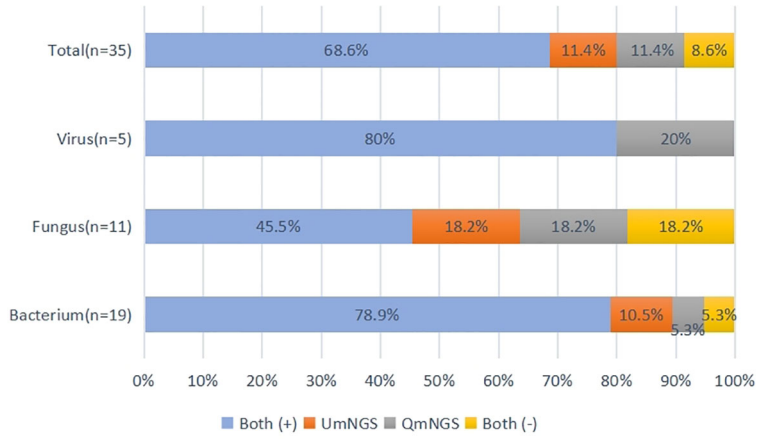

FIGURE 4
Concordance of QmNGS and UmNGS in the detection of a pathogen isolated from patients with a pulmonary infection. The coincidence rate of the two mNGS methods was 77.2%. Both (+), both methods detected the same pathogens in the same cases; both (-), both methods did not detect the same pathogens in the same cases.

pulmonary infection had bacterial infections, of which the most isolated strain was *Mycobacterium tuberculosis* (21.1%), which was inconsistent with common pathogens in hospital-acquired pneumonia (American Thoracic Society and Infectious Diseases Society of America, 2005). This may have been due to the different types of enrolled patients or the relatively small number of enrolled patients. Almost all enrolled patients (94.4%) were immunocompromised; they were much more susceptible to infection, and the pathogens may be uncommon and different from those of immunocompetent individuals (Thrikawala and Rosowski, 2020). Both QmNGS (72%) and UmNGS (76%) showed high sensitivity, similar to the results of a previous study (Huang et al., 2020). Our prospective study revealed that the specificities of UmNGS and QmNGS were 45.5% and 81.8%, respectively, and that the specificity of QmNGS was higher than that of UmNGS; however, the difference was not statistically significant. This may have been due to the limited number of patients that were enrolled in this study.

TABLE 4 The diagnostic performance of UmNGS and QmNGS in nonpulmonary infections.

Sample No.	QmNGS	UmNGS
S5	Negative	*Staphylococcus hemolyticus*
S6	Cytomegalovirus	Cytomegalovirus Acinetobacter Pitt
S7	Negative	Negative
S9	Human polyomavirus 4	Negative
S15	Negative	*Staphylococcus hominis*
S16	Negative	Negative
S17	Negative	Negative
S23	Negative	Human respirovirus 3 *Staphylococcus hominis*
S25	Negative	Cryptococcus neoformans
S29	Negative	Negative
S36	Negative	*Streptococcus pneumoniae*

A key technical difference between UmNGS and QmNGS is the library preparation method. QmNGS uses a library preparation method that is reaction-free of PCRs. Compared to traditional library preparation dependent on PCR, the pathogen detection response time can be reduced to approximately 12 h, which is important for the rapid diagnosis and precise treatment of patients with life-threatening diseases. Furthermore, a study showed that the PCR-free library preparation method can reduce manual operation by technicians, thus reducing possible sources of contamination (Luan et al., 2021). Furthermore, QmNGS using NGSmaster, which automates the wet lab workflow, can further reduce exogenous contamination. The above two differences may explain why QmNGS has a higher specificity and lower diagnostic error rate in noninfectious pneumonia than UmNGS. A study suggested that the sequencing output of mNGS subsamples in the original DNA content of a library, and any bias introduced by the PCR library building process, would inevitably change the original information, which can then affect the relative abundance of pathogens in the sample (Gu et al., 2019). However, according to our results, a p value was greater than 0.05 after comparing the relative abundance rankings of the detected pathogens between the two mNGS methods. This may have been due to the relatively limited number of cases enrolled in our study or an improvement in the current PCR-dependent library preparation technology.

An inherent drawback of mNGS is that the predominant portion of microbial nucleic acids in most patient samples is the human host, accounting for > 95% of reads, which limits mNGS sensitivity (Yang et al., 2011). This shortcoming is unbiased and inherent in mNGS, and although this may be partially mitigated by host depletion (Hasan et al., 2016), it may lead to nonspecific clearance of pathogens, an amplification of the background microbiome, and interference with the interpretation of the results (Charalampous et al., 2019). Although this study revealed

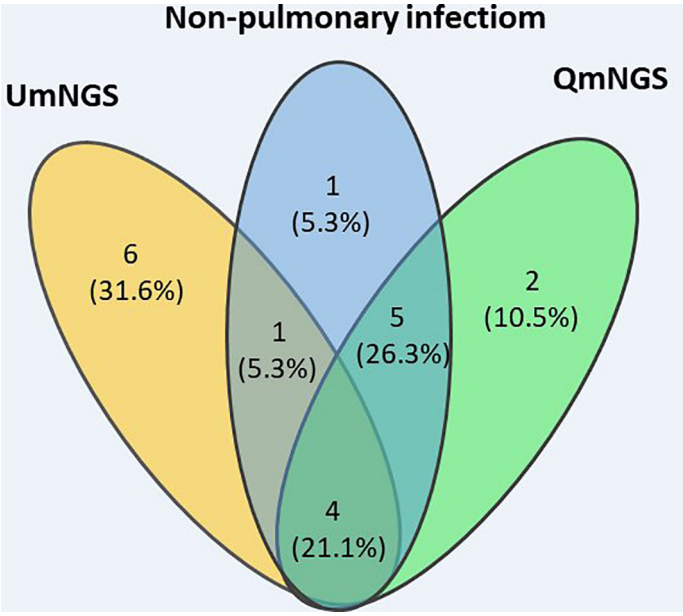

FIGURE 5
Wayne diagram describing the performances of QmNGS and UmNGS in patients with a nonpulmonary infection for pathogen detection. Blue represents eleven patients with nonpulmonary infection; yellow represents QmNGS; green represents UmNGS.

no differences were found between the two mNGSs regarding pathogen detection sensitivity, the specificity and negative LR tended to increase. Therefore, selective dehumanization of QmNGS did not cause a decrease in sensitivity compared with indifferent dehumanization of UmNGS but had a higher specificity. A study showed that the reads of the microorganisms identified by mNGS were not related to how the library was prepared but related to the concentration of host cells in the sample, which can decrease as the concentration of host cells increases (Luan et al., 2021). This was consistent with our finding that the pathogen reads were not significantly different between QmNGS and UmNGS.

Theoretically, our mNGS results are more reliable when the genome coverage and sequencing depth are higher (Li et al., 2021). Another study showed that samples from patients that were centrifuged to remove the cell precipitates before the library construction may reduce the proportion of the host genome proportion and increase the sequence coverage of pathogens significantly (Ji et al., 2020). Similarly, in our study, the sequencing depth and coverage of QmNGS were lower than those of UmNGS for co-detecting pathogens. However, neither the relative abundance ranking nor the sensitivity for detected pathogens were affected. However, the specificity showed an increasing trend, which may have been caused by the combined effect of the library construction method and the processing of human genes.

For the twenty-five patients with pulmonary infection, the concordance rate between the two mNGSs was 77.2% for pathogenic detection. Of the eleven patients with nonpulmonary infection, only four cases were detected using QmNGS and UmNGS. QmNGS detected viruses only, while UmNGS detected bacteria, viruses, and fungi, including *Staphylococcus* and *Cryptococcus neoformans*, which are classified more often as pathogens than viruses in clinics (Peng and Yang, 2021; Zhu et al., 2021). This may have provided a misleading anti-infection direction. Therefore, mNGS can detect not only the nucleic acids of the pathogens but also the nucleic acids of the colonized and contaminating pathogens, which is challenging to interpret. As the sensitivity of mNGS is improving, its specificity should be as high as possible to reduce any errors in diagnoses of nonpulmonary infections and has great significance for the rational use of antibiotics and avoidance of abuse. As shown in previous studies (Wang et al., 2019; Huang et al., 2020), mNGS has a higher false positive rate and higher cost compared to traditional pathogen detection methods, and traditional detection methods cannot be replaced.

As a limitation, due to the insufficient number of subjects included in this study, a true statistical difference between the two mNGS assays could not be established. However, the application value of QmNGS is promising.

In summary, this study conducted a comprehensive comparison of QmNGS and UmNGS in the detection of pathogens in BALF to understand the differences between the different mNGS technologies and offer a basis for the clinical selection of the diverse types of mNGS.

Data availability statement

The data presented in the study are deposited in the NCBI, accession number PRJNA940347 and PRJNA936669.

Ethics statement

The studies involving human participants were reviewed and approved by Ethics Review committee of Tianjin Medical University General Hospital (ChiCTR1900023727). The patients/participants provided their written informed consent to participate in this study.

Author contributions

YW and JF contributed to the research design and revision of the manuscript. ZZ and XC drafted the research protocol, analyzed the results, drafted the manuscript and deposited data in an acceptable repository. All authors approved the submitted version and agreed to be responsible for all aspects.

Funding

This research was supported by the Tianjin Key Medical Discipline (Specialty) Construction Project, the National Natural Science Foundation of China (82170097, 81970083, 81270144, 81570084, and 30800507 to JF; 82200100 to ZZ), National Key Technology R&D Program of China (2015BAI12B00 to JF), Natural Science Foundation of Inner Mongolia Autonomous Region of China (2021MS0801 to PX), Research Program of Science and Technology at the Universities of Inner Mongolia Autonomous Region (NJZY21584 to PX), Medical Program of Inner Mongolia Autonomous Region (202202198 to PX), Educational Reform Program of Inner Mongolia University (NYJXGG2021085 to PX), and General Program of Inner Mongolia University [YKD2020KJBW(LH)007 to PX].

Acknowledgments

We thank the respiratory endoscopy team of Tianjin Medical University General Hospital for technical support and suggestions.

Conflict of interest

The authors declare that the research was conducted in the absence of any commercial or financial relationships that could be construed as a potential conflict of interest.

Publisher's note

Supplementary material

The Supplementary Material for this article can be found online at: https://www.frontiersin.org/articles/10.3389/fcimb.2023.1184245/full#supplementary-material

References

American Thoracic Society and Infectious Diseases Society of America (2005). Guidelines for the management of adults with hospital-acquired, ventilator-associated, and healthcare-associated pneumonia. *Am. J. Respir. Crit. Care Med.* 171, 388–416. doi: 10.1164/rccm.200405-644ST

Charalampous, T., Kay, G. L., Richardson, H., Aydin, A., Baldan, R., Jeanes, C., et al. (2019). Nanopore metagenomics enables rapid clinical diagnosis of bacterial lower respiratory infection. *Nat. Biotechnol.* 37, 783–792. doi: 10.1038/s41587-019-0156-5

Chen, H., Yin, Y., Gao, H., Guo, Y., Dong, Z., Wang, X., et al. (2020). Clinical utility of in-house metagenomic next-generation sequencing for the diagnosis of lower respiratory tract infections and analysis of the host immune response. *Clin. Infect. Dis.* 71, S416–S426. doi: 10.1093/cid/ciaa1516

Chiu, C. Y., and Miller, S. A. (2019). Clinical metagenomics. *Nat. Rev. Genet.* 20 (6), 341–355. doi: 10.1038/s41576-019-0113-7

Colice, G. L., Morley, M. A., Asche, C., and Birnbaum, H. G. (2004). Treatment costs of community-acquired pneumonia in an employed population. *Chest* 125, 2140–2145. doi: 10.1378/chest.125.6.2140

Gu, W., Miller, S., and Chiu, C. Y. (2019). Clinical metagenomic next-generation sequencing for pathogen detection. *Annu. Rev. Pathol.* 14, 319–338. doi: 10.1146/annurev-pathmechdis-012418-012751

Hasan, M. R., Rawat, A., Tang, P., Jithesh, P. V., Thomas, E., Tan, R., et al. (2016). Depletion of human DNA in spiked clinical specimens for improvement of sensitivity of pathogen detection by next-generation sequencing. *J. Clin. Microbiol.* 54, 919–927. doi: 10.1128/JCM.03050-15

Huang, J., Jiang, E., Yang, D., Wei, J., Zhao, M., Feng, J., et al. (2020). Metagenomic next-generation sequencing versus traditional pathogen detection in the diagnosis of peripheral pulmonary infectious lesions. *Infect. Drug Resist.* 13, 567–576. doi: 10.2147/IDR.S235182

Ji, X. C., Zhou, L. F., Li, C. Y., Shi, Y. J., Wu, M. L., Zhang, Y., et al. (2020). Reduction of human DNA contamination in clinical cerebrospinal fluid specimens improves the sensitivity of metagenomic next-generation sequencing. *J. Mol. Neurosci.* 70, 659–666. doi: 10.1007/s12031-019-01472-z

Li, N., Cai, Q., Miao, Q., Song, Z., Fang, Y., and Hu, B. (2021). High-throughput metagenomics for identification of pathogens in the clinical settings. *Small Methods* 5, 2000792. doi: 10.1002/smtd.202000792

Luan, Y., Hu, H., Liu, C., Chen, B., Liu, X., Xu, Y., et al. (2021). A proof-of-concept study of an automated solution for clinical metagenomic next-generation sequencing. *J. Appl. Microbiol.* 131, 1007–1016. doi: 10.1111/jam.15003

Murdoch, D. R., O'Brien, K. L., Driscoll, A. J., Karron, R. A., Bhat, N.Pneumonia Methods Working Group, et al. (2012). Laboratory methods for determining pneumonia etiology in children. *Clin. Infect. Dis.* 54 (Suppl;2), S146–S152. doi: 10.1093/cid/cir1073

Peng, Q., and Yang, Q. (2021). Risk factors and management of pulmonary infection in elderly patients with heart failure: a retrospective analysis. *Medicine* 100, e27238. doi: 10.1097/MD.0000000000027238

Schlaberg, R., Chiu, C. Y., Miller, S., Procop, G. W., and Weinstock, G. (2017). Validation of metagenomic next-generation sequencing tests for universal pathogen detection. *Arch. Pathol. Lab. Med.* 141, 776–786. doi: 10.5858/arpa.2016-0539-RA

Thrikawala, S., and Rosowski, E. E. (2020). Infection of zebrafish larvae with aspergillus spores for analysis of host-pathogen interactions. *J. Vis. Exp.* 159, e61165.

Wang, J., Han, Y., and Feng, J. (2019). Metagenomic next-generation sequencing for mixed pulmonary infection diagnosis. *BMC pulmonary Med.* 19 (1), 252. doi: 10.1186/s12890-019-1022-4

Wunderink, R. G., and Waterer, G. (2017). Advances in the causes and management of community acquired pneumonia in adults. *BMJ* 358, j2471. doi: 10.1136/bmj.j2471

Yang, L., Song, J., Wang, Y., and Feng, J. (2021). Metagenomic next-generation sequencing for pulmonary fungal infection diagnosis: lung biopsy versus bronchoalveolar lavage fluid. *Infect. Drug Resist.* 14, 4333–4359. doi: 10.2147/IDR.S333818

Yang, J., Yang, F., Ren, L., Xiong, Z., Wu, Z., Dong, J., et al. (2011). Unbiased parallel detection of viral pathogens in clinical samples by use of a metagenomic approach. *J. Clin. Microbiol.* 49, 3463–3469. doi: 10.1128/JCM.00273-11

Zhang, R., Zhuang, Y., Xiao, Z. H., Li, C. Y., Zhang, F., Huang, W. Q., et al. (2022). Diagnosis and surveillance of neonatal infections by metagenomic next-generation sequencing. *Front. Microbiol.* 13, 855988. doi: 10.3389/fmicb.2022.855988

Zhao, Z., Song, J., Yang, C., Yang, L., Chen, J., Li, X., et al. (2021). Prevalence of fungal and bacterial co-infection in pulmonary fungal infections: a metagenomic next generation sequencing-based study. *Front. Cell Infect. Microbiol.* 11, 749905. doi: 10.3389/fcimb.2021.749905

Zhou, H., Ouyang, C., Han, X., Shen, L., Ye, J., Fang, Z., et al. (2022). Metagenomic sequencing with spiked-in internal control to monitor cellularity and diagnosis of pneumonia. *J. infect.* 84 (1), e13–e17. doi: 10.1016/j.jinf.2021.09.018

Zhu, S., Li, Y., Gao, H., Hou, G., Cui, X., Chen, S., et al. (2021). Identification and assessment of pulmonary *Cryptococcus neoformans* infection by blood serum surface-enhanced Raman spectroscopy. *Spectrochim Acta A Mol. Biomol Spectrosc* 260, 119978. doi: 10.1016/j.saa.2021.119978

frontiers | Frontiers in Cellular and Infection Microbiology

TYPE Original Research
PUBLISHED 03 August 2023
DOI 10.3389/fcimb.2023.1112229

OPEN ACCESS

EDITED BY
Jeyaprakash Rajendhran,
Madurai Kamaraj University, India

REVIEWED BY
Jiaxu Liang,
The Fifth Clinical Medical College of Henan University of Chinese Medicine, China
Jianmei Lin,
Sichuan Academy of Medical Sciences and Sichuan Provincial People's Hospital, China

*CORRESPONDENCE
Liyu Chen
14491291@qq.com
Ying Xiong
61711445@qq.com

RECEIVED 30 November 2022
ACCEPTED 18 July 2023
PUBLISHED 03 August 2023

CITATION
He S, Wei J, Feng J, Liu D, Wang N, Chen L and Xiong Y (2023) The application of metagenomic next-generation sequencing in pathogen diagnosis: a bibliometric analysis based on Web of Science. *Front. Cell. Infect. Microbiol.* 13:1112229. doi: 10.3389/fcimb.2023.1112229

The application of metagenomic next-generation sequencing in pathogen diagnosis: a bibliometric analysis based on Web of Science

Sike He[1], Jingwen Wei[1], Jiaming Feng[1], Dan Liu[2], Neng Wang[3], Liyu Chen[3]* and Ying Xiong[2]*

[1]West China School of Medicine, Sichuan University, Chengdu, China, [2]Department of Periodical Press, West China Hospital, Sichuan University, Chengdu, China, [3]Center of Infectious Diseases, West China Hospital, Sichuan University, Chengdu, China

Background: Infectious disease is a large burden on public health globally. Metagenomic next-generation sequencing (mNGS) has become popular as a new tool for pathogen diagnosis with numerous advantages compared to conventional methods. Recently, research on mNGS increases yearly. However, no bibliometric analysis has systematically presented the full spectrum of this research field. Therefore, we reviewed all the publications associated with this topic and performed this study to analyze the comprehensive status and future hotspots of mNGS for infectious disease diagnosis.

Methods: The literature was searched in the Web of Science Core Collection and screened without year or language restrictions, and the characteristics of the studies were also identified. The outcomes included publication years, study types, journals, countries, authorship, institutions, frontiers, and hotspots with trends. Statistical analysis and visualization were conducted using VOSviewer (version 1.6.16) and CiteSpace (version 6.1. R3).

Results: In total, 325 studies were included in the analysis after screening. Studies were published between 2009 and 2022 with a significantly increasing number from 1 to 118. Most of the studies were original articles and case reports. *Frontiers in Cellular and Infection Microbiology* and *Clinical Infectious Disease* were the most commonly cited and co-cited journals. Institutions and researchers from China contributed the most to this field, followed by those from the USA. The hotspots and frontiers of these studies are pneumonia, tuberculosis, and central nervous system infections.

Conclusion: This study determined that mNGS is a hot topic in the diagnosis of infectious diseases with development trends and provides insights into researchers, institutions, hotspots and frontiers in mNGS, which can offer references to related researchers and future research.

KEYWORDS

metagenomic next-generation sequencing, pathogen diagnosis, bibliometric analysis, Web of Science, VOSviewer, CiteSpace

1 Introduction

As a series of common and frequently occurring diseases, infectious diseases have always been a heavy burden to global health due to their high morbidity and mortality rate, especially in developing countries (McArthur, 2019). First, some ancient infectious diseases, such as tuberculosis (TB) caused by mycobacterium tuberculosis (MTB), have plagued mankind for thousands of years, and a quarter of the global population is infected with MTB (Kherabi et al., 2022). Additionally, some explosive epidemics, including seasonal influenza and COVID-19, have caused great losses in health, finances, and emotions (Calabrò et al., 2022; Schäfer et al., 2022; Xie et al., 2022). Precise pathogen diagnosis is a key part of infectious disease management. However, rare pathogens, emerging infectious diseases, and the prevalence of drug resistance present huge challenges to the diagnosis and further management (Mancuso et al., 2021; Vitiello, 2022).

Etiology is the gold standard for infectious disease diagnosis (Esposito, 2016). The detection technology of the traditional etiological method is culture with high positive predictive value. However, the limitations, including narrow pathogen spectrum, low positive rate, and long detection cycle, are nonnegligible. These drawbacks may lead to delays in diagnosis, the irrational use of antibiotics, etc., which can result in poor prognosis (Carbo et al., 2021; Chen et al., 2022). Metagenomic next-generation sequencing (mNGS), based on high-throughput sequencing technology, is a burgeoning unbiased pathogen detection method (Chiu and Miller, 2019; Gu et al., 2019). mNGS mainly consists of nucleic acid extraction, library preparation, host sequence exclusion and pathogen sequence enrichment (Jia et al., 2021). It can characterize all DNA or RNA in samples and analyze the entire microbiome, human host genome, and transcriptome in clinical samples (Chiu and Miller, 2019). The advantages, such as high throughput, wide coverage, high accuracy, and efficiency have brought new light to clinical use. According to the study by Duan et al., mNGS presented significantly higher sensitivity than the traditional culture method (67.4% vs 23.6%, $p < 0.001$) and similar specificity (68.8% vs 81.3%; $p = 0.41$) (Duan et al., 2021). Furthermore, mNGS is more effective than the conventional method that it required 3 days to identify 67.23% of cases of tuberculosis (TB), whereas 49.58% detected using conventional methods required over 90 days (Shi et al., 2020). Additionally, it can markedly increase the detection rate for some rare pathogens with a low positive rate of culture or insufficient clinical precedents (Simner et al., 2018). Therefore, it has been successfully applied in the diagnosis and treatment of difficult and critical infectious diseases, the identification of unknown pathogens, drug resistance gene monitoring, and epidemiological tracking investigations (Chiu and Miller, 2019; Han et al., 2019).

Bibliometrics is a new cross-science approach that can analyze all knowledge carriers using mathematical and statistical methods (Blakeman, 2018). It has been widely used to guide researchers in specific fields via the quantitative research assessment of academic output to improve research efficiency (Tang et al., 2018; Yeung et al., 2018). Citation analysis is the core part of bibliometric analysis because the number of citations can reflect the impact of an article to a certain extent (Feijoo et al., 2014; Xiong et al., 2022). Many medical articles have explored certain research fields via bibliometric analysis have been published, including diabetes (Zhao et al., 2016), tuberculosis (Xiong et al., 2022), and vaccines (Zhang et al., 2019). With the widespread use of mNGS, the number of studies about this topic has increased in recent years. However, there is no study concerning the overview of mNGS in pathogen diagnosis based on bibliometric analysis. Thus, we performed this study to identify the current status, future hotspots, and frontiers of mNGS by analyzing the publications from core collection in Web of Science (WoSCC).

2 Methods

2.1 Data collection

We extracted literature from the Science Citation Index database in the WoSCC via the Sichuan University Library website. The search strategy was "(TI= (metagenomic next-generation sequencing)) OR TI= (mNGS)," and we downloaded all data within one day on October 1, 2022. There were no restrictions on language or publication time to ensure comprehensive search results. Two researchers (SKH and JMF) screened the literature by excluding meeting abstracts, letters, book chapters, corrections, and articles not related to this topic. If two investigators have a discrepancy, the third author (LYC) will be consulted.

2.2 Data extraction

Two researchers (SKH and DL) extracted data from all the included studies. The extracted data included the title, abstract, keywords, references, source journal, publication date, total citations of all databases, authors with affiliation, country, and journal impact factor (IF). The institutions and countries were counted based on the corresponding authors. Journal IFs were obtained from Journal Citation Reports (JCR) 2022 to reflect the academic influence. Two researchers (NW and LYC) from the Center of Infectious Diseases in West China Hospital analyzed and screened the keywords, excluding some words without significant relevance, and merged synonyms (e.g., pcr and PCR). The third investigator (LYC) will be consulted when divergence occurs.

2.3 Data analysis and visualization

Microsoft (version 2022) was used to organize the publications and analyze their basic characteristics. The number of publications and citations annually were plotted by Stata (version 16.0). Bibliometric visualization was completed by VOSviewer (version 1.6.16) and CiteSpace (version 6.1. R3), including the journals, authors, countries, affiliations, and keywords in this research field regarding the use of mNGS in pathogen detection. VOSviewer was applied in co-citation and co-occurrence analysis. In the collaborative network map, each node represented one element (i.e., journal, country, author), and the size of each circle was weighted using document numbers and the line in the visualization reflected the relatedness of links. In the density map of keywords com-occurrence analysis, the colors ranged from blue to green to yellow. Yellow areas represented research hotspots and directions in this field. The "author keywords" was set in co-occurrence analysis. CiteSpace was applied to track the trend of keywords. The significance test was not used for statistical analysis because no control was involved.

3 Results

3.1 General information of the included literature

In total, 378 studies were conducted. After excluding meeting abstracts (26), letters (17), book chapters (4), corrections (4), and articles unrelated to the topic (2), we finally included 325 studies for further analysis (Figure 1). The study types (i.e., article, review, case report) were counted and the distribution is shown in Figure 2. Original article (n=214) and case report (n=96) accounted for the majority (65.8% and 29.5%). All the studies were published over 13 years from 2009 to 2022, and the number of publications increased during the past years, with an upwards trend (Figure 3A). The annual citation account was also conducted. From 2013 to 2020, the total citations increased significantly, which is consistent with the annual publications (Figure 3B). The top 20 most cited studies with details are displayed in Table 1.

3.2 Cited journals and co-cited journals

A total of 325 publications were published in 114 journals, and the top 10 cited journals are listed in Table 2. Most were published in *Frontiers in Cellular and Infection Microbiology* (n=28), followed by *Frontiers in Medicine* (n=22), *Infection and Drug Resistance* (n=21), *BMC Infectious Diseases* (n=20), *Frontiers in Microbiology* (n=20), *International Journal of Infectious Diseases* (n=15), *Journal of Clinical Microbiology* (n=9), *Frontiers in Public Health* (n=8), *Annals of Translational Medicine* (n=7), *BMC Pulmonary Medicine*

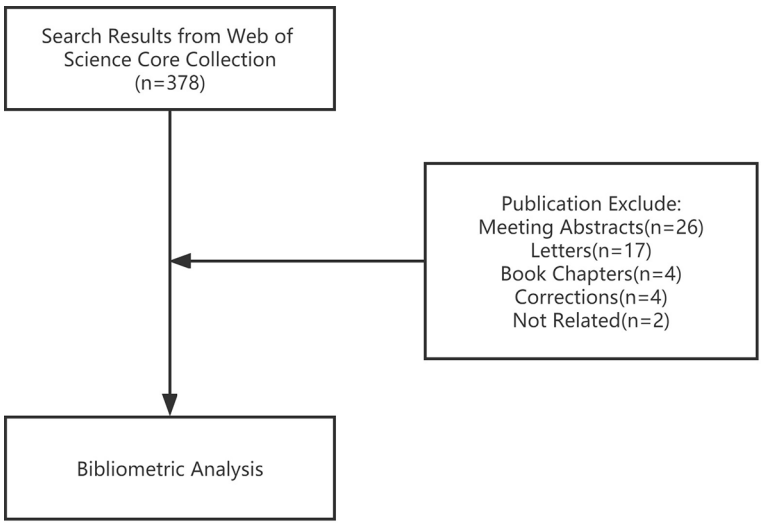

FIGURE 1
Flow chart of the study.

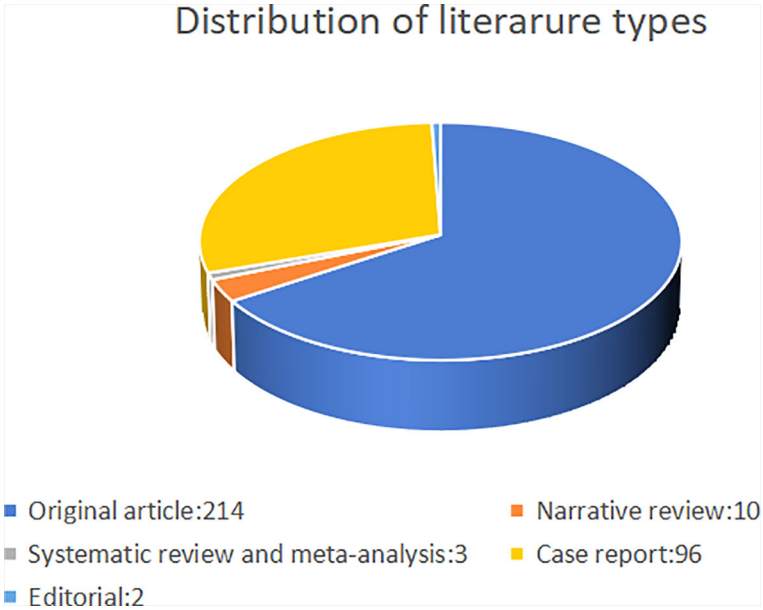

FIGURE 2
The distribution of the included studies.

(n=7), *and PLoS One* (n=7). The journals' IFs ranged from 11.677 to 3.320. The collaborative network of journals is shown in Figure 4A.

The top 10 co-cited journals are listed in Table 2. *Clinical Infectious Diseases* ranked first with 604 co-citations, followed by *Journal of Clinical Microbiology* (390), *New England Journal of Medicine* (288), *PLoS One* (241), and *Journal of Infection* (203). The network map of co-cited journals is shown in Figure 4B.

33 Distribution of contributing countries

We list the top 11 countries based on the corresponding authors who published at least two studies (Table 3). China occupies the majority of the contributing countries (70%), followed by the USA and France, respectively. In addition, India, the Netherlands, Switzerland, Japan, Brazil, England, Vietnam, and Germany also contributed significantly to this field. According to the total citations, England ranked the first, followed by the USA, France, and China. The collaborative network of contributing countries is shown in Figure 5. The strength of the lines shows that the USA connected with most countries and had a great impact on their research. People R China and England follow the USA with similar strengths.

3.4 Distributions of institutions

In Table 4, the institutions with a large number of publications are listed. Eight institutions (based on the corresponding authors) contributed more than 10 studies, from People R China (7) and the USA (1). The top five institutions are Zhejiang University (20), Fudan University (11), Fujian Medical University (10), Tianjin Medical University (10), and Zhengzhou University (10). The collaborative network is displayed in Figure 6

3.5 Authors and co-cited authors

Figure 7A presents the collaborative network of authors (authors who have published more than five studies) in the publications. Most of them were from China. These authors are divided into groups with quite a few collaborative works. The top 22 authors with large numbers of publications (≥5) are listed in Table 5. Han Xia from Hugobiotech in China ranked first with 14 publications, followed by Jing Feng (9), Charles Y Chiu (8), Bin Yang (8), Qing Miao (7), Hui Wang (7), and so on. In Figure 7B, the co-citation network map of authors is presented.

36 Keywords co-occurrence and clusters

Twenty-four keywords were retained and their co-occurrence frequencies were calculated. The keyword co-occurrence network map is shown in Figure 8A. From the density map of keyword co-occurrence in Figure 8B, the keywords mainly focused on diagnosis, infection, encephalitis, community-acquired pneumonia, viruses, pathogens, pneumonia, children, cerebrospinal fluid, MTB, and meningitis.

3.7 Trend of keywords

Figure 9 presents the top 14 keywords with the strongest citation burst. "Genome", "Encephalitis", "Next-generation

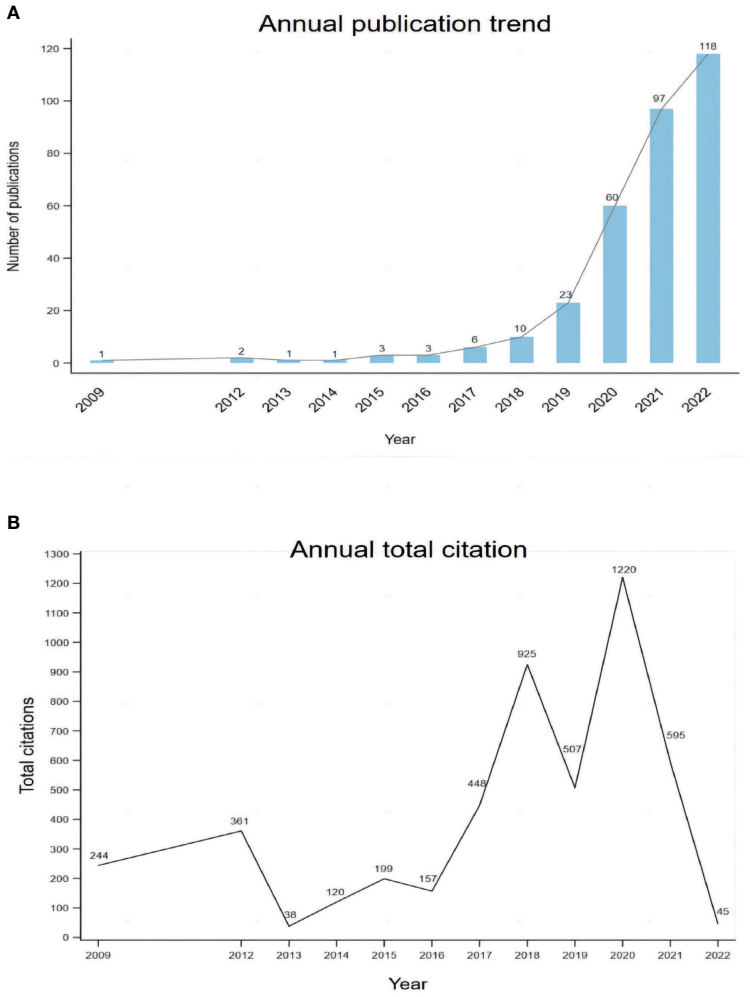

FIGURE 3
The trend of publications on mNGS in infectious diseases diagnosis from 2009 to 2022 **(A)** and the annual number of total citations **(B)**.

TABLE 1 The top 20 most cited studies.

Title	First author	Corresponding author	Year	Journal	IF	Total citations
RNA based mNGS approach identifies a novel human coronavirus from two individual pneumonia cases in 2019 Wuhan outbreak	Liangjun Chen	Yingle Liu, Ke Lan, Mang Shi, Yirong Li, Yu Chen	2020	EMERG MICROBES INFEC	19.568	344
Microbiological Diagnostic Performance of Metagenomic Next-generation Sequencing When Applied to Clinical Practice	Miao Qing	Bijie Hu	2018	CLIN INFECT DIS	20.999	267
Understanding the Promises and Hurdles of Metagenomic Next-Generation Sequencing as a Diagnostic Tool for Infectious Diseases	Simner PJ	Simner PJ	2018	CLIN INFECT DIS	20.999	254
Next-generation sequencing and metagenomic analysis: a universal diagnostic tool in plant virology	Adams IP	Adams IP	2009	MOL PLANT PATHOL	5.520	244
Validation of Metagenomic Next-Generation Sequencing Tests for Universal Pathogen Detection	Schlaberg R	Schlaberg R	2017	ARCH PATHOL LAB MED	5.686	239
Next generation sequencing and bioinformatic bottlenecks: the current state of metagenomic data analysis	Scholz MB	Chain PS	2012	CURR OPIN BIOTECH	10.279	213

(Continued)

TABLE 1 Continued

Title	First author	Corresponding author	Year	Journal	IF	Total citations
An ensemble strategy that significantly improves *de novo* assembly of microbial genomes from metagenomic next-generation sequencing data	Xutao Deng	Xutao Deng	2015	NUCLEIC ACIDS RES	19.190	168
Assessment of Metagenomic Assembly Using Simulated Next Generation Sequencing Data	Mende DR	Bork P	2012	PLOS ONE	3.752	148
Chronic Meningitis Investigated *via* Metagenomic Next-Generation Sequencing	Wilson MR	Wilson MR	2018	JAMA NEUROL	29.907	145
Comparison of three next-generation sequencing platforms for metagenomic sequencing and identification of pathogens in blood	Frey KG	Bishop-Lilly KA	2014	BMC GENOMICS	4.547	119
Rapid pathogen detection by metagenomic next-generation sequencing of infected body fluids	Wei GU	C.Y. Chiu	2021	NAT MED	87.241	116
Detection of Pulmonary Infectious Pathogens From Lung Biopsy Tissues by Metagenomic Next-Generation Sequencing	Henan Li	Hui Wang	2018	FRONT CELL INFECT MI	6.073	92
Coinfections of Zika and Chikungunya Viruses in Bahia, Brazil, Identified by Metagenomic Next-Generation Sequencing	Sardi SI	C.Y. Chiu	2016	J CLIN MICROBIOL	11.677	83
mNGS in clinical microbiology laboratories: on the road to maturity	Dongsheng Han	Jinming Li; Rui Zhang	2019	CRIT REV MICROBIOL	7.391	67
Rapid Metagenomic Next-Generation Sequencing during an Investigation of Hospital-Acquired Human Parainfluenza Virus 3 Infections	Greninger AL	Greninger AL	2017	J CLIN MICROBIOL	11.677	63
Neurobrucellosis: Unexpected Answer From Metagenomic Next-Generation Sequencing	Mongkolrattanothai K	C.Y. Chiu	2017	J PEDIATR INFECT DIS	5.235	60
Clinical Impact of Metagenomic Next-Generation Sequencing of Plasma Cell-Free DNA for the Diagnosis of Infectious Diseases: A Multicenter Retrospective Cohort Study	Hogan CA	Banaei N	2021	CLIN INFECT DIS	20.999	58
Metagenomic next-generation sequencing for mixed pulmonary infection diagnosis	Jiahui Wang	Jing Feng	2019	BMC PULM MED	3.320	57
Metagenomic Next-Generation Sequencing of Nasopharyngeal Specimens Collected from Confirmed and Suspect COVID-19 Patients	Mostafa HH	Simner PJ	2020	MBIO	7.786	57
Viral Surveillance in Serum Samples From Patients With Acute Liver Failure By Metagenomic Next-Generation Sequencing	Somasekar S	C.Y. Chiu	2017	CLIN INFECT DIS	20.999	54

TABLE 2 Top 10 cited and co-cited journals that published studies in this topic.

Cited Journal	Total citation	Impact factor (2022)	Co-cited journal	Total citation	Impact factor (2022)
Frontiers in Cellular and Infection Microbiology	222	6.073	*Clinical Infectious Disease*	604	20.999
Frontiers in Medicine	28	5.058	*Journal of Clinical Microbiology*	390	11.677
Infection and Drug Resistance	63	4.177	*New England Journal of Medicine*	288	176.079
BMC Infectious Diseases	146	3.667	*PLoS One*	241	3.752
Frontiers in Microbiology	140	6.064	*Journal of Infection*	203	38.637
International Journal of Infectious Diseases	115	12.074	*Bioinformatics*	181	6.931
Journal of Clinical Microbiology	276	11.677	*Frontiers in Cellular and Infection Microbiology*	162	6.073

(Continued)

TABLE 2 Continued

Cited Journal	Total citation	Impact factor (2022)	Co-cited journal	Total citation	Impact factor (2022)
Annals of Translational Medicine	19	3.616	*BMC Infectious Diseases*	159	3.667
BMC Pulmonary Medicine	81	3.320	*American Journal of Respiratory and Critical Care Medicine*	122	30.528
PLoS One	240	3.752	*Clinical Microbiology and Infection*	136	13.310

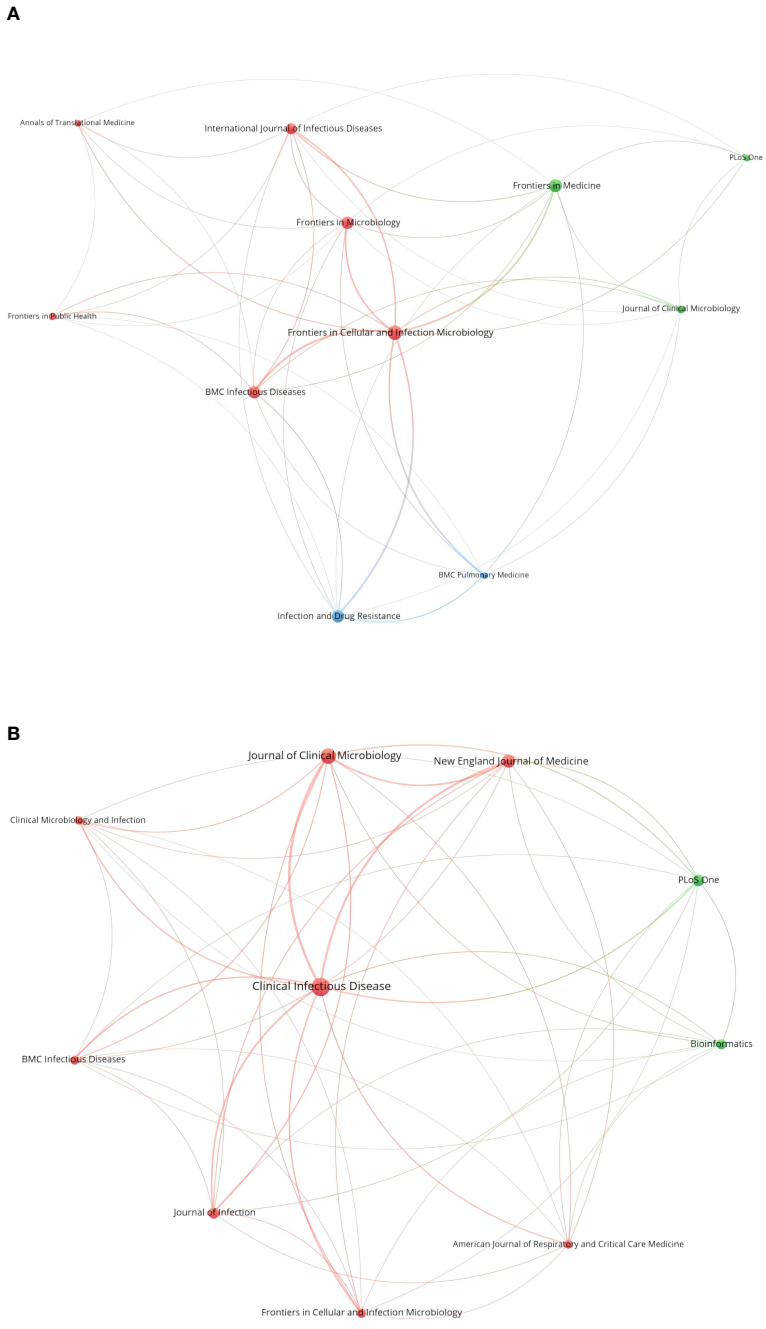

FIGURE 4
Collaborative network of the top 10 cited journals **(A)** and the top 10 co-cited journals **(B)**.

TABLE 3 Top 9 countries of the studies in mNGS (published at least 2 studies).

Country	Number of publication	Total citation	Average citation
People R China	249	2210	8.9
USA	43	1996	46.4
France	6	64	10.7
India	4	7	1.8
Netherlands	4	33	8.3
Japan	2	14	7
Switzerland	2	9	4.5
England	2	250	125
Vietnam	2	15	7.5

sequencing" and "Virus" were listed as the top 4 keywords with citation bursts of more than 3.50. The trend of some screened keywords and shows that some of them have been constantly heated thus far, such as genome and virus, while some of them have been focused on in recent years and can be considered as frontiers in the field, such as "children" (2017-2020), "meningoencephalitis" (2019-2020), "Mycobacterium tuberculosis (2019-2020)" and "cerebrospinal fluid (2019-2020)". There are similarities between hotspots and frontiers.

4 Discussion

Pathogenic infection is a leading cause of disease and remains a severe problem for public health, which is involved in more than 20% of deaths per year globally (GBD 2019 Antimicrobial Resistance Collaborators, 2022). To accurately identify pathogens and precisely treat the disease, mNGS was initiated at the right moment. The utility of mNGS in providing clinically actionable information was first approved in a 14-year-old boy with *neuroleptospirosis* in 2014 (Wilson et al., 2014). At present, an increasing number of clinical cohort studies and case reports have confirmed the value of mNGS in pathogen diagnosis (Chiu and Miller, 2019; Li et al., 2021). However, the studies on mNGS are mostly comprised of case reports and cohort studies. To the best of our knowledge, this is the first bibliometric analysis focused on mNGS in pathogen detection.

4.1 General information

The number of publications significantly increased since 2014. After the first clinical use, a large number of cases have been diagnosed using the new tool, and as a result, more studies were published. In addition to pathogen diagnosis, the use of mNGS in other fields also contributed to the increasing number of publications, such as the surveillance of antimicrobial resistance in the food supply (Oniciuc et al., 2018), prediction of the cause of infection, and evaluation of risk (Gliddon et al., 2018; Langelier et al., 2018). The total citations had a similar trend to the publications. However, there are some fluctuations that may be caused by some extremely highly cited studies in certain years. The classification of the study types revealed that researchers mainly focus on the utility of mNGS in some notable cases and assess the diagnostic performance in some infectious diseases via cohort studies, such as TB and meningitis. With the large number of original articles, some reviews and meta-analysis will be published to summarize the development or efficacy of mNGS in the future.

The studies were mostly published in journals related to general and integrative medicine (*Frontiers in Medicine*, *Annals of Translational Medicine*) and infectious diseases (*Frontiers in Cellular and Infection Microbiology*, *Infection and Drug Resistance*, *BMC Infectious Diseases*). This illustrates that the application of mNGS is currently limited in infectious diseases now. *Frontiers in Cellular and Infection Microbiology* was the most popular cited journal, and also ranked 6th in the co-cited journals, which means it is vital in this field. *Clinical Infectious Diseases* ranked first in co-cited journals with high IF (20.999). The average IF of the top 10 popular journals was 5.948 and that of the top 10 co-cited journals was 31.165. More articles can be published in more fields in the future based on these high-quality references.

Our study showed that the publications are from many countries. However, People R China and the USA showed such a powerful influence that publications from People R China accounted for approximately 70% of the total. This may be related to the

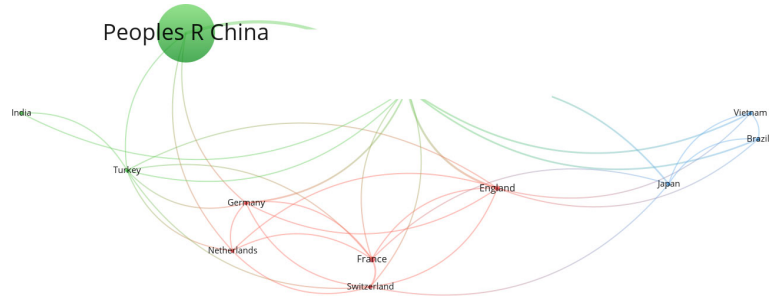

FIGURE 5
Collaborative network of the top 12 countries.

TABLE 4 Top 8 institutions of corresponding authors (published at least 10 studies).

Institution	Country	Number of publication
Zhejiang University	People R China	20
Fudan University	People R China	14
Fujian Medical University	People R China	11
Tianjin Medical University	People R China	11
Zhengzhou University	People R China	11
Central South University	People R China	10
Sun Yat Sen University	People R China	10
University of California, San Diego	USA	10

epidemiology in China. Although China has achieved great economic, public health, and healthcare development after the Severe Acute Respiratory Syndrome outbreak in 2003, there are still various infectious diseases (Lu et al., 2016; Liu et al., 2018). Second, owing to the complex ecological environment, the spectrum of pathogens is broad and includes many rare pathogens. Since mNGS is effective for pathogen identification and can aid doctors in rapid and accurate diagnosis, it has attracted a great deal of attention with plenty of literature published in China. The USA is the birthplace of mNGS for pathogen detection and has lead to extensive cohort studies to examine the efficacy. Furthermore, the USA and People R China have a strong relationship in cooperation with other countries. It can be speculated that mNGS is widely clinically applied in China, and the basic molecular mechanism has been studied extensively in the USA. Additionally, according to the average citations, England ranked the top. The study published in 2009 by Adams et al. from England was the first study to detect pathogens using mNGS in the world with 244 citations, which lead to the highest average citations of England (Adams et al., 2009). With the effort of many countries, mNGS can be improved for better application.

Considering the research institutions, Zhejiang University, Fudan University, and BGI in China contributed significantly to this field, while the University of California San Francisco in the USA also played a key role. It can be concluded that collaboration among authors is relatively fixed and independent. This is possibly because mNGS is used for detecting rare pathogens, which are distributed regionally, such as *leishmaniasis* in the central and western regions of China (Tang et al., 2022), hepatic *echinococcosis* in cattle-producing areas, and Dengue fever in tropical areas (Ren et al., 2022). Furthermore, mNGS is still in the development stage and there is currently no deep cross-team collaboration at the moment, and different teams have different research focuses. However, the lack of communication and cooperation among institutions certainly limited the development in this field. Therefore, the exchanges of research findings and more cooperation are essential and the academic barriers should be reduced to promote the development of mNGS.

Based on the results of author analysis, authors from China occupy the vast majority, which is similar to the distribution of

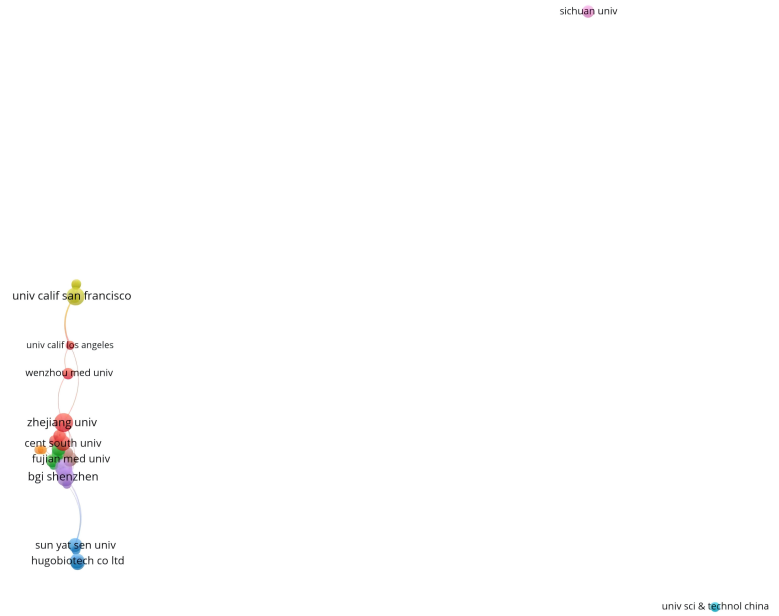

FIGURE 6
Collaborative network of institutions (published more than 5 articles).

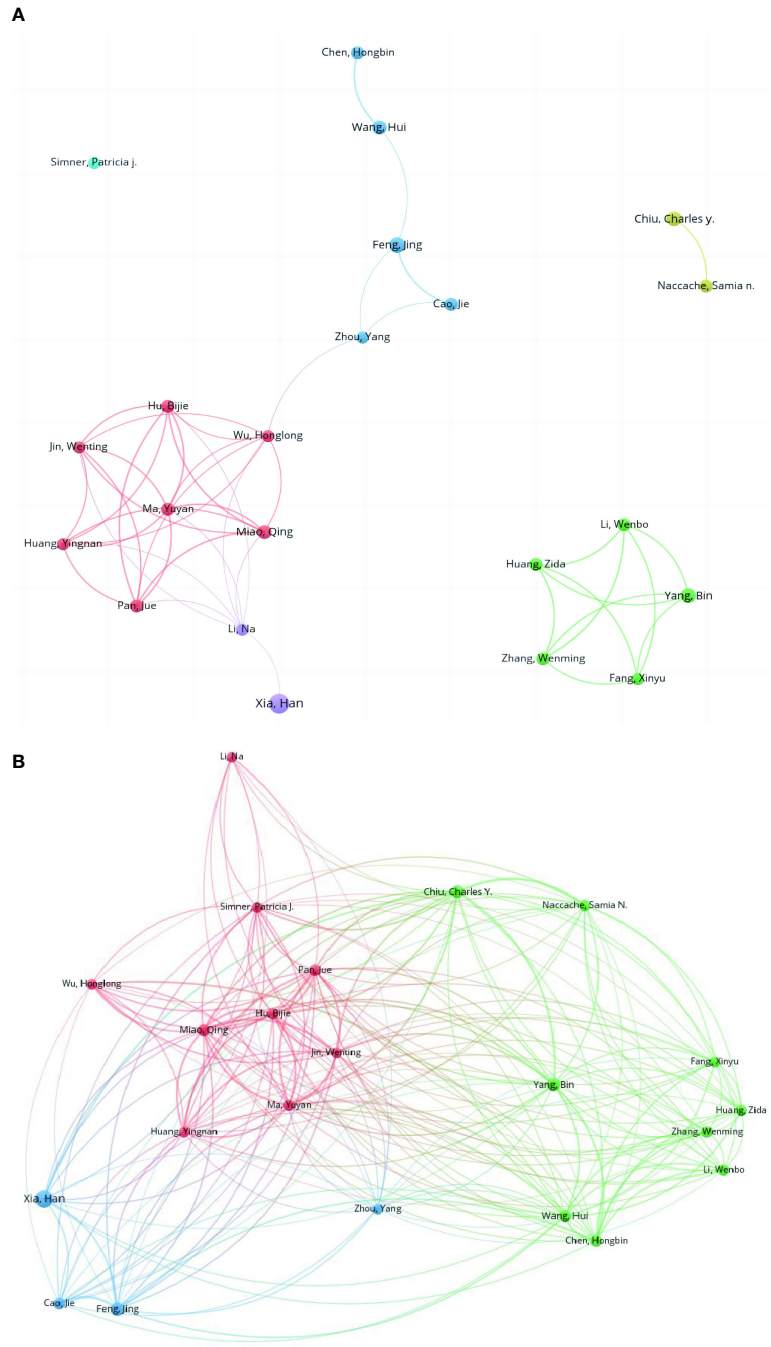

FIGURE 7
Collaborative network of the co-authorship **(A)** and co-citation relationships of authors **(B)**.

countries and institutions. Xia Han from Hugobiotech is the most productive with 14 publications, followed by Feng Jing from Beijing Chaoyang Hospital with 9. Chiu Charles from the University of California San Francisco is one the most influential researches in this field. He is the corresponding author of the first case report of mNGS by Wilson et al. which was published in *New England Journal of Medicine* as a milestone. Then, a clinical trial investigating the detection efficacy of mNGS in body fluids was published in *Nature Medicine* with a high IF (87.241) and citation (Gu et al., 2021).

4.2 Hotspots and frontiers

Keywords can reflect the core contents and topics of the studies. Through the keyword analysis, the results showed that pneumonia, tuberculosis, central nervous system (CNS) infection, and children had a high frequency or upwards trend.

4.2.1 Pneumonia

Pneumonia is one of the most common disease manifestations in respiratory infection and the leading cause of death, especially

TABLE 5 Top 22 corresponding authors of the publications (published at least 5 studies).

Name	Number of publications	Institution	Country
Han Xia	14	Hugobiotech	People R China
Jing Feng	9	Department of Ophthalmology, Beijing Chaoyang Hospital, Capital Medical University	People R China
Charles Y Chiu.	8	Department of Laboratory Medicine, University of California San Francisco	USA
Bin Yang	8	Department of Laboratory Medicine, The First Affiliated Hospital of Fujian Medical University	People R China
Qing Miao	7	Department of Infectious Diseases, Zhongshan Hospital, Fudan University	People R China
Hui Wang	7	Department of Ophthalmology, Beijing Chaoyang Hospital, Capital Medical University	People R China
Jie Cao	6	Department of Respiratory and Critical Care Medicine, Tianjin Medical University General Hospital	People R China
Hongbin Chen	6	Department of Clinical Laboratory, Peking University People's Hospital	People R China
Bijie Hu	6	Department of Infectious Diseases, Zhongshan Hospital, Fudan University	People R China
Zida Huang	6	Department of Orthopaedic Surgery, The First Affiliated Hospital of Fujian Medical University	People R China
Wenbo Li	6	Department of Orthopaedic Surgery, The First Affiliated Hospital of Fujian Medical University	People R China
Yuyuan Ma	6	Department of Infectious Diseases, Zhongshan Hospital, Fudan University	People R China
Samia N Naccache.	6	Department of Laboratory Medicine, University of California, San Francisco	USA
Jue Pan	6	Department of Infectious Diseases, Zhongshan Hospital of Fudan University	People R China
Wenming Zhang	6	Department of Orthopaedic Surgery, The First Affiliated Hospital of Fujian Medical University	People R China
Xinyu Fang	5	Department of Orthopedic Surgery, First Affiliated Hospital of Fujian Medical University	People R China
Yingnan Huang	5	Department of Infectious Diseases, Zhongshan Hospital, Fudan University	People R China
Wenting Jin	5	Department of Infectious Diseases, Zhongshan Hospital, Fudan University	People R China
Na Li	5	Department of Respiratory and Critical Care Medicine, The Second Affiliated Hospital of Chongqing Medical University	People R China
Patricia J Simner	5	Department of Pathology, Johns Hopkins University School of Medicine	USA
Honglong Wu	5	BGI PathoGenesis Pharmaceutical Technology,	People R China
Yang Zhou	5	BGI PathoGenesis Pharmaceutical Technology	People R China

community acquired pneumonia (Biscevic-Tokic et al., 2013; Wunderink and Waterer, 2017; Wang et al., 2022). Since a variety of pathogens can cause pneumonia and some of the symptoms are nonspecific, the detection rate of traditional culture combined with clinical experience is still low and ineffective (Schlaberg et al., 2017; Zhu et al., 2018). mNGS has shown better diagnostic efficiency for pneumonia and other respiratory system infections (Hogan et al., 2021; Zhan et al., 2021). Chen et al. demonstrated that mNGS had high diagnostic accuracy in bronchoalveolar lavage fluid (BALF) with 78% sensitivity and 77% specificity (Chen et al., 2022). In a

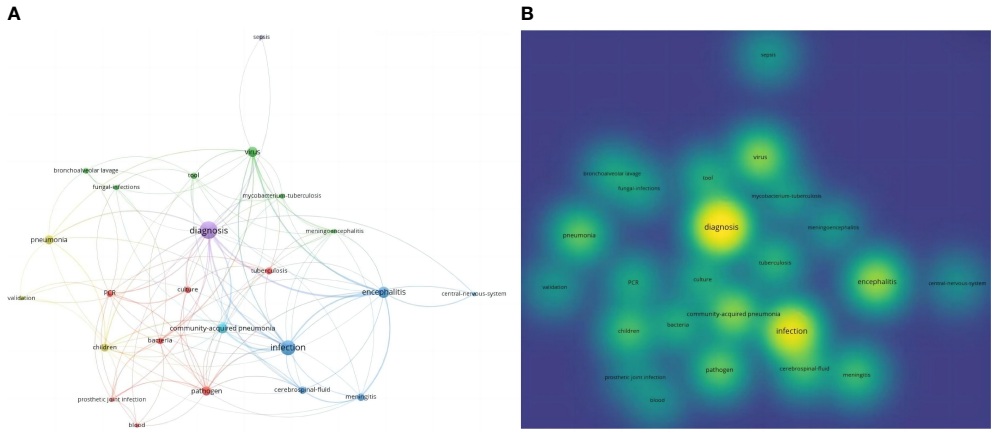

FIGURE 8
Cooccurrence network of key words **(A)** and cooccurrence density map of keywords **(B)**.

retrospective study focused on mixed respiratory infection cases, compared with the conventional method, the sensitivity was significantly higher (97.2% vs 13.9%, $p < 0.001$). However, the specificity was the opposite (63.2% vs 94.7%; $p = 0.07$) (Wang et al., 2019). Besides, the prevalence of coronavirus disease 2019 (COVID-19) has also contributed to making pneumonia a hotspot in recent years. This novel coronavirus was identified by RNA-based mNGS and the genome was revealed to provide insights for future research (Chen et al., 2020a). Additionally, acute respiratory distress syndrome (ARDS) in severe pneumonia, such as COVID-19, is critical and rapidly progresses, resulting in high morality and poor prognosis for survivors (Griffiths et al., 2019). mNGS is confirmed to be a valuable tool to improve the management of ARDS and provide better quality of life for survivors (Zhang et al., 2020). In summary, mNGS is a promising technique to detect pathogens in pneumonia and other respiratory infections.

4.2.2 Tuberculosis

Similar to pneumonia, TB caused by MTB is another hot topic in mNGS. MTB diagnosis has been a challenge for decades. Because of the specific biological properties of MTB, the positive rate of culture is low and takes a long time (Wang et al., 2020; Floyd et al., 2022). Thus, the diagnosis of TB is a problem that usually leads to TB-related death. mNGS was tested in pulmonary TB and showed outstanding performance in diagnosis with high sensitivity and specificity (Chen et al., 2020b). In addition, the multiorgan lesions also contribute to diagnosis difficulty, especially extrapulmonary TB (EPTB) (Suárez et al., 2019). Pang et al. revealed that the positive rate for EPTB by traditional tests was only 12.8% (Pang et al., 2019). A retrospective study in China assessed the clinical efficacy of mNGS in EPTB diagnosis and found that the positive rate was significantly higher than other routine methods ($p < 0.001$). Another meta-analysis also proved that mNGS is more effective than traditional tests in TB meningitis (Yu et al., 2020). However,

Keywords	Year	Strength	Begin	End	2009 - 2022
Genome	2009	4.01	**2009**	2020	
Dengue virus	2014	1.34	**2014**	2017	
Encephaliti	2017	3.73	**2017**	2020	
Next-generation sequencing	2015	3.69	**2015**	2020	
Virus	2009	3.52	**2015**	2020	
Children	2017	1.32	**2017**	2020	
Pathogen	2019	2.78	**2019**	2020	
Meningoencephaliti	2019	1.73	**2019**	2020	
Viral metagenomics	2018	1.7	**2018**	2020	
Mycobacterium tuberculosis	2019	1.46	**2019**	2020	
Epstein barr virus	2019	1.3	**2019**	2020	
Periprosthetic joint infection	2019	1.3	**2019**	2020	
Cerebrospinal fluid	2019	1.3	**2019**	2020	
Fever	2018	1.13	**2018**	2020	

FIGURE 9
The trend of screened key words.

the detection threshold and the efficacy in TB-related coinfection are still controversial and deserve further research (Shi et al., 2020). All of the evidence indicated that mNGS is a potential resolution for TB diagnosis and more research is necessary in the future.

4.2.3 CNS infection

CNS infections are life-threatening, usually resulting in poor prognosis (Yu et al., 2022). Because of the lack of specificity in clinical presentation and cerebrospinal fluid (CSF) parameters, as well as the low pathogen content in CSF, diagnosis remains a challenge (Leonard, 2017; Yu et al., 2022). Although the utility of mNGS matures in some samples such as blood and BALF, it remains unclear whether mNGS has better diagnostic efficiency in CSF. A meta-analysis focused on mNGS for bacterial meningoencephalitis elucidated that the diagnostic efficacy is satisfactory with an estimated AUC (area under curve) of the summary receiver operating characteristic curve of 0.91 (Kanaujia et al., 2022). However, since available evidence is divided and limited, more cohort studies or meta-analysis are expected to eliminate the discrepancy and present more comprehensive and reliable conclusions (Chen et al., 2021).

4.2.4 Children

For children or pediatrics, it is considered another frontier. Infectious disease is the leading cause of death in children, especially those under 5 years old. Because of the various pathogens, occult onset, atypical clinical symptoms, and rapid progression, pediatric infection is difficult to diagnose. Timely and accurate tools are necessary for the selection of effective medical interventions to improve the prognosis (Tao et al., 2022). Many studies elucidated that mNGS can provide useful information for suspected cases and identify infection or noninfection (Yan et al., 2021; Tao et al., 2022). Nowadays, large number of case report have demonstrated the successful use of mNGS in pediatric infection. However, the overall diagnostic performance has not been validated, which is worth illustrating in the future studies.

Summarily, all the hotspots and frontiers indicate that mNGS is a potential test and can be widely used.

4.3 Highlights and limitations

This bibliometric analysis presents the status of mNGS in pathogen detection, including journals, countries, contributors, institutions, research hotspots, and frontiers via data visualization, and the studies in this field can be rapidly accessed from the Supplementary Material. Scholars in the field can quickly understand the status by reading this study and contribute more to this field.

Our study has some limitations. First, the citation analysis was based on the Web of Science Core Collection, which might have missed some important literature indexed by other databases, such as Google Scholar and Scopus, resulting in biased results. Second, we used an accurate title search which means that a small number of publications that did not mention metagenomic next-generation sequencing may not have been included. Third, since bibliometrics includes several secondary studies (such as reviews), the keywords and research focus of the secondary research may be different from those of the original studies, which may also lead to bias. In addition, due to the purpose of the study, we can only describe the overview of this research field without a detailed mechanism.

5 Conclusion

In conclusion, this study determined that mNGS has become a current research hotspot and related research has grown exponentially. This study shows the research hotspots in mNGS, research institutions, and researchers of most related research that can provide useful references for workers in infectious diseases in the future.

Data availability statement

The original contributions presented in the study are included in the article/Supplementary Material. Further inquiries can be directed to the corresponding authors.

Author contributions

Conceptualization, YX. Methodology, SH, JW, JF. Software, SH, JW. Formal Analysis, YX, DL. Writing – Original Draft Preparation, SH. Writing – Review and Editing, YX, LC. All authors contributed to the article and approved the submitted version.

Acknowledgments

We thank all the authors who contributed to this article.

Conflict of interest

The authors declare that the research was conducted in the absence of any commercial or financial relationships that could be construed as a potential conflict of interest.

Publisher's note

Supplementary material

The Supplementary Material for this article can be found online at: https://www.frontiersin.org/articles/10.3389/fcimb.2023.1112229/full#supplementary-material

SUPPLEMENTARY TABLE 1
The 325 studies from the Web of Science Core Collection.

References

Adams, I. P., Glover, R. H., Monger, W. A., Mumford, R., Jackeviciene, E., Navalinskiene, M., et al. (2009). Next-generation sequencing and metagenomic analysis: a universal diagnostic tool in plant virology. *Mol. Plant Pathol.* 10, 537–545. doi: 10.1111/j.1364-3703.2009.00545.x

Biscevic-Tokic, J., Tokic, N., and Musanovic, A. (2013). Pneumonia as the most common lower respiratory tract infection. *Med. Arch.* 67, 442–445. doi: 10.5455/medarh.2013.67.442-445

Blakeman, K. (2018). Bibliometrics in a digital age: help or hindrance. *Sci. Prog.* 101, 293–310. doi: 10.3184/003685018X15337564592469

Calabrò, G. E., D'Ambrosio, F., Fallani, E., and Ricciardi, W. (2022). Influenza vaccination assessment according to a value-based health care approach. *Vaccines (Basel)* 10, 1675. doi: 10.3390/vaccines10101675

Carbo, E. C., Blankenspoor, I., Goeman, J. J., Kroes, A. C. M., Claas, E. C. J., and De Vries, J. J. C. (2021). Viral metagenomic sequencing in the diagnosis of meningoencephalitis: a review of technical advances and diagnostic yield. *Expert Rev. Mol. Diagn.* 21, 1139–1146. doi: 10.1080/14737159.2021.1985467

Chen, S., Kang, Y., Li, D., and Li, Z. (2022). Diagnostic performance of metagenomic next-generation sequencing for the detection of pathogens in bronchoalveolar lavage fluid in patients with pulmonary infections: Systematic review and meta-analysis. *Int. J. Infect. Dis.* 122, 867–873. doi: 10.1016/j.ijid.2022.07.054

Chen, L., Liu, W., Zhang, Q., Xu, K., Ye, G., Wu, W., et al. (2020a). RNA based mNGS approach identifies a novel human coronavirus from two individual pneumonia cases in 2019 Wuhan outbreak. *Emerg. Microbes Infect.* 9, 313–319. doi: 10.1080/22221751.2020.1725399

Chen, P., Sun, W., and He, Y. (2020b). Comparison of metagenomic next-generation sequencing technology, culture and GeneXpert MTB/RIF assay in the diagnosis of tuberculosis. *J. Thorac. Dis.* 12, 4014–4024. doi: 10.21037/jtd-20-1232

Chen, J., Zhang, R., Liu, L., Qi, T., Wang, Z., Song, W., et al. (2021). Clinical usefulness of metagenomic next-generation sequencing for the diagnosis of central nervous system infection in people living with HIV. *Int. J. Infect. Dis.* 107, 139–144. doi: 10.1016/j.ijid.2021.04.057

Chiu, C. Y., and Miller, S. A. (2019). Clinical metagenomics. *Nat. Rev. Genet.* 20, 341–355. doi: 10.1038/s41576-019-0113-7

Duan, H., Li, X., Mei, A., Li, P., Liu, Y., Li, X., et al. (2021). The diagnostic value of metagenomic next-generation sequencing in infectious diseases. *BMC Infect. Dis.* 21, 62. doi: 10.1186/s12879-020-05746-5

Esposito, S. (2016). Infectious diseases: pathophysiology, diagnostics and prevention. *Int. J. Mol. Sci.* 17, E1464. doi: 10.3390/ijms17091464

Feijoo, J. F., Limeres, J., Fernández-Varela, M., Ramos, I., and Diz, P. (2014). The 100 most cited articles in dentistry. *Clin. Oral. Investig.* 18, 699–706. doi: 10.1007/s00784-013-1017-0

Floyd, S., Klinkenberg, E., de Haas, P., Kosloff, B., Gachie, T., Dodd, P. J., et al. (2022). Optimising Xpert-Ultra and culture testing to reliably measure tuberculosis prevalence in the community: findings from surveys in Zambia and South Africa. *BMJ Open* 12, e058195. doi: 10.1136/bmjopen-2021-058195

GBD 2019 Antimicrobial Resistance Collaborators (2022). Global mortality associated with 33 bacterial pathogens in 2019: a systematic analysis for the Global Burden of Disease Study 2019. *Lancet* 400, 2221–2248. doi: 10.1016/S0140-6736(22)02185-7

Gliddon, H. D., Herberg, J. A., Levin, M., and Kaforou, M. (2018). Genome-wide host RNA signatures of infectious diseases: discovery and clinical translation. *Immunology* 153, 171–178. doi: 10.1111/imm.12841

Griffiths, M. J. D., McAuley, D. F., Perkins, G. D., Barrett, N., Blackwood, B., Boyle, A., et al. (2019). Guidelines on the management of acute respiratory distress syndrome. *BMJ Open Respir. Res.* 6, e000420. doi: 10.1136/bmjresp-2019-000420

Gu, W., Deng, X., Lee, M., Sucu, Y. D., Arevalo, S., Stryke, D., et al. (2021). Rapid pathogen detection by metagenomic next-generation sequencing of infected body fluids. *Nat. Med.* 27, 115–124. doi: 10.1038/s41591-020-1105-z

Gu, W., Miller, S., and Chiu, C. Y. (2019). Clinical metagenomic next-generation sequencing for pathogen detection. *Annu. Rev. Pathol.* 14, 319–338. doi: 10.1146/annurev-pathmechdis-012418-012751

Han, D., Li, Z., Li, R., Tan, P., Zhang, R., and Li, J. (2019). mNGS in clinical microbiology laboratories: on the road to maturity. *Crit. Rev. Microbiol.* 45, 668–685. doi: 10.1080/1040841X.2019.1681933

Hogan, C. A., Yang, S., Garner, O. B., Green, D. A., Gomez, C. A., Dien Bard, J., et al. (2021). Clinical impact of metagenomic next-generation sequencing of plasma cell-free DNA for the diagnosis of infectious diseases: A multicenter retrospective cohort study. *Clin. Infect. Dis.* 72, 239–245. doi: 10.1093/cid/ciaa035

Jia, X., Hu, L., Wu, M., Ling, Y., Wang, W., Lu, H., et al. (2021). A streamlined clinical metagenomic sequencing protocol for rapid pathogen identification. *Sci. Rep.* 11, 4405. doi: 10.1038/s41598-021-83812-x

Kanaujia, R., Biswal, M., Angrup, A., and Ray, P. (2022). Diagnostic accuracy of the metagenomic next-generation sequencing (mNGS) for detection of bacterial meningoencephalitis: a systematic review and meta-analysis. *Eur. J. Clin. Microbiol. Infect. Dis.* 41, 881–891. doi: 10.1007/s10096-022-04445-0

Kherabi, Y., Tunesi, S., Kay, A., and Guglielmetti, L. (2022). Preventive therapy for contacts of drug-resistant tuberculosis. *Pathogens* 11, 1189. doi: 10.3390/pathogens11101189

Langelier, C., Kalantar, K. L., Moazed, F., Wilson, M. R., Crawford, E. D., Deiss, T., et al. (2018). Integrating host response and unbiased microbe detection for lower respiratory tract infection diagnosis in critically ill adults. *Proc. Natl. Acad. Sci. U.S.A.* 115, E12353–E12362. doi: 10.1073/pnas.1809700115

Leonard, J. M. (2017). Central nervous system tuberculosis. *Microbiol. Spectr.* 5. doi: 10.1128/microbiolspec.TNMI7-0044-2017

Li, N., Cai, Q., Miao, Q., Song, Z., Fang, Y., and Hu, B. (2021). High-throughput metagenomics for identification of pathogens in the clinical settings. *Small Methods* 5, 2000792. doi: 10.1002/smtd.202000792

Liu, Q., Xu, W., Lu, S., Jiang, J., Zhou, J., Shao, Z., et al. (2018). Landscape of emerging and re-emerging infectious diseases in China: impact of ecology, climate, and behavior. *Front. Med.* 12, 3–22. doi: 10.1007/s11684-017-0605-9

Lu, J., Milinovich, G. J., and Hu, W. (2016). A brief historical overview of emerging infectious disease response in China and the need for a One Health approach in future responses. *One Health* 2, 99–102. doi: 10.1016/j.onehlt.2016.07.001

Mancuso, G., Midiri, A., Gerace, E., and Biondo, C. (2021). Bacterial antibiotic resistance: the most critical pathogens. *Pathogens* 10, 1310. doi: 10.3390/pathogens10101310

McArthur, D. B. (2019). Emerging infectious diseases. *Nurs. Clin. North Am.* 54, 297–311. doi: 10.1016/j.cnur.2019.02.006

Oniciuc, E. A., Likotrafiti, E., Alvarez-Molina, A., Prieto, M., Santos, J. A., and Alvarez-Ordóñez, A. (2018). The present and future of whole genome sequencing (WGS) and whole metagenome sequencing (WMS) for surveillance of antimicrobial resistant microorganisms and antimicrobial resistance genes across the food chain. *Genes (Basel)* 9, E268. doi: 10.3390/genes9050268

Pang, Y., An, J., Shu, W., Huo, F., Chu, N. , Gao, M., et al. (2019). Epidemiology of extrapulmonary tuberculosis among inpatients, China 2008-2017. *Emerg. Infect. Dis.* 25, 457–464. doi: 10.3201/eid2503.180572

Ren, Z.-Z., Zheng, Y., Sun, T., Wang, G.-Y., Chen, X.-M., and Zhou, Y.-M. (2022). A survey of clinical and laboratory characteristics of the dengue fever epidemic from 2017 to 2019 in Zhejiang, China. *Med. (Baltimore)* 101, e31143. doi: 10.1097/MD.0000000000031143

Schäfer, S. K., Kunzler, A. M., Kalisch, R., Tüscher, O., and Lieb, K. (2022). Trajectories of resilience and mental distress to global major disruptions. *Trends Cognit. Sci.* 1171–1189. doi: 10.1016/j.tics.2022.09.017.

Schlaberg, R., Chiu, C. Y., Miller, S., Procop, G. W., Weinstock, G.Professional Practice Committee and Committee on Laboratory Practices of the American Society for Microbiology, et al. (2017). Validation of metagenomic next-generation sequencing tests for universal pathogen detection. *Arch. Pathol. Lab. Med.* 141, 776–786. doi: 10.5858/arpa.2016-0539-RA

Shi, C.-L., Han, P., Tang, P.-J., Chen, M.-M., Ye, Z.-J., Wu, M.-Y., et al. (2020). Clinical metagenomic sequencing for diagnosis of pulmonary tuberculosis. *J. Infect.* 81, 567–574. doi: 10.1016/j.jinf.2020.08.004

Simner, P. J., Miller, S., and Carroll, K. C. (2018). Understanding the promises and hurdles of metagenomic next-generation sequencing as a diagnostic tool for infectious diseases. *Clin. Infect. Dis.* 66, 778–788. doi: 10.1093/cid/cix881

Suárez, I., Fünger, S. M., Kröger, S., Rademacher, J., Fätkenheuer, G., and Rybniker, J. (2019). The diagnosis and treatment of tuberculosis. *Dtsch Arztebl Int.* 116, 729–735. doi: 10.3238/arztebl.2019.0729

Tang, C., He, S., Wang, N., and Chen, L. (2022). A case report and literature review: diagnosis and treatment of human immunodeficiency virus coinfected with visceral leishmania by metagenomic next-generation sequencing in China. *Ann. Transl. Med.* 10, 497. doi: 10.21037/atm-22-1351

Tang, H., Huang, W., Ma, J., and Liu, L. (2018). SWOT analysis and revelation in traditional Chinese medicine internationalization. *Chin. Med.* 13, 5. doi: 10.1186/s13020-018-0165-1

Tao, Y., Yan, H., Liu, Y., Zhang, F., Luo, L., Zhou, Y., et al. (2022). Diagnostic performance of metagenomic next-generation sequencing in pediatric patients: A retrospective study in a large children's medical center. *Clin. Chem.* 68, 1031–1041. doi: 10.1093/clinchem/hvac067

Vitiello, A. (2022). Sars-Cov-2 and risk of antiviral drug resistance. *Ir J. Med. Sci.* 191, 2367–2368. doi: 10.1007/s11845-021-02820-y

Wang, J., Han, Y., and Feng, J. (2019). Metagenomic next-generation sequencing for mixed pulmonary infection diagnosis. *BMC Pulm Med.* 19, 252. doi: 10.1186/s12890-019-1022-4

Wang, W.-H., Takeuchi, R., Jain, S.-H., Jiang, Y.-H., Watanuki, S., Ohtaki, Y., et al. (2020). A novel, rapid (within hours) culture-free diagnostic method for detecting live Mycobacterium tuberculosis with high sensitivity. *EBioMedicine* 60, 103007. doi: 10.1016/j.ebiom.2020.103007

Wang, D., Willis, D. R., and Yih, Y. (2022). The pneumonia severity index: Assessment and comparison to popular machine learning classifiers. *Int. J. Med. Inf.* 163, 104778. doi: 10.1016/j.ijmedinf.2022.104778

Wilson, M. R., Naccache, S. N., Samayoa, E., Biagtan, M., Bashir, H., Yu, G., et al. (2014). Actionable diagnosis of neuroleptospirosis by next-generation sequencing. *N Engl. J. Med.* 370, 2408–2417. doi: 10.1056/NEJMoa1401268

Wunderink, R. G., and Waterer, G. (2017). Advances in the causes and management of community acquired pneumonia in adults. *BMJ* 358, j2471. doi: 10.1136/bmj.j2471

Xie, X., Zhang, N., Fu, J., Wang, Z., Ye, Z., and Liu, Z. (2022). The potential for traditional Chinese therapy in treating sleep disorders caused by COVID-19 through the cholinergic anti-inflammatory pathway. *Front. Pharmacol.* 13. doi: 10.3389/fphar.2022.1009527

Xiong, Y., Wei, J., Cai, Y., Zhang, Y., Feng, L., and Zhang, Y. (2022). Analysis of the research hotspot of drug treatment of tuberculosis: A bibliometric based on the top 50 cited literatures. *BioMed. Res. Int.* 2022, 9542756. doi: 10.1155/2022/9542756

Yan, G., Liu, J., Chen, W., Chen, Y., Cheng, Y., Tao, J., et al. (2021). Metagenomic next-generation sequencing of bloodstream microbial cell-free nucleic acid in children with suspected sepsis in pediatric intensive care unit. *Front. Cell Infect. Microbiol.* 11. doi: 10.3389/fcimb.2021.665226

Yeung, A. W. K., Heinrich, M., and Atanasov, A. G. (2018). Ethnopharmacology-A bibliometric analysis of a field of research meandering between medicine and food science? *Front. Pharmacol.* 9. doi: 10.3389/fphar.2018.00215

Yu, L., Zhang, Y., Zhou, J., Zhang, Y., Qi, X., Bai, K., et al. (2022). Metagenomic next-generation sequencing of cell-free and whole-cell DNA in diagnosing central nervous system infections. *Front. Cell Infect. Microbiol.* 12. doi: 10.3389/fcimb.2022.951703

Yu, G., Zhao, W., Shen, Y., Zhu, P., and Zheng, H. (2020). Metagenomic next generation sequencing for the diagnosis of tuberculosis meningitis: A systematic review and meta-analysis. *PloS One* 15, e0243161. doi: 10.1371/journal.pone.0243161

Zhan, Y., Xu, T., He, F., Guan, W.-J., Li, Z., Li, S., et al. (2021). Clinical evaluation of a metagenomics-based assay for pneumonia management. *Front. Microbiol.* 12. doi: 10.3389/fmicb.2021.751073

Zhang, P., Chen, Y., Li, S., Li, C., Zhang, S., Zheng, W., et al. (2020). Metagenomic next-generation sequencing for the clinical diagnosis and prognosis of acute respiratory distress syndrome caused by severe pneumonia: a retrospective study. *PeerJ* 8, e9623. doi: 10.7717/peerj.9623

Zhang, Y., Quan, L., Xiao, B., and Du, L. (2019). The 100 top-cited studies on vaccine: a bibliometric analysis. *Hum. Vaccin Immunother.* 15, 3024–3031. doi: 10.1080/21645515.2019.1614398

Zhao, X., Guo, L., Lin, Y., Wang, H., Gu, C., Zhao, L., et al. (2016). The top 100 most cited scientific reports focused on diabetes research. *Acta Diabetol.* 53, 13–26. doi: 10.1007/s00592-015-0813-1

Zhu, Y.-G., Tang, X.-D., Lu, Y.-T., Zhang, J., and Qu, J.-M. (2018). Contemporary situation of community-acquired pneumonia in China: A systematic review. *J. Transl. Int. Med.* 6, 26–31. doi: 10.2478/jtim-2018-0006

frontiers | Frontiers in Cellular and Infection Microbiology

TYPE Case Report
PUBLISHED 10 August 2023
DOI 10.3389/fcimb.2023.1214297

OPEN ACCESS

EDITED BY
Jeyaprakash Rajendhran,
Madurai Kamaraj University, India

REVIEWED BY
Tahereh Navidifar,
Ahvaz Jundishapur University of Medical Sciences, Iran
Ruotong Ren,
Matridx Biotechnology Co., Ltd, China

*CORRESPONDENCE
Limei He
helimei_1987@163.com

RECEIVED 29 April 2023
ACCEPTED 17 July 2023
PUBLISHED 10 August 2023

CITATION
Wu Y, Xu X, Liu Y, Jiang X, Wu H, Yang J and He L (2023) Case Report: Clinical analysis of a cluster outbreak of *chlamydia psittaci* pneumonia.
Front. Cell. Infect. Microbiol. 13:1214297.
doi: 10.3389/fcimb.2023.1214297

Case Report: Clinical analysis of a cluster outbreak of *chlamydia psittaci* pneumonia

Yinxia Wu[1], Xuemei Xu[1], Yun Liu[1], Xiangwei Jiang[1], Hongjing Wu[1], Jie Yang[1] and Limei He[2*]

[1]Department of Infectious Diseases, Lishui Municipal Central Hospital, Lishui, Zhejiang, China, [2]Department of Nephrology Diseases, Lishui Municipal Central Hospital, Lishui, Zhejiang, China

Objective: To explore the clinical characteristics and prognosis of clustered cases of psittacosis pneumonia.

Method: We retrospectively analyzed the clinical data of a cluster outbreak of psittacosis pneumonia. The analysis included epidemiological data, clinical symptoms, laboratory results, and prognosis. The diagnosis was made using mNGS and nested PCR technology.

Result: Of the four cases, two had direct contact with diseased poultry while the other two did not. All cases presented with more than 39.5 °C fever and chills. Additionally, significant increases in C-reactive protein, ferritin, creatine kinase, and lactate dehydrogenase were observed in all cases, while absolute lymphocyte count decreased. Case 2 also had increased calcitonin levels. Acute respiratory failure occurred during the treatment of case 1 and case 2, leading to tracheal intubation and ventilator-assisted ventilation. Unfortunately, case 2 passed away due to sepsis and multiple organ dysfunction, while the other cases had a positive prognosis.

Conclusion: mNGS facilitated the early diagnosis of psittacosis pneumonia. It is important to note that there is still a substantial risk of human-to-human transmission in psittacosis pneumonia. Absolute lymphocyte count and calcitonin levels can predict the severity and prognosis of the disease.

KEYWORDS

psittacosis, pneumonia, clustered onset, MNGs, clinical characteristics

Introduction

Chlamydia psittaci is a gram-negative intracellular parasite only found in poultry and known to cause zoonosis (Knittler and Saches, 2015). Parrot fever pneumonia is primarily transmitted through contact with infected birds or their excretions, with the most common cases being associated with parrots and poultry (Balsamo et al., 2017). The use of mNGS technology increased the reported cases of psittacosis pneumonia in recent years, but most

of these cases were solitary instances (Teng et al., 2021), and clustered outbreaks were rarely reported. This article reports 4 cases of a clustered outbreak of *chlamydia psittaci* pneumonia. The cases include 3 members of a single family and another individual who sold ducks to the family. The details of these cases are discussed below.

Basic information about the cases

This study included four cases, consisting of two males and two females aged 42 to 70 years. Case 1 had a history of hypertension and received long-term regular antihypertensive medications, while the other cases had no underlying diseases. None of them had immune system diseases. The onset dates for the cases were August 18th, August 18th, August 27th, and September 4th, 2021, respectively. Hospital stays occurred on August 21, August 28, August 30, and September 5, 2021.

Epidemiological data

Case 1 was a poultry seller who sold ducks to case 2. Case 2, case 3, and case 4 were a family of three (Table 1).

Clinical manifestation

All four cases presented with fever and chills, with the highest body temperature between 39.5 °C and 39.9 °C. Cases 1 and 2 experienced chest tightness and shortness of breath and developed acute respiratory failure on the third day (August 23) and the first day (August 28) after admission, respectively. Both cases underwent tracheal intubation and ventilator-assisted ventilation. Case 3 presented with chills, fatigue, and cough. Case 4 also presented with cough (Table 1).

Physical examination

Four cases came to the hospital with clear consciousness. Cases 1 and 2 received sedatives and analgesics after tracheal intubation, making their consciousness unmeasurable. Case 1 exhibited low breathing sounds in the right lung, coarse breathing sounds in the left lung, and audible moist rales in the left lung. Case 2 had coarse breathing sounds and moist rales in both lungs. Cases 3 and 4 had thick respiratory sounds in both lungs, with moist rales audible in the right lung. Physical examinations of the heart, abdomen, and nervous system in all four cases revealed no abnormalities.

Laboratory and imaging examinations

Both case 1 and case 2 were severe cases. On admission, all cases demonstrated significant elevations in C-reactive protein, ferritin, creatine kinase, and lactate dehydrogenase levels (Table 2). Additionally, absolute lymphocyte count decreased in all cases, with more clear decreases in case 1 and case 2 (Figure 1). Notably, no improvement in absolute lymphocyte count was observed in case 2 (Figure 2). Furthermore, the study found that calcitonin levels progressively increased in case 2, indicating a worsening condition. All cases underwent tests, including bronchoalveolar lavage fluid for acid-fast bacteria, fungal G (1,3β-D glucan) and GM (galactomannans) tests, and tumor marker tests, all of which were negative.

Except for case 2, who underwent bedside chest X-ray examination, all cases underwent chest CT after admission. The results revealed several infectious lesions in both lungs,

TABLE 1 Baseline characteristics and clinical manifestations of patients with Chlamydia psittaci pneumonia.

Case	1	2	3	4
Sex	Female	Male	Female	Male
Age	70	64	63	42
Occupation	Poultry salesperson	Farmer	Farmer	Worker
Past history	Hypertension	None	None	None
Contact history	Poultry (chicken and Ducks)	Purchased ducks from Case 1	Wife of Case 2	Son of Case 2
Time of onset	2021/8/18	2021/8/18	2021/8/27	2021/9/4
Admission time	2021/8/21	2021/8/28	2021/8/30	2021/9/5
Temperature Peak (°C)	39.9	39.8	39.5	39.6
Initial symptoms	Fever Cough	Fever	Fever	Fever
Concomitant symptoms	Chilly sensations blood-tinged sputurm chest tightness Shortness of breath	Cough blood-tinged sputurm chest tightness shortness of breath	Chilly sensations; Feeble; cough	Chilly sensations; dry cough

10.3389/fcimb.2023.1214297

TABLE 2 Laboratory findings in patients with Chlamydia psittaci pneumonia.

Main laboratory indicators	Case1	Case2	Case3	Case4
Serum chemistry				
Alanine aminotransferase, U/L	43	55	11	14
Glutamic oxaloacetic transaminase, U/L	54	59	20	16
Lactic dehydrogenase,U/L	811	696	751	246
Creatine kinase, U/L	888	67	414	128
Creatine kinase isoenzyme, ng/ml	11	14	3.53	15
Serum creatinine, μmol/L	40	193	46	69
Blood urea nitrogen, mmol/L	1.6	16.4	<1	4.4
Uric acid, μmol/L	87	308	106	207
Hypersensitive C-reaction protein,mg/L	302.53	272.42	220.05	36.89
Procalcitonin,ng/ml	0.73	6.35	0.16	0.07
Serum ferritin, ng/ml	>1675.6	>1675.6	327.2	427.6
Erythrocyte sedimentation rate,mm/h	72		108	30
Blood routine				
Leukocyte, 10^9/L	11	12.8	4.2	9
Percentage of neutrophils, %	92.6	96.6	80.4	73.8
Lymphocyte percentage, %	5.5	2.2	14.7	17.3
Absolute value of lymphocytes, 10^9/L	0.6	0.3	0.6	1.6
Erythrocyte,10^{12}/L	3.81	3.13	3.56	5.37
Hemoglobin, g/L	111	98	108	163
Platelet,10^{12}/L	207	185	159	200
Blood Gas Analysis				
PH value	7.474	7.434	7.502	
Partial pressure of carbon dioxide mmHg	32.7	30.5	33.7	
Oxygen partial pressure,mmHg	52.1	50.3	91.4	
Hydrogen carbonate concentration,mmol/L	23.8	20.1	26.2	
Base excess,mEq/L	1.1	-2.8	3.3	
Lactic acid,mmol/L	1.3	3.7	0.7	

predominantly lobular consolidation and atelectasis in the right lung, and slight flocculent and striped changes in the left lung. Pleural effusion was observed in case 1 and case 2. Following one week of treatment, pleural effusion markedly decreased in case 1 and case 2. Additionally, the infected lesions were significantly absorbed in case 3 and case 4 (Figure 3).

Pathogenic examination

All cases underwent mNGS testing on alveolar lavage fluid samples obtained through bronchoscopy. mNGS revealed *chlamydia psittaci* infection. Notably, cases 1 and 2 had higher gene sequence numbers than cases 3 and 4. Additionally, cases 1 and 2 underwent blood mNGS testing, which demonstrated a higher number of mNGS sequences in the alveolar lavage fluid compared to peripheral blood (Table 3). Phylogenetic analysis of genes in a study on disease control in Lishui City indicated that 11 sequences from four cases were closely related and clustered together on the same branch, indicating high homology (Yao et al., 2022).

Treatment and outcome

Case 1 was hospitalized on the third day of onset, while case 2 chose to rest at home and did not seek medical attention. On August 23, case 2 sought medical attention for a pulmonary infection at the

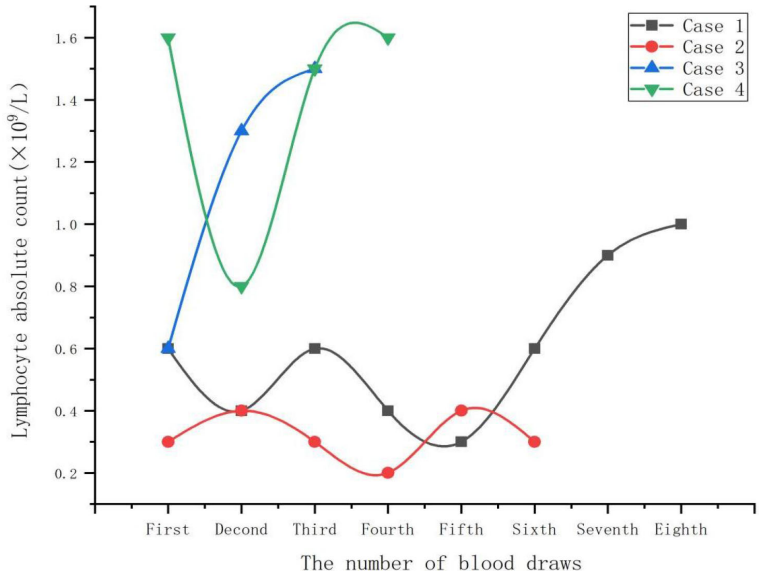

FIGURE 1
Lympocyte absolute count change curve.

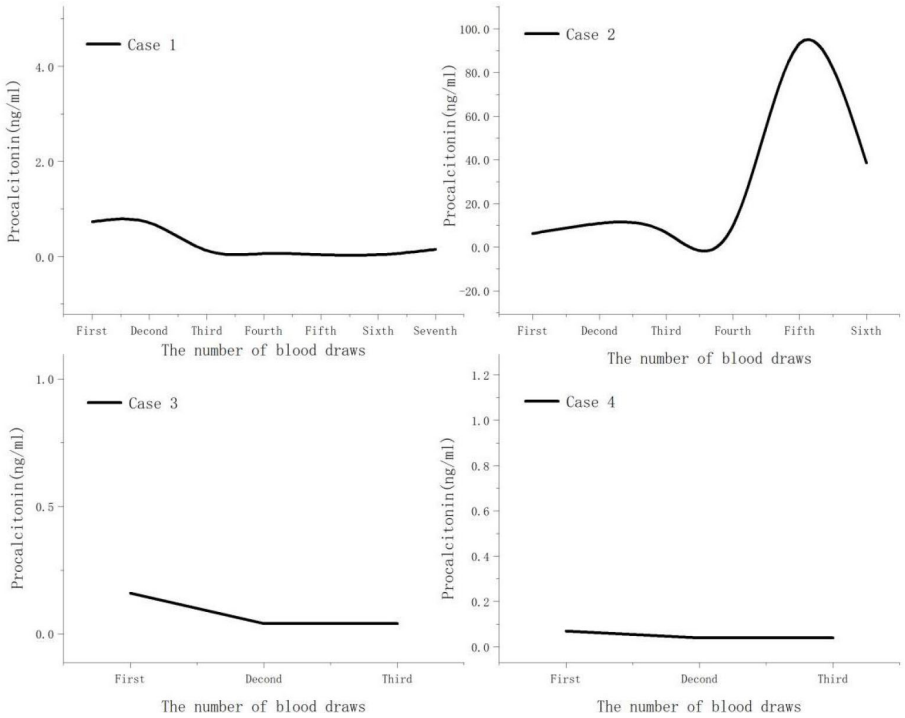

FIGURE 2
Procalcitonin change curve.

local county people's hospital. There, case 2 received ceftazidime 2.0g ivgtt q8h in combination with moxifloxacin 0.4g ivgtt qd for 5 days. On August 28th, case 2 developed new symptoms such as chest tightness, dyspnea, and difficulty breathing. Blood gas analysis revealed decreased blood oxygen saturation, and follow-up chest CT showed an increased number of pulmonary lesions. Therefore, case 2 was transferred to our hospital for further treatment. Both case 3 and case 4 developed symptoms and were directly hospitalized on the 3rd and 1st days of onset, respectively.

All four cases received combined antibacterial therapy with quinolones before their diagnosis. After being diagnosed with mNGS, levofloxacin was switched to azithromycin for case 1,

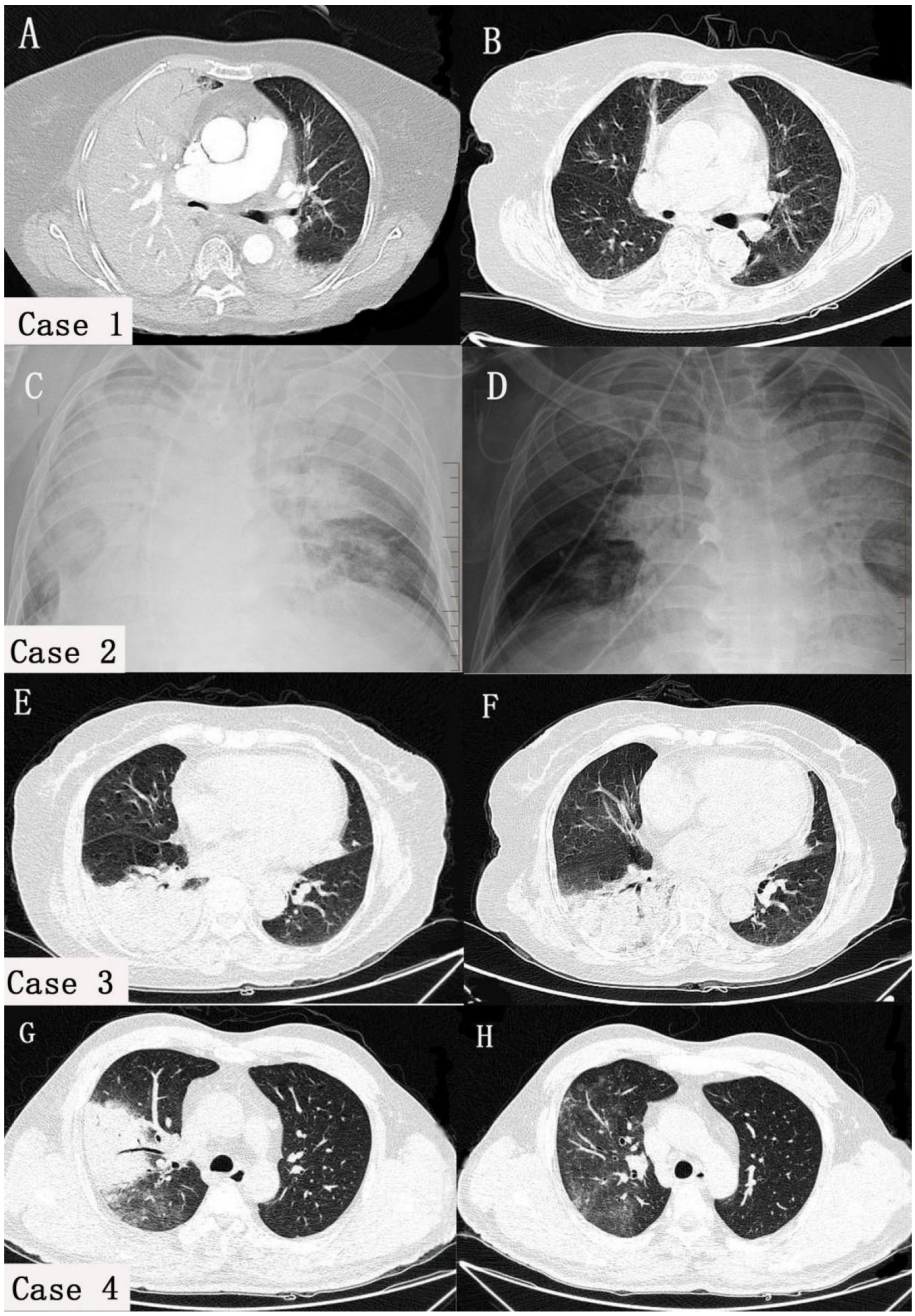

FIGURE 3
Comparison of chest Imaging scans before and after treatment in four cases. In case 1 **(A)** and case 2 **(C)**, both lungs had pleural effusion, atelectasis, and lesions, with the right lung being mainly affected. In cases 3 **(E)** and case 4 **(G)**, consolidation was predominantly observed in the right lung, with a few flocculent and striate changes in the left lung. After treatment, pleural effusion **(B, D)** and lung consolidation **(F, H)** significantly improved in all cases.

moxifloxacin was switched to azithromycin for case 2, no adjustments were considered for case 3, and minocycline was added to moxifloxacin for case 4. Following the changes in the treatment plan, the body temperature of all cases returned to normal the day before and after the change. During treatment, case 2 experienced gastrointestinal bleeding, sepsis, and multiple organ failure, which led to sudden cardiac arrest and subsequent death on September 13. On the other hand, case 1, case 3, and case 4 were discharged from the hospital on September 15, September 10, and September 23, respectively.

Discussion

In 1879, for the first time, J. Ritter reported seven cases of atypical pneumonia caused by Chlamydia psittaci infection (Harris and Williams, 1985). Since then, there have been outbreaks of varying scales in multiple locations. Psittacosis cases are predominantly sporadic, with rare instances of aggregation. Reports of human Psittacosis outbreaks have been documented in European countries, United States, Australia, Japan, and other locations. These outbreaks typically occur in poultry processing

TABLE 3 The mNGS results of BALF in patients with Chlamydia psittaci pneumonia.

	Time from onset to test (d)	Type of specimen	pathogen	Number of sequences	Relative abundance (%)	Type of specimen	pathogen	Number of sequences	Relative abundance (%)
Case1	5d	BALF	C.psittaci	7144	77.32	Blood	C.psittaci	71	64.55
Case2	12d	BALF	C. psittaci	7204	78.96	Blood	C.psittaci	6759	78.84
Case3	6d	BALF	C. psittaci	256	79.89				
Case4	4d	BALF	C.psittaci	4418	54.53				

BALF, Bronchoalveolar lavage fluid; C. psittaci, Chlamydia psittaci.

factories, bird fairs, and pet bird facilities (Hedberg et al., 1989; Hinton et al., 1993; Lederer and Mx Ller, 1999; Tiong et al., 2007; Berk et al., 2008; Matsui et al., 2008; Belchior et al., 2011; Williams et al., 2013). Reports of familial clustering are extremely rare (Bourke et al., 1989; Kaibu et al., 2006; Çiftçi et al., 2008; Boeck et al., 2016). In 2021, during the COVID-19 pandemic, China first reported a family outbreak of human psittacosis (Li et al., 2021), followed by two additional reports of family clusters experiencing the onset of the disease (Xiao et al., 2022; Jing et al., 2023). These reports all referred to parrots as the source of the disease, and patients were family members who had direct contact with the birds. This article discusses cases who got the infection from a duck. The four cases were not from the same family. One of them was a duck vendor, and the others were a family of three. It is worth noting that two members of the family did not have direct contact with the sick duck. Thus, the transmission of pathogens in this study is more complex and warrants further investigation.

Chlamydia psittaci pneumonia is a zoonosis that primarily affects the lungs but can also damage other organs such as the liver, kidney, circulatory system, and central nervous system, thereby leading to multiple organ failure (Zhang et al., 2020). According to statistics, approximately 1.03% (ranging from 0% to 6.7%) of community-acquired pneumonia is caused by Chlamydia psittaci annually (Hogerwerf et al., 2017). However, in countries such as the United States, the United Kingdom, and the Netherlands, pathogenic microorganisms are not typically tracked in uncomplicated common pneumonia (De Gier et al., 2018). This lack of tracking can lead to misdiagnosis and missed diagnoses of parrot fever pneumonia, and ultimately some patients do not receive effective treatment.

Psittacosis is usually transmitted from birds and poultry to humans, mainly through the respiratory tract or direct exposure to birds' excretion (Smith et al., 2011). Recent studies have indicated that chlamydia psittacosis can be isolated from mammals such as cattle and horses, which is also infectious (Lenny et al., 2020). Although interpersonal transmission of psittacosis pneumonia is rare, it is still possible. Researchers in China conducted a study on confirmed cases of psittacosis pneumonia and their close contacts in a hospital in Shandong Province. The study revealed that the epidemic originated from birds and was transmitted to humans, followed by second and third-level human-to-human transmission. The transmission also happened through several asymptomatic carriers and medical staff (Zhang et al., 2022). This study reports the first instance of human-to-human transmission of psittacosis pneumonia in China.

In this article, four cases were discussed. One of them was a duck vendor, and the others were family members who bought the duck. The disease manifested in a short period, with case 1 and case 2 starting on the same day. All four cases were confirmed to be infected with Chlamydia psittaci through alveolar lavage fluid mNGS.

Additionally, the disease control team confirmed the homology of the gene sequences of all four cases through nested PCR. The researchers collected 74 samples, including throat swabs, anal swabs, and poultry drinking water. Of these samples, 8 were positive (Yao et al., 2022). Therefore, the diagnosis of psittacosis was confirmed in all four cases. The disease simultaneously manifested in case 1 and case 2 due to contact with diseased ducks. However, the infection transmission in cases 3 and 4 may have been more complex due to various factors: 1) Case 3 and case 4 did not have direct contact with the infected duck; 2) The symptoms of case 3 and case 4 appeared several days after case 1 and case 2 (9 days later for case 3 and 17 days later for case 4). The incubation period of psittacosis is typically 1-2 weeks (Hogerwerf et al., 2020), and the time interval between the infection of cases 1 and 2 and case 4 exceeded the incubation period; 3) Cases 3 and 4 showed the first symptoms when case 2 was hospitalized. Based on the previous reports of person-to-person transmission of psittacosis, it is highly suspected that the infection was transmitted from case 2 to cases 3 and 4 through the respiratory tract. Case 3 and case 4 were also exposed to the home environment, and the disease control unit also confirmed that the environmental samples were positive. In addition, there are reports that the incubation period of psittacosis can be up to 45 days (Jenkins et al., 2018). Case 3 and case 4 might have been indirectly exposed to the contaminated environment. Further investigation into the infection pathways of these cases is warranted.

Once inhaled into the lung, Chlamydia psittaci enters the bloodstream and infects the macrophages in the liver and spleen (Fraeyman et al., 2010). From there, it spreads to other organs, manifesting with symptoms such as high-grade fever, chills, headaches, myalgia, and dyspnea. In severe cases, it can quickly progress to atypical or severe pneumonia and even affect other organs (Beeckman and Vanrompay, 2009; Cillóniz et al., 2016). In the absence of timely diagnosis or treatment+, the mortality rate can reach up to 10%-20% (Hogerwerf et al., 2017). In this study, all cases began with high-grade fever, with a peak body temperature of ≥39.5 °C. Cases 1 and 2 had noticeable chest tightness and dyspnea. Acute respiratory failure occurred within 3 days of admission, and tracheal

intubation and ventilator-assisted respiration were required. Case 2 ultimately died from cardiac arrest, while the symptoms of cases 3 and 4 were relatively mild. The severe symptoms of cases 1 and 2 were attributed to direct contact with infected ducks. The results of mNGS revealed that case 1 and case 2 had higher mNGS sequences compared to other cases. mNGS was performed for case 2, 12 days after the onset of symptoms, which was the longest interval, but case 2 had the highest sequence number and worst prognosis. The findings suggest that the quantity of mNGS sequences can potentially be utilized to assess the severity and prognosis of diseases. Notably, the numbers of mNGS sequences detected in the bronchoalveolar lavage fluid (BALF) of case 1 and case 2 were higher than that in peripheral blood, indicating that examining BALF via bronchoscopy may enhance the detection rate of pathogens in psittacosis pneumonia.

Metagenomic next-generation sequencing (mNGS) has emerged as a valuable tool in detecting infectious diseases, including psittacosis pneumonia (Expert, 2019). Although its detection rate is significantly higher than traditional methods, mNGS is expensive and not widely used in clinical practice. Typically, it is reserved for cases with undermined diagnosis and severe disease. Studies have shown that tetracyclines, macrolides, and quinolones are effective in treating mild cases of psittacosis. However, in some countries, the diagnosis and treatment guidelines for mild community-acquired pneumonia (CAP) do not require identification of the specific cause of the illness, which can result in delayed treatment of patients with psittacosis. For instance, in the Netherlands, amoxicillin is the conventional treatment for CAP (Postma et al., 2015), but it is not effective against psittacosis pneumonia.

Similar to other atypical pathogens, psittacosis pneumonia has characteristic features on CT imaging, such as localized nodules or patchy consolidation. These lesions progress rapidly to lobar consolidation within 2-5 days and are primarily distributed adjacent to the pleura. Commonly, they are accompanied by pleural effusion and show 'fine mesh' signs around them (Chunfang et al., 2023). The 'anti-halo sign' can be used as an imaging feature for psittacosis pneumonia (Rongju and Pingchao, 2023). The main findings on CT images were consolidation and atelectasis, and some of the patients had pleural effusion, without obvious "anti-halo sign".

We observed that CRP and ferritin levels increased to varying degrees in all cases, with the severity of the disease positively correlated with the degree and duration of the increase in these serum markers. This indicates that the pathogen can trigger systemic inflammatory reactions after entering the bloodstream, which may worsen the severity of the disease. Consistent with our findings, previous studies indicated that increased procalcitonin level is significantly associated with severe pneumonia (Simmons et al., 2017). In case 2, the procalcitonin levels progressively increased, ultimately resulting in patient's death.

Lymphopenia is a significant feature of severe psittacosis pneumonia. It is linked to the immune dysfunction and is usually proportional to the duration of the disease (Yang et al., 2022). In this study, all four cases had decreased absolute lymphocyte count, with cases 1 and 2 exhibiting a significant decrease. Additionally, case 2 showed no improvement in lymphocyte count, indicating severe immune dysfunction. In this study, the lymphocyte count of case 1 began to increase after 20 days of admission, while the lymphocyte count of case 3 and case 4 returned to normal after a week. The severity of the disease was associated with the degree of lymphopenia and recovery time in all patients. Hence, absolute lymphocyte count can serve as a crucial indicator for evaluating disease severity.

In summary, *chlamydia psittaci*, as a common pathogen of CAP, is severely underestimated in clinical practice, and mGNS can become an important means of its detection. Parrot fever pneumonia is mainly transmitted through poultry, but clustered outbreaks are increasing reported. Interpersonal transmission requires high attention and vigilance against the emergence of a human-to-human pandemic. Absolute lymphocyte count and PCT can be important indicators for predicting patients' prognosis.

Data availability statement

The original contributions presented in the study are included in the article/supplementary materials. Further inquiries can be directed to the corresponding author.

Ethics statement

Written informed consent was obtained from the individuals for the publication of any potentially identifiable images or data included in this article. Written informed consent was obtained from the participant/patient(s) for the publication of this case report.

Author contributions

YW dealt with the case and drafted the manuscript. XX, YL and XJ assisted collected case data and literature and carried out all the documentary and article work out. HW gave some constructive suggestions for this paper during the revision and production period. JY and LH contributed to conception, design, and critically revised the manuscript. All authors contributed to the article and approved the submitted version.

Acknowledgments

The authors would like to express their gratitude to EditSprings (https://www.editsprings.cn) for the expert linguistic services provided.

Conflict of interest

The authors declare that the research was conducted in the absence of any commercial or financial relationships that could be construed as a potential conflict of interest.

Publisher's note

References

Balsamo, G., Maxted, A. M., Midla, J. W., Murphy, J. M., Wohrle, R., Edling, T. M., et al. (2017). Compendium of measures to control chlamydia psittaci infection among humans (psittacosis) and pet birds (avian chlamydiosis), 2017. *J. Avian Med. Surg.* 31 (3), 262–282. doi: 10.1647/217-265

Beeckman, D. S., and Vanrompay, D. C. (2009). Zoonotic Chlamydophila psittaci infections from a clinical perspective. *Clin. Microbiol. Infect.* 15 (1), 11–17. doi: 10.1111/j.1469-0691.2008.02669.x

Belchior, E., Barataud, D., Ollivier, R., Capek, I., Laroucau, K., de Barbeyrac, B., et al. (2011). Psittacosis outbreak after participation in a bird fair, Western France, December 2008. *Epidemiol. Infect.* 139, 1637–1641. doi: 10.1017/S0950268811000409

Berk, Y., Klaassen, C. H., Mouton, J. W., and Meis, J. F. (2008). An outbreak of psittacosis at a bird-fanciers fair in the Netherlands. *Ned Tijdschr Geneeskd.* 152, 1889–1892. https://pubmed.ncbi.nlm.nih.gov/18788682/

Boeck, C. D., Dehollogne, C., Dumont, A., Spierenburg, M., Heijne, M., Gyssens, I., et al. (2016). Managing a cluster outbreak of psittacosis in Belgium linked to a pet shop visit in The Netherlands. *Epidemiol. Infect.* 144, 1710–1716. doi: 10.1017/S0950268815003106

Bourke, S., Carrington, D., Frew, C. E., Stevenson, R. D., and Banham, S. W. (1989). Serological cross-reactivity among chlamydial strains in a family outbreak of psittacosis. *J. Infect.* 19, 41–45. doi: 10.1016/S0163-4453(89)94824-X

Chunfang, L., Yi, Z., Jiajun, C., Guihan, L., Xue, C., Junguo, H., et al. (2023). Clinical and CT imaging features of Chlamydia psittaci pneumonia. *Chin. J. Radiol.* 57 (3), 315–318. doi: 10.3760/cma.j.cn112149-20220302-00187

Çiftçi, B., Güler, Z. M., Aydo Du, M., Konur, O., and Erdoğan, Y. (2008). Familial outbreak of psittacosis as the first Chlamydia psittaci infection reported from Turkey. *Tuberk Toraks.* 56, 215–220. https://pubmed.ncbi.nlm.nih.gov/18701984/

Cillóniz, C., Torres, A., Niederman, M., van der Eerden, M., Chalmers, J., Welte, T., et al. (2016). Community-acquired pneumonia related to intracellular pathogens. *Intensive Care Med.* 42 (9), 1374–1386. doi: 10.1007/s00134-016-4394-4

De Gier, B., Hogerwerf, L., Dijkstra, F., and van der Hoek, W. (2018). Disease burden of psittacosis in the Netherlands. *Epidemiol Infect* 146 (3), 303–305. doi: 10.1017/S0950268817003065

Expert (2019). Expert consensus on the application of macrogenomic analysis and diagnostic techniques in acute and critical infections. *Chin. J. Emergency Med.* 28 (2), 151–155. doi: 10.3760/cma.j.issn.1671-0282.2019.02.005

Fraeyman, A., Boel, A., Van Vaerenbergh, K., and De Beenhouwer, H. (2010). Atypical pneumonia due to Chlamydophila psittaci: 3 case reports and review of literature. *Acta Clin. Belg* 65(3), 192–196. doi: 10.1179/acb.2010.040

Harris, R. L., and Williams, T. W. (1985). "Contribution to the Question of Pneumotyphus": a discussion of the original article by J. Ritter in 1880. *Rev. Infect. Dis.* 7 (1), 119–122. doi: 10.1093/clinids/7.1.116

Hedberg, K., White, K., Forfang, J., Korlath, J. A., Friendshuh, K. A., Hedberg, C. W., et al. (1989). An outbreak of psittacosis in Minnesota Turkey industry workers: implications for modes of transmission and control. *Am. J. Epidemiol.* 130, 569–577. doi: 10.1093/oxfordjournals.aje.a115371

Hinton, D., Shipley, A., Galvin, J., Harkin, J. T., and Brunton, R. A. (1993). Chlamydiosis in workers at a duck farm and processing plant. *Aust. Vet. J.* 70, 174–176. doi: 10.1111/j.1751-0813.1993.tb06123.x

Hogerwerf, L., Gier B, D. E., Baan, B., and Van Der, H. W. (2017). Chlamydia psittaci (psittacosis) as a cause of community-acquired pneumonia: a systematic review and meta-analysis. *Epidemiol. Infect.* 145, 3096–3105. doi: 10.1017/S0950268817002060

Hogerwerf, L., Roof, I., de Jong, M. J. K., Dijkstra, F., and van der Hoek, W. (2020). Animal sources for zoonotic transmission of psittacosis:a systematic review. *BMC Infect. Dis.* 20 (1), 192. doi: 10.1186/s12879-020-4918-y

Jenkins, C., Jelocnik, M., Micallff, Ml, Galea, F., Taylor-Brown, A., Bogema, D. R., et al. (2018). An epizootic of chlamydia psittaci equine reproductive loss associated with suspected spillover from native Australian parrots. *Emerg. Microbes Infect.* 7 (1), 88. doi: 10.1038/s41426-018-0089-y

Jing, C., Ming, Lu, and Ning, S. (2023). Two cases of family cluster pneumonia caused by psittacosis. *Chin. Med. Case Repository* 5, e00225. doi: 10.3760/cma.j.cmcr.2023.e00225

Kaibu, H., Iida, K., Ueki, S., Ehara, H., Shimasaki, Y., Watanabe, S., et al. (2006). Psittacosis in all four members of a family in Nagasaki, Japan. *Jpn J. Infect. Dis.* 59, 349–350. https://pubmed.ncbi.nlm.nih.gov/17060709/

Knittler, M. R., and Saches, K. (2015). Chlamydia psittaci: up date on an underestimated zoonotic agent. *Pathog. Dis.* 73 (1), 115. doi: 10.1093/femspd/ftu007

Lederer, P., and Mx Ller, R. (1999). Ornithosis – studies in correlation with an outbreak. *Gesundheitswesen.* 61, 614–619. https://pubmed.ncbi.nlm.nih.gov/10666940/

Lenny, H., Inge, R., Marianne, J. K., de Jong, F. D., and van der Hoek, W. (2020). Animal sources for zoonotic transmission of psittacosis: a systematic review. *BMC Infect. Dis.* 20 (1), 192. doi: 10.1186/s12879-020-4918-y

Li, Na, Li, S., Tan, W., Wang, H., Xu, H., and Wang, D. (2021). Metagenomic next-generation sequencing in the family outbreak of psittacosis: the first reported family outbreak of psittacosis in China under COVID-19. *Emerging Microbes Infections* 10, 1418–1428. doi: 10.1080/22221751.2021.1948358

Matsui, T., Nakashima, K., Ohyama, T., Kobayashi, J., Arima, Y., Kishimoto, T., et al. (2008). An outbreak of psittacosis in a bird park in Japan. *Epidemiol. Infect.* 136, 492–495. doi: 10.1017/S0950268807008783

Postma, D. F., van Werkhoven, C. H., van Elden, L. J., Thijsen, S. F., Hoepelman, A. I., Kluytmans, J. A., et al. (2015). Antibiotic treatment strategies for community-acquired pneumonia in adults. *N Engl. J. Med.* 372 (14), 1312–1323. doi: 10.1056/NEJMoa1406330

Rongju, Wu, and Pingchao, X. (2023). Clinical analysis of Chlamydia psittaci pneumonia characterized by anti halo sign. *Chin. J. Med. Front.* 15 (1), 30–34. doi: 10.12037/YXQY.2023.01-07

Simmons, G. L., Chung, H. M., McCarty, J. M., Toor, A. A., Farkas, D., Miller, K., et al. (2017). Treatment of acute fibrinous organizing pneumonia following hematopoietic cell transplantation with etanercept. *Bone Marrow Transplant.* 52 (1), 141–143. doi: 10.1038/bmt.2016.197

Smith, K. A., Campbell, C. T., Murphy, J., Stobierski, M. G., and Tengelsen, L. A. (2011). Compendium of measures to control Chlamydophila psittaci infection among humans (psittacosis) and pet birds (avian chlamydiosis), 2010 National Association of State Public Health Veterinarians (NASPHV). *J. Exot Pet Med.* 20 (1), 32–45. doi: 10.1053/j.jepm.2010.11.007

Teng, X. Q., Gong, W. C., Qi, T. T., Li, G. H., Qu, Q., Lu, Q., et al. (2021). Clinical anlysis of metagenomic next generation sequencing confirmed Chlamydia psittaci pneumonia: a case series and lite rature review. *Infect. Drug Resist.* 14, 1481–1492. doi: 10.2147/IDR.S305790

Tiong, A., Vu, T., Counahan, M., Leydon, J., Tallis, G., and Lambert, S. (2007). Multiple sites of exposure in an outbreak of ornithosis in workers at a poultry abattoir and farm. *Epidemiol. Infect.* 135, 1184–1191. doi: 10.1017/S095026880700790X

Williams, C., Sillis, M., Fearne, V., Pezzoli, L., Beasley, G., Bracebridge, S., et al. (2013). Risk exposures for human ornithosis in a poultry processing plant modified by use of personal protective equipment: an analytical outbreak study. *Epidemiol. Infect.* 141, 1965–1974. doi: 10.1017/S0950268812002440

Xiaoyan, X., Wei, G., Jing, C., Xuan, S.Shuangshuang L., and Binghua, Z. (2022). Clinical features diagnosis and treatment of a family cluster of Chlamydia psittaci pneumonia. *Int. J. Respir.* 42, 14. doi: 10.3760/ cma.j.cn131368-20220126-00061

Yang, F. X., Li, J. J., Qi, B., Zou, L., Shi, Z., Lei, Y., et al. (2022). Clinical symptoms and outcomes of severe pneumonia caused by Chlamydia psittaci in Southwest China. *Front. Cell Infect. Microbiol.* 11, 727594. doi: 10.3389/fcimb.2021.727594

Yao, W., Chen, X., Wu, Z., Wang, L., Shi, G., Yang, Z., et al. (2022). A cluster of Psittacosis cases in Lishui, Zhejiang Province, China, in 2021. *Front. Cell. Infect. Microbiol.* 12, 1044984. doi: 10.3389/fcimb.2022.1044984

Zhang, H., Zhan, D., Chen, D., Huang, W., Yu, M., Li, Q., et al. (2020). Next generation sequencing diagnosis of severe pnumonia from fulminant psittacosis with multiple organ failure: a case report and literature review. *Ann. Transl. Med.* 8 (6), 401. doi: 10.21037/atm.2020.03.17

Zhang, Z., Zhou, H., Cao, H., Ji, J., Zhang, R., Li, W., et al. (2022). Human-to-human transmission of Chlamydia psittaci in China 2020: An epidemiological and aetiological investigation. *Lancet Microbe* 3, e512–e520. doi: 10.1016/S2666-5247(22)00064-7

frontiers | Frontiers in Cellular and Infection Microbiology

TYPE Original Research
PUBLISHED 01 December 2023
DOI 10.3389/fcimb.2023.1216339

OPEN ACCESS

EDITED BY
Jeyaprakash Rajendhran,
Madurai Kamaraj University, India

REVIEWED BY
Guoliang Zhang,
Shenzhen Third People's Hospital, China
Addy Cecilia Helguera-Repetto,
Instituto Nacional de Perinatología (INPER), Mexico

*CORRESPONDENCE
Yu Chen
chenyuzy@zju.edu.cn

†These authors have contributed equally to this work

RECEIVED 03 May 2023
ACCEPTED 07 November 2023
PUBLISHED 01 December 2023

CITATION
Zhang D, Yu F, Han D, Chen W, Yuan L, Xie M, Zheng J, Wang J, Lou B, Zheng S and Chen Y (2023) ddPCR provides a sensitive test compared with GeneXpert MTB/RIF and mNGS for suspected *Mycobacterium tuberculosis* infection. *Front. Cell. Infect. Microbiol.* 13:1216339. doi: 10.3389/fcimb.2023.1216339

ddPCR provides a sensitive test compared with GeneXpert MTB/RIF and mNGS for suspected *Mycobacterium tuberculosis* infection

Dan Zhang[1,2,3†], Fei Yu[1,2,3†], Dongsheng Han[1,2,3], Weizhen Chen[1,2,3], Lingjun Yuan[1], Mengxiao Xie[1], Jieyuan Zheng[1], Jingchao Wang[1], Bin Lou[1,2,3], Shufa Zheng[1,2,3] and Yu Chen[1,2,3*]

[1]Department of Laboratory Medicine, the First Affiliated Hospital, Zhejiang University School of Medicine, Hangzhou, China, [2]Key Laboratory of Clinical In Vitro Diagnostic Techniques of Zhejiang Province, Hangzhou, China, [3]Institute of Laboratory Medicine, Zhejiang University, Hangzhou, China

Introduction: The Metagenomics next-generation sequencing (mNGS) and GeneXpert MTB/RIF assay (Xpert) exhibited a sensitivity for tuberculosis (TB) diagnostic performance. Research that directly compared the clinical performance of ddPCR analysis, mNGS, and Xpert in *mycobacterium tuberculosis* complex (MTB) infection has not been conducted.

Methods: The study aimed to evaluate the diagnostic performance of ddPCR compared to mNGS and Xpert for the detection of MTB in multiple types of clinical samples. The final clinical diagnosis was used as the reference standard.

Results: Out of 236 patients with suspected active TB infection, 217 underwent synchronous testing for tuberculosis using ddPCR, Xpert, and mNGS on direct clinical samples. During follow-up, 100 out of 217 participants were diagnosed with MTB infection. Compared to the clinical final diagnosis, ddPCR produced the highest sensitivity of 99% compared with mNGS (86%) and Xpert (64%) for all active MTB cases.

Discussion: Twenty-two Xpert-negative samples were positive in mNGS tests, which confirmed the clinical diagnosis results from ddPCR and clinical manifestation, radiologic findings. Thirteen mNGS-negative samples were positive in ddPCR assays, which confirmed the clinical final diagnosis.ddPCR provides a higher sensitive compared to Xpert and mNGS for MTB diagnosis, as defined by the high concordance between ddPCR assay and clinical final diagnosis.

KEYWORDS

metagenomics next-generation sequencing, ddPCR, GeneXpert MTB/RIF, tuberculosis, latent TB infection

Introduction

Tuberculosis (TB) is a communicable disease that is one of the major causes of death. Until the coronavirus disease 2019 (COVID-19) pandemic, TB was the leading cause of death from a single infectious agent, ranking above acquired immune deficiency syndrome (AIDS) (World Health Organization, 2021). *Mycobacterium tuberculosis* complex (MTB) infection is a serious health issue with high infectivity, morbidity, and mortality. The microbiological detection of MTB is critical to the definitive diagnosis of TB. Among the TB-diagnosed cases, only 57% of pulmonary TB cases are bacteriologically confirmed by sputum smear microscopy, culture, or rapid MTB DNA tests (World Health Organization, 2020). The TB cases without bacteriological confirmation may result in ineffective treatment. Traditional mycobacterial culture is time-consuming, and the acid-fast bacilli (AFB) smear has low sensitivity (Li et al., 2022). Nucleic acid amplification tests (NAATs) have been widely applied in the rapid diagnosis of MTB (Zhang et al., 2021). Xpert MTB/RIF (Cepheid, United States) based on RT-PCR assays and Truenat MTB (Molbio, India) assays are recommended by the World Health Organization (WHO) as a rapid molecular diagnostic test for the case of extrapulmonary and pulmonary infections (Penn-Nicholson et al., 2021; World Health Organization, 2021; Hong et al., 2022).

In recent years, the mNGS technique has been applied to detect causative pathogens without any prior suspicion of certain pathogens and to guide targeted antimicrobial therapy. It can be used in multiple clinical diagnoses, including tuberculosis (Shi et al., 2020; Li et al., 2022). In terms of MTB diagnostic performance, mNGS shows high efficiency as compared with Xpert in these cohort (Shi et al., 2020; Li et al., 2022). These studies showed that mNGS is better in cerebrospinal fluid (CSF) and bronchoalveolar lavage fluid (BALF) samples, only slightly worse in pleural effusion, pericardial effusion, and ascites (Zhou et al., 2019). Normally, for Xpert-negative patients, experienced clinicians could identify the MTB infection by analyzing the mNGS-positive results to see whether they were in accordance with the patient's clinical manifestation and computed tomography (CT) images. For a high-priority pathogen like MTB, genus-specific read numbers ≥1 from mNGS-positive reporting threshold are normally considered to be credible reports. However, it was difficult to discriminate whether the false-positive results were caused by sampling contamination or by data analysis approaches (Miao et al., 2018). Additionally, mNGS has several drawbacks, including a long turnaround time, insufficient sensitivity in high background microorganisms, and cost-effectiveness considerations.

Compared with the conventional methods, the newly emerging droplet digital polymerase chain reaction (ddPCR) is observed with high sensitivity, precision, and accuracy for the identification of trace DNA in samples of low concentrations (Ushio et al., 2016; Li et al., 2020; Lyu et al., 2020). The ddPCR is proven to be fast enough to detect low-abundance MTB infection (Nyaruaba et al., 2019; Antonello et al., 2021). For suspected MTB infections without microbiological evidence, ddPCR is a good supplementary diagnosis for low-concentration MTB. Earlier studies have shown that mNGS and ddPCR demonstrate great promise in detecting MTB infections (Ushio et al., 2016; Nyaruaba et al., 2019; Cao et al., 2020; Yan et al., 2020; Liu et al., 2021; Zhu et al., 2021). However, the direct comparison of the ddPCR analysis with mNGS and Xpert in MTB infection is still scarce. The utility of ddPCR, mNGS, and Xpert for suspected clinical MTB infection has not been systematically evaluated.

In our study, a cohort of patients with suspected MTB infection was collected. The clinical application of ddPCR, mNGS, and Xpert methods for the accurate detection of MTB in the clinical samples was evaluated. The clinical diagnosis was used as the reference standard.

Materials and methods

Study participants

All patients with suspected of active MTB infections, including both pulmonary TB and extrapulmonary TB, were admitted to the First Affiliated Hospital, Zhejiang University School of Medicine from March 2021 to November 2021. Samples were collected from suspected infected sites of the enrolled patients. All clinical specimens were immediately sent for testing, including culture, Xpert, mNGS, ddPCR, and smear microscopy (for acid-fast bacilli). Fresh tissue, pleural effusion, pericardial effusion, CSF, ascites, and BALF samples were collected and divided into three aliquot parts for each sample.

The final clinical diagnosis of TB was made by infectious physicians or respiratory physicians based on the integration of the patient's medical history, radiological findings, and laboratory findings (microbiological, molecular, and immunological tests) according to the China Clinical Treatment Guide for Tuberculosis (Association CM, 2005). There are two types of confirmed TB cases: microbiological test-confirmed TB cases and clinically diagnosed TB cases. For microbiologically confirmed TB cases, the patients were classified as microbiologically confirmed TB cases by the following results: MTB biopsy-positive and culture-positive, mNGS-positive, or Xpert-positive. For patients without microbiological evidence, the attending physician can only clinically diagnose the active MTB infection by combining the patient's imaging findings, clinical manifestations, and other laboratory-related tests and exclude it from other diseases. The patient's TB was finally confirmed by its responsiveness to anti-TB treatment at 1-month follow-up. The non-TB group included infections other than TB, non-infectious inflammatory diseases, tumors, and miscellaneous causes.

This study conformed to the ethical guidelines of the 1975 Declaration of Helsinki and was approved by the ethics committee of the First Affiliated Hospital, Zhejiang University School of Medicine.

GeneXpert MTB/RIF detection

BALF samples were ground into a homogenate and liquefied. After centrifugating each BALF, pleural effusion, pericardial effusion, and ascites were collected as 2-mL sedimentation in

DNase-free tubes. Tissue was shredded using a blade and by grinding. The Xpert MTB/RIF assay was performed on the GeneXpert system (Cepheid, Sunnyvale, CA, USA) following the manufacturer's instructions. The results were determined by the fluorescence signal measured using the GeneXpert system and the built-in algorithm.

Sample processing and droplet digital PCR

Briefly, the same pre-processing was conducted with BALF and tissue, pleural effusion, pericardial effusion, and ascites. Pleural effusion, pericardial effusion, and ascites were collected as 2-mL sedimentation in DNase-free tubes. Bead-beating for cell lysis was required for all samples and using the host depletion approach before nucleic acid extraction. Following are additional details of bead-beating lysis: bead size: 1 mm and 3 mm zirconium beads; time setting: running time = 70 s, pause time = 30 s; number of cycles = 8; TGrinder H24 Tissue Homogenizer (Tiangen). After the bead-beating process, DNA was extracted using TIANamp Micro DNA Kit (DP316, Tiangen Biotech, Beijing, China) according to the manufacturer's protocol. DNA was eluted in 50 µL of elution buffer and used for the ddPCR assay and mNGS analysis promptly on the same day. The ddPCR analysis was performed using Targeting One Droplet Digital PCR System according to the manufacturer's protocol. Briefly, a 30-µL reaction mixture and 180 µL oil were loaded onto the droplet. The mixture was prepared for the emulsion generation using the TargetingOne Drop Maker M1 (TargetingOne, Beijing, China), and approximately 40,000 droplets were obtained. After 10 min at 95°C, a total of 40 cycles of the PCR reaction were carried out in a Bio-Rad PTC 200 thermal cycler according to the following procedure: 94°C for 30 s, 57°C for 1 min, and 12°C cooling for 5 min. The PCR droplets were then loaded onto Chip Reader R1 (TargetingOne, Beijing, China) to analyze the FAM (488-nm laser) fluorescence intensity for IS1081 and VIC (532-nm laser) for IS6110 fluorescence intensity for each droplet. The cluster plots were calculated using TargetingOne analysis software (TargetingOne, Beijing, China). Each sample was performed in duplicate. The threshold levels for selecting positive droplets were determined by the fluorescence intensities of the standard droplets. At least one copy of positive droplet MTB gene IS6110 or IS1081 was required for a positive test result. The threshold levels for selecting positive droplets were determined by a density-watershed algorithm method, which was developed for the accurate, automatic, and un-supervised classification of two/four-ddPCR data (Zhu et al., 2019).

Accuracy and limit of detection of droplet digital PCR assay

To verify the performance of MTB detection and quantification, a national reference for the PCR-based detection of *Mycobacterium tuberculosis* was purchased from the National Institutes for Food and Drug Control (Beijing, China; lot 230030-202004). The limits of detection (LODs) for the ddPCR assays were measured using four serial dilutions (1, 10, 10^2, and 10^3 copies/mL) of the MTB around the LOD. The LODs were calculated by using probit analysis for 95% positive result. The coefficient of determination of the MTB quantification was assessed for both IS6110 and IS1081 by using linear regression analysis. To determine the specificity and cross-reactivity of the MTB ddPCR assays, the DNA of cultured nontuberculous mycobacteria strains (NTMs), other bacterial strains, and negative controls, respectively, were also added in each run. The negative controls belonged to samples collected from individuals with no clinical and bacteriological signs of MTB infection.

Metagenomic next-generation sequencing and analysis

The synthesized DNA fragment was used as an internal control, and DNase-free water and samples from three healthy subjects were spiked with the internal control to monitor for external or reagent microbial contamination and cross-sample contamination. The same DNA was quantified using Qubit dsDNA HS Assay Kit (Life Technologies, CA, USA). DNA libraries were constructed by using Nextera XT Library Preparation Kit (Illumina, CA, USA) following the manufacturer's protocol. Sequencing was performed on an Illumina Nextseq CN550 platform (Illumina, CA, USA), resulting in 15–20 million reads (75 bp) for each sample. The sequence data was analyzed by using Weiyuan-MG v1.0 mNGS software (Weiyuan, Weiyuan Biotechnology, Guangzhou, China) which contains a proprietary curated database consisting of more than 20,000 reference microbial genomes.

Criteria for a positive mNGS result

The sequencing results of each sample are categorized into four tables, with each table representing bacteria, fungi, viruses, and parasites. The mNGS identified a microbe at the species level whose read count was among the top 10 in the complete list of species as well as a microbe at the species level whose coverage rate was 10 times greater than that of any other microbe. We identified the causative pathogen according to the pipeline described previously (Miao et al., 2018). MTB was considered positive when at least one read was mapped to either the species or genus level due to the difficulty of DNA extraction and the low possibility for contamination.

Statistical analysis

SPSS statistical package 22.0 software was used for database management and statistical analyses. Continuous variables were described by means when they conform to the *t*-test. The *t*-test was used to analyze normally distributed continuous variables, whereas the Mann–Whitney *U*-test was used to analyze nonnormally distributed continuous variables. Categorical variables were reported as frequencies and percentages and analyzed using chi-square test. The sensitivity and specificity of the different methods were assessed. The results were presented with a range of 95% confidence intervals. Analysis of variance test was applied to

compare differences across subgroups. A *P*-value less than 0.05 was considered statistically significant.

Results

Patients' characteristics

The demographic and clinical characteristics of the population included in the study are presented in Table 1. We enrolled 236 patients suspected to have active MTB infections. In total, 19 patients were excluded due to the limited specimen that was not enough for all three tests and the priority test that was chosen by their attending physician (Figure 1). Samples were retrieved mainly among male patients (68.2%) with a median age of 56.3 years (interquartile range: 50–68). A total of 217 patients initially suspected of having active pulmonary MTB infection underwent bronchoscopy during hospitalization, and 195 clinical lavage fluid samples and 22 other specimens (pleural effusion, pericardial effusion, CSF, ascites, and tissue) were obtained for the tests. All the clinical samples were subjected to tuberculous diagnosis using ddPCR, Xpert, mNGS, and traditional diagnostic methods (Figure 1). Moreover, 100 of 217 participants had a final clinical diagnosis of active pulmonary MTB infection.

Performance of droplet digital PCR-based assays

Assay linearity and limit of detection

The linearity of the IS6110 and IS1081 duplex ddPCR assays was tested by quantifying serial dilutions of a known amount of MTB DNA. The probit analysis of 95% positivity in 10 replicates in three different runs at five concentrations showed that the MTB ddPCR assays showed an LOD of three copies per reaction. Both IS6110 ($R^2 = 0.9661$, $p < 0.001$) and IS1081 ($R^2 = 0.9217$, $p < 0.001$) targeted tests were correlated with MTB DNA quantification (Figures 2A, B). No signal was detected in any of the 15 certainly negative samples nor in the added nontuberculous extract for both IS6110 and IS1081 targets. A representative example of Quanta soft panel for IS6110 and IS1081 was obtained by the positive MTB DNA control, and four positive samples were displayed. The specificities of IS6110 and IS1081 ddPCR for the MTB for the NTMs and other bacterial strains were confirmed (Table 2).

TABLE 1 Baseline characteristics of the population.

	TB (n=100)	Non-TB (n=117)
Age (mean), years	54.6	57.9
Sex-male, n (%)	77 (77%)	71 (60.7%)
T. SPOT TB (+), n (%)	69 (69%)	97 (82.90)
Pulmonary samples, n		
BALF	84	111
Lung biopsy tissue	6	0
Extrapulmonary samples, n		
CSF	2	7
Pleural fluid	2	0
Ascites	2	0
pericardial effusion	2	0
AFB (+)	26	6
Mycobacterial culture, n	22	6

Results of ddPCR in the detection of MTB DNA for clinical samples

As shown in Figures 3A, B, the number of copies detected in the TB group was significantly higher than that in the non-TB group: median (minimum, maximum) for IS6110, 79.7 (0.0, 248522.0) copies/30 µL of reaction mixture in the TB group vs. 0.0 (0.0, 4.7) copies/30 µL of reaction mixture in the non-TB group, $p < 0.001$. Similar results were also observed for the IS1081 assay: 22.4 (0.0, 248522.0) copies/30 µL of reaction mixture in the TB group vs. 0.0 (0.0, 1.6) copies/30 µL of reaction mixture in the non-TB group, $p < 0.001$ (Figures 3A, B). Our results also showed that the sensitivity of the IS6110-ddPCR assay for total TB was higher than that of the IS1081-ddPCR assay in the low loads MTB, especially in samples with only one read of detected MTB in the mNGS-positive samples and only in the ddPCR-positive samples (Figures 3C, D).

Diagnosis performance of ddPCR-based assays against Xpert and mNGS

To further measure the sensitivity and specificity of ddPCR-based assays against Xpert and mNGS, we assessed the diagnostic performance for ddPCR, Xpert, mNGS, and traditional methods and compared them with the final clinical diagnosis (Table 3; Figure 4). In total, 100 of 217 participants had a final clinical diagnosis of active pulmonary MTB infection. ddPCR produced the highest sensitivity of 99% among the three nucleic acid amplification tests, followed by mNGS (86%) and Xpert (64%), yet for the specificity results of the tests, mNGS had the highest specificity of 100%. With only four false-positive results, ddPCR had a specificity of 96.6% in our study. MTB was detected by ddPCR in 9.0% (9/100) Xpert- and mNGS-negative samples. Only three BAL and one ascites sample with Xpert-positive results were negative in the mNGS tests. A total of 22 Xpert-negative samples were positive in mNGS tests, which further confirmed the final clinical diagnosis results by ddPCR, clinical manifestation, and radiologic findings. Furthermore, 13 mNGS-negative samples were positive in ddPCR assays, which confirmed the final clinical diagnosis. The negative predictive value of ddPCR, mNGS, and Xpert for the detection of MTB was 99.1% (95%CI: 94.5–100%), 89.3% (95%CI: 82.4–93.8%), and 76.4% (95%CI: 68.8–82.8%), respectively. It also showed a higher sensitivity of ddPCR. Six cases of NTMs were simultaneously detected as negative both in mNGS and ddPCR. The diagnosis results were confirmed by using AFB smear and culture.

10.3389/fcimb.2023.1216339

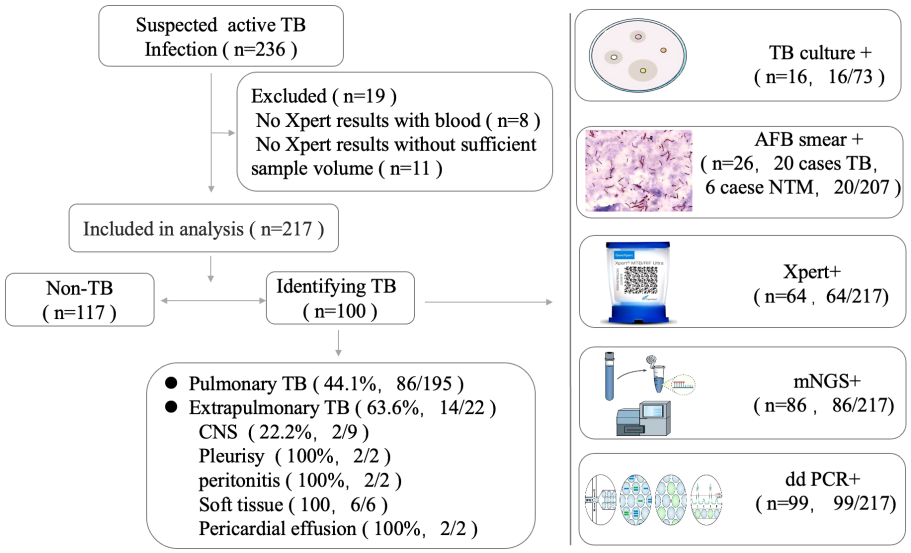

FIGURE 1
Study design.

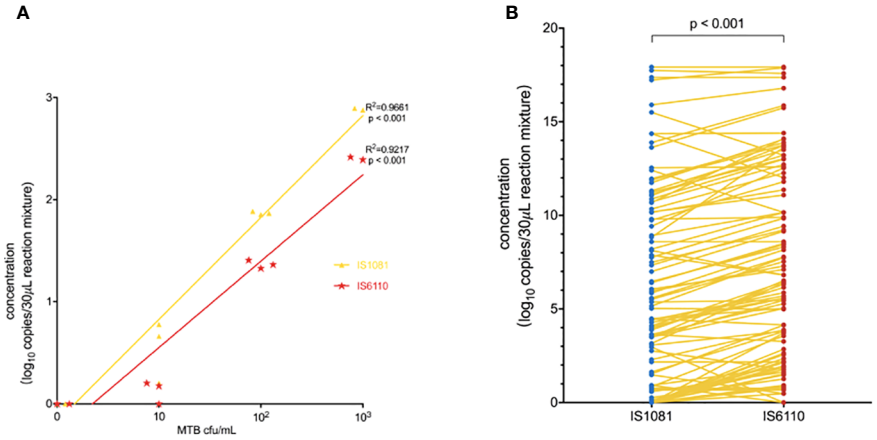

FIGURE 2
(A) Linear correlation of the observed IS1081 and IS6110 load, expressed as (log $_{10}$ copies/30 μL reaction mixture) concentration. **(B)** Duplex amplification of MTB IS6110 and IS1081 DNA in clinical samples by ddPCR. The differences in copy number of IS6110-dPCR and IS1081-dPCR were analyzed by using the Wilcoxon test.

Discussion

The current molecular diagnostic techniques for TB, including PCR and mNGS, have insufficient sensitivity to detect samples with low bacterial loads and showed limited efficacy, although the mNGS and Xpert assays exhibited a sensitivity for TB diagnostic performance. Some suspected tuberculosis diagnoses still lacked etiological evidence. ddPCR is an excellent nucleic acid quantification technique with high sensitivity (Zhao et al., 2022). However, directly evaluating the diagnostic performance of ddPCR with mNGS and Xpert in pulmonary MTB infection is still rare so far. To address this issue, we conducted a single-center study to analyze the performance of ddPCR for suspected clinical specimens of MTB infection and compared it with mNGS, Xpert, and the final clinical diagnosis. Our results proved that the performance of ddPCR-assays is a rapid and

TABLE 2 Amplification of NTMs and other bacterial strains in ddPCR.

Strain	Amplification Target	
	IS6110	IS1081
M. avium	N	N
M. kansasii	N	N
M.terraccomplex	N	N
M. shimoidei	N	N
M. asiaticum	N	N
M. scrofulaceum	N	N
M.gordonae	N	N

(Continued)

TABLE 2 Continued

Strain	Amplification Target	
	IS6110	IS1081
M.chelonei	N	N
M. Fortuitum	N	N
M. phlei	N	N
Nocardia brasiliensis	N	N
Corynebacterium pekinense	N	N
Streptococcus pneumoniae	N	N

NTM, nontuberculous mycobacteria.
N, negative.

sensitive molecular test for the detection of low-abundance MTB infection. Among these NAAT methods, the ddPCR results are in best accordance with the final clinical diagnosis of MTB infection, which could potentially improve the consistency of clinical diagnosis.

Although previous studies have shown the potential of the application of mNGS in identifying MTB infections (Zhou et al., 2019; Shi et al., 2020; Liu et al., 2021; Zhu et al., 2021), no consensus on the detection capacity of mNGS for MTB has been reached. For high-priority pathogens, MTB was considered positive when at least one read was assigned to the species or genus level due to the difficulty of DNA extraction and the low possibility of contamination (Miao et al., 2018; Shi et al., 2020). In our study, it was difficult for 11 clinical samples to detect one-read MTB by mNGS and identify MTB infections. Experienced clinics also

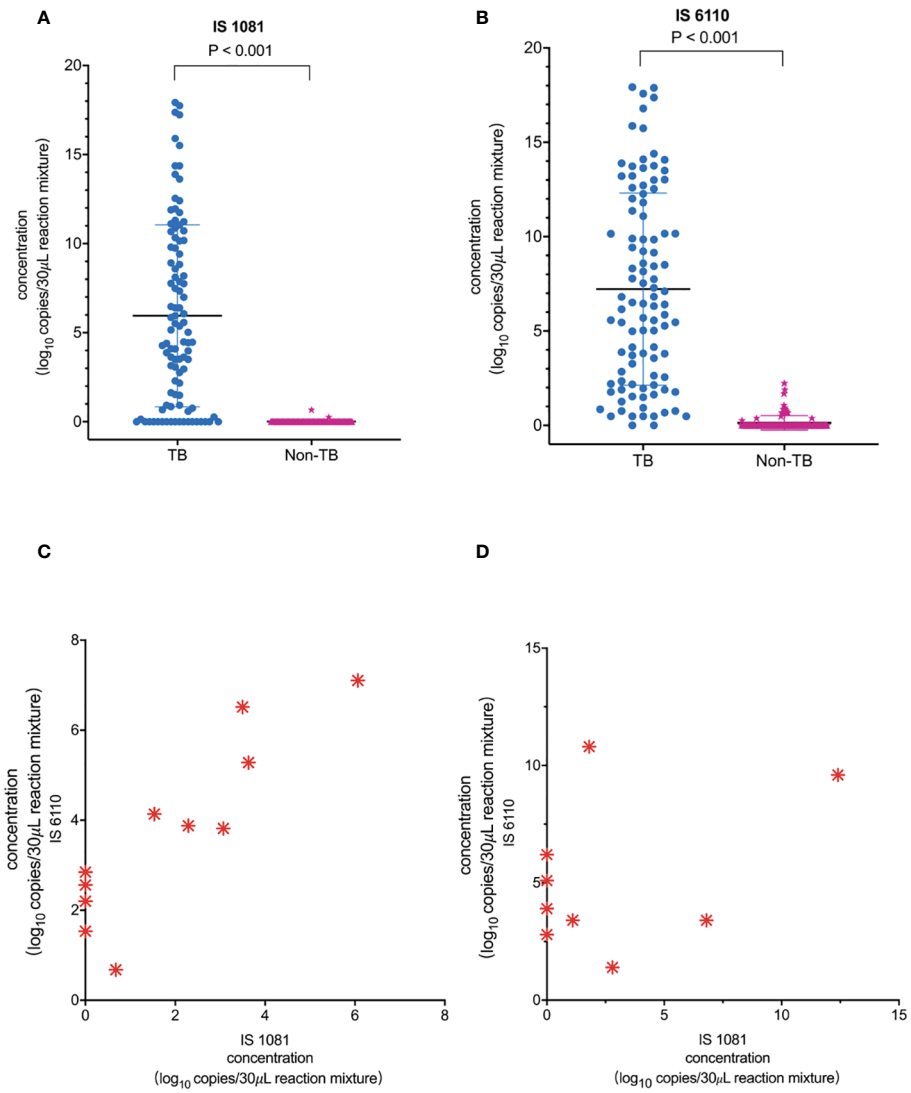

FIGURE 3
Quantification of MTB IS1081 and IS6110 DNA in clinical samples by ddPCR. **(A)** IS1081 and **(B)** IS6110 copy number in the clinical samples of total TB patients and non-TB patients, respectively (Mann–Whitney *U*-test). The results were considered significant when the *p*-value was 0.05 or lower. **(C)** All one-read MTB samples were detected by mNGS as positive and confirmed the final clinical diagnosis of TB. Only five of 11 one-read MTB samples were detected to be positive by Xpert. **(D)** Nine clinical samples were detected to be positive by ddPCR and confirmed the final clinical diagnosis of TB.

10.3389/fcimb.2023.1216339

TABLE 3 Diagnostic performance of MTB for mNGS, Xpert, ddPCR and traditional methods compared with the clinical final diagnosis.

Methods	samlpe size (n)	the final clinical diagnosis for TB		Statistical analysis			
		Yes, (n=100)	No, (n=117)	Sensitivity, % (95% CI)	Specificity, % (95% CI)	PPV, % (95% CI)	NPV, % (95% CI)
mNGS (Positive)	217	86	0	86 (77.2-91.8)	100 (96.0-100)	100 (94.6-100)	89.3 (82.4-93.8)
(Negative)		14	117				
Xpert (Positive)	217	64	0	64 (53.7-73.1)	100 (96.0-100)	100 (92.9-100)	76.4 (68.8-82.8)
(Negative)		36	117				
ddPCR (Positive)	217	99	4	99 (93.8-99.9)	96.6 (91.0-98.9)	100 (89.8-98.7)	99.1 (94.5-100)
(Negative)		1	113				
AFB smear (Positive)	207	20	0	22.4(14.6-32.8)	100 (95.6-100)	100 (80.0-100)	61.8(54.3-68.9)
(Negative)		74	117				
Culture (Positive)	73	16	0	43.2(27.5-60.4)	100 (88.0-100)	100 (75.9-100)	63.2 (49.3-75.2)
(Negative)		84	117				

NPV, negative predictive value; PPV, positive predictive value.

analyzed the mNGS results to see whether it was in accordance with the imaging findings, clinical manifestation, and diagnosis. MTB specimens with only one read were detected not only with low loads of IS6110 and IS1081 by ddPCR but also in six Xpert-negative specimens. It demonstrated that mNGS had an improved diagnostic performance in suspected MTB. mNGS was useful for the distinction between MTB and NTM.

In terms of TB diagnostic performance, mNGS is inferior to Xpert in our overall cohort, which is better in BAL. The sensitivity of ddPCR and mNGS using the same nucleic acid was higher than

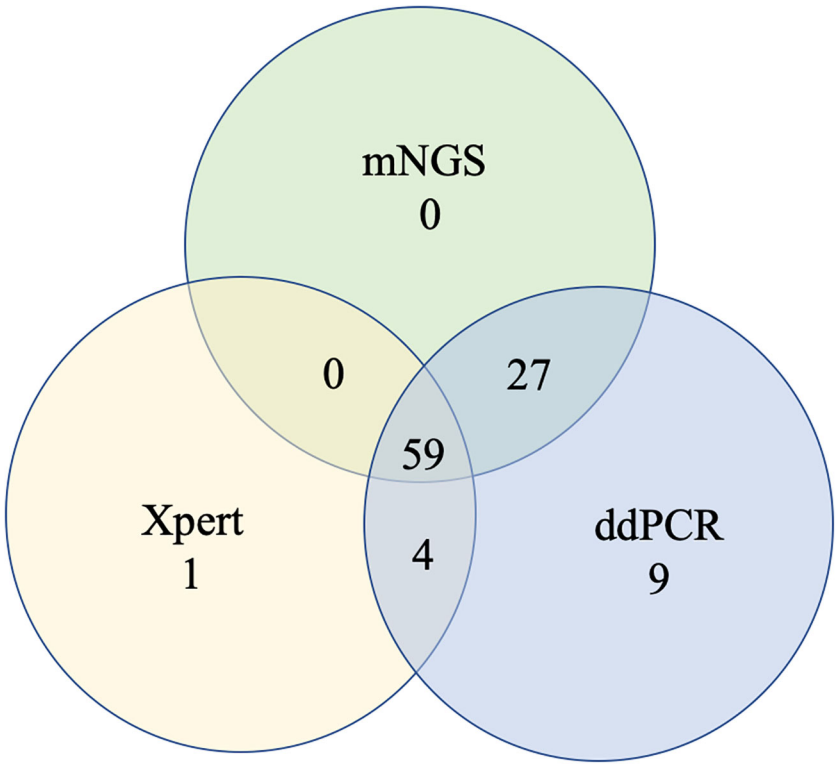

FIGURE 4
Venn diagram of overlap in TB diagnostics.

that of mycobacterial Xpert. Part of the reason may be in the sample DNA extraction with bead-beating processing. Previous studies have shown that the detection rate can be greatly improved in laboratories by adding a bead-beating process (Charalampous et al., 2019). Mechanical wall breaking can increase the yield of microbes at low concentrations, especially for MTB with a hard cell wall. However, some studies showed that mNGS is not superior to Xpert in detecting MTB (Shi et al., 2020; Liu et al., 2021). In our study, the sensitivity of mNGS (86%) was higher than that of Xpert (64%). mNGS is superior to Xpert in detecting MTB, which could be caused by adding a host DNA depletion process. The results indicated that adding a host DNA depletion process in an mNGS protocol might reduce the risk of false-negatives in testing low-microbial-biomass samples (Han et al., 2021) because different levels of background commensal/human DNA could potentially result in different LODs.

For suspected TB, some clinicians prescribe early empirical treatment based on the appearance of the patient's imaging findings and clinical manifestations which cannot replace an etiological confirmation. It is a challenge to detect low-abundance MTB samples for mNGS or Xpert. Therefore, the results of ddPCR were useful in providing appropriate treatment to patients in the early stage or latent TB infection (Song et al., 2018), supporting the clinical decision of treatment. In our study, ddPCR showed superior sensitivity in detecting pathogens compared with traditional diagnosis methods. Of the 14 false-negative findings with mNGS, ddPCR showed a higher sensitivity in probable MTB. For ddPCR specificity, 22 cases of NTM were detected by mNGS-positive and clinically diagnosed NTM cases, but only six cases were confirmed by culture and AFB smear. There were two false-positive ddPCR in the clinically diagnosed NTM cases. Only four IS6110 and IS1081 ddPCR-positive samples and were finally diagnosed with MTB infection after tracking the cases for half a year. These showed a higher sensitivity in probable and possible MTB. In addition, another four IS6110 and IS1081 ddPCR-positive samples which cannot be excluded as MTB were finally diagnosed after tracking the cases for half a year. It was demonstrated that ddPCR has a higher sensitivity.

In the IS6110 and IS1081 duplex ddPCR systems, IS6110 accounts for many more copies in the genome of clinical MTB samples than IS1081. It has been reported that the testing of IS6110 was not promising in clinical MTB samples from several areas such as Southeast Asia because some MTB strains only had one copy of IS6110 in their genome (Lyu et al., 2020). Some clinically isolated strains were found to have no IS6110 element, which accounts for approximately 5% of the total isolates (Huyen et al., 2013). Several studies have indicated MTB strains that typically contain multiple copies of IS6110 (up to 25 per genome), although strains with only a single copy or no copies have also been identified (Alonso et al., 2013). It can explain our results observed, such that IS6110-PCR has a higher sensitivity than IS1081 qPCR. It will need more advanced research in the future. Therefore, the sensitivity of joint detection was improved with the IS6110 and IS1081 assay for MTB with low loads. The disadvantages of ddPCR over other molecular methods need to be mentioned (1): higher chances of sample contamination and (2) ddPCR implementation needs specialized personnel.

Despite these promising results, our study has some limitations. First, our study had a relatively small extrapulmonary sample size; therefore, more future studies are required to understand the diagnostic value of mNGS in extrapulmonary TB. Due to interference, Xpert cannot detect tuberculosis in plasma, while mNGS and ddPCR were used for detecting TB and confirmed the final clinical diagnosis of MTB in four cases using plasma samples. Thus, plasma was not included in the study. Second, antibiotic resistance genes were not analyzed by mNGS and cannot help more targeted treatment for pulmonary TB. Third, the single-center study had limitations. Multi-center studies would be needed to explore universal criteria or guidelines of mNGS in active TB infections in the future. Finally, despite the low sensitivity of conventional methods, the study has not systematically included conventional methods such as culture and AFB. However, mNGS and Xpert showed an overall superior advantage over conventional methods and significantly improved the etiology diagnosis of both MTB.

In summary, our data show that the mNGS of the clinical sample represents a potential step forward in the MTB diagnosis of suspected pulmonary TB and extrapulmonary TB. ddPCR has been sensitive and has excellent accuracy for the rapid diagnosis of MTB in detecting low-pathogen-load samples. Among these methods, ddPCR is strongly recommended in clinical practice for the diagnosis of TB and the follow–up of positive patients.

Data availability statement

The original contributions presented in the study are included in the article/supplementary materials, further inquiries can be directed to the corresponding author/s.

Ethics statement

The study was conducted in accordance with the Declaration of Helsinki and was approved by FAHZU institutional review board (IIT20220714A).

Author contributions

YC and SZ conceived and designed the study. BL and DZ obtained clinical samples and defined the clinical labels. FY and DH performed statistical analysis. WC and DZ wrote the manuscript. LY, MX, JZ and JZ provided clinical expertise and guidance on the study design. YC supervised the project. All authors have accepted responsibility for the entire content of this manuscript and approved its submission.

Funding

The author(s) declare financial support was received for the research, authorship, and/or publication of this article. This study was supported by a grant from the National Natural Science Foundation of China (82300007).

Acknowledgments

The authors thank TargetingOne Corporation (Beijing) for the valuable technical assistance without, in any way, influencing the study design and data analysis.

Conflict of interest

The authors declare that the research was conducted in the absence of any commercial or financial relationships that could be construed as a potential conflict of interest.

Publisher's note

All claims expressed in this article are solely those of the authors and do not necessarily represent those of their affiliated organizations, or those of the publisher, the editors and the reviewers. Any product that may be evaluated in this article, or claim that may be made by its manufacturer, is not guaranteed or endorsed by the publisher.

References

Alonso, H., Samper, S., Martín, C., and Otal, I. (2013). Mapping IS6110 in high-copy number Mycobacterium tuberculosis strains shows specific insertion points in the Beijing genotype. *BMC Genomics* 14, 422. doi: 10.1186/1471-2164-14-422

Antonello, M., Scutari, R., Lauricella, C., Renica, S., Motta, V., Torri, S., et al. (2021). Rapid detection and quantification of *Mycobacterium tuberculosis* DNA in paraffinized samples by droplet digital pcr: a preliminary study. *Front. Microbiol.* 12, 727774. doi: 10.3389/fmicb.2021.727774

Association CM. (2005). *China clinical treatment guide for tuberculosis*. Beijing, China: People's Medical Publishing House.

Cao, Z., Wu, W., Wei, H., Gao, C., Zhang, L., Wu, C., et al. (2020). Using droplet digital PCR in the detection of Mycobacterium tuberculosis DNA in FFPE samples. *Int. J. Infect. Dis.* 99, 77–83. doi: 10.1016/j.ijid.2020.07.045

Charalampous, T., Kay, G., Richardson, H., Aydin, A., Baldan, R., Jeanes, C., et al. (2019). Nanopore metagenomics enables rapid clinical diagnosis of bacterial lower respiratory infection. *Nat. Biotechnol.* 37 (7), 783–792. doi: 10.1038/s41587-019-0156-5

Han, D., Diao, Z., Lai, H., Han, Y., Xie, J., Zhang, R., et al. (2021). Multilaboratory assessment of metagenomic next-generation sequencing for unbiased microbe detection. *J. Adv. Res.* 38, 213–222. doi: 10.1016/j.jare.2021.09.011

Hong, J., Lee, H., Menon, N., Lim, C., Lee, L., and Ong, C. (2022). Point-of-care diagnostic tests for tuberculosis disease. *Sci. Transl. Med.* 14 (639), eabj4124. doi: 10.1126/scitranslmed.abj4124

Huyen, M., Tiemersma, E., Kremer, K., de Haas, P., Lan, N., Buu, T., et al. (2013). Characterisation of Mycobacterium tuberculosis isolates lacking IS6110 in Viet Nam. *Int. Tuberc Lung Disease.* 17 (11), 1479–1485. doi: 10.5588/ijtld.13.0149

Li, Y., Jiao, M., Liu, Y., Ren, Z., and Li, A. (2022). Mycobacterium tuberculosisApplication of metagenomic next-generation sequencing in *Mycobacterium tuberculosis* infection. *Front. Med.* 9, 802719. doi: 10.3389/fmed.2022.802719

Li, Z., Pan, L., Lyu, L., Li, J., Jia, H., Du, B., et al. (2020). Diagnostic accuracy of droplet digital PCR analysis of cerebrospinal fluid for tuberculous meningitis in adult patients. *Clin. Microbiol. Infect.* 26 (2), 213–219. doi: 10.1016/j.cmi.2019.07.015

Liu, X., Chen, Y., Ouyang, H., Liu, J., Luo, X., Huang, Y., et al. (2021). Tuberculosis Diagnosis by Metagenomic Next-generation Sequencing on Bronchoalveolar Lavage Fluid: a cross-sectional analysis. *Int. J. Infect. Dis.* 104, 50–57. doi: 10.1016/j.ijid.2020.12.063

Lyu, L., Li, Z., Pan, L., Jia, H., Sun, Q., Liu, Q., et al. (2020). Evaluation of digital PCR assay in detection of M.tuberculosis IS6110 and IS1081 in tuberculosis patients plasma. *BMC Infect. Dis.* 20 (1), 657. doi: 10.1186/s12879-020-05375-y

Miao, Q., Ma, Y., Wang, Q., Pan, J., Zhang, Y., Jin, W., et al. (2018). Microbiological diagnostic performance of metagenomic next-generation sequencing when applied to clinical practice. *Clin. Infect. Dis.* 67 (suppl_2), S231–S240. doi: 10.1093/cid/ciy693

Nyaruaba, R., Mwaliko, C., Kering, K. K., and Wei, H. (2019). Droplet digital PCR applications in the tuberculosis world. *Tuberculosis (Edinb).* 117, 85–92. doi: 10.1016/j.tube.2019.07.001

Penn-Nicholson, A., Gomathi, S., Ugarte-Gil, C., Meaza, A., Lavu, E., Patel, P., et al. (2021). A prospective multicentre diagnostic accuracy study for the Truenat tuberculosis assays. *Eur. Respir. J.* 58, 2100526. doi: 10.1183/13993003.00526-2021

Shi, C. L., Han, P., Tang, P. J., Chen, M. M., Ye, Z. J., Wu, M. Y., et al. (2020). Clinical metagenomic sequencing for diagnosis of pulmonary tuberculosis. *J. Infect.* 81 (4), 567–574. doi: 10.1016/j.jinf.2020.08.004

Song, N., Tan, Y., Zhang, L., Luo, W., Guan, Q., Yan, M., et al. (2018). Detection of circulating Mycobacterium tuberculosis-specific DNA by droplet digital PCR for vaccine evaluation in challenged monkeys and TB diagnosis. *Emerging Microbes infections.* 7 (1), 78. doi: 10.1038/s41426-018-0076-3

Ushio, R., Yamamoto, M., Nakashima, K., Watanabe, H., Nagai, K., Shibata, Y., et al. (2016). Digital PCR assay detection of circulating Mycobacterium tuberculosis DNA in pulmonary tuberculosis patient plasma. *Tuberculosis (Edinb)* 99, 47–53. doi: 10.1016/j.tube.2016.04.004

World Health Organization. (2020). *Global tuberculosis report*. Geneva, Switzerland: World Health Organization.

World Health Organization. (2021). *Global tuberculosis report*. Geneva, Switzerland: World Health Organization.

Yan, L., Sun, W., Lu, Z., and Fan, L. (2020). Metagenomic Next-Generation Sequencing (mNGS) in cerebrospinal fluid for rapid diagnosis of Tuberculosis meningitis in HIV-negative population. *Int. J. Infect. Dis.* 96, 270–275. doi: 10.1016/j.ijid.2020.04.048

Zhang, Z., Du, J., Liu, T., Wang, F., Jia, J., Dong, L., et al. (2021). EasyNAT MTC assay: A simple, rapid, and low-cost cross-priming amplification method for the detection of mycobacterium tuberculosis suitable for point-of-care testing. *Emerg. Microbes infections.* 10 (1), 1530–1535. doi: 10.1080/22221751.2021.1959271

Zhao, Z., Wu, T., Wang, M., Chen, X., Liu, T., Si, Y., et al. (2022). A new droplet digital PCR assay: improving detection of paucibacillary smear-negative pulmonary tuberculosis. *Int. J. Infect. Dis.* 122, 820–828. doi: 10.1016/j.ijid.2022.07.041

Zhou, X., Wu, H., Ruan, Q., Jiang, N., Chen, X., Shen, Y., et al. (2019). Clinical Evaluation of Diagnosis Efficacy of Active Mycobacterium tuberculosis Complex Infection via Metagenomic Next-Generation Sequencing of Direct Clinical Samples. *Front. Cell Infect. Microbiol.* 9. doi: 10.3389/fcimb.2019.00351

Zhu, N., Zhou, D., and Li, S. (2021). Diagnostic accuracy of metagenomic next-generation sequencing in sputum-scarce or smear-negative cases with suspected pulmonary tuberculosis. *BioMed. Res. Int.* 2021, 9970817. doi: 10.1155/2021/9970817

Zhu, X., Su, S., Fu, M., Peng, Z., Wang, D., Rui, X., et al. (2019). A density-watershed algorithm (DWA) method for robust, accurate and automatic classification of dual-fluorescence and four-cluster droplet digital PCR data. *Analyst.* 144 (16), 4757–4771. doi: 10.1039/c9an00637k

frontiers | Frontiers in Cellular and Infection Microbiology

TYPE Original Research
PUBLISHED 20 February 2024
DOI 10.3389/fcimb.2023.1220012

OPEN ACCESS

EDITED BY
Pushpanathan Muthuirulan,
Harvard University, United States

REVIEWED BY
Carolina Henritta Pohl,
University of the Free State, South Africa
Sima Sadat Seyedjavadi,
Pasteur Institute of Iran (PII), Iran

*CORRESPONDENCE
Min Feng
fengmin612@sina.com
Wenzhi Guo
guowz66@163.com

†These authors have contributed equally to this work

RECEIVED 09 May 2023
ACCEPTED 31 December 2023
PUBLISHED 20 February 2024

CITATION
Huang C, Chang S, Ma R, Shang Y, Li Y, Wang Y, Feng M and Guo W (2024) COVID-19 in pulmonary critically ill patients: metagenomic identification of fungi and characterization of pathogenic microorganisms. *Front. Cell. Infect. Microbiol.* 13:1220012. doi: 10.3389/fcimb.2023.1220012

COVID-19 in pulmonary critically ill patients: metagenomic identification of fungi and characterization of pathogenic microorganisms

Changjun Huang[1†], Siyuan Chang[2†], Rui Ma[2], Yishu Shang[2], Yuexia Li[2], Yun Wang[1], Min Feng[2*] and Wenzhi Guo[1*]

[1]Department of Hepatobiliary Surgery, The First Affiliated Hospital of Zhengzhou University, Zhengzhou, China, [2]Department of Surgical Intensive Care Unit, The First Affiliated Hospital of Zhengzhou University, Zhengzhou, China

Background: Fungal co-infection is prevalent in critically ill patients with COVID-19. The conventional approach applied to fungal identification has relatively low sensitivity and is time-consuming. The metagenomic next-generation sequencing (mNGS) technology can simultaneously detect a variety of microorganisms, and is increasingly being used for the rapid detection and diagnosis of pathogens.

Methods: In this single-center retrospective study, we described the clinical presentation and outcomes of COVID-19 and mNGS positive for fungi in pulmonary critically ill patients during the outbreak of Omicron infection from December 2022 to January 2023.

Results: Among 43 COVID-19 patients with acute respiratory distress syndrome (ARDS) on a single intensive care unit (ICU), 10 were reported to be fungal positive using the mNGS test. The number of pathogenic microorganisms detected by mNGS was significantly higher than that via traditional methods, especially in the detection of fungi and viruses. *Aspergillus* infection was dominant, and most of these patients also had concurrent bacterial or viral infections. Probable or possible COVID-19-associated pulmonary aspergillosis (CAPA) was diagnosed in all 10 patients, and the prognosis was poor.

Conclusion: Patients with COVID-19 may be at increased risk of developing fungal infections as well as concurrent bacterial or viral infections, and mNGS can be a powerful tool in identifying these infections. Clinicians should be aware of the increased risk of fungal infections in COVID-19 patients, particularly those who have underlying immunocompromising conditions, and should monitor for early signs of infection.

KEYWORDS

COVID-19, SARS-CoV-2, aspergillosis, mNGS, CAPA

1 Introduction

The pandemic of an infectious disease named coronavirus disease 2019 (COVID-19) caused by severe acute respiratory syndrome coronavirus 2 (SARS-CoV-2) has become a worldwide threat (Shereen et al., 2020; Hu et al., 2021). COVID-19 infection has rapidly spread over China since December 2022 despite restrictive control measures by the government (The, 2023). As the infection continued to spread, severe pneumonia patients infected with SARS-CoV-2 requiring intensive care unit (ICU) admission gradually emerged.

The prevalence of fungal co-infection was reported in critically ill patients with COVID-19 and the mortality rate remains high (Bhatt et al., 2021; Seyedjavadi et al., 2022). A pre-Omicron outbreak retrospective observational study conducted in China revealed that 5.8% (3/52) of critically ill patients exhibited fungal co-infections (Yang et al., 2020). The identified infectious fungi included *Aspergillus flavus*, *Aspergillus fumigatus*, and *Candida albicans*. As far as our knowledge extends, following the emergence of the Omicron variant in China, substantial data encompassing a large sample size to characterize co-existing fungal infections in COVID-19 cases are currently lacking. Therefore, further clinical evidence in relation to the COVID-19 and fungal co-infection in critically ill patients is necessary. Rapid identification of pulmonary fungal infections facilitates the well-timed antifungal therapy. Despite the fact that microscopy and culture are the conventional approach applied to fungal identification, both methods have a relatively low sensitivity, and culture is a time-consuming process because of the long fungal growth time (Li, 2022). Histopathological diagnosis is still the gold standard for identifying invasive fungal infections (IFIs), despite it being a lengthy process (Mendonca et al., 2022). Immunological recognition of serum galactomannan and β-d-glucan antigen has significant auxiliary diagnostic efficacy, but there are many cofounding factors (Li, 2022). The metagenomic next-generation sequencing (mNGS) technology is a high-throughput DNA or RNA sequencing method that can simultaneously detect a variety of microorganisms, including bacteria, viruses, and fungi, and is widely used for the rapid detection and diagnosis of pathogens (Gu et al., 2021). Although mNGS has disadvantages such as its high cost, susceptibility to exogenous microbial contamination, and reduced efficiency in detecting thick-walled fungi, research has showcased its superior sensitivity and specificity in diagnosing invasive fungal diseases compared to traditional culture and histopathological methods (El-Kamand et al., 2019; Song et al., 2021; Wang et al., 2022). In certain circumstances, mNGS has a superior positive detection efficiency and can determine fungal pathogens that are difficult to diagnose via conventional diagnostic approaches (Zheng et al., 2021; Wu et al., 2023).

In this single-center retrospective study, we described the clinical presentation and outcomes of COVID-19 and mNGS positive for fungi in pulmonary critically ill patients during the outbreak of Omicron infection from December 2022 to January 2023.

2 Patients and methods

2.1 Study cohort

This is a retrospective single-center cohort study in China. Patients who were admitted to the ICU at the First Affiliated Hospital of Zhengzhou University between 29 December 2022 and 23 January 2023 were reviewed. All adult patients (aged > 18 years) who were diagnosed with COVID-19 and acute respiratory distress syndrome (ARDS), and who had undergone mNGS testing at least once, were screened. Furthermore, patients positive for fungi via mNGS testing were included in our study.

2.2 Data collection

Demographic, epidemiological, clinical, laboratory, treatment, and outcome data were retrieved from electronic medical records utilizing a standardized data collection form. All data were examined by two physicians (CH and SC), and a third researcher (YW) resolved contradictions between the two reviewers, if any.

2.3 Laboratory procedures

Methods for laboratory identification of SARS-CoV-2 infection have been described previously (Huang et al., 2020a). Briefly, the clinical laboratory of the First Affiliated Hospital of Zhengzhou University was responsible for SARS-CoV-2 detection in respiratory specimens using real-time RT-PCR or the antigen rapid detection test. SARS-CoV-2 and other pathogen detection in bronchoalveolar lavage fluid (BALF) or peripheral blood (PB) by mNGS was performed by the clinical laboratory of the First Affiliated Hospital of Zhengzhou University or Hangzhou Matridx Biotechnology Co., Ltd., Zhejiang, China. Initial data from the mNGS upon admission to the ICU were collected for analysis if the patient had multiple mNGS tests.

Results of the first examination after admission to ICU of routine blood examinations, procalcitonin (PCT), C-reactive protein (CRP), interleukin-6 (IL-6), N-terminal pro-brain natriuretic peptide (BNP), creatinine (Cr), urea, prothrombin time (PT), activated partial thromboplastin time (APTT), d-dimer, glucose (Glu), alanine aminotransferase (ALT), total bilirubin (TBIL), lactic acid (Lac), high-sensitivity cardiac troponin T (TNT), high-sensitivity cardiac troponin I (TNI), creatine kinase-MB (CK-MB), lymphocyte immunoassay, galactomannan, β-D-glucan, and microbial culture of PB, BALF, and sputum were collected for further analysis. Variables might be unavailable in some circumstances. Chest x-ray or CT scan was also performed for all patients. Frequency of examinations was determined by the managing physician. SOFA score, CURB-65 score, and APACHE II score were collected upon admission to the ICU.

2.4 mNGS detection protocol

Nucleic acid extraction, library preparation, and sequencing: For the BALF, cell walls of microbes were broken by vortex with glass beads. For the blood, the plasma was separated. DNA was extracted using the TIANamp micro DNA kit (DP316; Tiangen Biotech, Beijing, China) following the manufacturer's operation manual. Total RNA was extracted with a QIAamp® Viral RNA Kit (Qiagen) and ribosomal RNA was removed using a Ribo-Zero rRNA Removal Kit (Illumina). cDNA was generated using reverse transcriptase, random hexamer primers, and dNTPs (Thermo Fisher). Libraries were constructed for the DNA and cDNA samples using a Nextera XT DNA Library Prep Kit (Illumina, San Diego, CA). The library was purified and the fragments were selected by the magnetic beads. The library was quality assessed by the Qubit dsDNA HS Assay kit followed by the High Sensitivity DNA kit (Agilent) on an Agilent 2100 Bioanalyzer. The size of the qualified library was 300 to 500 bp without adapters and PCR dimers, and the concentration of the library was greater than 1 ng/mL. Library pools were then loaded onto an Illumina Nextseq 500CN sequencer for 75 cycles of single-end sequencing to generate approximately 20 million reads for each library. The internal control, named UMSI (unique molecular spiked-in), was added to the sample before the DNA extraction. The sequence of UMSI varied in different samples. Each mNGS assay run included an external negative control that ran in parallel with clinical samples. During analysis, the contamination between samples can be found if the UMSI sequence was the same or the reads of some pathogens in the external control were very high.

Bioinformatics analyses: High-quality sequencing data were generated by removing low-quality and short (length < 40 bp) reads, followed by computational subtraction of human host sequences mapped to the human reference genome (hg38 and YH sequences) using Burrows–Wheeler Alignment. After the removal of low-complexity reads, the remaining data were classified by simultaneously aligning them to four microbial genome databases, namely, viruses, bacteria, fungi, and parasites. The classification reference databases were downloaded and optimized from public databases such as NCBI, EBI, or Genbank. In the end, the multi-parameters of species in microbial genome databases were calculated and exported, and professionals with microbiology and clinical backgrounds interpreted the results.

2.5 Definitions

ARDS was diagnosed in accordance with the Berlin definition (Force et al., 2012). For the diagnosis of COVID-19-associated invasive pulmonary aspergillosis (CAPA), the modified ECMM/ISHAM 2020 consensus criteria were adopted (Fortun et al., 2023):

Probable CAPA: Compatible clinical and imaging manifestations (pulmonary infiltrate or nodules preferably documented by chest CT or cavitating infiltrate), along with microbiological isolation of *Aspergillus* in BALF, galactomannan in BALF > 1, or galactomannan in serum > 0.5.

Possible CAPA: Compatible clinical and imaging manifestations, along with microbiological isolation of *Aspergillus* in respiratory specimens in sputum. Possible pulmonary CAPA requires pulmonary infiltrates, well-circumscribed lesions(s) or nodules, preferably documented by chest CT, or cavitating infiltrate that cannot be attributed to another cause. In patients with bilateral, ground-glass opacities or other COVID-19-related manifestations, significant radiological changes as described above and confirmed by a specialized radiologist are necessary to consider the possibility of CAPA.

The study was conducted in accordance with the ethical principles of Good Clinical Practice and the Declaration of Helsinki. The study was approved by the ethics committee of the First Affiliated Hospital of Zhengzhou University (Identifier: 2023-KY-0139-001). This study was registered in chictr.org/cn (registry number: ChiCTR2300070926).

3 Results

A total of 43 successive ARDS patients with COVID-19 (34 male and 9 female patients; median age, 60 years [IQR 44–76]) were detected. Of the 43 patients, 10 patients who tested positive for fungi via mNGS were included (Table 1).

Patient #1: A 41-year-old man was admitted to the ICU because of severe ARDS with a Horowitz Index of 79 mm Hg. Nasopharyngeal swab PCR test showed that he was positive for SARS-CoV-2. He had a medical history of hypertension and type 2 diabetes. He underwent right kidney transplantation in 2003; tacrolimus, mycophenolate, and steroids were administered for immunosuppression therapy. Chest CT showed bilateral ground-glass opacities with mist-like high-density shadows (Supplementary Video S1; Figure 1A). PB was positive for *A. fumigatus*, and BALF was positive for *A. fumigatus, Aspergillus niger*, *Pneumocystis jeroveci, Enterococcus faecium, Leuconostoc lactis*, and *Tropheryma whipplei*, via the mNGS test. BALF culture tested positive for *A. flavus*. Intravenous voriconazole and inhalational amphotericin B were utilized for antifungal treatment. Sulfamethoxazole was administered as anti-pneumocystis prophylaxis. Meropenem and linezolid were adopted for antibacterial therapy. Penciclovir was adopted for antiviral therapy. Azvudine and Paxlovid were sequentially used for anti-COVID-19 therapy. Steroids were used to treat pneumonia, and prone positioning was also utilized. Because of acute renal failure, continuous renal replacement therapy (CRRT) was started.

Patient #2: A 55-year-old man was transferred to the ICU due to ARDS with a Horowitz Index of 97 mm Hg. Antigen rapid detection test revealed that he was SARS-CoV-2 positive (24 days before ICU admission). He had a medical history of acute kidney injury. He underwent liver transplantation owing to hepatitis B cirrhosis; tacrolimus and mycophenolate were administered for immunosuppression therapy. Chest CT showed bilateral decreased transparency and multiple nodular high-density shadows, with pulmonary consolidation (Supplementary Video S2; Figure 1B). *A. flavus*/*Aspergillus oryzae, Klebsiella pneumoniae*, and *Acinetobacter baumannii* were detected in BALF; *A. fumigatus, K. pneumoniae*, human alphaherpesvirus 1, and Epstein–Barr virus were

TABLE 1 Characteristics of pulmonary critically ill patients with COVID-19 and positive for fungi by metagenomic analysis.

Characteristics	Patient #1	Patient #2	Patient #3	Patient #4	Patient #5	Patient #6	Patient #7	Patient #8	Patient #9	Patient #10
Demographics and clinical characteristics										
Gender	M	M	F	M	M	F	M	M	M	M
Age (years)	41	55	62	54	53	44	32	76	73	83
Diagnosis for COVID-19	PCR, mNGS	Antigen	PCR	PCR	Antigen	PCR, mNGS	PCR	PCR, mNGS	PCR	PCR, mNGS
Medical history	Hypertension, type 2 diabetes, kidney transplant status	Acute kidney injury, liver transplant status	Hypertension, nephritic syndrome	Hypertension, type 2 diabetes, liver abscess after percutaneous drainage	Thymoma B3	Hypertension, kidney transplant status	No	Coronary atherosclerotic heart disease after PCI, liver cirrhosis, hypersplenism, old cerebral infarction, type 2 diabetes, hypertension	No	Hypertension, coronary heart disease
Current smoker	Yes	No	No	Yes	No	No	Yes	No	No	No
Underlying immunocompromising condition	Steroids, tacrolimus, mycophenolate	Tacrolimus, mycophenolate, sirolimus	Mycophenolate	No	Oxaliplatin + cyclophosphamide + doxorubicine chemotherapy	Steroids, tacrolimus, mycophenolate	No	No	No	No
Cause of admission to the ICU	ARDS	ARDS	ARDS	ARDS, cerebral infarction, cerebral hernia, septic shock	ARDS	ARDS	ARDS, acute pancreatitis	ARDS	ARDS	ARDS, cardiopulmonary arrest after cardiopulmonary resuscitation
Time from illness onset to ICU admission, days	14	24	10	4	3	42	1	11	30	20
ARDS	Yes	Yes	Yes	Yes	Yes	Yes	Yes	Yes	Yes	Yes
PaO_2 (ICU admission)	71	92	43	94	69	70	99	64	48	75
FIO_2 (ICU admission)	0.90	0.95	0.61	0.41	0.7	0.60	0.41	0.81	1.00	0.80
Horowitz Index (ICU admission)	79	97	70	229	99	117	241	79	48	94
Prone positioning	Yes	Yes	Yes	No	No	No	Yes	Yes	No	No
Tracheal intubation	Yes	Yes	Yes	Yes	Yes	Yes	Yes	Yes	Yes	Yes

(Continued)

10.3389/fcimb.2023.1220012

TABLE 1 Continued

Characteristics	Patient #1	Patient #2	Patient #3	Patient #4	Patient #5	Patient #6	Patient #7	Patient #8	Patient #9	Patient #10
SOFA score (ICU admission)	7	8	4	7	6	7	4	7	9	8
CURB-65 score (ICU admission)	2	2	2	2	1	2	1	2	3	3
APACHE II score (ICU admission)	12	34	18	22	19	12	11	14	24	35
CAPA classification	Probable	Possible	Probable	Probable	Possible	Probable	Probable	Probable	Possible	Possible
Laboratory findings										
mNGS (first time after ICU admission)										
Specimen	BALF & PB	BALF & PB	BALF	BALF	BALF	BALF	BALF	BALF	BALF	BALF
Fungus	*Aspergillus fumigatus* (PB & BALF) *Aspergillus niger* (BALF) *Pneumocystis jeroveci* (BALF)	*Aspergillus flavus/Aspergillus oryzae*(BALF) *Aspergillus fumigatus* (PB)	*Aspergillus fumigatus* *Aspergillus flavus*	*Aspergillus fumigatus*	*Aspergillus fumigatus*	*Aspergillus flavus* *Aspergillus fumigatus*	*Aspergillus flavus/ Aspergillus oryzae* *Rhizopus oryzae*	*Aspergillus flavus/Aspergillus oryzae* *Aspergillus fumigatus*	*Aspergillus flavus* *Aspergillus terreus* *Clavispora lusitaniae*	*Aspergillus fumigatus* *Candida albicans*
Bacteria	*Enterococcus faecium* (BALF) *Leuconostoc lactis* (BALF) *Tropheryma whipplei* (BALF)	*Klebsiella pneumoniae* (BALF & PB) *Acinetobacter baumannii* (BALF)	No	*Klebsiella pneumoniae* *Streptococcus pneumoniae* *Acinetobacter baumannii* *Enterococcus faecium*	*Acinetobacter baumannii*	*Enterococcus faecium* *Acinetobacter pittii*	*Escherichia coli* *Klebsiella pneumoniae*	*Acinetobacter baumannii*	*Klebsiella pneumoniae* *Enterococcus faecium*	No
Virology[1]	Epstein–Barr virus (PB) Human betaherpesvirus 5 (BALF) SARS-CoV-2 (BALF)	Human alphaherpesvirus 1 (PB) Epstein–Barr virus (PB)	No	Human alphaherpesvirus 1 Epstein–Barr virus	Human betaherpesvirus 5	Torque teno virus SARS-CoV-2	No	SARS-CoV-2	No	SARS-CoV-2
Serum galactomannan (μg/L) [<0.85][2]	0.43	0.47	0.31	0.12	0.81	0.84	1.94	0.96	NA	0.28
Serum β-D-glucan (pg/mL) [0-95]	<10	<10	<10	171.11	<10	294.35	126.97	<10	NA	<10
BALF galactomannan (pg/mL) [<1]	0.48	0.36	NA	NA	NA	0.36	3.87	1.26	NA	NA

(Continued)

10.3389/fcimb.2023.1220012

TABLE 1 Continued

Characteristics	Patient #1	Patient #2	Patient #3	Patient #4	Patient #5	Patient #6	Patient #7	Patient #8	Patient #9	Patient #10
Sputum culture	Negative	*Acinetobacter baumannii*	NA	*Acinetobacter baumannii*	Negative	Negative	*Acinetobacter baumannii*	*Acinetobacter baumannii*	NA	NA
BALF culture	*Aspergillus flavus*	*Acinetobacter baumannii*	*Aspergillus fumigatus Aspergillus flavus*	Negative	Negative	Negative	*Escherichia coli Aspergillus flavus*	*Acinetobacter baumannii*	*Klebsiella pneumoniae*	Negative
Pheripheral blood culture	Negative	*Enterococcus faecium Klebsiella pneumoniae*	Negative	Negative	Negative	Negative	Negative	Negative	*Enterococcus faecium*	*Candida albicans*
Treatment										
Steroids to treat pneumonia	Yes	Yes	No	Yes	Yes	Yes	No	Yes	Yes	No
Antifungal	Voriconazole, Amphotericin B, Sulfamethoxazole	Voriconazole, Amphotericin B	Voriconazole	Voriconazole	Voriconazole	Voriconazole	Isavuconazole Amphotericin B	Voriconazole	No	No
Antiviral (besides COVID-19)	Penciclovir	Ganciclovir	No	No	No	Ganciclovir	No	No	No	No
Anti-COVID-19	Azvudine, Paxlovid	Paxlovid	Azvudine, Paxlovid	No	No	Paxlovid	No	Azvudine, Paxlovid	Azvudine, Paxlovid	No
Antibacterial	Meropenem, Linezolid	Ceftazidime and Avibactam Sodium, Polymyxin B	Ceftizoxime	Meropenem, Ceftazidime, and Avibactam Sodium	Imipenem and cilastatin sodium, Teicoplanin	Biapenem, Linezolid	Imipenem and Cilastatin Sodium, Ceftazidime and Avibactam Sodium, Teicoplanin	Moxalactam Cefoperazone Sodium and Sulbactam Sodium	Cefoperazone Sodium and Sulbactam Sodium	Imipenem and Cilastatin Sodium
Outcomes										
Acute renal failure	Yes	Yes	No	No	Yes	No	No	No	No	Yes
Renal replacement therapy	Yes	Yes	No	No	Yes	No	No	No	No	Yes
Vasopressor	Yes	Yes	No	Yes	Yes	No	Yes	No	No	Yes
ECMO	No	No	No	No	Yes(V-A)	No	Yes (V-V)	No	No	Yes (V-V)
Outcome	Died	Survived	Survived	Died	Died	Survived	Survived	Died	Died	Died

APACHE, Acute Physiology and Chronic Health Evaluation; ARDS, acute respiratory distress syndrome; BALF, bronchoalveolar lavage fluid; CAPA, COVID-19-associated pulmonary aspergillosis; CURB-65, Confusion, Urea, Respiratory rate, Blood pressure plus age ≥ 65 years; ECMO, extracorporeal membrane oxygenation; FIO_2, fraction of inspiration oxygen; ICU, intensive care unit; mNGS, metagenomic next-generation sequencing; NA, not available; PaO_2, partial pressure of oxygen; PB, peripheral blood; PCI, percutaneous coronary intervention; PCR, polymerase chain reaction; SOFA, Sequential Organ Failure Assessment; V-A, venoarterial; V-V, venovenous.

[1]In patient #2, #3, #4, #5, #7, and #9, only DNA sequencing was performed and no SARS-CoV-2 was detected.

[2]Normal reference range of our laboratory was given in square brackets. The same below.

10.3389/fcimb.2023.1220012

10.3389/fcimb.2023.1220012

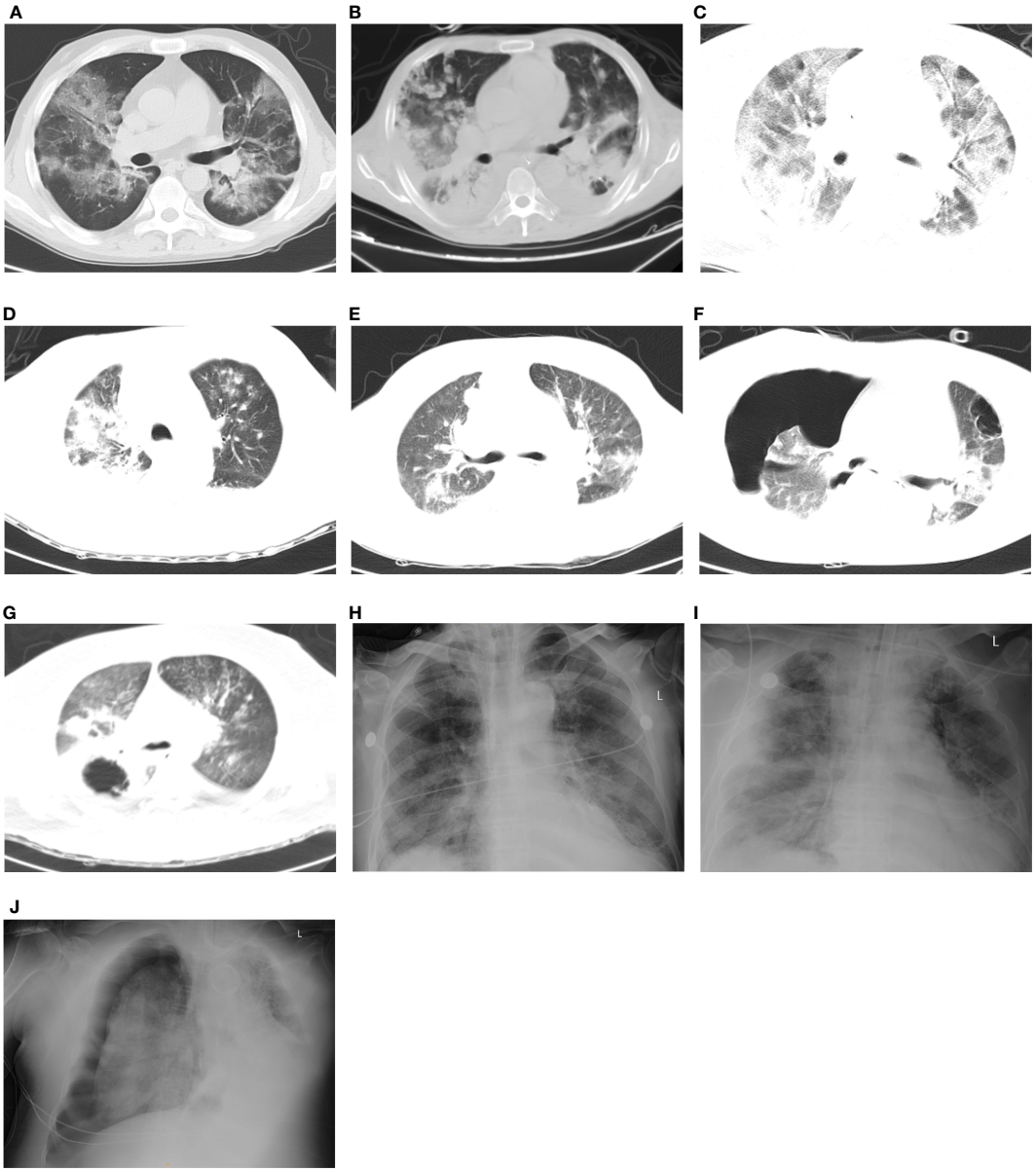

FIGURE 1
Thoracic CT-scan/x-ray of patients with COVID-19-associated pulmonary fungal infection. **(A)** Patient #1: Combined bilateral ground-glass opacities accompanied by mist-like shadows of high density. **(B)** Patient #2: Bilateral reductions in transparency with the presence of multiple nodular shadows of high density, accompanied by consolidations. **(C)** Patient #3: Bilateral multiple ground-glass opacities and patchy shadows. **(D)** Patient #4: The bronchovascular shadows bilaterally increased and blurred, accompanied by multiple patchy, cord-like, and round-like high-density shadows, as well as consolidations. **(E)** Patient #5: Bilateral ground-glass opacities present along with multiple patchy, cord-like high-density shadows. **(F)** Patient #6: Bilateral ground-glass opacities with patchy, cord-like high-density shadows, as well as cavities in both upper lung lobes. In addition, there was evidence of hydropneumothorax causing the right lung to collapse. **(G)** Patient #7: Bilateral ground-glass opacities with multiple small nodules and patchy, cord-like high-density shadows. Additionally, there were multiple cavities and consolidations observed in the right lung lobe. **(H)** Patient #8: Bilateral thickening of the lung texture and the presence of small exudation shadows. **(I)** Patient #9: Bilateral bronchovascular shadows that appeared increased and blurred, along with the presence of multiple exudations. **(J)** Patient #10: Bilateral increased thickening of the lung texture, with evidence of pleural effusion and atelectasis on the left side, as well as pneumothorax on the right side.

detected in PB, via the mNGS test. *A. baumannii* was grown in sputum and BALF culture. *E. faecium* and *K. pneumoniae* were detected in PB culture. Intravenous voriconazole and inhalational amphotericin B were used for antifungal therapy. Ceftazidime, avibactam sodium, and polymyxin B were administered for antibacterial therapy. Penciclovir was used for antiviral therapy. Paxlovid was adopted to treat COVID-19. Steroids and prone positioning were also commenced. Owing to acute renal failure, CRRT was initiated.

Patient #3: A 62-year-old woman was transferred to the ICU by virtue of ARDS and having tested positive for SARS-CoV-2 via PCR. Her Horowitz Index was 70 mm Hg. Previous medical history suggested hypertension and nephritic syndrome. Mycophenolate was taken regularly for 2 years. Chest CT scan exhibited multiple

ground-glass opacities and patchy shadows in both lungs (Supplementary Video S3; Figure 1C). *A. fumigatus* and *A. flavus* were both detected in BALF via mNGS and culture. Ceftizoxime was adopted for empirical treatment after ICU admission. Intravenous voriconazole was started after testing positive for *Aspergillus*. Azvudine and Paxlovid were successively commenced. Prone positioning was also put to use.

Patient #4: A 54-year-old man was admitted to the ICU because of mild ARDS (Horowitz Index of 229 mm Hg), coma, acute cerebral infarction, cerebral hernia, and septic shock. PCR test showed that he was positive for SARS-CoV-2. Previous medical history suggested hypertension, type 2 diabetes, and liver abscess after percutaneous drainage. Chest CT showed bilateral increased and blurred bronchovascular shadows with multiple patchy, cord-like, and round-like high-density shadows, as well as consolidations (Supplementary Video S4; Figure 1D). *A. fumigatus, K. pneumoniae*, *Streptococcus pneumoniae*, *A. baumannii, E. faecium*, human alphaherpesvirus 1, and Epstein–Barr virus were detected in BALF via mNGS analysis. Sputum culture grew *A. baumannii*, and drainage fluid of liver abscess culture grew *K. pneumoniae*. Intravenous voriconazole was commenced. Meropenem, ceftazidime, and avibactam sodium were utilized for antibacterial therapy.

Patient #5: A 53-year-old man presented with ARDS with a Horowitz Index of 99 mm Hg. Antigen rapid detection test suggested that he was SARS-CoV-2 positive. He was diagnosed with thymoma 20 days ago and was treated with oxaliplatin + cyclophosphamide + doxorubicine chemotherapy. Chest CT demonstrated bilateral ground-glass opacities and multiple patchy, cord-like high-density shadows (Supplementary Video S5; Figure 1E). *A. fumigatus, A. baumannii*, and human betaherpesvirus 5 were detected in BALF via the mNGS test. Imipenem, cilastatin sodium, and teicoplanin were adopted for antibacterial treatment. Intravenous voriconazole was started. On account of acute renal failure, CRRT was commenced. Owing to unsustainability of circulation, venoarterial (V-A) extracorporeal membrane oxygenation (ECMO) was put into use.

Patient #6: A 44-year-old woman was transferred to the ICU as a result of ARDS with a Horowitz Index of 117 mm Hg. PCR test suggested SARS-CoV-2 infection. She had a medical history of hypertension and uremia. She received kidney transplantation 10 years ago and was regularly taking tacrolimus and mycophenolate for antirejection therapy. Chest CT revealed ground-glass opacities with patchy, cord-like high-density shadows in both lungs, and cavity in the both upper lung lobes, as well as hydropneumothorax with a collapsed right lung (Supplementary Video S6; Figure 1F). *A. flavus, A. fumigatus, E. faecium, Acinetobacter pittii*, and Torque teno virus were detected in BALF via the mNGS test. Serum β-D-glucan also had a positive result. Intravenous voriconazole was utilized for antifungal therapy. Biapenem and linezolid were adopted for antibacterial therapy. Ganciclovir was used for antiviral therapy. Paxlovid was used for anti-COVID-19 treatment. Steroids were also started to treat pneumonia.

Patient #7: A 31-year-old man was admitted to the ICU because of mild ARDS (Horowitz Index: 79 mm Hg) and acute pancreatitis. PCR test showed that he was positive for SARS-CoV-2. Chest CT showed bilateral ground-glass opacities with multiple small nodules, patchy, cord-like high-density shadows, as well as multiple cavities and consolidations in the right lung lobe (Supplementary Video S7; Figure 1G). BALF was positive for *A. flavus*/*A. oryzae, Rhizopus oryzae, Escherichia coli*, and *K. pneumoniae*, via the mNGS test. *A. baumannii* was grown in sputum culture. *E. coli* and *A. flavus* were grown in BALF culture. Elevated galactomannan was seen in serum and BALF. Elevated serum β-D-glucan was also detected. Intravenous isavuconazole and inhalational amphotericin B were used for antifungal therapy. Imipenem, cilastatin sodium, ceftazidime, avibactam sodium, and teicoplanin were utilized for antibacterial treatment. Despite prone positioning, the patient required venovenous (V-V) ECMO supportive treatment to restore and maintain circulation stabilization.

Patient #8: A 76-year-old man was admitted to our ICU. He was intubated and developed severe ARDS with a Horowitz Index of 73 mm Hg. Nasopharyngeal swab PCR test showed that he was positive for SARS-CoV-2. He had a medical history of coronary atherosclerotic heart disease after percutaneous transluminal coronary intervention, liver cirrhosis, hypersplenism, old cerebral infarction, type 2 diabetes, and hypertension. X-ray radiography showed a combination of bilateral thickening of the lung texture and small exudation shadows (Figure 1H). The prehospital CT report suggested bilateral inferior pulmonary interstitial fibrosis and infection (no images available). *A. flavus*/*A. oryzae, A. fumigatus*, and *A. baumannii* were detected in BALF via the mNGS test. Elevated galactomannan in serum and BALF was detected. *A. baumannii* was detected in sputum and BALF culture. Intravenous voriconazole was used for antifungal treatment. Moxalactam or cefoperazone sodium and sulbactam sodium were used for antibacterial therapy. Azvudine or Paxlovid was separately adopted for anti-COVID-19 therapy. Steroids and prone positioning were also utilized. The patient eventually died of respiratory failure and respiratory cardiac arrest (Patient #1, Table 1).

Patient #9: A 73-year-old man presented with ARDS with a Horowitz Index of 48 mm Hg. PCR test revealed that he was SARS-CoV-2 positive. Chest x-ray imaged bilateral increased and blurred bronchovascular shadows, with multiple exudation (Figure 1I). Chest CT from the local hospital suggested bilateral ground-glass opacities (no images available). Azvudine and Paxlovid were already administered as anti-COVID-19 treatment at the local hospital. *A. flavus, Aspergillus terreus, Clavispora lusitaniae, K. pneumoniae*, and *E. faecium* were detected in BALF via mNGS. *K. pneumoniae* was grown in BALF and *E. faecium* was grown in PB. Cefoperazone sodium and sulbactam sodium were used for empirical treatment after ICU admission. The patient died of respiratory failure and malignant arrhythmias before the microbiological results became available.

Patient #10: An 83-year-old man was transferred to our ICU because of severe ARDS (Horowitz Index: 94 mm Hg) and cardiopulmonary arrest after cardiopulmonary resuscitation. PCR test suggested that he was SARS-CoV-2 positive. He had a medical history of hypertension and coronary heart disease. Chest x-ray radiography showed bilateral increased thickening of the lung

texture, with pleural effusion and atelectasis on the left side, as well as pneumothorax on the right side (Figure 1J). BALF mNGS test revealed positive results for *A. fumigatus* and *C. albicans*. *C. albicans* was also detected in PB culture. V-V ECMO was performed after cardiopulmonary resuscitation. CRRT was adopted for renal replacement and toxin clearance. Imipenem and cilastatin sodium were utilized for empirical treatment after ICU admission. The patient died of respiratory failure and multiple organ dysfunction syndrome before antifungal therapy.

Among the 10 patients, 6 patients died, with all fatalities attributed to pulmonary co-infections caused by COVID-19 and subsequent multi-organ dysfunction, while the remaining 4 patients survived following treatment. Detailed patient characteristics are given in Table 1. Hematological test results for the 10 patients are presented in Table 2.

4 Discussion

Patients with ARDS induced by SARS-CoV-2 infection are prone to fungal infections despite having no previous immunodeficiency conditions (Buil et al., 2020; Koehler et al., 2020). Among 43 COVID-19 patients with moderate to severe ARDS with or without underlying immunocompromising factors on a single ICU, 10 were reported to be fungal positive using the mNGS test.

In the past few years, mNGS has been increasingly utilized in clinical diagnosis and has remarkable practical application value in the diagnosis of pathogenic microbial infection (Gu et al., 2019; Duan et al., 2021; Tang et al., 2021). In our study, the number of pathogenic microorganisms detected by mNGS was significantly higher than that by traditional methods, especially in the detection of fungi and viruses, although some studies report that there was no significant difference in the specificity between mNGS and conventional methods (Chen et al., 2020b; Huang et al., 2020b). The combined application of mNGS and traditional methods may provide robust backup in the diagnosis of pulmonary pathogenic microorganism infections. Metagenomic sequencing is a powerful tool in identifying newly emerging, uncommon, and unexpected pathogens. In certain circumstances, it can even be a life-saving test and the most dependable way to detect disease-causing microorganisms (Wilson et al., 2014).

For patients with pulmonary infections, PB and sputum specimens are more readily obtainable. In our center, traditional culturing and immunological testing remain the preferred diagnostic methods. However, the overall diagnostic efficiency is relatively low, often necessitating repeated testing to yield positive results or with consistently negative results, particularly in cases where empirical antibiotic treatment has been administered. BALF is highly sensitive for pulmonary infection detection and is the preferred specimen type, particularly in critically ill patients requiring fiberoptic bronchoscopy. BALF can be used for microbial culture, biochemical testing, cytological examination, parasitological examination, and mNGS testing. In this study, mNGS test results were obtained for the first time after ICU admission, and in most cases, BALF specimens were predominantly used. Therefore, the time of mNGS specimen submission typically lags behind that of conventional culturing and immunological testing.

Our objective is quite clear: we aim to utilize mNGS technology for early and rapid screening of potential pathogenic microorganisms, thereby providing specific guidance for further antimicrobial treatment. In the analysis of these 10 cases, it is evident that COVID-19 patients have a significantly high occurrence of concurrent infections with other pathogenic microorganisms, and there is also a high probability of detecting fungi. However, it is not possible to diagnose IFIs solely through mNGS testing, as positive fungal detection in BALF samples may also indicate colonization. The gold standard for IFI diagnosis is histopathological biopsy. Nevertheless, patient conditions often render this approach unrealistic, and as such, we did not pursue it. COVID-19 patients who develop IFI exhibit poor treatment responsiveness and high mortality rates (Baddley et al., 2021; Fortun et al., 2023). Consequently, when we detected fungi in BALF through mNGS, antifungal treatment for the patients was subsequently initiated. However, owing to the limited number of cases, it is challenging to determine whether this combined anti-infective therapy decisively contributed to the patients' ultimate recovery. Given this limitation, it may be necessary to expand the sample size in future mNGS-related studies. Additionally, this highlights a shortcoming of mNGS, as it can detect a wide array of pathogenic species but cannot distinguish between pathogenic, colonizing, and contaminating microorganisms. Following pathogen detection, it is imperative to integrate other infection-related indicators in patients, such as blood PCT, CRP, BALF galactomannan, β-D-glucan, BALF cultures, and chest imaging, among others, to comprehensively evaluate the patient's infection status and thereby guide treatment decisions. Ultimately, treatment effectiveness should be assessed based on the patient's response to therapy.

There is a growing body of evidence suggesting that patients, especially those admitted to the ICU with COVID-19, may be at increased risk of developing fungal infections, such as aspergillosis, mucormycosis, candidiasis, and cryptococcosis (Amin et al., 2021; Doman and Banyai, 2022; Hoenigl et al., 2022). This association is likely due to several factors, including the immunocompromised effects of COVID-19, the use of corticosteroids and other immunomodulatory therapies in the treatment of severe COVID-19, and the use of invasive medical procedures such as mechanical ventilation, which can increase the risk of fungal colonization and infection (Baddley et al., 2021; Ezeokoli et al., 2021). *Aspergillus* infection was dominant in our study, as revealed by mNGS analysis indicating that all 10 patients were infected with or had co-infections involving *Aspergillus*. Likewise, some previous studies also documented a notable rise in the occurrence of aspergillosis among COVID-19 patients who were critically ill (Chen et al., 2020a; Koehler et al., 2020; Chong and Neu, 2021). It is important for clinicians to be aware of the increased risk of fungal infections in COVID-19 patients, particularly those who have underlying immunocompromising conditions, and to monitor for early signs of infection. Treatment of fungal infections in these patients may

TABLE 2 Hematological test results for the 10 cases included in the study.

Hematological tests[1]	Patient #1	Patient #2	Patient #3	Patient #4	Patient #5	Patient #6	Patient #7	Patient #8	Patient #9	Patient #10
Blood routine examination										
WBC (10^9/L) [3.5–9.5][2]	14.79	6.16	18.79	16.51	8.32	14.42	29.72	3.39	10.83	23.35
HGB (g/L) [130–175]	87	73	142	121	117	109	141	131	112	92
PLT (10^9/L) [125–350]	318	25	178	90	60	32	210	42	64	251
Lymphocyte ratio (%) [20–50]	1.9	4.8	1.8	6.7	9.9	0.5	4.2	3.5	1.5	8.7
Lymphocyte count (10^9/L) [1.1–3.2]	0.28	0.3	0.34	1.11	0.82	0.07	1.25	0.12	0.16	2.03
PCT (ng/mL) [<0.064]	2.7	2.5	0.13	23	22	0.44	3.5	0.59	<0.07	31
CRP (mg/L) [<5]	59.16	165	60	119	152	25	450	74	30	89
IL-6 (pg/mL) [0–11.09]	10.46	585.05	1.5	21.01	175	436.58	133.26	7.87	111.48	321.84
BNP (pg/mL) [age-adjusted][3]	5,110	20,500	1,930	248,000	161,000	1,450	735	1,565	797	7,930
Cr (μmol/L) [20–115]	315	244	66	73	238	55	52	60	107	101
Urea (mmol/L) [2.2–8.2]	19.33	24.12	9.9	10.38	17.2	20.68	7.63	10.4	19.71	12.77
PT (s) [8.8–13.6]	11	11.6	10.7	13.1	11.1	12.1	15.8	12.5	13.4	15.1
APTT (s) [26–40]	26.3	30.4	24.5	27.8	33.7	29.9	29	30	28.9	67.4
D-dimer (mg/L) DDU [0–0.55]	4.82	0.82	6.09	5.87	3.31	0.32	0.96	6.47	11.19	44.13
Glu (mmol/L) [3.6–6.1]	17.61	6.32	6.5	16.3	10.86	4.25	20.9	7.29	8.95	17.08
ALT (U/L) [0–40]	6	1	10	201	865	55	30	30	18	202
TBIL (μmol/L) [0–25]	10.4	8.6	13.3	16.6	10.6	28.3	29.3	18.5	7	14.6
Lac (mmol/L) [0.5–2.2]	1.1	1.1	1.6	1.5	2.6	1.2	1.8	1.7	1.2	15
TNT (ng/mL) [0–0.014]	0.064	0.066	0.018	0.1	9.53	0.06	0.013	0.015	NA	0
TNI (μg/L) [0.010–0.023]	0.019	0.02	<0.010	0.17	9.5	0.037	0.018	<0.010	0.021	0.062
CK-MB (ng/mL) [2–7.2]	4.2	<2	4.4	<2	395	10	3.01	3.8	<2	3.4
Lymphocyte analysis										
T (%) [50–81]	77.24	80.72	55.03	71.71	98.07	62.99	61.77	46.64	63.84	78.05
CD4+T (%) [27–51]	33.17	61.58	23.34	49.01	28.95	19.14	37.25	30.25	34.09	31.98
CD8+T (%) [15–44]	39.2	18.12	27.23	21.91	66.5	43.21	22.83	16.96	28.93	41.32
B (%) [5–8]	17.23	17.28	35.2	14.72	0	13.43	33.62	44.29	18.39	11.05

(Continued)

10.3389/fcimb.2023.1220012

10.3389/fcimb.2023.1220012

TABLE 2 Continued

Hematological tests[1]	Patient #1	Patient #2	Patient #3	Patient #4	Patient #5	Patient #6	Patient #7	Patient #8	Patient #9	Patient #10
NK (%) [7–40]	12.5	1.36	9.49	12.53	1.56	50.41	3.17	5.48	11.47	5.86
CD4+T/CD8+T [0.71–2.78]	0.85	3.4	8.11	2.24	0.44	0.44	1.63	1.78	1.18	0.68
Lym (/μL) [1,530–3,700]	434.07	263	319.81	883	1,909	63.74	1,169.07	219	142.36	340.34
T (/μL) [955–2,860]	335.28	213	174.69	632	1,872	40.15	703.91	102	90.89	265.62
CD4+T (/μL) [550–1,440]	170.37	156	74.08	430	563	12.1	424.48	65	48.53	108.84
CD8+T (/μL) [320–1,250]	201.37	46	86.44	191	1,288	27.32	260.11	37	41.18	161.05
B (/μL) [90–560]	74.81	47	111.74	132	0	8.56	379.69	99	26.18	33.97
NK (/μL) [150–1,100]	12.28	4	30.13	112	29	11.8	36.16	12	16.32	18.02

ALT, alanine aminotransferase; APTT, activated partial thromboplastin time; ARDS, acute respiratory distress syndrome; B, B lymphocyte; BNP, N-terminal pro-brain natriuretic peptide; CK-MB, creatine kinase-MB; Cr, creatinine; CRP, C-reactive protein; Glu, glucose; HGB, hemoglobin; IL-6, interleukin-6; Lac, lactic acid; Lym, Lymphocyte; NA, not available; NK, natural killer cell; PCT, procalcitonin; PLT, platelet; PT, prothrombin time; T, T lymphocyte; TBIL, total bilirubin; TNI, high-sensitivity cardiac troponin I; TNT, high-sensitivity cardiac troponin T; WBC, white blood cell.

[1]The case sequence is identical to Table 1.

[2]Normal reference range of our laboratory was given in square brackets. The same below.

[3]Normal reference range of BNP in our laboratory: <300 pg/mL (<50 years); <900 pg/mL (50–75 years); <1,800 pg/mL (>75 years).

require aggressive antifungal therapy and invasive intervention in some cases. The results of mNGS and conventional diagnostic methods suggest that most of these patients also had concurrent bacterial or viral infections. Elevated inflammatory marks, such as white blood cell count, CRP, PCT, or IL-6, also suggest the possibility of concurrent infection. These patients progressed rapidly and had a poor prognosis; empirical use of antibiotics or antivirals before obtaining microbiological results may be reasonable.

The incidence of COVID-19-associated CAPA among patients who have been admitted to the ICU has been documented to vary from 19.6% to 33.3% (Fortun et al., 2023). Patients with CAPA had poorer prognoses, as evidenced by higher ordinal disease severity scores and longer recovery times, with mortality rates estimated to be approximately 50%, despite the widespread use of antifungals (Chong and Neu, 2021). In our study, of the 10 fungal-positive patients by mNGS testing, probable CAPA was diagnosed in 6 patients and possible CAPA was diagnosed in the remaining 4 patients. It is suggested that the results of mNGS testing and conventional diagnostic methods are largely consistent.

Lymphocyte analysis serves as a means to evaluate the immune system function, which includes the number and proportion of different types of lymphocytes in the blood (Luo et al., 2019). Lymphocyte analysis is of great significance for the diagnosis and prognosis evaluation of COVID-19 infection. COVID-19 infection may result in a decrease in lymphocyte count, especially CD8+ T, CD4+ T, and natural killer (NK) cells, which may lead to an impaired immune response to pathogens and aggravate the disease (Carsetti et al., 2020; Diao et al., 2020). Dysregulation of lymphocyte subsets may also be one of the reasons for the occurrence of dangerous and uncontrollable inflammatory response, namely, “cytokine storm”, in COVID-19 patients (Ghasemzadeh et al., 2022; Zanza et al., 2022). Some studies have found that the abnormal distribution of lymphocyte subpopulations may be associated with the severity of COVID-19 infection (Tan et al., 2020; Cantenys-Molina et al., 2021; Liu et al., 2021). We retrospectively reviewed the proportions and counts of T cells from the 10 patients (Table 2). Apart from one patient with thymoma (Patient #5), the T, CD4+ T, CD8+ T, and NK cell proportions in the other nine patients were mostly within the normal range or close to the normal range. However, the T, CD4+ T, CD8+ T, and NK cell counts of these patients were significantly decreased. These findings are consistent with literature reports, indicating that the immune system of patients with ARDS complicated by COVID-19 infection is significantly impaired. The lymphocyte ratio and count in blood routine examination also confirmed the immune system damage in these patients.

The SOFA scoring system has been widely applied in clinical research and critical care fields, especially in evaluating the condition and prognosis of patients with severe infections and ARDS. In our study, all 10 patients had a SOFA score greater than 2 upon admission to the ICU, indicating a high incidence of sepsis in patients with COVID-19 and ARDS. The CRB-65 score is used to assess the severity of community-acquired pneumonia and can help guide clinical decision-making for hospitalization and predict mortality. Interestingly, among the 10 patients, 8 patients

had a CURB-65 score of less than 3 upon ICU admission. This suggests that for COVID-19 patients with ARDS, the CURB-65 score may need to be dynamically evaluated after admission. The Acute Physiology and Chronic Health Evaluation (APACHE) II score is a widely used clinical prediction tool that assesses the severity of critical illness in patients admitted to ICUs. Of the 10 patients, 6 patients had an APACHE II score greater than 15 upon ICU admission, indicating the severity of the disease.

In addition to respiratory symptoms, COVID-19 has been reported to cause damage to other organs, including the heart, liver, kidney, and the nervous system (Jain, 2020). Our study also supports the findings mentioned above. For example, some patients required renal replacement therapy or ECMO support (Table 1), while others exhibited abnormal coagulation, liver, kidney, or cardiac function indicators (Table 2). These extra-pulmonary manifestations highlight the systemic nature of COVID-19 and the need for comprehensive clinical management.

This study also has some limitations: (1) the sample size is relatively small, and (2) the data came from a single center during the outbreak of Omicron infection. Our findings need to be confirmed in clinical trials to elucidate the role of mNGS and COVID-19 in pulmonary critically ill patients in the future.

5 Conclusion

It is possible for COVID-19 patients to have a higher chance of developing fungal infections, along with simultaneous viral or bacterial infections. The utilization of mNGS can aid in detecting these infections effectively. Healthcare providers must be mindful of the heightened risk of fungal infections among COVID-19 patients, especially those with existing immunocompromised states. Early infection signs should be closely monitored.

Data availability statement

The raw data supporting the conclusions of this article will be made available by the authors, without undue reservation.

Ethics statement

The studies involving humans were approved by Ethic committee of the First Affiliated Hospital of Zhengzhou University. The studies were conducted in accordance with the local legislation and institutional requirements. The ethics committee/institutional review board waived the requirement of written informed consent for participation from the participants or the participants' legal guardians/next of kin because (1) The research involves risks no greater than minimal risk, exclusively involves retrospective data collection, and does not interfere with clinical diagnosis and treatment; (2) Waiving informed consent will not adversely affect the rights or benefits of the subjects; (3) Patients have been discharged, and some have died. Without waiving informed consent, the research cannot proceed.

Author contributions

Conceptualization, WG and MF; methodology, CH and SC; validation, RM, YS, and YL; data curation, YW; writing-original draft preparation, CH and RM; writing-review and editing, SC, YS, and YL; supervision, WG and MF. All authors contributed to the article and approved the submitted version.

Funding

The author(s) declare financial support was received for the research, authorship, and/or publication of this article. This study was supported by the "Joint Construction Project of Medical Science and Technology of Henan Province" (No. LHGJ20220316) and the "Liver and Biliary Mutual Aid Fund of Henan Province Charity Federation" (No. GDXZ2023004).

Acknowledgments

The authors thank Huifang Sun for technical assistance.

Conflict of interest

The authors declare that the research was conducted in the absence of any commercial or financial relationships that could be construed as a potential conflict of interest.

Publisher's note

Supplementary material

The Supplementary Material for this article can be found online at: https://www.frontiersin.org/articles/10.3389/fcimb.2023.1220012/full#supplementary-material

References

Amin, A., Vartanian, A., Poladian, N., Voloshko, A., Yegiazaryan, A., Al-Kassir, A. L., et al. (2021). Root causes of fungal coinfections in COVID-19 infected patients. *Infect. Dis. Rep.* 13, 1018–1035. doi: 10.3390/idr13040093

Baddley, J. W., Thompson, G. R. 3rd, Chen, S. C., White, P. L., Johnson, M. D., Nguyen, M. H., et al. (2021). Coronavirus disease 2019-associated invasive fungal infection. *Open Forum Infect. Dis.* 8, ofab510. doi: 10.1093/ofid/ofab510

Bhatt, K., Agolli, A., Patel, M. H., Garimella, R., Devi, M., Garcia, E., et al. (2021). High mortality co-infections of COVID-19 patients: mucormycosis and other fungal infections. *Discoveries (Craiova)* 9, e126. doi: 10.15190/d.2021.5

Buil, J. B., Meijer, E. F. J., Denning, D. W., Verweij, P. E., and Meis, J. F. (2020). Burden of serious fungal infections in the Netherlands. *Mycoses* 63, 625–631. doi: 10.1111/myc.13089

Cantenys-Molina, S., Fernandez-Cruz, E., Francos, P., Lopez Bernaldo De Quiros, J. C., Munoz, P., and Gil-Herrera, J. (2021). Lymphocyte subsets early predict mortality in a large series of hospitalized COVID-19 patients in Spain. *Clin. Exp. Immunol.* 203, 424–432. doi: 10.1111/cei.13547

Carsetti, R., Zaffina, S., Piano Mortari, E., Terreri, S., Corrente, F., Capponi, C., et al. (2020). Different innate and adaptive immune responses to SARS-CoV-2 infection of asymptomatic, mild, and severe cases. *Front. Immunol.* 11, 610300. doi: 10.3389/fimmu.2020.610300

Chen, N., Zhou, M., Dong, X., Qu, J., Gong, F., Han, Y., et al. (2020a). Epidemiological and clinical characteristics of 99 cases of 2019 novel coronavirus pneumonia in Wuhan, China: a descriptive study. *Lancet* 395, 507–513. doi: 10.1016/S0140-6736(20)30211-7

Chen, X., Ding, S., Lei, C., Qin, J., Guo, T., Yang, D., et al. (2020b). Blood and bronchoalveolar lavage fluid metagenomic next-generation sequencing in pneumonia. *Can. J. Infect. Dis. Med. Microbiol.* 2020, 6839103. doi: 10.1155/2020/6839103

Chong, W. H., and Neu, K. P. (2021). Incidence, diagnosis and outcomes of COVID-19-associated pulmonary aspergillosis (CAPA): a systematic review. *J. Hosp Infect.* 113, 115–129. doi: 10.1016/j.jhin.2021.04.012

Diao, B., Wang, C., Tan, Y., Chen, X., Liu, Y., Ning, L., et al. (2020). Reduction and functional exhaustion of T cells in patients with coronavirus disease 2019 (COVID-19). *Front. Immunol.* 11, 827. doi: 10.3389/fimmu.2020.00827

Doman, M., and Banyai, K. (2022). COVID-19-associated fungal infections: an urgent need for alternative therapeutic approach? *Front. Microbiol.* 13, 919501. doi: 10.3389/fmicb.2022.919501

Duan, H., Li, X., Mei, A., Li, P., Liu, Y., Li, X., et al. (2021). The diagnostic value of metagenomic next rectanglegeneration sequencing in infectious diseases. *BMC Infect. Dis.* 21, 62. doi: 10.1186/s12879-020-05746-5

El-Kamand, S., Papanicolaou, A., and Morton, C. O. (2019). The use of whole genome and next-generation sequencing in the diagnosis of invasive fungal disease. *Curr. Fungal Infection Rep.* 13, 284–291. doi: 10.1007/s12281-019-00363-5

Ezeokoli, O. T., Gcilitshana, O., and Pohl, C. H. (2021). Risk factors for fungal co-infections in critically ill COVID-19 patients, with a focus on immunosuppressants. *J. Fungi (Basel)* 7, 545. doi: 10.3390/jof7070545

Force, A. D. T., Ranieri, V. M., Rubenfeld, G. D., Thompson, B. T., Ferguson, N. D., Caldwell, E., et al. (2012). Acute respiratory distress syndrome: the Berlin Definition. *JAMA* 307, 2526–2533. doi: 10.1001/jama.2012.5669

Fortun, J., Mateos, M., de la Pedrosa, E. G., Soriano, C., Pestana, D., Palacios, J., et al. (2023). Invasive pulmonary aspergillosis in patients with and without SARS-CoV-2 infection. *J. Fungi (Basel)* 9, 130. doi: 10.3390/jof9020130

Ghasemzadeh, M., Ghasemzadeh, A., and Hosseini, E. (2022). Exhausted NK cells and cytokine storms in COVID-19: Whether NK cell therapy could be a therapeutic choice. *Hum. Immunol.* 83, 86–98. doi: 10.1016/j.humimm.2021.09.004

Gu, W., Deng, X., Lee, M., Sucu, Y. D., Arevalo, S., Stryke, D., et al. (2021). Rapid pathogen detection by metagenomic next-generation sequencing of infected body fluids. *Nat. Med.* 27, 115–124. doi: 10.1038/s41591-020-1105-z

Gu, W., Miller, S., and Chiu, C. Y. (2019). Clinical metagenomic next-generation sequencing for pathogen detection. *Annu. Rev. Pathol.* 14, 319–338. doi: 10.1146/annurev-pathmechdis-012418-012751

Hoenigl, M., Seidel, D., Sprute, R., Cunha, C., Oliverio, M., Goldman, G. H., et al. (2022). COVID-19-associated fungal infections. *Nat. Microbiol.* 7, 1127–1140. doi: 10.1038/s41564-022-01172-2

Hu, B., Guo, H., Zhou, P., and Shi, Z. L. (2021). Characteristics of SARS-CoV-2 and COVID-19. *Nat. Rev. Microbiol.* 19, 141–154. doi: 10.1038/s41579-020-00459-7

Huang, C., Wang, Y., Li, X., Ren, L., Zhao, J., Hu, Y., et al. (2020a). Clinical features of patients infected with 2019 novel coronavirus in Wuhan, China. *Lancet* 395, 497–506. doi: 10.1016/S0140-6736(20)30183-5

Huang, J., Jiang, E., Yang, D., Wei, J., Zhao, M., Feng, J., et al. (2020b). Metagenomic next-generation sequencing versus traditional pathogen detection in the diagnosis of peripheral pulmonary infectious lesions. *Infect. Drug Resist.* 13, 567–576. doi: 10.2147/IDR.S235182

Jain, U. (2020). Effect of COVID-19 on the organs. *Cureus* 12, e9540. doi: 10.7759/cureus.9540

Koehler, P., Cornely, O. A., Bottiger, B. W., Dusse, F., Eichenauer, D. A., Fuchs, F., et al. (2020). COVID-19 associated pulmonary aspergillosis. *Mycoses* 63, 528–534. doi: 10.1111/myc.13096

Li, H. (2022). Editorial: mNGS for fungal pulmonary infection diagnostics. *Front. Cell Infect. Microbiol.* 12, 864163. doi: 10.3389/fcimb.2022.864163

Liu, G., Jiang, X., Zeng, X., Pan, Y., and Xu, H. (2021). Analysis of lymphocyte subpopulations and cytokines in COVID-19-associated pneumonia and community-acquired pneumonia. *J. Immunol. Res.* 2021, 6657894. doi: 10.1155/2021/6657894

Luo, Y., Xie, Y., Zhang, W., Lin, Q., Tang, G., Wu, S., et al. (2019). Combination of lymphocyte number and function in evaluating host immunity. *Aging (Albany NY)* 11, 12685–12707. doi: 10.18632/aging.102595

Mendonca, A., Santos, H., Franco-Duarte, R., and Sampaio, P. (2022). Fungal infections diagnosis - Past, present and future. *Res. Microbiol.* 173, 103915. doi: 10.1016/j.resmic.2021.103915

Seyedjavadi, S. S., Bagheri, P., Nasiri, M. J., Razzaghi-Abyaneh, M., and Goudarzi, M. (2022). Fungal infection in co-infected patients with COVID-19: an overview of case reports/case series and systematic review. *Front. Microbiol.* 13, 888452. doi: 10.3389/fmicb.2022.888452

Shereen, M. A., Khan, S., Kazmi, A., Bashir, N., and Siddique, R. (2020). COVID-19 infection: Origin, transmission, and characteristics of human coronaviruses. *J. Adv. Res.* 24, 91–98. doi: 10.1016/j.jare.2020.03.005

Song, N., Li, X., Liu, W. J. J. O. L., and Medicine, P. (2021). Metagenomic next-generation sequencing (mNGS) for diagnosis of invasive fungal infectious diseases: a narrative review. *Transl. Cancer Res.* 10, 966–976. doi: 10.21037/jlpm-21-25

Tan, L., Wang, Q., Zhang, D., Ding, J., Huang, Q., Tang, Y. Q., et al. (2020). Lymphopenia predicts disease severity of COVID-19: a descriptive and predictive study. *Signal Transduct Target Ther.* 5, 33. doi: 10.1038/s41392-020-0148-4

Tang, W., Zhang, Y., Luo, C., Zhou, L., Zhang, Z., Tang, X., et al. (2021). Clinical application of metagenomic next-generation sequencing for suspected infections in patients with primary immunodeficiency disease. *Front. Immunol.* 12, 696403. doi: 10.3389/fimmu.2021.696403

The, L. (2023). The COVID-19 pandemic in 2023: far from over. *Lancet* 401, 79.

Wang, C., You, Z., Fu, J., Chen, S., Bai, D., Zhao, H., et al. (2022). Application of metagenomic next-generation sequencing in the diagnosis of pulmonary invasive fungal disease. *Front. Cell Infect. Microbiol.* 12, 949505. doi: 10.3389/fcimb.2022.949505

Wilson, M. R., Naccache, S. N., Samayoa, E., Biagtan, M., Bashir, H., Yu, G., et al. (2014). Actionable diagnosis of neuroleptospirosis by next-generation sequencing. *N Engl. J. Med.* 370, 2408–2417. doi: 10.1056/NEJMoa1401268

Wu, S., Song, J., Hu, F., Li, H., Tian, Y., Cheng, W., et al. (2023). Pneumonia during the COVID-19 pandemic in hubei province, China: a case report of mucormycosis. *Clin. Lab.* 69. doi: 10.7754/Clin.Lab.2022.220905

Yang, X., Yu, Y., Xu, J., Shu, H., Xia, J., Liu, H., et al. (2020). Clinical course and outcomes of critically ill patients with SARS-CoV-2 pneumonia in Wuhan, China: a single-centered, retrospective, observational study. *Lancet Respir. Med.* 8, 475–481. doi: 10.1016/S2213-2600(20)30079-5

Zanza, C., Romenskaya, T., Manetti, A. C., Franceschi, F., La Russa, R., Bertozzi, G., et al. (2022). Cytokine storm in COVID-19: immunopathogenesis and therapy. *Medicina (Kaunas)* 58, 144. doi: 10.3390/medicina58020144

Zheng, Y., Qiu, X., Wang, T., and Zhang, J. (2021). The diagnostic value of metagenomic next-generation sequencing in lower respiratory tract infection. *Front. Cell Infect. Microbiol.* 11, 694756. doi: 10.3389/fcimb.2021.694756

Frontiers in
Cellular and Infection Microbiology

Investigates how microorganisms interact with their hosts

Explores bacteria, fungi, parasites, viruses, endosymbionts, prions and all microbial pathogens as well as the microbiota and its effect on health and disease in various hosts.

Discover the latest Research Topics

See more →

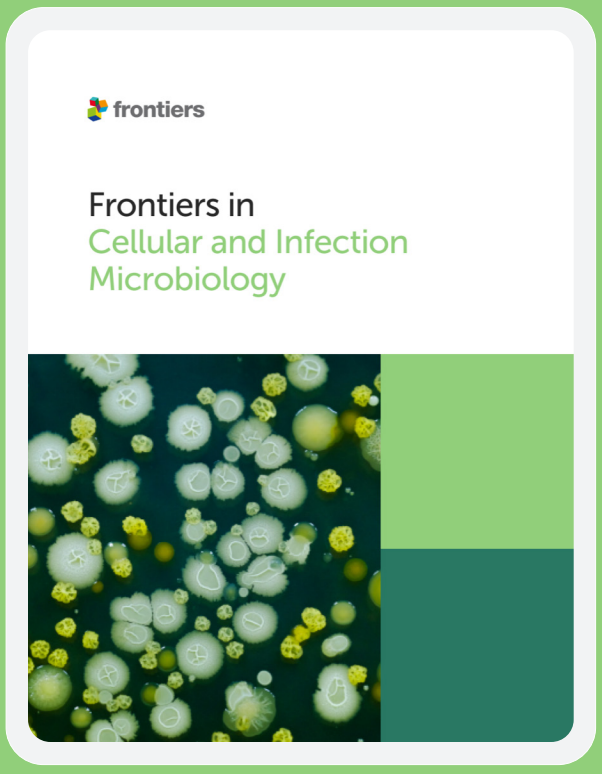

Frontiers

Avenue du Tribunal-Fédéral 34
1005 Lausanne, Switzerland
frontiersin.org

Contact us

+41 (0)21 510 17 00
frontiersin.org/about/contact